Annual Issue 2012

The Journal on Advanced Studies in Theoretical and Experimental Physics, including Related Themes from Mathematics

PROGRESS IN PHYSICS

"All scientists shall have the right to present their scientific research results, in whole or in part, at relevant scientific conferences, and to publish the same in printed scientific journals, electronic archives, and any other media."
— Declaration of Academic Freedom, Article 8

ISSN 1555-5534

The Journal on Advanced Studies in Theoretical and Experimental Physics, including Related Themes from Mathematics

PROGRESS IN PHYSICS

A quarterly issue scientific journal, registered with the Library of Congress (DC, USA). This journal is peer reviewed and included in the abstracting and indexing coverage of: Mathematical Reviews and MathSciNet (AMS, USA), DOAJ of Lund University (Sweden), Zentralblatt MATH (Germany), Scientific Commons of the University of St. Gallen (Switzerland), Open-J-Gate (India), Referativnyi Zhurnal VINITI (Russia), etc.

Electronic version of this journal:
http://www.ptep-online.com

Postal Address

Department of Mathematics and Science,
University of New Mexico,
200 College Road, Gallup, NM 87301, USA

ISSN: 1555-5534 (print)
ISSN: 1555-5615 (online)

Standard Address Number: 297-5092
Printed in the United States of America

JANUARY 2012 **VOLUME 1**

CONTENTS

Information for Authors and Subscribers

Progress in Physics has been created for publications on advanced studies in theoretical and experimental physics, including related themes from mathematics and astronomy. All submitted papers should be professional, in good English, containing a brief review of a problem and obtained results.

All submissions should be designed in LaTeX format using *Progress in Physics* template. This template can be downloaded from *Progress in Physics* home page http://www.ptep-online.com. Abstract and the necessary information about author(s) should be included into the papers. To submit a paper, mail the file(s) to the Editor-in-Chief.

All submitted papers should be as brief as possible. We accept brief papers, no larger than 8 typeset journal pages. Short articles are preferable. Large papers can be considered in exceptional cases to the section *Special Reports* intended for such publications in the journal. Letters related to the publications in the journal or to the events among the science community can be applied to the section *Letters to Progress in Physics*.

All that has been accepted for the online issue of *Progress in Physics* is printed in the paper version of the journal. To order printed issues, contact the Editors.

This journal is non-commercial, academic edition. It is printed from private donations. (Look for the current author fee in the online version of the journal.)

A New Theoretical Derivation of the Fine Structure Constant

Eckart Schönfeld* and Peter Wilde†

*Physikalisch Technische Bundesanstalt (PTB) Braunschweig (retired), Kritzower Straße 4, 19412 Weberin, Germany.
†University of Applied Sciences Jena, Carl-Zeiss-Promenade 2, 07745 Jena, Germany. E-mail: Peter.Wilde@TU-Ilmenau.de

The present paper is devoted to a new derivation of the expression given already earlier for the fine structure constant α. This expression is exactly the same as that what we published several times since 1986. The equation $1/\alpha = \pi^4 \sqrt{2}\ m_{qm}/m_0$ (m_0 being the rest mass of the electron and m_{qm} the quantum-mechanical fraction of it) is precisely confirmed. The new derivation is based on relations for the energy density in the interior of a macroscopically resting electron within the framework of our standing wave model. This model is strongly supported by the present investigation. Two equations for the energy density inside of an electron were set equal, one of them is taken from classical electrodynamics, the other uses relations from quantum mechanics, special relativity theory and four-dimensional space. As the final theoretical equation for the fine structure constant is unchanged, the numerical value as published in 2008 is still maintained: $1/\alpha = 137.035\,999\,252$.

1 Introduction

In the fine structure constant $\alpha = e^2/\hbar c$ the constants of the electron charge e, Planck's constant h and the light velocity c are flowing together. These fundamental constants play a leading role in electrodynamics (ED), quantum mechanics (QM) and special relativity theory (SRT). Pauli [1] has called the explanation of the fine structure constant one of the most important problems of modern atomic physics. Mac Gregor 1971 [2] discussed α as an universal scaling factor. Here we present a new derivation for the fine structure constant obtained by equalizing two expressions for the energy density of the electromagnetic field inside the electron. One of these relations is based on ED, the other one is based on QM and SRT. In our opinion the new derivation is extraordinarily beautiful, simple and elegant.

We have developed a model of a macroscopically resting extended electron, called standing wave model. This model is based on the assumption that there is an internal energy flux along a closed curve of everywhere the same curvature. The energy flux takes place with velocity of light and is located on the surface of a sphere with radius r_m. The curve is denoted as spherical loop. It has an arc length $4\pi\rho_m$, where $\rho_m = r_m/\sqrt{2}$ is its radius of curvature and it consists of four semi circles. The internal motion produces the spin, magnetic moment and the electromagnetic field of the electron. In a set of publications [3–5] the authors have reported about these subjects.

Moreover, a study of the internal energy transport allowed us to derive a relation for the fine structure constant by investigating longitudinal and transversal standing waves inside of the electron. Here a new explanation of the fine structure constant is presented, also based on the standing wave model of the macroscopically resting electron but following a way which is essentially new.

We are convinced the new way of deriving α is of peculiar interest in understanding the structure of elementary particles. Therefore, we would like to open a discussion about our ideas and procedures.

2 Energy density based on electrodynamics

From classical electrodynamics applied to our standing wave model we were able to calculate the energy contributions of the electromagnetic field to the self-energy of an electron in the whole space. The energy flux is located on the surface of a sphere with the radius [5]

$$r_m = \frac{\hbar}{\sqrt{2} m_{qm} c}, \tag{1}$$

where m_{qm} denotes the quantum-mechanical fraction of the rest mass m_0 of the electron. Quantities which have a subscript m are related to the surface or the interior of a sphere with radius r_m and a subscript qm shall indicate that the corresponding quantity is related to quantum mechanics. Inside the sphere there are a transversal electric field with a field strength $\mathbf{E^t_m}$, and a magnetic field with a field strength $\mathbf{H_m}$. The absolute values of both field strengths are equal inside the sphere of radius r_m [5]:

$$\frac{e}{r_m^2} = |\mathbf{E^t_m}| = |\mathbf{H_m}|. \tag{2}$$

These fields are supposed to be homogeneous inside, i.e. the magnitudes of the field strenghts do not depend on the position. The volume of the sphere is given by

$$V_m = \frac{4}{3}\pi r_m^3. \tag{3}$$

The energy densities of the electric and magnetic fields can be taken from the field strength squares [6]:

$$u_E = \frac{1}{8\pi}|\mathbf{E^t_m}|^2 \tag{4}$$

$$u_H = \frac{1}{8\pi}|\mathbf{H_m}|^2. \tag{5}$$

The total energy density u_s of the electromagnetic field inside the electron is

$$u_s = u_E + u_H = \frac{2}{8\pi}\frac{e^2}{r_m^4}. \tag{6}$$

By integration over the sphere and using eq. (1) as well as the definition of the fine structure constant, the corresponding field energy is obtained

$$\begin{aligned} W_s &= \frac{2}{8\pi}\int_0^{r_m}\int_0^{\pi}\int_0^{2\pi}\frac{e^2}{r_m^4}r^2\sin\varphi\, d\theta\, d\varphi\, dr \\ &= \frac{2}{3}\frac{e^2}{2r_m} = \frac{2}{3}\frac{\alpha}{\sqrt{2}}m_{qm}c^2. \end{aligned} \tag{7}$$

The subscript s shall indicate that the corresponding quantities are related to the standing wave model.

3 Energy density based on QM, SRT and four dimensional space

We start from the three dimensional surface $S_{qm} = 2\pi^2 R^3$ of a four dimensional sphere (cf Schmutzer 1958 [7]). Choosing for the radius $R = \pi r_m$ there follows

$$S_{qm} = 2\pi^5 r_m^3. \tag{8}$$

The zero point energy inside this sphere is given by

$$W_{qm} = \frac{1}{2}\hbar\omega_0, \tag{9}$$

where ω_0 is the lowest possible, positive eigen frequency of the corresponding basic harmonic oscillator. According to the standing wave model this harmonic oscillator describes the electron. From the de Broglie relation

$$E = \hbar\omega_0 = m_0c^2 \tag{10}$$

there follows

$$W_{qm} = \frac{1}{2}m_0c^2, \tag{11}$$

and the energy density can be obtained from (8) and (11)

$$u_{qm} = \frac{W_{qm}}{S_{qm}} = \frac{m_0c^2}{4\pi^5 r_m^3}. \tag{12}$$

4 Fine structure constant

A calculation of the values of u_s and u_{qm} show that they are very close to each other. This stimulated us to set

$$u_s = u_{qm}. \tag{13}$$

Indeed, using (1), (6) and (12), we obtain

$$u_s = u_{qm} \Leftrightarrow \frac{e^2}{\hbar c} = \frac{1}{\sqrt{2}\pi^4}\frac{m_0}{m_{qm}}. \tag{14}$$

Now, using the definition of the fine structure constant, for the inverse of it there follows immediately

$$\frac{1}{\alpha} = \pi^4\sqrt{2}\frac{m_{qm}}{m_0}, \tag{15}$$

where m_0 denotes the rest mass of the electron and m_{qm} its quantum-mechanical fraction. Just the same relation has been found earlier in an other way [3–5]. There, we have shown that both, m_0 and m_{qm}, are depending on α. Solving equation (15) the latest theoretical value of the inverse fine structure constant is [5]

$$\frac{1}{\alpha} = 137.035\,999\,252. \tag{16}$$

This value has to be compared with the semi experimental value 137.035 999 084(51) obtained by combining theory and experiment of the anomalous magnetic moment of the electron [8], as well as with the value 137.035 999 074(44), which is the latest CODATA value [9] from 2010. Furthermore, the ratio m_0/m_{qm} is obtained to be

$$\frac{m_0}{m_{qm}} = 1.005\,263\,277. \tag{17}$$

If we replace (as an alternative) m_0 in (11) by m_{qm} and simultaneously e^2 in (6) by e_i^2 (e_i is the intrinsic or bare charge of the electron) then we have exactly the wonderful relation

$$\frac{\hbar c}{e_i^2} = \pi^4\sqrt{2} = 137.757\,257... \tag{18}$$

The equations (15) and (18) are identical if

$$\frac{m_0}{m_{qm}} = \frac{e^2}{e_i^2}. \tag{19}$$

5 Discussion and conclusions

The numerical value of the fine-structure constant α was often denoted to be a mystery, a magic number and an enigma. A lot of more or less obscure relations have been published with the aim to understand the origin, theoretical background and the numerical value of the fine structure constant, see for example the comprehensive compilation of Kragh 2003 [10]. Why a derivation like the present one has not been carried out earlier? Probably it was the lack of an accurate model of an extended electron. No such model was available, see for example Mac Gregor 1992 [11]. We are convinced that without an understanding of the geometry and inner dynamics of the electron, a consistent understanding of the fine structure constant will not be possible. The simplicity of the present explanation of the fine structure constant is really surprising. Nevertheless, a more detailed discussion and interpretation of the roots of the fine structure constant would be very desirable. So far it concerns the history it should be remarked that already König 1951 [12] found as a byproduct in a rather

complicated argumentation the same expression for α as we found here but without the factor m_{qm}/m_0. A difference between the theoretical and the experimental value of 0.53 % might be the reason that his paper, entitled "An electromagnetic wave picture of micro processes", have found very little attention.

We do not intend to give here a comprehensive discussion of the many aspects which are coupled with the fine structure constant. Several essays have been published devoted to to different aspects (Bahcall and Schmidt 1967 [13] (variation of α with time), Jehle 1972 [14] and 1977 [15] (flux quantization, loops, general discussion), Wilczek 2007 [16] (fundamental constants), Jordan 1939 [17] (cosmological constancy), Peik et al 2004 [18] (temporal limit), Dehnen et al. 1961 [19] (independence on gravitation field), Srianand et al. 2004 [20] (limits on time variation), Schönfeld 1996 [21] (self-energy analysis, see also [3–5])). We would like to remark and underline only two aspects of the present results: one is the exponent four at π which is obviously connected to the four dimensions of our world, the other is that the present result supports strongly the independence of the fine structure constant on time and space, i.e. expresses the cosmological constancy of alpha which was studied by theory and experiment in the last time. Naturally an experiment can give only an upper limit of time or position variation, compare [17–20].

Acknowledgements

The authors are very much indebted to Dr. Harald Hein (Jena) for his critical review, comprehensive discussion and contributions.

Submitted on October 4, 2011 / Accepted on October 13, 2011

References

1. Pauli W. Sommerfelds Beiträge zur Quantentheorie. *Naturwissenschaften*, 1948, v. 35, 129–132.
2. Mac Gregor M. H. The fine-structure constant $\alpha = e^2/\hbar c$ as a universal scaling factor. *Lettere al Nuovo Cimento* 1971, v. 1 (18), 759–764.
3. Schönfeld E. Versuch einer Deutung des Zahlenwertes der Feinstrukturkonstante auf der Basis eines Teilchenmodells. *Experimentelle Technik der Physik (Jena)*, 1986, v. 34, 433–437.
4. Schönfeld E. Electron and Fine Structure Constant. *Metrologia*, 1990, v. 27, 117–125.
5. Schönfeld E., Wilde P. Electron and fine structure constant II. *Metrologia*, 2008, v. 45, 342–355.
6. Jackson J. D. Classical Electrodynamics. Wiley, New York, 1998.
7. Schmutzer E. Spezielle relativistische Auswertung einer Variante der projektiven Relativitätstheorie. *Annalen der Physik*, 1958, v. 7, 136–144.
8. Hanneke D., Fogwell S., Gabrielse G. New measurement of the electron magnetic moment and the fine-structure constant. *Physical Review Letters*, 2008, v. 100, 120801–120805.
9. http://physics.nist.gov/
10. Kragh H. Magic number: A partial history of the fine-structure constant. *Archive for History of Exact Sciences*, 2003, v. 57, 395–431.
11. Mac Gregor M. H. The enigmatic electron. Kluver Acad. Publ., Dordrecht, 1992.
12. König H. W. Zu einem elektromagnetischen Wellenbild von Mikrovorgängen. *Acta Physica Austriaca*, 1951, v. 5. 286–318.
13. Bahcall J. N., Schmidt M. Does the fine-structure constant vary with time? *Physical Review Letters*, 1967, v. 19, 1294–1295.
14. Jehle H. Relationship of flux quantization and the electro magnetic coupling constant. *Physical Review D*, 1972, v. 3, 306–345.
15. Jehle H. Electron muon puzzle and the electromagnetic coupling constant. *Physical Review D*, 1977, v. 15, 3727–3759.
16. Wilczek F. Fundamental constants. arXiv: hep-ph/0708.4361v1.
17. Jordan P. Über die kosmologische Konstanz der Feinstrukturkonstante. *Zeitschrift für Physik*, 1939, v. 113, 660–662.
18. Peik E. et al. Limit on the temporal variation of the fine-structure constant. *Physical Review Letters*, 2004, v. 93, 170801–170805.
19. Dehnen H., Hönl H., Westpfahl K. Über die Unabhängigkeit der Feinstrukturkonstante vom Gravitationsfeld. *Zeitschrift für Physik*, 1961, v. 164, 486–493.
20. Srianand R., Chand H., Petitjean P. and Aracil B. Limits on the time variation of the electromagnetic fine-structure constant in the low energy limit from absorption lines in the spectra of distant quasars. *Physical Review Letters*, 2004, v. 92 (12), 121302–121306.
21. Schönfeld E. Contributions to the Self-energy of a Macroscopically Resting Electron within the Framework of the Standing Wave Model. *PTB Report* (Monograph series issued by the "Physikalisch Technische Bundesanstalt" in Braunschweig, Germany), 1996, PTB-RA-40.

Redshift Adjustment to the Distance Modulus

Yuri Heymann

3 rue Chandieu, 1202 Geneva, Switzerland
E-mail: y.heymann@yahoo.com

The distance modulus is derived from the logarithm of the ratio of observed fluxes of astronomical objects. The observed fluxes need to be corrected for the redshift as the ratio of observed to the emitted energy flux is proportional to the wavelength ratio of the emitted to observed light according to Planck's law for the energy of the photon. By introducing this redshift adjustment to the distance modulus, we find out that the apparent "acceleration" of the expansion of the Universe that was obtained from observations of supernovae cancels out.

1 Introduction

In the present study a redshift adjustment to the distance modulus was introduced. The rationale is that the observed fluxes of astronomical objects with respect to the emitting body are being reduced by the effect of redshift. According to Planck's law, the energy of the photon is inversely proportional to the wavelength of light; therefore, the ratio of observed to emitted fluxes should be multiplied by the wavelength ratio of emitted to observed light.

2 Model development

Below is shown the derivation of the redshift adjusted distance modulus.

Let us recall the derivation of the distance modulus. The magnitude as defined by Pogson [1] is:

$$m = -2.5 \log F + K, \tag{1}$$

where m is the magnitude, F the flux or brightness of the light source, and K a constant. The absolute magnitude is defined as the apparent magnitude measured at 10 parsecs from the source.

By definition, the brightness is a measure of the energy flux from an astronomical object and depends on distance. Therefore, a redshift correction to the flux is derived from Planck's law for the energy of the photon

$$E = \frac{h \cdot c}{\lambda}, \tag{2}$$

where E is the energy of the photon, h the Planck's constant, and λ the light wavelength.

The ratio of observed to emitted energy flux is derived from eq. (2), leading to

$$\frac{E_{obs}}{E_{emit}} = \frac{\lambda_{emit}}{\lambda_{obs}} = \frac{1}{1+z}, \tag{3}$$

where E_{obs} and E_{emit} are respectively the observed and emitted energy fluxes, λ_{obs} and λ_{emit} are respectively the observed and emitted light wavelengths, and z the redshift.

As light is emitted from a source, it is spread out uniformly over a sphere of area $4\pi d^2$. Excluding the redshift effect, the brightness – expressed in units of energy per time and surface area – diminishes with a relationship proportional to the inverse of square distance from the source of light. Therefore, taking into account the redshift effect, the following relationship is obtained for the brightness:

$$F_{obs} \propto \frac{L_{emit}}{d^2} \cdot \frac{E_{obs}}{E_{emit}}, \tag{4}$$

where L_{emit} is the emitted luminosity, and d the distance to the source of light.

Combining eq. (1), (3) and (4), we obtain

$$m = -2.5 \log \left(\frac{L_{emit}}{d^2 \cdot (1+z)} \right) + K. \tag{5}$$

And, because z is close to zero at 10 Parsec:

$$M = -2.5 \log \left(\frac{L_{emit}}{100} \right) + K, \tag{6}$$

where M is the absolute magnitude.

Hence, the redshift adjusted distance modulus, eq. (5) minus eq. (6) is:

$$m - M = -5 + 5 \log d + 2.5 \log(1+z) \tag{7}$$

with d in parsec, and log is the logarithm in base 10.

3 Discussion

In the present study the distance modulus was adjusted to take into account the effect of redshifts on the observed fluxes of astronomical objects. Evidence of an "accelerating" Universe expansion was established based on the observation of supernovae [2]. This result was obtained by detecting a deviation from linearity on the distance modulus versus redshift plot in log scale for supernovae. In order to account for the redshift adjustment, the adjusted distance modulus $m - M - 2.5log(1+z)$ should be plotted againt redshifts for the supernovae. A deviation of $m - M$ of about +0.5 magnitude was obtained at redshift 0.6. The redshift adjustment

$2.5log(1+z)$ is roughly equal to this deviation. By introducing the redshift adjusted distance modulus eq. (7) this deviation cancels out, and one may no longer conclude that the expansion of the Universe is accelerating.

Submitted on October 4, 2011 / Accepted on October 12, 2011

References

1. Pogson N. Magnitudes of Thirty-six of the Minor Planets for the first day of each month of the year 1857. *Monthly Notices of the Royal Astronomical Society*, 1857, v. 17, 12–15.
2. Riess A.G., Filippenko A.V., Challis P., Clocchiatti A., Diercks A., Garnavich P.M., Gilliand R.L., Hogan C.J., Jha S., Kirshner R.P., Leibundgut B., Phillips M.M., Reiss D., Schmidt B.P., Schommer R.A., Smith R.C., Spyromilio J.S., Stubbs C., Suntzeff N.B., Tonry J. Observational Evidence from Supernovae for an Accelerating Universe and a Cosmological Constant. *The Astronomical Journal*, 1998, v. 116 1009–1038.

A Comment on arXiv:1110.2685

Armando V.D.B. Assis
Departamento de Física, Universidade Federal de Santa Catarina – UFSC, Trindade 88040-900, Florianópolis, SC, Brazil
armando.assis@pgfsc.ufsc.br

This brief paper traces comments on the article [2]. This article, a preprint, has recently received an attention, raising errors related to the timing process within the OPERA Collaboration results in [1], that turns out to be a wrong route by which serious science should not be accomplished. A peer-reviewed status should be previously considered to assert that [2] claims a solution for the superluminal results in [1]. Within [2], it seems there is an intrinsical misconception within its claimed solution, since an intrinsical proper time reasoning leads to the assumption the OPERA collaboration interprets a time variation as a proper time when correcting time intervals between a GPS frame and the grounded baseline frame. Furthermore, the author of [2] seems to double radio signals, doubling the alleged half of the truly observed time of flight, since the Lorentz transformations do consider radio signals intrinsically by construction.

1 An intrinsical proper time reasoning? A misconception from the OPERA collaboration, or from the author of [2]? What is actually observed, τ_{clock}/γ?

The author of the article [2]* used, *ab initio*, the designation: *from the perspective of the clock...* Within the approach used by the author, via special relativity, the GPS frame of reference must use ***two*** distinct but synchronized clocks to tag the instants at A and B. The eq. (2) in [2] was, intrinsically, obtained via the Lorentz transformations for the neutrino events of departure from A and arrival to B, but this was not clearly specified within [2], being the construction of the Eq. (2) in [2] crudely accomplished under what would be being seen from the perspective of the clock, in the author of [2] words:

- ***From the perspective of the clock the detector at B moves towards location A at a speed v. And we find that the foton will reach the detector when the sum of the distances covered by the detector and the foton equals the original separation...***; [2].

This reasoning, *ab initio*, leads, as it very seems, to an intrinsical proper time reasoning under the perspective of what was being seen, locally, by the satellite at its very location. Let (x_A, t_A) and (x_B, t_B) be the spacetime events of departure and arrival of the neutrino in the baseline reference frame K, respectively. The time interval spent by the neutrino to accomplish the travel in the [2] GPS reference frame K' is:

$$\delta t' = \left(1 - v^2/c^2\right)^{-1/2} \left[(t_B - t_A) - \frac{v}{c^2}(x_B - x_A)\right], \qquad (1)$$

in virtue of the canonical Lorentz transformation for time in K' as a function of the spacetime coordinates in K, where v is the assumed boost of K' in relation to K in the baseline direction AB, c the speed of light in the empty space. With $\delta t = t_B - t_A$, $\delta x = x_B - x_A = S_{baseline}$, $\delta x = v_\nu \delta t$, where v_ν is the neutrino velocity along the AB direction, the eq. (1) reads:

$$\delta t' = \left(1 - v^2/c^2\right)^{-1/2} S_{baseline} \left(\frac{1}{v_\nu} - \frac{v}{c^2}\right). \qquad (2)$$

With $v_\nu = c$, $\gamma = \sqrt{1 - v^2/c^2}$, $\delta t' \stackrel{!}{=} \tau_{clock}$, as defined in [2], the eq. (2) here becomes the eq. (2) in [2]:

$$\tau_{clock} = \frac{\gamma S_{baseline}}{c + v} \Rightarrow c\tau_{clock} + v\tau_{clock} = \gamma S_{baseline}. \qquad (3)$$

But:

- $\delta t' \stackrel{!}{=} \tau_{clock}$ is not a proper time (it is a time interval measured by distinct clocks at different spatial positions in K'); hence: why would the OPERA collaboration correct $\delta t' \stackrel{!}{=} \tau_{clock}$ via $\delta t = \delta t'/\gamma$, as claimed via the eq. (5) in [2]?
- Such correction would be plausible if the events of departure and arrival of the neutrino had the same spatial coordinate $x'_A = x'_B$ in the GPS K' frame of reference, but it is not the case.

Hence, as asserted before, the claimed solution supposes an intrinsical proper time reasoning, but there is no reason for this, since the $\delta t'$ is not a proper time. Thus, the claimed solution turns out to be constructed on an erroneous correction. The correction that should be done by the OPERA Collaboration, if the [2] GPS reference frame was to be taken in consideration, would read:

$$\delta t = \left(1 - v^2/c^2\right)^{-1/2} \left[(t'_B - t'_A) + \frac{v}{c^2}(x'_B - x'_A)\right], \qquad (4)$$

and this correction would read: $\delta t = \delta t'/\gamma$, with the $\gamma = \sqrt{1 - v^2/c^2}$ defined in [2], ***if and only if***: $x'_B - x'_A = 0$, but it is not the case.

*The comments we raise here are related to the first version of [2], v1, uploaded to arXiv. Recently, the author uploaded an updated version, but the misconceptions seem to persist. The root of the arguments within [2] to obtain the alleged 64 ns seems to be flawed *ab initio*.

Furthermore, I would like to assert that, related to the K' reference frame, the frame taken by the author of [2] to explain the relevance of the GPS reference frame in terms of special relativity: the radio signals turn out to be irrelevant to be taken into consideration once the clocks within K' are synchronized, viz., the Lorentz transformations for events do consider radio signals intrinsically under the synchronization of clocks in a given reference frame. This said, the factor 2 the author uses to reach 64 ns seems misconcepted. Remembering, the τ_{clock} is the time interval in K', it is not a proper time interval, and this time interval totally accounts for the entire process of emission and detection of the neutrino at A and B, respectively, departure and arrival, from which there are not two corrections to be accomplished at the points A and B related to radio signals. The radio signals related to the events at A and B in the GPS reference frame in [2], K', were taken into consideration *ab initio*, in [2], since the clocks at A and B in this reference frame tagging the events of departure and arrival were previously synchronized by the very radio signals the author of [2] refers at the end of his article, due to the intrinsical use of the Lorentz transformations, *ab initio*, within the eq. (2) in [2], albeit the author of [2] had not written down his eq. (2) in [2] under a Lorentzian reasoning. Hence, once the Lorentz transformations provided the τ_{clock}, the radio signals should not be considered twice.

I would like to furtherly comment the root of misconceptions, by which the author of [2] seems to have carried his reasonings to raise his arguments. Related to my previous comments, as asseverated before (see footnote 1), these ones are related to the first version of the mentioned article uploaded to arXiv. The author uploaded an updated version, but the root of misconceptions persists within his primordial reasoning related to the Lorentz transformations. It very seems the author had in mind that the time interval to be corrected $\delta t' = \tau_{clock}$ (here, we continue to consider the notations within the first version of [2], since there are not substantial modifications throughout the updated version to avoid the criticisms raised) was a proper interval. Constructing his arguments, the author refers to what is observed in the satellite reference frame. Suppose, following the author of [2] reasonings, the satellite sends a radio signal to the event at A to see the departure of the neutrino when this radio signal is sent back to the satellite. Be t'_{ESA} (E denotes emission, S denotes satellite, and A denotes the location of the CERN at the instant, read in the satellite local clock, the neutrino starts the travel to Gran Sasso) the instant this signal is sent to reach the event of the neutrino departure; t'_{RSA} (R detotes reception) the instant the signal comes back to the satellite, read in the satellite local clock. These instants are related by:

$$t'_{RSA} = t'_{ESA} + 2d'_{SA}(t'_A)/c, \tag{5}$$

where $d'_{SA}(t'_A)$ is the distance between the satellite and the CERN location at A, at the instant the signal (radio signal) reaches A, viz., $d'_{SA}(t'_A)$ is the distance between the satellite and the CERN location at A at the instant t'_A the neutrino is sent to Gran Sasso in the satellite frame. Analogous reasoning related to the neutrino arrival at Gran Sasso, at B, leads to:

$$t'_{RSB} = t'_{ESB} + 2d'_{SB}(t'_B)/c, \tag{6}$$

where $d'_{SB}(t'_B)$ is the distance between the satellite and the Gran Sasso location at B, at the instant another signal previously sent by the satellite at instant t'_{ESB} read in the satellite local clock (another radio signal) reaches B, viz., $d'_{SB}(t'_B)$ is the distance between the satellite and the Gran Sasso location at B at the instant t'_B the neutrino arrives to Gran Sasso in the satellite frame. The instants t'_A and t'_B are respectively given by:

$$t'_A = \frac{t'_{ESA} + t'_{RSA}}{2}, \tag{7}$$

and:

$$t'_B = \frac{t'_{ESB} + t'_{RSB}}{2}. \tag{8}$$

From these relations, the proper time interval between the instants the satellite ***sees*** the events of departure and arrival, $t'_{RSB} - t'_{RSA}$, is given by:

$$t'_{RSB} - t'_{RSA} = t'_B - t'_A + \frac{d'_{SB}(t'_B)}{c} - \frac{d'_{SA}(t'_A)}{c}, \tag{9}$$

therefore, since $t'_B - t'_A = \delta t' = \tau_{clock}$, see my previous comments:

$$\tau_{clock} = t'_{RSB} - t'_{RSA} - \left(\frac{d'_{SB}(t'_B)}{c} - \frac{d'_{SA}(t'_A)}{c}\right), \tag{10}$$

from which: τ_{clock} ***does take into consideration*** the radio signals travelling, encapsulated within the time intervals within:

$$\tau_{signals} = \frac{d'_{SB}(t'_B)}{c} - \frac{d'_{SA}(t'_A)}{c}. \tag{11}$$

The problem within the reasonings of the author of [2] seems to be this author was thinking that τ_{clock} would be the proper interval related to what was being seen by the satellite, $t'_{RSB} - t'_{RSA}$. Hence, at the end of his article, this author applies a correction related to radio signals to account for the time interval $t'_B - t'_A$, but this process was already done when the author obtained $\delta t' = t'_B - t'_A$, viz., as said before within my previous comments, the Lorentz transformations have got radio signals intrinsically, by construction, to deal with events in spacetime. Thus, when the author of [2] applies the factor 2, this author seems to erroneously account for radio signals twice, and the factor 2 seems misconcepted. Even if the OPERA Collaboration had done the correction the author of [2] refers to, such discrepancy would be 32 ns, but not this value twice. The factor 2 seems to have not got logical explanation within the [2] reasoning, mostly being putted a fortiori.

2 Conclusions

Respectfully, the reasoning that led the author of [2] to the factor 2 is not clear. I think this reasoning should be putted under a fairly crystalline terms, as far as possible, in virtue of the importance given to this article, in virtue of the importance given to the subject. Furthermore, what would be being observed, $\delta t'/\gamma$ (this gamma is the original one used by the author of [2]), or this value twice? Why does not the author of [2] provide spacetime diagrams showing the process related to the radio signals that doubles the alleged half of the truly observed time of flight?

Concluding, it seems unlikely that the OPERA collaboration has misinterpreted a GPS time interval within the terms of [2].

Acknowledgments

A.V.D.B.A is grateful to Y.H.V.H and CNPq for financial support.

Submitted on October 16, 2011 / Accepted on October 20, 2011

References

1. The OPERA collaboration: T. Adam et al. Measurement of the neutrino velocity with the OPERA detector in the CNGS beam http://arxiv.org/abs/1109.4897 *arXiv:1109.4897*, 2011.
2. Ronald A.J. van Elburg. Times of Flight between a Source and a Detector observed from a GPS satelite http://arxiv.org/abs/1110.2685 *arXiv:1110.2685*, 2011.

Spooky Action at a Distance or Action at a Spooky Distance?

Sebastiano Tosto

Italy. E-mail: stosto@inwind.it

The paper demonstrates that the non-locality and non-reality of the quantum world are direct consequences of the concept of uncertainty. It is also shown that the analysis of states in the phase space entails the operator formalism of wave mechanics. While being well known that the uncertainty principle is a consequence of the commutation rules of operators, the paper shows that the reverse path is also possible; i.e. the uncertainty equations entails themselves the operators and wave equations of energy and momentum. The same theoretical approach has been eventually extended to infer significant results of the special relativity.

1 Introduction

Einstein never liked the weirdness and the conceptual limit of the quantum mechanics due to its probabilistic character; for instance, he disliked the incomplete knowledge about position and momentum of a particle, about all components of angular momentum and so forth. Paradoxically, just his theory of the specific heat and its explanation of the photoelectric effect were the strongest support to the energy quantization early introduced by Plank to explain the black body radiation. In fact to the quantum theory we owe not only the ability to explain weird experimental data, e.g. the dual wave/particle behavior of matter and the tunnel effect, but also important discoveries like the laser, the transistor and the superconductivity. Further experimental evidences recently obtained compelled however accepting besides its weird character other aspects even more counterintuitive of quantum behavior. Mostly important are in this respect the non-localism and non-realism: according to the former, exchange of information is allowed even between particles separated by a superluminal distance; according to the latter, the experimental measurements do not reveal preexisting properties of particles but concur to define themselves the measured properties. The EPR gedanken experiment [1] tried to overcome the conceptual incompleteness of quantum mechanics by hypothesizing "hidden variables" in the wave function, i.e. variables not accessible to experimental evidence but able to improve our extent of knowledge and to overcome the difficulty of a "spooky action at a distance" between correlated couples of particles. Yet, several experiments were able to exclude the existence of hidden variables while demonstrating instead non-local effects [2, 3]. The theoretical apparatus of quantum mechanics acknowledges the non-local behavior of the quantum particles through the concept of entanglement [4, 5]. This term was early introduced by Schrodinger [6] to describe the possibility of correlating quantum systems even though spatially separated; the most controversial point concerns of course the difficulty arising from the requirements of relativity. Even today the concept of entanglement has different interpretations: the most acknowledged point of view is the quantum superposition of states, according which two correlated particles share a single quantum state until a measurement is carried out. The quantum mechanics is founded on a set of mathematical rules, which however do not incorporate themselves since the beginning the non-locality and non-reality in its fundamental conceptual structure, in order to include and rationalize per se these effects. For this reason the EPR paper appears legitimate from a rational point of view, although in fact wrong from a physical point of view; indeed a separate theoretical tool, the Bell inequality [7], was necessary to evidence the inconsistency of the EPR attempt [8, 9]: the predictions of local realism on which is based the Bell inequality conflict with the results obtained in various experiments, e.g. [10, 11, 12]. It is worth noticing that no theoretical foundation of the wave mechanics can be considered really general without containing inherently the non-realism and non-localism of the quantum world. It is therefore interesting to examine in this respect the approach followed in previous papers [13, 14], where results consistent with that of wave mechanics have been inferred exploiting the following equations only

$$\Delta x \Delta p_x = n\hbar = \Delta\varepsilon\Delta t. \qquad (1,1)$$

The second equality is consequence of the first one defining formally $\Delta t = \Delta x/v_x$ and $\Delta\varepsilon = \Delta p_x v_x$, where v_x is the average velocity with which any particle travels through Δx; the equalities share the common number n of allowed states. The equations (1,1) do not require any assumption about the ranges, about the motion of the particle and even about its wave/corpuscle nature; this latter will be inferred as a corollary in section 6. The present paper aims to contribute some ideas about how to regard the non-locality and non-reality uniquely according to eqs. (1,1). For reasons that will be clear below, it is useful to introduce shortly in section 2 the way of exploiting these equations to infer the quantum angular momentum; the remarks at the end of this section, which has a preliminary worth, are essential to discuss subsequently the weirdness of the quantum world. Although the angular momentum has been already introduced in [13], its elucidation is so straightforward and elementary that it deser-

ves being shortly sketched here; in doing so, indeed, it introduces reference concepts that will be further developed in the following sections 3 and 4 that concern the non-reality and non-locality. Eventually, the connection between quantum theory and special relativity is also sketched in sections 5 and 7; the link between eqs. (1,1) and the operator formalism of wave mechanics is discussed in section 6.

2 The non-relativistic angular momentum

The non-relativistic quantization of the classical angular momentum M^2 and of one of its components M_w along an arbitrary direction defined by the unit vector $\mathbf{w}$ starts from the classical scalar $\mathbf{r} \times \mathbf{p} \cdot \mathbf{w}$; here $\mathbf{r}$ is the radial distance of any particle from the origin O of an arbitrary reference system R and $\mathbf{p}$ its momentum. For instance, this could be the case of an electron in the field of a nucleus centered in O. As introduced in [15], the positions

$$\mathbf{r} \rightarrow \Delta\mathbf{r} \qquad \mathbf{p} \rightarrow \Delta\mathbf{p} \tag{2,1}$$

enable the number l of quantum states to be calculated as a function of the ranges $\Delta\mathbf{r}$ and $\Delta\mathbf{p}$ of all local distances and momenta physically allowed to the particle. These ranges only, and not the random local values $\mathbf{r}$ and $\mathbf{p}$ themselves, are considered in the following. The first step yields $M_w = (\Delta\mathbf{r} \times \Delta\mathbf{p}) \cdot \mathbf{w} = (\mathbf{w} \times \Delta\mathbf{r}) \cdot \Delta\mathbf{p}$ and so $M_w = \Delta\mathbf{I} \cdot \Delta\mathbf{p}$, where $\Delta\mathbf{I} = \mathbf{w} \times \Delta\mathbf{r}$. If $\Delta\mathbf{p}$ and $\Delta\mathbf{I}$ are orthogonal, then $M_w = 0$; else, writing $\Delta\mathbf{I} \cdot \Delta\mathbf{p}$ as $(\Delta\mathbf{p} \cdot \Delta\mathbf{I}/\Delta I)\,\Delta I$ with $\Delta I = |\Delta\mathbf{I}|$, the component $\pm\Delta p_I = \Delta\mathbf{p} \cdot \Delta\mathbf{I}/\Delta I$ of $\Delta\mathbf{p}$ along $\Delta\mathbf{I}$ yields $M_w = \pm\Delta I \Delta p_I$. In turn this latter equation yields according to eqs. (1,1) $M_w = \pm l\hbar$, being l the usual notation for the number of states of the angular momentum; l is positive integer including zero. As expected, M_w is not a single valued function because of the uncertainties initially postulated for $\mathbf{r}$ and $\mathbf{p}$. One component of $\mathbf{M}$ only, e.g. along the z-axis, is knowable; repeating the same approach for the y and x components would trivially mean changing $\mathbf{w}$. Just this conclusion suggests that the average values $< M_x^2 >$, $< M_y^2 >$ and $< M_z^2 >$ should be equal; so the quantity of physical interest to describe the properties of quantum angular momentum is l, as a function of which M^2 is indeed inferred as well. Let us calculate these average components over the possible states summing $(l\hbar)^2$ from $-L$ to $+L$, where L is an arbitrary maximum value of l. Being by definition $< M_i^2 >= \sum_{l_i=-L}^{l_i=L} (\hbar l)^2/(2L+1)$, one finds $M^2 = \sum_{i=1}^{3} < M_i^2 >= L(L+1)\hbar^2$. Note that the mere physical definition of angular momentum is enough to find quantum results completely analogous to that of wave mechanics; any local detail of motion, like that of electron "orbit" around the nucleus, is utterly unnecessary. The quantization of the classical values appears merely introducing the delocalisation ranges into the definition of angular momentum and then exploiting eqs. (1,1). The reason of it is evident: after the steps (2,1), the unique information available comes from the uncertainty ranges of coordinates and momentum, rather than from the local values of these latter; then the quantities thereafter calculated concern the number of allowed states only, which have in fact the same physical meaning of the quantum number defined by the solution of the pertinent wave equation. An analogous approach shows that the non-relativistic hydrogenlike energy levels depend on a further integer n because of the radial uncertainty equation $\Delta p_\rho \Delta\rho = n\hbar$ of an electron from the nucleus [13]; again, even without specifying any local detail of motion, the numbers of states l and n related to the angular and radial uncertainties of the electron in the field of nucleus correspond to the respective quantum numbers that characterize the energy levels. This preliminary introduction on how to exploit eqs. (1,1) was included in the present paper to emphasize several points useful in the following, i.e.: (i) the replacements (2,1) that allow to exploit eqs. (1,1) are enough to plug the classical physical definition $\mathbf{r} \times \mathbf{p}$ of angular momentum into the quantum world; (ii) no hypothesis is necessary about the geometrical properties of motion of the particle nor about its wave/matter nature to infer the quantum result; (iii) trivial algebraic manipulations replace the solution of the pertinent wave equation; (iv) the information inferred through eqs. (1,1) only is fully consistent with that of the wave mechanics; (v) the local momentum and distance between the particles concerned in the "orbiting" system do not play any role in determining l; (vi) as found elsewhere, [15, 17], the number of allowed states plays actually the role of the quantum numbers of the operator formalism of wave mechanics; (vii) the amount of information accessible for the angular momentum is not complete like that expected in the classical physics; (viii) eqs. (1,1) rule out "a priori" any possibility of "hidden variables" that could in principle enhance our knowledge about M_w and M^2 in order to obtain a more complete description of the orbiting quantum system.

It is worth mentioning that the validity of the point (i) has been checked and extended in the papers [13, 14] also to more complex quantum systems like many electron atoms/ions and diatomic molecules. The fact that eqs. (1,1) efficiently replace the standard approach of wave mechanics has central interest for the topics introduced in following sections, especially as concerns the very important point (viii). In principle one could not exclude that the wave function, from which is extracted all physical information allowed about the quantum systems, could actually contain hidden variables; indeed this chance, reasonably suspected in the famous EPR paper, has been excluded later thanks to a separate theoretical tool only, the Bell inequality. In the present approach, instead, the quantization of angular momentum is more "transparent" in that it explicitly displays variables and steps that lead to the quantum result; in other words, the present approach excludes any possibility of hidden variables because it works with actual quantities inherent the mere definition of angular momentum only. In conclusion the present section aimed mostly to ensure that sensible results are obtained regarding the uncertainty as a fundamental principle of nature itself, rather than

as a by-product of the operator formalism of wave mechanics. It is necessary however to better understand eqs. (1,1). To ascertain "a posteriori" that these equations work well has no heuristic worth. Therefore, after having checked their validity, the remainder of the paper starts from a step behind them, i.e. to highlight the more profound physical basis rooted in the concept of space-time uncertainty.

3 Non-realism and non-localism of eqs. (1,1)

Let us introduce a reference system R to define the ranges of eqs. (1,1). In the simplest 1D case, R is represented by an arbitrary axis where are defined two coordinates x_o and x_t with respect to an arbitrary origin O: the former describes the position of the range $\Delta x = x_t - x_o$ with respect to O, the latter describes its size. The postulated arbitrariness of size makes Δx consistent with the local coordinate x_o in the limit case $x_t \to x_o$ and with any other coordinate if is also allowed the limit size $\Delta x \to \infty$. If neither boundary coordinate is time dependent, then the section 2 and the papers [15, 16] show that this is all we need to know to define an observable physical property of the concerned quantum system: indeed, with the help of an analogous reasoning for the momentum range, this approach is enough to find the number of allowed states i.e. the quantum numbers that define the eigenvalues of the observable. If instead x_o and x_t are in general time dependent, then Δx expands or shrinks as a function of time, while possibly shifting with respect to O too, depending on how are mutually related the displacements of x_o and x_t. Actually the paper [15] shows that such a detailed information about how both of them displace with respect to O is physically redundant; all we need to know is the resulting $\Delta\dot{x}$ only. If Δx is an empty range, the chance of displacement in principle possible for x_o and x_t entails the presence of a force field within Δx; in the absence of a particle delocalized in it, however, this conclusion has a self-contained worth only that concerns a property of the the range itself in R. Instead consequences of physical interest are expected when a free particle is possibly therein delocalized; first of all because this presence requires itself highlighting the physical meaning of x_o and x_t to justify why these boundary coordinates, although remaining in principle completely arbitrary, can in fact include all values of dynamical variables allowed to the particle. Assume for instance two infinite potential barriers at x_o and x_t: if the size of the delocalization range changes from Δx_1 to Δx_2 during the time range $\Delta t = t_2 - t_1$, it means that necessarily the properties of the particle are affected during Δt as well; at the time t_1 the particle was constrained bouncing within Δx_1 with average frequency $\nu_1 = v_x \Delta x_1^{-1}$, at the time t_2 with average frequency $\nu_2 = v'_x \Delta x_2^{-1}$. The average displacement velocity v_x of the particle has been regarded different at the times t_1 and t_2 for sake of generality; however this fact is not essential, since $\Delta x_2 \neq \Delta x_1$ is enough to ensure $\nu_2 \neq \nu_1$. Hence the deformation of Δx as a function of time entails changing average displacement velocity, bouncing frequency of the particle and thus its momentum as well. To draw such a conclusion two essential elements have implemented the initial definition of delocalization range: the presence of a particle and the size change of Δx. Since however no assumption has been made about times and range sizes, nor about v_x and v'_x, these properties do not define themselves any state allowed to the particle; nothing about arbitrary range sizes, frequencies and velocities can be related to an integer number. Despite the intuitive fact that the particle dynamics has changed, n still appears unexplainable. This conclusion is important because, for the reasons introduced in section 2, just n entails the chance of measuring a physical observable of the particle. Overcoming this indeterminacy requires thus a further condition or constraint on ν_1 and ν_2, e.g. on the change of energy or momentum of the particle during the aforesaid time range. In effect, this condition is a crucial step to allow the transition from an unphysical "virtual" state towards an observable state: if for instance to define n concur the values of momentum or energy related to ν_1 and ν_2, then the sought number of states should correspondingly represent just the allowed eigenvalues of momentum or energy of the particle. The fact that a unique range is inadequate to define n, justifies reasonably the idea of introducing a further range ancillary to Δx able to represent in R the values of a second dynamical variable. Apart from this intuitive conclusion, it is necessary to explain why two arbitrary ranges of allowed dynamical variables are necessary to define the sought observable state of the particle. A reasonable idea is to examine the concept itself of measurement process. It is known that this concept is replaced in quantum mechanics by that of interaction, whose effect is to perturb the early state of the particle under test. The dynamical variables of the unperturbed free particle in R represent the initial boundary condition as a function of which is determined the effect of the interaction between particle and observer. Let the intensity of the local perturbation, whatever it might be, depend in general on the current local position and momentum of the particle; then the observer records an outcome somehow related to the boundary condition describing the particle before the measurement process. Since however the initial dynamical variables were unknown, they remain unpredictable and unknown after the measurement process as well; any correlation between initial and final state of the particle is impossible, simply because the former is in fact undefined. Renouncing "a priori" to know the local values of conjugate dynamical variables compels thus introducing ranges of their allowed values. Despite the lack of information about the sought correlation and kind of interaction, let us show that even so the concept of measurement allows defining the number of states, which in fact makes actual the properties of the particles. Regard to this purpose the aforesaid x_o and x_t respectively as coordinates of the particle before and after the measurement process; in agreement with eqs. (1,1), both are random, unknown and unpredictable, whereas du-

ring the interaction even intermediate values are expected to fall between these extremal boundaries. Considerations analogous to $x_t - x_o$ hold also for the conjugate momentum range $p_t - p_o$, whose boundary values p_o and p_t are related to the momentum of the particle before and after the measurement process. However $x_t - x_o$ and $p_t - p_o$, although fulfilling the requirements of both measurement process and eqs. (1,1), cannot be directly related themselves to Δx and Δp_x; the former are indeed uncorrelated and thus still unable to justify n, the central aim of the present discussion. Let us introduce thus the probabilities Π_x and Π_{p_x} that the values of both dynamical variables change during the measurement process in such a way that

$$x_t - x_o \rightarrow measurement \rightarrow \Delta x$$

$$p_t - p_o \rightarrow measurement \rightarrow \Delta p_x$$

where the usual notations Δx and Δp_x refer to ranges compliant with eqs. (1,1). This suggests writing

$$\Pi_x = \Delta x/(\Delta x + \Delta x'), \quad \Pi_{p_x} = \Delta p_x/(\Delta p_x + \Delta p'_x), \qquad (3,1)$$

where $\Delta x'$ and $\Delta p'_x$ are ancillary ranges consistent with the conditions $\Pi_x \rightarrow 0$ for $\Delta x \rightarrow 0$ and $\Pi_x \rightarrow 1$ for $\Delta x \rightarrow \infty$; analogous considerations hold of course for the momentum probability too. By definition therefore $\Delta x' > 0$ and $\Delta p'_x > 0$, in agreement with the idea that all ranges in the present model are positive. The physical meaning of $\Delta x'$ and $\Delta p'_x$ appears noting that initially, i.e. before defining n, space delocalization and momentum ranges are unrelated. Let us regard then $\Delta x + \Delta x' = x_t - x_o$ and $\Delta p_x + \Delta p'_x = p_t - p_o$ as the unperturbed early ranges, whose respective final sizes are just Δx and Δp_x of eqs. (1,1). So eqs. (3,1) concern the probability that the particle is eventually in Δx resulting after the measurement driven perturbation of the early $\Delta x + \Delta x'$, whereas an analogous explanation holds of course for Π_{p_x} as well. The total probability $\Pi_n = \Pi_x \Pi_{p_x}$ for space delocalization and momentum ranges fulfilling eqs. (1,1) is thus

$$\Pi_n = \Delta x \Delta p_x/(\Delta x \Delta p_x + \Delta x \Delta p'_x + \Delta p_x \Delta x' + \Delta p'_x \Delta x'). \quad (3,2)$$

In eq. (3,2) Π_n is expressed as a function of Δx and Δp_x that will bring us to eqs. (1,1) although starting from initial larger ranges still unrelated, whence the notation. First of all note that eq. (3,2) requires $(\Delta x/\sqrt{\Pi_n})(\Delta p_x/\sqrt{\Pi_n}) > \Delta x' \Delta p'_x$. Since all ranges appearing in this inequality are arbitrary, the left hand side can be shortly written as $\delta x \delta p_x$ whatever the specific values of $\Pi_x \neq 0$ and $\Pi_{p_x} \neq 0$ might be; these last positions are straightforward consequences of the previous considerations. Second, also note that the probability of quantum interest is the square root $\sqrt{\Pi_n} = \sqrt{\Pi_x \Pi_{p_x}}$ of that defined classically as ratio between favorable and total chances; this point will be further concerned in section 6. Third, by definition the product of ranges at right hand side of the inequality cannot be made equal to zero; this would contradict the concept of uncertainty, which must hold for any ranges of any size not simultaneously vanishing. So $\delta x \delta p_x > 0$ requires the existence of a value $const' > 0$ such that

$$\delta x \delta p_x > const' \qquad \Rightarrow \qquad \delta \varepsilon \delta t > const'. \qquad (3,3)$$

The second equation is obtained from the first likewise as in eqs. (1,1). This is in effect the uncertainty principle with the value of $const'$ of the order of the Plank constant; this inequality is then direct consequence of the probabilistic definition of eqs. (3,1) and supports the idea that the perturbation induced by the measurement process shrinks the initial uncorrelated ranges $\Delta x + \Delta x'$ and $\Delta p_x + \Delta p'_x$ to the correlated ones Δx and Δp_x of eqs. (1,1). The fact that eqs. (3,3) concern by definition observable states ensures that effectively $\sqrt{\Pi_n} \neq 0$. Eventually, together with eq. (3,2) must in principle exist also the probability

$$\Pi'_n = 1 - \Pi_n. \qquad (3,4)$$

Note that eq. (3,2) admits in principle $\Delta x' << \Delta x$ and $\Delta x' >> \Delta x$, together with analogous features of $\Delta p'_x$; so both limit probabilities can tend to 0 or to 1. Thus it is possible to regard eq. (3,2) as the effective chance of getting an eigenvalue from the measurement process and eq. (3,4) as that of not getting any eigenvalue. Both account for well known outcomes of wave mechanics, e.g.: (i) eq. (3,4) accounts for eigenvalues that actually do not exist, see for instance the previous conclusions about the x and y components of angular momentum once having determined M_z; (ii) when a quantum states is described by a superposition of several eigenfunctions, several eigenvalues exist whose respective actual occurrence is probabilistic, and so on. These chances must be inferred case by case when exploiting eqs. (1,1) through specific reasonings like that of section 2. The physical meaning of $\sqrt{\Pi_n}$ will also be shortly discussed in the next section 6; so eqs. (3,2) and (3,4) do not deserve further comments here. Now instead let us pose a question before proceeding on: why just shrinking and not expanding further the initial unrelated ranges? Apart from ther fact that the ranges are by definition all positive, the second chance would mean $\Delta x + \Delta x'$ and $\Delta p_x + \Delta p'_x$ defined by negative $\Delta x'$ and $\Delta p'_x$, which in turn would exclude the possibility of defining the probabilities Π_x and Π_{p_x} themselves. Besides this inconsistency, a plain consideration further clarifies the question. The measurement process tries to determine a physical property. Expanding the early unrelated ranges would mean decreasing our degree of knowledge about the particle, whose dynamical variables would oscillate within wider ranges of possible values; if so, the concept of measurement would be itself an oxymoron. Shrinking the early ranges, instead, is the best compromise offered by the nature to us during what we call "measurement process": while being forbidden the exact local values of the classical physics we must content ourselves,

at least, of reduced ranges of values for conjugate dynamical variables to which correspond however numbers of states. We must accept therefore the probabilities of eqs. (3,1) as the best we can get from a measurement process; this is what tells us the Heisenberg inequality just obtained from our probabilistic knowledge of the reality around us. To proceed further exploit again the arbitrariness of all ranges so far introduced in order to rewrite eq. (3,2) in various possible ways. In the first way $\Pi = \Delta x\Delta p_x/(\Delta x''\Delta p_x'')$, being $\Delta x''\Delta p_x'' \geq \Delta x\Delta p_x$ the sum of all addends at denominator. This suggests that $\Delta x\Delta p_x = \alpha const$, where *const* is a constant and α a parameter to be defined consistently with the actual product of the resulting uncertainties. Indeed this position allows writing in general

$$\Delta x''\Delta p_x'' = \alpha'' const, \quad \Delta x'''\Delta p_x''' = \alpha''' const \tag{3,5}$$

and so forth, depending on the values of the range products at left hand side. Let for instance be $\alpha''' \leq \alpha''$; eliminating *const* from these equations one finds $\Delta x'''\Delta p_x'''/(\Delta x''\Delta p_x'') = \alpha'''/\alpha''$ i.e. the sought form of Π_n. A further possibility of rewriting eq. (3,2) is $\Pi_n = \Delta x\Delta p_x/(4\Delta x^{\S}\Delta p_x^{\S})$ in the particular case where all terms at denominator of eq. (3,2) are equal to that here indicated with the unique notation $\Delta x^{\S}\Delta p_x^{\S}$; there is indeed no reason to discard also this chance, which must be therefore included in our definition of Π_n. Eventually, another consequence of the arbitrariness in defining $\Delta x'$ and thus $\Delta x''$ and $\Delta x'''$ of eqs. (3,5) must be taken into account: $\Delta x'$ could have been even rewritten itself as $\Delta x' = \Delta x^{\S} + \Delta x^{\S\S} + \cdots$, with several addends again arbitrary; in this case the number of addends at denominator of eq. (3,2) would have been any integer n rather than 4. All these requirements are easily included in the definition of Π_n simply putting $\alpha \equiv n$, so that eqs. (3,5) read $\Delta x''\Delta p_x'' = n''const$ and so forth with n arbitrary integer; in other words, n corresponds to the arbitrary number of possible subdivisions of the early ranges induced by the measurement process. This result effectively leads to both eqs. (1,1), which merely specify the value of *const* as that of $\hbar$. Note eventually that dividing more and more the initial interval $\Delta x'$ into an increasing number of intervals $\Delta x^{\S}$, $\Delta x^{\S\S}$, ... means considering smaller and smaller sized ranges, to which corresponds an increasing number n; since a smaller and smaller range actually tends to the limit of a local coordinate better and better defined, one realizes that $n \to \infty$ corresponds to the deterministic limit of the classical physics. Once more, the same holds for the other ranges. Since eqs. (1,1) are adequate to describe the existence of eigenvalues, one concludes that the measurement process is in fact consistent with the existence of experimental observables despite the initial uncertainties of both dynamical variables. Note that the reasoning above did not exploit any specific feature of the momentum; in other words, instead of the momentum range the reasoning could have identically exploited directly the perturbation of the velocity v_x of the particle under observation, i.e. a velocity range. The question about why we have in fact introduced just the momentum is irrelevant, as it rests merely on the particular choice of the physical dimension of *const*; regarding this latter as a product $const^{\S}m$, involving m times another constant, one would still find eqs. (3,5) with the form $\Delta x''\Delta p_x'' = n''const^{\S}m$ i.e. $\Delta x''\Delta v_x'' = n''const^{\S}$. Two further considerations are instead by far more relevant. The first is that eqs. (1,1) compel regarding any observable as the consequence of the measurement process itself, rather than as intrinsic feature of matter; no pre-existing state, and thus n, was indeed definable for the particle before the measurement. The conclusion that n characterizing the eigenvalues is consequence of the measurement process, rules the realism out of the quantum world. The second relevant feature of eqs.(1,1), which clearly appears recalling the results of section 2, concerns the localism. The particular example of the angular momentum has been introduced before any further consideration of central interest for the purposes of the present paper just to show that the local dynamical variables do not play any role in determining the observable properties of reality around us, as the experimental properties we measure are related to the eigenvalues and thus to the number of allowed states only. So the local values of dynamical variables become unphysical once accepting eqs. (1,1) to formulate quantum problems: nothing measurable corresponds to the local values. Hence, in lack of local information, the concept of distance is unphysical itself in the quantum world. For instance, in [15] the Newton and Coulomb forces between two interacting masses or charges have been inferred replacing the dependence on their classical distance x_{12}^{-2} with the dependence on Δx^{-2}: according to eqs. (1,1), the space range includes all possible local distances between the interacting particles whose coordinates fall within Δx. Regarded from this point of view, the EPR paradox is unphysical itself: it is impossible to define a superluminal distance conflicting with the exchange of information about the spin orientation of two particles arbitrarily apart each other. Whatever their distance might be, a range Δx including both of them certainly exists because its size is by definition arbitrary. Once regarding two particles within Δx, however, the concept of their local distance fails together with that of the respective local coordinates; in principle nobody knows or can measure how far they might actually be. For this reason it would be appropriate to describe the EPR gedankenexperiment as an action at a spooky distance, instead of a spooky action at a distance. Moreover the concept of entanglement appears itself implicitly inherent the present approach, as even particles at superluminal distance must behave consistently with their chance of being anywhere and thus of exchanging information as if they would actually be at very short distance. In this respect, just the quantum entanglement is itself the best demonstration of the correctness of the present point of view based exclusively on the eqs. (1,1), which thus exclude "a priori" both realism and localism from the quantum world; all this clearly appears in section 2. Also the Aharonov-Bohm effect is immediately understandable in the

frame of the present reasoning: an electrically charged particle is affected by an electro-magnetic field even when it is confined in a region where both electric and magnetic fields are zero. Actually it is here *and* there just like a wave propagating through, and thus filling, all available delocalization range. The previous considerations show indeed that regarding a quantum particle here *or* there is physically illusory; assigning a specific location is an idea arbitrarily and incorrectly extrapolated from the classical physics to the quantum world.

4 The Bell inequality

At this point, the exposition brings unavoidably into the mind the Bell inequality. The non-locality and non-reality of the results inferred from eqs. (1,1) suggest emphasizing the connection between the considerations of section 3 and the Bell inequality. To highlight this link let us rewrite the eqs. (1,1) as

$$\frac{\Delta x}{\Delta x_1}\frac{\Delta p_x}{\Delta p_1} = n, \qquad \frac{\Delta t}{\Delta t_1}\frac{\Delta \varepsilon}{\Delta \varepsilon_1} = n, \qquad n \geq 1, \tag{4,1}$$

where the subscript "1" means $n = 1$. In this way $\hbar$ does no longer appear explicitly in the expression of the number of states. Eqs. (4,1) appear therefore as an appropriate starting point to examine the relationship between eqs. (1,1) and Bell inequality, which has indeed general character not specifically related to the quantum theory. Considering for sake of brevity the first equation only (the second is indeed its straightforward consequence) and taking the logarithms of both sides one finds

$$\log\left(\frac{\Delta x}{\Delta x_1}\right) + \log\left(\frac{\Delta p_x}{\Delta p_1}\right) \geq 0. \tag{4,2}$$

This equation presents a formal analogy with the Bell-like inequality, [9]

$$N(A, B_{\rm n}) + N(B, C_{\rm n}) \geq N(A, C_{\rm n}), \tag{4,3}$$

where the subscript "n" stands for "not". Its demonstration is amazingly simple. Whatever the properties A, B and C might represent, the inequality $N(A, B_{\rm n}, C) + N(A_{\rm n}, B, C_{\rm n}) \geq 0$ expressing the sum of the respective numbers of occurrences/non-occurrences possible for A, B and C is self-evident. Add to both sides the sum $N(A, B_{\rm n}, C_{\rm n}) + N(A, B, C_{\rm n})$ expressing further numbers of occurrences/non-occurrences possible for B and C and note that terms like $N(A, B_{\rm n}, C) + N(A, B_{\rm n}, C_{\rm n})$ read actually $N(A, B_{\rm n})$; the notation emphasizes a resulting term no longer distinguished according to either property C, i.e. the sum including both chances allowed for C with the same A and $B_{\rm n}$ discriminates in fact the occurrences/non-occurrences of A and B only. So one infers immediately the inequality (4,3) that can be more expressively rewritten as

$$N_n(A, B_{\rm n}) + (N_n(B, C_{\rm n}) - N_n(A, C_{\rm n})) \geq 0 \tag{4,4}$$

with notations N_n for reasons that will be clear soon. Comparing the inequalities (4,2) and (4,4) requires emphasizing first of all what "not" stands for. In eqs. (3,1) the ranges $\Delta x'$ and $\Delta p'_x$ additional to Δx and Δp_x have been introduced to define the probability Π_x that after the measurement interaction the particle delocalization is described by Δx and no longer by $\Delta x + \Delta x'$, while an analogous idea holds also for Π_{p_x}; as we have shown, just the probabilities that both initial ranges shrink to new ranges fulfilling eqs. (1,1) entail the numbers of states n and thus the existence of the respective eigenvalues. This suggests that B and $B_{\rm n}$ describe respectively the chances of leaving the initial delocalization range unchanged or not after the perturbation induced by the observer, whereas C and $C_{\rm n}$ concern in an analogous way the momentum ranges of the particle. As regards A, it represents the existence of an eigenvalue of the particle; of course $A_{\rm n}$ means that delocalization and momentum ranges of the particle remain unchanged and so unrelated, thus not corresponding to any number of states. The notation N_n relates thus the inequality (4,4) to any possible eigenvalue. For instance: since n requires that are verified both favorable probabilities (3,1), it is reasonable to think that the various probabilities P_n corresponding to eq. (4,4) fulfill also the condition

$$P_n(A, B_{\rm n})P_n(A, C_{\rm n}) + P_n(A_{\rm n}, B)P_n(A_{\rm n}, C) = 1. \tag{4,5}$$

In effect, it is possible to normalize eq. (4,4) be means of an appropriate numerical factor in order to express the various numbers N_n of occurrences/non-occurrences through their respective probabilities P_n for one particle only. The first addend of eq. (4,5) represents the probability of getting an eigenvalue as a consequence of the measurement process, the second does not; in fact this idea was already introduced through the probabilities Π_n and Π'_n of eqs. (3,2) and (3,4). The sum of both chances that correspond to the Bell-like inequality

$$P_n(A, B_{\rm n}) + P_n(B, C_{\rm n}) - P_n(A, C_{\rm n}) \geq 0$$

must be of course equal to 1 in eq. (4,5). Let us try now to correlate term by term eqs. (4,2) and (4,4); the latter concerns directly the numbers of occurrences/non-occurrences leading to the n-th number of states allowed for one particle. This correlation yields

$$\Delta x = \Delta x_1 \exp\left(N_n(A, B_{\rm n})\right),$$

$$\Delta p_x = \Delta p_1 \exp\left(N_n(B, C_{\rm n}) - N_n(A, C_{\rm n})\right).$$

To verify if these equations can be simultaneously fulfilled, let us multiply them side by side; recalling that by definition $\Delta x_1 \Delta p_1 = \hbar$, one obtains

$$n = \exp\left(Q_n\right),$$

$$Q_n = N_n(A, B_{\rm n}) + N_n(B, C_{\rm n}) - N_n(A, C_{\rm n}) \geq 0. \tag{4,6}$$

So the result is that n must be equal just to the exponential of the number Q_n of occurrences/non-occurrences of the Bell-like inequality. It is clear however that in general the first equation (4,6) is false. Even admitting the chance that it is effectively verified for one among the possible numbers of states, say $n^{\S}$, by an appropriate value $Q_{n^{\S}}$, what about other numbers of states like for instance $n^{\S} - 1$ or $n^{\S} + 1$? It is clear that a hypothesis should be made on the respective $Q_{n^{\S}-1}$ and $Q_{n^{\S}+1}$. However the Bell-like inequality (4,3) does not prospect itself any indication about such a hypothesis, which therefore would require an "ad hoc" assumption valid for all arbitrary integers n progressively increasing from 1 by steps of 1 until to infinity. Note in this respect that the impossibility of eqs. (1,1) to fulfil the Bell-like inequality is in fact due to the quantization of n; if this latter could take any non-quantized value, then eq. (4,6) would be fulfilled in principle whatever Q_n might be. Hence is just the quantization of the eigenvalues that makes itself non-real and non-local the quantum world. In effect for $n \to \infty$ the number n approximates better and better a continuous variable of the classical physics, whence the realism and localism of the macroscopic classical world.

5 Uncertainty and special relativity

After having justified why the uncertainty ranges of position and momentum entail non-locality and non-reality, remains the concept of time and energy uncertainty to be better explained in the frame of such a conceptual context. Consider that also the time measurement requires a macroscopic apparatus, whose outcome is nothing else but the time of the observer. The question arises: is the observer time coincident with that of the particle? This question can be answered considering first that during the measurement process eqs. (1,1) apply to different reference systems, about which no hypothesis is made. Suppose that eqs. (1,1) refer to the particle; we must rewrite them as $\Delta x' \Delta p'_x = n'\hbar = \Delta\varepsilon' \Delta t'$ for the observer. Let R and R' be the respective reference systems; in both cases the ranges are completely arbitrary by definition, as concerns their sizes and analytical form. For instance it is not possible to establish if $\Delta x = x_o + v_x \Delta t$ or if $\Delta x = \sqrt{x_o^2 + (v_x \Delta t)^2}$ or anything else. The same holds also for the momentum range and for the energy range. Moreover n and n' are not assigned values, rather they are mere notations to indicate any integer unspecified and unspecifiable. So n and n' remain indistinguishable despite any integer of either reference system might turn into a different integer in the other reference system. Hence the arbitrariness of the analytical form of the ranges does not contradict the validity of eqs. (1,1) in different reference systems despite the chance of their possible size changes; the uncertainty equations (1,1) hold identically in R and in R', regardless of whether they refer to particle and observer in the respective reference systems. So, whatever the sizes of Δx of the particle and $\Delta x'$ of the observer might be, in principle eqs. (1,1) do not require that the time ranges Δt and $\Delta t'$ coincide. Recall now that the time range was introduced in section 1 to infer eqs. (1,1) through the positions $\Delta t = \Delta x / v_x$, which thus requires analogously $\Delta t' = \Delta x' / v'_x$, and note that both signs are allowed for the velocity components v_x and v'_x defined in R and R'. This means that with respect to the origin O of R we expect $\Delta x \pm v_x \Delta t = 0$ depending on whether the particle moves leftwards or rightwards. A possible position to summarize into a unique equation these chances regardless of either sign of v_x is $\Delta x^2 - v_x^2 \Delta t^2 = 0$; to this result corresponds of course an analogous expression in R', i.e. $\Delta x'^2 - v'^2_x \Delta t'^2 = 0$. Hence it is possible to write

$$\Delta x'^2 - v'^2_x \Delta t'^2 = 0 = \Delta x^2 - v_x^2 \Delta t^2. \qquad (5,1)$$

Both v_x and v'_x are reminiscent of the respective reference systems where they have been initially defined. Since no constraint is required for these velocities, both arbitrary by definition, the last equation allows replacing v_x and v'_x with any other values of velocity still defined in R and R'; so

$$\Delta x'^2 - v''^2_x \Delta t'^2 = \delta s^2_{v'',v'''} = \Delta x^2 - v'''^2_x \Delta t^2 \quad \delta s^2_{v'',v'''} \neq 0. \qquad (5,2)$$

Being unchanged the delocalization range sizes at right hand side, the interval $\delta s^2_{v'',v'''}$ is no longer equal to zero once having replaced v_x^2 with v'''^2_x; yet this does not hinder that this interval is still equal to the expression at left hand side if v'_x is replaced by another appropriate velocity v''_x also defined in R'; thus remains unchanged the analytical form of eqs. (5,1) and (5,2). In this way we have found a unique interval $\delta s^2_{v'',v'''}$ common to both reference systems R and R'. Yet this result is not a property of an interval defined by uncertainty ranges only, as it involves the presence of a particle through its displacement velocity; however it is interesting the fact that $\delta s^2_{v',v'''}$ does not require specific values of v''^2_x and v'''^2_x, which are indeed arbitrary like the ranges themselves. In the paper [15], was identified a velocity invariant in any reference system, called $v_x^{\max}$, i.e. the maximum average velocity with which any particle can displace in any Δx. This suggest the chance of expressing eqs. (5,2) just through this velocity, which will be called from now on c. If in particular we replace v''^2_x and v'''^2_x with c, then

$$\Delta x'^2_c - c^2 \Delta t'^2_c = \delta s^2_c = \Delta x_c^2 - c^2 \Delta t_c^2 \quad \delta s_c \neq 0. \qquad (5,3)$$

This result contains new delocalization ranges that can be chosen in order to generalize the previous result; this can be certainly done in agreement with this appropriate choice of the velocity, to which refers indeed the subscript c. In general eq. (5,3) holds for δs_c not necessarily equal to zero and represents a real step onwards with respect to eq. (5,2) because of the peculiar property of c, which is defined regardless of a specific reference system. The only quantities that depend on R are Δx_c and Δt_c that define δs_c regardless of the presence itself of any kind of particle thanks to the universal character of c. In conclusion, the present discussion allowed to find a

relationship that describes the form of an interval invariant in R and R', thus in any other reference system. Since this result has been obtained from eqs. (1,1), it is also compliant with the requirements of non-locality and non-reality previously introduced. The interval rule is a fundamental statement of special relativity, for instance it allows to infer the Lorentz transformations of space, time, momentum and energy [18]. However, apart from the formal analogy, the ranges introduced here have fully quantum physical meaning, i.e. they are uncertainty ranges; instead the ranges of relativity have the deterministic character of classical physics, i.e. they are defined as a function of selected local coordinates in principle exactly known. Therefore eq. (5,3) shows that even the relativity can be made compliant with the requirements of the quantum world provided that the local dynamical variables be discarded as done here and the macroscopic deterministic ranges take the physical meaning of uncertainty ranges. This crucial step, although abstractly simple, is certainly non-trivial as concerns the different way of regarding the conceptual basis of relativity. The next considerations concern just the consequences of this conclusion. From eq. (5,3) and according to eqs. (1,1) one infers, omitting for simplicity the subscripts c and x from now on but still intending that v is a component of average velocity along an arbitrary axis,

$$\frac{c^2\Delta t'^2}{c^2\Delta t^2} = \frac{(v/c)^2 - 1}{(v'/c)^2 - 1}, \qquad v = \Delta x/\Delta t, \qquad v' = \Delta x'/\Delta t'. \tag{5,4}$$

Putting in this equation $c \to \infty$, i.e. in the non-relativistic limit, $\Delta t' \to \Delta t$; as expected, without a finite light speed one finds the absolute time of Newton. Suppose now R and R' displacing each other at constant rate V such that in either of them, say in R, the particle is at rest. In the particular case $v = 0$, therefore, v' is just the rate V with which R displaces with respect to R'; of course it is also identically possible to put $v' = 0$, in which case $v = -V$. Since we have two equivalent ways to regard v and v', let us exploit for instance the first chance to find the transformation properties of the time range and the second chance for the space range; in the latter case it is convenient to put in eq. (5,3) $\delta s_c = 0$ to infer directly $c\Delta t_c = \Delta x_c$ and $c\Delta t'_c = \Delta x'_c$. One finds then

$$\Delta t' = \Delta t\Big(1 - (V/c)^2\Big)^{-1/2}, \qquad \Delta x'_c = \Delta x_c\Big(1 - (V/c)^2\Big)^{1/2}. \tag{5,5}$$

Actually the subscript c could have been omitted in the second equation; being arbitrary both time ranges of eq. (5,3), it holds in fact for any Δx and $\Delta x'$. The relevant remark is however that to time dilation corresponds length contraction in the primed reference system. It is also immediate to find the expressions of momentum and energy of a free particle. Let us consider first the following equalities obtained from eqs. (1,1) in the particular case $n = 1$

$$\Delta p^{(v)}\Delta x^{(v)} = \Delta t^{(v)}\Delta\varepsilon^{(v)} = \Delta t^{(c)}\Delta\varepsilon^{(c)} = \hbar,$$

$$\Delta t^{(c)} = \Delta t_{\min}, \qquad \Delta\varepsilon^{(c)} = \Delta\varepsilon_{\max}.$$

The superscripts emphasize the values taken by the velocity v in the various cases; the subscripts emphasize that when $v = c$ the traveling time is minimum whereas $\Delta\varepsilon$ is maximum, both consistently with $\hbar$ and with the arbitrary $\Delta p^{(v)}$ and $\Delta x^{(v)}$ describing a slower massive particle. These positions are important as they compel specifying how, in a given reference system, $\Delta p^{(v)}$ and $\Delta\varepsilon^{(v)}$ scale with respect to $\Delta p^{(c)}$ and $\Delta\varepsilon^{(c)}$ when $v < c$. Since $\Delta\varepsilon^{(c)} = cp_2^{(c)} - cp_1^{(c)}$, then $\varepsilon^{(c)} = cp^{(c)}$ by definition; here $\varepsilon^{(c)}$ and $p^{(c)}$ are random local values of energy and momentum within their own uncertainty ranges. For a slower massive particle $\Delta t^{(v)}$ and $\Delta\varepsilon^{(v)}$ scale like c/v and v/c with respect to $\Delta t^{(c)}$ and $\varepsilon^{(c)}$; hence, according to the former equality, $\varepsilon^{(v)} = \varepsilon^{(c)}v/c$ requires $p^{(v)}$ scaling with respect to $p^{(c)}$ like $cp^{(v)} = \varepsilon^{(c)}v/c$, i.e. $p^{(v)} = \varepsilon^{(c)}v/c^2$. Being $p^{(v)}$ and $\varepsilon^{(c)}$ random local quantities within the respective ranges, the functional relationship between any possible value of momentum and energy must be

$$p = \varepsilon v/c^2. \tag{5,6}$$

Momentum and energy of a free particle are constants both in classical physics and in special relativity. However eq. (5,6) is here a quantum result, which therefore must be accordingly handled. Let us admit that during a short time range δt even the energy of a free particle is allowed to fluctuate randomly by $\delta\varepsilon$. Eq. (5,6) is thus exploited to calculate the link between $\delta\varepsilon$ and related values of δp and δv during the time transient where the fluctuation allows the particle moving in altered way. Differentiating eq. (5,6) one finds $\delta\varepsilon = c^2\delta p/v - p(c/v)^2\delta v$: once having fixed p and v, this result defines the functional dependence of $\delta\varepsilon$ upon arbitrary δp and $\delta v = v_2 - v_1$ defined by two arbitrary values v_1 and v_1. Summing $\delta\varepsilon$ and eq. (5,6) one finds $\varepsilon + \delta\varepsilon = c^2(p + \delta p)/v - \varepsilon\delta v/v$. Note now that in general $\delta p\delta x = n\hbar$ reads identically $(\delta p)^2 = n\hbar\delta p/\delta x$, whereas in an analogous way $(\delta\varepsilon)^2 = n\hbar\delta\varepsilon/\delta t$. Regard in this way just the new ranges $\varepsilon + \delta\varepsilon$ and $p + \delta p$; putting $\delta x = v\delta t$ and replacing in the last expression to calculate $\delta(\varepsilon + \delta\varepsilon)/\delta t$, one finds

$$(n\hbar)^{-1}(\Delta\varepsilon)^2 = (n\hbar)^{-1}(\Delta pc)^2 - \varepsilon\delta\omega, \tag{5,7}$$

$$\Delta\varepsilon = \varepsilon + \delta\varepsilon, \qquad \Delta p = p + \delta p.$$

The last addend results because $v/\delta x$ has physical dimensions of a frequency ω, so that $\delta v/\delta x = \omega_2 - \omega_1$. Since $n\hbar\omega\delta\varepsilon = \delta(\varepsilon n\hbar\omega) - \varepsilon\delta(n\hbar\omega)$, replacing this identity in the last equation one finds $(\Delta\varepsilon)^2 = (\Delta pc)^2 + n\hbar\omega\delta\varepsilon - \delta(\varepsilon n\hbar\omega)$. Let us specify this result via the position

$$n\hbar\omega = \delta\varepsilon \tag{5,8}$$

which yields also $(\Delta\varepsilon)^2 - (\Delta pc)^2 = (\delta\varepsilon)^2 - \delta(\varepsilon\delta\varepsilon)$. At left hand side appear terms containing the ranges $\varepsilon + \delta\varepsilon$ and $p + \delta p$ only, at right hand side the ranges $\delta\varepsilon$ and δp only; so it is reasonable

to expect that the last equation splits into two equations linked by a constant energy ε_o

$$(\Delta\varepsilon)^2 - (\Delta pc)^2 = \varepsilon_o^2 = (\delta\varepsilon)^2 - \delta(\varepsilon\delta\varepsilon).$$

Indeed ε_o agrees with both of them just because it does not depend upon neither of them. Trivial manipulations show that the first equation yields

$$p = \pm\frac{\varepsilon_o v/c^2}{\sqrt{r_\varepsilon^2 - r_p^2(v/c)^2}}, \qquad \varepsilon = \pm\frac{\varepsilon_o}{\sqrt{r_\varepsilon^2 - r_p^2(v/c)^2}}, \quad (5,9)$$

$$r_p = 1 + \frac{\delta p}{p}, \qquad r_\varepsilon = 1 + \frac{\delta\varepsilon}{\varepsilon}.$$

As expected, eq. (5,6) results fulfilled even during the transient. The value of the constant ε_o is immediately found through the following boundary condition consequence of eq. (5,6)

$$\lim_{v\to 0}\frac{p}{v} = \frac{\varepsilon_{rest}}{c^2} = m. \qquad (5,10)$$

Then $\varepsilon_o^2 = \varepsilon_{rest}^2$. Eqs. (5,9) hold during the time transient allowing $\delta\varepsilon$; before and after that transient one must put $\delta\varepsilon = 0$ and $\delta p = 0$ which yields the "standard" Einstein momentum and energy of the particle, which are of course

$$\varepsilon_{Ein}^2 = c^2 p_{Ein}^2 + \varepsilon_{rest}^2, \qquad \varepsilon_{rest} = mc^2, \qquad (5,11)$$

$$p_{Ein} = \pm\frac{mv}{\sqrt{1-(v/c)^2}}, \qquad \varepsilon_{Ein} = \pm\frac{mc^2}{\sqrt{1-(v/c)^2}}.$$

It is easy now to calculate the energy and momentum gaps $\varepsilon - \varepsilon_{Ein}$ and $p - p_{Ein}$ during the time transient δt as a function of $\delta p/p$ and $\delta\varepsilon/\varepsilon$ as follows

$$\frac{mv}{\sqrt{r_\varepsilon^2 - r_p^2(v/c)^2}} - \frac{mv}{\sqrt{1-(v/c)^2}} = \frac{\hbar}{\delta l}, \qquad (5,12)$$

$$\frac{mc^2}{\sqrt{r_\varepsilon^2 - r_p^2(v/c)^2}} - \frac{mc^2}{\sqrt{1-(v/c)^2}} = \frac{\hbar}{\delta t}.$$

These equations, which are nothing else but the uncertainty equations of the fluctuation gaps, will be commented and exploited in section 7. The chance of obtaining the eqs. (5,6), (5,10) and (5,11) could be reasonably expected; in the paper [15] it was shown that eqs. (1,1) only are enough to infer the following corollaries: (i) equivalence of all inertial reference systems in describing the physical laws, (ii) existence of a maximum average displacement rate allowed for any particle in its delocalization range and (iii) invariance in all reference systems of such a maximum velocity. These corollaries are in fact the basic statements of special relativity. Five further remarks are crucial in this respect: (i) the mass m is not introduced here as the familiar concept of everyday common experience, rather the mass is inferred itself as a consequence of the uncertainty; (ii) the analytical expressions of energy and momentum have been obtained without need of any hypothesis additional to eqs. (1,1); (iii) the most representative formulas of special relativity are here obtained as straightforward consequences of the quantum uncertainty through trivial algebraic manipulations of eqs. (1,1) only; (iv) eqs. (5,11) are typical expressions of particle behaviour of matter, eq. (5,8) involves instead the wave behavior of matter too, because the frequency ω is a typical property of waves; unifying both properties into a unique equation leads to the well known relativistic formulas; (v) uncertainty ranges only appear in formulas coincident with that, well known, of the special relativity.

Note in this respect that the Einstein deterministic approach excludes the random fluctuation of velocity, energy and momentum, which is a typical quantum phenomenon; here instead the well known eqs. (5,11) are particular cases only of the more general eqs. (5,9) taking into account the possibility of fluctuations, in agreement with the fact that here the Einstein intervals here are actually quantum uncertainty ranges. Just this last statement opens the way to further considerations, carried out in section 7. Before exploiting the results of the present section, however, the next section 6 will concern a further topic previously introduced: the possibility of defining uncertainty sub-ranges included in larger ranges. The aim is to clarify the physical meaning of such a further way to regard the quantum uncertainty.

6 Uncertainty and operator formalism of wave mechanics

It is well known that the uncertainty principle is a consequence of the operator formalism of wave mechanics. This section aims to emphasize that the reverse path is also possible: here we show how to infer the momentum and energy wave equations starting from eqs. (1,1). This result is nontrivial: it emphasizes that the fundamental basis of the present theoretical approach leads also to the early wave equations from which has been developed the modern formulation of quantum mechanics. The uncertainty inherent Δx does not prevent to define in principle the probability $\Pi = \Pi(x,t)$ that the particle be in an arbitrary sub-range δx inside the total range

$$\frac{\delta x}{\Delta x} = \Pi, \qquad \delta x = x - x_o, \qquad \delta x \le \Delta x, \qquad (6,1)$$

provided that hold for δx the same uncertainty features of Δx; so no hypothesis is made about δx. Moreover x and x_o are both arbitrary and unknown likewise that of Δx; there is no chance of defining width or location of δx within Δx or distinguishing δx with respect to any other possible sub-range. In general Π is expected to depend on space coordinate and time; yet we consider first the explicit dependence of Π on x only, i.e. t is regarded as fixed parameter in correspondence to which are examined the properties of Π as a function of

x. Regard the width of δx variable, with x current coordinate and x_o constant. The couples of coordinates defining Δx and Δp_x are instead considered fixed. Eqs. (6,1) yield

$$\frac{1}{\Delta x} = \frac{\partial \Pi}{\partial x}, \qquad \Pi = \Pi(x, t). \tag{6,2}$$

Let Π and $1 - \Pi$ be the chances for the particle to be or not within δx and be n_+ and n_- the arbitrary numbers of states consistent with the respective probabilities. Putting

$$\delta x \Delta p = n_+ \hbar, \qquad (\Delta x - \delta x)\Delta p = n_- \hbar, \qquad n_+ + n_- = n, \tag{6,3}$$

then $n_+/n + n_-/n = 1$; also, eq. (6,3) yields the identity

$$(1 - \Pi)\Pi \Delta p^2 = n_- n_+ \hbar^2 \left(\frac{\partial \Pi}{\partial x}\right)^2. \tag{6,4}$$

Putting $n_+ n_- = n' + n''$, where n' and n'' are further arbitrary integers, eq. (6,4) splits as follows

$$\Pi \Delta p^2 = n' \hbar^2 \left(\frac{\partial \Pi}{\partial x}\right)^2, \tag{6,5a}$$

$$\Pi^2 \Delta p^2 = -n'' \hbar^2 \left(\frac{\partial \Pi}{\partial x}\right)^2. \tag{6,5b}$$

Since n_+ and n_- are by definition positive, at least one among n' and n'' or even both must be positive. Consider separately the possible signs of n' and n''.

Case (i) $n' > 0$ and $n'' < 0$. Eqs. (6,5) read also $\delta x \Delta p = (n'/n)\hbar$ and $\delta x^2 \Delta p^2 = |n''| \hbar^2$ because of eqs. (6,1) and (6,2). Moreover multiplying both sides of the latter by $|n''|$ and both sides of the former by $n^{\S} n/n'$, with $n^{\S}$ arbitrary integer, one finds

$$\delta x'' \Delta p = n'' \hbar, \qquad \delta x^{\S} \Delta p = n^{\S} \hbar,$$

where $\delta x'' = \sqrt{|n''|}\delta x$ and $\delta x^{\S} = (n^{\S} n/n')\delta x$. Also, $(n'/n)^2 = |n''|$ and $\Pi = |n''|/n'$. These results are mutually consistent for any integers at right hand sides, because are arbitrary not only n' and n'' but also δx; indeed the new uncertainty equations have an analogous form and physical meaning. Hence eqs. (6,5) do not exclude each other and are both acceptable; yet they are both formally analogous also to the initial eq. (1,1), the only difference being the size of their space uncertainty ranges only. In conclusion, being the sizes arbitrary by definition, this combination of signs of n' and n'' does not entails anything new with respect to eq. (1,1), and thus has no physical interest.

Case (ii) $n' < 0$ and $n'' > 0$. The right hand sides of both eqs. (6,5) have negative sign, so neither of them can have the same physical meaning of the initial eq. (1,1); they read $\Pi = -|n'|/n^2$ and $\Pi^2 = -n''/n^2$ because of eq. (6,2). Yet the result $\Pi = n''/|n'| = -|n'|/n^2$ is clearly absurd, so also this combination of signs has no physical interest.

Case (iii) $n' > 0$ and $n'' > 0$. Eqs. (6,5) are now physically different, because their ratio would entail Π negative. Thus these equations cannot be combined together, because of their different ways to describe the particle delocalized in Δx; they must be considered separately. Eq. (6,5a) is conceptually analogous to eq. (1,1); eq. (6,5b) excludes eq. (6,2) and admits the solution $\Pi = A' \exp(\pm i(x - x_o)\Delta p/\hbar \sqrt{n''})$, being A' the integration constant. Rewriting $\Pi = A \exp(\pm i\varphi \delta x/\Delta x)$ with $\varphi = n/\sqrt{n''}$, the probability Π inferred here significantly differs from Π of eq. (6,5a) despite the same notation; the former is indeed a complex function, the latter coincides instead with eq. (6,1). Both are however definable in principle.Thus eq. (6,5b) still retains the essential concept of delocalization within an arbitrary uncertainty range, yet without concerning itself the ability of regarding the particle as a corpuscle in any specific point of Δx.

The following discussion concerns the case (iii). To accept both eqs. (6,5) together, we must acknowledge their different form, i.e. their different way to describe the particle delocalization inside Δx. This dual outcome reveals however the inadequacy of regarding the particle as mere corpuscle delocalized somewhere in its uncertainty range, as required by eqs. (1,1). Despite the particle must be anyway randomly moving in Δx, eq. (6,5b) is incompatible with the corpuscle-like behaviour of eq. (6,5a). A further difficulty to regard together eqs. (6,5a) and (6,5b) is that Π defined by this latter is not real, as instead $\Pi^* \Pi = |const|^2$ does. Yet just this property suggests a possible way out from this difficulty, i.e. supposing that eq. (6,5b) requires a wave-like propagation of the particle: so $\Pi^* \Pi$ could stand for particle wave amplitude whereas A', in fact regarded here as $A_0 A(t)$ without contradicting any previous step, could define frequency and phase of the particle wave. This idea is confirmed rewriting the exponential $x\Delta p$ of Π as $t\Delta\varepsilon$ dividing and multiplying by an arbitrary velocity v in order that $\pm ix\Delta p/\hbar\sqrt{n''}$ turns into $\pm it\Delta\varepsilon/\hbar\sqrt{n''}$. So $A(t)$ results defined just by this requirement, i.e.

$$\Pi = A_0 \exp[\pm i(c_x(x - x_o)\Delta p + c_t(t - t_o)\Delta\varepsilon)/\hbar\sqrt{n''}], \tag{6,6}$$

being c_x and c_t arbitrary coefficients of the linear combination expressing the most general way to unify the space and time functions. Calculate $\partial^2\Pi/\partial x^2 = -(c_x\Delta p)^2\Pi$ to extract the real quantity $c_x\Delta p$ from Π, and then by analogy $\partial^2\Pi/\partial t^2 = -(c_t\Delta\varepsilon)^2\Pi$ too; eliminating Π between these equations and noting that by dimensional reasons $(c_x\Delta p/c_t\Delta\varepsilon)^2 = v^{-2}$, the result $\partial^2\Pi/\partial x^2 - v^{-2}\partial^2\Pi/\partial t^2 = 0$ confirms, whatever v might be, the wave-like character of particle delocalization provided by eq. (6,5b). A similar wave equation could not be inferred from eq. (6,5a), according which the physical properties of the particle are related directly to the probability Π of eq. (6,1); instead, owing to the complex form of Π resulting from eq. (6,5b), the physical properties of the wave are related to $\Pi^*\Pi$. It is possible to eliminate this discrepancy introducing the complex function $\sqrt{\Pi}$ in place of Π and rewriting eq. (6,5b) as a function of the former instead of the latter; this idea agrees with that already exploited to find eqs.

(3,3). Dividing both sides by Π, eq. (6,5b) reads

$$\left(\pm\hbar\frac{\partial\sqrt{\Pi}}{\partial x}\right)^2 = -\left(p^{\S}\sqrt{\Pi}\right)^2, \qquad p^{\S} = \pm\frac{\Delta p}{2\sqrt{n''}}. \quad (6,7)$$

The notation emphasizes that $p^{\S}$ does not depend on x and is not a range; being defined as solution of the differential equation (6,7) only, its value is not longer related to Δp, i.e. it is an eigenvalue of $\sqrt{\Pi}$. This is possible because n'' is arbitrary like Δp, which allows that the ratio $\Delta p/2\sqrt{n''}$ behaves as a well determined quantity specified just by $p^{\S}$, whose value and signs correspond to either component of momentum along the x-axis where are defined positive δx and Δx. Thus eq. (6,7) reads

$$\pm\frac{\hbar}{i}\frac{\partial\sqrt{\Pi}}{\partial x} = p^{\S}\sqrt{\Pi}, \qquad \sqrt{\Pi} = \sqrt{A}\sqrt{\exp(\pm i\varphi\delta x/\Delta x)}. \quad (6,8)$$

So $\sqrt{\Pi}\sqrt{\Pi^*}$ expresses the probability to find the particle so-mewhere in Δx. Write thus

$$\sqrt{\Pi}\sqrt{\Pi^*} = \pm\frac{\hbar}{ip^{\S}}\frac{\sqrt{\Pi^*}\partial\sqrt{\Pi}}{\partial x}.$$

The right hand side is real and yields $\sqrt{\Pi}\sqrt{\Pi^*} = \delta x_0/\Delta x = A_0$, being $\delta x_0 = A_0\hbar\varphi/2p^{\S}$. As a proper value of A_0 certainly exists such that $\delta x_0 \le \Delta x$, then $\sqrt{\Pi}\sqrt{\Pi^*}$ agrees with a concept of probability similar to that of the initial definition $\delta x/\Delta x$ of eq. (6,1); yet this latter is replaced in the last equation by a constant value, which entails thus equal probability to find the particle in any sub-range δx_0 regardless of its size and position within Δx. The physical meaning of this result is emphasized integrating both sides of eq. (6,8) with respect to x in the sub-range $\delta x_0 = x_{02} - x_{01}$, which yields

$$p^{\S} = \pm\left(\int_{x_{01}}^{x_{02}}\sqrt{\Pi}\sqrt{\Pi^*}dx\right)^{-1}\int_{x_{01}}^{x_{02}}\left(\sqrt{\Pi^*}\frac{\hbar}{i}\frac{\partial}{\partial x}\sqrt{\Pi}\right)dx. \quad (6,9)$$

The average value of momentum is thus equal to the eigenvalue expected for the steady motion of a free particle (Ehre-nfest's theorem), which suggests regarding $\delta x_0/\Delta x$ as average probability that the particle is in the sub-range δx_0. It is clearly convenient therefore to define A_0 in order that $\delta x_0 = \Delta x$ through $\int\sqrt{\Pi}\sqrt{\Pi^*}dx = 1$, i.e. the momentum eigenvalue concerns the certainty that the particle is really delocalized in the total range Δx. Being this latter arbitrary, it allows considering in general the particle from $-\infty$ to ∞. The physical information provided by eq. (6,5b) is thus really different from that of eq. (6,5a), although being unquestionable the consistency of eqs. (6,8) and (6,9) with the initial eq. (6,1) despite their different formulation: both come indeed from the same uncertainty equations (1,1). So it is not surprising that the uncertainty is still inherent $\sqrt{\Pi}$ and consistent with the eigenvalue $p^{\S}$. It is evident at this point that the results hitherto inferred concern just the basic ideas through which has been formulated the early quantum mechanics; it is enough to regard in general the wave functions in analogous way, e.g. as it is shown below for the energy eigenfunction. So, write $\psi = const\sqrt{\Pi}$ and $\psi^* = const\sqrt{\Pi^*}$ to define the probability density of the particle within the volume $\Delta x\Delta y\Delta z$; this is just the volume to normalize $\psi\psi^*$. Being the uncertainty ranges arbitrary, this probability density concerns actually the whole space allowed to the particle. The normalization constant is inessential for the purposes of the present paper and not explicitly concerned hereafter. The result of interest is that, after having introduced the probability Π of eq. (1,1), one finds two distinct equations concurrently inferred from the respective eqs. (6,5)

$$\Delta p^{\S}\Delta x^{\S} = n^{\S}\hbar, \quad (6,10a)$$

$$\frac{\hbar}{i}\frac{\partial\sqrt{\Pi}}{\partial x} = \pm p^{\S}\sqrt{\Pi}. \quad (6,10b)$$

Two comments about eqs. (6,10):

(i) eq. (6,10a) is conceptually equal to the initial eq. (1,1), from which it trivially differs because of the size of the uncertainty ranges and related number of states; (ii) eq. (6,10b) defines a differential equation that calculates an eigenvalue of momentum through the probability that the particle be in a given point of its allowed range $\Delta x^{\S}$.

Eq. (6,10a) does not consider explicitly the particle, but only its delocalization inside $\Delta x^{\S}$ and thus its phase space; the same holds also for the momentum, whence the positions (2,1) and the indistinguishability of identical particles whose specific properties are disregarded "a priori". The unique information available concerns indeed the number of states $n^{\S}$ consistent with $\Delta x^{\S}$ and $\Delta p^{\S}$ for any delocalized particle; nothing requires considering the local dynamical variables themselves. The point of view of eq. (6,10b) is different: it considers explicitly the sub-range δx through $\sqrt{\Pi}$ and thus, even without any hypothesis about size and position of δx within $\Delta x^{\S}$, concerns directly the particle itself through its properties $\sqrt{\Pi}\sqrt{\Pi^*}$ and $p^{\S}$; both these latter are explicitly calculated solving the differential equation. Yet the common derivation of both eqs. (6,10) from the initial eq. (1,1) shows that actually the respective ways to describe the particle must be consistent and conceptually equivalent, as in effect it has been verified in section 2. This coincidence evidences the conceptual link between properties of the particles and phase space; it also clarifies why the quantum eigenvalues do not depend on the current values of the dynamical variables of the particles, even though calculated solving the differential equation (6,10b). Initially Π was introduced in eq. (6,1) as mere function of uncertainty ranges and sub-ranges of the phase space; thereafter, however, it has taken through the steps from eqs. (6,2) to (6,10) the physical meaning of wave function $\sqrt{\Pi}$ of the particle defining the momentum eigenvalue $p^{\S}$, which involves the mass of the particle. Eq.

(6,10b) introduces the operator formalism of wave mechanics. The approach starting directly from eqs. (1,1) has therefore more general character than the latter, which starts just postulating eq. (6,10b) here found instead as a corollary: the basic reason is that eq. (6,10a) contains less information than eq. (6,10b). These equations can be now regarded together once having acknowledged the kind of information inferred from eqs. (1,1). On the one side eqs. (6,10) introduce the wave/corpuscle dual nature of particles: eq. (6,10a) admits that the particle is somewhere in Δx, even though renouncing to know exactly where because of the delocalization; eq. (6,10b) instead regards the particle as a wave propagating within Δx thus still delocalized but excluding in principle the unknown position of a material corpuscle. On the other side eqs. (6,10) confirm that properties of particles and properties of phase space must not be regarded separately, rather they are intrinsically correlated: just for this reason the results of section 2 show that the numbers of quantum states (properties of the phase space) coincide with the quantum numbers that define the eigenvalues (properties of the wave function of the particle). Further properties of $\sqrt{\Pi} = \psi$ could be easily found, e.g. the concept of parity or the fact that the arbitrariness of the coefficients c_x and c_t previously introduced in the early expression $\Pi = A_0 \exp[\pm i(c_x x\Delta p + c_t t\Delta\varepsilon)/\hbar\sqrt{n''}]$ allows to write the more general form for this equation

$$\Pi = \sum_j A_{0j} \exp[\pm i(c_{xj} x\Delta p_j + c_{tj} t\Delta\varepsilon_j)/\hbar\sqrt{n''_j}].$$

All these assertions are well known since the early birth of the quantum theory and do not need further consideration here for sake of brevity; their evolution brings the theory up to today's formulation. It is more interesting to examine the same problem considering the time instead of the space coordinate. The steps to find the energy operator are conceptually identical to those so far reported; yet one regards the probability for the particle to be in δx at the time t, i.e. Π is defined as ratio between the time range $\delta t = t - t_o$ spent within a fixed δx and the total time range $\Delta t = t_2 - t_1$ spent elsewhere within Δx. Let us write then $\Pi = \delta t/\Delta t$ at fixed coordinate x; eqs. (6,2) and (6,4) read now $\Delta t^{-1} = \partial\Pi/\partial t$ and $(1-\Pi)\Pi\Delta\varepsilon^2 = n_- n_+ \hbar^2 (\partial\Pi/\partial t)^2$. Replacing position and momentum with time and energy in eq. (6,2), eqs. (6,7) read

$$\left(\pm\hbar\frac{\partial\sqrt{\Pi}}{\partial t}\right)^2 = -\left(\varepsilon^{\S}\sqrt{\Pi}\right)^2, \qquad \varepsilon^{\S} = \pm\frac{\Delta\varepsilon}{2\sqrt{n''}}. \quad (6,11)$$

The second eq. (6,8) reads now $\sqrt{A}\sqrt{\exp(\pm i\varphi\delta t/\Delta t)}$, which however is disregarded here because it appears included in eq. (6,6); the first eq. (6,8) becomes

$$-\frac{\hbar}{i}\frac{\partial\sqrt{\Pi}}{\partial t} = \pm\varepsilon^{\S}\sqrt{\Pi}. \quad (6,12)$$

With the upper sign at right hand side of eq. (6,12), the classical Hamiltonian written with the help of eq. (6,8) is consistent with the result $\varepsilon^{\S} = p^{\S 2}/2m$ in the particular case of a free particle having mass m and momentum $p^{\S}$. Yet the lower sign, also allowed as a consequence of eq. (6,11), shows the possibility of states with negative energy as well. The couple of equations (6,10) turns into

$$\Delta t^{\S}\Delta\varepsilon^{\S} = n^{\S}\hbar, \quad (6,13a)$$

$$-\frac{\hbar}{i}\frac{\partial\sqrt{\Pi}}{\partial t} = \pm\varepsilon^{\S}\sqrt{\Pi}. \quad (6,13b)$$

For this couple of equations hold the same considerations carried out for the corresponding eqs. (6,10). This section has shown that the operator formalism of wave mechanics is consequence itself of the concept of uncertainty. On the one side this result explains why the properties of quantum particles can be obtained as shown in section 2 even without solving any wave equation. On the other side it appears clearly that both chances of describing the quantum world are nothing else but mirror consequences of the dual wave/corpuscle behavior of particles. All considerations so far carried out do not require knowing anything about the concerned uncertainty ranges.

7 Heuristic aspects of quantum special relativity

Let us introduce now some comments about eqs. (5,9) and (5,11) before exploiting eqs. (5,12). The momentum and energy equations during the quantum fluctuation transient rewritten identically as follows

$$p(t) = \pm\frac{mv_{eff}/r_p}{\sqrt{1-(v_{eff}/c)^2}}, \quad \varepsilon(t) = \pm\frac{mc^2/r_\varepsilon}{\sqrt{1-(v_{eff}/c)^2}}, \quad (7,1)$$

$$v_{eff} = r_p v/r_\varepsilon, \qquad r_p = r_p(t), \qquad r_\varepsilon = r_\varepsilon(t),$$

evidence that the Einstein quantities of eqs. (5,11) turn into new constant expressions calculated with an effective velocity and multiplied by the respective functions of time; the previous velocity v does not longer appear explicitly into the equations. If v_{eff} is regarded as a constant, then v turns into a time variable without contradicting the Einstein equations, whose deterministic character does not admit any fluctuation and requires a steady value of v; the fluctuation has been instead introduced by admitting the quantum meaning of $\delta\varepsilon$, δp and δv. The notation of eqs. (7,1) emphasizes that energy and momentum are functions of time during the transient; regarding r_ε and r_p like time variables is reasonable, because according to eqs. (5,9) $\delta\varepsilon$ and δp are related to r_ε and r_p during the fluctuation. The physical meaning of r_ε and r_p is that of describing the cycle of values of energy and momentum, whereas r_p/r_ε controls the range of transient values allowed for the velocity. To be more specific, any energy fluctuation is characterized by an initial time t_{in} where $\varepsilon(t_{in}) = \varepsilon_{Ein}$ that successively increases to $\varepsilon(t) > \varepsilon_{Ein}$ at $t > t_{in}$ and then decreases down to the initial value ε_{Ein} at the time t_{end}. Note now that during the fluctuation transient must hold the inequality $r_p < r_\varepsilon$; otherwise, being v arbitrary e.g. very close

to c, the chance $r_p > r_\varepsilon$ could entail $\varepsilon(t)$ imaginary although being real ε_{Ein}. This would actually mean that the fluctuation is not allowed to occur. Thanks to the former inequality, instead, v can increase in principle even beyond c while still keeping $v_{eff} < c$; this can happen during the time range between t_{in} and t_{end} without divergent or imaginary quantities because under square root of the transient formulas appears v_{eff} only. This point is easily verified noting that $\varepsilon(t)/p(t) = c^2/v$, as already emphasized in section 5. Thus it must be also true that $\varepsilon(t)^2 = c^2 p(t)^2 + (mc^2)^2$ likewise eq. (5,11). Trivial manipulations yield $(v/c)^2 = (r_\varepsilon^2 - 1)/(r_p^2 - 1)$; so if $r_\varepsilon > r_p$ then is even allowed a value $v_* > c$ without contradicting neither eqs. (5,5) nor (5,11) that describe a steady behavior of the particle. According to eqs. (5,7), $r_p < r_\varepsilon$ requires

$$\delta\varepsilon(t)/\delta p(t) > \varepsilon_{Ein}/p_{Ein}. \qquad (7,2)$$

From an intuitive point of view, the transient proceeds for an observer in the lab frame according to the following steps: (i) $r_p = r_\varepsilon = 1$ at $t = t_{in}$, i.e. hold eqs. (5,11) with a value of $v_{eff} = v < c$ uniquely fixed by the initial motion of the particle; (ii) when r_p and r_ε start changing at $t > t_{in}$, the value of v_{eff} is still constrained by $v_{eff} < c$ but now $v > v_{eff}$ according to the inequality (7,2); (iii) at a later time $t_* < t_{end}$ it could even happen that $v_* > c$, although still being $v_{eff} < c$; (iv) subsequently r_p and r_ε tend again to 1 when the fluctuation cycle ends at $t \to t_{end}$ while $p(t) \to p_{Ein}$ and $\varepsilon(t) \to \varepsilon_{Ein}$, i.e. $v \to v_{eff} < c$. Thanks to the concept of quantum fluctuation, therefore, the increase of velocity $v_* > c$ in the step (iii) does not involve directly the value of v appearing in the steady formulas of ε_{Ein} and p_{Ein}, as indeed it results in eqs. (5,12); so the superluminal step (iii) is in principle possible. However, what about the chance of detecting it experimentally? Certainly the answer is not found via eqs. (7,1), which describe local quantities at the random and unspecified time t; on the other hand, since the particle travels, t is related to a corresponding x, random and unspecified as well. Throughout this paper it has been emphasized that information of physical interest is obtainable through uncertainty ranges only; thus the considerations just carried out, based on time and space local coordinates, have worth only to guess and assess the possible behavior of the particle at any $t_{in} \le t \le t_{end}$ and better understand the physical results inferred by consequence. Coherently with the approach so far followed, we discard once again the local dynamical variables and pay attention to the respective uncertainty ranges only. Exploit thus eqs. (5,12) to get information comparable with the experience, putting $\delta t = t_{end} - t_{in}$ and δl equal to the distance across which is measured the velocity. In this way we can calculate an *average* velocity $\delta l/\delta t$ whose value depends upon how the experiment is carried out. If δt is shorter than the time τ for the particle to travel the distance δl, then the superluminal effect it is not detectable, because the fluctuation starts and ends while the particle is still traveling within δl; this means that the fluctuation is an event entirely occurring within a space delocalization range. Yet nothing is known about what happens within this uncertainty range. In this case, when considering the average velocity of the particle, we can only acknowledge that this latter is anyway smaller than c, whereas any information about any possible event allowed to occur within δl remains in fact unaccessible; moreover eqs. (5,12) do not have themselves physical meaning, as they attempt to get physical insight within an uncertainty range. If however δt is longer than τ, then the superluminal effect is at least in principle detectable without contradicting the previous reasoning, because now the fluctuation extends throughout all the range δl and beyond; it is no longer a local event hidden by the uncertainty. So if the average velocity is measured in these experimental conditions, i.e. with δl sufficiently short or δt sufficiently long, the superluminal effect is in principle detectable. Note in this respect that a small value of m in the second eq. (5,12) corresponds to a longer time at right hand side, so the inequality (7,2) is more easily fulfilled for a particle not too heavy than for a heavy particle; indeed the former typically travels with values of v closer to c than the latter for energy reasons and also entails a longer δt, so it could effectively overcome the superluminal transition threshold fulfilling more likely the condition $\delta t > \tau$. Once fulfilling these conditions, a light particle appears traveling the space range $\delta l = v_* \delta t$ at speed $v_* > c$ in the laboratory reference system even during a moderate energy fluctuation and without violating any principle of quantum special relativity formulated in section 5; indeed $\delta l/\delta t$ does not calculate v_{eff} but the average transient of v. As a clarifying comparison recall that $\delta\varepsilon$ does not violate the energy conservation, it is simply a temporary derogation to this latter allowed by the uncertainty principle only; why not should something similar happen also for the velocity, if this latter does not cause divergent or imaginary results? Anyway, for the comparison with the experiment are enough just the two equations (5,12) that relate in the laboratory frame the distance δl traveled by the particle to the time δt during which the transient is still in progress; their ratio, assumed physically consistent with the time length of the fluctuation transient, reads

$$\frac{\delta l}{\delta t} = \frac{\frac{mc^2}{\sqrt{r_\varepsilon^2 - (r_p v/c)^2}} - \frac{mc^2}{\sqrt{1-(v/c)^2}}}{\frac{mv}{\sqrt{r_\varepsilon^2 - (r_p v/c)^2}} - \frac{mv}{\sqrt{1-(v/c)^2}}} = c\frac{c}{v}.$$

Since $v < c$, then $\delta l/\delta t > c$, which demonstrates a superluminal particle transfer during the quantum fluctuation cycle. If for instance $v = 0.99c$ then $\delta l/\delta t = 1.01c$. Note that instead the speed of the photon $v = c$ remains identically, universally and invariantly equal to c. Eqs. (5,5) have been written through time and space uncertainty ranges only. The Einstein relativity specifies the time range $\Delta t = t - t_o$ through a current time coordinate t and a lower boundary $t_o = x_o V/c^2$; both times have a deterministic physical meaning. This last result could be easily guessed also here, thinking that even t_o must depend on V/c and must be related to

the corresponding x_o. Thus a value $V > c$ would change the signs of Δt and $\Delta t'$ in eq. (5,5), i.e. the concept itself of sequence "before" and "after". Apart from the fact that such a conclusion would be illusory in the present theoretical frame because the uncertainty discards "a priori" the local coordinates, it is also essential in this respect a further remark. As shown before, the lack of physical information about t and t_o and $t - t_o$ does not prevent to infer the relativistic formulas of energy and momentum: yet, even specifying $t_o = x_o V/c^2$, the possible time-reversal during the quantum fluctuation cycle does not affect any result previously obtained. First of all because actually this cycle has not been specified, i.e. exchanging t_{end} with t_{in} does not change any step of the previous reasoning; moreover if the cycle starts with an initial energy ε_{Ein} and ends with the same final energy ε_{Ein}, any discrimination between beginning and ending of the cycle seems unphysical. Therefore, since the possible time reversal should be a local effect concerning the quantum fluctuation only, all the conclusions hitherto obtained still hold. Also note that $\delta l/\delta t = \varepsilon_{Ein}/p_{Ein} = c^2/v$; so the inequality (7,2) reads $\delta\varepsilon/\delta p > \delta l/\delta t$ as well, i.e. $\delta\varepsilon/\delta l > \delta p/\delta t$: the left hand side represents the force acting on the particle due to its fluctuation driven energy gap along its path, the right hand side represents the force due to the momentum change during the fluctuation time length. Saying that the former is greater than the latter means an excess force with respect to the mere momentum change having fully quantum origin, necessarily due to nothing else but the fluctuation in the case of a free particle. It seems reasonable to assume that just this excess force justifies the superluminal effect. As expected, neither δl nor δt enter explicitly into the calculation of the velocity; the ratio between two uncertainty ranges provides of course an average value during the transient, which is in effect allowed in the frame of the present approach. It is interesting to emphasize that a given $\delta\varepsilon/\delta l$, related to the energy growing along the path traveled by the particle, could be at increasing δl not greater than $\delta p/\delta t$, related to the given fluctuation time length; this is because δl and δt are two independent quantities, the former related to the experimental apparatus, the latter to a feature of the fluctuation. If δl increases up to a larger value Δl such that $\delta\varepsilon/\Delta l < \delta p/\delta t$ the superluminal effect is not observable. Indeed this is just in line with the previous considerations recalling that: (i) the effect is detectable if at the end of the path of the particle within δl the fluctuation is still in progress; (ii) if instead the fluctuation cycle ends while the particle is still traveling inside δl, then it becomes an event occurring within an uncertainty range and thus, as such, unobservable. If the model is correct, this is what to expect imagining to increase the size of δl up to Δl: the same kind of observation should yield a positive outcome if carried out in the experimental situation (i), but certainly a negative outcome if carried out in the experimental situation (ii). This also suggests a possible way to verify the considerations just carried out: to detect the same velocity fluctuation event of not-heavy particles with two detectors located in two different laboratories. Although the concept of their respective "distances" from the source is illusory for the reasons introduced in sections 3, it remains nevertheless still true that different locations, wherever they might be, provide different chances for the uncertainty of revealing or hiding experimentally the superluminal transition. Thus the random occurring/non-occurring of the superluminal effect should not be ascribed to human experimental errors but to a further probabilistic weirdness of the quantum world.

8 Discussion

The ordinary formulation of quantum mechanics contains the classical physics as a limit case but needs this latter to be formulated [17]. Regarding instead eqs. (1,1) as expressions of a fundamental principle of nature, and not as mere by-products of the commutation rules of operators, this ambiguous link between classical and quantum physics is bypassed. Section 6 has shown that eqs. (1,1) entail as a corollary the operator formalism of wave mechanics; yet the present approach appears more general than that based on this latter. As shown in sections 4 and 5, it automatically introduces since the beginning the non-locality and non-reality into the description of quantum systems. In principle the quantum uncertainty does not prevent knowing exactly one dynamical variable only; being the size of all ranges arbitrary by definition, one must admit even the chance $\Delta x \to 0$ that means local position of a particle exactly known. The same reasoning holds separately for the momentum as well. Independent ranges however do not provide physical information on the observable properties of the quantum world. These observables require abandoning separate certainties independently allowed; the physical meaning of the ranges changes when considering together two conjugate dynamical variables, which also means discarding the classical realism and localism as well but gaining the eigenvalues. Does the moon exist regardless of whether one observes it? According to the approach sketched in section 2 this question should be better reformulated, for instance as follows: do the properties of the moon we know exist regardless of a possible observer? Yet if nobody observes the moon, nobody could define the properties "we know"; these latter are the outcomes of some kind of measurement, i.e. they are triggered themselves by a previous measurement interaction. Repeating this reasoning back in the time the conclusion is that before the first recording of light beam escaping from the moon nobody would even know the existence of the moon; in which case would become physically irrelevant the prospective physical properties of an object still to be discovered. In this sense it appears understandable that the properties we know exist when observations are carried out. Hence what we call moon is just the result of an interaction between an observer and an object sufficiently close to the Earth to be observable. As concerns the localism it is appro-

priate to think about an action at a spooky distance, since the local coordinates defining the distance are actually an arbitrary extrapolation to the quantum world of a classical way of thinking. This idea appeared since the early times of birth of quantum mechanics, when the deterministic concept of trajectory was irreversibly abandoned. The operator formalism requires a wave function of time and space coordinates; these latter identify in turn a region of space where however has physical meaning the mere probability density to find the particle only. Thus the wave function denies the classical meaning of the local coordinates, e.g. position and momentum or energy and time, as a function of which is however itself calculated. In this respect the present approach formulates an even more indeterministic and drastic view of the reality: to discard the local values since the beginning. In this sense, eqs. (1,1) seem a step ahead with respect to the operator formalism; even though seemingly more agnostic, they avoid handling the local variables to define and solve the appropriate wave equations from which are extracted the eigenvalues, i.e. the observables, in a probabilistic conceptual context. Here indeed we refuse "a priori" the physical usefulness of introducing time and space local coordinates and, in general, local quantities that do no longer appear in the eigenvalues; yet, even so the results are identical. This suggests that actually is the uncertainty the fundamental concept behind the results, a sort of essential information directly related to the knowledge we can afford; for instance, the arbitrariness of the quantum numbers of wave mechanics, due to the mathematical features of the solutions of differential equations, is replaced by that of the number of states; indeed the results show that the latter have a physical meaning identical to the former. Eqs. (1,1) provide these numbers since the beginning. This is the reason of the straightforward character of the present approach, which indeed does not require solving any differential equation but proceeds through trivial algebraic manipulations of the formulae. The arbitrariness seems a concept with negative valence, especially in science; yet it played an essential role in deriving eqs. (3,5) from eq. (3,2); on this step are based eqs. (1,1). The section 2 shows that these equations plug the classical definition of angular momentum into the quantum world thanks to two concepts: introducing the number of states and eliminating local information. The section 6 has shown why the indistinguishability of identical particles is a natural consequence of these premises; in the operator formalism instead it must be purposely introduced as a postulate and appropriately handled from a mathematical point of view, recall for instance the early Slater determinants. Moreover the section 4 has shown why the present approach entails inherently even the non-locality and the non-reality of the quantum world: while evidencing their link with the quantization of the physical observables, these weird features are automatically required by eqs. (1,1) through n. Eventually, let us emphasize that the present way of regarding the quantum world is compatible with the special relativity. The paper [15] has inferred its basic principles as corollaries, in section 7 some results particularly significant have been obtained: the invariant interval, the Lorentz transformations of time and length, the energy and momentum equations of a free particle, the rest energy of particle, the existence of antimatter and the concept of mass itself. The key idea underlying these results is the way to regard the relativistic intervals: to discard their deterministic definition, early introduced by Einstein, and regard them as uncertainty ranges. As shown before, this simple conceptual step is enough to plug into the quantum world even the special relativity. Moreover, the quantum way to infer the relativistic equations has opened the way to admit a typical quantum phenomenon, the energy fluctuation, able to account for unexpected effects otherwise precluded by the early deterministic basis of special relativity formulated by Einstein.

9 Conclusion

The approach based uniquely on eqs. (1,1) contains inherently the requirements of non-locality and non-reality that characterize the quantum world. This kind of approach is also consistent with the special relativity, whose basic statements were found as corollaries in previous paper.

Submitted on October 18, 2011 / Accepted on October 23, 2011

References

1. Einstein A., Podolski B., Rosen N. Can Quantum-Mechanical Description of Physical Reality be Considered Complete? *Physical Review*, 1935, v. 47, 777–780.
2. Aspect A., Dalibard J., Roger G. Experimental realization of Einstein-Podolski-Rosen-Bohm gedanken experiment; a new violation of Bell's inequalities. *Physical Review Letters*, 1982, v. 49, 91–94.
3. Clauser J.F., Horne M.A., Shimony S., Holt R.A. Proposed experiment to test local hidden-variable theories. *Physical Review Letters*, 1969, 23, pp. 880-884
4. Keller E.T., Rubin M.H. Theory of two photon entanglement for spontaneous parametric down-conversion driven by a narrow pump pulse. *Physical Review A*, 1997, v. 56, 1534–1541.
5. Rubin M. H. Locality in the Everett Interpretation of Heisenberg-Picture Quantum Mechanics. *Foundation of Physics Letters*, 2001, v. 14(4), 301–322.
6. Schrödinger E. Discussion of Probability Relations between Separated Systems. *Proceedings of the Cambridge Philosophical Society*, 1935, v. 31, 555–563.
7. Bell J.S. Speakable and Unspeakable in quantum mechanics, Cambridge University Press, 1987, pp. 14–21.
8. Bell J.S. On the Einstein Podolsky Rosen Paradox. *Physics*, 1964, v. 1(3), 195–200.
9. Eberly J.H. Bell inequalities and quantum mechanics. *American Journal of Physics*, 2002, v. 70(3), 276–279.
10. Aspect A., Dalibard J., Roger G. Experimental test of Bell's inequalities using time-varying analizers. *Physical Review Letters*, 1982, v. 49, 1804–1807.
11. Weichs G., Jennewein T., Simon C., Weinfurter H., Zeilinger A. Violation of Bell's inequality under strict Einstein locality conditions. *Physical Review Letters*, 1998, v. 81, 5039–5043.

12. Clauser J.F., Shimony A., Bell's theorem: experimental tests and implications. *Reports on Progress in Physics*, 1978, v. 41, 1881–1927.
13. Tosto S. An analysis of states in the phase space: the energy levels of quantum systems. *Il Nuovo Cimento B*, 1996, v. 111(2), 193–215.
14. Tosto S. An analysis of states in the phase space: the diatomic molecules. *Il Nuovo Cimento D*, 1996, v. 18(12), 1363–1394.
15. Tosto S. An analysis of states in the phase space: uncertainty, entropy and diffusion. *Progress in Physics*, 2011, v. 4, 68–78.
16. Tosto S. An analysis of states in the phase space: the anharmonic oscillator. *Progress in Physics*, 2011, v. 4, 29–36.
17. Landau L., Lifchitz E. Mechanique quantique; theorie non relativiste, 1967, (In French), Editions MIR, Moscow, p. 10.
18. Landau L., Lifchitz E. Theorie du Champ (in French), 1966, Editions MIR, Moscow, p. 286 and ff.

Thermodynamics and Scale Relativity

Robert Carroll
University of Illinois, Urbana, IL 61801
rcarroll@math.uiuc.edu

It is shown how the fractal paths of SR = scale relativity (following Nottale) can be introduced into a TD = thermodynamic context (following Asadov-Kechkin).

1 Preliminary remarks

The SR program of Nottale et al (cf. [1]) has produced a marvelous structure for describing quantum phenomena on the QM type paths of Hausdorff dimension two (see below). Due to a standard Hamiltonian TD dictionary (cf. [2]) an extension to TD phenomena seems plausible. However among the various extensive and intensive variables of TD it seems unclear which to embelish with fractality. We avoid this feature by going to [3] which describes the arrow of time in connection with QM and gravity. This introduces a complex time (**1A**) $\tau = t - (i\hbar/2)\beta$ where $\beta = 1/kT$ with $k = k_B$ the Bolzmann constant and a complex Hamiltonian (**1B**) $\mathfrak{H} = \mathfrak{E} - (i\hbar\Gamma/2)$ where $\mathfrak{E}$ is a standard energy term, e.g. (**1C**) $\mathfrak{E} \sim (1/2)mv^2 + \mathfrak{W}(x)$. One recalls that complex time has appeared frequently in mathematical physics. We will show how fractality can be introduced into the equations of [3] without resorting to several complex variables or quaternions.

Thus from [3] one has equations

$$\mathfrak{H} = \mathfrak{E} - \left(\frac{i\hbar}{2}\Gamma\right);\ \tau = t - \frac{i\hbar}{2}\beta;\ [\mathfrak{E}, \Gamma] = [\mathfrak{H}, \mathfrak{H}^\dagger] = 0; \quad (1.1)$$

$$\Psi = exp^{-\frac{i\mathfrak{S}\tau}{\hbar}}\psi; P_n = \frac{w_n}{Z}; w_n = \rho_n exp^{[-\mathfrak{E}_n\beta + \Gamma_n t]};$$

$$i\hbar\partial_\tau\Psi = \mathfrak{H}\Psi; \Psi = \sum C_n\psi_n;$$

$$\mathfrak{H}_n = \mathfrak{E}_n - \frac{i\hbar}{2}\Gamma_n; [\mathfrak{H}, \mathfrak{H}^\dagger] = 0;$$

$$\mathfrak{E}\psi_n = \mathfrak{E}_n\psi_n; \Gamma\psi_n = \Gamma_n\psi_n; (\psi_n, \psi_k) = \delta_{nk}.$$

One could introduce another complex variable here, say j with $j^2 = -1$, but this can be avoided.

Now go to the SR theory and recall the equations

$$\frac{\hat{d}}{dt} = \frac{1}{2}\left(\frac{d_+}{dt} + \frac{d_-}{dt}\right) - \frac{i}{2}\left(\frac{d_+}{dt} - \frac{d_-}{dt}\right); \quad (1.2)$$

$$\mathcal{V} = \frac{\hat{d}x}{dt} = V - iU = \frac{1}{2}(v_+ + v_-) - \frac{i}{2}(v_+ - v_-);$$

$$\frac{\hat{d}}{dt} = \partial_t + \mathcal{V}\cdot\nabla - i\mathcal{D}\Delta;$$

$$\mathcal{H} = \frac{m}{2}\mathcal{V}^2 - im\mathcal{D}\nabla\cdot\mathcal{V} + \mathcal{W} = \frac{1}{2m}\mathcal{P}^2 - i\mathcal{D}\cdot\mathcal{P} + \mathcal{W}; \quad (1.3)$$

$$\mathcal{H} = \mathcal{V}\cdot\mathcal{P} - i\mathcal{D}\nabla\cdot\mathcal{P} - \mathcal{L};$$

$$\hat{\mathcal{V}} = \mathcal{V} - i\mathcal{D}\nabla; \quad (\partial_t + \hat{\mathcal{V}}\cdot\nabla)\mathcal{V} = -\frac{\nabla\mathcal{W}}{m}; \quad (1.4)$$

$$U = \mathcal{D}\nabla log(P); \quad P = |\psi|^2; \quad \psi = e^{i\Xi/2m\mathcal{D}};$$

$$\mathfrak{Q} = -2m\mathcal{D}^2\frac{\Delta\sqrt{P}}{\sqrt{P}}; \quad (1.5)$$

$$\mathcal{V} = -2i\mathcal{D}\nabla[log(\psi)]; \quad \Xi_0 = 2m\mathcal{D};$$

$$\mathcal{D}^2\Delta\psi + i\mathcal{D}\partial_t\psi - \frac{\mathcal{W}}{2m}\psi = 0; \quad (1.6)$$

$$\frac{dV}{dt} = \frac{F}{m} = U\cdot\nabla U + \mathcal{D}\Delta U.$$

This has been written for 3 space dimensions but we will restrict attention to a 1-D space based on x below.

We will combine the ideas in (1.1) and (1.2) in Section 2 below. Note here $\mathfrak{Q}$ is the QP = quantum potential (see e.g. [5–8] for background).

2 Combination and interaction

From (1.2)-(1.6) we see that the fractal paths in one space dimension have Hausdorff dimension 2 and we note that U in (1.2) is related to an osmotic velocity and completely determines the QP $\mathfrak{Q}$. Note that these equations (1.2)-(1.6) produce a macro-quantum mechanics (where $\mathcal{D} = \hbar/2m$ for QM). It is known that a QP represents a stabilizing organizational anti-diffusion force which suggests an important connection between the fractal picture above and biological processes involving life (cf. [1, 9–13]). We also refer to [14–16] for probabalistic aspects of quantum mechanics and entropy and recommend a number of papers of Agop et al (cf. [17]) which deal with fractality (usually involving Hausdorff dimension 2 or 3) in differential equations such as Ginzburg-Landau, Korteweg de-Vries, and Navier-Stokes; this work

includes some formulations in Weyl-Dirac geometry (Feoli-Gregorash-Papini-Wood formulation) involving superconductivity in a gravitational context.

Now let us imagine that $\mathcal{W} \sim \mathfrak{W}$ and $V \sim v$ so that the energy terms in the real part of the SE arising from (1.2)-(1.6) will take the form

$$\mathfrak{E} \sim \frac{1}{2}mV^2 + \mathfrak{W} + \mathfrak{Q} \tag{2.1}$$

and we identify this with $\mathfrak{E}$ in the TD problem where

$$\mathfrak{Q} = -2m\mathcal{D}^2\frac{\Delta\sqrt{P}}{\sqrt{P}}; \quad P = |\Psi|^2. \tag{2.2}$$

One arrives at QM for $\mathcal{D} = \hbar/2m$ as mentioned above and one notes that the mean value $\bar{\mathfrak{E}}$ used in the analysis of [3] will now have the form

$$\bar{\mathfrak{E}} = \frac{1}{2}\int mV^2Pdx + \int |\mathfrak{W}|^2Pdx + \int \mathfrak{Q}Pdx \tag{2.3}$$

and the last term $\int \mathfrak{Q}Pdx$ has a special meaning in terms of Fisher information as developed in [5–7, 19–21]. In fact one has

$$\int \mathfrak{Q}Pdx = -2m\mathcal{D}^2\int \frac{\partial_x^2\sqrt{P}}{\sqrt{P}}Pdx = \tag{2.4}$$

$$= -\frac{\mathcal{D}^2}{2}\int\left[\frac{2P''}{P} - \left(\frac{P'}{P}\right)^2\right]Pdx = \frac{m\mathcal{D}^2}{2}\int\frac{(P')^2}{P}dx$$

In the quantum situation $\mathcal{D} = \hbar/2m$ leading to

$$\int \mathfrak{Q}Pdx = \frac{\hbar^2}{8m}\int\frac{(P')^2}{P}dx = \frac{\hbar^2}{8m}FI \tag{2.5}$$

where FI denotes Fisher information (cf. [7, 21]). And this term can be construed as a contribution from fractality.

One can now sketch very briefly the treatment of [3] based on (1.1). Thus one constructs a generalized QM (with arrow of time and connections to gravity for which we refer to [3]). The eigenvalues $\mathfrak{E}_n$, Γ_n, in (1.1) are exploited with

$$\rho_n = |C_n|^2; \quad P_n = \frac{w_n}{Z};$$

$$\Psi = \sum C_n\psi_n; \quad w_n = \rho_n e^{-\mathfrak{E}_n\beta + \Gamma_n t}. \tag{2.6}$$

One considers two special systems:

1. First let the eigenvectors Γ_n all be the same (decay free system) and then $w_n = \rho_n exp[-\mathfrak{E}_n\beta]$ which means that β is actually the inverse absolute temperature (multiplied by k_B) when $\mathfrak{E}_n$ is identified with the n-th energy level and the system is decay free.
2. Next let all the $\mathfrak{E}_n$ be the same so $w_n = \rho_n exp[-\Gamma_n t]$ and all the Γ_N have the sense of decay parameters if t is the conventional physical time.

Thus the solution space of the theory space can be decomposed into the direct sum of subspaces which have a given value of the energy or of the decay parameter. It is seen that for $\beta = constant$ the dynamical equation for the basis probabilities is

$$\frac{dP_n}{dt} = -(\Gamma_n - \bar{\Gamma})P_n; \quad \frac{d\bar{\Gamma}}{dt} = -D_\Gamma^2; \quad D_\Gamma^2 = \overline{(\Gamma - \bar{\Gamma})^2}. \tag{2.7}$$

From (2.7) one sees that $\bar{\Gamma}(t)$ is not increasing which means that the isothermal regime of evolution has an arrow of time, which is related to the average value of the decay operator. Thus P_n increases if $\bar{\Gamma} > \Gamma_n$ and decreases when $\bar{\Gamma} < \Gamma_n$. One can also show that in the general case of $\beta = \beta(t)$ the dynamical equations for the P_n have the form

$$\frac{dP_n}{dt} = -\left[\Gamma_n - \bar{\Gamma} + (\mathfrak{E}_n - \bar{\mathfrak{E}})\frac{d\beta}{dt}\right]P_n. \tag{2.8}$$

Here the specific function $d\beta/dt$ must be specified or extracted from a regime condition $f(t, \beta, \bar{\mathfrak{A}}(t, \beta)) = 0$ for some observable $\mathfrak{A}$ (e.g. $\bar{\mathfrak{E}} = constant$ is an adiabatic condition). In the adiabatic case for example when $\bar{\mathfrak{E}} = \sum_n \mathfrak{E}_n P_n = constant$ there results

$$\frac{d\beta}{dt} = -\frac{\overline{\mathfrak{E}T} - \bar{\mathfrak{E}}\bar{T}}{D_{\mathfrak{E}}^2} \tag{2.9}$$

where $D_{\mathfrak{E}}$ denotes a dispersion of the energy operator $\mathfrak{E}$. Using (2.8)-(2.9) one obtains

$$\frac{d\bar{\Gamma}}{dt} = -D_\Gamma^2\left[1 - \frac{(\overline{\mathfrak{E}T} - \bar{\mathfrak{E}}\bar{T})^2}{D_{\mathfrak{E}}^2 D_\Gamma^2}\right] \geq 0. \tag{2.10}$$

Subsequently classical dynamics is considered for $\hbar \to 0$ and connections to gravity are indicated with kinematically independent geometric and thermal times (cf. [3]).

Submitted on October 12, 2011 / Accepted on October 23, 2011

References

1. Nottale L. Scale relativity and fractal space-time, Imperial College Press, 2011.
2. Peterson M. *American Journal of Physics*, 1979, v. 47, 488–490.
3. Asadov V., Kechkin O. *arXiv* hep-th 0608148, 0612122, 0612123, 0612162, 0702022, and 0702046; *Moscow University Physics Bulletin*, 2008, v. 63, 105–108; *Gravity and Cosmology*, 2009, v. 15, 295–301.
4. Acosta D., Fernandez de Cordoba P., Isidro J., Santandar J. *arXiv* hep-th 1107.1898.
5. Carroll R. Fluctuations, information, gravity, and the quantum potential, Springer, 2006.
6. Carroll R. On the quantum potential, Arima Publ., 2007.
7. Carroll R. On the emergence theme of physics, World Scientific, 2010.
8. Carroll R. *arXiv* math-ph 1007.4744; gr-qc 1010.1732 and 1104.0383.
9. Auffray C., Nottale L. Progress in Biophysics and Molecular Biology, 97, 79 and 115.
10. Roman-Roldan R., Bernaola-Galvan P., Oliver J. *Pattern Recognition*, 1996, v. 7, 1187–1194.

11. Sanchez I. *Journal of Modern Physics*, 2011, v. 2, 1–4.
12. Zak M. *International Journal of Theoretical Physics (IJTP)*, 1992, v. 32, 159–190; v. 33, 2215–2280; *Chaos, Solitons, and Fractals*, 1998, v. 9, 113–1116; 1999, v. 10, 1583-1620; 2000, v. 11, 2325–2390; 2002, v. 13, 39–41; 2007, v. 32, 1154–1167 and 2306; *Physics Letters A*, 1989, v. 133, 18–22; 1999, v. 255, 110–118; *Information Sciences*, 2000, v. 128, 199–215 and 2000, v. 129, 61–79; 2004, v. 165, 149–169.
13. Zak M. *International Journal of Theoretical Physics*, 1994, v. 33, 1113–1116; 2000, v. 39, 2107–2140; *Chaos, Solitons, and Fractals*, 2002, v. 14, 745–758; 2004, v. 19, 645–666; 2005, v. 26, 1019–1033, 2006, v. 28, 616–626; 2007, v. 32, 1154–1167; 2007, v. 34, 344–352; 2009, v. 41, 1136–1149 and 2306–2312; 2009, v. 42, 306–315; *Foundations of Physics Letters*, 2002, v. 15, 229–243.
14. Caticha A. *arXiv* quant-ph 1005.2357, 1011.0723, and 1011.9746.
15. Nagasawa M. Schrödinger equations and diffusion theory, Birkhäuser, 1993; Stochastic processes in quantum physics, Birkhäuser, 2000.
16. Nelson E. Quantum fluctuations, Princeton Univ. Press, 1985; *Physical Review*, 1966, v. 130, 1079; Dynamical theory of Brownian motion, Princeton Univ. Press, 1967.
17. Agop M. et al, *Chaos, Solitons, and Fractals*, 1999, v. 8, 1295; 1999, v. 16, 3367; 2000, v. 17, 3527; 2003, v. 16, 321; 2006, v. 30, 441; 2006, v. 32, 30; 2007, v. 34, 172; 2008, v. 38, 1243; *Journal of Mathematical Physics*, 2005, v. 46, 062110; *Classical and Quantum Gravity*, 1999, v. 16, 3367, 2000, v. 17, 3627, 2001, v. 18, 4743; *European Physics Journal D*, 2008, v. 49, 35; 2010, v. 56, 239; *General Relativity and Gravity*, 2008, v. 40, 35.
18. Gregorash D., Papini G. *Nuovo Cimento B* 1980, v. 55, 37–51, 1980, v. 56, 21–38, and 1981, v. 63, 487–509.
19. Frieden B., Physics from Fisher information, Cambridge Univ. Press, 1998; Science from Fisher information, Springer, 2004.
20. Frieden B., Gatenby R. Exploratory data analysis using Fisher information, Springer, 2007.
21. Frieden B., Plastino A., Plastino A.R., Soffer B. *Physical Review E*, 1999, v. 60, 48–53 and 2002, v. 60, 046128; *Physics Letters A*, 2002, v. 304, 73–78.
22. Lebon G., Jou D., Casas-Vazquez J. Understanding non-equilibrium TD, Springer, 2008.
23. Ottinger H. Beyond equilibrium TD, Wiley, 2005; *Physical Review E*, 2006, v. 73, 036126.

Van Aubel's Theorem in the Einstein Relativistic Velocity Model of Hyperbolic Geometry

Cătălin Barbu
"Vasile Alecsandri" National College - Bacău, str. Vasile Alecsandri, nr. 37, 600011, Bacău, Romania
E-mail: kafka_mate@yahoo.com

In this note, we present a proof to the Van Aubel Theorem in the Einstein Relativistic Velocity Model of Hyperbolic Geometry.

1 Introduction

Hyperbolic Geometry appeared in the first half of the 19^{th} century as an attempt to understand Euclid's axiomatic basis of Geometry. It is also known as a type of non-Euclidean Geometry, being in many respects similar to Euclidean Geometry. Hyperbolic Geometry includes similar concepts as distance and angle. Both these geometries have many results in common but many are different. There are known many models for Hyperbolic Geometry, such as: Poincaré disc model, Poincaré half-plane, Klein model, Einstein relativistic velocity model, etc. Here, in this study, we give hyperbolic version of Van Aubel theorem. The well-known Van Aubel theorem states that if ABC is a triangle and AD, BE, CF are concurrent cevians at P, then $\frac{AP}{PD} = \frac{AE}{EC} + \frac{AF}{FB}$ (see [1, p. 271]).

Let D denote the complex unit disc in complex z - plane, i.e.

$$D = \{z \in \mathbb{C} : |z| < 1\}.$$

The most general Möbius transformation of D is

$$z \to e^{i\theta}\frac{z_0 + z}{1 + \overline{z_0}z} = e^{i\theta}(z_0 \oplus z),$$

which induces the Möbius addition $\oplus$ in D, allowing the Möbius transformation of the disc to be viewed as a Möbius left gyrotranslation

$$z \to z_0 \oplus z = \frac{z_0 + z}{1 + \overline{z_0}z}$$

followed by a rotation. Here $\theta \in \mathbb{R}$ is a real number, $z, z_0 \in D$, and $\overline{z_0}$ is the complex conjugate of z_0. Let $Aut(D, \oplus)$ be the automorphism group of the grupoid $(D, \oplus)$. If we define

$$gyr : D \times D \to Aut(D, \oplus), gyr[a, b] = \frac{a \oplus b}{b \oplus a} = \frac{1 + a\overline{b}}{1 + \overline{a}b},$$

then is true gyrocommutative law

$$a \oplus b = gyr[a, b](b \oplus a).$$

A gyrovector space $(G, \oplus, \otimes)$ is a gyrocommutative gyrogroup $(G, \oplus)$ that obeys the following axioms:

1. $gyr[\mathbf{u}, \mathbf{v}]\mathbf{a} \cdot gyr[\mathbf{u}, \mathbf{v}]\mathbf{b} = \mathbf{a} \cdot \mathbf{b}$ for all points $\mathbf{a}, \mathbf{b}, \mathbf{u}, \mathbf{v} \in G$.
2. G admits a scalar multiplication, $\otimes$, possessing the following properties. For all real numbers $r, r_1, r_2 \in \mathbb{R}$ and all points $\mathbf{a} \in G$:

   (G1) $1 \otimes \mathbf{a} = \mathbf{a}$

   (G2) $(r_1 + r_2) \otimes \mathbf{a} = r_1 \otimes \mathbf{a} \oplus r_2 \otimes \mathbf{a}$

   (G3) $(r_1 r_2) \otimes \mathbf{a} = r_1 \otimes (r_2 \otimes \mathbf{a})$

   (G4) $\frac{|r| \otimes \mathbf{a}}{\|r \otimes \mathbf{a}\|} = \frac{\mathbf{a}}{\|\mathbf{a}\|}$

   (G5) $gyr[\mathbf{u}, \mathbf{v}](r \otimes \mathbf{a}) = r \otimes gyr[\mathbf{u}, \mathbf{v}]\mathbf{a}$

   (G6) $gyr[r_1 \otimes \mathbf{v}, r_1 \otimes \mathbf{v}] = I$
3. Real vector space structure $(\|G\|, \oplus, \otimes)$ for the set $\|G\|$ of onedimensional "vectors"

   $$\|G\| = \{\pm\|\mathbf{a}\| : \mathbf{a} \in G\} \subset \mathbb{R}$$

   with vector addition $\oplus$ and scalar multiplication $\otimes$, such that for all $r \in \mathbb{R}$ and $\mathbf{a}, \mathbf{b} \in G$,

   (G7) $\|r \otimes \mathbf{a}\| = |r| \otimes \|\mathbf{a}\|$

   (G8) $\|\mathbf{a} \oplus \mathbf{b}\| \leq \|\mathbf{a}\| \oplus \|\mathbf{b}\|$

Definition 1. *Let ABC be a gyrotriangle with sides a, b, c in an Einstein gyrovector space $(V_s, \oplus, \otimes)$, and let h_a, h_b, h_c be three altitudes of ABC drawn from vertices A, B, C perpendicular to their opposite sides a, b, c or their extension, respectively. The number*

$$S_{ABC} = \gamma_a a \gamma_{h_a} h_a = \gamma_b b \gamma_{h_b} h_b = \gamma_c c \gamma_{h_c} h_c$$

is called the gyrotriangle constant of gyrotriangle ABC (here $\gamma_{\mathbf{v}} = \frac{1}{\sqrt{1 - \frac{\|\mathbf{v}\|^2}{s^2}}}$ is the gamma factor).

(See [2, p. 558].)

Theorem 1. ***(The Gyrotriangle Constant Principle)*** *Let A_1BC and A_2BC be two gyrotriangles in a Einstein gyrovector plane $(\mathbb{R}^2_s, \oplus, \otimes)$, $A_1 \neq A_2$ such that the two gyrosegments A_1A_2 and BC, or their extensions, intersect at a point $P \in \mathbb{R}^2_s$. Then,*

$$\frac{\gamma_{|A_1P|}\,|A_1P|}{\gamma_{|A_2P|}\,|A_2P|} = \frac{S_{A_1BC}}{S_{A_2BC}}.$$

(See [2, p. 563].)

Theorem 2. ***(The Hyperbolic Theorem of Menelaus in Einstein Gyrovector Space)*** *Let $\mathbf{a}_1, \mathbf{a}_2$, and $\mathbf{a}_3$ be three non-gyrocollinear points in an Einstein gyrovector space $(V_s, \oplus, \otimes)$. If a gyroline meets the sides of gyrotriangle $\mathbf{a}_1\mathbf{a}_2\mathbf{a}_3$ at points $\mathbf{a}_{12}, \mathbf{a}_{13}, \mathbf{a}_{23}$, then*

$$\frac{\gamma_{\ominus\mathbf{a}_1\oplus\mathbf{a}_{12}}\,\|\ominus\mathbf{a}_1\oplus\mathbf{a}_{12}\|}{\gamma_{\ominus\mathbf{a}_2\oplus\mathbf{a}_{12}}\,\|\ominus\mathbf{a}_2\oplus\mathbf{a}_{12}\|}\cdot\frac{\gamma_{\ominus\mathbf{a}_2\oplus\mathbf{a}_{23}}\,\|\ominus\mathbf{a}_2\oplus\mathbf{a}_{23}\|}{\gamma_{\ominus\mathbf{a}_3\oplus\mathbf{a}_{23}}\,\|\ominus\mathbf{a}_3\oplus\mathbf{a}_{23}\|}\cdot$$

$$\frac{\gamma_{\ominus\mathbf{a}_3\oplus\mathbf{a}_{13}}\,\|\ominus\mathbf{a}_3\oplus\mathbf{a}_{13}\|}{\gamma_{\ominus\mathbf{a}_1\oplus\mathbf{a}_{13}}\,\|\ominus\mathbf{a}_1\oplus\mathbf{a}_{13}\|} = 1$$

(See [2, p. 463].)

Theorem 3. ***(The Gyrotriangle Bisector Theorem)*** *Let ABC be a gyrotriangle in an Einstein gyrovector space $(V_s, \oplus, \otimes)$, and let P be a point lying on side BC of the gyrotriangle such that AP is a bisector of gyroangle $\measuredangle BAC$. Then,*

$$\frac{\gamma_{|BP|}\,|BP|}{\gamma_{|PC|}\,|PC|} = \frac{\gamma_{|AB|}\,|AB|}{\gamma_{|AC|}\,|AC|}$$

(See [3, p. 150].) For further details we refer to the recent book of A. Ungar [2].

2 Main results

In this section, we prove Van Aubel's theorem in hyperbolic geometry.

Theorem 4. *If the point P does lie on any side of the hyperbolic triangle ABC, and BC meets AP in D, CA meets BP in E, and AB meets CP in F, then*

$$\frac{\gamma_{|AP|}\,|AP|}{\gamma_{|PD|}\,|PD|} = \frac{\gamma_{|BC|}\,|BC|}{2}\cdot\frac{\gamma_{|AE|}\,|AE|}{\gamma_{|EC|}\,|EC|}\cdot\frac{1}{\gamma_{|BD|}\,|BD|}+$$

$$\frac{\gamma_{|BC|}\,|BC|}{2}\cdot\frac{\gamma_{|FA|}\,|FA|}{\gamma_{|FB|}\,|FB|}\cdot\frac{1}{\gamma_{|CD|}\,|CD|}.$$

Proof. If we use the Menelaus's theorem in the h-triangles ADC and ABD for the h-lines BPE, and CPF respectively, then

$$\frac{\gamma_{|AP|}\,|AP|}{\gamma_{|PD|}\,|PD|} = \frac{\gamma_{|AE|}\,|AE|}{\gamma_{|EC|}\,|EC|}\cdot\frac{\gamma_{|BC|}\,|BC|}{\gamma_{|BD|}\,|BD|} \tag{1}$$

and

$$\frac{\gamma_{|AP|}\,|AP|}{\gamma_{|PD|}\,|PD|} = \frac{\gamma_{|FB|}\,|FB|}{\gamma_{|FA|}\,|FA|}\cdot\frac{\gamma_{|BC|}\,|BC|}{\gamma_{|CD|}\,|CD|} \tag{2}$$

From (1) and (2), we have

$$2\cdot\frac{\gamma_{|AP|}\,|AP|}{\gamma_{|PD|}\,|PD|} = \frac{\gamma_{|AE|}\,|AE|}{\gamma_{|EC|}\,|EC|}\cdot\frac{\gamma_{|BC|}\,|BC|}{\gamma_{|BD|}\,|BD|}+$$

$$\frac{\gamma_{|FA|}\,|FA|}{\gamma_{|FB|}\,|FB|}\cdot\frac{\gamma_{|BC|}\,|BC|}{\gamma_{|CD|}\,|CD|},$$

the conclusion follows. □

Corollary 1. *Let G be the centroid of the hyperbolic triangle ABC, and D, E, F are the midpoints of hyperbolic sides BC, CA, and AC respectively. Then,*

$$\frac{\gamma_{|AG|}\,|AG|}{\gamma_{|GD|}\,|GD|} = \frac{\gamma_{|BC|}\,|BC|}{2}\left[\frac{1}{\gamma_{|BD|}\,|BD|}+\frac{1}{\gamma_{|CD|}\,|CD|}\right]. \tag{3}$$

Proof. If we use theorem 4 for the triangle ABC and the centroid G, we have

$$\frac{\gamma_{|AG|}\,|AG|}{\gamma_{|GD|}\,|GD|} = \frac{\gamma_{|BC|}\,|BC|}{2}\cdot\frac{\gamma_{|AE|}\,|AE|}{\gamma_{|EC|}\,|EC|}\cdot\frac{1}{\gamma_{|BD|}\,|BD|}+$$

$$\frac{\gamma_{|BC|}\,|BC|}{2}\cdot\frac{\gamma_{|FA|}\,|FA|}{\gamma_{|FB|}\,|FB|}\cdot\frac{1}{\gamma_{|CD|}\,|CD|},$$

the conclusion follows. □

Corollary 2. *Let I be the incenter of the hyperbolic triangle ABC, and let the angle bisectors be AD, BE, and CF. Then,*

$$\frac{\gamma_{|AI|}\,|AI|}{\gamma_{|ID|}\,|ID|} = \frac{1}{2}\left[\frac{\gamma_{|AB|}\,|AB|}{\gamma_{|BD|}\,|BD|}+\frac{\gamma_{|AC|}\,|AC|}{\gamma_{|CD|}\,|CD|}\right]. \tag{4}$$

Proof. If we use theorem 3 for the triangle ABC, we have

$$\frac{\gamma_{|AE|}\,|AE|}{\gamma_{|EC|}\,|EC|} = \frac{\gamma_{|AB|}\,|AB|}{\gamma_{|BC|}\,|BC|}, \text{ and}$$

$$\frac{\gamma_{|AF|}\,|AF|}{\gamma_{|FB|}\,|FB|} = \frac{\gamma_{|AC|}\,|AC|}{\gamma_{|BC|}\,|BC|}. \tag{5}$$

If we use theorem 4 for the triangle ABC and the incenter I, we have

$$\begin{aligned}\frac{\gamma_{|AI|}\,|AI|}{\gamma_{|ID|}\,|ID|} = {} & \frac{\gamma_{|BC|}\,|BC|}{2}\cdot\frac{\gamma_{|AE|}\,|AE|}{\gamma_{|EC|}\,|EC|}\cdot\frac{1}{\gamma_{|BD|}\,|BD|}+\\ & \frac{\gamma_{|BC|}\,|BC|}{2}\cdot\frac{\gamma_{|FA|}\,|FA|}{\gamma_{|FB|}\,|FB|}\cdot\frac{1}{\gamma_{|CD|}\,|CD|}.\end{aligned} \tag{6}$$

From (5) and (6), we have

$$\frac{\gamma_{|AI|}\,|AI|}{\gamma_{|ID|}\,|ID|} = \frac{\gamma_{|BC|}\,|BC|}{2}\cdot\frac{\gamma_{|AB|}\,|AB|}{\gamma_{|BC|}\,|BC|}\cdot\frac{1}{\gamma_{|BD|}\,|BD|}+$$

$$\frac{\gamma_{|BC|}\,|BC|}{2}\cdot\frac{\gamma_{|AC|}\,|AC|}{\gamma_{|BC|}\,|BC|}\cdot\frac{1}{\gamma_{|CD|}\,|CD|},$$

the conclusion follows. □

The Einstein relativistic velocity model is another model of hyperbolic geometry. Many of the theorems of Euclidean geometry are relatively similar form in the Einstein relativistic velocity model, Aubel's theorem for gyrotriangle is an example in this respect. In the Euclidean limit of large s, $s \to \infty$, gamma factor γ_v reduces to 1, so that the gyroequality (1) reduces to the

$$\frac{|AP|}{|PD|} = \frac{|BC|}{2}\left[\frac{|AE|}{|EC|}\cdot\frac{1}{|BD|} + \frac{|FA|}{|FB|}\cdot\frac{1}{|CD|}\right]$$

in Euclidean geometry. We observe that the previous equality is a equivalent form to the Van Aubel's theorem of euclidian geometry.

Submitted on October 25, 2011 / Accepted on October 28, 2011

References

1. Barbu C. Fundamental Theorems of Triangle Geometry, Ed. Unique, Bacău, 2008 (in Romanian).
2. Ungar A.A. Analytic Hyperbolic Geometry and Albert Einstein's Special Theory of Relativity, Hackensack, World Scientific Publishing Co. Pte. Ltd., 2008.
3. Ungar A.A. A Gyrovector Space Approach to Hyperbolic Geometry, Morgan & Claypool Publishers, 2009.
4. Ungar A.A. Analytic Hyperbolic Geometry Mathematical Foundations and Applications, Hackensack, World Scientific Publishing Co. Pte. Ltd., 2005.

Rossi's Reactors – Reality or Fiction?

Ludwik Kowalski
Montclair State University, New Jersey, USA
E-mail: kowalskil@mail.montclair.edu

A tabletop prototype of a new kind of nuclear device was demonstrated at the University of Bologna, several months ago. It generated thermal energy at the rate of 12 kW. A set of one hundred of such interconnected devices, able to generate energy at a much higher rate (up to 1000 kW) is said to be now commercially available. The inventor claims that the energy was produced via nuclear fusion of hydrogen and nickel. This note addresses conceptual difficulties associated with such interpretation. Experimental facts reported by the inventor seem to conflict with accepted knowledge. This, however, should not be a justification for the rejection of experimental data. Refutations and confirmations should be based on independently performed experiments.

1 Introduction

An interesting website, describing an ongoing research project, has been created by an Italian engineer Andrea Rossi [1]. He is the inventor of a tabletop device in which powdered nickel, mixed with common hydrogen, reported to generate thermal energy at the rate of 12 kW, for six months. A large percentage of nickel was said to be converted into copper, during that time. The device was recently demonstrated at the University of Bologna. The most obvious questions, raised by the reported features of the reactor are:

1. What lowers the coulomb barrier, between the atomic nuclei of hydrogen and nickel?
2. Is the reported accumulation of copper consistent with the well known half-lives of radioactive copper byproducts?
3. Is the measurable isotopic composition of nickel, in spent fuel, consistent with the amount of released energy?
4. The radiation level, outside the operating 12 kW reactor, was said to be comparable to that due to cosmic rays. Spent fuel, removed from the reactor, one hour after the shutdown, was found to be not radioactive [1]. How can these purported facts be explained?

Results from earlier experiments (2008 and 2009) are described in [2]. In one case the device was used to heat a "small factory" (probably two or three rooms) for one year.

2 Reported 2011 results

One demonstration of the device – January 14, 2011, at the University of Bologna – is described in [3–5]. Subsequent experiments – February 10, and March 29, 2011 – are described in [6–8]. In both cases the apparatus consisted of a cylinder containing nickel. Pure hydrogen was forced to flow through the hot nickel powder. The amount of powder was 100 grams [8, 9], or slightly more than one cubic inch, depending on the level of compression. Reactions between nickel and hydrogen turned out to be extremely exothermic, generating thermal energy at the rate of about 12.4 kW. This was 31 times higher than the rate at which electric energy was supplied, to operate the equipment [4].

In the February experiment the amount of thermal energy was determined from the flow rate of cooling water, and the difference between its input and output temperature. In the January experiment the water flow rate was slower; the entering water was a liquid, the escaping water was a vapor. The amount of thermal energy released was determined from the amount of liquid water (initially at 15 ^{o}C) transformed into 101 ^{o}C vapor. Rossi claims that most heat is produced from nuclear reactions:

$$p + Ni \rightarrow Cu,$$

where p is nothing but ionized hydrogen. This is very surprising because the temperature of hydrogen was below the melting point of nickel. Addressing this issue in [10] Rossi reported that about 30% of nickel was turned into copper, after six months of uninterrupted operation. A schematc diagram of the reactor, and additional details are in [11, 12].

Comment 1
Many physicists have studied fusion of protons with nickel nuclei. But their protons had much higher energies, such as 14.3 MeV [13]. Rossi's protons, by contrast, had very low energies, close to 0.04 eV. The probability of nuclear fusion, expressed in terms of measurable cross sections, is known to decrease rapidly when the energy is lowered. How can 0.04 eV protons fuse with nickel, whose atomic number is 28? Rossi is convinced that this is due a catalyst added to the powdered nickel. The nature of the catalyst has not been disclosed. This prevents attempts to replicate the experiments, or to discuss the topic theoretically. Secrecy might make sense in some business situations, but it is not consistent with scientific methodology.

Comment 2
How can 30% of nickel in Rossi's reactor be transmuted into

copper? This seems to be impossible, even if the coulomb barrier is somehow reduced to zero by his catalyst. To justify this let us focus on the ^{58}Ni and ^{60}Ni isotopes–they constitute 94.1% of the nickel initially loaded into the device. The reactions, by which copper is produced, from these isotopes, would be:

$$p + \ ^{58}Ni \rightarrow \ ^{59}Cu \quad \text{(half-life is 3.2 s)} \qquad \text{(A)}$$

and

$$p + \ ^{60}Ni \rightarrow \ ^{61}Cu \quad \text{(half-life is 3.3 h)} \qquad \text{(B)}$$

The reported amount of accumulated copper – 30% of the initial nickel being turned into copper, after six months of operation–would indeed be possible, via reactions (A) and (B), if the produced copper isotopes were stable, or had half-lives much longer than six months. But this is not the case, as shown above. The produced copper isotopes, ^{59}Cu and ^{61}Cu, rapidly decay into ^{59}Ni and ^{61}Ni. Each reaction, in other words, would lead to accumulation of these isotopes of nickel, not to accumulation of copper, as reported by Rossi. The accumulation of copper would practically stop after several half-lives. Note that ^{63}Cu and ^{65}Cu, if produced from fusion of protons with ^{62}Ni and ^{64}Ni, would be stable. But natural abundance of these isotopes of nickel, 3.63% and 0.92%, respectively, is too low to be consistent with the claimed accumulation of 30% of copper.

Comment 3

How much of the original ^{58}Ni should be destroyed, after six months of continuous operation, in order to generate thermal energy at the rate of 12 kW? Let us again assume that Coulomb barriers are somehow reduced to zero by Rossi's secret catalyst. The ^{58}Ni is 68% of the total. On that basis one can assume that 68% of 12 kW is due to the radioactive decay of ^{59}Cu, and its radioactive daughter, ^{59}Ni. Thus $P_1' = 0.68 \times 12 = 8.16$ kW. This is the thermal power. The nuclear power P_1 must be larger, because neutrinos and some gamma rays do escape from the vessel. As a rough estimate, assume that the nuclear power is

$$P_1 = 16 \text{ kW} = 16{,}000 \text{ J/s} = 10^{17} \text{ MeV/s}.$$

The excited ^{59}Cu, from the reaction (A), releases 3.8 MeV of energy, as one can verify using a table of known atomic masses. In the same way one can verify that the energy released from its radioactive daughter, ^{59}Ni, is 4.8 MeV. In other words, each transformation of ^{58}Ni into ^{60}Ni releases 3.8 + 4.8 = 8.6 MeV of nuclear energy.

The number of reactions (A) should thus be equal to $10^{17}/8.6 = 1.16 \times 10^{16}$ per second. Multiplying this result by the number of seconds in six months (1.55×10^7) one finds that the total number of destroyed ^{58}Ni nuclei is 1.80×10^{23}, or 17.4 grams. A similar estimate can be made for other initially present nickel isotopes. The overall conclusion is that the isotopic composition of nickel, after six months of operation, at the 12 kW level, would change drastically, if the reaction A were responsible for the heat produced in the reactor invented by Rossi.

The amount of ^{59}Ni, for example, would increase from 0% (natural abundance) to 17.4%. The amount of ^{58}Ni, on the other hand, would be reduced from 68% (natural abundance) to 50.6%. The isotopic composition of nickel in spent fuel was measured, according to [1], but results remain "privileged information".

Comment 4

The level of radioactivity, next to the reactor generating heat at the rate of 12 kW, was reported as not much higher than the natural background [5]. Is this consistent with reaction (A) being responsible for most of the heat? The answer is negative. How can this be justified? In the steady state the rate at which radioactive atoms, in this case ^{59}Cu, are decaying is the same as the rate at which they are produced. That rate, as shown in Comment 3, is 1.16×10^{16} atoms per second. In other words, the expected activity is

$$1.16 \times 10^{16}/3.7 \times 10^{10} = 313{,}000 \text{ Curies}.$$

The emitted radiation would include gamma rays of 1.3 MeV, able to escape. The level of radiation, next to the reactor, would depend on the wall thickness. It would certainly exceed the background by many orders of magnitude. Absence of excessive gamma radiation might be an indication that the reactions producing heat were different from the p+Ni fusion.

3 Addendum

Note that the reported fuel power density of 120 W/g would be at least ten times higher than in a fuel element of a nuclear reactor based on ^{235}U. What can be more desirable than higher safety and lower cost? Did Rossi really invent a new kind of nuclear reactor? Logical speculations, such as those above, are not sufficient to answer this question. Only independently performed experiments can do this.

Rossi's claims, if confirmed, would present a challenge to theoretical physicists. Physics, unlike mathematics, is based on confirmed experimental facts, not on axioms. Newly discovered facts often lead to improvements of accepted theories. Let's hope that Rossi's incredible results can be independently confirmed in the near future.

Submitted on November 7, 2011 / Accepted on November 12, 2011

References

1. Rossi A. http://www.journal-of-nuclear-physics.com
2. Rossi A. *Journal of Nuclear Physics* http://www.journal-of-nuclear-physics.com/?p=62
3. Celani F. New Energy Times http://newenergytimes.com/v2/news/2011/36/3623rf-celani.shtml

4. Mills H.
http://pesn.com/2011/03/07/9501782_Cold_Fusion_
Steams_Ahead_at_Worlds_Oldest_University/
5. Macy M.
http://pesn.com/2011/01/19/9501747_
cold-fusion-journals_warming_to_Rossi_breakthrough/
6. Lewan M.
http://www.nyteknik.se/nyheter/energi_miljo/energi/
article3108242.ece
7. Rothwell J. http://www.lenr-canr.org/News.htm
8. Lewan M.
http://www.nyteknik.se/nyheter/energi_miljo/energi/
article3144827.ece
9. Rossi A.
http://www.journal-of-nuclear-physics.com/?p=338#
more-338
10. Rossi A.
http://www.journal-of-nuclear-physics.com/?p=
62&cpage=2
11. Chubb S. *Infinite Energy*, 2011, issue 96,
http://www.infinite-energy.com/images/pdfs/IE96Rossi.
pdf
12. Allan S.D.
http://pesn.com/2011/10/28/9501940_1_MW_E-Cat_Test_
Successful/
13. Miller J. et al. *Physical Review*, 1967, v. 163, 107411.

Photon-assisted Spectroscopy of Dirac Electrons in Graphene

Ahmed S. Abdelrazek*, Walid A. Zein†, and Adel H. Phillips†

*Faculty of Engineering, Kafr-Elsheikh University, Kafr-Elsheikh, Egypt
†Faculty of Engineering, Ain-Shams University, Cairo, Egypt. E-mail: adel.phillips@gmail.com

The quantum Goos-Hanchen effect in graphene is investigated. The Goos-Hanchen phase shift is derived by solving the Dirac eigenvalue differential equation. This phase shift varies with the angle of incidence of the quasiparticle Dirac fermions on the barrier. Calculations show that the dependence of the phase shift on the angle of incidence is sensitive to the variation of the energy gap of graphene, the applied magnetic field and the frequency of the electromagnetic waves. The present results show that the conducting states in the sidebands is very effective in the phase shift for frequencies of the applied electromagnetic field. This investigation is very important for the application of graphene in nanoelectronics and nanophotonics.

1 Introduction

In recent years, the interest in novel device structures able to surmount the miniaturization limits imposed by silicon based transistors has led researchers to explore alternative technologies such as those originated in the field of semiconducting quantum dots, nanowire, graphene and carbon nanotubes [1, 2]. Graphene [3, 4] consists of a monolayer of carbon atoms forming a two-dimensional honeycomb lattice.

Graphene has been intensively studied due to its fascinating physical properties and potential applications in the field of nanoelectronics and another different field, for example, biosensor, hydrogen storage, and so on [5, 6]. In graphene, the energy bands touch the Fermi energy at six discrete points at the edges of the hexagonal Brillouin zone. Out of these six Fermi points, only two are inequivalent, they are commonly referred to as K and K´ points [7]. The quasiparticle excitation about K & K´ points obey linear Dirac like energy dispersion [8]. The presence of such Dirac like quasiparticle is expected to lead to a number of unusual electronic properties in graphene including relativistic quantum Hall effect [9], quasi-relativistic Klein tunneling [10, 11] and the lateral shift of these Dirac quasi-particles in graphene, which is known as Goos-Hanchen effect, Bragg reflector and wave guides [12–15]. The present paper is devoted to investigate the quantum Goos-Hanchen effect in graphene, taking into consideration the effect of electromagnetic waves of wide range of frequencies and magnetic field.

2 The Model

The transport of quasiparticle Dirac Fermions in monolayer graphene through a barrier of height, V_b, and width, d, is described by the following Dirac Hamiltonian, H_o, which is given as [4, 16]:

$$H_o = -i\hbar v_f \sigma \nabla + V_b, \tag{1}$$

where v_f is the Fermi velocity and $\sigma = (\sigma_x, \sigma_y)$ are the Pauli matrices. Since the graphene is connected to two leads and applying a top gate with gate voltage, V_g. Also, the transport of quasiparticle Dirac fermions are influenced by applying both magnetic field, B, and an electromagnetic field of amplitude, V_{ac}, and of wide range of frequencies, ω. So, accordingly Eq. (1) can be rewritten as follows:

$$H = -i\hbar v_f \sigma \nabla + V_b + eV_{sd} + eV_g + eV_{ac}\cos(\omega t) + \frac{\hbar eB}{2m^*}, \tag{2}$$

where V_{sd} is the bias voltage, $\hbar$ is reduced Planck's constant and m^* is the effective mass of quasiparticle Dirac fermions. Now, due to transmission of these quasi-particles Dirac fermions, a transition from central band to side-bands at energies [11, 17] $E \pm n\hbar\omega$, where n is an integer with values $0, \pm 1, \pm 2, \ldots$. The Dirac fermions Hamiltonian, H, (Eq. 2) operates in space of the two-component eigenfunction, Ψ, where Dirac eigenvalue differential equation is given by [11]:

$$H\Psi(r) = E\Psi(r), \tag{3}$$

where E is the scattered energy of quasi-particle Dirac fermions. The solution of Eq. (3) gives the following eigenfunctions [11,18]. The eigenfunction of incident quasi-particle Dirac fermions is

$$\Psi_{in}(r) = \sum_{n=1}^{\infty} J_n\left(\frac{eV_{ac}}{\hbar\omega}\right)[A + B], \tag{4}$$

where

$$A = \begin{pmatrix} 1 \\ se^{i\varphi} \end{pmatrix} \exp\left(i(k_x x + k_y y)\right),$$

$$B = r\begin{pmatrix} 1 \\ -se^{-i\varphi} \end{pmatrix} \exp\left(i(-k_x x + k_y y)\right),$$

J_n is the n^{th} order of Bessel function of first kind and the eigenfunction for the transmitted quasiparticle Dirac fermions through the barrier is given by:

$$\Psi_{tr}(r) = \sum_{n=1}^{\infty} J_n\left(\frac{eV_{ac}}{\hbar\omega}\right) t\begin{pmatrix} 1 \\ se^{i\varphi} \end{pmatrix} \exp\left(i(k_x x + k_y y)\right) \tag{5}$$

In Eqs. (4, 5), r and t are the reflection and transmission amplitude respectively and S = Sgn(E) is the signum function of E. The components of the wave vectors k_x and k_y outside the barrier are expressed in terms of the angle of incidence, φ, of the quasiparticles Dirac fermions as:

$$k_x = k_f \cos\varphi, \quad k_y = k_f \sin\varphi, \tag{6}$$

where k_f is the Fermi wave vector. The eigenfunction Ψ_b inside the region of the barrier is given by:

$$\Psi_b(r) = \sum_{n=1}^{\infty} J_n\left(\frac{eV_{ac}}{\hbar\omega}\right)[C + D], \tag{7}$$

where

$$C = \begin{pmatrix} \alpha \\ s'\beta e^{i\theta} \end{pmatrix} \exp\left(i(q_x x + k_y y)\right),$$

$$D = r\begin{pmatrix} \alpha \\ -s'\beta e^{-i\theta} \end{pmatrix} \exp\left(i(-q_x x + k_y y)\right),$$

$$q_x = (k_f'^2 - k_y^2)^{\frac{1}{2}}, \tag{8a}$$

and

$$\theta = \tan^{-1}\left(\frac{k_y}{q_x}\right) \tag{8b}$$

in which

$$k_f' = \frac{\sqrt{(V_b - \varepsilon)^2 - \dfrac{\varepsilon_g^2}{2}}}{\hbar v_f}, \tag{9}$$

where ε_g is the energy gap and ε is expressed as

$$\varepsilon = E - eV_g - n\hbar\omega - eV_{sd} - V_b + \frac{\hbar eB}{2m^*} \tag{10}$$

In Eq. (7), the parameters s', α, and β are given by:

$$s' = sgn\,(E - V_b) \tag{11}$$

$$\alpha = \sqrt{1 + \frac{\dfrac{s'\varepsilon_g}{2\hbar v_f}}{\sqrt{k_f'^2 + \dfrac{\varepsilon_g^2}{4(\hbar v_f)^2}}}} \tag{12}$$

This parameter, α, corresponds to K-point. Also, β is given by

$$\beta = \sqrt{1 - \frac{\dfrac{s'\varepsilon_g}{2\hbar v_f}}{\sqrt{k_f'^2 + \dfrac{\varepsilon_g^2}{4(\hbar v_f)^2}}}} \tag{13}$$

This parameter, β, corresponds to K'-point. Now, in order to find an expression for both the transmission coefficient, t, (Eq. 5) and the corresponding Goos-Hanchen phase shift, Φ, this is done by applying the boundary conditions at the boundaries of the barrier [11, 18]. This gives the transmission coefficient, t, as:

$$t = \sum_{n=1}^{\infty} J_n\left(\frac{eV_{ac}}{\hbar\omega}\right) \times \left[\frac{1}{\cos(q_x d) - F}\right], \tag{14}$$

where

$$F = i(s' s\gamma \sec(\varphi)\sec(\theta) + \tan(\varphi)\tan(\theta))\sin(q_x d)$$

and γ is expressed as:

$$\gamma = \frac{\sqrt{\dfrac{\varepsilon_g^2}{4(\hbar v_f)^2} + k_f'^2}}{k_f'} \tag{15}$$

The transmission coefficient, t, is related to the Goos-Hanchen phase shift, Φ, [12, 18] as:

$$t = \frac{e^{i\phi}}{f}, \tag{16}$$

where f is the Gaussian envelop of the shifted wave of quasiparticle Dirac fermions [12, 18, 19]. So, the expression for the phase shift is given by:

$$\Phi = \tan^{-1}\left[\frac{\sin(\theta)\sin(\varphi) + ss'\gamma}{\cos(\theta)\cos(\varphi)}\tan(q_x d)\right], \tag{17}$$

where d is the width of the barrier. We notice that the phase shift, Φ (Eq. 17) depends on the angle of incidence, ϕ of the quasiparticle Dirac fermion and on the barrier of height, V_b, and its width, d, and other parameters considered, for example, the energy gap, ε_g, the magnetic field, B, gate voltage, V_g, and the external pulsed photons of wide range of frequencies.

3 Results and Discussion

Numerical calculations are performed for phase shift, Φ, (Eq. 17) as shown below. For monolayer graphene, the values of both barrier height, V_b, and its width are respectively V_b = 120 meV and d = 80 nm [16, 18, 19]. Also, the value of the Fermi-velocity, v_f is approximately 10^6 m/s, and the effective mass of quasiparticle Dirac fermions is approximately m^* = 0.054 me [16, 18, 19]. The engineering of band gap of graphene generates a pathway for possible graphene-based nanoelectronics and nanophotonics devices. It is possible to open and tune the band gap of graphene by applying electric field [20] or by doping [21]. So, in our calculations we take the value of the energy gap of graphene to be ε_g = 0 eV, 0.03 eV, 0.05 eV [22].

The features of our results are the following:

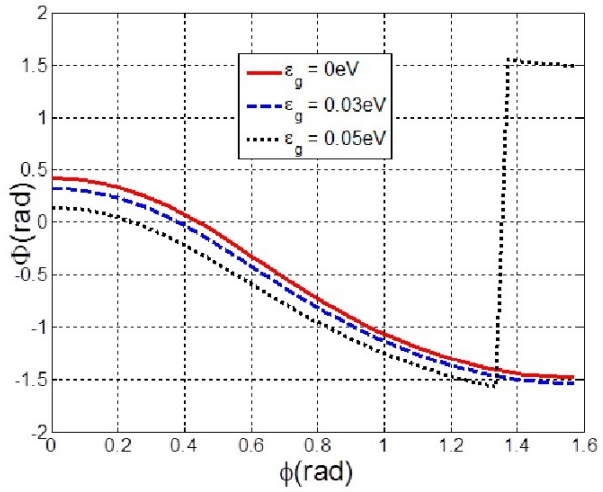

Fig. 1: The variation of Goos-Hanchen phase shift, Φ, with angle of incidence, ϕ, at different values of energy gap.

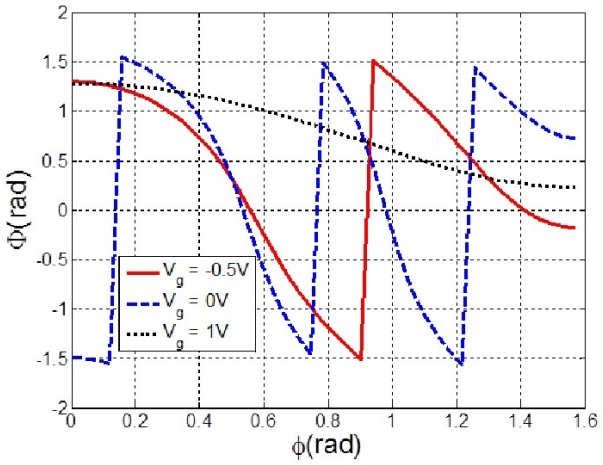

Fig. 2: The variation of Goos- Hanchen phase shift, Φ, with angle of incidence, ϕ, at different values of gate voltage.

1. Fig. 1, shows the dependence of the Goos-Hanchen phase shift, Φ, on the angle of incidence ϕ at different values of energy gap, ε_g. As shown from the figure that the phase shift, Φ, decreases as the angle of incidence, ϕ, increase for the considered values of the energy gap, ε_g. It must be noticed that for ε_g = 0.05eV, for angle of incidence $\phi \approx$1.335 rad, the phase shift, Φ , increases from -1.571 rad to 1.549 rad and then slightly decreases. This result shows the strong dependence of Goos-Hanchen phase shift on the engineered band gap of graphene [18, 23]. This result shows that the phase shift, Φ , can be enhanced by certain energy gap at the Dirac points.
2. Fig. 2 shows the dependence of the phase shift, Φ, on the angle of incidence, ϕ , at different values of the gate voltage, V_g. As shown from the figure that for large values of gate voltage, V_g, for example, V_g = 1V, the phase shift, Φ , decreases as the angle of incidence, ϕ, increase and phase shift takes only positive values. While for values of V_g = 0V or V_g = -0.5V, the value of phase shift oscillates between negative and positive values. It is well known that the tunneling of quasiparticle Dirac fermions could be controlled by changing the barrier height, V_b, this could be easily implemented by applying a gate voltage, V_g, to graphene [11,24–26].
3. Fig. 3 shows the dependence of the phase shift, Φ, on the angle of incidence, ϕ ,at different values of magnetic field, B. As shown from the figure that for B = 0.5 T, the phase shift decreases gradually as the angle of incidence, ϕ , increases to value Φ = 1.335 rad and then increases to Φ = 1.549 rad at ϕ = 1.374 rad and very slightly decreases. While for values B = 5 T and 10 T the value of the phase shift, Φ, is negative and decreases up to *Phi* = -1.561 rad when ϕ = 0.8635rad (when B = 5T) and then increases to Φ = 1.529 rad when ϕ = 0.902 rad and then decreases as the angle of incidence increases. For B = 10 T, the value of phase shift is negative and decreases as the value of ϕ increases up to ϕ = 0.432 rad and increases up to Φ = 1.547 rad and ϕ = 0.471 rad and decreases as the angle of incidence increases. This result shows that how a magnetic field modifies the transport of quasiparticle Dirac fermions in graphene with certain barrier height and certain energy gap [26].
4. Fig. 4 shows the variation of the phase shift, Φ, at different values of frequencies, ν , of the pulsed electromagnetic field. As shown from the figure, for higher frequencies 400 THz, 800 THz and 1000 THz, the value of the phase shift, Φ, decreases as the angle of incidence increases. We notice that in this range of frequencies, the value of phase shift is negative. While for microwave frequencies, MW = 300 GHz the value of the phase shift, Φ, decreases as the angle of incidence increases up to ϕ = 1.021 rad and then the phase shift increases up to Φ = 1.55 rad and ϕ = 1.06 rad and then decreases gradually.

This result shows that the conducting states in the side bands can be effective in the Goos-Hanchen phase shift for a certain frequency of the applied electromagnetic signal [27]. This result is very important for tailoring graphene for photonic nano-devices.

The present results show that the Goos-Hanchen phase shift can be modulated by both intrinsic parameters, for example, the barrier height, the energy gap and the extrinsic parameters, for example, magnetic field and the induced photons of electromagnetic field. The present research is very important for the applications of graphene in different nanoelectronics and nanophotonic devices.

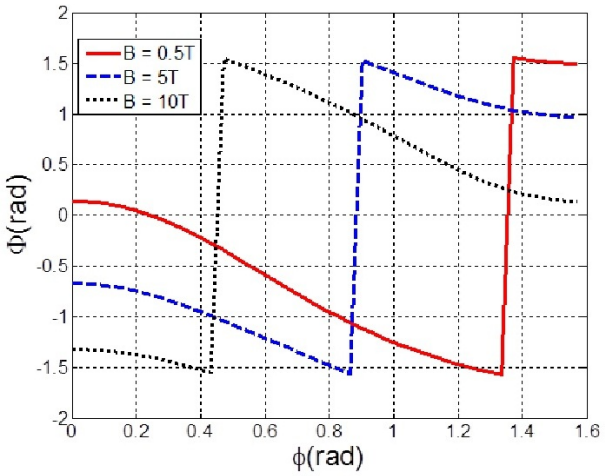

Fig. 3: The variation of Goos-Hanchen phase shift, Φ, with angle of incidence, ϕ, at different values of magnetic field.

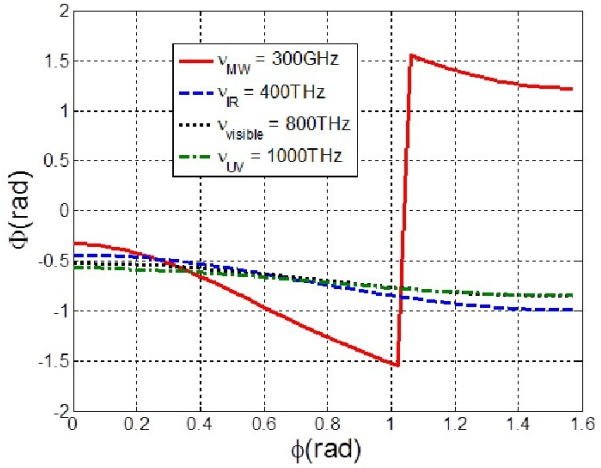

Fig. 4: The variation of Goos-Hanchen phase shift, Φ, with angle of incidence, ϕ, at different values of electromagnetic wave frequencies.

Submitted on November 20, 2011 / Accepted on November 26, 2011

References

1. Phillips A.H. Nanotechnology & semiconductor Nanodevices, Book chapter in Hadron model Models and related New Energy Issues, edited by Smarandache F., Christianto V. Info-Learn Quest. USA, November 2007, 308.
2. Bergmann C.P., de Andrado M.J. Nanostructured material for Engineering Applications. Springer-verlog Berlin Heidelberg, 2011.
3. Novoselov K.S., Geim A.K., Morozov S.V., Jiang D., Zhang Y., Dubonos S.V, Grigorieva I.V., Firsov A.A. Electric field effect in atomically thin carbon films. *Science*, 2004, v. 306, 666.
4. Castro Netro A., Guineer F., Novoselov K., Geim A. The electronic properties of graphene. *Review of Modern Physics*, 2009, v. 81, 109.
5. Geim A.K. Graphene: Status and prospecrts. *Science*, 2009, v. 324, 1530.
6. Geim A.K., Novoselov K.S. The rise of graphene. *Nature materials*, 2007, v. 6(3), 183.
7. Ando T. Theory of Electronic states and Transport in carbon nanotubes. *Journal of physical society Japan*, 2005, v. 74, 777.
8. Peres N.M.R. The electronic properties of graphene and its bilayer. *Vacuum*, 2009, v. 83, 1248.
9. Gusynin V.P., Sharapov S.G. Unconventional integer quantum Hall effect in graphene. *Physical Review Letters*, 2005, v. 95, 146801.
10. Yamakage A., Imura K.I., Cayssol J., Kuramoto Y. Klein tunneling in graphene under substrate electric field. *Physics Procedia*, 2010, v. 3, 1243.
11. Mina A.N., Phillips A.H. Photon-assisted resonant chiral tunneling through a bilayer graphene barrier. *Progress in Physics*, 2011, v. 1, 112.
12. Beeenakker C.W.J., Sepkhanov R.A., Akhmerov A.R., Tworzydlo J. Quantum Goos-Hanchen effect in graphene. *Physical Review Letters*, 2009, v. 102, 146804.
13. Wu Zhenhua, Zhai F., Peeters F.M., Xu H.Q., Chang Kai. Valley-dependent Brewster angles and Goos-Hanchen effect in strained graphene. *Physical Review Letters*, 2011, v. 106, 176802.
14. Ghosh S., Sharma M. Electron optics with magnetic vector potential barrier in graphene. *Journal of Physics: condensed matter*, 2009, v. 21, 292204.
15. Zhang F.M., He Y., Chen X. Guided modes in graphene waveguides. *Applied Physics Letters*, 2009, v. 94, 212105.
16. Katsnelson M.I, Novoselov K.S., Geim A.K. Chiral tunneling and the Klein paradox in graphene. *Nature Physics*, 2006, v. 2, 620.
17. Ryzhii V., Ryzhii M. Graphene Bilayer field effect phototransistor for terahertz and infrared detection. *Physical Review B*, 2009, v. 79, 245311.
18. Sharma M., Ghosh S. Electronic transport and Goos-Hanchen shift in graphene with electric and magnetic barriers: optical analogy and band structure. *Journal of physics: condensed matter*, 2011, v. 23(5), 055501.
19. Zhao L., Yelin S.F. Proposal for graphene based coherent buffers and memories. *Physical Review B*, 2010, v. 81(11), 115441.
20. Zhang Y., Tang T.T., Girit C., Hao Z., Martin M., Zettle A., Crommie M.F., Shen Y.R., Wang F. Direct observation of a widely tunable band gap in bilayer graphene. *Nature*, 2009, v. 459, 820–823.
21. Ohta T., Bostwick A., Seyller T., Horn K., Rotenberg E. Controlling the electronic structure of bilayer graphene. *Science*, 2006, v. 313, 951–954.
22. Dubois S.M.M., Zanolliz., Declerck X., Charlier J.C. Electronic properties and quantum transport in graphene-based nanostructures. *European Physical Journal B*, 2009, v. 72(1), 1–24.
23. Zhou S.Y., Gweon G.H., Federov A.V., First P.N., de Heer W.A., Lee D.H., Guinea F., Castro Neto A.H., Lanzera A. Origin of energy gap in epitaxial graphene. *Nature Materials*, 2008, v. 7, 259.
24. Awadallah A.A., Phillips A.H., Mina A.N., Ahmed R.R. Photon-assisted transport in carbon nanotube mesoscopic device. *International Journal of Nanoscience*, 2011, v. 10(3), 419.
25. Mina A.N., Awadallah A.A., Phillips A.H., Ahmed R.R. Microwave spectroscopy of carbon nanotube field effect transistor. *Progress in Physics*, 2010, v. 4, 61.
26. Huard B., Sulpizio J.A., Stander N., Todd K., Yang B., Gold haber-Gordon D. Transport measurements across a tunable potential barrier in graphene. *Physical Review Letters*, 2007, v. 98, 236803.
27. Rocha G., Pacheco M., Foa-Torres L.E.F., Cunilberti G., Latge' A. Transport respose of carbon-based resonant cavities under time-dependent potential and magnetic fields. *European Physics Letters*, 2011, v. 94, 47002.

Coherent Spin Polarization in an AC-Driven Mesoscopic Device

Mina Danial Asham*, Walid A. Zein†, and Adel H. Phillips†
*Faculty of Engineering, Benha University, Benha, Egypt
E-mail: minadanial@yahoo.com
†Faculty of Engineering, Ain-Shams University, Cairo, Egypt
E-mail: adel.phillips@gmail.com

The spin transport characteristics through a mesoscopic device are investigated under the effect of an AC-field. This device consists of two-diluted magnetic semiconductor (DMS) leads and a nonmagnetic semiconducting quantum dot. The conductance for both spin parallel and antiparallel alignment in the two DMS leads is deduced. The corresponding equations for giant magnetoresistance (GMR) and spin polarization (SP) are also deduced. Calculations show an oscillatory behavior of the present studied parameters. These oscillations are due to the coupling of photon energy and spin-up & spin-down subbands and also due to Fano-resonance. This research work is very important for spintronic devices.

1 Introduction

The field of semiconductor spintronics has attracted a great deal of attention during the past decade because of its potential applications in new generations of nanoelectronic devices, lasers, and integrated magnetic sensors [1, 2]. In addition, magnetic resonant tunneling diodes (RTDs) can also help us to more deeply understand the role of spin degree of freedom of the tunneling electron and the quantum size effects on spin transport processes [3–5]. By employing such a magnetic RTD, an effective injection of spin-polarized electrons into nonmagnetic semiconductors can be demonstrated [6]. A unique combination of magnetic and semiconducting properties makes diluted magnetic semiconductors (DMSs) very attractive for various spintronics applications [7, 8]. The II-VI diluted magnetic semiconductors are known to be good candidates for effective spin injection into a non-magnetic semiconductor because their spin polarization can be easily detected [9, 10]. The authors investigated the spin transport characteristics through mesoscopic devices under the effect of an electromagnetic field of wide range of frequencies [11–14].

The aim of the present paper is to investigate the spin transport characteristics through a mesoscopic device under the effect of both electromagnetic field of different frequencies and magnetic field. This investigated device is made of diluted magnetic semiconductor and semiconducting quantum dot.

2 The Model

The investigated mesoscopic device in the present paper is consisted of a semiconducting quantum dot connected to two diluted magnetic semiconductor leads. The spin-transport of electrons through such device is conducted under the effect of both electromagnetic wave of wide range of frequencies and magnetic effect. It is desired to deduce an expression for spin-polarization and giant magnetoresistance. This is done as follows:

The Hamiltonian, H, describing the spin transport of electrons through such device can be written as:

$$\begin{aligned} H &= -\frac{\hbar^2}{2m^*}\frac{d^2}{dx^2} + eV_{sd} + eV_g + E_F + V_b \\ &\quad + eV_{ac}\cos(\omega t) \pm \frac{1}{2}g\mu_B\sigma B + \frac{N^2e^2}{2C} \pm \sigma h_o, \end{aligned} \tag{1}$$

where m^* is the effective mass of electron, $\hbar$ is the reduced Planck's constant, V_{sd} is the source-drain voltage (bias voltage), V_g is the gate voltage, E_F is the Fermi-energy, V_b is the barrier height at the interface between the leads and the quantum dot, V_{ac} is the amplitude of the applied AC-field with frequency ω, g is the Landé factor of the diluted magnetic semiconductor, μ_B is Bohr magneton, B is the applied magnetic field, σ-Pauli matrices of spin, and h_o is the exchange field of the diluted magnetic semiconductor. In eq. (1), the term $(N^2e^2/2C)$ represents the Coulomb charging energy of the quantum dot in which e is the electron charge, N is the number of electrons tunneled through the quantum dot, and C is the capacitance of the quantum dot. So, the corresponding Schrödinger equation for such transport is

$$H\psi = E\psi, \tag{2}$$

with the solution for the eigenfunction, $\psi(x)$, in the corresponding regions of the device can be expressed as [15]:

$$\psi(x) = \begin{cases} \left[A_1 e^{ik_1 x} + B_1 e^{-ik_1 x}\right] J_n\left(\frac{eV_{ac}}{\hbar\omega}\right) e^{-in\omega t}, x < 0 \\ \left[A_2 Ai(\rho(x)) + B_2 Bi(\rho(x))\right] J_n\left(\frac{eV_{ac}}{\hbar\omega}\right) \\ \times e^{-in\omega t}, 0 < x < d \\ A_3 e^{ik_2 x} J_n\left(\frac{eV_{ac}}{\hbar\omega}\right) e^{-in\omega t}, x > d \end{cases} \tag{3}$$

where $Ai(\rho(x))$ is the Airy function and its complement is $Bi(\rho(x))$ [16]. In eqs. (3), the parameter $J_n(eVac/\hbar\omega)$ represents the n^{th} order Bessel function of the first kind. The

solutions of eqs. (3) must be generated by the presence of the different side-bands "n" which come with phase factor $e^{-in\omega t}$ [11–14], and d represents the diameter of the quantum dot. Also, the parameters k_1, k_2 and $\rho(x)$ in eqs. (3) are:

$$k_1 = \sqrt{\frac{2m^*}{\hbar^2}\left(E + n\hbar\omega + V_b + \sigma h_o\right)}, \tag{4}$$

n = 0, ± 1, ± 2, ± 3 ...

$$k_2 = \sqrt{\frac{2m^*}{\hbar^2}(V_b + eV_{sd} + eV_g + E_F + \frac{N^2e^2}{2C} + n\hbar\omega \pm \frac{1}{2}g\mu_B B\sigma \pm \sigma h_o)} \tag{5}$$

and

$$\rho(x) = \frac{d}{eV_{sd}\Phi}\left(E_F + V_b + eV_{sd}\left(\frac{x}{d}\right) + eV_g + \frac{N^2e^2}{2C} + \frac{1}{2}g\mu_B B\sigma + E\right) \tag{6}$$

in which Φ is given by

$$\Phi = \sqrt[3]{\frac{\hbar^2 d}{2m^* eV_{sd}}}. \tag{7}$$

Now, the tunneling probability, $\Gamma(E)$, could be obtained by applying the boundary conditions to the eigenfunctions (eq. (3)) and their derivative at the boundaries of the junction [11–14]. We get the following expression for the tunneling probability, $\Gamma(E)$, which is:

$$\Gamma(E) = \sum_{n=1}^{\infty} J_n^2\left(\frac{eV_{ac}}{\hbar\omega}\right)\cdot\left\{\frac{4k_1k_2}{\pi^2\Phi^2}\left[\alpha^2k_1^2k_2^2 + \beta^2{m^*}^2k_1^2\right]^{-1}\right\}, \tag{8}$$

where α and β are given by:

$$\alpha = Ai(\rho(0))\cdot Bi(\rho(d)) - Bi(\rho(0))\cdot Ai(\rho(d)), \tag{9}$$

and

$$\beta = \frac{1}{\Phi m^*}\left[Ai(\rho(0))\cdot Bi'(\rho(d)) - Bi(\rho(0))\cdot Ai'(\rho(d))\right], \tag{10}$$

where $Ai'(\rho(x))$ is the first derivative of the Airy function and $Bi'(\rho(x))$ is the first derivative of its complement. Now, the conductance, G, of the present device is expressed in terms of the tunneling probability, $\Gamma(E)$, through the following equation as [11–14, 17]:

$$G = \frac{2e^2}{h}\sin(\varphi)\int_{E_F}^{E_F+n\hbar\omega} dE\left(-\frac{\partial f_{FD}}{\partial E}\right)\cdot\Gamma(E), \tag{11}$$

where ϕ is the phase of the scattered electrons and the factor $(-\partial f_{FD}/\partial E)$ is the first derivative of the Fermi-Dirac distribution function and it is given by:

$$\left(-\frac{\partial f_{FD}}{\partial E}\right) = (4k_BT)^{-1}\cosh^{-2}\left(\frac{E - E_F + n\hbar\omega}{2k_BT}\right), \tag{12}$$

where k_B is the Boltzmann constant and T is the absolute temperature. The spin polarization, SP, and giant magnetoresistance, GMR, are expressed in terms of the conductance, G, as follows [18]:

$$Sp = \frac{G_{\uparrow\uparrow} - G_{\uparrow\downarrow}}{G_{\uparrow\uparrow} + G_{\uparrow\downarrow}}, \tag{13}$$

and

$$GMR = \frac{G_{\uparrow\uparrow} - G_{\uparrow\downarrow}}{G_{\uparrow\uparrow}}, \tag{14}$$

where $G_{\uparrow\uparrow}$ is the conductance when the magnetization of the two diluted magnetic-semiconductor leads are in parallel alignments, while $G_{\uparrow\downarrow}$ is the conductance for the case of antiparallel alignment of the magnetization in the leads. The indicator ↑ corresponds to spin up and also ↓ corresponds to spin down.

3 Results and Discussion

Numerical calculations to eqs. (11, 13 and 14), taking into consideration the two cases for parallel and antiparallel spins of quasiparticles in the two leads. In the present calculations, we take the case of quantum dot as GaAs and the two leads as diluted magnetic semiconductors GaMnAs. The values for the quantum dot are [11–14, 19–21]: E_F = 0.75 eV, C = 10^{-16} F and d = 2 nm, V_b = 0.3 eV. The value of the exchange field, h_o, for GaMnAs is -1 eV and g = 2 [18–22].

The features of the present results:

1. Figs. 1a, 1b show the variation of the conductance with the induced photon of the frequency range $10^{12} - 10^{14}$ Hz. The range of frequency is in the infra-red range at different values of gate voltage, V_g. Fig. 1a is for the case of the parallel alignment of spin in the two diluted magnetic semiconductor leads, while Fig. 1b for antiparallel case. As shown from these figures that an oscillatory behavior of the conductance with the frequency for the two cases. It must be noted the peak height of the conductance (for the two cases) increases as the frequency of the induced photons. Also, the trend of the dependence is a Lorentzian shape for each range of frequencies. These results are due to photon-spin-up and spin-down subbands coupling. This coupling will be enhanced as the frequency of the induced photon increases.
2. Fig. 2a shows the variation of the giant magnetoresistance, GMR, with the frequency of the induced photon at different values of gate voltage, V_g. As shown from the figure, random oscillations of GMR with random peak heights. GMR attains a maximum value ∼ 30%

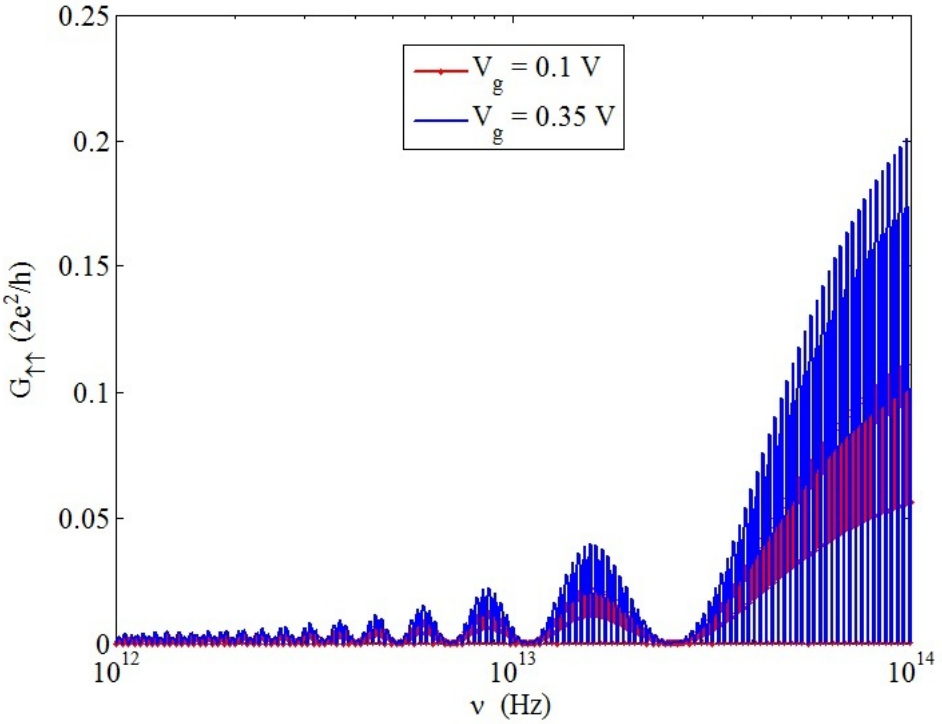

(a)

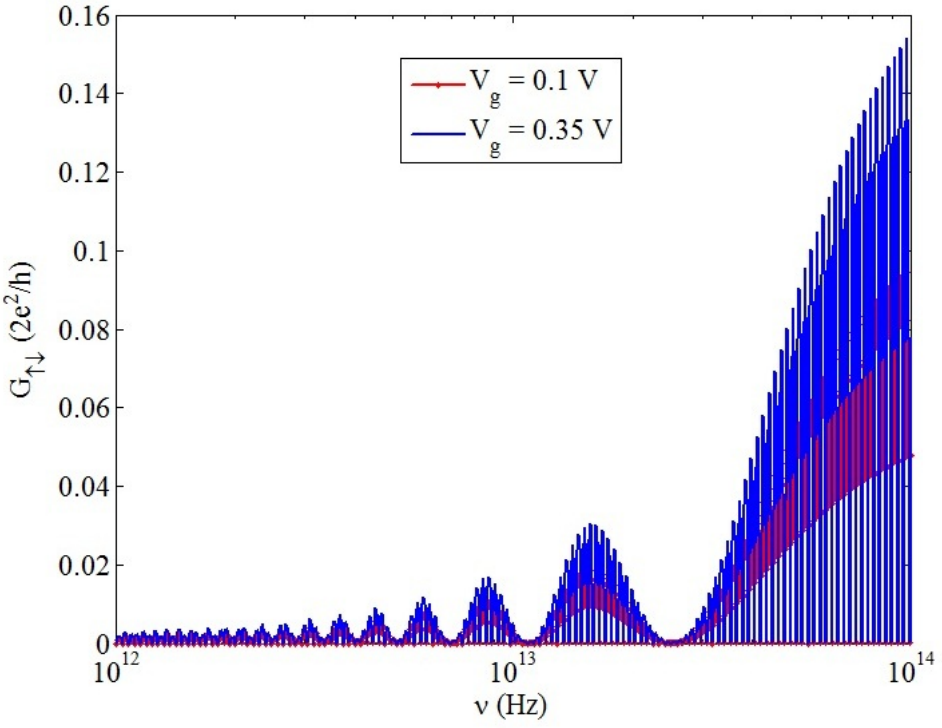

(b)

Fig. 1: The variation of conductance with frequency at two different gate voltages for (a) parallel spin alignment and (b) antiparallel spin alignment.

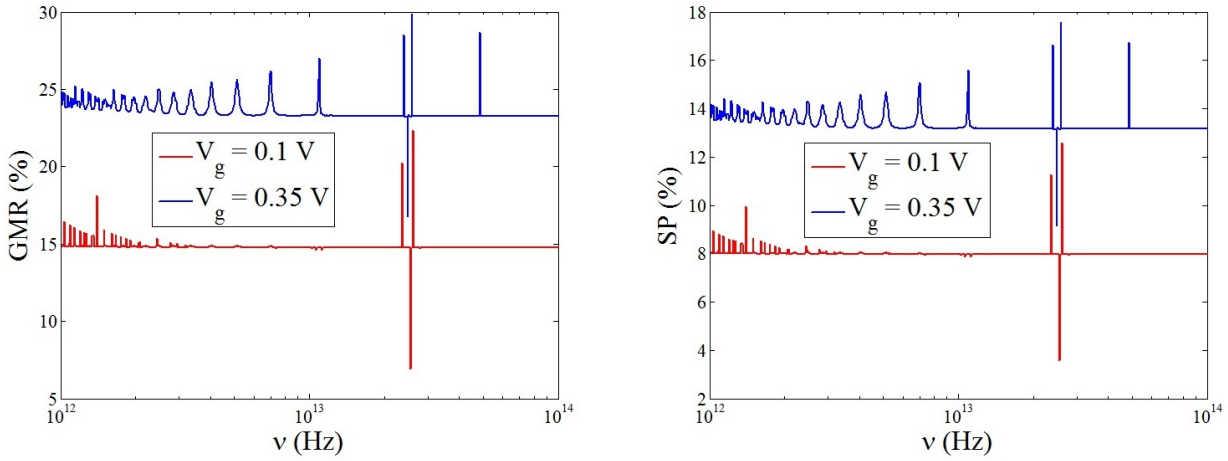

(a) (b)

Fig. 2: The variation of (a) GMR and (b) SP with frequency at two different gate voltages.

at $\nu = 2.585\times10^{13}$ Hz ($V_g = 0.35$ V) and GMR attains a maximum value ~ 22% at $\nu = 2.615\times 10^{13}$ Hz ($V_g = 0.1$ V).

3. Fig. 2b shows the variation of the spin polarization, SP, with the frequency of the induced photon at different values of gate voltage, V_g. As shown from the figure, random oscillations of spin polarization with random peak heights. SP attains a maximum value ~ 17.6% at $\nu = 2.585\times10^{13}$ Hz ($V_g = 0.35$ V), and also SP attains a maximum value ~ 12.6% at $\nu = 2.615\times10^{13}$ Hz ($V_g = 0.1$ V).

These random oscillations for both GMR & SP might be due to spin precession and spin flip of quasiparticles which are influenced strongly as the coupling between the photon energy and spin-up & spin-down subbands in quantum dot.

Also, these results show that the position and line shape of the resonance are very sensitive to the spin relaxation rate of the tunneled quasiparticles [23,24] through the whole junction.

In general, the oscillatory behavior of the investigated physical quantities might be due to Fano-resonance as the spin transport is performed from continuum states of dilute magnetic semiconductor leads to the discrete states of non-magnetic semiconducting quantum dots [14, 25].

So, our analysis of the spin polarization and giant magnetoresistance can be potentially useful to achieve a coherent spintronic device by optimally adjusting the material parameters. The present research is practically very useful in digital storage and magneto-optic sensor technology.

Submitted on November 18, 2011 / Accepted on November 26, 2011

References

1. Fabian J., Matos-Abiaguea A., Ertlea C., Stano P., Zutic I. Semiconductor spintronics. *Acta Physica Slovaca*, 2007, v. 57, 565.
2. Awschalom D. D., and Flatte M. E. Challenges for semiconductor spintronics. *Nature Physics*, 2007, v. 3, 153.
3. Beletskii N. N., Bermann G. P., Borysenko S. A. Controlling the spin polarization of the electron current in semimagnetic resonant-tunneling diode. *Physical Review B*, 2005, v. 71, 125325.
4. Ertler C. Magnetoelectric bistabilities in ferromagnetic resonant tunneling structures. *Applied Physics Letters*, 2008, v. 93, 142104.
5. Ohya S., Hai P. N., Mizuno Y., Tanaka M. Quantum size effect and tunneling magnetoresistance in ferromagnetic semiconductor quantum heterostructures. *Physical Review B*, 2007, v. 75, 155328.
6. Petukhov A. G., Demchenko D. O., Chantis A. N. Electron spin polarization in resonant interband tunneling devices. *Physical Review B*, 2003, v. 68, 125332.
7. Ohno H. Making nonmagnetic semiconductor magnetic. *Science*, 1998, v. 281, 951.
8. Zutic I., Fabian J., Das Sarma S. Spintronics: Fundamentals and Applications. *Reviews of Modern Physics*, 2004, v. 76, 323.
9. Bejar M., Sanchez D., Platero G., McDonald A. H. Spin-polarized current oscillations in diluted magnetic semiconductor multiple quantum wells. *Physical Review B*, 2003, v. 67, 045324.
10. Guo Y., Han L., Zhu R., Xu W. Spin-dependentshot noise in diluted magnetic semiconductor / semiconductor hetero-structures. *European Physical Journal B*, 2008, v. 62, 45.
11. Amin A. F., Li G. Q., Phillips A. H., Kleinekathofer U. Coherent control of the spin current through a quantum dot. *European Physical Journal B*, 2009, v. 68, 103.
12. Zein W. A., Ibrahim N. A., Phillips A. H. Spin-dependent transport through Aharanov-Casher ring irradiated by an electromagnetic field. *Progress in Physics*, 2010, v. 4, 78.
13. Zein W. A., Ibrahim N. A., Phillips A. H. Noise and Fano factor control in AC-driven Aharonov-Casher ring. *Progress in Physics*, 2011, v. 1, 65.
14. Zein W. A., Ibrahim N. A., Phillips A. H. Spin polarized transport in an AC-driven quantum curved nanowire. *Physics Research International*, 2011, article ID-505091, 5 pages, doi: 10.1155/2011/505091.
15. Manasreh O. Semiconductor heterojunctions and nanostructures. McGraw-Hill, 2005.
16. Abramowitz M., Stegun I. A. Handbook of mathematical functions, Dover-New York, 1965.

17. Heinzel T. Mesoscopic electronics in solid state nanostructures. Wiley-VCH Verlag Weinheim, 2003.

18. Spin-dependent Transport in magnetic nanostructures. Editors: Maekawa S., Shinjo T. CRC-Press LLC, 2002.

19. Aly A. H., Phillips A. H. Quantum transport in a superconductor-semiconductor mesoscopic system. *Physica Status Solidi B*, 2002, v. 232, no. 2, 283.

20. Aly A. H., Hang J., Phillips A. H. Study of the anomaly phenomena for the hybrid superconductor-semiconductor junctions. *International Journal of Modern Physics B*, 2006, v. 20, no. 16, 2305.

21. Phillips A. H., Mina A. N., Sobhy M. S.,Fouad E. A. Responsivity of quantum dot photodetector at terahertz detection frequencies. *Journal of Computational and Theoretical Nanoscience*, 2007, v. 4, 174.

22. Sanvito S., Theurich G., Hill N. A. Density functional calculations for III-V dilutedferro-magnetic semiconductors: A Review. *Journal of Superconductivity: Incorporating Novel Magnetism*, 2002, v. 15, no. 1, 85.

23. Singley E. J., Burch K. S., Kawakami R., Stephens J., Awschalom D. D., Basov D. N. Electronic structure and carrier dynamics of the ferromagnetic semiconductor Ga1-xMnxAs. *Physical Review B*, 2003, v. 68, 165204.

24. Kyrychenko F. V., Ullrich C. A. Response properties of III-V dilute magnetic semiconductors including disorder, dynamical electron-electron interactions and band structure effects. *Physical Review B*, 2011, v. 83, 205206.

25. Microshnichenko A. E., Flach S., Kivshar Y. S. Fano resonances in nanoscale structures. *Reviews of Modern Physics*, 2010, v. 82, 2257.

The Upper Limit of the Periodic Table of Elements Points out to the "Long" Version of the Table, Instead of the "Short" One

Albert Khazan

E-mail: albkhazan@gmail.com

Herein we present an analysis of the internal constitution of the "short" and "long" forms of the Periodic Table of Elements. As a result, we conclude that the second (long) version is more correct. We also suggest a long version of the Table consisting of 8 periods and 18 groups, with the last (heaviest) element being element No. 155, which closes the Table.

1 Introduction

Many research papers have been written about the discovery of the Periodic Law of Elements. Many spectacular versions of this law have likewise been suggested. However the main representation of this law is still now a two-dimensional table consisting of cells (each single cell manifests a single element). The cells are joined into periods along the horizontal axis (each row represents a single period), while the cells are joined into groups along the vertical axis (each column represents a single group). The resulting system is represented in three different forms: the "short version" (short-period version); the "long version" (long-period version); and the "super-long version" (extended version), wherein each single period occupies a whole row.

Our task in this paper is the consideration of the first two versions of the Periodic System.

There are hundreds of papers discussing the different versions of the Periodic Table, most of whom have been suggested by Mark R. Leach [1].

To avoid any form of misunderstanding of the terminology, we should keep in mind that, in each individual case, the Periodic Law sets up the fundamental dependence between the numerical value of the atomic nucleus and the properties of the element, while the Periodic System shows how we should use this law in particular conditions. The Periodic Table is a graphical manifestation of this system.

On March 1, 1869, Dmitri Mendeleev suggested the first "long" version of his Table of Elements. Later, in December of 1970, he published another, "short" version of the Table. His theory was based on atomic masses of the elements. Therefore, he formulated the Periodic Law as follows:

"*Properties of plain bodies, and also forms and properties of compounds of the elements, have a periodic dependence on the numerical values of the atomic masses of the elements*".

After the internal constitution of each individual atom had been discovered, this formulation was changed to:

"*Properties of plain substances, and also forms and properties of compounds of the elements, have a periodic dependence from the numerical value of the electric charge of the respective nucleus*".

All elements in the Periodic Table have been numbered, beginning with number one. These are the so-called atomic numbers. Further, we will use our data about the upper limit of the Periodic Table [2–4], when continuing both the short and long versions of the Table upto their natural end, which is manifested by element No. 155.

2 The short version of the Periodic Table

2.1 The Periods

The Periodic System of Elements is presented with the Periodic Table (see Table 1), wherein the horizontal rows are known as Periods. The first three Periods are referred to as "short ones", while the last five — "long ones". The elements are distributed in the Periods as follows: Period 1 — by 2 elements, Periods 2 and 3 — by 8 elements in each, Periods 4 and 5 — by 18 elements in each, Periods 6 and 7 — by 32 elements in each, Period 8 — by 37 elements. Herein we mean that Period 7 is full upto its end, while Period 8 has been introduced according to our calculation. Each single Period (except for Hydrogen) starts with an alkaline metal and then ends with a noble gas. In Periods 6 and 7, within the numbers 58–71 and 90–103, families of Lanthanoids and Actinides are located, respectively. They are placed on the bottom of the Table, and are marked by stars. Chemical properties of Lanthanides are similar to each other: for instance, they all are "reaction-possible" metals — they react with water, while producing Hydroxide and Hydrogen. Proceeding from this fact we conclude that Lanthanides have a very manifested horizontal analogy in the Table. Actinides, in their compounds, manifest more different orders of oxidation. For instance, Actinium has the oxidation order +3, while Uranium — only +3, +4, +5, and +6. Experimentally studying chemical properties of Actinides is a very complicate task due to very high instability of their nuclei. Elements of the same Period have very close numerical values of their atomic masses, but different physical and chemical properties. With these, and depending on the length of the particular Period — each small one consists of one row, while each long one consists of two rows (the upper even row, and the lower odd row), — the rate of change of the properties is smoother and slower

in the second case. In the even rows of the long Periods (the rows 4, 6, 8, and 10 of the Table), only metals are located. In the odd rows of the long Periods (these are the rows 5, 7, and 9), properties of the elements change from left to right in the same row as well as those of the typical elements of the Table.

The main sign according to which the elements of the long Periods are split into two rows is their oxidation order: the same numerical values of it are repeated in the same Period with increase of atomic mass of the elements. For instance, in Period 4, the oxidation order of the elements from K to Mn changes from +1 to +7, then a triad of Fe, Co, Ni follows (they are elements of an odd row), after whom the same increase of the oxidation order is observed in the elements from Cu to Br (these are elements of an odd row). Such distribution of the elements is also repeated in the other long Periods. Forms of compounds of the elements are twice repeated in them as well. As is known, the number of each single Period of the Table is determined by the number of electronic shells (energetic levels) of the elements. The energetic levels are then split into sub-levels, which differ from each one by the coupling energy with the nucleus. According to the modern reference data, the number of the sub-levels is n, but not bigger than 4. However, if taking Seaborg's suggestion about two additional Periods of 50 elements in each into account, then the ultimate high number of the electrons at an energetic level, according to the formula $N = 2n^2$, should be 50 (under $n = 5$). Hence, the quantum mechanical calculations require correction.

2.2 The Groups

The Periodic Table of Elements contains 8 Groups of the elements. The Groups are numbered by Roman numbers. They are located along the vertical axis of the Table. Number of each single Group is connected with the oxidation order of the elements consisting it (the oxidation number is manifested in the compounds of the elements). As a rule, the positive highest oxidation order of the elements is equal to the number of that Group which covers them. An exception is Fluorine: its oxidation number is -1. Of the elements of Group VIII, the oxidation order +8 is only known for Osmium, Ruthenium, and Xenon. Number of each single Group depends on the number of the valence electrons in the external shell of the atom. However it is equally possible to Hydrogen, due to the possibility of its atom to loose or catch the electron, to be equally located in Group I or Group VII. Rest elements in their Groups are split into the *main* and *auxiliary* sub-groups. Groups I, II, II include the elements of the left side of all Periods, while Groups V, VI, VII — the elements located in the right side. The elements which occupy the middle side of the long Periods are known as the transferring elements. They have properties which differ from the properties of the elements of the short Periods. They are considered, separately, as Groups IVa, Va, VIa, VIII, which include by three elements of each respective long Period Ib, IIb, IIIb, IVb. The main sub-groups consist of the typical elements (the elements of Periods 2 and 3) and those elements of the long Periods which are similar to them according to their chemical properties. The auxiliary sub-groups consist of only metals — the elements f the long Periods. Group VIII differs from the others. Aside for the main sub-group of Helium (noble gases), it contains three shell sub-groups of Fe, Co, and Ni. Chemical properties of the elements of the main and auxilary subgroups differ very much. For instance, in Group VII, the main sub-group consists of non-metals F, Cl, Br, I, At, while the auxiliary subgroup consists of metals Mn, Tc, Re. Thus, the sub-groups join most similar elements of the Table altogether. Properties of the elements in the sub-groups change, respectively: from up to down, the metalic properties strengthen, while the non-metalic properties become weak. It is obvious that the metalic properties are most expressed on Fr then on Cs, while the non-metalic properties are most expressed on F then on O [5].

2.3 Electron configuration of the atoms, and the Periodic Table

The periodic change of the properties of the elements by increase of the ordinal number is explained as the periodic change of their atoms' structure, namely by a number of electrons at their outer energetic levels. Elements are divided into *seven periods* (*eight according to our dates*) in accordance with energetic levels in electron shells. The electron shell of Period 1 contains one energetic level, Period 2 contains two energetic levels, Period 3 — three, Period 4 — 4, and so on. Every Period of the Periodic System of Elements begins with elements whose atoms, each, have one electron at the outer level, and ends with elements whose atoms, each, have at the outer shell 2 (for Period 1) or 8 electrons (for all subsequent Periods). Outer shells of elements (Li, Na, Ka, Rb, Cs); (Be, Mg, Ca, Sr); (F, Cl, Br, I); (He, Ne, Ar, Kr, Xe) have a similar structure. The number of the *main sub-Groups* is determined by the maximal number of elements at the energetic level which equals 8. The number of common elements (elements of auxiliary sub-Groups) is determined by maximal electrons at d-sub-level, and it equals 10 for every large Period (see Table 2).

As far as one of auxiliary sub-Groups of the Periodic Table of Elements contains at once three common elements with similar chemical properties (so called triads Fe-Co-Ni, Ru-Rh-Pd, Os-Ir-Pt), then the number, as of common sub-Groups as main ones, equals 8. The number of Lanthanoids and Actinides placed at the foot of the Periodic Table as independent rows equals the maximum number of electrons at the f-Sublevel in analogy with common elements, i.e. it equals 14.

A Period begins with an element the atom of which contains one s-electron at the outer level: this is hydrogen in Pe-

Group → Period ↓	**1**	**2**	**3**	**4**	**5**	**6**	**7**	**8**	**9**	**10**	**11**	**12**	**13**	**14**	**15**	**16**	**17**	**18**
1	1 H																	2 He
2	3 Li	4 Be											5 B	6 C	7 N	8 O	9 F	10 Ne
3	11 Na	12 Mg											13 Al	14 Si	15 P	16 S	17 Cl	18 Ar
4	19 K	20 Ca	21 Sc	22 Ti	23 V	24 Cr	25 Mn	26 Fe	27 Co	28 Ni	29 Cu	30 Zn	31 Ga	32 Ge	33 As	34 Se	35 Br	36 Kr
5	37 Rb	38 Sr	39 Y	40 Zr	41 Nb	42 Mo	43 Tc	44 Ru	45 Rh	46 Pd	47 Ag	48 Cd	49 In	50 Sn	51 Sb	52 Te	53 I	54 Xe
6	55 Cs	56 Ba	*	72 Hf	73 Ta	74 W	75 Re	76 Os	77 Ir	78 Pt	79 Au	80 Hg	81 Tl	82 Pb	83 Bi	84 Po	85 At	86 Rn
7	87 Fr	88 Ra	**	104 Rf	105 Db	106 Sg	107 Bh	108 Hs	109 Mt	110 Ds	111 Rg	112 Cn	113 Uut	114 Uuq	115 Uup	116 Uuh	117 Uus	118 Uuo
8	119 Uue	120 Ubn	***															
	155																	
Lanthanides *				57 La	58 Ce	59 Pr	60 Nd	61 Pm	62 Sm	63 Eu	64 Gd	65 Tb	66 Dy	67 Ho	68 Er	69 Tm	70 Yb	71 Lu
Actinides **				89 Ac	90 Th	91 Pa	92 U	93 Np	94 Pu	95 Am	96 Cm	97 Bk	98 Cf	99 Es	100 Fm	101 Md	102 No	103 Lr
g-elements ***				121 Ubu	122 Ubb	123 Ubt	124 Ubq											
f-elements				125	126	127	128	129	130	131	132	133	134	135	136	137	138	139
Ubb-series				140	141	142	143	144	145	146	147	148	149	150	151	152	153	154

Table 1: The standard (long) version of the Periodic Table of Elements.

Period	Row	a I b						aVIIb	a VIII b		
1	1	H 1	a II b	a III b	a IV b	a V b	a VI b	(H)	He 2		
2	2	Li 3	Be 4	B 5	C 6	N 7	O 8	F 9	Ne 10		
3	3	Na 11	Mg 12	Al 13	Si 14	P 15	S 16	Cl 17	Ar 18		
4	4	K 19	Ca 20	Sc 21	Ti 22	V 23	Cr 24	Mn 25	Fe 26	Co 27	Ni 28
	5	Cu 29	Zn 30	Ga 31	Ge 32	As 33	Se 34	Br 35	Kr 36		
5	6	Rb 37	Sr 38	Y 39	Zr 40	Nb 41	Mo 42	Tc 43	Ru 44	Rh 45	Pd 46
	7	Ag 47	Cd 48	In 49	Sn 50	Sb 51	Te 52	I 53	Xe 54		
6	8	Cs 55	Ba 56	La* 57	Hf 72	Ta 73	W 74	Re 75	Os 76	Ir 77	Pt 78
	9	Au 79	Hg 80	Tl 81	Pb 82	Bi 83	Po 84	At 85	Rn 86		
7	10	Fr 87	Ra 88	Ac† 89	Rf 104	Db 105	Sg 106	Bh 107	Hs 108	Mt 109	Ds 110
	11	Rg 111	Uub 112	Uut 113	Uuq 114	Uup 115	Uuh 116	Uus 117	Uuo 118		

Lanthanides (the upper row) and Actinides (the lower row)

Ce 58	Pr 59	Nd 60	Pm 61	Sm 62	Eu 63	Gd 64	Tb 65	Dy 66	Ho 67	Er 68	Tm 69	Yb 70	Lu 71
Th 90	Pa 91	U 92	Np 93	Pu 94	Am 95	Cm 96	Bk 97	Cf 98	Es 99	Fm 100	Md 101	No 102	Lr 103

Period 8

8	12	119 Uue	120 Ubn	121 Ubu	122 Ubb	123 Ubt	124 Ubq	125 Ubp	126 Ubh	127 Ubs	128 Ubo
	13	129 Ube	130 Utn	131 Utu	132 Utb	133 Utt	134 Utq	135 Utp	136 Uth		
	14	137 Uts	138 Uto	139 Ute	140 Uqn	141 Uqu	142 Uqb	143 Uqt	144 Uqq	145 Uqp	146 Uqh
	15	147 Uqs	148 Uqo	149 Uqe	150 Upn	151 Upu	152 Upb	153 Upt	154 Upq		
	16	**155**									

121-124—g-elements
125-138---f-elements
155-Upp (Unpentpentium)—Last element

Table 2: The suggested (short) version of the Periodic Table of Elements, up to No. 155.

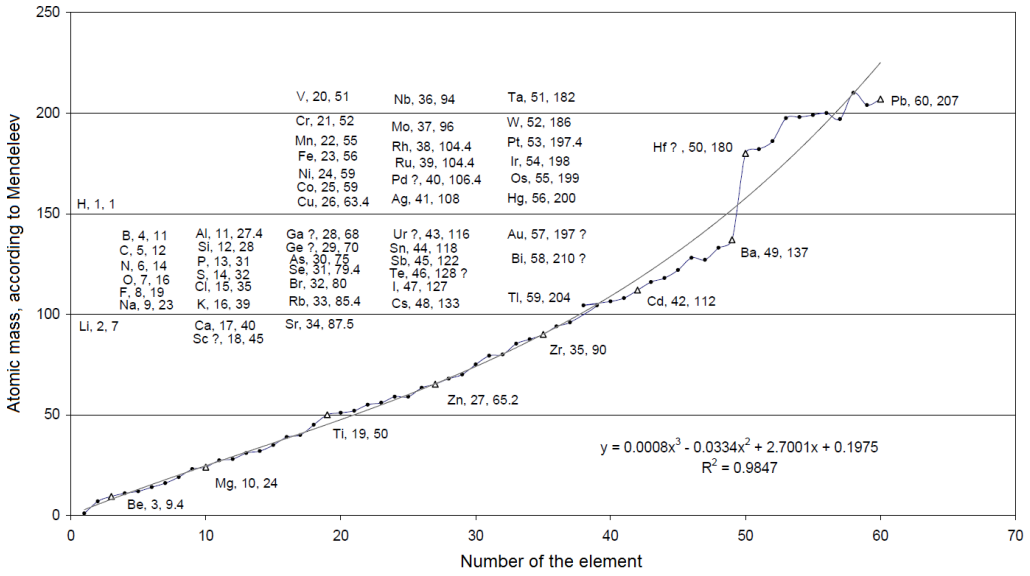

Fig. 1: Experience of the System of the Elements, based on their atomic mass (the table, according to Mendeleev). Dependence of the atomic mass from the number of the elements (the graphs, according to the suggested formulation). The triangles mean the beginning of each Period.

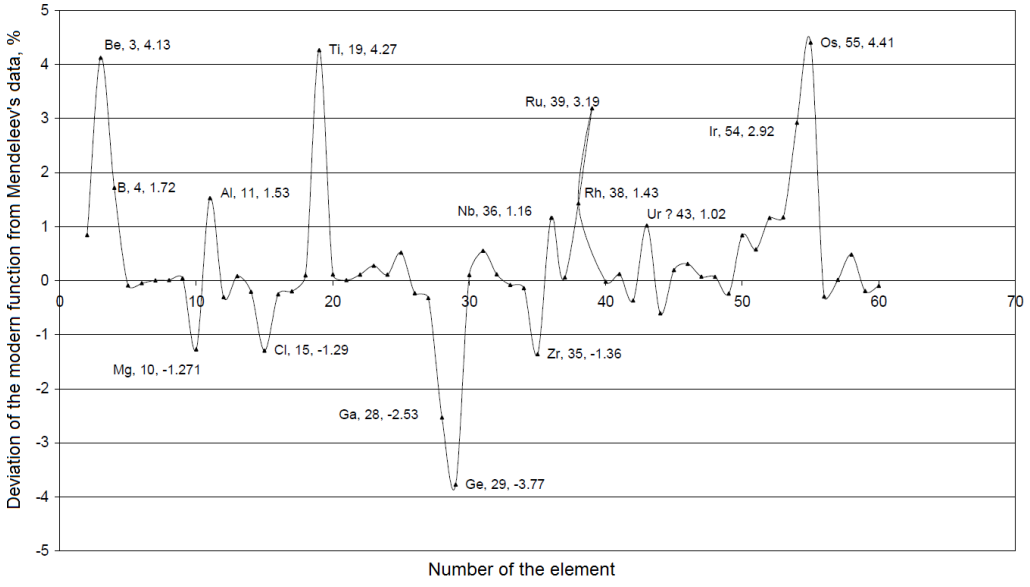

Fig. 2: Deviation of the modern (suggested) dependence of the atomic mass from the number of the elements from Mendeleev's data.

riod 1, and alkaline metals in the others. A Period ends with precious gas: helium ($1s^2$) in Period 1.

Detailed studies of the structure of an atom are not the aim of our paper, therefore we draw common conclusions concerning the corresponding locations of **elements in blocks**:

1. **s-elements**: electrons fill s-sub-shells of the outer level; two first elements of every Period are related to them;
2. **p-elements**: electrons fill p-sub-shells of the outer level; six last elements of every Period are related to them;
3. **d-elements**: electrons fill s-sub-shells of the outer level; they are elements of inserted decades of big Periods placed between s- and p-elements (they are called also common elements);
4. **f-elements**: electrons fill f-sub-shells; they are Lanthanoids and Actinides.

3 Drawbacks of the short version and advantages of the long version of the Periodic Table

The "short" form of the Table was cancelled officially by IUPAC in 1989. But it is still used in Russian information and educational literature, must probably, according to a tradition. But it follows by detailed consideration that it contains some moot points.

In particular, Group VIII contains in the common Group, together with precious gases (the main sub-Group), triads of elements, which have precisely expressed the properties of metals. The contradiction here is that the triad Fe, Co, Ni is near families of platinum metals although their properties differ from the properties of Groups of iron. Group I contains alkaline metals having very strong chemical activity, but simultaneously the sub-Group "b" contains copper, silver and gold which have not these properties but possess excellent electric conductivity. Besides gold, silver and platinum, metals have very weak chemical activity.

Group VII, where nearby halogens such metals as manganese, technezium and renium are placed, is also incorrect, because in the same Group two sub-Groups of elements possessing absolutely different properties are collected.

The "short" Table is sufficiently informative but it is difficult in terms of use due to the presence of the "long" and the "short" Groups, i.e. the small and big Periods divided by even and odd lines. It is very difficult to place f-elements inside eight Groups.

The "long" form of the Table consisting of 18 Groups was confirmed by IUPAC in 1989. Defect characteristics of the "short" Table were removed here: the sub-Groups are excepted, Periods consist of one stitch, elements are composed of blocks, the families of iron and platinum metals have disappeared, and so on.

The known Periodic Table consisting of 118 elements and 7 Periods where our dates for Period 8 are added must contain: 17 s-elements, 42 p-elements, 50 d-elements, 42 f-elements, and 4 g-elements.

The number 17 for s-elements follows from the fact that two of them are in Group I and Group II of Period 8, while element No. 155 (the last s-element, 17-th) is in Period 9 and Group I (the sole) closes the Table.

The extended Table consisting of blocks containing the number of elements calculated by us is published in [4].

3.1 From the Periodic Law to the Hyperbolic Law and the upper limit of the Periodic System

A note by Mendeleev, in March of 1869, was published and sent in Russian and French to scientists, titled "Experience of Systems of Elements Founded on Their Atomic Weights and Chemical Similarity" (with "atomic weight" to be understood as "atomic mass" here and in the future). This date is considered as the discovery date of the periodic law of chemical elements. The author dedicated the next two years to the work in this direction, which was a correction of atomic masses, an elaboration of studies about the periodical properties of elements, about the rôle of Groups, of big and small Periods, as well as about the places of chemical combinations in the Table. As a result, "Mendeleev's Natural System of Elements" which was the first periodic table of chemical elements was published in the first edition of his book "The Foundations of Chemistry", in 1871.

It is necessary to note that the dates published in the table of "Experience of Systems of Elements Founded on Their Atomic Weights and Chemical Similarity" permits us to use them in order to prove the correctness of Mendeleev's work.

The comprehensive table based the book "Experience of System of Element Found on Their Atomic Weight and Chemical Similarity", in terms of the dependence of each atomic mass on the number of the corresponding element, has been built by us and showed on Fig. 1. Because then it was not known yet that the ordinal number of each element characterizes its charge, it was simply the case that an element possessing a minimal mass was allowed to be designed as No. 1, and this order is conserved in the future: the next, in terms of mass, element will be designated as No. 2, the third as No. 3, and so on. Thus the ordinal number, which was attributed to the element after the theory of the atom was constructed has here another numerical value — symbolizing order of priority. The Table on Fig. 1 is the same as the one composed by Mendeleev, and the elements and the numbers are placed as the points on the arc where the triangles designate the beginning of the Periods. As is clear, the arc goes smoothly, preceding the elements and the atomic mass ~100, and after that it deviates preceding Ba. The trend line equation can be easily described by the multinomial of the third degree, i.e. by $R^2 = 0.9847$, in spite of a strong jump in the region of Lantanides. It should be noted that the part of the arc preceding Ba has $R^2 = 0.999$. It means that the direction

of the trend line after Ba reflects correctly the further course of our dependence, which allows us to calculate easily the atomic weights of other elements.

It should be noted that the trend line of the curve constructed according to contemporary dates has $R^2 = 0.9868$. In order that compare the dependence of the atomic mass from the ordinal number according to contemporary dates and the dates of Mendeleev the graph of was constructed (see Fig. 2). As is clear, the maximal deviations (3–4%) are observed for 6 cases, (1–1.5%) — for 8 cases, the others are placed lower. Because the common number of elements is 60, this spread is negligible for the those time.

As follows from the indicated dates, Mendeleev showed by means of his works concerning the Periodic Law that it is true for 60–70 elements, opening the way for the extension of the Table up to No. 118.

But our studies of the Periodic Table distinctly show that a hyperbolic law takes place in it. The law determines the upper limit of the Table through element No. 155. This fact is indisputable and it is justified by numerous publications.

4 Conclusion

If it was allowed in the 1950s that a maximum value of an ordinal number in Periodic Table could not exceed the value $Z = 110$ due to a spontaneous division of the nucleus, then in the 1960s theoreticians proposed the hypothesis that the atomic nucleus could have anomalously high stability. Seaborg called these regions "islands of stability" in a "sea of instability". He hoped for a possible synthesis of superelements inside these regions, **"... but until [now] the problem of the upper bound of the Periodic System [remains] unsolved"** (and so: at that time)!

Since in order to solve any problem it is necessary to know a final goal and to define its bounds, we have realized experimental studies and constructed a mathematical apparatus for the determination of the upper bound of the Periodic Table. According to our calculations, the last element is estimated and its location is determined: Period 9, Group I, with atomic mass of 411.66 (approximately), for which $Z = 155$. The earlier-proposed extended tables by Seaborg for 168 and 216 elements simply cannot be realized, because **only 155 elements can be in the Table, in its entirety**.

Submitted on June 23, 2011 / Accepted on June 30, 2011
After re-submission, December 09, 2011

References

1. http://www.meta-synthesis.com/webbook/35_pt/pt_database.php
2. Khazan A. Upper limit in the Periodic Table of Elements. *Progress in Physics*, 2007, v. 1, 38–41.
3. Khazan A. Upper Limit in Mendeleev's Table — Element No. 155. 2nd edition, Svenska fysikarkivet, Stockholm, 2010.
4. Khazan A. Isotopes and the Electron Configuration of the Blocks in the Periodic Table of Elements, upto the Last Element No. 155. *Progress in Physics*, 2011, v. 2, 55–57.
5. Pauling L. General Chemistry. 3rd edition, W. H. Freeman & Co., San Francisco, 1970, p. 843.

Kepler-16 Circumbinary System Validates Quantum Celestial Mechanics

Franklin Potter* and Howard G. Preston†

*Sciencegems.com, 8642 Marvale Drive, Huntington Beach, CA 92646, USA. E-mail: frank11hb@yahoo.com
†15 Vista del Sol, Laguna Beach, CA 92651, USA.

We report the application of quantum celestial mechanics (QCM) to the Kepler-16 circumbinary system which has a single planet orbiting binary stars with the important system parameters known to within one percent. Other gravitationally bound systems such as the Solar System of planets and the Jovian satellite systems have large uncertainties in their total angular momentum. Therefore, Kepler-16 allows us for the first time to determine whether the QCM predicted angular momentum *per mass* quantization is valid.

1 Introduction

We report a precision test of quantum celestial mechanics (QCM) in the Kepler-16 circumbinary system that has planet-b orbiting its two central stars at a distance of 0.70 AU from the barycenter. QCM, proposed in 2003 by H.G. Preston and F. Potter [1] as an extension of Einstein's general theory of relativity, predicts angular momentum *per mass* quantization states for bodies orbiting a central mass in all gravitationally bound systems with the defining equation in the Schwarzschild metric being

$$\frac{L}{\mu} = m\frac{L_T}{M_T}. \qquad (1)$$

Here μ is the mass of the orbiting body with orbital angular momentum L and M_T is the total mass of the bound system with total angular momentum L_T. We calculate that the quantization integer m = 10, an amazing result with about a 1% uncertainty. Note that in all systems tested, we assume that the orbiting bodies have been in stable orbits for at least a 100 million years.

Kepler-16 is the first solar system type for which the total mass and the total angular momentum are *both* known accurately enough to allow a test of the angular momentum per mass quantization condition to within a few percent. The advantage this system has over all others is that the binary stars in revolution at its center contribute more than 99.5% of the system's total angular momentum. Moreover, more orbiting bodies may be detected in the future to provide the acid test of the theory because our precision result should improve.

2 Brief Review

Contrary to popular statements in the literature about planetary orbital angular momentum, the angular momentum of the Oort Cloud dominates the total angular momentum of the Solar System, being about 60 times the angular momentum of the orbiting planets, but its value has high uncertainty. The Jovian planets have differential internal rotations which bring their angular momentum uncertainties to more than 10% also. The Earth-Moon and Pluto-Charon systems have known values and a fit can be made to m = 65 and m = 9, respectively, but the application of the Schwarzschild metric is questionable in systems for which a reduced mass must be used. In addition, there is not another orbiting body for prediction purposes.

The Mars-Phobos-Deimos system offers a test of the angular momentum condition. We find that m = 61 for Phobos and m = 97 for Deimos, with uncertainties less than about 4%. The Schwarzschild metric is a good approximation here but the integers are very large and therefore somewhat unsatisfactory for a definitive test. We would prefer to find a system for which the m values that fit are small integers, if possible.

We have applied the equation to many multiplanet exosystems and found that the fits all predict additional undetected angular momentum. Such solar systems can be expected to have an additional planet and/or the equivalent of an Oort Cloud that contributes significant orbital angular momentum. Examples include: Kepler-18, HR 8799, HIP 57274, Gliese 581, 55Cnc, Kepler-11, PSR 1257, HD 10180, HD 125612, HD 69830, 47 Uma, and 61 Vir.

Other confirmed circumbinary systems with one or two known planets are either dominated by the planetary angular momentum or the planets contribute about 50%, rendering their fits unsuitable for a precision test: HW Virginis, NNSerpentis, and DP Leonis.

Our original article [1] contains the derivation of QCM from the general relativistic Hamilton-Jacobi equation and its new gravitational wave equation for any metric. Our first application, to the Solar System without knowledge of the Oort Cloud angular momentum, predicted that all the planetary orbits should be within the Sun's radius! Subsequently, we learned about the Oort Cloud and were able to produce two excellent QCM linear regression fits with $R^2 > 0.999$ for m sets (1) 2,3,4,5,9,13,19,24,28; (2) 3,4,5,6,11,15,21,26,30. Therefore, we predict a total angular momentum for the Solar System $L_{SS} \approx 1.9 \times 10^{45}$ kg m^2/s with the planets contributing only $L_{pl} = 3.1 \times 10^{43}$ kg m^2/s.

Several follow-up articles verify its application to galaxies without requiring 'dark matter' for gravitational lensing by the galaxy quantization states [2], the quantization state of baryonic mass in clusters of galaxies [3], and how the cosmo-

logical redshift is interpreted as a gravitational redshift that agrees with the accelerated expansion of the Universe [4]. That is, QCM applied to the Universe with the interior metric dictates that every observer at distance r from the source sees the light originating from an effective negative potential $V(r) \approx -kr^2 c^2/[2(1-kr^2)^2]$, meaning the clocks run slower at the distant source.

In the Schwarzschild metric the QCM wave equation reduces to a Schrödinger-like equation that predicts quantization states for the angular momentum per mass and for the energy per mass. There is no Planck's constant per se but instead each system has its unique constant $H = L_T/M_T c$, a characteristic distance for the gravitationally bound system. Important physical quantities can be related to H and the Schwarzschild radius. In the single free particle limit, such as a free electron, the QCM equation reduces to the standard quantum mechanical Schrödinger equation. Note that QCM is not quantum gravity.

3 The Kepler-16 System

We have been waiting about 10 years for a gravitationally bound system for which its total angular momentum per total mass is known to about 1%. Finally, in September, 2011, the Kepler-16 system was reported [5] with two stars, star A and star B, separated by 0.22 AU and a planet called planet-b orbiting their barycenter at 0.70 AU. The list below provides the important physical parameters of this system.

Star A:

Mass = 0.6897 ± 0.0035 solar masses

Orbital radius = 0.05092 ± 0.00027 AU

Period = 41.079220 ± 0.000078 days

Angular momentum = (1.4247 ± 0.0170) x 10^{44} m^2/s

Star B:

Mass = 0.20255 ± 0.00066 solar masses

Orbital radius = 0.17339 ± 0.00115 AU

Period = 41.079220 ± 0.000078 days

Angular momentum = (4.8514 ± 0.0632) x 10^{44} m^2/s

planet-b:

Mass = 0.333 ± 0.0016 Jupiter masses

Orbital radius = 0.7048 ± 0.0011 AU

Period = 228.776 ± 0.037 days

Angular momentum = (2.2479 ± 0.1080) x 10^{42} m^2/s

Kepler-16 system:

L_T/M_T = (3.517± 0.011) x 10^{14} m^2/s

L_b/M_b = (3.555± 0.036) x 10^{15} m^2/s

Note that although the planet mass value has about a 5% uncertainty, this large uncertainty is excluded from the equation because the planet mass divides out in L_b/μ_b. Our result for the QCM angular momentum per mass quantization integer is

$$m = 10.1 \pm 0.1. \quad (2)$$

Therefore, we have determined that planet-b is in the $m = 10$ quantization state with a maximum uncertainty of less than 2%. In Einstein's general theory of relativity and in Newtonian gravitation there is no a priori reason for m to be an integer, so its value could have been anywhere.

4 Comments

As good as this result has been, the acid test for QCM is yet to come. We need to detect at least one more planet in the Kepler-16 system to determine whether the QCM prediction leads to its correct angular momentum value, i.e., an integer multiple of L_T/M_T equal to the classical value at radius r.

Assuming that QCM passes the acid test, we wish to point out that the existence of quantization states of angular momentum per mass and energy per mass are important concepts for the formation of stars, planets, solar systems, galaxies, and clusters of galaxies. Models ignoring QCM will be incomplete and will need speculative inventions such as dark matter and perhaps dark energy to preserve traditional incomplete approaches toward 'understanding' these gravitational systems.

An additional gravitational test of QCM would be a laboratory experiment with a slowly rotating attractor mass producing a repulsive effect to counteract the Newtonian attraction at specific rotation frequencies for the given separation distance to the affected mass. We are in the process of searching for this behavior.

Acknowledgements

One of us (F. P.) thanks physicist Gregory Endo of Endo Engineering for recently suggesting that we apply QCM to a binary star system.

Submitted on December 5, 2011 / Accepted on December 10, 2011

References

1. Preston H. G. and Potter F. Exploring large-scale gravitational quantization without $\hbar$ in planetary systems, galaxies, and the Universe. arXiv: gr-qc/0303112.
2. Potter F. and Preston H. G. Gravitational lensing by galaxy quantization states. arXiv: gr-qc/0405025.
3. Potter F. and Preston H. G. Quantization states of baryonic mass in clusters of galaxies. *Progress in Physics*, 2007, v. 1, 61–63.
4. Potter F. and Preston H. G. Cosmological Redshift interpreted as Gravitational Redshift. *Progress in Physics*, 2007, v. 2, 31–33.
5. Doyle L. R. et al. Kepler-16: A Transiting Circumbinary Planet. arXiv: 1109.3432v1.

Nuclear Structure of $^{122\text{-}134}$Xe Isotopes

Salah A. Eid† and Sohair M. Diab*

†Faculty of Engineering, Phys. Dept., Ain Shams University, Cairo, Egypt
*Faculty of Education, Phys. Dept., Ain Shams University, Cairo, Egypt
E-mail: mppe2@yahoo.co.uk

The potential energy surfaces, $V(\beta,\gamma)$, for a series of Xenon isotopes $^{122-134}$Xe have been calculated. The relatively flat potential to ^{130}Xe and energy ratio $E^+_{4_1}/E^+_{2_1} = 2.2$ show $E(5)$ symmetry to the nucleus which is laying in the transition region from γ-soft to vibrational characters. The interacting boson approximation model ($IBA-1$) has been used in calculating levels energy and electromagnetic transition probabilities $B(E2)'s$. Back bending is observed for $^{122-130}$Xe. The calculated values are compared to the available experimental data and show reasonable agreement.

1 Introduction

The chain of $^{122-134}$Xe isotopes is of great interest because of the existence of transitional nuclei where the nuclear structure changes from rotational to vibrational shapes. Many authors studied this area of isotopes experimentally and theoretically.

Experimentally, the mass of $^{122-134}$Xe isotopes [1] were detected on line using mass separator ISOLDE/CERN while the lifetimes of the low lying states in $^{122-134}$Xe were measured using Doppler-Shift [2] technique.

Theoretically, many authors studied this series of isotopes useing different theoretical models as algebric $sp(4)$ shell model [3], cranked Strutinsky method [4], relativistic mean field theory [5, 6], isospin-dependent lattice gas model [7, 8], general Bohr Hamiltonian [9], quadrupole-quadrupole plus pairing model [10], cranked Hartree-Fock-Bogoliubov model [11, 12] and interacting boson approximation model [13, 17]. They reported:

1. the reduced transition probabilities for Yrast spectra up to $I^+ = 10$;
2. the existance of shape transitions as well as $E(5)$ and $X(5)$ symmetry nuclei,
3. the occurrence of backbending in $^{122-130}$Xe nuclei, and
4. M1 transition probabilities between the mixed-symmetry and fully symmetric states.

2 Interacting Boson Approximation Model

The IBA-1 model [18] was applied to the positive parity low-lying states in even-even $^{122-134}$Xe isotopes. The proton, π, and neutron, ν, bosons are treated as one boson and the system is considered as an interaction between s-bosons and d-bosons. Creation ($s^\dagger d^\dagger$) and annihilation ($s\tilde{d}$) operators are for s and d bosons. The Hamiltonian employed for the present calculation is given as:

$$\begin{aligned} H &= EPS\cdot n_d + PAIR\cdot(P\cdot P)+ \\ &\quad +\tfrac{1}{2}\,ELL\cdot(L\cdot L)+\tfrac{1}{2}\,QQ\cdot(Q\cdot Q)+ \\ &\quad +5\,OCT\cdot(T_3\cdot T_3)+5HEX\cdot(T_4\cdot T_4), \end{aligned} \tag{1}$$

where

$$P\cdot p = \frac{1}{2}\begin{bmatrix} \left\{(s^\dagger s^\dagger)^{(0)}_0 - \sqrt{5}(d^\dagger d^\dagger)^{(0)}_0\right\} x \\ \left\{(ss)^{(0)}_0 - \sqrt{5}(\tilde{d}\tilde{d})^{(0)}_0\right\} \end{bmatrix}^{(0)}_0, \tag{2}$$

$$L\cdot L = -10\sqrt{3}\left[(d^\dagger\tilde{d})^{(1)} x\,(d^\dagger\tilde{d})^{(1)}\right]^{(0)}_0, \tag{3}$$

$$Q\cdot Q = \sqrt{5}\begin{bmatrix} \left\{(S^\dagger\tilde{d}+d^\dagger s)^{(2)} - \dfrac{\sqrt{7}}{2}(d^\dagger\tilde{d})^{(2)}\right\} x \\ \left\{(s^\dagger\tilde{d}+\tilde{d}s)^{(2)} - \dfrac{\sqrt{7}}{2}(d^\dagger\tilde{d})^{(2)}\right\} \end{bmatrix}^{(0)}_0, \tag{4}$$

$$T_3\cdot T_3 = -\sqrt{7}\left[(d^\dagger\tilde{d})^{(2)} x\,(d^\dagger\tilde{d})^{(2)}\right]^{(0)}_0, \tag{5}$$

$$T_4\cdot T_4 = 3\left[(d^\dagger\tilde{d})^{(4)} x\,(d^\dagger\tilde{d})^{(4)}\right]^{(0)}_0. \tag{6}$$

In the previous formulas, n_d is the number of bosons; $P\cdot P$, $L\cdot L$, $Q\cdot Q$, $T_3\cdot T_3$ and $T_4\cdot T_4$ represent pairing, angular momentum, quadrupole, octupole and hexadecupole interactions between the bosons; EPS is the boson energy; and $PAIR$, ELL, QQ, OCT, HEX are the strengths of the pairing, angular momentum, quadrupole, octupole and hexadecupole interactions.

3 Results and discussion

3.1 The potential energy surfaces, (PESs)

The PESs [19], $V(\beta,\gamma)$, for Xenon isotopes as a function of the deformation parameters β and γ have been calculated using :

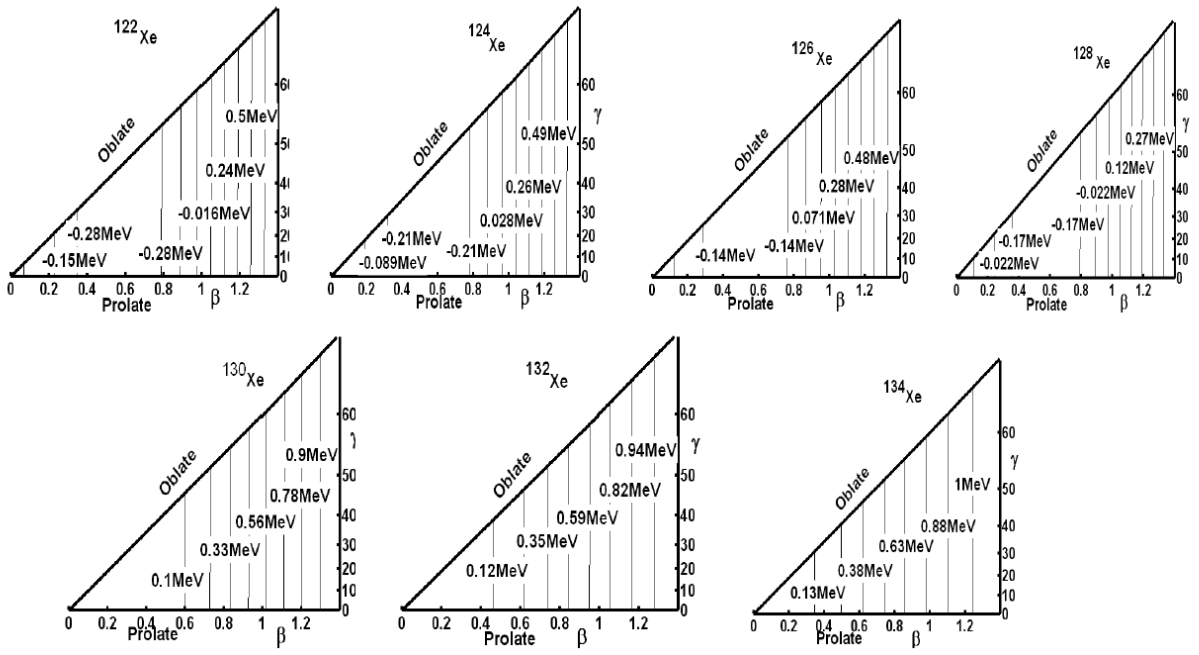

Fig. 1: Contour plot of the potential energy surfaces for $^{122-134}$Xe nuclei.

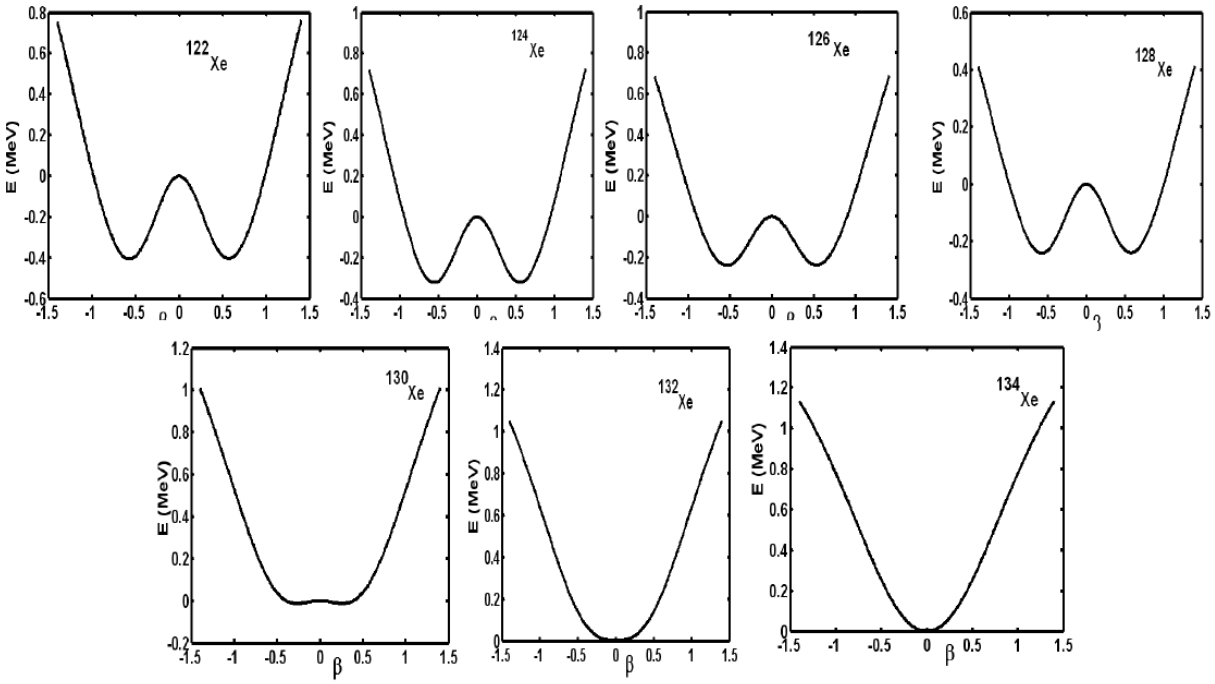

Fig. 2: Potential energy surfaces for $^{122-134}$Xe nuclei at $\gamma = 0^o$ (Prolate) and $\gamma = 60^o$ (Oblate).

nucleus	*EPS*	*PAIR*	*ELL*	*QQ*	*OCT*	*HEX*	$E2SD(eb)$	$E2DD(eb)$
^{122}Xe	0.4700	0.0000	0.0216	−0.0200	0.0000	0.00000	0.1390	−0.4112
^{124}Xe	0.4680	0.0000	0.0216	−0.0200	0.0000	0.0000	0.1280	−0.3786
^{126}Xe	0.4490	0.0000	0.0216	−0.0200	0.0000	0.0000	0.1260	−0.3727
^{128}Xe	0.4720	0.0000	0.0216	−0.0200	0.0000	0.0000	0.1410	−0.4171
^{130}Xe	0.5420	0.0000	0.0216	−0.0200	0.0000	0.0000	0.1500	−0.4437
^{132}Xe	0.6450	0.0000	0.0216	−0.0200	0.0000	0.0000	0.1460	−0.4319
^{134}Xe	0.8020	0.0000	0.0216	−0.0200	0.0000	0.0000	0.1480	−0.4378

Table 1: Parameters used in IBA-1 Hamiltonian (all in MeV).

I_i^+ I_f^+	^{122}Xe	^{124}Xe	^{126}Xe	^{128}Xe	^{130}Xe	^{132}Xe	^{134}Xe
$0_1{}^*Exp.\ 2_1$	1.40(6)	0.96(6)	0.770(25)	0.750(40)	0.65(5)	0.460(30)	0.34(6)
0_1 Theo. 2_1	1.4038	0.9651	0.7691	0.7575	0.6575	0.4684	0.3451
$2_1\ 0_1$	0.2808	0.1930	0.1538	0.1515	0.1315	0.0937	0.0690
$2_2\ 0_1$	0.0057	0.0033	0.0022	0.0015	0.0007	0.0002	0.0001
$2_2\ 0_2$	0.1552	0.0979	0.0741	0.0684	0.0567	0.0412	0.0343
$2_3\ 0_1$	0.0009	0.0003	0.0001	0.0000	0.0000	0.0000	0.0000
$2_3\ 0_2$	0.1640	0.1278	0.1047	0.1077	0.0926	0.0583	0.0298
$2_3\ 0_3$	0.0465	0.0248	0.0161	0.0133	0.0113	0.0091	0.0086
$2_4\ 0_3$	0.0766	0.0355	0.0198	0.0121	0.0064	0.0025	——
$2_4\ 0_4$	0.1031	0.0886	0.0784	0.0867	0.0839	0.0683	——
$4_1\ 2_1$	0.5297	0.3583	0.2787	0.2650	0.2186	0.1447	0.0941
$4_1\ 2_2$	0.0487	0.0316	0.0239	0.0227	0.0194	0.0145	0.0124
$4_1\ 2_3$	0.0737	0.0562	0.0452	0.0456	0.0386	0.0240	0.0122
$6_1\ 4_1$	0.6735	0.4529	0.3448	0.3183	0.2482	0.1465	0.0714
$6_1\ 4_2$	0.0476	0.0326	0.0254	0.0259	0.0244	0.0198	0.0182
$6_1\ 4_3$	0.0563	0.0428	0.0337	0.0332	0.0261	0.0127	——
$8_1\ 6_1$	0.7369	0.4875	0.3586	0.3139	0.2199	0.0979	——
$8_1\ 6_2$	0.0409	0.0290	0.0230	0.0246	0.0248	0.0214	——
$8_1\ 6_3$	0.0438	0.0319	0.0237	0.0210	0.0127	——	——
$10_1\ 8_1$	0.7363	0.4717	0.3269	0.2567	0.1362	——	——
$10_1\ 8_2$	0.0347	0.0252	0.0202	0.0223	0.0237	——	——

Table 2: Theoretically calculated reduced transition probabilities, $B(E2)'s$ in $e^2\,b^2$. *Ref. [27]

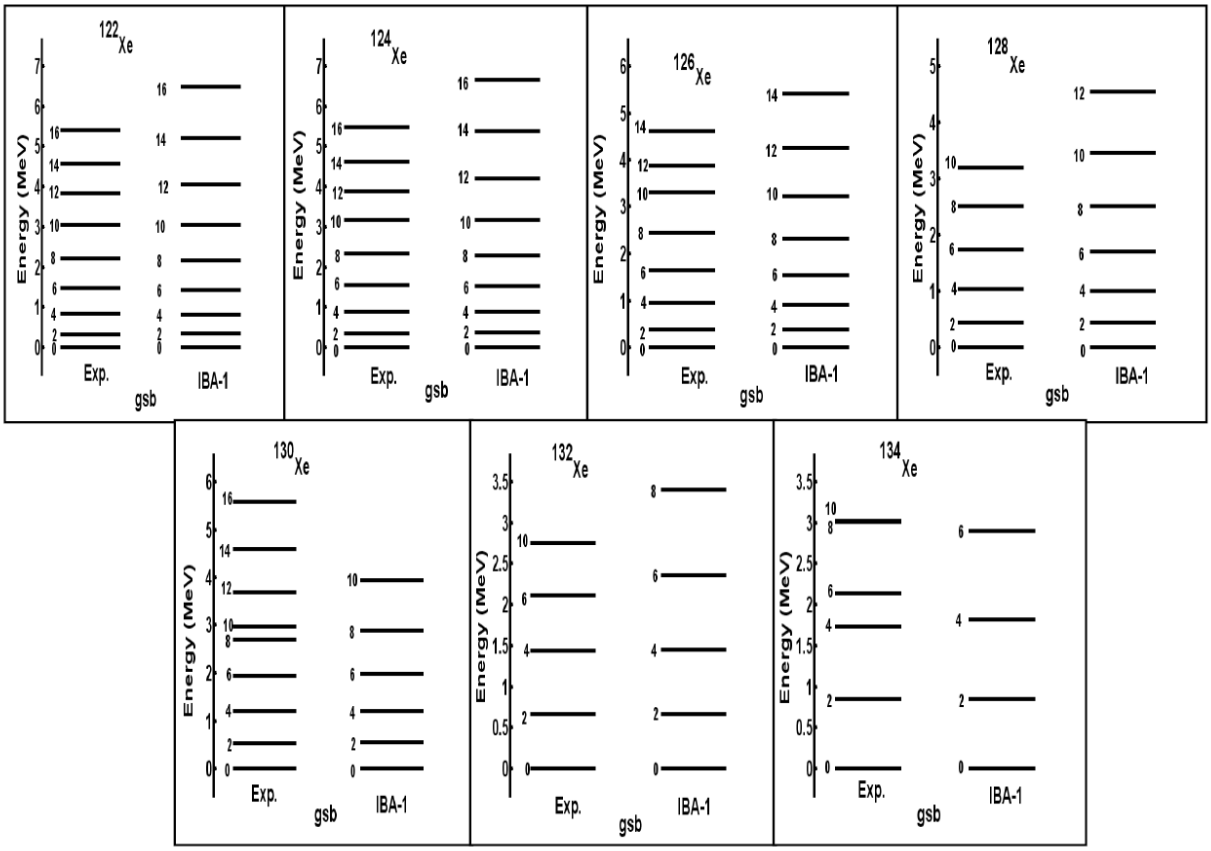

Fig. 3: Comparison between experimental [20–26] and theoretical (IBA) energy levels.

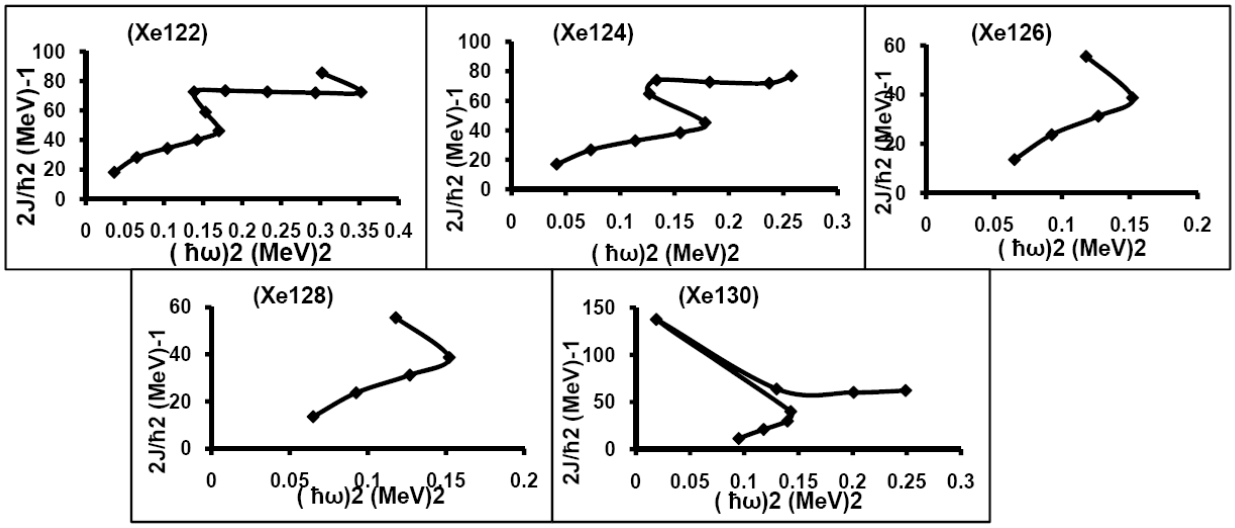

Fig. 4: Back bending in $^{122-134}$Xe isotopes.

$$
\begin{aligned}
E_{N_\Pi N_\nu}(\beta,\gamma) &= <N_\pi N_\nu;\beta\gamma|H_{\pi\nu}|N_\pi N_\nu;\beta\gamma> = \\
&= \zeta_d(N_\nu N_\pi)\beta^2(1+\beta^2)+\beta^2(1+\beta^2)^{-2}\times \\
&\times\left\{kN_\nu N_\pi[4-(\bar{X}_\pi\bar{X}_\nu)\beta\cos 3\gamma]\right\}+ \\
&+\left\{[\bar{X}_\pi\bar{X}_\nu\beta^2]+N_\nu(N_\nu-1)\left(\frac{1}{10}\,c_0+\frac{1}{7}\,c_2\right)\beta^2\right\},
\end{aligned}
\tag{7}
$$

where

$$
\bar{X}_\rho=\left(\frac{2}{7}\right)^{0.5}X_\rho,\quad \rho=\pi\,or\nu\,. \tag{8}
$$

The calculated PESs, $V(\beta,\gamma)$, for Xenon series of isotopes are presented in Fig. 1 and Fig. 2. They show that $^{122-128}$Xe nuclei are deformed and the two wells on both oblate and prolate sides are nearly equals and O(6) characters is expected to these nuclei. ^{130}Xe has flat potential energy, Fig. 2, which indicates that the nucleus is $E(5)$ symmetry and confirmed by the energy ratio $R=E^+_{4_1}/E^+_{2_1}=2.2$ as well as it is laying also in the transition from γ- unstable, $O(6)$, to vibrational, $U(5)$, nuclei while, $^{132,134}Xe$ are vibrational like nuclei.

3.2 Energy spectra and transition rates

IBA-1 model has been used in calculating the energy of the positive parity low-lying levels of Xenon series of isotopes. Comparison between the experimental spectra [20–26] and our calculations, using values of the model parameters given in Table 1, are illustrated in Fig. 3. The agreement between the low-laying calculated energy levels and their corresponding experimental values is fairly good but for higher states theoretical values are slightly higher. We believe that is due to the change of the projection of the angular momentum which may be due to band crossing and change in angular momentum.

The electric quadrupole transition operator [18] employed in this study is given by:

$$
T^{(E2)}=E2S\,D\cdot(s^\dagger\tilde{d}+d^\dagger s)^{(2)}+\frac{1}{\sqrt{5}}\,E2DD\cdot(d^\dagger\tilde{d})^{(2)}\,. \tag{9}
$$

The reduced electric quadrupole transition rates between $I_i\to I_f$ states are given by

$$
B(E_2,I_i-I_f)=\frac{[<I_f\parallel T^{(E_2)}\parallel I_i>]^2}{2I_i+1}\,. \tag{10}
$$

Unfortunately there is no enough measurements of electromagnetic transition rates $B(E2)$ for these series of nuclei. The only measured $B(E2,0^+_1\to 2^+_1)$'s are presented, in Table 2 for comparison to the calculated values. The parameters $E2S\,D$ and $E2DD$, displayed in Table 1, are used in the present calculation of the transition rates $B(E2)'s$ and then normalized to the experimentally known ones [27]. In our calculations we did not introduce any new parameters.

3.3 Back bending

The moment of inertia J and energy parameters $\hbar\omega$ are calculated [28]using equations (11, 12):

$$
\frac{2J}{\hbar^2}=\frac{4I-2}{\Delta E(I\to I-2)}\,, \tag{11}
$$

$$
(\hbar\omega)^2=(I^2-I+1)\left[\frac{\Delta E(I\to I-2)}{(2I-1)}\right]^2\,. \tag{12}
$$

The plots in Fig. 4 show back bending for $^{122-126}$Xe at $I^+=10$ while at $I^+=12$ for ^{128,130}Xe and this is in agreement with the work done by other authors [29]. Back bending in Xenon isotopes in higher states is explained [10] as due to partial rotational alignment of a pair of neutrons in the $1h_{1/2}$ neutron orbit near the Fermi surface.

4 Conclusions

The IBA-1 model has been applied successfully to $^{122-134}$Xe isotopes and we have got:

1. The ground state bands are successfully reproduced;
2. The potential energy surfaces are calculated and show $O(6)$ characters to $^{122-128}$Xe isotopes where the prolate and oblate depths are equal;
3. Flat potential energy to ^{130}Xe and energy ratios confirmed that the nucleus is an $E(5)$ symmetry;
4. ^{132,134}Xe nuclei show vibrational-like characters;
5. Electromagnetic transition rates, $B(E2)'s$, are calculated, then normalized to experimental B(E2, 0_1-2_1) values and then compared to the available data, and
6. Back bending for $^{122-126}$Xe have been observed at angular momentum $I^+=10$ and at $I^+=12$ for ^{128,130}Xe.

Submitted on December 6, 2011 / Accepted on December 16, 2011

References

1. Dilling J., Audi G., Beck D., Bollen G., Henry S., Herfurth F., Kellerbauer A., Kluge H.J., Lunney D., Moore R.B., Scheidenberger C., Schwarz S. , Sikler G., Szerypo J. and ISOLDE collaboration. Direct mass measurements of neutron-deficient xenon isotopes with the ISOLTRAP mass spectrometer. *Nuclear Physics A* , 2002, v. 701, 520–523.
2. Govil I.M., Kumar A. and Iyer H. Recoil distance lifetime measurements in ^{122,124}Xe. *Physical Review C*, 1998, v. 57, 632–636.
3. Sviratcheva K.D., Georgieva A.I. and Draayer J.P. Staggering behavior of $^+0$ state energies in the Sp(4) pairing model. *Physical Review C*, 2004, v. 69, 024313–024323.
4. Chasman R.R. Very extended nuclear shapes near A=100. *Physical Review C*, 2001, v. 64, 024311–024316.
5. Fossion R., Bonatsos D. and Lalazissis G.A. E(5), X(5) and prolate to oblate shape phase transitions in relativistic Hartree-Bogoliubov theory. *Physical Review C*, 2006, v. 73, 044310–044319.
6. Schunck N., Dudek J. and Herskind B. Nuclear hyperdeformation and the jacobi shape transition. *Physical Review C*, 2007, v. 75, 054304–054319.

7. Ma Y.G., Shen W.Q., Han D.D., Su Q.M., Wang J.S., Cai X.Z., Fang D.Q. and Zhang H.Y. Isospin effect on particle emission in nuclear dissociation. *Journal of Physics G*, 1999, v. 25, 1559–1570.
8. Ma Y.G., Su Q.M., Shen W.Q., Han D.D., Wang J.S., Cai X.Z., Fang D.Q. and Zhang H.Y. Isospin influence on particle emission and critical phenomena in nuclear dissociation. *Physical Review C*, 1999, v. 60, 024607–024616.
9. Prochniak L., Zajac K., Pomorski K., Rohozinski S.G. and Srebrny J. Collective quadrupole excitations in the $50\angle Z, N\angle 82$, nuclei with the general Bohr Hamiltonian. *Nuclear Physics A*, 1999, v. 648, 181–202.
10. Sarswat S.P., Bharti A. and Khosa S.K. Backbending and breaking of axial symmetry in the yrast bands of $^{114\text{-}130}$Xe isotopes. *Physical Review C*, 1998, v. 58, 2041–2048.
11. Sarkar M.S. and Sen S. Cranked Hartree-Fock Bogoliubov calculations in the Xe-Ba region. *Physical Review C*, 1997, v. 56, 3140–3151.
12. Devi R., Sarswat S.P., Bharti A. and Khosa S.K. E2 transition and Q_{J^+} systematics of even mass xenon nuclei. *Physical Review C*, 1997, v. 55, 2433–2440.
13. Vogel O., Van Isacker P., Gelberg A., Brentano P.V. and Dewald A. Effective γ deformation near A= 130 in the interacting boson model. *Physical Review C*, 1996, v. 53, 1660–1663.
14. Mittal H.M. and Devi V. Evidence for possible $O(6)$ symmetry in $A = 120 - 200$ mass region. *Armmenian Journal of Physics*, 2009, v. 2, 146–156.
15. Pascu S., Zamfir N.V., Cata-Danil Gh. and Marginean N. Structural evolution of the $Z = 52 - 62$ neutron-deficient nuclei in the interacting boson approximation framework. *Physical Review C*, 2010, v. 81, 054321–054329.
16. Jolos R.V., Pietralla N., Shirikova N. Yu. and Voronov V.V. Schematic microscopic approach to the description of $M1$ transitions between mixed-symmetry and fully symmetric collective states in $\gamma-$soft nuclei based on RPA-IBM boson mapping. *Physical Review C*, 2011, v. 84, 014315–014324.
17. Higashiyama K. and Yoshinaga N. Pair-truncated shell-model analysis of nuclei around mass 130. *Physical Review C*, 2011, v. 83, 034321–034339.
18. Scholten O. The program package PHINT, 1979, Internal report K.V.I-63.
19. Ginocchio J.N. and Kirson M.W. An intrinsic state for the interacting boson model and its relationship to the Bohr-M0ttelson model. *Nuclear Physics A*, 1980, v. 350, 31–60.
20. Tamura T. *Nuclear Data Sheets A=122*, 2007, v. 108, 455–632.
21. Iimura H., Katakura J., Kitaok K. and Tamura T. *Nuclear Data Sheets A; eq 124*, 1997, v. 80, 895–1068.
22. Katakura J. and Kitao K. *Nuclear Data Sheets A=126*, 2002, v. 97, 765–926.
23. Kanbe M. and Kitao K. *Nuclear Data Sheets A=128*, 2001, v. 94, 227–395.
24. Singh B. *Nuclear Data Sheets A=130*, 2001, v. 93, 33–242.
25. Khazov Y., Rodionov A.A., Sakharov S. and Singh B. *Nuclear Data Sheets A=132*, 2005, v. 104, 497–790.
26. Sonzogni A.A. *Nuclear Data Sheets A=134*, 2004, v. 103, 1–182.
27. Raman S., Nestor J.R.C.W., and Tikkanen P. Transition probability from the ground to the first excited 2^+ state of even-even nuclei. *Atomic Data and Nuclear Data Tables*, 2001, v. 78, 1–128.
28. Tripathi P.N., Sharma S.K. and Khosa S.K. Backbending anomaly in some highly neutron-rich molybdenum isotopes. *Physical Review C*, 1984, v. 29, 1951–1954.
29. Kusakari H., Kitao K., Sato K., Sugawara M. and Katsuragawa H. High spin states in even-mass Xe nuclei and backbending phenomena. *Nuclear Physics A*, 1983, v. 401, 445–459.

The Crucial Role of Multi-Configuration States of Bound Fermions

Eliahu Comay

Charactell Ltd. P.O. Box 39019, Tel Aviv 61390, Israel
E-mail: elicomay@post.tau.ac.il

The structure of a bound state of several Dirac particles is discussed. Relying on solid mathematical arguments of the Wigner-Racah algebra, it is proved the a non-negligible number of configurations is required for a description of this kind of systems. At present, the main results are not widely known and this is the underlying reason for the phenomenon called the proton spin crisis.

1 Introduction

Once upon a midnight dreary,
while I pondered weak and weary,
Over many a quaint and curious
volume of forgotten lore... [1].

The main objective if this work is to prove that the multi-configuration structure of a bound state of several Dirac particles plays an extremely important role. The existence of such a multi-configuration structure was already known many decades ago [2, 3] and early electronic computers were used for providing a numerical proof of this issue [4]. (Note that the first edition of [2] was published in 1935.) Unfortunately, this scientific evidence has not found its way to contemporary textbooks of physics and has become a kind of a forgotten lore. For example, [5] uses a single configuration and remarks that the error is about 5 per cent [5, see a comment on p. 234]. Here [6, see p. 116] is a notable exception. The paper proves the main points of this issue and shows its far reaching meaning and its relevance to physical problems that are still unsettled. In doing so the paper aims to make a contribution to the correction of this situation.

It is well known that quantum mechanics explains the Mendeleev periodic table of chemical elements. The shell structure of electrons provides an easy interpretation of chemical properties of noble gases (a full shell), halogens (a full shell minus 1), alkali metals (a full shell + 1) etc. The standard explanation of the Mendeleev periodic table uses a single configuration for a description of the electronic states of each chemical element. Thus, for example, the helium and the lithium atoms are described by the $1s^2$ and $1s^2 2s$ configurations, respectively. At this point the following problem arises: Does the unique configuration structure of an atomic ground state make an acceptable description of its quantum mechanical system or is it just a useful pedagogical explanation of the Mendeleev periodic table? The answer to this problem certainly must be obtained from a mathematical analysis of the quantum mechanical state of systems that contain more than one electron. By describing an outline of this task, the present work proves beyond any doubt that an atomic state of more than one electron has a multi-configuration structure and that no single configuration dominates the system.

The conclusion stated above has two important aspects. First, It is clear that a correct understanding of the structure of any fundamental physical system is a vital theoretical asset for every physicist. Next, it turns out that the lack of an adequate awareness of this physical evidence has already caused the phenomenon called the "proton spin crisis" [7] which haunts the particle physics community for decades. The measurements published in [7] show that quarks carry a very small portion of the proton's spin and this evidence has been regarded as a surprise. Now, it is shown in this work that the multiconfiguration structure found in atomic states is not a specific property of the Coulomb interaction. Thus, it is expected to be also found in any bound state of three spin 1/2 quarks, like it is found in bound states of several spin 1/2 electrons. For this reason, one can state that if the experiment described in [7] would have shown that *quarks carry the entire proton's spin then this result should have been regarded as a real crisis of fundamental quantum mechanical principles.*

In this work, units where $\hbar = c = 1$ are used. The second section contains a brief description of the main properties of a bound state of several Dirac particles that are required for the discussion. The underlying mathematical reasons for the multiconfiguration structure of states are discussed in the third section. Some aspects of the results are pointed out in the last section.

2 General Arguments

The main objective of this work is to find a reliable mathematical method for describing the ground state of a bound system of spin 1/2 particles. Applying Wigner's analysis of the Poincare group [8, 9], one concludes that the total mass (namely, energy) and the total spin are good quantum numbers. Thus, one assumes that an energy operator (namely, a Hamiltonian) exists. For this reason, one can construct a Hilbert space of functions that can be used for describing the given system as an eigenfunction of the Hamiltonian. Evidently, in the system's rest frame, an energy eigenfunction has the time dependent factor $\exp(-iEt)$. This factor can be removed and the basis of the Hilbert space contains time independent functions.

The fact that every relatively stable state has a well de-

fined total spin J can be used for making a considerable simplification of the problem. Thus, one uses a basis for the Hilbert space that is made of functions that have the required spin J and ignores all functions that do not satisfy this condition. Evidently, a smaller Hilbert space reduces the amount of technical work needed for finding the Hamiltonian's eigenfunctions. An additional argument holds for systems whose state is determined by a parity conserving interaction, like the strong and the electromagnetic interactions. Thus, one can use functions that have a well defined parity and build the Hilbert space only from functions that have the required parity. This procedure makes a further simplification of the problem.

The notion of a configuration of a system of several Dirac particles is a useful mathematical tool that satisfies the two requirements stated above [2, see p. 113] and [10, see p. 245]. A configuration is written in the form of a product of single particle wave functions describing the corresponding radial and orbital state of each particle belonging to the system (the m quantum number is ignored). For atomic systems a non-relativistic notation is commonly used and the values of the nl quantum numbers denote a configuration, like $1s^2 2s^1$. In relativistic cases the variables nlj [10, see p. 245] are used. In the latter case, the variables nj^π (here π denotes parity and it takes the values ± 1) is an equivalent notation for a relativistic configuration because $l = j \pm 1/2$ and the numerical parity of the l-value of a Dirac spinor upper part defines the single particle's parity. (This work uses the nj^π notation.) Evidently, any acceptable configuration must be consistent with the Pauli exclusion principle.

For any given state where the total spin J and parity are given, one can use configurations that are consistent with J and the product of the single-particle parity equals the parity of the system. The total angular momentum J is obtained from an application of the law of vector addition of angular momentum [2, see p. 56] and [10, see p. 95]. Here the triangular condition holds [10, see p. 98]. Thus, for example, an acceptable configuration for the two-electron 0^+ ground state of the helium atom must take the form $n_1 j_1^{\pi_1}\, n_2 j_2^{\pi_2}$, where $j_1 = j_2$ and $\pi_1 = \pi_2$. Similarly, a description of a 2-electron state where $J^\pi = 3^+$ *cannot* contain a configuration of the form $n_1 \frac{1}{2}^+\, n_2 \frac{3}{2}^+$, because the two J values 1/2 and 3/2 can only yield a total $J = 1$ or $J = 2$.

At this point the structure of the relevant Hilbert space is known. It is made of configurations that satisfy certain requirements. This is one of the useful properties of using configurations - the relevant Hilbert space is smaller because many configurations can be ignored due to the total spin and parity requirements. Obviously, a smaller Hilbert space indicates shorter computational efforts. Thus, the framework needed for the analysis is established. The problem of finding how many configurations are required for an acceptable description of an atomic state is discussed in the following section.

3 The Multi-Configuration Structure of Atomic States

The purpose of this section is to outline a proof that shows why a bound state of several electrons takes the form of a linear combination of terms, each of which belongs to a specific configuration. For this purpose, the Hamiltonian matrix is constructed for a Hilbert space whose basis is made of functions that take a configuration form. Evidently, non-vanishing off-diagonal matrix elements prove that the required state is a linear combination of configurations. It is shown that this property holds even for the simplest atomic state of more than one electron, namely the $J^\pi = 0^+$ ground state of the 2-electron Helium atom.

It is explained in the previous section that the required Hilbert space contains functions that have the given total spin and parity. The form of a two electron function is written as follows

$$\chi(\mathbf{r}_1, \mathbf{r}_2) = F_i(r_1) F_k(r_2) (j_1^{\pi_1}\, j_2^{\pi_2} JM). \tag{1}$$

Here, $F_i(r_1)$, $F_k(r_2)$ denote radial functions of the appropriate electron, j_1, j_2, π_1, π_2 denote the single particle spin and parity of the electrons, respectively, J is the total spin obtained by using the appropriate Clebsch-Gordan coefficients [2, 10] and M denotes the magnetic quantum number of the total angular momentum,

Let us use the principles described in the previous section and try to find the structure of the helium atom ground state. Thus, due to the triangular rule [10, see p. 98] and in order to be consistent with $J = 0$, we must use configurations where $j_1 = j_2$. Similarly, in order to have an even total parity, we must use configurations where the two electrons have the same parity. Thus, the required Hilbert space contains functions of the following form

$$\chi(\mathbf{r}_1, \mathbf{r}_2) = F_i(r_1) F_k(r_2) (j^\pi j^\pi 00), \tag{2}$$

where j is a positive number of the form $j = n + 1/2$, n is an integer and $\pi = \pm 1$.

The angular parts of any two different functions of (2) are orthogonal. Hence, off-diagonal matrix elements of any pure radial operator vanish. Since the following discussion is focused on finding off-diagonal matrix elements of the Hamiltonian, radial coordinates and radial operators are not always shown explicitly in expressions.

At this point one can use a given Hamiltonian and construct its matrix. Before doing this assignment one has to find a practical procedure that can be used for overcoming the infinite number of configurations that can be obtained from the different values of n, j and π. For this purpose one organizes the configurations of (2) in an ascending order of j and examines a Hilbert subspace made of the first N_0 functions, where N_0 is a positive integer. Here a finite Hamiltonian matrix is obtained and one can diagonalize it, find the smallest eigenvalue E_0 and its associated eigenfunction Ψ_0. The quantities

found here represent an approximation for the required solution. Let this approximate solution be denoted in this form

$$\{E_0, \Psi_0\}. \tag{3}$$

In order to evaluate the goodness of this approximation, one replaces N_0 by $N_1 = N_0 + 1$ and repeats the procedure. The new solution $\{E_1, \Psi_1\}$ is a better approximation because it relies on a larger Hilbert subspace. The difference between these solutions provides an estimate for the goodness of the solutions obtained. This procedure can be repeated for an increasing value of N_i. Thus, if a satisfactory approximation is reached for a certain value of N_i then one may terminate the calculation and use the solution obtained from this procedure as a good approximation to the accurate solution.

Now we are ready to examine the Hamiltonian's matrix elements. This examination demonstrates the advantage of using configurations as a basis for the Hilbert space. Thus, the angular part of the kinetic energy of each electron takes the form found for the hydrogen atom and only diagonal matrix elements do not vanish. The same result is obtained for the spherically symmetric radial potential operator Ze^2/r of the nucleus. It follows that off-diagonal matrix elements can be obtained only from the interaction between the two electrons. (This quantity does not exist for the one electron hydrogen atom and for this reason, each of the hydrogen atom eigenfunctions takes the form of a unique configuration.) In a full relativistic case the two-electron interaction takes the form of Breit interaction [11, see p. 170]. which contains the instantaneous ordinary Coulomb term and a velocity-dependent term. The existence and the results of the Hamiltonian's off-diagonal matrix elements are the main objective of this discussion and it is shown below that for this purpose the examination of the relatively simple Coulomb term is enough.

Thus, one has to write the $1/r_{12}$ operator in a form that is suitable for a calculation that uses the single particle independent variables $\mathbf{r}_1, \mathbf{r}_2$ of the configurations (2). This objective is achieved by carrying out a tensor expansion of the interaction [10, see p. 208]. For the specific case of the Coulomb interaction, one obtains [12, see p. 114]

$$\frac{1}{r_{12}} = \sum_{k=0}^{\infty} \frac{r_<^k}{r_>^{k+1}} P_k(\cos\theta_{12}). \tag{4}$$

Here $r_<$ and $r_>$ denote the smaller and the larger values of r_1 and r_2, respectively and θ_{12} is the angle between them. $P_k(\cos\theta_{12})$ is the Legendre polynomial of order k. At this point one uses the addition theorem for spherical harmonics [10, see p. 113]

$$P_k(\cos\theta_{12}) = \frac{4\pi}{2k+1} \sum_{m=-k}^{k} (-1)^m Y_{k,-m}(\theta_1, \phi_1) Y_{k,m}(\theta_2, \phi_2) \tag{5}$$

and obtains an expansion of the appropriate Legendre polynomial $P_k(\cos\theta_{12})$ of (4) in terms of spherical harmonics that depend on single particle angular variables. This analysis shows how matrix elements can be obtained for a Hilbert space whose basis is made of functions that are an appropriate set of configurations.

At this point the wave functions of the Hilbert space basis as well as the Hamiltonian operator depend on the radial and the angular coordinates of single particle functions. The main objective of this section is to explain why the electronic states are described as a linear combination of configurations. It is shown above that the configurations of the Hilbert space basis are eigenfunctions of the operators representing the kinetic energy and the interaction with the spherically symmetric potential of the nucleus. Hence, the discussion is limited to the two particle operator (4) that depends on the expansion (5).

Let us find, for example, the off-diagonal matrix element of the configurations $((1\frac{1}{2}^+)^2 00)$ and $((2\frac{3}{2}^-)^2 00)$ of the Hilbert space basis (2). Consider the 2-electron Coulomb interaction obtained for the upper (large) component of the Dirac spinor. Thus, $\frac{1}{2}^+$ is a spatial s-wave and $\frac{3}{2}^-$ is a spatial p-wave. The Wigner-Racah algebra provides explicit formulas for expressions that depend on the angular coordinates. Now, as stated above, the main objective of the discussion is to show that off-diagonal matrix elements do not vanish. For this purpose, only the main points of the calculation are written and readers can use explicit reference for working out the details.

The formal form of the angular component of the off-diagonal matrix element is

$$H_{ij} = < j_1 j_2 JM | \frac{1}{r_{12}} | j'_1 j'_2 JM > . \tag{6}$$

Here j_1, j_2 of the ket are angular momentum values of the first and the second electron, respectively and they are coupled to a total J, M. The bra has an analogous structure. In the particular case discussed here $J = M = 0$ and (6) takes the form

$$H_{ij} = < \tfrac{1}{2}\tfrac{1}{2}00 | \frac{1}{r_{12}} | \tfrac{3}{2}\tfrac{3}{2}00 > . \tag{7}$$

The following points describe the steps used in the calculation of (7).

1. The Wigner-Eckart theorem shows that (6) can be cast into a product of a *Wigner 3j symbol* and a *reduced matrix element* [10, see p. 117]
2. In (4), the expansion (5) of $1/r_{12}$ is a *scalar product of two tensors* [10, see p. 128].
3. The reduced matrix element of such a scalar product can be put in the form of a product of a *Racah coefficient* and two reduced matrix elements that depend on the first and the second electron, respectively [10, see p. 129].
4. Each of these reduced matrix elements takes the form $< sl\,j \| Y_k \| sl'\,j' >$ where sl denote single particle spin and spatial angular momentum that are coupled to the

particle's total angular momentum j. In the specific case discussed here it is $< \frac{1}{2}0\frac{1}{2}\|Y_1\|\frac{1}{2}1\frac{3}{2} >$. The value of the last expression can be readily obtained as a product of a square root of an integer and a Wigner $3j$ symbol [10, see p. 521]. The final value is

$$< \tfrac{1}{2}0\tfrac{1}{2}\|Y_1\|\tfrac{1}{2}1\tfrac{3}{2} >= \frac{-2}{\sqrt{4\pi}}. \quad (8)$$

This discussion shows that the Hamiltonian's off diagonal matrix elements do not vanish for the $J = 0$ ground state of the He atom. It means that a single configuration does not describe accurately this state. The next step is to carry out an explicit calculation and find out how good is the usage of a single configuration. This task has already been carried out [4] and it was proved that the description of the ground state of the He atom requires many configurations. Here radial and angular excitations take place and no single configuration plays a dominant role.

4 Discussion

Several aspects of the conclusion obtained in the previous section are discussed below.

Intuitively, the multiconfiguration structure of the ground state may be regarded as a mistake. Indeed, the ground state takes the lowest energy possible. Hence, how can a mixture of a lower energy state and a higher energy state yield a combined state whose energy is lower than either of the two single mono-configuration states? The answer to this question relies on a solid mathematical basis. Thus, a diagonalization of a Hermitian matrix reduces the lowest eigenvalue and increases the highest eigenvalue [12, see e.g. pp. 420–423]. Hence, *for a Hermitian matrix, any off-diagonal matrix element increases the difference between the corresponding diagonal elements*. It means that the smaller diagonal element decreases and the larger diagonal element increases. Since the Hamiltonian is a Hermitian operator, one concludes that if the Hilbert space basis yields a non-diagonal Hamiltonian matrix then the lowest eigenvalue "favors" eigenfunctions that are a linear combination of the Hilbert space basis functions.

It is shown in the previous section that the non-vanishing off-diagonal matrix elements rely on the two body Coulomb interaction between electrons. Thus, the tensor expansion of the interaction (4) casts the 2-body Coulomb interaction into a series of Legendre polynomials where $cos\theta_{12}$ is the polynomial's argument. Evidently, any physically meaningful interaction depends on the distance between the interacting particles. Hence, an expansion in terms of the Legendre polynomials can be obtained. This expansion proves that the mathematical procedure described in the previous section has a comprehensive validity [10, see p. 208]. Thus, what is found in the previous section for electrons in the He atom ground state also holds for quarks in the proton. Moreover, the proton is an extremely relativistic system of quarks and, as such, its spin-dependent interactions are expected to be quite strong. Evidently, spin dependent interactions make a contribution to off-diagonal matrix elements. On the basis of this conclusion, one infers that the proton's quark state must be described by a linear combination of many configurations.

A polarized proton experiment has been carried out where the instantaneous spin direction of quarks was measured [7]. The measurements have shown that *the total quark spin constitutes a rather small fraction of the proton's spin.* This result is in a complete agreement with the mathematical analysis carried out above. Thus, the relativistic proton dynamics indicates that the jj-coupling provides a better approach (and this is the reason for the usage of this notation here). In each quark configuration, spin and spatial angular momentum are coupled to a total single particle j-value and the Clebsch-Gordan coefficients determine the portion of spin-up and spin-down of the quark. Next, The relativistic quark state indicates that, unlike the case of the hydrogen atom, the lower part of the Dirac spinor of quarks is quite large. As is well known, if in the upper part of a Dirac spinor is $l = j \pm 1/2$ then its lower part is $l = j \mp 1/2$. Hence, different Clebsch-Gordan coefficients are used for the upper and the lower parts of the Dirac spinor. Furthermore, in different configurations, different Clebsch-Gordan coefficients are used for the single particle coupling of the three quarks to the total proton's spin and the overall weight of the spin-up and spin-down components takes a similar value. This argument indicates that the outcome of [7] is quite obvious and that if the experiment would have yielded a different conclusion where *quarks carry the entire proton's spin then this result should have been regarded as a real crisis of fundamental quantum mechanical principles.* This discussion also shows that the quite frequently used description of the results of [7] as "the proton spin crisis" is unjustified.

Computers are based on quantum mechanical processes that take place in solid state devices. Hence, it is clear that people who have established the laws of quantum mechanics had no access to the computational power of computers. For this reason, several approximations have been contrived in order to get an insight into atomic structure. A method that deals with configurations is called *central field approximation* [5, see p. 225]. Here, for every electron, the actual field of all other electrons is replaced by an approximate spherically symmetric radial field. Evidently, as explained in the third section, such a radial field does not cause a configuration mixture and, in this approximation, a single configuration is used for describing atomic states. This approach is frequently used in a description of the Mendeleev's periodic table [5, see pp. 240–247].

However, even in the early days of quantum mechanics, the central field approximation has been regarded as an approximation and people have constructed mathematical tools for treating the multi-configuration atomic structure which is known as the Wigner-Racah algebra of angular momentum. These mathematical tools have been used in the early days of

electronic computers [4] and the result is quite clear: *many configurations are required even for the simplest case of the ground state $J = 0$ of the 2-electron He atom and no single configuration plays a dominant role.* Today, this outcome is still known [6, see p. 116] but unfortunately not widely known. Thus, [6] is based on lectures delivered in a chemistry department. On the other hand, the birth and the long duration of the idea concerning *the proton spin crisis* prove that this fundamental physical issue is indeed not widely known. This paper has been written for the purpose of improving the present status.

Submitted on December 25, 2011 / Accepted on January 6, 2012

References

1. Poe E. A. The Raven. 1845.
2. Condon E. V., Shortley G. H., The Theory of Atomic Spectra. University Press, Cambridge, 1964.
3. Taylor G. R., Parr R. G. Superposition of Configurations: The Helium Atom. *Proceedings of the National Academy of Sciences, USA* 1952, v. 38 (3), 154–160.
4. Weiss A. W. Configuration Interaction in Simple Atomic Systems. *Physical Review*, 1961, v. 122 (6), 1826–1836.
5. Landau L. D., Lifshitz E. M. Quantum Mechanics. Pergamon, London, 1959.
6. Zare R. N. Angular Momentum. Wiley, New York, 1988.
7. Ashman J. et al. (EMC) A measurement of the spin asymmetry and determination of the structure function g1 in deep inelastic muon-proton scattering. *Physics Letters B* 1988, v. 206 (2), 364–370.
8. Wigner E. On unitary representations of the inhomogeneous Lorentz group. *Annals of Mathematics* 1939, v. 40, 149–204.
9. Schweber S. S. An introduction to relativistic quantum field theory. Harper & Row, New York, 1964.
10. de-Shalit A., Talmi I. Nuclear Shell Theory, Academic Press, New York, 1963.
11. Bethe H. A., Salpeter E. E. Quantum Mechanics of One and Two-Electron Atoms, Springer, Berlin, 1957.
12. Cohen-Tannoudji C., Diu B., Laloe F. Quantum Mechanics. V. 1, Wiley, New York, 2005.

Discovery of Uniformly Expanding Universe

Reginald T. Cahill and David Rothall

School of Chemical and Physical Sciences, Flinders University, Adelaide 5001, Australia
E-mail: Reg.Cahill@flinders.edu.au, David.Rothall@flinders.edu.au

Saul Perlmutter and the Brian Schmidt – Adam Riess teams reported that their Friedmann-model GR-based analysis of their supernovae magnitude-redshift data revealed a new phenomenon of "dark energy" which, it is claimed, forms 73% of the energy/matter density of the present-epoch universe, and which is linked to the further claim of an accelerating expansion of the universe. In 2011 Perlmutter, Schmidt and Riess received the Nobel Prize in Physics "for the discovery of the accelerating expansion of the Universe through observations of distant supernovae". Here it is shown that (i) a generic model-independent analysis of this data reveals a uniformly expanding universe, (ii) their analysis actually used Newtonian gravity, and finally (iii) the data, as well as the CMB fluctuation data, does not require "dark energy" nor "dark matter", but instead reveals the phenomenon of a dynamical space, which is absent from the Friedmann model.

1 Introduction

Observational determination of the time evolution of the scale factor $a(t)$ of the universe is fundamental to understanding the dynamics of the universe. Measurement [1, 2] of supernovae magnitude-redshifts provided that critical data, and it is a simple procedure to determine $a(t)$ from that data. A secondary process is then to test different dynamical theories of the universe against that data. However this did not happen, and not for the 1st time in the history of astronomy was one predetermined theory forced into the data fitting.

The 1st example was Ptolemy's fitting of his geocentric model of the solar system to the Babylonian planetary orbit data. This then required, and correctly so, that the orbits have epicycle components. This model persisted for some 1400 years, until the heliocentric model replaced the geocentric model, and for which the epicycle phenomenon then evaporated - it was merely an artifact of the incorrect geocentric model. It now appears that a similar confusion of data and model has reappeared in analysing the supernovae data, for again a simple and manifestly inadequate model of the universe, namely Newtonian gravity (NG), has been used. A generic model-independent analysis of the data reveals that the universe is undergoing a uniform expansion, see sect.2. However use of the Newtonian gravity model has resulted in a new collection of model-induced artifacts, namely "dark energy", "dark matter", and a claim that the universe expansion is accelerating. These artifacts also disappear once we use a model that replaces Newtonian gravity.

It is usually argued that General Relativity (GR) in the form of the Friedmann equation is superior to NG, and it was the Friedmann equation that was used in analysing the supernovae data [1, 2]. However in sect.3 we derive the Friedmann equation from NG in a few simple steps. This happens because GR was constructed as a generalisation of NG, and reduces to NG in the limit of low matter densities and low speeds. Alternatively, in sect.4, we show in a few simple steps, that the dynamical 3-space theory of space and gravity yields a uniformly expanding universe, and so dispenses with the "dark energy" and "dark matter" artifacts. The implication here, and in previous analyses of the dynamics of space itself, shows that NG is a flawed model of gravity, even at the level of laboratory measurements of G, bore-hole g anomalies, galactic rotation, and so on. So the Friedmann equation is based upon a flawed theory. This is in fact a major outcome of the observations of supernova events, and needs to be understood.

2 Model Independent Analysis Reveals Uniform Expansion

The scale factor $a(t) = r(t)/r(t_0)$; ($a(t_0) \equiv 1$ by definition), where $r(t)$ are galactic separations on a sufficiently large scale, and t_0 is the present moment age of the universe. It describes the time evolution of the universe assuming a homogeneous and isotropic description. In principle it may be directly extracted from magnitude-redshift data without the use of any particular dynamical model for $a(t)$. The redshift is $z = 1/a(t) - 1$, and the Hubble function is $H(t) = \dot{a}/a$. We define $H(z)$ by changing variables from t to z. A dimensionless luminosity distance is given by (see appendix)

$$d_L(z) = (1 + z) \int_0^z \frac{H_0 dz'}{H(z')}. \quad (1)$$

$d_L(z)$ takes account of the reduced photon flux and energy loss caused by the expansion. Then the magnitude-redshift observables are computable from $a(t)$

$$\mu(z) = 5 \log_{10} d_L(z) + m, \quad (2)$$

where m is determined by the intrinsic brightness of the SNe Ia supernova. In principle this can be inverted to yield $a(t)$, without reference to any dynamical theory for $a(t)$. A simple

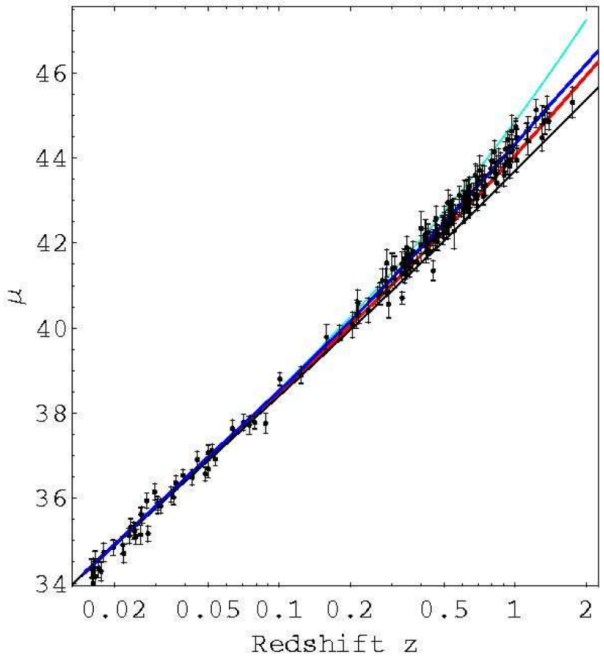

Fig. 1: Supernovae magnitude-redshift data. Upper curve (light blue) is "dark energy" only $\Omega_\Lambda = 1$. Next curve (blue) is best fit of "dark energy"-"dark-matter" $\Omega_\Lambda = 0.73$. Lowest curve (black) is "dark matter" only $\Omega_\Lambda = 0$. 2nd lowest curve (red) is generic uniformly expanding universe.

first analysis of the data tries a uniform expansion $a(t) = t/t_0$, which involves one parameter $t_0 = 1/H_0$, which sets the time scale. Fig.1 shows that this uniform expansion (shown by red plot) gives an excellent account of the data. We conclude that the supernovae magnitude-redshift data reveals a uniformly expanding universe. So why did [1, 2] report an accelerating expansion for the universe? The answer, according to the Nobel Prize briefing notes, is because "the evolution of the Universe is described by Einstein's theory of general relativity" [3]. To the contrary we argue that the data should be used to test possible theories of the universe, as in the usual scientific method, and not *a priori* demand that one theory, with *ad hoc* adjustments, be defined to be the only correct theory.

3 Newtonian Gravity Universe Model

The analysis in [1, 2] used the GR-based Friedmann equation for $a(t)$

$$\dot{a}^2 = \frac{8}{3}\pi G a(t)^2 \rho(t), \tag{3}$$

where $\rho(t)$ is the matter/energy density. However this equation follows trivially from Newtonian gravity. Consider a uniform density of matter moving radially with speed $v(r, t)$, at distance r, away from an origin. The kinetic + gravitational potential energy, with total energy E, of a test particle of mass m is given by

$$\frac{1}{2}mv^2 - \frac{GmM(r)}{r} = E, \tag{4}$$

where $M(r) = \frac{4}{3}\pi r^3 \rho$ is the mass enclosed within radius r - this follows simply from Newton's Inverse Square Law. Using $r(t) = a(t)r_0, v = \dot{r}$ and the so-called critical case $E = 0$, immediately gives (3). The reason for this simple derivation is that GR was constructed as a generalisation of NG that reduces to NG in the limit of low speeds and matter densities. So the Friedmann equation inherits all of the known failures of NG. As well the redshift z is a Doppler shift, caused by the motion of the source relative to the observer. Consider then some of the implications of (3): (i) if $\rho = 0$, i.e. no matter, then there is no expanding universe possible: $\dot{a} = 0$. This arises because (3) is about the effects of matter-matter gravitational attraction, and without matter there are no gravitational effects. (ii) (3) is not about the expansion of space, for it arises from NG in which matter moves through a Euclidean and unchanging space, (iii) (3) requires, at $t = t_0$, that

$$H_0^2 = \frac{8}{3}\pi G \rho_c, \tag{5}$$

where ρ_c is the so-called critical density. However (5) is strongly violated by the data: the observed baryonic matter density is some 20 times smaller than ρ_c, and so ρ must be padded out to satisfy (5), and (iv) (3) does not posses uniformly expanding solutions, unless $\rho \sim 1/a^2$, a form not considered in [1, 2]. To fit the data [1, 2] used the restricted *ad hoc* form

$$\rho(a) = (\frac{\Omega_M}{a^3} + \Omega_\Lambda)\rho_c, \tag{6}$$

where Ω_Λ is the "dark energy" composition parameter, and Ω_M is the "matter" composition parameter. There is no theoretical underpinning for this "dark energy". The above $H_0 - \rho_c$ (5) relationship requires that $\Omega_\Lambda + \Omega_M = 1$, resulting in a two parameter model: H_0 and Ω_Λ. Fitting the data, by solving (3), and then using (1) and (2), gives $\Omega_\Lambda = 0.73$, and so $\Omega_M = 0.27$. This fitting is shown in Fig. 1. Essentially $\Omega_\Lambda = 0.73$ is the value for which NG best mimics a uniformly expanding universe, despite its inherent weakness as a model of a universe. The known baryonic matter density, corresponding to $\Omega_m = 0.05$, then requires that $\Omega_M - \Omega_m = 0.22$ be interpreted as the "dark matter" composition. However (3) has another strange feature, namely that $a(t)$, as a consequence of the "dark energy" parametrisation, possess an exponential component: neglecting Ω_M, which becomes increasingly valid into the future we get

$$a(t) \sim e^{H_0 \sqrt{\Omega_\Lambda} t}. \tag{7}$$

The Nobel Prize for Physics in 2011 was awarded for the discovery of this "accelerated expansion of the universe", despite the fact that the model-independent analysis in sect. 2 shows no such effect.

4 Dynamical Space Universe Model

A newer dynamical model of space describes the velocity of this structured space, relative to an observer using coordinate system $\mathbf{r}$ and t, by [5]

$$\nabla\cdot\left(\frac{\partial\mathbf{v}}{\partial t}+(\mathbf{v}\cdot\nabla)\mathbf{v}\right)+\frac{\alpha}{8}\left((trD)^2-tr(D^2)\right)+$$
$$+\frac{\delta^2}{8}\nabla^2\left((trD)^2-tr(D^2)\right)+...=-4\pi G\rho$$

$$\nabla\times\mathbf{v}=\mathbf{0},\quad D_{ij}=\frac{\partial v_i}{\partial x_j}. \tag{8}$$

The 1st term involves the Euler constituent acceleration, while the $\alpha-$ and $\delta-$ terms contain higher order derivative terms. This dynamical theory is conjectured to arise from a derivative expansion of a quantum foam theory of space. Laboratory, geophysical and astronomical data show that α is the fine structure constant, while δ appears to be a very small Planck-like length. Quantum theory determines the "gravitational" acceleration of quantum matter to be, as a quantum wave refraction effect,

$$\mathbf{g}=\frac{\partial\mathbf{v}}{\partial t}+(\mathbf{v}\cdot\nabla)\mathbf{v}+(\nabla\times\mathbf{v})\times\mathbf{v}_R-\frac{\mathbf{v}_R}{1-\dfrac{\mathbf{v}_R^2}{c^2}}\frac{1}{2}\frac{d}{dt}\left(\frac{\mathbf{v}_R^2}{c^2}\right)+..., \tag{9}$$

where $\mathbf{v}_R=\mathbf{v}_0-\mathbf{v}$ is the velocity of matter relative to the local space. Substituting the Hubble form $\mathbf{v}(\mathbf{r},t)=H(t)\mathbf{r}$, and then $H(t)=\dot{a}/a$, we obtain

$$4a\ddot{a}+\alpha\dot{a}^2=-\frac{16}{3}\pi G a^2\rho. \tag{10}$$

This has a number of key features: (i) even when $\rho=0$, i.e. no matter, $a(t)\neq 0$ and monotonically increasing. This is because the space itself is a dynamical system, and the (small) amount of actual baryonic matter merely slightly slows that expansion, as the matter dissipates space. As well relation (5) no longer applies, and so there is no "critical density", (ii) the redshift z is no longer a Doppler shift; now it is caused by the expansion of the space removing energy from photons. Because of the small value of $\alpha=1/137$, the α term only plays a significant role in extremely early epochs, but only if the space is completely homogeneous*. In the limit $\rho\to 0$ and neglecting the α term, we obtain the solution $a(t)=t/t_0$. This uniformly expanding universe solution is exactly the form directly determined in sect.2 from the supernovae data. It requires neither "dark energy" nor "dark matter" – these effects have evaporated, and are clearly revealed as nothing more than artifacts of the NG model. The "accelerating expansion of the universe" in the future has also disappeared.

*Keeping the α term we obtain $a(t)=(t/t_0)^{1/(1+\alpha/4)}$

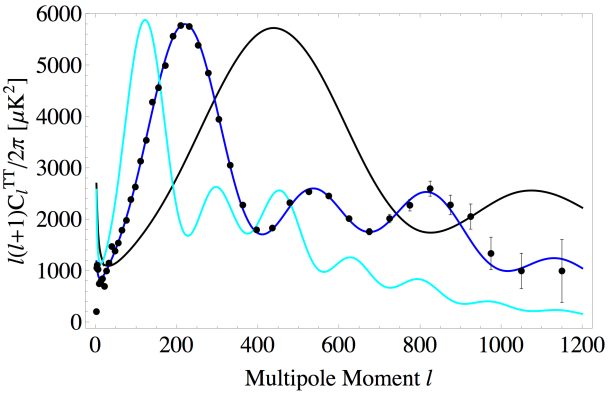

Fig. 2: CMB angular power spectrum for (i) $\Omega_\Lambda=1$ (light blue curve), (ii) = 0.73 (dark blue curve), and (iii) = 0 (black curve), confirming that the background space is uniformly expanding.

5 CMB Fluctuations

Another technique for determining the expansion rate of the universe is to use the Cosmic Microwave Background (CMB) temperature angular fluctuation spectrum. This spectrum is computed as a perturbation of the plasma relative to an assumed homogeneous background universe dynamical model. The background model used is the Friedmann equation (3). We show in Fig. 2 the angular fluctuation power spectrum from CAMB (Code for Anisotropies in the Microwave Background), [6, 7], for the same three values $\Omega_\Lambda=0$, 0.73 and 1, as also used in Fig. 1. However, as already noted in sect. 3, this homogeneous background dynamics is merely a Newtonian gravity model, with "dark energy" and "dark matter" used to pad out the critical density and mimic a uniform expansion. The Newtonian model and the dynamical 3-space model give the same age for the universe, 13.7 Gyr, as they both describe the same uniform expansion rate, with the minor variations in the Newtonian model expansion rate cancelling out. However they give different decoupling times, 0.38 Myr for the Newtonian model and 1.4 Myr for the dynamical 3-space. So it is important to note that the decoupling time is very model dependent.

6 Conclusions

The supernovae magnitude-redshift data is of great significance to cosmology. It reveals, using a model-independent analysis, that the universe is undergoing a uniform expansion. This represents a major challenge to theories of the universe, particularly as GR does not have such solutions. We have also noted that GR, via the Friedmann equation, is nothing more than Newtonian gravity applied to the gravitational force between matter, essentially with galaxies as that matter. To mimic the uniform expansion the canonical value $\Omega_\Lambda=0.73$ emerges by fitting the NG model to either the data, or more revealingly, by fitting to the dynamical 3-space the-

ory. However the *ad hoc* introduction of the "dark energy" parameter results in a spurious accelerating expansion. These spurious effects, "dark energy", "dark matter", and "accelerating expansion", are reminiscent of Ptolemy's epicycles when an incorrect model of the solar system was forced to fit the data, rather than using the data to test different models of the solar system. This recurring failure to use the scientific method resulted, in both cases, in deeply wrong theories being embellished and promoted as orthodoxy, with astronomers now committing major resources to "explaining" these new epicycles. The dynamical 3-space theory has been extensively tested, from bore hole g anomalies, to supermassive black holes and cosmic filaments. It gives a uniformly expanding universe without the introduction of any *ad hoc* parameters, and disagrees in general with Newtonian gravity, even in the low matter density, low speed limits, while nevertheless reproducing the NG restricted successes within the solar system. Introducing "dark matter" and "dark energy" amounts to the belief that Newton had correctly and completely described space and gravity some 300 years ago, requiring only the identification of new matter/energy. The supernova data is informing us that this is not so [8]. The use of the *ad hoc* parametrisation in (6) is not sufficiently general to give an unbiased fitting procedure, forcing an exponential growth term which is not present in the data.

7 Acknowledgments

We acknowledge the use of the Legacy Archive for Microwave Background Data Analysis (LAMBDA). We also acknowledge use of the CAMB (Lewis et al. 2000) package.

8 Appendix: Luminosity Distance

To extract $a(t)$ we need to describe the relationship between the cosmological observables: the apparent energy-flux magnitudes and redshifts, and in a model independent manner. We use the dynamical space formalism, although the result, in (1) & (15), is generic and was used in [1, 2]. First we take account of the reduction in photon count caused by the expanding 3-space, as well as the accompanying reduction in photon energy. To that end we first determine the distance travelled by the light from a supernova event before detection. Using a choice of embedding-space coordinate system, with $r = 0$ at the location of a supernova event at time t_1, the speed of light relative to this embedding space frame is $c + v(r(t; t_1), t)$, i.e. c wrt the space itself, where $r(t; t_1)$ is the photon embedding-space distance from the source. Then the distance travelled by the light at time t, after emission at time t_1, is determined implicitly by

$$r(t; t_1) = \int_{t_1}^{t} dt'(c + v(r(t'; t_1), t'), \tag{11}$$

which has the solution, on using $v(r, t) = H(t)r$,

$$r(t; t_1) = ca(t) \int_{t_1}^{t} \frac{dt'}{a(t')}. \tag{12}$$

This distance gives directly the surface area $4\pi r(t; t_1)^2$ of the expanding sphere and so the decreasing photon count per unit area on that surface. With $t \to t_0$ (and then dropping t_0 in the notation), $a(t_0) = 1$ and $a(t_1) = 1/(1 + z(t_1))$ we obtain

$$r(z) = c \int_0^z \frac{dz'}{H(z')}. \tag{13}$$

However because of the expansion the flux of photons is reduced by the factor $1/(1 + z)$ simply because they become spaced further apart by the expansion. The photon flux is then given by $\mathcal{F}_P = \mathcal{L}_P/4\pi(1 + z)r(z)^2$ where $\mathcal{L}_P$ is the source photon-number luminosity. However usually the energy flux is measured, and the energy of each photon is reduced by the factor $1/(1 + z)$ because of the redshift. Then the energy flux is, in terms of the source energy luminosity $\mathcal{L}_E$: $\mathcal{F}_E = \mathcal{L}_E/4\pi(1 + z)^2 r(z)^2 \equiv \mathcal{L}_E/4\pi r_L(z)^2$ which defines the effective energy-flux luminosity distance $r_L(z)$. Then the energy-flux luminosity effective distance is

$$r_L(z) = (1 + z)r(z) = c(1 + z) \int_0^z \frac{dz'}{H(z')} \tag{14}$$

The dimensionless "energy-flux" luminosity effective distance is then given by

$$d_L(z) = (1 + z) \int_0^z \frac{H_0 dz'}{H(z')}. \tag{15}$$

For the uniformly expanding universe $H(z) = (1 + z)H_0$ and $d_L(z) = (1 + z) \ln(1 + z)$.

Submitted on December 31, 2011 / Accepted on January 9, 2012

References

1. Riess A.G., Filippenko A.V., Challis P., Clocchiattia A., Diercks A., Garnavich P.M., Gilliland R.L., Hogan C.J., Jha S., Kirshne R.P., Leibundgut B., Phillips M.M., Reiss D., Schmidt B.P., Schommer R.A., Smith R.C., Spyromilio J., Stubbs C., Suntzeff N.B. and Tonry J. Observational Evidence from Supernovae for an Accelerating Universe and Cosmological Constant. *Astronomical Journal*, 1998, v. 116, 1009–1038.
2. Perlmutter S., Aldering G., Goldhaber G., Knop R.A., Nugent P., Castro P.G., Deustua S., Fabbro S., Goobar A., Groom D.E., Hook I.M., Kim A.G., Kim M.Y., Lee J.C., Nunes N.J., Pain R., Pennypacker C.R., Quimby R., Lidman C., Ellis R.S., Irwin M., McMahon R.G., Ruiz-Lapuente P., Walton N., Schaefer B., Boyle B.J., Filippenko A.V., Matheson T., Fruchter A.S., Panagia N., Newberg H.J.M. and Couch W.J. Measurement of Ω and Λ from 42 High-Redshift Supernovae. *Astrophysical Journal*, 1999, v. 517, 565–586.
3. Class for Physics of the Royal Swedish Academy of Sciences, *The Accelerating Universe*, http://www.nobelprize.org/nobel_prizes/physics/laureates/2011/advanced-physicsprize2011.pdf
4. Cahill, R.T. Unravelling the Dark Matter – Dark Energy Paradigm. *Apeiron*, 2009, v. 16, no. 3, 323–375.
5. Cahill R.T., Kerrigan D. Dynamical Space: Supermassive Galactic Black Holes and Cosmic Filaments. *Progress in Physics*, 2011, v. 4, 79–82.
6. Larson D. *The Astrophysical Journal Supplement Series*, 2011, v. 192 (2), 16.
7. Lewis A., Challinor A., Lasenby A. Efficient computation of cosmic microwave background anisotropies in closed Friedmann-Robertson-Walker models. *Astrophysical Journal*, 2000, v. 538 (2), 473–476.
8. Cahill R.T. *Dynamical 3-Space: Emergent Gravity*, in: *Should the Laws of Gravitation be Reconsidered?* Múnera H. (Editor), *Aperion*, Montreal, 2011, 363–376.

LETTERS TO PROGRESS IN PHYSICS

On the Epistemological Nature of Genius and Individual Scientific Creation

Indranu Suhendro
http://www.zelmanov.org; e-mail: wings.of.solitude@gmail.com

This brief exposition summarizes a universally over-arching deepening of the epistemology of aesthetics (especially as regards the nature of Genius) as outlined in a particular section of the Author's work on an all-embracing, post-Kantian epistemological theory of Reality and the Universe called "The Surjective Monad Theory of Reality" (SMTR), which generalizes, in the utmost ontological sense, Kantianism, phenomenology, and a paradigm of Reality called "Reflexive Monism" (RM).

Most people, both eruditically trained and untrained, are profoundly mistaken in their belief about the nature of Genius, especially in relation to the mere prevalence of talent and the dominant structure of pedantry (i.e., a dominant world-paradigm of mass-education, as opposed to authentic individual education), the epistemological nature of the so-called "scientific research", and the entire psychologism thereof. By "psychologism", we mean an ultimately solipsistic, super-tautological basis that manages to present science and scientific-technological progress (let alone revolution in the sciences), among others, to the world at large in the image of a homogeneously working contingency of non-independent scientists, political factors, and industrial games, as opposed to single creative individuals in the profoundest sense.

Such a semi-popular image replete with "democratic-spiritism" (not to be confused with democracy in and of itself), which easily captures unassuming, aspiring talents into the underlying system, cannot be denuded for what it is, what it is not, and what is universally, utterly other than it, except by (advances in) epistemology. Until then, the utmost critical attitude towards the world of informative representations (e.g., in the sense of Wittgenstein), if not the most universal nature of philosophy, science, and art, is found among individual epistemic geniuses alone — who know just "what is what" absolutely independently of all "otherness".

In the sense of the post-Kantian epistemological theory of Reality outlined in [1], Genius is indeed not even a "superlative of talent" and is separated from all else by an entire world of noumena. In terms of the ontological, multi-teleological reality alluded to therein, which embraces also the eidetic-noumenal "surject" (or "qualon", which is beyond mere "omnijectivity" and "inter-subjectivity") in addition to the usual reflection ("object"), projection ("subject"), and annihilation ("abject") in a certain domain of epistemological dimensionality ("prefect"), Genius is said to be "noumenal-reflective" ("surjective"), while talent is termed "reflective-projective" ("phenomenal-reflexive"). Thus, by itself, the said epistemological framework qualifies itself as being post-Hegelian in its sector of dialectics: by the very presence of "surjection", Genius is beyond the usual triplicity of thesis, anti-thesis, and synthesis — and so beyond all multiplicity-dependent, contingent, linear progression.

The universal logic (i.e., meta-logic) thereof, by which our epistemological meta-structure surpasses Kantian philosophy and Socratic-Hegelian dialectics entirely is four-fold, anholonomic, and asymmetric in that the general surjective representation of a universal entity, as regards its "place" in Reality, is as follows:

(without, within, within-the-within, without-the-without).

Thus, for a given complete ontological entity A (and not merely a phenomenologically abstract and concrete entity), there exists the following four-fold eidetic representation:

$$\{\mathrm{A}\} = \{\mathrm{A},\ \text{non-A},\ \text{non-non-A},\ \text{none of these}\}\,.$$

The above, being "twice-qualified ontological", is not to be confused with both four-fold phenomenological Buddhist logic (of phenomena embedded in infinite contingency) and Whiteheadian process philosophy. Rather, the first two elements, i.e., A ("without") and non-A ("within") are of the phenomenological level (in the self-dual concrete and abstract sense): given an object of contemplation ("without"), it is impossible to discern its causal, formative "interior" ("within") without considering the abstract contingency (interconnectedness) of all possible phenomenal existents; while the last two ontologically, surjectively denote Universality ("within-the-within") and Reality ("without-the-without"), respectively. These four constituents are hereby called "ontological categories" for simplicity. Therefore, an entity or instance is called "universal" if and only if it is "four-fold eidetically qualified", and not just "two-fold phenomenologically qualified".

That which is surely universally qualified as such is the Universe itself, for which we have the following representation:

$$\{\text{the Universe}\} = \{\text{the Material Universe, the Abstract Universe, the Universe-in-itself, Reality}\}\,.$$

Meanwhile, for Thought itself, we have

$$\{\text{Thought}\} = \{\text{Thought, Anti-Thought, Unthought, Reality}\}\,,$$

i.e., the Universe-in-itself corresponds to Unthought (not to be confused arbitrarily with "irrationality") in the sense that the Universe as Unthought is a direct presentation ("surdetermination") of Reality and not a mere (phenomenological-reflective) representation, rendering Reality unthinkable in the first place, and so it is beyond both the Material Universe and the Abstract Universe, which are the domains of the traditional sciences (with respect to which, therefore, progress always seems endlessly "infinite"). Note that, especially when an arbitrary "thought" other than a "truly universal thought" (peculiar to Genius) is considered, "thought" and "anti-thought" always exist in a single phenomenological contingency while their directions of causality ("momenta") differ.

This way, the Cartesian dictum, "I think therefore I am", should be replaced by a twice-qualified ontological thinker (and universal observer) as follows: "I think therefore I am, I am not, I am not-not, and none of these".

Accordingly, Reality is such that: 1. It is One-Singular and cannot be reduced to Unreality simply because "Reality-in-itself does not mingle with Unreality" in the first place, whether by necessity or by chance (i.e., unlike arbitrary phenomenological entities mingling across time and space), for otherwise (noumenal and phenomenal) "things", even the Universe itself, would cease to exist "as one and at once" (at one "Now") — and both Reality and Unreality too would be Not —, which is absurd in a four-fold manner: before, during, after, and without time. 2. It contains "things" and yet these "things" contain it not, not merely in the spatio-temporal sense but in the sense that Reality, as Moment, always precedes and surpasses "things" behind, within, and ahead of them, and "none of these at all". 3. The "distance", i.e., meta-logical foliage, between the four ontological categories is thus asymmetric and anholonomic: phenomenally approaching Reality (M) from the transitive entirety of phenomena (O) will be substantially different from approaching such phenomenal entirety (O) directly from Reality (M). In other words: $\{OM\} \neq \{MO\}$. 4. There exists a meta-logical exception in that there are surjective instances with respect to which Reality is their exception just as they are Reality's exceptions (singularities) everywhere in the Universe, i.e., they, unlike others, exist in sheer eidetic-noumenal symmetry with Reality and the Universe. Such an instance is none other than Genius. 5. In the surjective-deterministic sense of Reality, there exists an ultimate observer in the twice-qualified ontological sense of Genius, as opposed to an arbitrary observer: whether or not a leaf falls in a forest with apparently no observer around, it still falls simply because the Universe, in its capacity as an ultimate observer, observes it. This is because the universal meta-structure is such that the Universe is without both "inside" and "outside" with respect to the (noumenal) entirety of the laws of Nature. This saves both common-sense objectivity while, up to such non-arbitrary ontological qualification, keeping intact the unification of observers and observables as found in both quantum mechanics and the monad formalism of General Relativity (e.g., of Abraham Zelmanov). Otherwise, without such universal determination, one is left with mere surrealism and omnijectivity, which, as we have said, can in no way be a direct presentation of Reality-in-itself.

All that, in a word, is symbolically-noumenally written in a single "Reality equation" as follows:

$$\mathbf{M{:}\ N\big(U(g,\, dg)\big) \sim S}$$

where M stands for Reality (Reality-in-itself, "Being-qua-Being"), N for the Qualic Monad (Reality's entirely pre-reflexive, self-singular presentation of itself, i.e., with or without the Universe and reflective world-foliages, or "Multiverse"), U for the noumenal Universe (the Universe-in-itself), (g, dg) for Surjectivity and infinite self-differentiation (isomorphic to Genius — which is none other than surjective, archetypal insight and motion — and the "interior" of the Universe), and S for Suchness (Eidos).

Thus, by "Universe" — in this truly qualified sense of Reality — we always mean "Such Universe", where "Such" is "Twice-That/There" (in terms of the phenomenal "without" and the noumenal "without-the-without") and "Universe" is "Twice-This/Here" (in terms of the phenomenal "within" and the noumenal "within-the-within").

In this epistemology, the Universe — in the likeness of Reality itself — is therefore most tangible and most elusive at once: it is "that which draws near from farness and draws far from nearness". It takes Genius to truly comprehend this as it is, for the relationship between the Universe and Genius in this respect is like that between the entire cosmos and the monopolar meta-particle.

Such is how our framework generalizes Kantianism (and what not) by the presence of the self-singular monad ("surject" or "qualon", i.e., the ultimate pre-reflexive singularity) free of the inconsistent inner state of "singularity in and of multiplicity" when it comes to phenomenologically defining traditional "Kantian oneness" (due to which Kantianism ultimately fails to distinguish between — or simply transcend — "a thing-in-itself" and "another thing-in-itself", let alone between all noumena). In addition, it also effortlessly surpasses the analytical rigor of Wittgensteinian logic and eradicates all discrepancies between "essentialism" and "existentialism" on a highest possible ontological level.

As such, Genius belongs to a self-singular nature (self-constitution) of not just psychological thought, but also of Reality itself, independently of the entire contingency (and, often, over-determination) of tautologically constructed world-representations by the majority of sentient beings. Such strictly individual determination, of Genius, is thus called "surjective". This, while talent is always info-cognitively co-dependent on the entirety of prevailing contingencies, i.e., on the way a specific world is represented by them as "multiple intelligences" (through theses and anti-theses).

In other words, with respect to the Universe, Genius is Reality's very exception just as Reality is the very exception of Genius. Just as Reality is One-Singular beyond reducibility and reflexivity (mere reflection and projection), so is Genius, and so is the "mirror", i.e., the mirror in which the surjective instance of Genius appears: the Universe itself. As such, unlike the case of talent, there is indeed no such a thing as "mathematical genius", "physical genius", "philosophical genius", "musical genius", etc. as people are commonly, partially, phenomenally used to these terms. Rather, Genius is always universal and, by that very universality, it is solitary and chanceless: such is the nature of universal creation known as art, which is the quintessence (sine qua non) of genuine philosophical, artistic, and scientific creation.

In physics especially, the universal weight of an instance of scientific creation by an individual of Genius inevitably differs from the rest of physicists simply because the former moves — without residue and mere chance — as an epistemically solitary artist at the very universal level of "science-in-itself", and thus at the Universal Moment, by whose act the artist is immensely self-rewarded without even seeking recognition other than the necessity to move as the Universe categorically moves from the noumenal category to the phenomenal domain, while at best the latter is merely tautologically interested in "the problems that are important according to others" — ever at the risk of genuine originality (although, as we have seen, Genius is not a matter of merely being situational, but of the pan-Kierkegaardian infinite single-mindedness of "I cannot do otherwise", in contrast to talent).

Hence, silently in the face of Reality, Genius happens to the Universe as much as the Universe happens to it, while others can hardly notice, let alone imbibe, this epistemological degree of universal solitariness.

That is, to paraphrase Einstein somehow,

> "True science, if not art itself, consists in the following: apply yourself entirely and fearlessly to what deeply interests you the most, and not simply to what others — no matter who — are interested in, as this is between you and the Universe, not you and people. This is because every true philosopher (or profound thinker and creator), who truly understands his own moments, has his own Kant".

Of course, depending on the epistemological dimensionality of a given human endeavor or science, there are instances where "working as a group" is important and essential to progress (e.g., medicine, experimental psychology, and engineering). But in fundamental abstract sciences, as fundamental as they are in relation to art and philosophy, there should be no excuse as to the arbitrary, non-epistemological "peer-group treatment" and "machination" to which true individual geniuses are often subject, precisely because such individuals alone carry the very archetype of Universality and Revolution, which is absolutely not a matter of societal training and progress. Intrinsically, such an individual may indeed refuse the entirety of conventions of a particular society of people and their agendas in order to infinitely eye the noumenal-creative "science-in-itself", instead of just participating in "big scientism" and its often excessive relative loudness.

For instance, aside from the creation of fundamental theories or mathematical methods, the eminent general relativist who spear-headed the Soviet cosmological school, Abraham Zelmanov, is said to have regarded writing mere academic articles as a "waste of time" [5]. Also Einstein himself is known to have principally disregarded the anonymous "peer-review" system prevalent in the American system, as opposed to the way things were done rather transparently, epistemologically, and dialectically in Europe at the time his theories flourished: so long as there are no mathematical and other fundamental flaws in a submitted scientific thesis containing some genuine novelty, a corresponding anti-thesis would simply be presented by the scientific editor(s), and thereafter a common synthesis should likely be reached by both the individual scientist and the universally capable editor(s): such is the epistemologically universal way of disseminating novel scientific ideas and progress, and of championing true academic freedom, as greatly opposed to all superficial excuses (especially those made by fallible, anonymous observers). It was also Einstein's single-mindedness which made him unable to accept "quantum theory as Copenhagen sees it", strongly believing in a more deterministic (geometric) fashion thereof — a "fate" he shared with even de Broglie (who envisioned a kind of hidden "thermostat medium" in quantum physics) and Bohm (with his hidden-variable quantum theory), among others.

This, while mere "crackpots" are easily seen in broad daylight for themselves, and yet Genius is not even visible in the blazing sun of the day as in the mirrorless depths of the night — unless by way of sheer deliberation on the part of the individual of Genius himself. Indeed, of this — and after a lengthy, peripheral epistemic discourse and logical ascension — Wittgenstein himself would have said, "Up there, I am senseless: you must understand me senselessly". (See, e.g., [6]; during his entire solitary life, Wittgenstein only cared to produce two condensed philosophical works — each being a self-complete fundamental treatise written in a very unorthodox style — instead of writing mere philosophical "documentaries".)

However, the situation with "Genius and people" is rather helpless in any age due to the anholonomic, asymmetric nature of Genius — and the entire Universe itself — with respect to the rest of otherness, of which individuals of Genius are acutely conscious: just as the distance between Reality and "things" is not the same as that between "things" and Reality, as we have seen, the distance between Genius and people is not the same as that between people and Genius. Thus, mere sense-projection often only makes things worse.

To understand Genius, one must understand the noumenal Universe within its very own solitary instant, while most people, merely existing in groups and in definite contingency of both stances of the "dogmatist" (of objective dogmatism) and the "relativist" (of subjective relativism), are still far away from such cognizance, not just in the phenomenal-progressive sense, but in the entire ontological-noumenal sense. Still, one must know the noumenal even better than Kant himself understood it (and his entire epistemology), hence the phrase, "to understand Kant is to simply surpass him, there is no other way". Needless to say, the same seems to hold for most known physical theories as well — such as relativity and quantum theory, — especially in terms of the truly epistemological-universal construction of quantum gravity and unified field theories.

Indeed, while some of the known geniuses of the past are rather belatedly celebrated by people today (only to superficially project themselves on the past and to aggrandize their own sense of historical continuity as such), they always tend to neglect the geniuses of the present. This is precisely because they themselves, no matter how talented and bright, are not geniuses and have no substantial resemblance with them whatsoever: they are merely the product of the age. It is in this rather secluded Schopenhauerian-Weiningerian sense and infinite, silent understanding that Genius, more than others, embraces tragedy willingly: he is absolutely not the product of the age in the first place and he suffers most intuitively amidst people.

Hence, in any cosmic epoch, the so-called "Renaissance" is that infinitely solitary period of Genius before everyone else is capable of naming it, and not merely its subsequent, timely crumbs as received by a particular culture (society). It is the "mysterious" (as Einstein would have called it), not "public space".

A man of Genius is simply a universal volunteer on the canvas of Reality, without ulterior motives whatsoever, and without him, Reality would never "archetypally act upon itself" in and of the Universe: as such, he is most capable of infinite differentiation ("noema" and creation) peculiar to his singular Genus alone. Such Genus ("Kudos") is transcendent — not simply parallel or anti-parallel — with respect to all species.

As long as the four-fold logic behind Reality, the Universe, the manifold world-imagery, and Genius is not realized, an "objective dogmatist" will always fall into a "subjective relativist" (and mere sophist) soon enough, and vice versa, for the horizon-forming duality of phenomenological things remains as such, according to traditional "two-dimensional" (or "two-and-a-half" at most) eruditic logic. Such, then, only serves to yield a fallible observer, of whom Genius has no need whatsoever. In this sense, art is indeed most suitable to most geniuses than is academic science, precisely due to the more solitary noumenal-epistemological nature (richness) of art and its practicality at large. But, whenever such a universal mind appears in scientific territories, one must intimate the art of it all, without any "sophisticated pretention" whatsoever, rather than simply dismiss the emergent qualic unorthodoxy peculiar to Genius (for, as history has shown, such only results in one's shameful chagrin in the face of Reality, whether immediately or eventually), of which that one has no true understanding whether in short or at length. (In this respect, one can simply imagine Kant and Goethe — rather than Euler and Gauss — doing some particular sciences, apart from philosophy and art, and the predictable neglect and cold calculation of those who feel their territories have been violated. Fortunately, this particular case involving the two men and the rest of the world does not seem to have taken place.)

Undoubtedly, the foregoing epistemological discourse fully capable of mirroring "worlds", "anti-worlds", and "non-worlds", (by "world", of course we also mean "thought" or "paradigm") from the universal standpoint of Reality itself, is particularly relevant to the championing of scientific human rights as outlined in [2] as well as to the importance of aprioristic and dialectical thinking in physics (and science in general) as reflected, e.g., in [3] and [4].

All that — the Universe itself — is inevitably opposed to mere communalism, especially in the post-modern era of "big scientism".

Submitted on October 26, 2011 / Accepted on October 30, 2011

References

1. Suhendro I. The Surjective Monad Theory of Reality: A Qualified Generalization of Reflexive Monism. Original Draft (in press), 2011.
2. Rabounski D. Declaration of Academic Freedom (Scientific Human Rights). *Prog. Phys.*, 2006, v.1, 57–60.
3. Isaeva E. Rational Thinking and Reasonable Thinking in Physics. *Prog. Phys.*, 2008, v.2, 169–170.
4. Kuhn T. The Structure of Scientific Revolution. The University of Chicago Press, 2nd Edition, 1970.
5. Rabounski D. Biography of Abraham Zelmanov. *The Abraham Zelmanov Journal*, 2008, v.1, xx–xxvi.
6. Wittgenstein L. Tractatus Logico-Philosophicus. Original Draft (in a recent online version), 1918.

LETTERS TO PROGRESS IN PHYSICS

From the Chloride of Tungsten to the Upper Limit of the Periodic Table of Elements

Albert Khazan
E-mail: albkhazan@gmail.com

Experimental study of the physical chemical properties and the technology of manufacturing chemically clean hexachloride of tungsten has led to unexpected results. It was found that each element of the Periodic Table of Elements has its own hyperbola in the graph "molecular mass — content of the element". The hyperbolas differ according to the atomic mass of the elements. Lagrange's theorem shows that the tops of the hyperbolas approach to an upper limit. This upper limit means the heaviest element, which is possible in the Table. According to the calculation, its atomic mass is 411.66, while its number is 155.

1 Introduction

In the early 1960's, I and my research group worked in the Department of Rare, Radioactive Metals and Powder Metallurgy at Moscow Institute of Steel and Alloys, Russia. We looked for a better technology of manufacturing the chemically clean hexachlorid of tungsten (WCl_6) through chlorination of ferrotungsten. Then, in the 1970's, I continued this experimental research study at the Baikov Institute of Metallurgy, Russian Academy of Sciences.

Our main task in this experimental search was to obtain a purely oxygen-free product. Because the raw material we worked with was resented as a many-component gaseous mix, we studied behaviour of the vaporous medleys during filtering them by saline method, distillation, and rectification. As a result, the percent of mass of the metal we have obtained in vaporous medley was 99.9% for W, 20.0% for Mo, 2.0% for Fe [1–3].

After cleaning the obtained condensate with the aforementioned methods, we have found a small inclusion of the chloride compound of tungsten in it. This chloride compound of tungsten differs from the hexachloride of tungsten in colour and the boiling temperature, which was 348°C for WCl_6, 286°C for WCl_5, and 224°C for $WOCl_4$ [4]. The cleaned hexachloride of tungsten recovers to the powder metallic state by hydrogen in the boiling layer, in plasma, precipitates as a thin cover on a base in use. It is used for manufacturing alloys with other metals through metalthermic method, etc. [5].

2 Results

In development of this technology, it was found that the theoretical (expected) results of the chemical analysis of the vaporous medleys do not match the experimental results for a little. This occurred due to some quantity of WO_2Cl_2 and $WOCl_4$ obtained in the process, which were used further for manufacturing a high clean WO_3 [6]. In order to keep control on the product of the chemical reactions, we have drawn dependencies of the content of tungsten, chlorine, and oxygen in the compounds (per one gram-atom of each element). This is necessary because, for example, the common quantity of the chloride of tungsten in chlorides is presented with a broken line (see Fig. 1) whose mathematical equation is impossible. As was found, after our Fig. 1, the arc of the content of tungsten is presented with an equilateral hyperbola $Y = K/X$ wherein its different compounds (in particular WO_3) are located. In analogy to this graph, the respective arcs were obtained for chlorine and oxygen, which appeared as hyperbolas as well.

Further checking for the possibility of creating similar functions for the other chemical elements manifested the fact that each element of the Periodic Table of Elements has its own hyperbola, which differs from the others according to the atomic mass of the element. As an example, Fig. 2 shows the hyperbolas created for the elements of Group 2, including the hypothetical elements No.126 and No.164. As is known, an equilateral hyperbola is symmetric with respect to the bisector of the angle XOY in the first quarter. Besides, the bisector coincides with the real axis, while the point of intersection of it with the hyperbola (the top point) is determined as the square root from $K(X_0 = Y_0)$. Respectively, for instance, the top point of the hyperbola of beryllium (atomic mass 9.0122) is located at $X_0 = Y_0 = 3.00203$.

In chemistry, it is commonly assumed to calculate the quantity of a reacted element in the parts of unit. Therefore, the hyperbola of each element begins from the mass of the element and $Y = 1$. From here, through Lagrange's theorem, we calculate the top of the hyperbola of beryllium: $X = 60.9097$, $Y = 0.14796$. Comparing the obtained coordinates, it is easy to see that $X/X_0 = 20.2895$ and $Y_0/Y = 20.2895$, which is the inverse proportionality with a respective scaling coefficient. Tangent of the angle of inclination of the real axis in the other (scaled) coordinates is $Y/X = 0.14796/60.9097 = 0.00242917$. The scaling coefficient al-

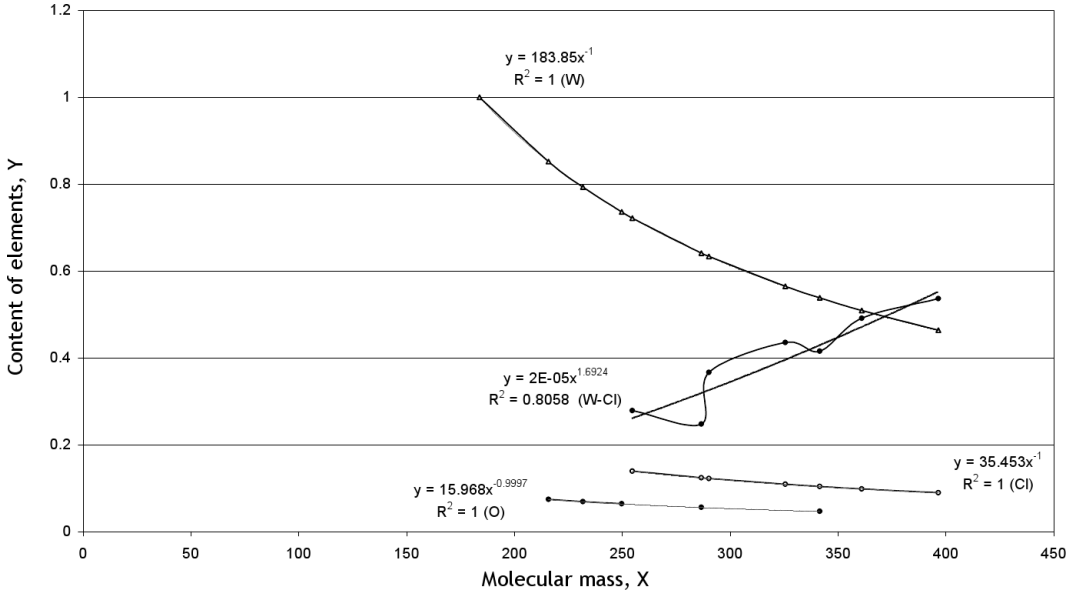

Fig. 1: The common quantity of the chloride of tungsten in chlorides.

lowed us to create a line joining the tops of the hyperbolas, located in the real axis (see Fig. 3). This is a straight crossing the line $Y = 1$, where the atomic and molecular masses of an element described by the hyperbolas are equal to each other ($K = X$). This is only possible if the origin of the hyperbola and its top meet each other at a single point where the content Y takes maximal numerical value (according to the equation $Y = K/X$). Atomic mass of this «ultimate» element, determined by the crossing point, was calculated with use of the scaling coefficient and the tangent of inclination of the real axis: $X = Y/\tan\alpha = 1/0.00242917 = 411.663243$. This calculated element is the last (heaviest of all theoretically possible elements) in the Periodic Table of Elements because Y cannot exceed 1. The second important characteristic of the element – its atomic number – was calculated through the equation of the exponent $Y = 1.6089\exp^{1.0993x}$ ($R^2 = 0.9966$). The calculated number of the last element is 155. With use of these equations, the respective parameters of all other elements of the Periodic Table can be calculated, including in the interval of super-heavy elements No.114–No.155 [7, 8].

3 Discussion

We see that on the basis of the initially experimental studies of the chloride of tungsten, a new law was found in the Periodic Table of Elements. This is the hyperbolic law, according to which the content Y of any element (per 1 gram-atom) in any chemical compound of a molecular mass X can be described by the equation of the positive branches of an equilateral hyperbola of the kind $Y = K/X$ (where $Y \leqslant 1$ and $K \leqslant X$). The hyperbolas of the respective chemical elements lie in the order of the increasing nuclear charge, and have a common real axis which meets their tops. The tops, with distance from the origin of the coordinates, approach the location $Y = 1$ and $K = X$ wherein atomic mass takes its maximally possible numerical value, which indicates the last (heaviest) element of the Periodic Table.

It should be noted that the new dependencies we pointed out here have provided not only better conditions of applied research, but also a possibility for re-considering our views on the conditions of synthesis of super-heavy elements. If already in 2003 theoretical physicists discussed properties of elements with number near 400 whose nuclei contain until 900 neutrons each [9], in February 2009, after primary publication of our studies, they discuss the elements with numbers not higher than 150–200 [10].

Submitted on November 18, 2011 / Accepted on November 22, 2011

References

1. Zelikman A. N., Stephanyuk S. L., and KhazanA. Z. *Russ. J. Non-Ferrous Metals*, 1969, no.5, 72.
2. Zelikman A. N., Stephanyuk S. L., and Khazan A. Z. *Russ. J. Non-Ferrous Metals*, 1970, no.1, 69.
3. Zelikman A. N., Stephanyuk S. L., Khazan A. Z., and Ivanov M. I. *Metallurgiya*, 1972, v.75, 60.
4. Zelikman A. N. and Nikitina L. S. Tungsten. Metallurgiya Press, Moscow, 1978.
5. Khazan A. Z. Study of the Experimental Method of Manufacturing the Hexachloride of Tungsten through Chlorination of Ferrotungsten and Tungsten. Baikov Inst. of Metallurgy and Materials Science, Moscow, 1971.
6. Zelikman A. N., Dmitriev Yu. M., and Khazan A. Z. *Izvestiya Acad. Sci. USSR Inorganic Materials*, 1965, v.1, 1582.

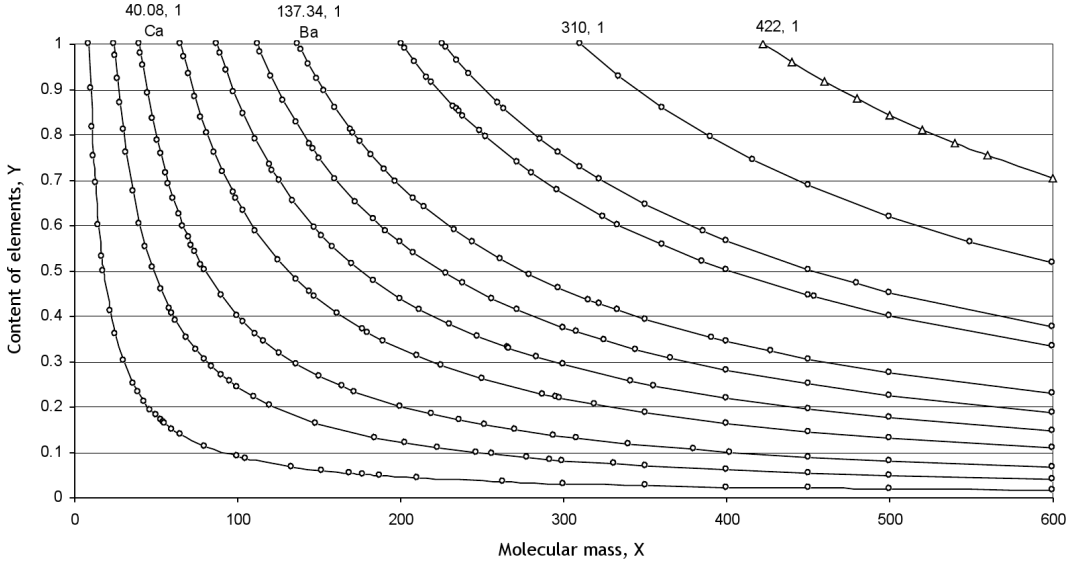

Fig. 2: The hyperbolas created for the elements of Group 2, including the hypothetical elements No.126 and No.164.

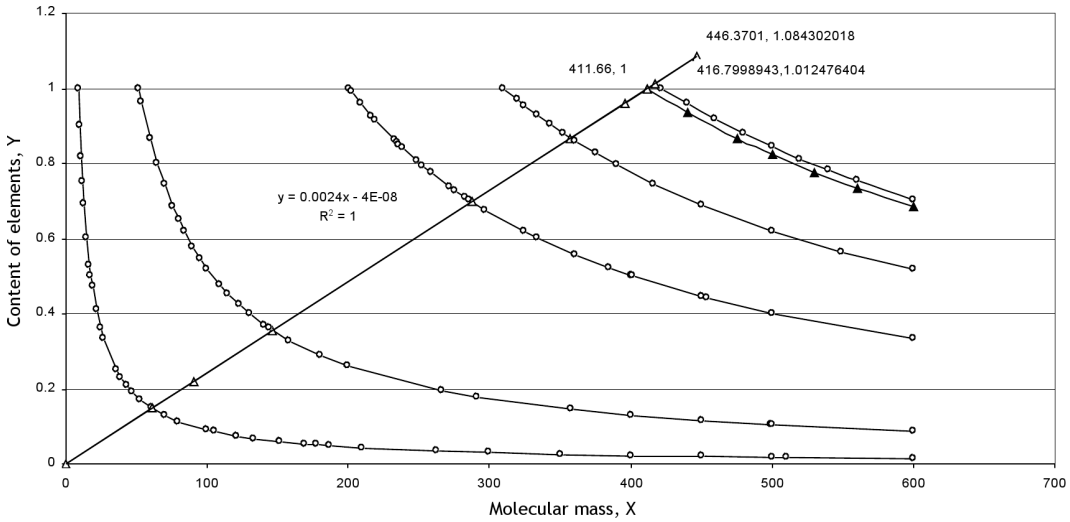

Fig. 3: The upper limit of the Periodic Table of Elements.

7. Khazan A. *Progress in Physics*, 2007, v.1, 38.
8. Khazan A. Upper Limit in Mendeleev's Periodic Table — Element No.155. Svenska fysikarkivet, Stockholm, 2010.
9. Oganesyan Yu. T. *Atomium*, 2003, v.1, 5.
10. *Weekly Bulletin of the Joint Inst. of Nuclear Research* (*Dubna*), 2009, no.3944.

LETTERS TO PROGRESS IN PHYSICS

Superluminal Physics and Instantaneous Physics as New Trends in Research

Florentin Smarandache
Department of Mathematics and Sciences, University of New Mexico, 200 College Road, Gallup, NM 87301, USA
Email: smarand@unm.edu

In a similar way as passing from Euclidean Geometry to Non-Euclidean Geometry, we can pass from Subluminal Physics to Superluminal Physics, and further to Instantaneous Physics. In the lights of two consecutive successful CERN experiments with superluminal particles in the Fall of 2011, we believe that these two new fields of research should begin developing.

1 Introduction

Let's start by recalling the history of geometry in order to connect it with the history of physics.

Then we present the way of S-denying a law (or theory) and building a spectrum of spaces where the same physical law (or theory) has different forms, then we mention the S-multispace with its multistructure that may be used to the Unified Field Theory by employing a *multifield*.

It is believed that the S-multispace with its multistructure is the best candidate for 21st century *Theory of Everything* in any domain.

2 Geometry's history

As in Non-Euclidean Geometry, there are models that validate the hyperbolic geometric and of course invalidate the Euclidean geometry, or models that validate the elliptic geometry and in consequence they invalidate the Euclidean geometry and the hyperbolic geometry.

Now, we can mix these geometries and construct a model in which an axiom is partially validated and partially invalidated, or the axiom is only invalidated but in multiple different ways [1]. This operation produces a degree of negation of an axiom, and such geometries are hybrid. We can in general talk about the *degree of negation of a scientific entity* P, where P can be a theorem, lemma, property, theory, law, etc.

3 S-denying of a theory

Let's consider a physical space S endowed with a set of physical laws L, noted by (S, L), such that all physical laws L are valid in this space S.

Then, we construct another physical space (or model) S_1 where a given law has a different form, afterwards another space S_2 where the same law has another form, and so on until getting a spectrum of spaces where this law is different.

We thus investigate spaces where anomalies occur [2].

4 Multispace theory

In any domain of knowledge, multispace (or S-multispace) with its multistructure is a finite or infinite (countable or uncountable) union of many spaces that have various structures. The spaces may overlap [3].

The notions of multispace (also spelt multi-space) and multistructure (also spelt multi-structure) were introduced by the author in 1969 under his idea of hybrid science: combining different fields into a unifying field (in particular combinations of different geometric spaces such that at least one geometric axiom behaves differently in each such space), which is closer to our real life world since we live in a heterogeneous multispace. Today, this idea is accepted by the world of sciences. S-multispace is a qualitative notion, since it is too large and includes both metric and non-metric spaces.

A such multispace can be used for example in physics for the Unified Field Theory that tries to unite the gravitational, electromagnetic, weak and strong interactions by constructing a *multifield* formed by a gravitational field united with an electromagnetic field united with a weak-interactions field and united with a strong-interactions field.

Or in the parallel quantum computing and in the mu-bit theory, in multi-entangled states or particles and up to multi-entangles objects.

We also mention: the algebraic multispaces (multi-groups, multi-rings, multi-vector spaces, multi-operation systems and multi-manifolds, also multi-voltage graphs, multi-embedding of a graph in an n-manifold, etc.) or structures included in other structures, geometric multispaces (combinations of Euclidean and Non-Euclidean geometries into one space as in S-geometries), theoretical physics, including the Relativity Theory [4], the M-theory and the cosmology, then multi-space models for p-branes and cosmology, etc.

The multispace is an extension of the neutrosophic logic and set, which derived from neutrosophy. Neutrosophy (1995) is a generalization of dialectics in philosophy, and takes into consideration not only an entity <A> and its opposite <antiA> as dialectics does, but also the neutralities <neutA> in between. Neutrosophy combines all these three <A>, <antiA>, and <neutA> together. Neutrosophy is a metaphilosophy.

Neutrosophic logic (1995), neutrosophic set (1995), and

neutrosophic probability (1995) have, behind the classical values of truth and falsehood, a third component called indeterminacy (or neutrality, which is neither true nor false, or is both true and false simultaneously — again a combination of opposites: true and false in indeterminacy).

Neutrosophy and its derivatives are generalizations of the paradoxism (1980), which is a vanguard in literature, arts, and science, based on finding common things to opposite ideas (i.e. combination of contradictory fields).

5 Physics history and the future

a) With respect to the size of space there are: *Quantum Physics* which is referring to the subatomic space, the *Classical Physics* to our intuitive living space, while *Cosmology* to the giant universe;

b) With respect to the direct influence: the *Locality*, when an object is directly influenced by its immediate surroundings only, and the *Nonlocality*, when an object is directly influenced by another distant object without any interaction mediator;

c) With respect to the speed: the *Newtonian Physics* is referred to low speeds, the *Theory of Relativity* to subluminal speeds near to the speed of light, while *Superluminal Physics* will be referred to speeds greater than c, and *Instantaneous Physics* to instantaneous motions (infinite speeds).

A physical law has a form in Newtonian physics, another form in Relativity Theory, and different form at Superluminal theory, or at Infinite (Instantaneous) speeds — as above in the S-Denying Theory spectrum.

We get new physics at superluminal speeds and other physics at a very very big speed ($v \gg c$) speeds or at instantaneous (infinite) traveling.

At the beginning we have to extend physical laws and formulas to superluminal traveling and afterwards to instantaneous traveling.

For example, what/how would be Doppler effect if the motion of an emitting source relative to an observer is greater than c, or $v \gg c$ (much greater than c), or even at instantaneous speed?

Also, what addition rule should be used for superluminal speeds?

Then little by little we should extend existing classical physical theories from subluminal to superluminal and instantaneous traveling.

For example: if possible how would the Theory of Relativity be adjusted to superluminal speeds?

Lately we need to found a general theory that unites all theories at: law speeds, relativistic speeds, superluminal speeds, and instantaneous speeds — as in the S-Multispace Theory.

6 Conclusion

Today, with many contradictory theories, we can reconcile them by using the S-Multispace Theory.

We also propose investigating new research trends such as Superluminal Physics and Instantaneous Physics. Papers in these new fields of research should be e-mailed to the author by July 01, 2012, to be published in a collective volume.

Submitted on December 02, 2011 / Accepted on December 05, 2011

References

1. Linfan Mao. Automorphism groups of maps, surfaces and Smarandache geometries. arXiv: math/0505318.
2. Smarandache F. S-Denying a Theory. *Progress in Physics*, 2011, v.1, 71–74.
3. Smarandache F. Multispace and Multistructure as a Theory of Everything. *13th Annual Meeting of the Northwest Section of the APS*, Session D1, LaSells Stewart Center, Public Gallery (room), Oregon State University, Corvallis, Oregon, USA, 04:30 PM on Friday, October 21, 2011.
4. Rabounski D. Smarandache Spaces as a New Extension of the Basic Space-Time of General Relativity. *Progress in Physics*, 2010, v.2, L1–L2.

LETTERS TO PROGRESS IN PHYSICS

A More Elegant Argument that *P≠NP*

Craig Alan Feinstein
2712 Willow Glen Drive, Baltimore, Maryland 21209
Email: cafeinst@msn.com

In April 2011, Craig Alan Feinstein published a paper in *Progress in Physics* entitled "An elegant argument that $P \neq NP$". Since then, Craig Alan Feinstein has discovered how to make that argument much simpler. In this letter, we present this argument.

In April 2011, I published a paper in *Progress in Physics* entitled "An elegant argument that $P \neq NP$" [1]. Since then, I have discovered how to make that argument much simpler. In this letter, I present this argument.

Consider the following problem: Let $\{s_1, \ldots, s_n\}$ be a set of n integers and t be another integer. We want to determine whether there exists a subset of $\{s_1, \ldots, s_n\}$ for which the sum of its elements equals t. We shall consider the sum of the elements of the empty set to be zero. This problem is called the SUBSET-SUM problem [2].

Let $k \in \{1, \ldots, n\}$. Then the SUBSET-SUM problem is equivalent to determining whether there exist sets $I^+ \subseteq \{1, \ldots, k\}$ and $I^- \subseteq \{k+1, \ldots, n\}$ such that

$$\sum_{i \in I^+} s_i = t - \sum_{i \in I^-} s_i \, .$$

There is nothing that can be done to make this equation simpler. Then since there are 2^k possible expressions on the left-hand side of this equation and 2^{n-k} possible expressions on the right-hand side of this equation, we can find a lower-bound for the worst-case running-time of an algorithm that solves the SUBSET-SUM problem by minimizing $2^k + 2^{n-k}$ subject to $k \in \{1, \ldots, n\}$.

When we do this, we find that $2^k + 2^{n-k} = 2^{\lfloor n/2 \rfloor} + 2^{n-\lfloor n/2 \rfloor} = \Theta(\sqrt{2^n})$ is the solution, so it is impossible to solve the SUBSET-SUM problem in $o(\sqrt{2^n})$ time with a deterministic and exact algorithm. This lower-bound is tight [1]. And this conclusion implies that $P \neq NP$ [2].

Submitted on December 11, 2011 / Accepted on December 20, 2011

References

1. Feinstein C.A. An elegant argument that $P \neq NP$. *Progress in Physics*, 2011, v. 2, 30–31.
2. Cormen T.H., Leiserson C.E., and Rivest R.L. Introduction to Algorithms. McGraw-Hill, 1990.

The Journal on Advanced Studies in Theoretical and Experimental Physics, including Related Themes from Mathematics

PROGRESS IN PHYSICS

A quarterly issue scientific journal, registered with the Library of Congress (DC, USA). This journal is peer reviewed and included in the abstracting and indexing coverage of: Mathematical Reviews and MathSciNet (AMS, USA), DOAJ of Lund University (Sweden), Zentralblatt MATH (Germany), Scientific Commons of the University of St. Gallen (Switzerland), Open-J-Gate (India), Referativnyi Zhurnal VINITI (Russia), etc.

Electronic version of this journal:
http://www.ptep-online.com

Postal Address

Department of Mathematics and Science,
University of New Mexico,
705 Gurley Ave., Gallup, NM 87301, USA

ISSN: 1555-5534 (print)
ISSN: 1555-5615 (online)

Standard Address Number: 297-5092
Printed in the United States of America

APRIL 2012 **VOLUME 2**

CONTENTS

Information for Authors and Subscribers

Progress in Physics has been created for publications on advanced studies in theoretical and experimental physics, including related themes from mathematics and astronomy. All submitted papers should be professional, in good English, containing a brief review of a problem and obtained results.

All submissions should be designed in LaTeX format using *Progress in Physics* template. This template can be downloaded from *Progress in Physics* home page http://www.ptep-online.com. Abstract and the necessary information about author(s) should be included into the papers. To submit a paper, mail the file(s) to the Editor-in-Chief.

All submitted papers should be as brief as possible. We accept brief papers, no larger than 8 typeset journal pages. Short articles are preferable. Large papers can be considered in exceptional cases to the section *Special Reports* intended for such publications in the journal. Letters related to the publications in the journal or to the events among the science community can be applied to the section *Letters to Progress in Physics*.

All that has been accepted for the online issue of *Progress in Physics* is printed in the paper version of the journal. To order printed issues, contact the Editors.

This journal is non-commercial, academic edition. It is printed from private donations. (Look for the current author fee in the online version of the journal.)

Relativistic Dynamical Theory for Test Particles and Photons in Static Spherically Symmetric Gravitational Fields

Chifu Ebenezer Ndikilar

Gombe State University, Faculty of Science, Physics Department, P.M.B. 127, Gombe, Gombe State, Nigeria
E-mail: ebenechifu@yahoo.com

The gravitational line element in this field is used to postulate the four spacetime element of arc vector, volume element, del operator and divergence operator for space-time gravitational fields. A relativistic dynamical theory is then established for static spherically symmetric gravitational fields. Equations of motion for test particles and photons are obtained with post Newton and post Einstein correction terms of all orders of c^{-2}.

1 Introduction

Schwarzschild in 1916 constructed the first exact solution of Einstein's gravitational field equations. It was the metric due to a static spherically symmetric body situated in empty space such as the Sun or a star [1].

In this article, we establish a link between Schwarzschild's metric and Newton's dynamical theory of gravitation. The consequence of this approach is the emergence of complete expressions for the velocity, acceleration and total energy with post Newton and post Einstein correction terms to all orders of c^{-2} [2].

2 Euclidean Geometry in Static Spherically Symmetric Fields

Recall that the scalar world line element dS^2 in Schwarzschild's gravitational field is given as

$$dS^2 = -g_{11}dr^2 - g_{22}d\theta^2 - g_{33}d\phi^2 + g_{00}(dx^0)^2 \qquad (2.1)$$

where

$$g_{00} = \left(1 - \frac{2GM}{c^2 r}\right),$$

$$g_{11} = \left(1 - \frac{2GM}{c^2 r}\right)^{-1},$$

$$g_{22} = r^2,$$

$$g_{33} = r^2 \sin^2\theta.$$

G is the universal gravitational constant, c is the speed of light in vacuum and M is the mass of the static homogeneous spherical mass (Schwarzschild's mass) [3, 4]. Now, also recall that the world line element dS^2 from which the metric tensor is formulated is obtained from the fundamental line element $d\overline{S}(r,\theta,\phi)$. Also, from vector analysis, it is well known that $d\overline{S}(r,\theta,\phi)$ is the most fundamental quantity from which all vector and scalar quantities required for the formulation of the dynamical theory of classical mechanics are derived.

2.1 Element of arc vector

From equation (2.1), we realise that Schwarzschild's gravitational field is a four dimensional orthogonal vector space with coordinates (r,θ,ϕ,x^0) and unit vectors $(\widehat{r},\widehat{\theta},\widehat{\phi},\widehat{x^0})$ and hence the element of arc vector $d\overline{S}$ is given as

$$\begin{aligned} d\overline{S} &= [-g_{11}]^{1/2}(dr)\widehat{r} + [-g_{22}]^{1/2}(d\theta)\widehat{\theta} \\ &+[-g_{33}]^{1/2}(d\phi)\widehat{\phi} + [g_{00}]^{1/2}(dx^0)\widehat{x^0} \end{aligned} \qquad (2.2)$$

with scale factors h_r, h_θ, h_ϕ and h_{x^0} defined as

$$h_r = [-g_{11}]^{1/2},$$

$$h_\theta = [-g_{22}]^{1/2},$$

$$h_\phi = [-g_{33}]^{1/2},$$

$$h_{x^0} = [g_{00}]^{1/2}.$$

2.2 Volume element and Gradient operators

As in Eulidean geometry in three dimensional vector space, we postulate that the volume element dV in Schwarzschild's gravitational field is given by

$$dV = dS_r dS_\theta dS_\phi dS_{x^0} \qquad (2.3)$$

and the corresponding space element of volume

$$dV = dS_r dS_\theta dS_\phi, \qquad (2.4)$$

where

$$\begin{aligned} dS_r &= h_r dr, \\ dS_\theta &= h_\theta d\theta, \\ dS_\phi &= h_\phi d\phi, \\ dS_{x^0} &= h_{x^0} dx^0. \end{aligned}$$

We postulate that our complete spacetime del operator in Schwarzschild's gravitational field is given as

$$\overline{\nabla} = \frac{\widehat{r}}{h_r}\frac{\partial}{\partial r} + \frac{\widehat{\theta}}{h_\theta}\frac{\partial}{\partial\theta} + \frac{\widehat{\phi}}{h_\phi}\frac{\partial}{\partial\phi} + \frac{\widehat{x^0}}{h_{x^0}}\frac{\partial}{\partial x^0}. \qquad (2.5)$$

The complete spacetime divergence, curl and laplacian operators can be defined in a similar manner[2].

3 Relativistic Dynamical Theory for Test Particles

From the spacetime line element, the instantaneous spacetime velocity vector in the gravitational field can be defined[2] as

$$\overline{u} = \frac{d\overline{S}}{d\tau} \tag{3.1}$$

or

$$\overline{u} = u_r\hat{r} + u_\theta\hat{\theta} + u_\phi\hat{\phi} + u_{x^0}\hat{x}^0, \tag{3.2}$$

where τ is the proper time,

$$u_r = \left(1 - \frac{2GM}{c^2 r}\right)^{-1/2} \dot{r},$$

$$u_\theta = r\dot{\theta},$$

$$u_\phi = r\sin\theta\dot{\phi}$$

and

$$u_{x^0} = \left(1 - \frac{2GM}{c^2 r}\right)^{1/2} \dot{x}^0.$$

Hence, the instantaneous speed u is

$$u^2 = \left(1 - \frac{2GM}{c^2 r}\right)^{-1} \dot{r}^2 + r^2\dot{\theta}^2 + r^2\sin^2\theta\dot{\phi}^2 + \left(1 - \frac{2GM}{c^2 r}\right)(\dot{x}^0)^2. \tag{3.3}$$

Also the instantaneous spacetime acceleration vector is given as

$$\overline{a} = \frac{d\overline{u}}{d\tau} \tag{3.4}$$

or

$$\overline{a} = a_r\hat{r} + a_\theta\hat{\theta} + a_\phi\hat{\phi} + a_{x^0}\hat{x}^0, \tag{3.5}$$

where

$$a_r = \left(1 - \frac{2GM}{c^2 r}\right)^{-1/2} \ddot{r} - \frac{GM}{c^2 r^2}\left(1 - \frac{2GM}{c^2 r}\right)^{-3/2} \dot{r}^2,$$

$$a_\theta = r\ddot{\theta} + \dot{r}\dot{\theta},$$

$$a_\phi = \dot{r}\sin\theta\dot{\phi} + r\cos\theta\dot{\theta}\dot{\phi} + r\sin\theta\ddot{\phi}$$

and

$$a_{x^0} = \frac{d}{d\tau}\left[\left(1 - \frac{2GM}{c^2 r}\right)^{1/2} \dot{x}^0\right].$$

Now, recall that the inertial mass m_I and passive mass m_p are related to the rest mass m_0 of a particle by

$$m_I = m_p = \left(1 - \frac{u^2}{c^2}\right)^{-1/2} m_0 \tag{3.6}$$

where in this gravitational field, u^2 is as defined in equation (3.3). Also, the linear momentum of a particle of nonzero rest mass is defined as

$$\overline{P} = m_I\overline{u} \tag{3.7}$$

or

$$\overline{P} = \left(1 - \frac{u^2}{c^2}\right)^{-1/2} m_0\overline{u}. \tag{3.8}$$

The instantaneous relativistic kinetic energy (T) of a particle of nonzero rest mass is given as

$$T = (m_I - m_0)\,c^2 \tag{3.9}$$

or

$$T = \left[\left(1 - \frac{u^2}{c^2}\right)^{-1/2} - 1\right] m_0 c^2 \tag{3.10}$$

and the instantaneous relativistic gravitational potential energy (V_g) for a particle of nonzero rest mass is

$$V_g = m_p\Phi = -\left(1 - \frac{u^2}{c^2}\right)^{-1/2} \frac{GMm_0}{r}, \tag{3.11}$$

where $\Phi = \frac{-GM}{r}$ is the gravitational scalar potential in Schwarzschild's gravitational field. Thus, the total relativistic mechanical energy E for a particle of nonzero rest mass is given as

$$E = T + V_g \tag{3.12}$$

or

$$E = m_0 c^2\left[\left(1 - \frac{GM}{c^2 r}\right)\left(1 - \frac{u^2}{c^2}\right)^{-1/2} - 1\right]. \tag{3.13}$$

Thus, our expression for total energy has post Newton and post Einstein correction terms of all orders of c^{-2}.

The relativistic dynamical equation of motion for particles of non-zero rest mass[2] is given as

$$\frac{d}{d\tau}\overline{P} = -m_p\overline{\nabla}\Phi \tag{3.14}$$

or

$$\frac{d}{d\tau}\left[\left(1 - \frac{u^2}{c^2}\right)^{-1/2} m_0\overline{u}\right] = -\left(1 - \frac{u^2}{c^2}\right)^{-1/2} m_0\overline{\nabla}\Phi \tag{3.15}$$

or

$$\overline{a} + \frac{1}{2c^2}\left(1 - \frac{u^2}{c^2}\right)^{-1} \frac{d}{d\tau}(u^2)\overline{u} = -\overline{\nabla}\Phi. \tag{3.16}$$

Thus, the spacetime relativistic dynamical equations of motion in static spherically symmetric gravitational field can be obtained from (3.16). The time equation of motion is obtained as

$$a_{x_0} + \frac{1}{2c^2}\left(1 - \frac{u^2}{c^2}\right)^{-1} \frac{d}{d\tau}(u^2)u_{x^0} = 0 \tag{3.17}$$

or

$$\frac{d}{d\tau}\left[\left(1 - \frac{2GM}{c^2 r}\right)^{1/2} \dot{x}^0\right] + \frac{1}{2c^2}\left(1 - \frac{u^2}{c^2}\right)^{-1} \frac{d}{d\tau}(u^2)u_{x^0} = 0. \tag{3.18}$$

Notice that the first term of equation (3.18) is exactly the expression obtained for the general relativistic time dilation and hence the second term is a correction term obtained from our dynamical approach in Schwarzschild's gravitational field.

Also, the respective azimuthal, polar and radial equations of motion are obtained as

$$\begin{aligned} &\dot{r}\sin\theta\dot{\phi} + r\cos\theta\dot{\theta}\dot{\phi} + r\sin\theta\ddot{\phi} \\ &+\frac{1}{2c^2}\left(1-\frac{u^2}{c^2}\right)^{-1}\frac{d}{d\tau}(u^2)u_\phi \;=\; 0, \end{aligned} \tag{3.19}$$

$$r\ddot{\theta} + \dot{r}\dot{\theta} + \frac{1}{2c^2}\left(1-\frac{u^2}{c^2}\right)^{-1}\frac{d}{d\tau}(u^2)u_\theta \;=\; 0 \tag{3.20}$$

and

$$\begin{aligned} &a_r + \frac{1}{2c^2}\left(1-\frac{u^2}{c^2}\right)^{-1}\frac{d}{d\tau}(u^2)u_r \\ &= -\frac{GM}{r^2}\left(1-\frac{2GM}{c^2 r}\right)^{-1/2} \end{aligned} \tag{3.21}$$

with correction terms not found in the general relativistic approach.

4 Relativistic Dynamical Theory for Photons

The instantaneous passive and inertial mass of photons is given as

$$m_p = m_I = \frac{h\nu}{c^2}, \tag{4.1}$$

where h is Planck's constant. Precisely, as in Special Relativity, we postulate that the relativistic dynamical linear momentum of photons is given as

$$\overline{P} = \frac{h\nu}{c^2}\overline{u}, \tag{4.2}$$

where $\overline{u}$ is as defined in (3.2). The relativistic dynamical kinetic energy for photons is given as

$$T = (m_I - m_0)c^2 \tag{4.3}$$

or

$$T = h(\nu - \nu_0). \tag{4.4}$$

Also, as in Newton's dynamical theory of classical mechanics, the relativistic dynamical gravitational potential energy of photons(V_g) is postulated to be given by

$$V_g = m_p\Phi. \tag{4.5}$$

Hence, in static spherically symmetric gravitational fields

$$V_g = -\frac{h\nu}{c^2}\frac{GM}{r}. \tag{4.6}$$

Thus, the total mechanical energy E of a photon is given as

$$E \;=\; h(\nu - \nu_0) - \frac{h\nu}{c^2}\frac{GM}{r}. \tag{4.7}$$

If the mechanical energy of the photon is E_0 at $r = r_0$ then using the principle of conservation of mechanical energy it can be deduced that

$$\nu \;=\; \frac{E_0}{h}\left(1-\frac{GM}{c^2 r}\right)^{-1} \tag{4.8}$$

or

$$\nu \;=\; \nu_0\left(1-\frac{GM}{c^2 r_0}\right)\left(1-\frac{GM}{c^2 r}\right)^{-1}. \tag{4.9}$$

Equation (4.9) is our newly derived expression for gravitational spectral shift for static spherically symmetric mass distributions with post Newtonian and post Einstein corrections of all orders of c^{-2}.

Also, the relativistic dynamical equation of motion for photons in static spherically symmetric gravitational fields can be obtained as

$$\frac{d}{d\tau}\left[\left(1-\frac{GM}{c^2 r}\right)^{-1}\overline{u}\right] \;=\; -\left(1-\frac{GM}{c^2 r}\right)^{-1}\overline{\nabla}\Phi \tag{4.10}$$

from which the instaneous velocity and acceleration vectors can be obtained.

5 Conclusion

Instructively, this approach unifies the dynamical and geometrical theories of gravitation for test particles and photons in static spherically symmetric gravitational fields. It is hoped that if it is well developed it can account for most corrections of theoretical results in gravitational fields. It is also hoped that this approach can also be used to establish the long desired unification of gravitational fields with other fundamental fields in nature.

Submitted on October 4, 2011 / Accepted on October 13, 2011

References

1. Bergmann P.G. Introduction to the Theory of Relativity, Prentice Hall, New Delhi, 1987.
2. Howusu S.X.K. Complete Dynamical Theories of Physics, Jos University Press, Jos, 2010.
3. Howusu S.X.K. The 210 astrophysical solutions plus 210 cosmological solutions of Einstein's geometrical gravitational field equations. Jos University Press, Jos, 2007.
4. Schwarzschild K. Über das Gravitationsfeld eines Massenpunktes nach der Einsteinschen Theorie. *Sitzungsberichte der Königlich Preussischen Akademie der Wissenschaften*, 1916, 189–196 (published in English as: Schwarzschild K. On the gravitational field of a point mass according to Einstein's theory. *Abraham Zelmanov Journal*, 2008, v. 1, 10–19).

The Turning Point for the Recent Acceleration of the Universe with a Cosmological Constant

T. X. Zhang

Department of Physics, Alabama A & M University, Normal, Alabama, U.S.A.
E-mail: tianxi.zhang@aamu.edu

The turning point and acceleration expansion of the universe are investigated according to the standard cosmological theory with a non-zero cosmological constant. Choosing the Hubble constant H_0, the radius of the present universe R_0, and the density parameter in matter $\Omega_{M,0}$ as three independent parameters, we have analytically examined the other properties of the universe such as the density parameter in dark energy, the cosmological constant, the mass of the universe, the turning point redshift, the age of the present universe, and the time-dependent radius, expansion rate, velocity, and acceleration parameter of the universe. It is shown that the turning point redshift is only dependent of the density parameter in matter, not explicitly on the Hubble constant and the radius of the present universe. The universe turned its expansion from past deceleration to recent acceleration at the moment when its size was about 3/5 of the present size if the density parameter in matter is about 0.3 (or the turning point redshift is 0.67). The expansion rate is very large in the early period and decreases with time to approach the Hubble constant at the present time. The expansion velocity exceeds the light speed in the early period. It decreases to the minimum at the turning point and then increases with time. The minimum and present expansion velocities are determined with the independent parameters. The solution of time-dependent radius shows the universe expands all the time. The universe with a larger present radius, smaller Hubble constant, and/or smaller density parameter in matter is elder. The universe with smaller density parameter in matter accelerates recently in a larger rate but less than unity.

1 Introduction

The measurements of type Ia supernovae to appear fainter and thus further away than expected have indicated that the universe turned its expansion from past deceleration to recent acceleration [1-4]. The dark energy, a hypothetical form of negative pressure, is generally suggested to be the cause for the universe to accelerate recently. The Einsteinian cosmological constant Λ, initially assumed for a static model of the universe, is the simplest candidate of the dark energy [5]. Quintessence such as the scalar field from the scalar-tensor theory or the five-dimensional Kaluza-Klein unification theory is usually considered as another candidate of the dark energy [6-9]. In the black hole universe model, proposed recently by the author, the dark energy is nothing but the accretion of mass in an increasing time rate from outside space, the mother universe [10-17]. In the black hole universe model, the cosmological constant can be represented as $\Lambda = 3(\dot{M}/M)^2$, where M is the universe mass and $\dot{M}$ is the time rate of the universe mass. However, when the universe turns or what the redshift of the turning point for the universe to turn its expansion from past deceleration to recent acceleration has not yet been consistently and precisely determined.

The turning point redshift $Z_{\rm TP}$ was determined to be ~ 0.5 by combining the redshift and luminosity observations of type Ia supernovae with the standard model of cosmology [2, 4]. The universe was considered to be flat (i.e., $k = 0$ with k the curvature of the universe) with a cold dark matter (CDM) and a constant dark energy density (i.e., the cosmological constant). To explain the measurements of type Ia supernovae with the flat universe model, the density parameters in matter and dark energy ($\Omega_{M,0}$ and $\Omega_{\Lambda,0}$) at the present time (t_0) were chosen to be

$$\Omega_{M,0} \equiv \frac{8\pi G\rho_M(t_0)}{3H_0^2} = 0.3, \tag{1}$$

$$\Omega_{\Lambda,0} \equiv \frac{\Lambda}{3H_0^2} = 0.7, \tag{2}$$

where G is the gravitational constant, $\rho_{M,0}$ is the mass density, and $H_0 \sim 50 - 70$ km/s/Mpc is the Hubble constant [18-21]. For a holographic dark energy, the turning point redshift depends on a free parameter [22]. The turning point redshift is $Z_{\rm TP} \sim 0.72$ if the free parameter is chosen to be unity. For the best fit to the type Ia supernova data, the free parameter is around 0.2, which leads to a smaller turning point redshift, $Z_{\rm TP} \sim 0.28$.

To combine the measurements of type Ia supernovae with the cosmological model, a redshift-luminosity distance relation is required. The often used relation is, however, a linearly approximate relation,

$$d_L(Z) \simeq c(1+Z)\int_0^Z \frac{du}{H(u)}, \tag{3}$$

which is only good for nearby objects (see the detail of the standard derivation given by [23]. Using this approximate redshift-luminosity distance relation to study the expansion of the universe constrained by the measurements of type Ia supernovae with redshift greater than unity, one cannot accurately determine the turning point redshift [24] (Zhang and tan 2007). In Eq. (3), c is the light speed, Z is the redshift of light from the object, and d_L is the luminosity, which is usually defined by

$$F = \frac{L}{4\pi d_L^2}, \tag{4}$$

where L is the luminosity of the object such as a supernova, F is the apparent brightness of the object (i.e., the object emission flux measured at the Earth).

In this study, we analytically derive the turning point redshift only from the cosmological model without combining the model with the type Ia supernova data of measurements and thus without using the approximate redshift-luminosity distance relation. The simplest cosmological model that describes the recent acceleration of the universe is governed by the Friedmann equation with a non-zero Einsteinian cosmological constant [1-2, 5]. The expansion characteristics of the universe described by this constant ΛCDM model depend on three independent parameters. There are many different ways or combinations to choose the three independent parameters. But no matter how to combine, the number of independent parameters is always three. We have chosen the Hubble constant H_0, the radius of the present universe R_0, and the density parameter in matter $\Omega_{M,0}$ as the three independent parameters and have further derived the turning point redshift. The derived turning point redshift is only dependent of the density parameter in matter $\Omega_{M,0}$, not dependent of the other two independent parameters R_0 and H_0 if the universe is flat.

Exact solutions of the Friedmann equation [25-26] with the cosmological constant were obtained by [27-28]. The physical solutions, however, have not yet been analyzed with the recent measurements of the universe, especially on the turning point redshift.

The objective of this study is to quantitatively study the turning point and expansion characteristics of the recent acceleration universe through analyzing and numerically solving the Friedmann equation with a non-zero cosmological constant. First, for each set of H_0, $\Omega_{M,0}$, and R_0, we analytically obtain the turning point redshift $Z_{\rm TP}$ and other cosmological parameters such as the density parameter in dark energy $\Omega_{\Lambda,0}$, the cosmological constant Λ, and the mass of the universe M. Then, we substitute the obtained M and Λ into the Friedmann equation to numerically solve the time-dependent expansion rate or Hubble parameter $H(t)$, velocity $v(t)$, radius $R(t)$, and acceleration parameter $q(t)$ of the universe. Third, from the solutions, we determine the age of the present universe. Finally, we discuss the significant results and summarize our concluding remarks.

2 Turning Point and Expansion Characteristics of the Universe

According to the standard cosmological theory, the expansion of the universe is governed by the Friedmann equation [25-26, 29]

$$H^2(t) \equiv \frac{\dot{R}^2(t)}{R^2(t)} = \frac{8\pi G\rho_M(t)}{3} - \frac{kc^2}{R^2(t)} + \frac{\Lambda}{3}, \tag{5}$$

(Friedmann 1922, 1924; Carroll et al. 1992) where the dot refers to the derivative with respect to time, G is the gravitational constant, $\rho_M(t)$ is the density of matter given by

$$\rho_M(t) = \frac{3M}{4\pi R^3(t)}, \tag{6}$$

and k is the curvature of the space given by -1, 0, 1 for the universe to be open, flat, and closed, respectively. For the flat universe (i.e., $k = 0$), Eq. (5) becomes

$$H^2(t) \equiv \frac{\dot{R}^2(t)}{R^2(t)} = \frac{2GM}{R^3(t)} + \frac{\Lambda}{3}. \tag{7}$$

The solution of Eq. (7) depends on three independent parameters: R_0, M, and Λ. There are many different combinations that can be considered as the three independent parameters such as (R_0, H_0, Λ), (R_0, H_0, $\Omega_{M,0}$), etc. In this study, we have chosen R_0, H_0, and $\Omega_{M,0}$ as the three independent parameters.

To describe the acceleration of the universe, we define the acceleration parameter as

$$q(t) \equiv \frac{R(t)\ddot{R}(t)}{\dot{R}^2(t)} = 1 + \frac{\dot{H}(t)}{H^2(t)}. \tag{8}$$

Traditionally, a negative sign is inserted in Eq. (8) for the deceleration parameter.

A light that was emitted at time t is generally shifted towards the red when it is observed at the present time t_0 due to the expansion of the universe. The redshift of the light is given by

$$Z_H = \frac{R(t_0)}{R(t)} - 1. \tag{9}$$

The recent acceleration universe turned its expansion from past deceleration to recent acceleration at the moment when the acceleration parameter is equal to zero, i.e.,

$$q(t_{\rm TP}) = 0, \tag{10}$$

where $t_{\rm TP}$ is defined as the turning point - the time when the universe neither accelerates nor decelerates. It has been recognized for years but not yet theoretically determined.

Differentiating Eq. (7) with respect to time to get $\dot{H}(t)$ and using the turning point condition (10), we have the following relation

$$\Lambda = \frac{3GM}{R^3(t_{\rm TP})}. \tag{11}$$

Then, using Eq. (9), we have

$$\Lambda = \frac{3GM}{R^3(t_0)}\left(\frac{R^3(t_0)}{R^3(t_{\rm TP})}\right) = \frac{3GM}{R_0^3}(Z_{\rm TP}+1)^3, \qquad (12)$$

where we have replaced $R(t_0)$ by R_0 and denoted the redshift of observed light that was emitted at the turning point by $Z_{\rm TP}$ - the turning point redshift. From Eq. (12), the turning point redshift can be written as

$$Z_{\rm TP} = \left(\frac{\Lambda R_0^3}{3GM}\right)^{1/3} - 1. \qquad (13)$$

At the present time t_0, Eq. (7) can be written as

$$1 = \Omega_{M,0} + \Omega_{\Lambda,0}, \qquad (14)$$

where the density parameters in matter and dark energy are defined respectively by

$$\Omega_{M,0} = \frac{8\pi G\rho_M(t_0)}{3H_0^2} = \frac{2GM}{H_0^2R_0^3}, \qquad (15)$$

and

$$\Omega_{\Lambda,0} = \frac{\Lambda}{3H_0^2}. \qquad (16)$$

From Eqs. (15)-(16), we obtain

$$\frac{\Lambda R_0^3}{3GM} = 2\frac{1-\Omega_{M,0}}{\Omega_{M,0}}. \qquad (17)$$

Then, Eq. (13) reduces

$$Z_{\rm TP} = \left(2\frac{1-\Omega_{M,0}}{\Omega_{M,0}}\right)^{1/3} - 1. \qquad (18)$$

Eq. (18) is a new result and has not been obtained before by any one. It is seen from Eq. (18) that the turning point redshift $Z_{\rm TP}$ is only dependent of the density parameter in matter Ω_M, not explicitly on another two independent parameter H_0 and R_0.

Figure 1 plots $Z_{\rm TP}$ as a function of Ω_M. The result indicates that, for the universe to be recently turned (i.e., $Z_{\rm TP} > 0$), the density parameter in matter must be $\Omega_{M,0} < 2/3$ (or $\Omega_{\Lambda,0} > 1/3$). For the universe to be turned at $1 \gtrsim Z_{\rm TP} \gtrsim 0.5$, the density parameter in matter must be $0.2 \lesssim \Omega_M \lesssim 0.4$. When $\Omega_{M,0} = 1$, we have $Z_{\rm TP} = -1$, which implies that the flat universe will never be accelerated if the cosmological constant is zero. This is consistent with the gravitational physics because gravity always attracts.

Considering H_0, R_0, and $\Omega_{M,0}$ as three independent parameters in the flat universe model, we can determine Ω_Λ, M, Λ, and $Z_{\rm TP}$ by Eqs. (14)-(16) and (18). Substituting the determined M and Λ into Eq. (7), we can numerically solve the expansion parameters of the recent acceleration universe

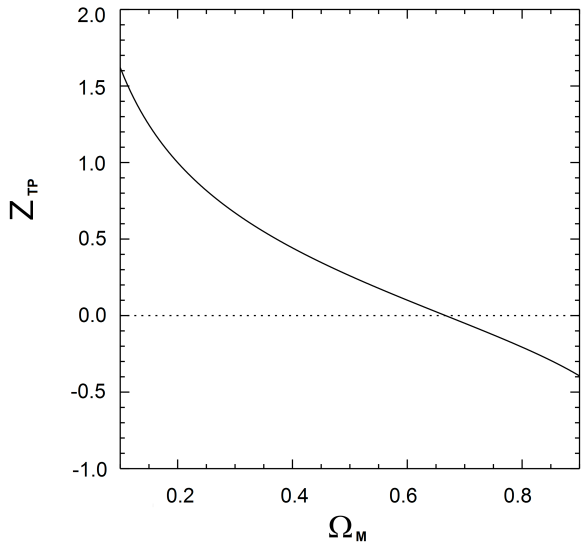

Fig. 1: Turning point redshift $Z_{\rm TP}$ versus density parameter in matter $\Omega_{M,0}$.

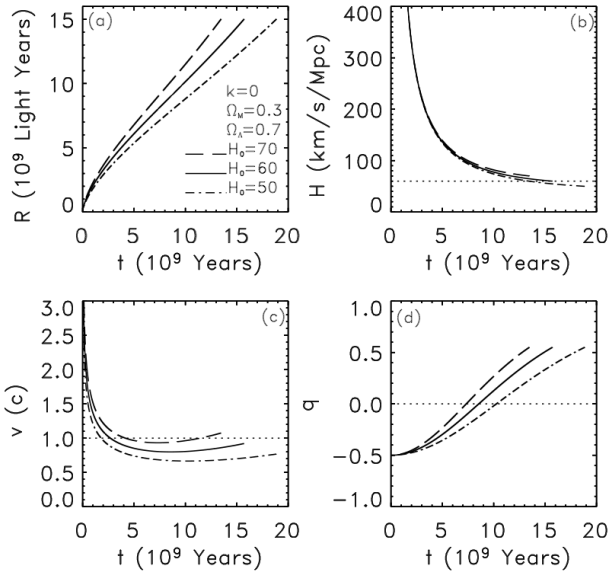

Fig. 2: Expansion characteristics of the universe when $\Omega_{M,0} = 0.3$, $R_0 = 15$ billion light years, and $H_0 = 50, 60, 70$ km/s/Mpc. (a) Radius of the universe $R(t)$, (b) expansion rate $H(t)$, (c) expansion velocity $v(t)$, (d) acceleration parameter $q(t)$.

including the radius $R(t)$, expansion rate $H(t)$, expansion velocity $v(t)$, and acceleration parameter $q(t)$.

Figure 2 plots these expansion parameters – $R(t)$, $H(t)$, $v(t)$, and $q(t)$ – as functions of time. We have chosen $H_0 = 50, 60, 70$ km/s/Mpc, $\Omega_{M,0} = 0.3$, and $R_0 = 15$ billion light years, which are displayed in Figure 2a. Three types of lines (dotted-dashed, solid, and dashed) correspond to the results with three different Hubble constants. With these three sets

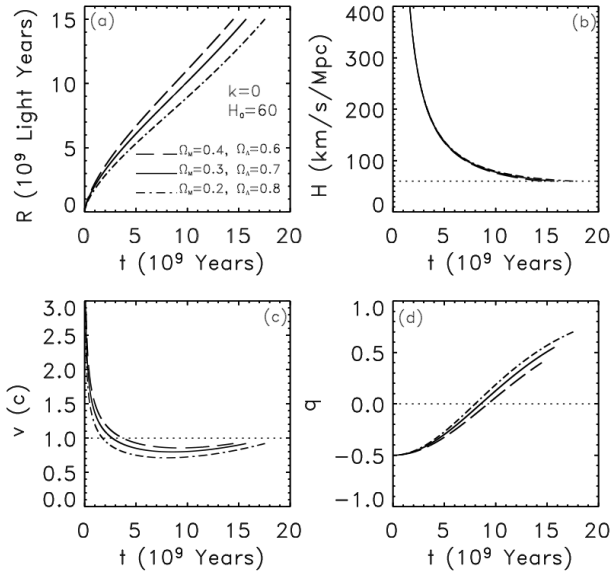

Fig. 3: Expansion characteristics of the universe when $\Omega_{M,0} = 0.2, 0.3, 0.4$ and $H_0 = 60$ km/s/Mpc with the same R_0. (a) Radius of the universe $R(t)$, (b) expansion rate $H(t)$, (c) expansion velocity $v(t)$, (d) acceleration parameter $q(t)$.

of parameters, we have $M = 1.7, 2.4, 3.3 \times 10^{53}$ kg, $\Lambda = 5.5, 8.0, 10.8 \times 10^{-36}$ s^{-2}, $\Omega_{\Lambda,0} = 0.7$, and $Z_{\rm TP} = 0.67$.

Figure 2a shows that $R(t)$ increases with time to approach R_0 at the present time t_0. In comparison with a linear relation, the radius-time curves bend down at $R \lesssim 3R_0/5$ and then slightly go up at $R \gtrsim 3R_0/5$. The flat universe turned its expansion from past deceleration to recent acceleration at the time when the size of the universe was about three-fifth of the present universe (i.e., at $Z_{\rm TP} \simeq 2/3$) due to the dark energy or non-zero cosmological constant. Figure 2b indicates that the expansion rate or Hubble parameter $H(t)$ decreases with time (or $\dot{H}(t) < 0$) to approach the Hubble constant H_0 at the present time. The dotted line refers to $H_0 = 60$ km/s/Mpc. Figure 2c shows that the expansion velocity decreases with time to the minimum at the turning point and then increases with time to approach $v_0 = H_0 R_0$, which exceeds the light speed in the case of $H_0 = 70$ km/s/Mpc and $R_0 = 15$ billion light years. In the early period, the expansion velocity can be much greater than the light speed. The minimum expansion velocity is determined by $v_{\rm min} = (2GM)^{1/3}\Lambda^{1/6}$. From Figure 2d, that the universe turned its expansion from past deceleration to recent acceleration can be seen in more obviously. The dotted line refers to $q = 0$. Each curve of $q(t)$ intersects with the dotted line at the turning point. For a different Hubble constant, the turning point $t_{\rm TP}$ is different. The acceleration parameter is negative (i.e., deceleration) before the turning point and positive (i.e., acceleration) after the turning point. At the present time, the acceleration parameter is slightly over 0.5.

Figure 3 also plots the four expansion parameters $R(t)$, $H(t)$, $v(t)$, and $q(t)$ as functions of time. In this plot, we have chosen a single $H_0 = 60$ km/s/Mpc but three $\Omega_M = 0.2, 0.3, 0.4$ with the same R_0. The three types of lines correspond to the results with three different density parameters. With these three sets of parameters, we have $M = 2.4 \times 10^{53}$ kg, $\Lambda = 8.0 \times 10^{-36}$ s^{-2}, $\Omega_{\Lambda,0} = 0.8, 0.7, 0.6$, and $Z_{\rm TP} = 1, 0.67, 0.5$. The results are basically similar to Figure 2. The turning point redshift is single in the case of Figure 2 but multiple in the case of Figure 3. The radius-time curves (Figure 3a) also bend down relative to the linear relation in the past and go up recently, which implies that the flat universe was decelerated in the past and accelerated recently. The decreasing profiles of expansion rate $H(t)$ with time only slightly different among different density parameters (Figure 3b). The expansion velocity reaches the minimum $v_{\rm min}$ at the turning point and approaches v_0 at t_0 (Figure 3c). The acceleration parameter at t_0 is greater if the universe contains more dark energy relative to matter (Figure 3d). For a different density parameter, the turning point $t_{\rm TP}$ is different. The acceleration parameter is negative (i.e., deceleration) before the turning point and positive (i.e., acceleration) after the turning point.

From Figures 2 and 3, we can find the present time or the age of the present universe with $R_0 = 15$ billion light year. For a different H_0 or $\Omega_{M,0}$, the age of the present universe should be different. The age of the present universe determined based on Figures 2 and 3 is plotted as a function of H_0 in Figure 4a and as a function of $\Omega_{M,0}$ in Figure 4b. It is seen that the age of the present universe decreases with H_0 and $\Omega_{M,0}$ when R_0 is fixed. For $R_0 = 15$ billion light year, $H_0 = 50 - 70$ km/s/Mpc, and $\Omega_{M,0} = 0.3$, the age of the universe is in the range of $\sim 13 - 19$ billion years, slightly less than H_0^{-1}. The universe is elder if it turned earlier (i.e., smaller $\Omega_{M,0}$) or has a smaller expansion rate.

3 Discussions and Conclusions

The open or closed universe can also be recently accelerated by the dark energy. Since k is not zero, the density parameters will be quite different in order for the universe to be turned from deceleration to acceleration at a similar turning point. The details on the turning point and expansion characteristics of the open and closed universes will be studied in future.

Consequently, the turning point and accelerating expansion of the flat universe has been investigated according to the cosmological theory with a non-zero cosmological constant. Choosing six sets of H_0, R_0, and $\Omega_{M,0}$, we have quantitatively determined $\Omega_{M,0}$, Λ, M, $Z_{\rm TP}$, t_0, $R(t)$, $H(t)$, $v(t)$, and $q(t)$. Analyzing these results, we can conclude the following remarks.

To turn the expansion from deceleration to acceleration, the flat universe must contain enough amount of dark energy $\Omega_{\Lambda,0} > 1/3$. The turning point redshift depends only on the density parameter in matter $Z_{\rm TP} = [2(1 - \Omega_{M,0})/\Omega_{M,0}]^{1/3} - 1$. The flat universe will never be accelerated if the cosmologi-

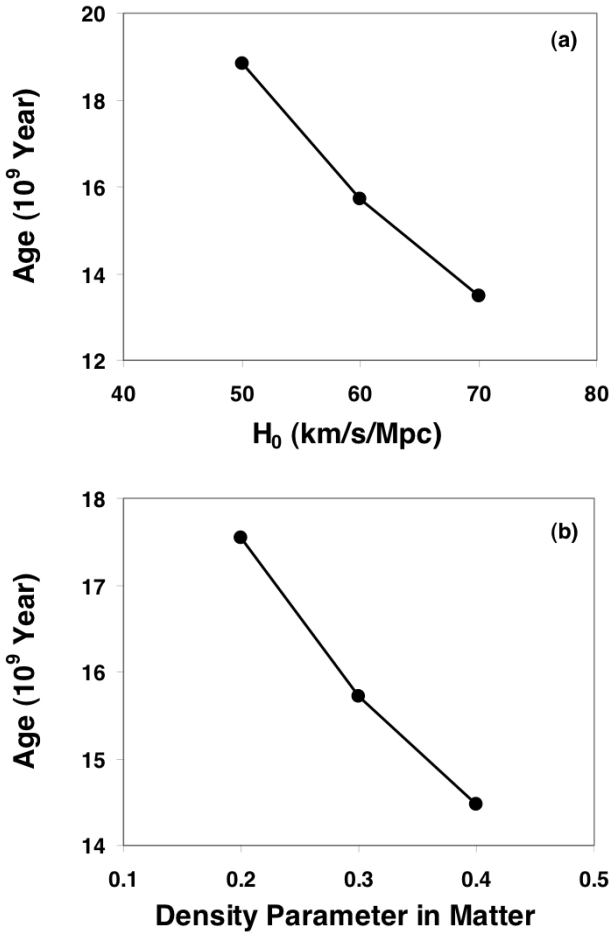

Fig. 4: Age of the universe as a function of H_0 (a) and $\Omega_{M,0}$ (b).

cal constant is zero. For the flat universe to be turned from deceleration to acceleration at $0.5 \lesssim Z_{\rm TP} \lesssim 1$, the density parameter in matter must be $0.4 \gtrsim \Omega_{M,0} \gtrsim 0.2$. The radius of the universe generally increases with time. The expanding profiles are belong to the M_1 type of exact solutions given by [27-28]. The expansion rate of the universe rapidly decreases with time to approach the Hubble constant. The expansion velocity decreases with time to the minimum $v_{\rm min} = (2GM)^{1/3}\Lambda^{1/6}$ at the turning point and then increases with time to approach $v_0 = H_0 R_0$. The acceleration parameter also increases with time and changes from negative to positive at the turning point. The acceleration of the present universe is larger if it contains more dark energy. The age of the universe depends on all of R_0, H_0, and $\Omega_{M,0}$. The flat universe with a fixed R_0 should be elder for smaller H_0 or $\Omega_{M,0}$ due to the expansion velocity smaller.

Overall, this study has shown the constraints and characteristics of the recent acceleration universe, which deepens our understanding of the turning and accelerating of the universe from past deceleration to recent acceleration.

Acknowledgement

This work was supported by the NASA research and education program (NNG04GD59G), NASA EPSCoR program (NNX07AL52A), NSF CISM program, Alabama A & M University Title III program, National Natural Science Foundation of China (G40890161).

Submitted on January 26, 2012 / Accepted on February 3, 2012

References

1. Riess, A.G. et al. Observational Evidence from Supernovae for an Accelerating Universe and a Cosmological Constant. *Astronomical Journal*, 1998, v. 116, 1009–1038.
2. Riess, A.G. et al. Type Ia Supernova Discoveries at Z > 1 from the Hubble Space Telescope Evidence for Past Deceleration and Constraints on Dark Energy Evolution. *Astrophysical Journal*, 2004, v. 607, 665–687.
3. Perlmutter, S. et al. Measurements of Omega and Lambda from 42 High-Redshift Supernovae. *Astrophysical Journal*, 1999, v. 517, 565–586.
4. Turner, M.S. and Riess, A.G. Do Type Ia Supernovae Provide Direct Evidence for Past Deceleration of the Universe? *Astrophysical Journal*, 2002, v. 569, 18–22.
5. Peebles, P.J. and Ratra, B. The Cosmological Constant and Dark Energy. *Reviews of Modern Physics*, 2003, v. 75, 559–606.
6. Brans, C.H. and Dicke, R. H. Mach's Principle and a Relativistic Theory of Gravitation. *Physical Review*, 1961, v. 124, 925–935. s
7. Arik, M. and Calik, M.C. Can Brans-Dicke Scalar Field Account for Dark Energy and Dark Matter? *Modern Physics Letters A*, 2006, v. 21, 1241–1248.
8. Sharif, M. and Khanum, F. Kaluza-Klein Cosmology with Modified Holographic Dark Energy. *General Relativity and Gravitation*, 2011, v. 43, 2885–2894.
9. Jadhav, M., Zhang, T.X. and Winebarger, A. Modified Friedmann Equation with a Scalar Field. *AAMU STEM Day*, 2009, v. 3, 66–66.
10. Zhang, T.X. A New Cosmological Model: Black Hole Universe. *BAAS*, 2007, v. 39, 1004–1004.
11. Zhang, T.X. Anisotrpic Expansion of the Black Hole Universe. *BAAS*, 2009, v. 41, 499–499.
12. Zhang, T.X. A New Cosmological Model: Black Hole Universe. *Progress in Physics*, 2009, v. 2, 3–11.
13. Zhang, T.X. Cosmic Microwave Background Radiation of Black Hole Universe. *BAAS*, 2009, v. 41, 754–754.
14. Zhang, T.X. Observational Evidences of Black Hole Universe. *BAAS*, 2010, v. 42, 314–314.
15. Zhang, T.X. Cosmic Microwave Background Radiation of Black Hole Universe. *ApSS*, 2010, v. 330, 157–165.
16. Zhang, T.X. Black Hole Universe and Dark Energy. *BAAS*, 2011, v. 43, 2011–2011.
17. Zhang, T.X. Mechanism for Gamma Ray Bursts and Black Hole Universe Model. *AAS 219th Meeting*, 2012, Abstract # 310.02.
18. Hughes, J.P. and Birkinshaw, M. A Measurement of Hubble Constant from the X-Ray Properties and the Sunyaev-Zeldovich Effect of CL 0016+16. *Astrophysical Journal*, 1998, v. 501, 1–14.
19. Mauskopf, P.D. et al. A Determination of the Hubble Constant Using Measurements of X-Ray Emission and the Sunyaev-Zeldovich Effect at Millimeter Wavelengths in the Cluster Abell 1835. *Astrophysical Journal*, 2000, v. 538, 505–516.
20. Macri, L.M., Stanek, K.Z., Bersier, D., Greenhill, L.J., and Reid, M.J. A New Cepheid Distance to the Maser-Host Galaxy NGC 4258 and Its Implications for the Hubble Constant. *Astrophysical Journal*, 2006, v. 652, 1133–1149.

21. Sandage, A., Tammann, G.A., Saha, A., Reindl, B., Macchetto, F.D., and Panagia, N. The Hubble Constant: A Summary of the Hubble Space Telescope Program for the Luminosity Calibration of Type Ia Supernovae by Means of Cepheids. *Astrophysical Journal*, 2006, v. 653, 843–860.
22. Huang, Q.G., Gong, Y.G. Supernova Constraints on a Holographic Dark Energy Model. *JCAP*, 2004, v. 8, 6–10.
23. Weinberg, S. Gravitation and Cosmology. John Wiley and Sons, New York, 1972, pp.419-422.
24. Zhang, T.X., and Tan, A. The Turning and Evolution of the Recent Acceleration Universe. *BAAS*, 2007, v. 38, 241–241.
25. Friedmann, A.A. Über die Krümmung des Raumes, *Zeitschrift für Physik*, 1922, v. 10, 377–386.
26. Friedmann, A.A. Über die Möglichkeit einer Welt mit konstanter negativer Krümmung des Raumes. *Zeitschrift für Physik*, 1924, v. 21, 326–332.
27. Kharbediya, L.I. Some Exact Solutions of the Friedmann Equations with the Cosmological Term. *Soviet Astronomy*, 1976, v. 20, 647.
28. Kharbediya, L.I. Solutions to the Friedmann Equations with the Lambda Term for a Dust-Radiation Universe. *Soviet Astronomy*, 1983, v. 27, 380–383.
29. Carroll, S.M., Press, W.H., Turner, E.L. The Cosmological Constant. *AR&AA*, 1992, v. 30, 499–542.

Anisotropic to Isotropic Phase Transitions in the Early Universe

Muhammad Adeel Ajaib

Department of Physics and Astronomy, University of Delaware, Newark, Delaware 19716
E-mail: adeel@udel.edu

We attempt to develop a minimal formalism to describe an anisotropic to isotropic transition in the early Universe. Assuming an underlying theory that violates Lorentz invariance, we start with a Dirac like equation, involving four massless fields, and which does not exhibit Lorentz invariance. We then perform transformations that restore it to its covariant form along with a mass term for the fermion field. It is proposed that these transformations can be visualized as waves traveling in an anisotropic media. The transformation $it/\hbar \rightarrow \beta$ is then utilized to transit to a statistical thermodynamics system and the partition function then gives a better insight into the character of this transition. The statistical system hence realized is a two level system with each state doubly degenerate. We propose that modeling the transition this way can help explain the matter antimatter asymmetry of the Universe.

1 Introduction

The idea that the Universe is homogeneous, isotropic and that space-time is Lorentz invariant are important pillars of theoretical physics. Whereas the cosmological principal assumes the Universe to be homogeneous and isotropic, Lorentz invariance is required to be a symmetry of any relativistic quantum field theory. These requirements have robust footings, but there can possibly be scenarios where these ideas are not sufficient to describe the dynamics of a system. Temperature fluctuations in the Cosmic Microwave Background (CMB) radiation indicate that the assumptions made by the cosmological principal are not perfect. There is no conclusive evidence of Lorentz violation to date but this has been a topic of considerable interest and the Standard Model Extension (SME) has been constructed which includes various terms that preserve observer Lorentz transformations but violate particle Lorentz transformations [1]. Limits have been placed on the coefficients of various terms in the SME as well [2]. Another important question is the matter-antimatter asymmetry of the Universe which is not completely resolved. Sakharov, in 1967 derived three conditions (baryon violation, C and CP violation and out of thermal equilibrium) for a theory to satisfy in order to explain the baryon asymmetry of the Universe.

Origin of fermion masses is also one of the most intriguing questions which is now close to be answered by the ATLAS and CMS experiments at the Large Hadron Collider. Hints of this particle have been seen and we will know for sure this year, hopefully mid 2012, whether it exists or not. If the Higgs does not exist than the formalism presented in this article can also serve as a possible explanation for the origin of mass of fermions.

In this paper we intend to describe the evolution of a theory that violates Lorentz invariance to a theory that preserves it. The fields that are involved in the Lorentz violating theory can be viewed in analogy with fields traveling in an anisotropic medium. When the system evolves from the anisotropic to isotropic phase the symmetry of the theory is restored and the partition function formalism can be used to better understand how this transition takes place. This formalism, we propose, can help explain the matter-antimatter asymmetry of the Universe. The paper is organized as follows: In section 2 and 3 we describe these transformations and propose a way to interpret them as plane wave transitions into anisotropic media. In section 4 the partition function is used to get a better insight into how the transformations in section 2 occur and we conclude in section 5.

2 Transformations leading to Covariant Dirac equation

In this section we outline a set of transformations that lead to the Dirac equation for a QED (Quantum Electrodynamics) like theory with no interaction terms. We start with a Dirac-like equation which involves four fields $(\chi_a, \chi_b, \chi_c, \chi_d)$. These fields can be redefined in a simple way such that the covariant form of the Dirac equation is restored along with a mass term. We assume a minimal scenario and consider just the kinetic terms for the fields in the underlying theory. If we start with the following equation ($\hbar = c = 1$):

$$i\bar{\chi_a}\gamma^0\partial_0\chi_a + i\bar{\chi_b}\gamma^1\partial_1\chi_b + i\bar{\chi_c}\gamma^2\partial_2\chi_c + i\bar{\chi_d}\gamma^3\partial_3\chi_d = 0, \quad (1)$$

and transform each of the χ fields in the following manner,

$$\begin{aligned} &\chi_a(x) \rightarrow e^{i\alpha m\gamma^0 x_0}\psi(x), \;\; \chi_b(x) \rightarrow e^{i\beta m\gamma^1 x_1}\psi(x), \\ &\chi_c(x) \rightarrow e^{i\delta m\gamma^2 x_2}\psi(x), \;\; \chi_d(x) \rightarrow e^{i\sigma m\gamma^3 x_3}\psi(x), \end{aligned} \quad (2)$$

we get the Dirac equation in covariant form, along with a mass term (using, for e.g., $e^{i\beta m\gamma^1 x_1}\gamma_0 = \gamma_0 e^{-i\beta m\gamma^1 x_1}$),

$$\overline{\psi}[i\gamma^\mu\partial_\mu - (\alpha+\beta+\delta+\sigma)m]\psi = 0, \quad (3)$$

where $\alpha, \beta, \delta and \sigma$ are real positive constants. For plane wave solution for particles, $\psi = e^{-ip.x}u(p)$, the above redefinition

for the field χ_a, for example, is a solution of the following equation:

$$\frac{\partial}{\partial t}\chi_a(x) = -i(E - \alpha m\gamma_0)\chi_a(x), \tag{4}$$

with similar equations for the other fields. Equation (4), is similar to equation (27) in reference [3] which is a solution of the differential equation governing linear elastic motions in an anisotropic medium (with a constant matrix, see section III of the reference). With $\alpha = 0$ the left hand side is just the Hamiltonian with the plane wave its eigenstate.

Note that the manner in which we can transform equation (1) to (3) is not unique and there are various ways to do this with different combinations of the χ fields along with the field ψ. A mass term ($m\bar{\chi}\chi$) for the χ fields could have been added to equation (1), but the redefinitions (2) can be used to eliminate it. So, if we want our resulting equation to describe a massive fermion, these fields should be massless or cannot have mass term of the form $m\bar{\chi}\chi$. This argument will be further corroborated with the results we present in section 4. The transformation matrices in equation (2) are not all unitary, the matrix $e^{i\alpha m\gamma^0 x_0}$ is unitary while the rest ($e^{i\beta m\gamma^i x_i}$) are hermitian.

The fields in equation (1) can be considered as independent degrees of freedom satisfying equation (4) in an underlying theory that violates Lorentz invariance. The transformations (2) can, therefore, be seen as reducing the degrees of freedom of the theory from four to one. In such an underlying theory, various interaction terms can be written for these fields. Since we intend to obtain the free Dirac equation, we have considered only kinetic terms involving the fields χ. A quadratic term involving different χ fields ($m\bar{\chi}_i\chi_j$) can be added to equation (1) but this leads to a term that violates Lorentz invariance in the resulting Dirac equation. A quartic term ($c\bar{\chi}_i\chi_i\bar{\chi}_j\chi_j$) is possible and would result in a dimension 6 operator for the field ψ with the constant c suppressed by the square of a cutoff scale. So, with the restriction that the resulting Dirac equation only contains terms that are Lorentz scalars the number of terms we can write for the χ fields can be limited. In other words we impose Lorentz symmetry in the resulting equation so that various terms vanish or have very small coefficients.

3 Visualizing field Redefinitions

Space-time dependent field redefinitions in the usual Dirac Lagrangian result in violation of Lorentz invariance. For example, the field redefinition $\psi \to e^{-i\alpha^\mu x_\mu}\psi$ leads to the Lorentz violating terms in the Lagrangian [1]. This particular redefinition, however, would not lead to physically observable effects for a single fermion. A transformation of this type amounts to shifting the four momentum of the field. It can also be viewed in analogy with plane waves entering another medium of a different refractive index which results in a change in the wave number of the transmitted wave. Similarly, transformations (2) can be interpreted as transitions of a wave from an anisotropic to isotropic medium or vice versa as done in the Stroh's matrix formalism [3]. For plane wave solutions of ψ, the χ fields have propagative, exponentially decaying and increasing solutions (for example, $e^{\pm imx}$, $e^{\pm mx}$). This wave behavior is similar to that in an anisotropic medium or a medium made of layers of anisotropic medium. The eigenvalues of the Dirac matrices being the wave numbers of these waves in this case. The coefficients in the exponent relates to how fast the wave oscillates, decays and/or increases exponentially. The transfer matrix in Stroh's formalism describe the properties of the material and in this case can possibly represent the properties of the anisotropic phase from which the transition to the isotropic phase occurs.

Therefore, we can visualize a global and local transformation as transitions of plane waves to different types of media. The wave function of a particle ($E > V$) which comes across a potential barrier of a finite width and height undergoes a phase rotation ($e^{ikl}\psi$) upon transmission. If the width of the barrier extends to infinity, the wave function can be viewed as undergoing a position dependent phase rotation ($e^{ikx}\psi$). The transformations (2) can similarly be seen as a plane wave entering an anisotropic medium. Another phenomenon called birefringence in optics can be used to explain why these four fields map on to the same field ψ. Birefringence results in a plane wave splitting into two distinct waves inside a medium having different refractive indices along different directions in a crystal. These analogies can serve as crude sketches to visualize how the transformations in equation (2) can occur.

In the usual symmetry breaking mechanism a Higgs field acquires a vacuum expectation value (VEV) and the resulting mass term does not respect the symmetry of the underlying group. For example, in the Standard Model, due to its chiral nature, a Higgs field is introduced in order to manifest gauge invariance. Once the Higgs field acquires a VEV the mass term only respects the symmetry of the resulting group which is $U(1)_{EM}$. In our case the mass term arises after symmetry of the Dirac equation is restored. Consider the simple case where we have one field χ_a in addition to the field ψ:

$$i\bar{\chi_a}\gamma^0\partial_0\chi_a + i\bar{\psi}\gamma^i\partial_i\psi = 0, \tag{5}$$

and this field transforms to the field ψ as $\chi_a(x) \to e^{i\alpha m\gamma^0 x_0}\psi(x)$, leading to the Dirac equation. In order to discuss the symmetries of the above equation let's assume that the two independent degrees of freedom are described by the above equation. Equation (5) then has two independent global U(1) symmetries and the resulting equation has one. In fact, there is a list of symmetries of equation (5) not possessed by (3), for example invariance under local transformations, $\chi_a \to e^{ib^i\theta(x_i)}\chi'_a$ ($i, j = 1, 2, 3$), where b_i can be a constant vector, the matrix γ_0 or any matrix that commutes with γ_0 (e.g., σ_{ij}, $\gamma_5\gamma_i$). This implies invariance under global and local SO(3) transformations (rotations of the fields χ_a but not boosts). Similarly, $\psi \to e^{iA\ \theta(t)}\psi'$ is a symmetry, where A can be a constant or the

matrix $i\gamma_0\gamma_5$ which commutes with the three Dirac matrices γ_i. After the transformation $\chi_a \rightarrow e^{im\gamma_0 t}\psi$ the equation is no more invariant under these symmetries and the SO(1,3) symmetry of the Dirac equation is restored along with a global U(1) symmetry.

4 Partition Function as a Transfer Matrix

In the early Universe, a transition from a Lorentz asymmetric to a symmetric phase could possibly induce transformations of the form (2). Let's again consider the simple example in equation (5). For this case the eigenvalues of the Dirac matrix γ_0 define the wave numbers of the waves traveling in the anisotropic medium. The direction of anisotropy in this case is the temporal direction, which means that the time evolution of these waves is not like usual plane waves. It is not straight forward to visualize the fields, the dynamics of whom are described by the anisotropy of space time, but we can use the partition function method to get a better insight into this. We can, by using this formalism, calculate the temperature at which the transformations in equation (2) occur.

We next perform a transition to a thermodynamics system by making the transformation $it \rightarrow \beta$, where $\beta = 1/k_B T$ [4]. The partition function is then given by the trace of the transformation matrix $e^{im\gamma_0 t}$,

$$Z = \mathrm{Tr}(e^{m\beta\gamma_0}) = 2e^{\beta m} + 2e^{-\beta m}. \tag{6}$$

This partition function is similar to that of a two-level system of spin 1/2 particles localized on a lattice and placed in a magnetic field with each state, in this case, having a degeneracy of two. The lower energy state corresponding to spin parallel to the field ($E = -m, Z_1 = e^{\beta m}$). In this case the doubly degenerate states correspond to spins up and down of the particle or anti-particle. For N distinguishable particles the partition function is Z^N, N here is the total number of particles and antiparticles of a particular species. So, we are modeling our system as being on a lattice with the spin along the field as representing a particle and spin opposite to the field representing an antiparticle.

The evolution of this system with temperature represents the time evolution of the system in equation (1). In other words the partition function describes the evolution of these waves from anisotropic to isotropic phase as the temperature decreases. For a two level system the orientation of the dipole moments becomes completely random for large enough temperatures so that there is no net magnetization. In our case we can introduce another quantity, namely a gravitational dipole, which would imply that the four states (particle/antiparticle, spin up/down) of N such particles at high enough temperatures orient themselves in a way that the system is massless. This just serves as an analogy and does not mean that the masses are orientating themselves the same way as dipoles would do in space. The anisotropic character can be seen as mimicking the behavior of the field in a two level system. The population of a particular energy level is given by

$$n_{p(\overline{p})} = \frac{Ne^{\pm\beta m}}{e^{\beta m} + e^{-\beta m}}, \tag{7}$$

which shows that the number density of particles and antiparticles vary in a different way with respect to temperature. In the early Universe, therefore the anisotropic character of space-time seems to play an important role such that particles and anti-particles behave in different manners. As the temperature decreases the number density of the anti-particles decreases and is vanishingly small for small temperatures ($\sim e^{-2\beta m}$). When the decoupling temperature is attained there is a difference in the number density of the particles and antiparticles as described by equation (7). This leads to an excess of particles over antiparticles. The decoupling temperature of a particular species of particle with mass m and which is non-relativistic is given by, $k_B T \lesssim 2m$. Below this temperature the particles annihilate to photons but the photons do not have enough energy to produce the pair. This can be used to get the ratio of antiparticles over particles (matter radiation decoupling). For $\beta m \approx 0.5$, we get

$$\frac{n_p - n_{\overline{p}}}{n_p} \approx 0.6\,, \tag{8}$$

which implies an excess of particles over antiparticles and thus can serve as another possible way to explain the matter antimatter asymmetry of the Universe. This number is very large compared to the one predicted by standard cosmology ($\sim 10^{-9}$). The above expression yields this order for $\beta m \approx 10^{-9}$ which implies a large temperature. For electrons this would imply a temperature of the order 10^{18}K which is large and the electrons are relativistic. So if we assume that the decoupling takes place at a higher temperature, the baryon asymmetry can be explained. Even without this assumption the conditions proposed by Sakharov can also enhance the number of particles over the antiparticles. Sakharov's conditions involve the interaction dynamics of the fields in the early Universe whereas in our case the statistical system serves more as a model describing the dynamics of space-time to a more ordered phase.

Statistical mechanics, therefore, enables us to visualize this transition in a rather lucid way. In a two level system the net magnetization at any given temperature is analogous to the excess of particles over antiparticles in the early Universe. The time evolution of this anisotropic to isotropic transition is modeled on the evolution of a statistical thermodynamics system with particles on a lattice placed in a magnetic field. The particles on the lattice are localized, static and have no mutual interaction. The free energy of the system is given by:

$$F = -Nk_B T \ln\{4\cosh[m\beta]\}. \tag{9}$$

From this we can calculate the entropy S, heat capacity

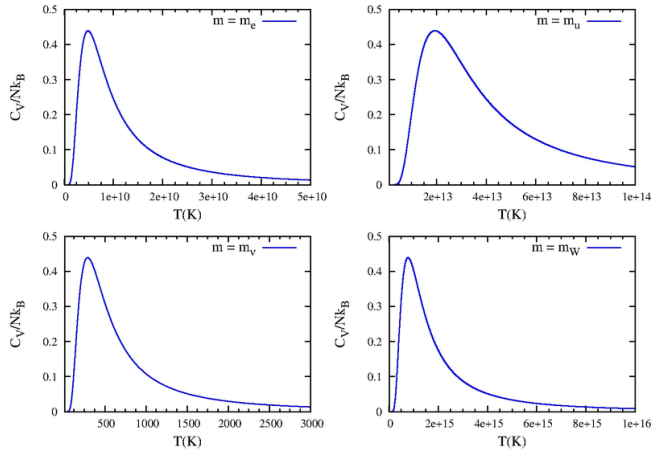

Fig. 1: Plot of heat capacity C_V for the mass of electron, up quark, neutrino and W boson. The maximum of the heat capacity of the electron occurs at 4.8×10^9K, for the up quarks is 1.9×10^{13}K, for neutrinos is 291K and for the W bosons is 7.8×10^{14}K. We use $k_B = 8.6 \times 10^{-5}$ eV/K and $m_\nu = 0.03$ eV.

C_V and mean energy U of the system:

$$S = -\left(\frac{\partial F}{\partial T}\right)_V = Nk_B \ln\{4\cosh[m\beta]\} - Nmk_B\beta\tanh[m\beta] \quad (10)$$

$$U = F + TS = -Nm\tanh[m\beta] \quad (11)$$

$$C_V = \left(\frac{\partial U}{\partial T}\right)_V = Nk_B m^2\beta^2\mathrm{sech}^2[m\beta] \quad (12)$$

In Fig. 1, the peaks in the heat capacity represent phase transition of a particular particle species. These are second order phase transitions and the peak in the heat capacity is usually referred to as the Schottky anomaly [5]. Note that the phase transition we model our system on is a magnetic one. So, modeling the complex system in the early Universe on a lattice with spin 1/2 particles can reduce the complications of the actual system by a considerable amount.

The Schottky anomaly of such a magnetic system, therefore, represents phase transitions in the early Universe. For a particular species of particles the Schottky anomaly shows a peak around $mc^2 \approx kT$. The phase transition for the electrons occurs at the temperature where nuclei start forming in the early Universe. For the quarks the transition temperature refers to confinement into protons and neutrons. Similarly, W boson's transition occurs at the electroweak breaking scale. The W boson, being a spin 1 particle, is not described by the Dirac equation, but the heat capacity entails this feature of showing a phase transition for the energy scale relevant to the mass of a particle.

The curve for neutrinos implies that the transition temperature for neutrinos is around 291 K, which means that the density of antineutrinos from the big bang for present neutrino background temperatures (~ 2 K) is not negligible. The ratio of antineutrinos over neutrinos for $T = 2$ K, is $n_{\bar{\nu}}/n_\nu \sim 10^{-15000}$ ($m_\nu = 2$ eV) and for an even lower neutrino mass $m_\nu = 0.1$ eV the ratio is $n_{\bar{\nu}}/n_\nu \sim 10^{-500}$, which for other more massive particles is much smaller. A cosmic neutrino and antineutrino background is one of the predictions of standard cosmology but is still unobserved. This model predicts an antineutrino background much less than the neutrino one.

In Fig. 2, the plots of mean energy and entropy are shown in dimensionless units. In the massless limit for fermions the entropy attains its maximum value of $Nk_B\ln 4$. The plots show that the energy of the system approaches zero as the temperature approaches infinity. This situation is analogous to the spins being completely random at high temperatures for the two level system. The same way that the magnetic energy of the system on the lattice is zero at high temperatures, the mass of this system is zero in the very early Universe. As the temperature decreases the energy of the system attains it minimum value ($U = -Nm$) and the particles become massive at the temperature less than the value given by the peak of the heat capacity. The entropy for high temperatures asymptotically approaches its maximum value of $Nk_B\ln 4$.

According to the statistical thermodynamics model that describes this transition, as this phase transition occurs antiparticles will start changing into particles and as can be seen from the figure the system will move towards all spins aligned parallel with the "field", i.e., towards being particles. From Fig. 2 we can see that the energy of the system starts attaining the minimum value as the temperature decreases where all particles are aligned with the field and are "particles". The plot of entropy vs. temperature also represents an important feature of these transformations. The entropy decreases with decreasing temperature and this represents the transition to a more ordered phase using equations (2). The plots of energy of the system U in Fig. 2 show that the system will eventually settle down to the lowest energy state which in this case means that the system will have almost all particles with negligible number of antiparticles. In short, the plot of the heat capacity reflects the phase transitions, the plot of energy U represents the transition from massless to massive states and the plot of entropy represents the transition of space time to a more ordered phase.

The Big Bang theory is one of the most promising candidates to describe how the Universe began. According to this theory, the Universe expanded from a singularity where curved space-time, being locally Minkowskian, eventually became flat. It is possible that there even was a transition to the Minkowski space from a non-Minkowski one. If the Universe began with a state of maximum entropy than we can very well assume that space-time was not Minkowskian even locally. The fields that dwell in space-time are representation of the symmetry group that describes it. The χ fields in the underlying theory, described by equation (1), are therefore, not rep-

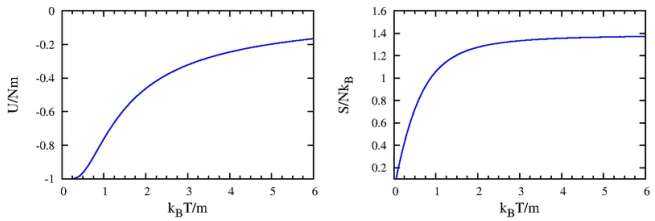

Fig. 2: Plot of entropy and energy for a particle of mass m. For large enough temperatures the energy of the system approaches zero and the entropy approaches the limiting value of Nk_Bln4.

resentations of the Lorentz group. The CPT theorem assumes symmetries of Minkowski space-time in implying the similarities between particles and antiparticles. If the underlying theory is not Minkowskian than particles and antiparticles can behave differently and this is what the model described in this section implies.

Finally, we would like to point out that the occurrence of the Schottky anomaly has motivated the study of negative temperatures [6]. Note that the partition functions is invariant under the transformation $T \rightarrow -T$ but the equations for the free energy, entropy and energy are not. The existence of negative temperatures has been observed in experiments. Negative temperatures, for example, can be realized in a system of spins if the direction of the magnetic field is suddenly reversed for a system of spins initially aligned with the magnetic field [5]. Similarly, as described in reference [6] the allowed states of the system must have an upper limit. Whereas this is not the case for the actual particles in the early Universe, the statistical mechanics system on which it can be modeled on has this property. A negative temperature system would eventually settle down to the lower energy state ($U = Nm$) which in our case would mean that the Universe would ends up having more antiparticles than particles. This is yet another interesting insight we get by modeling the early Universe on a two state system.

5 Conclusions

We analyzed transformations that restore the Dirac equation to its covariant form from an underlying theory that violates Lorentz invariance. The fields in the underlying theory are massless and the transformations yielding the Dirac equation describe a massive fermion field. The transformations performed, we suggest, can be interpreted as waves traveling in an anisotropic medium. The partition function formalism then, enabled us to model these transformations on the evolution of a system of spin 1/2 particles on a lattice placed in a magnetic field. Symmetry breaking in this case takes place in this lattice, the partition function of which characterizes the transition. Also, since space-time is not Minkowskian in the underlying theory, the CPT theorem does not hold, implying a difference in the behavior of particles and antiparticles. This is in agreement with the analogy created with the statistical system whereby spin up and down particles behave in different ways with the evolution of the system. This formalism can arguably serve as another possible way to explain the origin of fermion masses till the final results related to the Higgs boson are presented in 2012.

We then showed that this model can describe the anisotropic to isotropic phase transitions in the early Universe. Three important features of the early Universe are depicted in this model: (1) The heat capacity shows the occurrence of phase transitions. (2) The mean energy of the system shows how the particles become massive from being massless. (3) The plot of entropy shows that the transition to a Lorentz symmetric phase occurred from an asymmetric one. At any given temperature the net magnetization measures the excess of particles over antiparticles. We then suggest that this model can be used to explain the matter antimatter asymmetry of the Universe.

Acknowledgements

I would like to thank Fariha Nasir, Hassnain Jaffari and Ilia Gogoladze for useful discussions and comments.

Submitted on January 24, 2012 / Accepted on February 4, 2012

References

1. Colladay D., Kostelecky V.A. Lorentz violating Extension of the Standard Model. *Physical Review D*, 1998, v. 58, 116002–116025.
2. Kostelecky V.A. and Russell N. Data Tables for Lorentz and CPT Violation. *Reviews in Modern Physics*, 2011, v. 83, 11–31.
3. Braga M.B. and Hermann G. Floquet waves in anisotropic periodically layered composites. *Journal of the Acoustical Society of America*, 1992, v. 91, 1211–1227.
4. Zee A. Quantum Field Theory in a Nutshell. Princeton University Press, Princeton, NJ, 2003.
5. Pathria R.K. Statistical Mechanics. Butterworth-Heinemann, Oxford, 1996; Greiner W. Thermodynamics and Statistical Mechanics. Springer, New York, 1995.
6. Ramsey N.F. Thermodynamics and Statistical Mechanics at Negative Absolute Temperatures. *Physical Review*, 1956, v. 103, 20–28.

Local Doppler Effect, Index of Refraction through the Earth Crust, PDF and the CNGS Neutrino Anomaly?

Armando V.D.B. Assis

Departamento de Física, Universidade Federal de Santa Catarina – UFSC, Trindade 88040-900, Florianópolis, SC, Brazil
E-mail: armando.assis@pgfsc.ufsc.br

In this brief paper, we show the neutrino velocity discrepancy obtained in the OPERA experiment may be due to the local Doppler effect between a local clock attached to a given detector at Gran Sasso, say C_G, and the respective instantaneous clock crossing C_G, say C_C, being this latter at rest in the instantaneous inertial frame having got the velocity of rotation of CERN about Earth's axis in relation to the fixed stars. With this effect, the index of refraction of the Earth crust may accomplish a refractive effect by which the neutrino velocity through the Earth crust turns out to be small in relation to the speed of light in the empty space, leading to an encrusted discrepancy that may have contamined the data obtained from the block of detectors at Gran Sasso, leading to a time interval excess ϵ that did not provide an exact match between the shift of the protons PDF (probability distribution function) by TOF_c and the detection data at Gran Sasso via the maximum likelihood matching.

1 Definitions and Solution

Firstly, the effect investigated here is not the same one that was investigated in [2], but, throughout this paper, we will use some useful configurations defined in [2]. The relative velocity between Gran Sasso and CERN due to the Earth daily rotation may be written:

$$\vec{v}_G - \vec{v}_C = 2\omega R \sin\alpha \hat{e}_z, \tag{1}$$

where $\hat{e}_z$ is a convenient unitary vector, the same used in [2], ω is the norm of the Earth angular velocity vector about its daily rotation axis, being R given by:

$$R_E = \frac{R}{\cos\lambda}, \tag{2}$$

where R_E is the radius of the Earth, its averaged value $R_E = 6.37 \times 10^6$ m, and α given by:

$$\alpha = \frac{1}{2}(\alpha_G - \alpha_C), \tag{3}$$

where α_C and α_G are, respectively, CERN's and Gran Sasso's longitudes ($\leftarrow WE \rightarrow$). Consider the inertial (in relation to the fixed stars) reference frame $O_C x_C y_C z_C \equiv Oxyz$ in [2]. This is the lab reference frame and consider this frame with its local clocks at each spatial position as being ideally synchronized, viz., under an ideal situation of synchronicity between the clocks of $O_C x_C y_C z_C \equiv Oxyz$. This situation is the expected ideal situation for the OPERA collaboration regarding synchronicity in the instantaneous lab (CERN) frame.

Now, consider an interaction between a single neutrino and a local detector at Gran Sasso. This event occurs at a given spacetime point $(t_\nu, x_\nu, y_\nu, z_\nu)$ in $O_C x_C y_C z_C \equiv Oxyz$. The interaction instant t_ν is measured by a local clock C_C at rest at (x_ν, y_ν, z_ν) in the lab frame, viz., in the $O_C x_C y_C z_C \equiv Oxyz$ frame. But, under gedanken, at this instant t_ν, according to $O_C x_C y_C z_C \equiv Oxyz$, there is a clock C_G attached to the detector at Gran Sasso that crosses the point $(t_\nu, x_\nu, y_\nu, z_\nu)$ with velocity given by Eq. (1). Since C_G crosses C_C, the Doppler effect between the proper tic-tac rates measured at each location of C_C and C_G, viz., measured at their respective locations in their respective reference frames (the reference frame of C_G is the $O_G x_G y_G z_G \equiv \tilde{O}\tilde{x}\tilde{y}\tilde{z}$ in [2], also inertial in relation to the fixed stars), regarding a gedanken control tic-tac rate continuosly sent by C_C, say via electromagnetic pulses from C_C, is not transverse. Since the points at which C_C and C_G are at rest in their respective reference frames will instantaneously coincide, better saying, will instantaneously intersect, at t_ν accordingly to C_C, they must be previously approximating, shortening their mutual distance during the interval $t_\nu - \delta t_\nu << t_\nu$ along the line passing through these clocks as described in the C_C world.

Suppose C_C sends $\mathcal{N}$ electromagnetic pulses to C_G. During the C_C proper time interval $(t_\nu - \delta t_\nu) - 0 = t_\nu - \delta t_\nu$ * within which C_C emits the N electromagnetic pulses, the first emitted pulse travels the distance $c(t_\nu - \delta t_\nu)$ and reaches the clock C_G, as described by C_C. Within this distance, there are $\mathcal{N}$ equally spaced distances between consecutive pulses as

*The initial instant C_C starts to emit the electromagnetic pulses is set to zero in both the frames $O_C x_C y_C z_C \equiv Oxyz$ and $O_G x_G y_G z_G \equiv \tilde{O}\tilde{x}\tilde{y}\tilde{z}$; zero also is the instant the neutrino starts the travel to Gran Sasso in $O_C x_C y_C z_C \equiv Oxyz$; hence the instant the neutrino starts the travel to Gran Sasso and the emission of the first pulse by C_C are simultaneous events in $O_C x_C y_C z_C \equiv Oxyz$. These events are simultaneous in $O_G x_G y_G z_G \equiv \tilde{O}\tilde{x}\tilde{y}\tilde{z}$ too, since they have got the same spatial coordinate $z_c = z = 0$ along the $O_C z_C \equiv Oz$ direction as defined in [2]. The relative motion between CERN and Gran Sasso is parallel to this direction. The only one difference between these events is the difference in their $x_C = x$ coordinates, being $x_C = 0$ for the neutrino departure and $x_C = L = 7.3 \times 10^5$ m for C_C, being these locations perpendicularly located in relation to the relative velocity given by the Eq. (1).

described in the C_C world, say λ_C:

$$\mathcal{N}\lambda_C = c\,(t_\nu - \delta t_\nu)\,. \tag{4}$$

Also, since the clocks C_C and C_G will intersect at t_ν, as described in $O_C x_C y_C z_C \equiv Oxyz$, during the interval δt_ν, the clock C_G must travel the distance $2\omega R\sin\alpha\,\delta t_\nu$ in the C_C world to accomplish the matching spatial intersection at the instant t_ν, hence the clock C_G travels the $2\omega R\sin\alpha\,\delta t_\nu$ in the C_C world, viz., as described by C_C in $O_C x_C y_C z_C \equiv Oxyz$:

$$\mathcal{N}\lambda_C = 2\omega R\sin\alpha\,\delta t_\nu \Rightarrow \delta t_\nu = \mathcal{N}\frac{\lambda_C}{2\omega R\sin\alpha}. \tag{5}$$

Solving for t_ν, from the Eqs. (4) and (5), one reaches:

$$t_\nu = \frac{\mathcal{N}\lambda_C}{c}\left(1 + \frac{c}{2\omega R\sin\alpha}\right). \tag{6}$$

Now, from the perspective of C_G, in $O_G x_G y_G z_G \equiv \tilde{O}\tilde{x}\tilde{y}\tilde{z}$, there must be $\mathcal{N}$ electromagnetic pulses covering the distance:

$$c\left(t_\nu^G - \delta t_\nu^G\right) - 2\omega R\sin\alpha\,\left(t_\nu^G - \delta t_\nu^G\right), \tag{7}$$

where $t_\nu^G - \delta t_\nu^G$ is the time interval between the non-proper instants $t^G = t_\nu = 0$, at which the C_C clock sends the first pulse, and the instant $t_\nu^G - \delta t_\nu^G$, at which this first pulse reaches C_G, as described by C_G in its world $O_G x_G y_G z_G \equiv \tilde{O}\tilde{x}\tilde{y}\tilde{z}$. Within this time interval, $t_\nu^G - \delta t_\nu^G$, C_G describes, in its $O_G x_G y_G z_G \equiv \tilde{O}\tilde{x}\tilde{y}\tilde{z}$ world, the clock C_C approximating the distance:

$$2\omega R\sin\alpha\,\left(t_\nu^G - \delta t_\nu^G\right), \tag{8}$$

with the first pulse traveling:

$$c\left(t_\nu^G - \delta t_\nu^G\right), \tag{9}$$

giving the distance within which there must be $\mathcal{N}$ equally spaced pulses, say, spaced by λ_G, as described by C_G in its $O_G x_G y_G z_G \equiv \tilde{O}\tilde{x}\tilde{y}\tilde{z}$ world:

$$\mathcal{N}\lambda_G = (c - 2\omega R\sin\alpha)\left(t_\nu^G - \delta t_\nu^G\right). \tag{10}$$

With similar reasoning that led to the Eq. (5), now in the $O_G x_G y_G z_G \equiv \tilde{O}\tilde{x}\tilde{y}\tilde{z}$ C_G world, prior to the spatial matching intersection between C_C and C_G, the C_C clock must travel the distance $\mathcal{N}\lambda_G$ during the time interval δt_ν^G, with the C_C approximation velocity $2\omega R\sin\alpha$:

$$\mathcal{N}\lambda_G = 2\omega R\sin\alpha\,\delta t_\nu^G \Rightarrow \delta t_\nu^G = \mathcal{N}\frac{\lambda_G}{2\omega R\sin\alpha}. \tag{11}$$

From Eqs. (10) and (11), we solve for t_ν^G:

$$t_\nu^G = \mathcal{N}\frac{\lambda_G}{2\omega R\sin\alpha}\frac{1}{[1 - (2\omega R\sin\alpha)/c]}. \tag{12}$$

From the Eqs. (6) and (12), we have got the relation between the neutrino arrival instant t_ν as measured by the CERN reference frame, $O_C x_C y_C z_C \equiv Oxyz$, and the neutrino arrival instant t_ν^G as measured by the Gran Sasso reference frame, $O_G x_G y_G z_G \equiv \tilde{O}\tilde{x}\tilde{y}\tilde{z}$, at the exact location of the interaction at an interation location within the Gran Sasso block of detectors, provided the effect of the Earth daily rotation under the assumptions we are taking in relation to the intantaneous movements of these locations in relation to the fixed stars as previously discussed:

$$\frac{t_\nu^G}{t_\nu} = \frac{\lambda_G}{\lambda_C}\left[1 - (2\omega R\sin\alpha)^2/c^2\right]^{-1} = \gamma^2\frac{\lambda_G}{\lambda_C}, \tag{13}$$

where $\gamma \geq 1$ is the usual relativity factor as defined above.

Now, λ_G/λ_C is simply the ratio between the spatial displacement between our consecutive gedanken control pulses, being these displacements defined through our previous paragraphs, leading to the Eqs. (4) and (10). Of course, this ratio is simply given by the relativistic Doppler effect under an approximation case in which C_C is the source and C_G the detector. The ratio between the Eqs. (10) and (4) gives:

$$\frac{\lambda_G}{\lambda_C} = [1 - (2\omega R\sin\alpha)/c]\,\frac{\left(t_\nu^G - \delta t_\nu^G\right)}{(t_\nu - \delta t_\nu)}. \tag{14}$$

But the time interval $(t_\nu - \delta t_\nu)$ is a proper time interval measured by the source clock C_C, as previously discussed. It accounts for the time interval between the first pulse sent and the last pulse sent as locally described by C_C is its $O_C x_C y_C z_C \equiv Oxyz$ world. These two events accur at different spatial locations in the C_G detector clock world $O_G x_G y_G z_G \equiv \tilde{O}\tilde{x}\tilde{y}\tilde{z}$, since C_C is approximating to C_G is this latter world. Hence, $t_\nu - \delta t_\nu$ is the Lorentz time contraction of $t_\nu^G - \delta t_\nu^G$, viz.:

$$t_\nu - \delta t_\nu = \gamma^{-1}\left(t_\nu^G - \delta t_\nu^G\right) \quad \therefore$$

$$\frac{\left(t_\nu^G - \delta t_\nu^G\right)}{t_\nu - \delta t_\nu} = \gamma = \left[1 - (2\omega R\sin\alpha)^2/c^2\right]^{-1/2}. \tag{15}$$

With the Eqs. (14) and (15), one reaches the usual relativistic Doppler effect expression for the approximation case:

$$\frac{\lambda_G}{\lambda_C} = \sqrt{\frac{1 - (2\omega R\sin\alpha)/c}{1 + (2\omega R\sin\alpha)/c}}. \tag{16}$$

With the Eq. (16), the Eq. (13) reads:

$$\frac{t_\nu^G}{t_\nu} = \left[1 - (2\omega R\sin\alpha)^2/c^2\right]^{-1/2}[1 + (2\omega R\sin\alpha)/c]^{-1} =$$

$$= \frac{\gamma}{1 + (2\omega R\sin\alpha)/c}. \tag{17}$$

Since $(2\omega R\sin\alpha)/c << 1$, we may apply an approximation for the Eq. (17), viz.:

$$\gamma \approx 1 + \frac{1}{2}\frac{(2\omega R\sin\alpha)^2}{c^2}, \tag{18}$$

and:

$$[1 + (2\omega R \sin\alpha)/c]^{-1} \approx 1 - (2\omega R \sin\alpha)/c, \qquad (19)$$

from which, neglecting the higher order terms, the Eq. (17) reads:

$$\frac{t_\nu^G}{t_\nu} \approx 1 - \frac{2\omega R \sin\alpha}{c} \quad \therefore \qquad (20)$$

$$t_\nu^G - t_\nu = -\frac{2\omega R \sin\alpha}{c} t_\nu. \qquad (21)$$

From this result, the clock that tag the arrival interaction instant t_ν^G in Gran Sasso turns out to measure an arrival time that is shorter than the correct one, this latter given by t_ν. With the discrepancy, ϵ, given by the value measured by the OPERA Collaboration [1], since t_ν is simply given by L/v_ν, where L is the baseline distance between the CERN and Gran Sasso, v_ν the speed of neutrino through the Earth crust, one obtains a value for v_ν. We rewrite the Eq. (21):

$$\epsilon = t_\nu^G - t_\nu = -\frac{2\omega R \sin\alpha}{c}\frac{L}{v_\nu}. \qquad (22)$$

With the values* $\omega = 7.3 \times 10^{-5}\,\mathrm{s}^{-1}$, $R = R_E \cos\lambda \approx 6.4 \times 10^6\,\mathrm{m} \times \cos(\pi/4) = 4.5 \times 10^6\,\mathrm{m}$, $\sin\alpha \approx \sin(7\pi/180) = 1.2 \times 10^{-1}$, $c = 3.0 \times 10^8\,\mathrm{ms}^{-1}$ and $L = 7.3 \times 10^5\,\mathrm{m}$, also with the discrepancy ϵ, given by the Eq. (22), being, say, $\epsilon = -62 \times 10^{-9}\,\mathrm{s}$, the neutrino velocity through the Earth crust reads:

$$v_\nu \approx 3.1 \times 10^6\,\mathrm{ms}^{-1}, \qquad (23)$$

being the refraction index of the Earth crust for neutrino given by:

$$n_{c|\nu} = \frac{c}{v_\nu} \approx 97. \qquad (24)$$

In reference to the matching PDF (probability distribution function) in the OPERA experiment, one would have a discrepancy between the maximum likelihood distribution obtained from the block of detectors at Gran Sasso and the translation of the PDF due to the protons distribution by TOF_c given by, in virtue of the Eq. (22):

$$\mathrm{TOF}_\nu = \mathrm{TOF}_c + \epsilon = \mathrm{TOF}_c - \frac{2\omega R \sin\alpha}{c}\frac{L}{v_\nu} \quad \therefore$$

$$\mathrm{TOF}_\nu - \mathrm{TOF}_c \approx -62\,\mathrm{ns}, \qquad (25)$$

under the reasoning and simplifications throughout this paper. One should notice the resoning here holds if the discrepancy turns out to be encrusted within the time translation of the PDF data, but such effect would not arise if the time interval TOF_ν were directly measured, since, in this latter situation, such interval would only read L/v_ν.

*See the Eqs. (2) and (3). The latitudes of CERN and Gran Sasso are, respectively: $46^{\mathrm{deg}}14^{\mathrm{min}}3^{\mathrm{sec}}$(N) and $42^{\mathrm{deg}}28^{\mathrm{min}}12^{\mathrm{sec}}$(N). The longitudes of CERN and Gran Sasso are, respectively: $6^{\mathrm{deg}}3^{\mathrm{min}}19^{\mathrm{sec}}$(E) and $13^{\mathrm{deg}}33^{\mathrm{min}}0^{\mathrm{sec}}$(E).

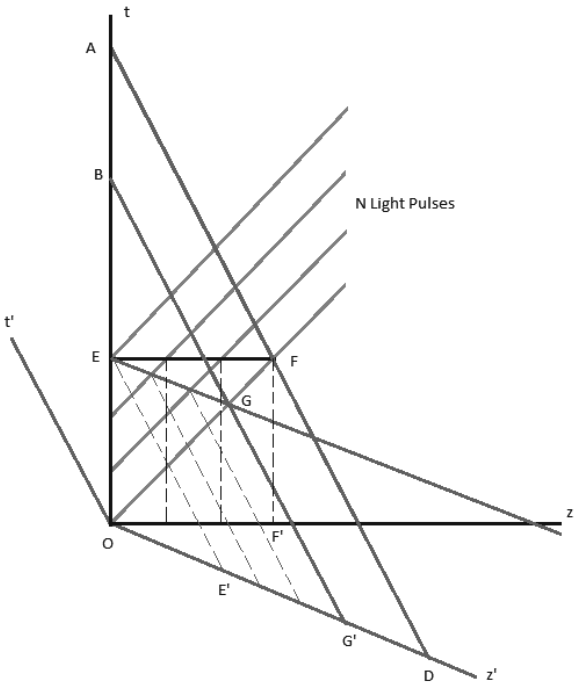

Fig. 1: Spacetime diagram for the phenomenon previously discussed. The Oz and Oz' axes depict the negative portions, respectively, of our previously defined Oz and $\tilde{O}\tilde{z}$ axes.

2 Spacetime diagram: a detailed explanation

Fig. 1 depicts the results we previously obtained, to which we will provide interpretation throughout this section.

The method we had used as a gedankenexperiment to send $\mathcal{N}$ light pulses is depicted via the Fig. 1. There are two different situations, since we want to determine, via the application of $\mathcal{N}$ gedanken pulses, in which reference frame the interaction of a neutrino at a point within the block of detectors at Gran Sasso actually had its interaction instant tagged. One should notice the Opera Collaboration shifted the PDF of the protons distribution to the time location of the interactions at Gran Sasso, but one must notice the proton PDF was not at the same instantaneous reference frame the block of detectors was. Hence, when one shifts the proton PDF distribution, one is assuming this shifted distribution represents the interactions at Gran Sasso in the same reference frame of the produced protons. This latter situation of shifting the PDF data of the protons is represented by the point A in the Fig. 1, viz., the point A represents the protons PDF distribution at its shifted position, and the clock that measures the shifting process is at rest in the CERN reference frame previously discussed, $O_C x_C y_C z_C \equiv Oxyz$, being our previously obtained t_ν given by the line segment OA in the Fig. 1, with the method of N sent pulses firstly accomplished in this reference frame. Note that $t_\nu \equiv OA$ is not the time a photon

would spend to accomplish the shift *, since one would expect this from the shifting the OPERA Collaboration statistically accomplished, once the Collaboration would be intrinsically assuming the time shift TOF_c as actually being the time interval the protons PDF would spend to match the distribution at the detection location, which would lead to a neutral shift in comparison with the detected distribution obtained from the Gran Sasso detectors in a case in which the protons PDF travelled at c, viz., a fortuitous shift would be simply pointing out to a velocity discrepancy in relation to c. The time interval the protons PDF actually spent to reach the Gran Sasso detectors was not directly measured, and the physical shift that actually occurred was, by the reasonings of this paper, t_ν. Now, since the interactions at Gran Sasso occurred in the $O_G x_G y_G z_G \equiv \tilde{O}\tilde{x}\tilde{y}\tilde{z}$ reference frame, the clock that tagged a neutrino interaction, measured via our gedanken method of $\mathcal{N}$ sent pulses, now being applied in the Gran Sasso reference frame, has its world line $G'B$ in the Fig. 1, viz, $t_\nu^G \equiv G'B$, i.e., the line segment $G'B$ in the Fig. 1 has our previously obtained t_ν^G as its lenght. Hence, once the OPERA Collaboration tried to match t_ν and t_ν^G, they, unfortunately, would obtain a discrepancy given by the Eq. (22), since two *different* frames raise and do not match. Finally, we would like to point out that, in the Fig. 1: OE is our previously defined $t_\nu - \delta t_\nu$, EA is our previously defined δt_ν, $G'G$ is our previously defined $t_\nu^G - \delta t_\nu^G$ and GB is our previously defined δt_ν^G. Also, as said before, A is the time location the proton PDF was actually shifted by the OPERA Collaboration, although they had aprioristically assumed a TOF_c shift for the protons PDF, and B the time location a Gran Sasso local clock actually tagged a neutrino event.

3 Conclusion

It is interesting to observe that even with a velocity having got two orders of magnitude lesser than c a neutrino may be interpreted as having got a velocity greater than c, depending on the method used to measure neutrino's time of flight, with the Earth crust presenting an index of refraction $n_{c|\nu} > 1$, due, also, to the local Doppler effect between the clocks attached to Gran Sasso and the respective intersecting ones in the CERN reference frame, as discussed throughout this paper, in virtue of the Earth daily rotation.

Acknowledgments

A.V.D.B. A. is grateful to Y.H.V. H. and CNPq for financial support.

Submitted on February 11, 2012 / Accepted on February 12, 2012

*the propagation axis of this photon does not appear in Fig. 1, since its propagation axis, Ox, is not depicted in the Fig. 1, which is not relevant for our analysis here. This same irrelevance for the propagation axis of the neutrinos holds here.

References

1. The OPERA collaboration: Adam T. et al. Measurement of the neutrino velocity with the OPERA detector in the CNGS beam. *arXiv:1109.4897*, 2011 (http://arxiv.org/abs/1109.4897).
2. Assis A.V.D.B. On the Neutrino Opera in the CNGS Beam. *Progress in Physics*, 2011, v. 4, 85–90.

A Way to Revised Quantum Electrodynamics

Bo Lehnert

Alfvn Laboratory, Royal Institute of Technology, 10044 Stockholm, Sweden
E-mail: Bo.Lehnert@ee.kth.se

In conventional theoretical physics and its Standard Model the guiding principle is that the equations are symmetrical. This limitation leads to a number of difficulties, because it does not permit masses for leptons and quarks, the electron tends to "explode" under the action of its self-charge, a corresponding photon model has no spin, and such a model cannot account for the "needle radiation" proposed by Einstein and observed in the photoelectric effect and in two-slit experiments. This paper summarizes a revised Lorentz and gauge invariant quantum electrodynamic theory based on a nonzero electric field divergence in the vacuum and characterized by linear intrinsic broken symmetry. It thus provides an alternative to the Higgs concept of nonlinear spontaneous broken symmetry, for solving the difficulties of the Standard Model. New results are obtained, such as nonzero and finite lepton rest masses, a point-charge-like behavior of the electron due to a revised renormalization procedure, a magnetic volume force which counteracts the electrostatic eigen-force of the electron, a nonzero spin of the photon and of light beams, needle radiation, and an improved understanding of the photoelectric effect, two-slit experiments, electron-positron pair formation, and cork-screw-shaped light beams.

1 Introduction

Conventional electromagnetic theory based on Maxwell's equations and quantum mechanics has been successful in its applications to numerous problems in physics, and has sometimes manifested itself in an extremely good agreement with experiments. Nevertheless there exist areas within which these joint theories do not provide fully adequate descriptions of physical reality. As already stated by Feynman [1], there are unsolved problems leading to difficulties with Maxwell's equations that are not removed by and not directly associated with quantum mechanics. It has thus to be remembered that these equations have served as a guideline and basis for the development of quantum electrodynamics (QED) in the vacuum state. Therefore QED also becomes subject to the typical shortcomings of electromagnetics in its conventional form.

A way to revised quantum electrodynamics is described in this paper, having a background in the concept of a vacuum that is not merely an empty space. There is thus a nonzero level of the vacuum ground state, the zero point energy, which derives from the quantum mechanical energy states of the harmonic oscillator. Part of the associated quantum fluctuations are also carrying electric charge. The observed electron-positron pair formation from an energetic photon presents a further indication that electric charges can be created out of an electrically neutral vacuum state. In this way the present approach becomes based on the hypothesis of a nonzero electric charge density and an associated electric field divergence in the vacuum state. This nonzero divergence should not become less conceivable than the nonzero curl of the magnetic field related to Maxwell's displacement current.

The present treatise starts in Section 2 with a discussion on quantization of the field equations. This is followed in Section 3 by a description of the difficulties which remain in conventional theory and its associated Standard Model. An outline of the present revised theory is then given in Section 4, and its potentialities are presented in Section 5. A number of fundamental applications and new consequences of the same theory are finally summarized in Sections 6 and 7.

2 Quantization of the field equations

As stated by Schiff [2] among others, Maxwell's equations are used as a guideline for proper interpretation of conventional quantum electrodynamical theory. To convert in an analogous way the present extended field equations into their quantum electrodynamical counterpart, the most complete way would imply that the quantum conditions are included already from the outset.

In this treatise, however, a simplified procedure is applied, by first determining the general solutions of the basic field equations, and then imposing the relevant quantum conditions afterwards. This is at least justified by the fact that the quantized electrodynamic equations become identically equal to the original equations in which the potentials and currents are merely replaced by their expectation values, as shown by Heitler [3]. The result of such a procedure should therefore not be too far from the truth, by using the most probable trajectories and states in a first approximation.

3 Difficulties in conventional theory

As pointed out by Quigg [4] among others, the guiding principle of the Standard Model in theoretical physics is that its equations are symmetrical, and this does not permit masses for leptons and quarks. Such a feature also reveals itself in the symmetry of the conventional field equations of QED in

which there are vanishing divergences of both the electric and magnetic fields in the vacuum, as given e.g. by Schiff [2].

In the Dirac wave equation of a single particle like the electron, the problem of nonzero mass and charge is circumambulated by introducing given values of its mass m_e and charge e. With an electrostatic potential ϕ and a magnetic vector potential $\mathbf{A}$, the equation for the relativistic wave function has the form

$$\alpha_0 m_e c\Psi + \boldsymbol{\alpha}\cdot[(\hbar/i)\nabla\Psi - (e/c)\mathbf{A}\Psi] + e\phi\Psi = -\frac{\hbar}{ic}\frac{\partial}{\partial t}\Psi \quad (1)$$

where α_i are the Dirac matrices given e.g. by Morse and Feshbach [5].

To fulfill the demand of a nonzero particle mass, the symmetry of the field equations has to be *broken*. One such possibility was worked out in the mid 1960s by Higgs [6] among others. From the corresponding equations a Higgs particle was predicted which should have a nonzero rest mass. Due to Ryder [7] the corresponding Lagrangian then takes the form

$$\mathcal{L} = -\frac{1}{4}F_{\mu\nu}F^{\mu\nu} + \left|\left(\partial_\mu + icA_\mu\right)\phi\right|^2 - m^2\phi^*\phi - \lambda(\phi^*\phi)^2 \quad (2)$$

where ϕ represents a scalar field, A_μ a vector field, and $F_{\mu\nu} = \partial_\mu A_\nu - \partial_\nu A_\mu$ is the electromagnetic field tensor. The quantity m further stands for a parameter where $m^2 < 0$ in the case of *spontaneous symmetry breaking*, and the parameter λ is related to a minimized potential. The symmetry breaking is due to the two last terms of the Lagrangian (2). The latter is *nonlinear* in its character, and corresponds to a deduced relation for the minimum of the vacuum potential. Experimental confirmation of this mechanism does not rule out the applicability of the present theory to the problem areas treated in this paper.

3.1 Steady states

Conventional theory based on Maxwell's equations in the vacuum is symmetric in respect to the field strengths **E** and **B**. In the absence of external sources, such as for a self-consistent particle-like configuration, the charge density $\bar{\rho}$, div**E** and curl**B** all vanish. Then there is no scope for a local nonzero energy density in a steady state which would otherwise be the condition for a particle configuration having a nonzero rest mass. This is consistent with the statement by Quigg [4] that the symmetric conventional field equations do not permit masses for leptons and quarks.

The fundamental description of a charged particle is in conventional theory deficient also in the respect that an equilibrium cannot be maintained by the classical electrostatic forces, but has been assumed to require extra forces of a non-electromagnetic origin, as proposed e.g. by Heitler [3] and Jackson [8]. In other words, the electron would otherwise "explode" under the action of its electric self-charge.

The electron behaves like a point charge with a very small radius. Standard theory is confronted with the infinite self-energy of such a system. A quantum electromagnetic renormalization procedure has then been applied to yield a finite result, by adding an infinite ad hoc term to the Lagrangian, such as to obtain a finite result from the difference between two "infinities" [7]. Even if such a procedure has turned out to be successful, it can be questioned from the logical and physical points of view.

3.2 Wave modes

In a state of explicit time dependence, the conventional symmetric wave equations by Maxwell in the vacuum with vanishing electric and magnetic field divergences can be recast in terms of a Hertz vector $\mathbf{\Pi}$, as described by Stratton [9] and Halln [10] among others. These equations result in two partial solutions, $\mathbf{\Pi}_1$ and $\mathbf{\Pi}_2$, denoted as an electric and a magnetic type which are given by the fields

$$\mathbf{E_1} = \nabla(\mathrm{div}\mathbf{\Pi}_1) - (1/c^2)\partial^2\mathbf{\Pi}_1/\partial t^2 \quad (3)$$

$$\mathbf{B_1} = (1/c^2)\mathrm{curl}(\partial\mathbf{\Pi}_1/\partial t) \quad (4)$$

and

$$\mathbf{E_2} = -\mu_0\mathrm{curl}(\partial\mathbf{\Pi}_2/\partial t) \quad (5)$$

$$\mathbf{B_2} = \mu_0\nabla(\mathrm{div}\mathbf{\Pi}_2) - (\mu_0/c^2)\partial^2\mathbf{\Pi}_2/\partial t^2. \quad (6)$$

Here $c^2 = 1/\mu_0\epsilon_0$ with μ_0 denoting the magnetic permeability and ϵ_0 the dielectric constant in the vacuum. Using the results obtained from equations (3)-(6) and given in current literature, the integrated angular momentum in the direction of propagation (spin) can be evaluated for plane, cylindrical, and spherical wave modes. This is made in terms of the electromagnetic momentum density

$$\mathbf{g} = \epsilon_0\mathbf{E}\times\mathbf{B} = \frac{1}{c^2}\mathbf{S} \quad (7)$$

where **S** is the Poynting vector, and of the density

$$\mathbf{s} = \mathbf{r}\times\frac{\mathbf{S}}{c^2} \quad (8)$$

with **r** standing for the radius vector. The results are summarized as described by the author [11]:

- For plane waves propagating in the direction of a rectangular frame (x, y, z) the field components E_z and B_z vanish as well as the spin. A three-dimensional disturbance of arbitrary shape at a given instant can in principle be constructed by Fourier analysis from a spectrum of plane waves. At later instants, however, such a disturbance would rapidly disintegrate [9].
- Cylindrical geometry has the advantage of providing a starting point for waves which propagate with conserved shape in a defined direction like a photon, at

the same time as it can have limited dimensions in the transverse directions under certain conditions. With an elementary wave form $f(r)\exp[i(-\omega t + kz + n\varphi)]$ in a cylindrical frame (r, φ, z) with z in the direction of propagation, the dispersion relation becomes

$$K^2 = (\omega/c)^2 - k^2 \tag{9}$$

This leads to local spin densities s_{z1} and s_{z2} of equation (8) in respect to the z axis where

$$|s_{z1}| \text{ and } |s_{z2}| \propto K^2 n\,[J_n(Kr)]^2 \sin 2n\varphi \tag{10}$$

for the two types of equations (3)-(6), and with $J_n(Kr)$ as Bessel functions. Consequently, the local contribution to the spin vanishes both when $n = 0$ and $K = 0$. With nonzero n and K the total integrated spin also vanishes.

- When considering spherical waves which propagate along r in a spherical frame (r, θ, φ) of unbounded space at the phase velocity $\omega/k = c$ with a periodic variation $\exp(in\varphi)$, the field components are obtained in terms of associated Legendre functions, spherical Bessel functions, and factors $\sin(n\varphi)$ and $\cos(n\varphi)$ [9]. The asymptotic behavior of the components of the momentum density (7) then becomes

$$g_r \propto 1/r^2 \quad g_\theta \propto 1/r^3 \quad g_\varphi \propto 1/r^3 \tag{11}$$

The momentum g_r along the direction of propagation is the remaining one at large distances r for which the spin thus vanishes. From the conservation of angular momentum there is then no integrated spin in the near-field region as well. This is confirmed by its total integrated value.

From these results is thus shown that the conventional symmetric equations by Maxwell in the vacuum, and the related equations in quantized field theory, do not become reconcilable with a physically relevant photon model having nonzero spin.

In addition, a conventional theoretical concept of the photon as given by equations (3)-(6) cannot account for the needle-like behavior proposed by Einstein and being required for knocking out an atomic electron in the photoelectric effect. Nor can such a concept become reconcilable with the dot-shaped marks which occur at the screen of two-slit experiments from individual photon impacts, as observed e.g. by Tsuchiya et al. [12].

4 An outline of present revised theory

As stated in the introduction, the present theory is based on the hypothesis of a nonzero electric charge density in the vacuum. The detailed evaluation of the basic concepts of this theory has been reported by the author [13, 14] and is shortly outlined here. The general four-dimensional Lorentz invariant form of the corresponding Proca-type field equations reads

$$\left(\frac{1}{c^2}\frac{\partial^2}{\partial t^2} - \nabla^2\right) A_\mu = \mu_0 J_\mu, \quad \mu = 1, 2, 3, 4 \tag{12}$$

where

$$A_\mu = \left(\mathbf{A}, \frac{i\phi}{c}\right) \tag{13}$$

with $\mathbf{A}$ and ϕ standing for the magnetic vector potential and the electrostatic potential in three-space,

$$J_\mu = (\mathbf{j}, ic\bar{\rho}) = \bar{\rho}(\mathbf{C}, ic) \quad \mathbf{j} = \bar{\rho}\mathbf{C} = \epsilon_0(\mathrm{div}\mathbf{E})\mathbf{C} \tag{14}$$

and $\mathbf{C}$ being a velocity vector having a modulus equal to the velocity constant c of light, i.e. $\mathbf{C}^2 = c^2$. Consequently this becomes a *generalization* of Einsteins relativistic velocity limit. In three dimensions equation (12) in the vacuum results in

$$\frac{\mathrm{curl}\mathbf{B}}{\mu_0} = \epsilon_0(\mathrm{div}\mathbf{E})\mathbf{C} + \frac{\epsilon_0\partial\mathbf{E}}{\partial t} \tag{15}$$

$$\mathrm{curl}\mathbf{E} = -\frac{\partial\mathbf{B}}{\partial t} \tag{16}$$

$$\mathbf{B} = \mathrm{curl}\mathbf{A}, \ \mathrm{div}\mathbf{B} = 0 \tag{17}$$

$$\mathbf{E} = -\nabla\phi - \frac{\partial\mathbf{A}}{\partial t} \tag{18}$$

$$\mathrm{div}\mathbf{E} = \frac{\bar{\rho}}{\epsilon_0}. \tag{19}$$

These equations differ from the conventional form, by a nonzero electric field divergence in equation (19) and by the additional first term of the right-hand member in equation (15) which represents a "space-charge current density" in addition to the displacement current. Due to the form (14) there is a similarity between the current density and that by Dirac [5]. The extended field equations (15)-(19) are easily found also to become invariant to a gauge transformation. The same equations can further be derived from a Lagrangian density

$$\mathcal{L} = \frac{1}{2}\epsilon_0(\mathbf{E}^2 - c^2\mathbf{B}^2) - \bar{\rho}\phi + \mathbf{j}\cdot\mathbf{A}. \tag{20}$$

In this context special attention will be paid to steady states for which the field equations reduce to

$$c^2\mathrm{curlcurl}\mathbf{A} = -\mathbf{C}(\nabla^2\phi) = \frac{\bar{\rho}}{\epsilon_0}\mathbf{C} \tag{21}$$

and to wave modes for which

$$\left(\frac{\partial^2}{\partial t^2} - c^2\nabla^2\right)\mathbf{E} + \left(c^2\nabla + \mathbf{C}\frac{\partial}{\partial t}\right)(\mathrm{div}\mathbf{E}) = 0. \tag{22}$$

The main characteristic new features of the present theory can be summarized as follows:

- The hypothesis of a nonzero electric field divergence in the vacuum introduces an *additional* degree of freedom, leading to new physical phenomena. The associated nonzero electric charge density thereby acts somewhat like a "hidden variable".
- This also abolishes the symmetry between the electric and magnetic fields, and the field equations then obtain the character of *intrinsic linear symmetry breaking*.
- The theory is both Lorentz and gauge *invariant*.
- The velocity of light is no longer a scalar quantity, but is represented by a velocity *vector* of the modulus c.

5 Potentialities of present theory

Maxwell's equations in the vacuum, and their quantized counterparts, are heavily constrained. Considerable parts of this limitation can be removed by the present theory. Thus the characteristic features described in Section 4 debouch into a number of potentialities:

- The present linear field equations are characterized by an intrinsic broken symmetry. The Lagrangian (20) differs from the form (2) by Higgs. The present approach can therefore become an *alternative* to the Higgs concept of nonlinear spontaneous broken symmetry.
- In the theory by Dirac the mass and electric charge of the electron have been introduced as given parameters in the wave equation (1), whereas nonzero and finite masses and charges *result* from the solutions of the present field equations. This is due to the symmetry breaking of these equations which include *steady* electromagnetic states, not being present in conventional theory.
- As a further consequence of this symmetry breaking, the electromagnetic wave solutions result in photon models having *nonzero* angular momentum (spin), not being deducible from conventional theory, and being due to the current density $\mathbf{j}$ in equations (14) and (15) which gives a contribution to the momentum density (7).
- This broken symmetry also renders possible a *revised* renormalization process, providing an alternative to the conventional one in a physically more surveyable way of solving the infinite self-energy problem. This alternative is based on the nonzero charge density of equation (19).
- In analogy with conventional theory, a local momentum equation including a volume force term is obtained from vector multiplication of equation (15) by $\mathbf{B}$ and equation (16) by $\epsilon_0\mathbf{E}$, and adding the obtained equations. This results in a volume force density which does not only include the well-known electrostatic part $\bar{\rho}\mathbf{E}$, but also a *magnetic* part $\bar{\rho}\mathbf{C}\times\mathbf{B}$ not being present in conventional theory.

6 Fundamental applications

A number of concrete results are obtained from the present theory, as fundamental applications to models of leptons and photons and to be shortly summarized in this section.

6.1 An Electron Model

Aiming at a model of the electron at rest, a steady axisymmetric state is considered in a spherical frame (r,θ,φ) where $\mathbf{A}=(0,0,A)$ and $\mathbf{j}=(0,0,c\bar{\rho})$ with $C=\pm c$ representing the two spin directions. Equations (21) can be shown to have a general solution being derivable from a separable generating function

$$F(r,\theta)=CA-\phi=G_0G(\rho,\theta)=G_0R(\rho)T(\theta) \qquad (23)$$

where G_0 stands for a characteristic amplitude, $\rho=r/r_0$ is a normalized radial coordinate, and r_0 is a characteristic radial dimension. The potentials $\mathbf{A}$ and ϕ as well as the charge density $\bar{\rho}$ can be uniquely expressed in terms of F and its derivatives. This, in its turn, results in forms for the spatially integrated net values of electric charge q_0, magnetic moment M_0, mass m_0 obtained from the mass-energy relation by Einstein, and spin s_0.

A detailed analysis of the integrals of q_0 and M_0 shows that an electron model having nonzero q_0 and M_0 only becomes possible for radial functions $R(\rho)$ being divergent at the origin $\rho=0$, in combination with a polar function $T(\theta)$ having top-bottom symmetry with respect to the midplane $\theta=\pi/2$. Neutrino models with vanishing q_0 and M_0 become on the other hand possible in three other cases. The observed point-charge-like behavior of the electron thus comes out as a consequence of the present theory, due to the requirement of a nonzero net electric charge.

The necessary divergence of the radial function R leads to the question how to obtain finite and nonzero values of all related field quantities. This problem can be solved in terms of a revised renormalization procedure, being an alternative to the conventional process of tackling the self-energy problem. Here we consider a generating function with the parts

$$R=\rho^{-\gamma}e^{-\rho},\quad \gamma>0 \qquad (24)$$

$$\begin{aligned} T &= 1+\sum_{\nu=1}^{n}\{a_{2\nu-1}\sin[(2\nu-1)\theta]+a_{2\nu}\cos(2\nu\theta)\} \\ &= 1+a_1\sin\theta+a_2\cos 2\theta+a_3\sin 3\theta+\ldots \end{aligned} \qquad (25)$$

where R is divergent at $\rho=0$ and T is symmetric in respect to $\theta=\pi/2$. In the present renormalization procedure the lower radial limits of the integrals in (q_0,M_0,m_0,s_0) are taken to be $\rho=\epsilon$ where $0<\epsilon\ll 1$. Further the concepts of first and second counter-factors are introduced and defined by the author [13,15], i.e.

$$f_1=c_{rG}\epsilon=r_0G_0\quad f_2=c_G\epsilon^2=G_0 \qquad (26)$$

where c_{rG} and c_G are corresponding constants. Consequently all field quantities (q_0, M_0, m_0, s_0) then become nonzero and finite at small ϵ. This revised renormalization procedure implies that the "infinities" of the field quantities due to the divergence of R at $\rho = 0$ are outbalanced by the "zeros" of the counter-factors f_1 and f_2 .

The quantum conditions to be imposed on the general solutions are the spin condition

$$s_0 = \pm h/4\pi \tag{27}$$

of a fermion particle, the magnetic moment relation

$$M_0 m_0/q_0 s_0 = 1 + \delta_M \quad \delta_M = 1/2\pi f_0 = 0.00116 \tag{28}$$

given e.g. by Feynman [16], and the magnetic flux condition

$$\Gamma_{tot} = |s_0/q_0| \tag{29}$$

where Γ_{tot} stands for the total magnetic flux being generated by the electric current system.

From these conditions the normalized electric charge $q^* \equiv |q_0/e|$, with $q^* = 1$ as its experimental value, can be obtained in terms of the expansion (25). In the four-amplitude case (a_1, a_2, a_3, a_4) the normalized charge q^* is then found to be limited at large a_3 and a_4 in the a_3a_4-plane to a narrow "plateau-like" channel, localized around the experimental value $q^* = 1$ as shown by Lehnert and Scheffel [17] and Lehnert and Hk [18]. As final results of these deductions all quantum conditions and all experimentally relevant values of charge, magnetic moment, mass, and spin can thus be reproduced by the single choices of only two scalar free parameters, i.e. the counter-factors f_1 and f_2 [15,17,18]. This theory should also apply to the muon and tauon and corresponding antiparticles.

With correct values of the magnetic flux (29) including magnetic island formation, as well as the correct magnetic moment relation (28) including its Land factor, the plateau in a_3a_4-space thus contains the correct experimental value $q^* = 1$ of the elementary charge. There are deviations of only a few percent from this value within the plateau region. This could at a first sight merely be considered as fortunate coincidence. What speaks against this is, however, that changes in the basic conditions result in normalized charges which differ fundamentally from the experimental value, this within an accuracy of about one percent. Consequently, omission of the magnetic islands yields an incorrect value $q^* \approx 1.55$, and an additional change to half of the correct Land factor results in $q^* \approx 1.77$. That the correct forms of the magnetic flux and the magnetic moment become connected with a correct value of the deduced elementary charge, can therefore be taken as a strong support of the present theory. Moreover, with wrong values of the magnetic flux and Land factors, also the values of magnetic moment M_0 and mass m_0 would disagree with experiments.

The Lorentz invariance of the electron radius can be formally satisfied, in the case where this radius is allowed to shrink to that of a point charge. The obtained results can on the other hand also apply to the physically relevant situation of a small but nonzero radius of a configuration having an internal structure.

The configuration of the electron model can be prevented from "exploding" under the influence of its eigencharge and the electrostatic volume force $\bar{\rho}\mathbf{E}$. This is due to the presence of the magnetically confining volume force $\bar{\rho}\mathbf{C} \times \mathbf{B}$ [18].

6.2 A Photon Model

Cylindrical waves appear to be a convenient starting point for a photon model, due to the aims of a conserved shape in a defined direction of propagation and of limited spatial extensions in the transverse directions. In a cylindrical frame (r, φ, z) the velocity vector is here given by the form

$$\mathbf{C} = c(0, \cos\alpha, \sin\alpha) \tag{30}$$

where $\sin\alpha$ will be associated with the propagation and $\cos\alpha$ with the spin. In the case of axisymmetric waves, equation (22) yields

$$\omega = k\nu, \quad \nu = c(\sin\alpha) \tag{31}$$

for normal modes which vary as $f(r)\exp[i(-\omega t + kz)]$. The angle α should be constant since astronomical observations indicate that light from distant objects has no dispersion. The basic equations result in general solutions for the components of $\mathbf{E}$ and $\mathbf{B}$, in terms of a generating function

$$F(r, z, t) = E_z + (\cot\alpha)E_\varphi = G_0 G, \qquad G = R(\rho)\exp[i(-\omega t + kz)] \tag{32}$$

and its derivatives. The dispersion relation (31) shows that the phase and group velocities along the z direction of propagation are smaller than c. Not to get in conflict with the experiments by Michelson and Moreley, we then have to restrict ourselves to a condition on the spin parameter $\cos\alpha$, in the form

$$0 < \cos\alpha \ll 1 \quad \nu/c \approx 1 - \frac{1}{2}(\cos\alpha)^2. \tag{33}$$

From the normal mode solutions, wave-packets of narrow line width can be deduced, providing expressions for the corresponding spectrally integrated field strengths $\bar{\mathbf{E}}$ and $\bar{\mathbf{B}}$. The latter are further used in spatial integrations which lead to a net electric charge $q = 0$ and net magnetic moment $M = 0$, as expected, and into a nonzero total mass $m \neq 0$ due to the mass-energy relation by Einstein, as well as to a nonzero spin $s \neq 0$ obtained from the Poynting vector and equation (8). There is also an associated very small photon rest mass $m_0 = m(\cos\alpha)$. Thus a nonzero spin and a nonzero photon rest mass become two sides of the same intrinsic property

which vanishes with the parameter $\cos\alpha$, i.e. with div$\mathbf{E}$. Due to the requirement of Lorentz invariance, a nonzero $\cos\alpha$ thus implies that a nonzero spin arises at the expense of a slightly reduced momentum and velocity in the direction of propagation. This is a consequence of the generalized Lorentz invariance in Section 4.

In this connection it has to be added that the alternative concept of a momentum operator $\mathbf{p} = -i\hbar\nabla$ has been applied to a massive particle in the Schrdinger equation [2]. As compared to the momentum density $\mathbf{g}$ of equation (7), however, the operator $\mathbf{p}$ leads to physically unrealistic transverse components for a cylindrically symmetric and spatially limited wave-packet model of the photon.

With a radial part of the generating function (32) being of the form

$$R(\rho) = \rho^{\gamma} e^{-\rho} \tag{34}$$

there are two options, namely the convergent case of $\gamma > 0$ and the divergent one of $\gamma < 0$. In the convergent case combination of the wave-packet solutions for a main wavelength λ_0 with the quantum conditions

$$m = h/c\lambda_0 \quad s = h/2\pi \tag{35}$$

results in an effective transverse photon radius

$$\hat{r} = \frac{\lambda_0}{2\pi(\cos\alpha)} \quad \gamma > 0. \tag{36}$$

In the divergent case a corresponding procedure has to be applied, but with inclusion of a revised renormalization being analogous to that applied to the electron. With the corresponding smallness parameter ϵ the effective photon radius then becomes

$$\hat{r} = \frac{\epsilon\lambda_0}{2\pi(\cos\alpha)} \quad \gamma < 0. \tag{37}$$

The results (36) and (37) can be considered to represent two modes. The first has relatively large radial extensions as compared to atomic dimensions, and for $\epsilon/(\cos\alpha) \leqslant 1$ the second mode leads to very small such extensions, in the form of "needle radiation". Such radiation provides explanations of the photoelectric effect, and of the occurrence of the dot-shaped marks on a screen in double-slit experiments [12]. The two modes (36) and (37) are based on the broken symmetry and have no counterpart in conventional theory. They can also contribute to an understanding of the two-slit experiments, somewhat in the sense of the Copenhagen school of Bohr and where an individual photon makes a transition between the present modes, in a form of "photon oscillations" including both a particle behavior and that of wave interference, as stated by the author [19]. Such oscillations would become analogous to those of neutrinos which have nonzero rest masses.

The nonzero electric field divergence further leads to insintric electric charges of alternating polarity within the body of an individual photon wave packet. This contributes to the understanding of electron-positron pair formation through the impact of an external electric field from an atomic nucleus or from an electron, as proposed by the author [20].

There is experimental evidence for the angular momentum of a light beam of spatially limited cross-section, as mentioned by Ditchburn [21]. This can be explained by contributions from its boundary layers, in terms of the present approach.

The wave equations of this theory can also be applied to cork-screw-shaped light beams in which the field quantities vary as $f(r)\exp[i(-\omega t + \bar{m}\varphi + kz)]$ and where the parameter $\bar{m}$ is a positive or negative integer. The dispersion relation then becomes

$$\omega/k = c(\sin\alpha) + (\bar{m}/kr)c(\cos\alpha). \tag{38}$$

The normal modes and their spectrally integrated screw-shaped configurations then result in a radially hollow beam geometry, as observed in experiments described by Battersby [22] among others.

For the W^+, W^- and Z^0 bosons, a Proca-type equation being analogous to that of the present theory can possibly be applied in the weak-field case. This would then provide the bosons with a nonzero rest mass, as an alternative to the Higgs concept.

With the present theory of the vacuum state as a background, fermions like the electron and neutrino, and bosons like the photon, could be taken as concepts with the following characteristics. The fermions can be made to originate from the steady-state field equations, represent "bound" states, and have an explicit rest mass being associated with their spin. This does not exclude that moving fermions also can have wave properties. The bosons originate on the other hand from the dynamic wavelike field equations, represent "free" states, and have an implicit rest mass associated with their spin. They occur as quantized waves of the field which describe the interaction between the particles of matter.

7 New consequences of present theory

Among the fundamental new consequences which only come out of the present theory and also strongly support its relevance, the following should be emphasized:

- Steady electromagnetic states lead to rest masses of leptons.
- A nonzero electronic charge is by necessity connected with a point-charge-like geometry.
- A deduced electronic charge agreeing with the experimental value results from correct forms of the magnetic moment and magnetic flux, but not from other forms.
- A confining magnetic force prevents the electron from "exploding" under the influence of its eigencharge.

- Electromagnetic waves and their photon models possess spin.
- There are needle-like wave solutions contributing to the understanding of the photoelectric effect and of two-slit experiments.
- The angular momentum of a light beam can be explained.

Submitted on February 7, 2012 / Accepted on February 17, 2012

References

1. Feynmann R. P. Lectures on Physics: Mainly Electromagnetism and Matter. Addison-Wesley, Reading, MA, 1964, 28.
2. Schiff L. I. Quantum Mechanics. McGraw-Hill Book Comp., Inc., New York-Toronto-London, 1949, Ch. XIV; Ch. II, Sec. 6.
3. Heitler W. The Quantum Theory of Radiation. Third edition, Oxford, Clarendon Press, 1954, Appendix, 409; 31.
4. Quigg C. The coming revolution in particle physics. *Scientific American*, February 2008, 38–45.
5. Morse P. M. and Feshbach H. Methods of Theoretical Physics. McGraw-Hill Book Comp., Inc., New York-Toronto-London, 1953, Part I, 260–261.
6. Higgs P. W. Spontaneous symmetry breakdown without massless bosons. *Physical Review*, 1966, v. 145, 1156–1163.
7. Ryder L. H. Quantum Field Theory. Second edition, Cambridge University Press, 1996, 397; Ch.9.
8. Jackson J. D. Classical Electrodynamics. John Wiley & Sons, Inc., New York, London, Sydney, 1962, Sec. 17.4.
9. Stratton J. A. Electromagnetic Theory. First edition, McGraw-Hill Book Comp., Inc., New York-Toronto-London 1941, Ch. I, Sec. 11. 1; Sec. 6. 7.
10. Halln E. Electromagnetic Theory. Chapman and Hall, London, 1962, Sec. 34.
11. Lehnert B. The failure of Maxwell's equations as a basis for a photon model in the vacuum state. *International Review of Physics*, 2008, v. 2, no. 6, 337–340.
12. Tsuchiya Y., Inuzuka E., Kurono T., and Hosoda M. Photo-counting imaging and its application. *Advances in Electronics and Electron Physics*, 1985, v. 64A, 21–31.
13. Lehnert B. A Revised Electromagnetic Theory with Fundamental Applications. Edited by Z. I. Vakhnenko and A. Z. Zagorodny, Bogolyubov Instutute for Theoretical Physics, Kiev 2008; Edited by D. Rabounski, Swedish Physics Archive, The National Library of Sweden, Stockholm 2008; Revised Quantum Electrodynamics. In the series "Contemporary Fundamental Physics" edited by V. V. Dvoeglazov, Nova Science Publishers, Inc., Hauppange 2012, New York, USA.
14. Lehnert B. Revised Quantum Electrodynamics with Fundamental Applications. In *New Aspects of Plasma Physics*, Edited by P. K. Shukla, L. Stenflo and B. Eliasson, World Scientific Publishing Co. Pte. Ltd., Singapore 2008, 52–36.
15. Lehnert B. Deduced fundamental properties of the electron. *International Review of Physics*, 2010, v. 4, no. 1, 1–6.
16. Feynman R. QED: The Strange Theory of Light and Matter. Penguin, London, 1990.
17. Lehnert B. and Scheffel J. On the minimum elementary charge of an extended electromagnetic theory. *Physica Scripta*, 2002, v. 65, 200–207.
18. Lehnert B. and Hk L. J. An electron model with elementary charge. *Journal of Plasma Physics*, 2010, v. 76, 419–428.
19. Lehnert B. The individual photon in two-slit experiments. *International Review of Physics*, 2011, v. 5, no. 1, 15–18.
20. Lehnert B. Wave-particle properties and pair formation of the photon. In *Frontiers of Modern Plasma Physics*, Edited by P. K. Shukla, B. Eliasson and L. Stenflo, American Institute of Physics, Melville, NY, USA, 2008, 282–291.
21. Ditchburn R. W. Light. Academic Press, London, New York, San Francisco, 1976, Third edition, Sec. 17. 24.
22. Battersby S. Twisting the light away. *New Scientist*, 12 June 2004, 37–40.

Parameterized Special Theory of Relativity (PSTR)

Florentin Smarandache
University of New Mexico, Gallup, NM 87301, USA
E-mail: smarand@unm.edu

We have parameterized Einstein's thought experiment with atomic clocks, supposing that we knew neither if the space and time are relative or absolute, nor if the speed of light was ultimate speed or not. We have obtained a Parameterized Special Theory of Relativity (PSTR), first introduced in 1982. Our PSTR generalized not only Einstein's Special Theory of Relativity, but also our Absolute Theory of Relativity, and introduced three more possible Relativities to be studied in the future. After the 2011 CERN's superluminal neutrino experiments, we recall our ideas and invite researchers to deepen the study of PSTR, ATR, and check the three new mathematically emerged Relativities 4.3, 4.4, and 4.5.

1 Einstein's thought experiment with the light clocks

There are two identical clocks, one is placed aboard of a rocket, which travels at a constant speed v with respect to the Earth, and the second one is on the Earth. In the rocket, a light pulse is emitted by a source from A to a mirror B that reflects it back to A where it is detected. The rocket's movement and the light pulse's movement are orthogonal. There is an observer in the rocket (the astronaut) and an observer on the Earth. The trajectory of light pulse (and implicitly the distance traveled by the light pulse), the elapsed time it needs to travel this distance, and the speed of the light pulse at which is travels are perceived differently by the two observers (depending on the theories used — see below in this paper).

According to the astronaut (see Fig. 1):

$$\Delta t' = \frac{2\,d}{c}\,, \tag{1}$$

where $\Delta t'$ time interval, as measured by the astronaut, for the light to follow the path of double distance $2d$, while c is the speed of light.

According to the observer on the Earth (see Fig. 2):

$$\left.\begin{aligned} 2\,l &= v\,\Delta t\,, \quad s = |AB| = |BA'| \\ d &= |BB'|\,, \quad l = |AB'| = |b'A'| \end{aligned}\right\}, \tag{2}$$

where Δt is the time interval as measured by the observer on the Earth. And using the Pythagoras' Theorem in the right triangle $\Delta ABB'$, one has

$$2s = 2\,\sqrt{d^2 + l^2} = 2\,\sqrt{d^2 + \left(\frac{v\,\Delta t}{2}\right)^2}\,, \tag{3}$$

but $2s = c\,\Delta t$, whence

$$c\,\Delta t = 2\,\sqrt{d^2 + \left(\frac{v\,\Delta t}{2}\right)^2}\,. \tag{4}$$

Squaring and computing for Δt one gets:

$$\Delta t = \frac{2\,d}{c}\,\frac{1}{\sqrt{1 - \frac{v^2}{c^2}}}\,. \tag{5}$$

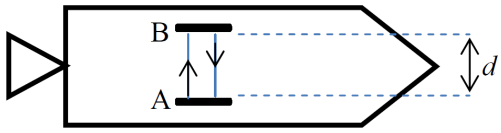

Figure 1

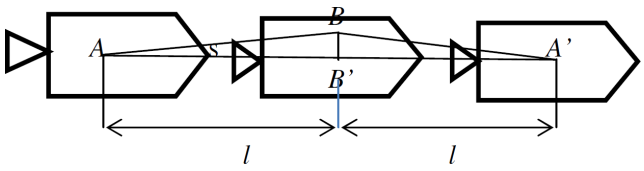

Figure 2

Whence Einstein gets the following time dilation:

$$\Delta t = \frac{\Delta t'}{\sqrt{1 - \frac{v^2}{c^2}}}\,. \tag{6}$$

where $\Delta t > \Delta t'$

2 Parameterized Special Theory of Relativity (PSTR)

In a more general case when we don't know the speed x of the light as seen by the observer on Earth, nor the relationship between $\Delta t'$ and Δt, we get:

$$x\,\Delta t = 2\,\sqrt{d^2 + \left(\frac{v\,\Delta t}{2}\right)^2}\,. \tag{7}$$

But $d = \frac{c\,\Delta t'}{2}$, therefore:

$$x\,\Delta t = 2\,\sqrt{\left(\frac{c\,\Delta t}{2}\right)^2 + \left(\frac{v\,\Delta t}{2}\right)^2}\,, \tag{8}$$

or

$$x\,\Delta t = \sqrt{c^2(\Delta t')^2 + v^2(\Delta t')^2}\,. \tag{9}$$

Dividing the whole equality by Δt we obtain:

$$x = \sqrt{v^2 + c^2 \left(\frac{\Delta t'}{\Delta t}\right)^2}\,. \tag{10}$$

which is the *PSTR Equation*.

3 PSTR elapsed time ratio τ (parameter)

We now substitute in a general case

$$\frac{\Delta t'}{\Delta t} = \tau \in (0, +\infty)\,, \tag{11}$$

where τ is the PSTR elapsed time ratio. Therefore we split the Special Theory of Relativity (STR) in the below ways.

4 PSTR extends STR, ATR, and introduces three more Relativities

4.1 If $\tau = \sqrt{1 - \frac{v^2}{c^2}}$ we get the STR (see [1]), since replacing x by c, one has

$$c^2 = v^2 + c^2 \left(\frac{\Delta t'}{\Delta t}\right)^2, \tag{12}$$

$$\frac{c^2}{c^2} - \frac{v^2}{c^2} = \left(\frac{\Delta t'}{\Delta t}\right)^2, \tag{13}$$

or $\frac{\Delta t'}{\Delta t} = \sqrt{1 - \frac{v^2}{c^2}} \in [0, 1]$ as in the STR.

4.2 If $\tau = 1$, we get our *Absolute Theory of Relativity* (see [2]) in the particular case when the two trajectory vectors are perpendicular, i.e.

$$X = \sqrt{v^2 + c^2} = |\vec{v} + \vec{c}|\,. \tag{14}$$

4.3 If $0 < \tau < \sqrt{1 - \frac{v^2}{c^2}}$, the time dilation is increased with respect to that of the STR, therefore the speed x as seen by the observer on the Earth is decreased (becomes subluminal) while in STR it is c.

4.4 If $\sqrt{1 - \frac{v^2}{c^2}} < \tau < 0$, there is still time dilation, but less than STR's time dilation, yet the speed x as seen by the observer on the Earth becomes superluminal (yet less than in our Absolute Theory of Relativity). About superluminal velocities see [3] and [4].

4.5 If $\tau > 1$, we get an *opposite time dilation* (i.e. $\Delta t' > \Delta t$) with respect to the STR (instead of $\Delta t' < \Delta t$), and the speed x as seen by the observer on earth increases even more than in our ATR.

5 Further research

The reader might be interested in studying these new Relativities mathematically resulted from the above 4.3, 4.4, and 4.5 cases.

Submitted on February 6, 2012 / Accepted on February 12, 2012

References

1. Einstein A. Zur Eletrodynamik bewegter Körper. *Annalen der Physik*, 1905, v. 17, 891–921.
2. Smarandache F. Absolute Theory of Relativity and Parameterized Special Theory of Relativity and Noninertial Multirelativity. Somipress, 1982, 92 p.
3. Smarandache F. There is No Speed Barrier in the Universe. Liceul Pedagogic Rm. Vâlcea, Physics Prof. Elena Albu, 1972.
4. Rabounski D. A blind pilot: who is a super-luminal observer? *Progress in Physics*, 2008, v. 2, 171.

The Surjective Monad Theory of Reality: A Qualified Generalization of Reflexive Monism

Indranu Suhendro
www.zelmanov.org

What remains of presence and use in the universal dark (or perhaps, after all, in a too luminous, sight-blinding place), when mirrors are traceless as if without glass, when eyes are both mindfully and senselessly strained: wakeful but not ultimately cognizant enough — being a splendid spark at best, but incapable of self-illumination and shedding light on existents as if (situated) in themselves —, when no reflection remains within and without? Indeed, only that exceedingly singular, somewhat pre-existent (i.e., pre-reflexive) Motion and Moment without reflection inheres, which is our characteristic redefinition of Noesis or Surjectivity. This, since Reality can in no way be reduced to Unreality, even in such noumenal darkness where existence and non-existence are both flimsy, for otherwise at once — at one universal Now and Here — all would cease to exist, "before before" and "after after"; and yet all that, nay Being itself, already exists with or without (the multiplicity of) reflective attributes, i.e., without the slightest chance to mingle, by both necessity and chance, with Non-Being and hence with multiplicity! That is simply how chanceless Reality is in itself, suddenly beyond both the possible and the impossible, such that even Unreality (as it is, without history), which is a lingering "backwater part" of the Universe after all, can only be (i.e., be "there", even if that simply means "nothing", "nowhere") if and only if Reality IS, i.e., if Reality is One even without operational-situational sign or space in the first place, and not the other way around. Such, then, is what chance, i.e., the chance of reflection, may mean in the Universe — and not elsewhere: Reality is such that if it weren't Such, both Reality and Unreality would be Not, ever. He who fails to see this at once — as One — will not be able to understand the rest of the tale, Here and Now (or, as some say, "Now-Here", "Nowhere", or as Wittgenstein would have put it, "senselessly"), with or without the Universe as we commonly know it. — A first self-query in epistemic solitude.

1 Introduction: silently in the loud background of things

> *"Come, like a gush of early bewilderment abruptly arriving at the edge of time. Let us sort ourselves out from the loudness of things here."*

The present elucidation is not a "consciousness study". It is a conscious expression of Reality. It is a symptom of consciousness, a deliberation of knowing. Or, as some would say, "it's a proof, like music, rain, or a tempest". It is a self-orchestrated pulsation and presencing without truncation even by silent objectivity, just as one may paint certain scenes of Sun-brushed magnolia eyes and long coral noons, or perhaps the deep winter rain and the seamless Moon-lit snow — simply like a mindful artist reminded of nudity during certain cavernous moments, nearly without a mirror capturing his inward constellation of motions. And so he moves, as it is, simultaneously before and after reflection, as if moving away from time itself. And so it moves, the entire reflection included.

Despite the possibly glacial theoretical sounding of the title and the way the text shall proceed from here (perhaps inconsistently), it is essentially not another viscid gathering of scholastic words on monism, let alone an ecstatic, bemused first-time attempt at modeling Reality. It is not a theory in the sense of mental speculation and inspirational belief: it is Presence and Idea before and after philosophy, and a direct presentation and "surdetermination" during philosophy. Thus, it is not a mere representation, for it does not even begin with reflection. Rather, the entirety of reflection is but momentous and strengthened only by what truly precedes and surpasses it. It is not a psychological documentary multi-linearly tinged with philosophical armor and scientific draping. It is not a predictable philosophy in the rear. It is not a lucrative science as the world knows it. It is a mirror for worlds, anti-worlds, and all the non-worlds. And sometimes this very mirror does vanish, for absolute certainty's sake.

This is an exposition to be enjoyed the most by self-similar "stray falcons", who can't help with their epistemic-intellectual speed and Genius, whose taste — upon the wind and beyond distant hills — is beyond that of the herd and the faltering, image-dependent, super-tautological world as a whole. It is not intended to be a secure throne in the sky nor a comfy haven on the Earth. Also, it is definitely not for the hideous, vainly copious one-dimensional intellect devoid of the valley's affection and the seasons' intimation. It is a silence-breaking tempest and a self-sustaining root in the most evident evening, entirely independent of the small

sparks of the present age of thought. It calls upon witnessing the Witness (and the Witnessed) in infinite exhaustiveness, intimidation, and silence.

It is incumbent upon the reader to acknowledge that the present exposition's veracity is to be grasped not by merely studying it, but by "studying it, not studying it, not-not studying it, and by none of these" (as to why, it shall be clear later). While Reality is not situational (as we shall see), the surreptitious meta-situation here is that, while there is an entire history of human ideas in the background of the world at any instant, its content moves not on any regularly known ground of being, so basically even the intrepid reader cannot compete with its velocity and vortex, for it is ahead of his reading, behind it, within it, and without it. And it is none of these.

Still, let the burning lines of the night and the time-span of the intellect's long orbit be epistemologically intimated. For even if there is nothing to be seen and understood by the reader here, that one shall still see "seeing" itself, beyond mere "spiritism", however indifferent.

And so here falls headlong the platitudinous introductory tone first. Granted, it shall evaporate away soon enough, once the most unlikely epistemic sensitivity happens to the reader.

At the forefront of humanity — which is definitely a conscious, self-reflective episode in the evolution of the cosmos, according to the famous Anthropic Principle of cosmology and cosmogony — there is no need to explain why one needs to fully explore the nature of consciousness philosophically and scientifically, i.e., unless one is a dead-end dogmatist who, however taut, probably dares not "swear upon his own life, as to whether or not his beliefs are universally true after all".

The present semantic-ontological exposition centers around a further (or furthest possible) development of the theory of consciousness called "Reflexive Monism" (*RM*) — hereby referred to as the "Surjective Monad Theory of Reality" (*SMTR*).

By contrast, the version of realism called "Biological Naturalism" (*BN*) posits that consciousness is merely an emergent property of inanimate matter: everything that exists is necessarily inside the material brain, possibly as a quantum state. Thus, there is "no world inside the mind" — and so there is no "mind" (only a material brain) — and consciousness is but a field (electromagnetic, perhaps) activity involving the neuronal circuitry. Connected to this (and the theory of "Artificial Intelligence", *AI*), is the theory of Multiple Intelligences (*MI*), which advocates "consciousness" as a collective state of material brains via a global circuit mechanism, necessitating the existence of multiple participants — ultimately leaving no room for an individual brain, let alone an individual mind in the Universe (and hence, one could say, no room for a real solitary Genius at all, since *MI*-consciousness is always a collective pseudo-democratic state, no matter how transparent), for phenomenal multiplicity (rather than the self-cognizant, inhering presence of a single universal intelligence) is at the very core of this form of materialism. Yet, consider this now-generic example as, e.g., conveyed by Velmans [1]. Suppose, convinced like many merely collectivistic scientists today, one accepts *BN*, then by definition one also accepts the whole world (nay, the Universe) as contained in the material brain. But most of every-day objects, including the skies and the horizons, seem to be located "out there" — that is, outside the brain. Thus, in order to encapsulate all that in a single material brain, one must accept that there is a "real skull" (whether or not certain "noumena" are known to one here) whose size is beyond that of the skies and the horizons, since physically the brain is contained in a skull. The "real skull" would then be related to individual skulls through some kind of "statistical-holographic averaging". The difference between "is" and "seems" becomes so arbitrary here, as we can easily see.

On the other hand, the history of human thought presents us with "Pure Idealism" (*PI*) — such as that advocated by Berkeley in one of its versions — where the world is but a mental entity, purely located inside the mind. By "world", we mean all that can exist as a single situational adage and corollary of reflective facts, including qualia (the trans-optical reality of color) and psychosomatic sensations. According to *PI*, there is "no world out there". In this approach, the mind is distinguished from the material brain, with the brain being a material self-representation of the mind, and everything is necessarily contained in the mind — yet with serious troubles for, like *BN*, it is without clear epistemic qualifications regarding the notion of individual and multiple entities: according to this theory, one might be tempted to see whether or not the Universe too ceases to exist, when an arbitrary mind (anyone's mind) dies out. Non-epistemologically positing essentially "eternal souls" does not really help either. (As regards qualia, we shall readily generalize this notion to include not just color, but also subsume it in the category spanned by the pre-reflexive "Surject", i.e., "Qualon" — precisely so as not to take the abstract phenomenological entity for granted.)

Such radical, self-limited approaches leave room for both "dogmatism" and "relativism", and consequently have their own drawbacks as shown, e.g., in Velmans' studies. Indeed in the face of Reality, one cannot help but be radical and isolated, whether shivering or rasping, but true epistemological qualification (herein to be referred to as "eidetic qualification") is quite profoundly something else. Velmans himself — formerly a proponent of *BN* — is a cogent philosophical proponent of *RM* and has indeed very extensively explored this reality theory, especially its aspects pertaining to cognitive psychology. Yet, we shall naturally go even beyond him in "imbibing Reality", hence the present theory as our basic ontological paradigm.

As is evident, *RM* is a version of realism adopted by thinkers such as Spinoza, Einstein (but not specifically its associated pantheism), and Velmans — which goes beyond *BN* and *PI*. Reality is said to isomorphically partake of events

(mental and material instances) both inside and outside the brain — and the mind.

Let us attempt to paraphrase *RM* as follows: the most fundamental "stuff" of the Universe is a self-intelligent, self-reflexive ("autocameral") substance beyond both (the commonly known) mind and matter, possibly without an "outside" and an "inside" in the absolute sense (think of a Möbius strip or a Klein bottle, for instance). And yet, locally and "conspansively" (for the original use of this term, see also [2]: here "conspansion" is to be understood as self-expression and self-expansion within the semantics and syntax of universal logic), it produces intrinsic mind and extrinsic matter — as we know them.

In our present theory, this underlying substance is further identified as a non-composite self-intelligent Monad ("*Nous*"), without any known attribute whatsoever other than "surjective, conscious Being-in-itself": we can make no mention of extensivity, multiplicity, and the entire notion of knowledge set at this "level" of Reality, whether subjectively or objectively, or both simultaneously. Otherwise, inconsistent inner multiplicity associated with reflection would somehow always have to qualify (i.e., ontologically precede) Being not only as being self-situational or self-representational, but also as being "accidentally none of these". Such is absurd, for then it must also hold in the sheer case of Non-Being, i.e., without both existence and such multiplicity-in-itself and -for-itself. Being pre-reflexive, and hence pre-holographic and pre-homotopic, the true meaning of this point shall be effortlessly self-evident as we proceed from here. This is the reason why our *Nous* has no superficial resemblance with arbitrary phenomenal intelligence, let alone substance.

And yet the very same Monad sets out the emergent properties of reflexivity, holography, and homotopy with respect to the Universe it emergently, consciously sees (or "observes", as per the essential element of quantum mechanics: the observer and elementary particles are both fundamental to the theory). It is necessarily, inevitably "intelligent" since it positively spans (knows) the difference between existence and non-existence and thereby fully augments this distinction in that which we refer to as the Universe or Reality's Trace, which individual intelligences may reflect in various degrees of "motion" and "observation". Otherwise, no one in extension would ever know (or have the slightest conscious power to know) the distinction between existence and non-existence; between the conscious and the unconscious — and further between absolute singular existence and various epistemological categories of multiplicity. Verily, this forms the basis of our paradigm for a fully intelligent cosmos — and further qualified versions of the Anthropic Principle.

Furthermore, our framework manifests a theory of Reality via four-fold universal (trans-Heraclitean) logic, which is beyond both conventional (binary) and fuzzy logics — as well as beyond Kantian categorical analysis. Given a super-set $(\{A, B\})$, where $\{A\}$ is a collection of abstract principles, $\{B\}$ is a collection of emergent realities isomorphic to the entirety of $\{A\}$, and the super-set ( ) is "eidetically symmetric" (the meaning of which shall become clear later) with respect to its elements, it contains the full logical span of "*A*", "non-*A*", "non-non-*A*", and that which is "none of these" (how it differs from traditional Buddhist logic will become clear later as well). As such, one may inclusively mention a maximum span of truly qualified universals, including ontological neutralities. This gives us a "surjective determination of Reality", whose fundamental objects are related to it via infinite self-differentiation, as distinguished from Unreality.

While so far the reader is rigged with limited equipment — for, at this point, we have not introduced the essence and logical tools of the present theory to the reader — we can nevertheless roughly depict Reality accordingly, i.e., we shall start with "thinking of thinking itself" and "imagining the dark". For this we will need one to imagine an eye, a mirror, a pitch-dark room (or infinite dark space), and circumferential light. Then, the following self-conclusive propositions follow:

P_1. In the pitch-dark room ("Unreality"), there exists an Ultimate Observer ("Eye") that sees the pure, luminous mirror. The mirror is the Universe — henceforth called the "Mirror-Universe" —, which is a "bare singularity" with respect to itself, but which is otherwise multi-dimensional (for instance, n-fold with respect to the four categorical dimensions of space-time, matter, energy, and consciousness, let alone the Universe itself).

P_2. The circumferential light augments both the mirror and the sense of staring at it, resulting in the image of an "eye" (or "eyes", due to the multiple dimensions of the Mirror-Universe) and a whole range of "eye-varied fantasies" — which is the individual mind and a variational synthesis of that very image with the dark background — where that which is anyhow materialized readily borders with Unreality.

P_3. The circumferential light is, by way of infinite self-differentiation (and transfinite, self-dual consciousness), none other than (universal) consciousness.

P_4. Reality is the Eye, the Consciousness, the Mirror, the Image, and the "Eye-without-Eye". This can only be understood later by our four-fold universal logic encompassing the so-called "Surjectivity" (*Noesis*) — with the introduction of "Surject" at first overwhelming both "Subject" and "Object" (in addition to "Dimension") in this framework, but as we shall see, only this very "Surject" ultimately defines "Moment" (and not just a universal continuum of three-dimensional space and sequential time) and "Uniqueness" (and not just the "totality of consistent and inconsistent facts") four-fold: "within", "without", "within-the-within", and "without-the-without", ultimately corresponding to the paramount qualification of Reality for itself and, subsequently, its associated "class of Surjects" in the noumenal and phenomenal world-realms.

Before we proceed further by the utilization of the above

similes, we note in passing that the underlying monad of any reflexive model of the Universe is none other than mind and matter at once, when seen from its phenomenal-organizational-relational aspect, a property which constitutes — or so it seems — both the semantics and syntax of the Universe, especially when involving conscious observers such as human beings. That is, noumenally (in-it-self, for instance in the Kantian sense), the Universe is consciousness-in-itself, and phenomenally (in relation to the way its intelligibility inheres by means of extensive objects), it is a self-dual reality with a multiverse of material and mental modes of existence. But, as we shall see, there is a lot more to our adventure than just this: hence our generalization.

So much for a rather self-effacing introduction, in anticipation of the irregular dawning of things on the reader's mental window. Before we proceed further, let us remark on the rather speculative nature of "excess things" regarding the subject of *RM* in general: while, in general, mind cannot be reduced (transformed) into matter and vice versa, there exists subtle interactive links between them that should be crucially discerned by pensive research activities so as to maximally relate the philosophical dialectics of consciousness and technological endeavors, i.e., without causing philosophy, yet again, to get the "last mention". For, to partake of Reality as much as possible, humans must simply be as conscious as possible.

2 The gist of the present epistemology: the surjective qualon

> "*Mere eruditic logic often turns — as has been generically said — philosophy into folly, science into superstition, and art into pedantry. How far away from creation and solitude, from play and imagination, from day and night, from noon and silhouette it is! How Genius is precisely everything other than being merely situational, alone as the Universe.*"

Herein we present a four-fold asymmetric theory of Reality whose essence — especially when properly, spontaneously understood — goes beyond the internal constitutions and extensive limitations of continental and analytic philosophies, including classical philosophy in its entirety (most notably: Platonism, neo-Platonism, atomism, dualism, and peripatetic traditions), monism (Spinoza-like and others), sophistic relativism and solipsism (which, as we know, has nothing to do with the actuality of the Einsteinian physical theory of relativity), dogmatic empiricism and materialism, Kantianism and neo-Kantianism, Hegelianism and non-Hegelian dialectics (existentialism), Gestalt psychologism, symbolic logic, hermeneutics, and all phenomenology. This, while leaving the rather arbitrary self-triviality of major super-tautological (collectivistic, ulterior, inter-subjective) and post-modern, post-structural strands of thought in deliberate non-residual negligence — for, abruptly starting at the level of axiology and being generically "not even wrong" in short or at length, these are devoid of real ontological-epistemological weight in our view.

The new ontological constitution under consideration is four-fold and asymmetric in the sense that there exist four levels necessitating both the Universe and Unreality, i.e., Reality, the Reflexive Mirror-Universe, the Projective World-Multiplicity, and Unreality, whose *eidetic connective distances* (i.e., "foliages" or "reality strengths") are *telically* (i.e., multi-teleologically) direction-dependent and not arbitrarily symmetric among themselves unless by means of *Noesis*, by which the very theory is said to be *eidetically qualified* (i.e., qualified by *Eidos*, or Suchness — be it Alone without even specific reference to the Universe at all, or when noumenally and associatively designated as All or All-in-All) — and hence self-unified and self-unifying with respect to an entirely vast range of phenomenological considerations.

It is to be noted that Surjectivity, as implied by the very term *Noesis*, in our own specific terminology is associated with *Nous*, or the Universal Monad, which is none other than the *First Self-Evident Essence* through whose first qualitative "Being-There" (*Ontos qua Qualon*) the ontological level, and not just the spatio-temporal level, is possible at all, especially as a definite, non-falsifiable concentration of knowledge.

Thus, in particular, the classical Socratic-Hegelian dialectics of thesis, anti-thesis, and synthesis is herein generalized to include also *Noesis*, but rather in the following *asymmetric, anholonimic* order: *Noesis* (via the Ontological Surjective "*Surject*", i.e., "*Qualon*"), *Synthesis* (via the Epistemological Reflexive "*Dimension*", i.e., "*Prefect*"), Thesis (via the Reflective Dimensional "*Object-Subject*", i.e., "*Affect*"), *Anti-Thesis* (via the Projective Dimensional "*Subject-Object*", i.e., "*Defect*"). This corresponds to the full creation of a new philosophical concept, let alone the Logos, by the presence of self-singular points and infinitely expansive perimeters.

The ontic (i.e., single monad) origin of the noumenal Universe is Reality itself, i.e., Reality-in-itself (Being-qua-Being) without any normatively conceivable notion of an internally extensive (self-reflexive) contingency (e.g., the usual context of cognition, information, syntax, simplex, and evolution) of inter-reflective, isomorphic, homotopic unity and multiplicity at all, let alone the immediate self-dual presence of subjects and objects (i.e., representational and observational categories, such as space-time and observers).

Thereafter, extensively, upon the emergence of the notion of a universe along with *universality*, i.e., *reflexivity* (encompassing, by noumenal and phenomenal extension, both *reflection* and *projection* — with the former being universal, ultimately akin to singularity and non-dual perception but still, in an austere sense, other than Reality itself, and with the latter being somewhat more inter-subjective and arbitrary, still bordering with the dark, shadowy vanity of Unreality), Reality is said to encompass primal, pre-geometric (i.e., "mirrorless", trans-imaginary, or *qualic*) singularities and transformational multiplicities (modalities) at successive levels capa-

ble of fully reflecting essence and existence in the four-fold Suchness of "*within*", "*without*", "*within-the-within*", and "*without-the-without*", where original noumena inhere only by means of *eidetic-noetic instance* (*Surjection*) without the necessity of phenomena whatsoever, but only the presence of the so-called "*Surject*" — that which is not known to regular epistemologies, for in a sense it is other than "subject", "object", and "dimension". Only then do both noumena and phenomena appear *info-cognitively* by means of reflexive omnijectivity involving arbitrary subjects, objects, and epistemological dimensions (i.e., in fundamental semantic triplicity), which in turn is responsible for the reflective and projective self-dual modes of all abstract and concrete phenomenal existences — hence the emergence of the universal syntax, nearly as circular self-causality.

In elaborating upon the above allusions, we shall also introduce a post-Kantian four-fold universal logic (not to be confused with four-fold Buddhist logic or that which is associated with non-relativistic, semantics-based process philosophy) associated with an eidetically qualified kind of *non-composite consciousness*, which enables us to epistemologically generalize and elucidate the metaphysics (logical interior) of the so far sound-enough theory of Reflexive Monism (i.e., "sound-enough" at least at the "mesoscopic" stage of things, and in comparison with the majority of competing paradigms).

In connection with the elucidatory nature of this exposition, we shall adopt a style of narration as intuitive, lucid, and prosaic as possible — while being terse whenever necessary —, due to the otherwise simple ambiguity inherent in the association of Reality with a potentially inert scholastic theory (while there is subtle isomorphism between Reality and language at a descriptive stage, to the Wittgensteinian extent, as recorded in [5], that "that which can be spoken of, must be spoken of clearly, and that which cannot, must be withheld in utter silence", how can Reality only be a "theory" or "philosophy" after all?): the profundity of the former is ultimately senseless and immediate, with or without deliberate systemization on our part, while the latter is but a singular, cognition-based contingency-in-itself (a logical enveloping singularity and yet always not devoid of the multiplicity of perceptual things, including those of plain syntactical undecidability).

3 Peculiar eidetic re-definitions: aprioristic terminology and essence

> "*May I suspect, friend, you know — arbitrarily — what appears. But, tell me, what IS?*"

It is important to note that some of the eclectic terms employed throughout this exposition do not essentially depend on their scholastic historicity. It is immaterial whether or not they have come into existence through the collective jargon of the multifarious schools of all-time philosophers. (Needless to say, the same applies to scientific-sounding terms, without any attempt towards imparting to the reader's mind a sense of "pseudo-science" whenever touching upon aspects other than traditional science, for one must be most acutely aware of the profound tedium prevalent in much of the arbitrary literature of post-modernism and so-called "theosophy" in actual relation to pseudo-science, pseudo-spirituality, pseudo-philosophy, and pseudo-artistry.) Rather, whenever we use these terms, we would only like to further present them in the twice-innermost and twice-outermost sense: phenomenological instances have inner and outer meaning, and yet we wish to also encompass the "twice-inward" (twice-Unseen, twice-Real within-the-within) and "twice-outward" (twice-Manifest, twice-Real without-the-without) akin to Reality beyond simple constitutional duality and arbitrary individual fragments. This is simply a prelude to an amiable over-all description of the four-fold Suchness of Reality and its self-qualified primal noumena, which is not attributable to simple, eidetically unqualified "bi-dimensional" entities (whose common qualification is solely based on "this" and "other", "yes" and "no", or at most "yes and/or no").

Now, in order to be trans-phenomenally readable, we may give the following list of five primary eidetic redefinitions (corollaries) essential to the outline of things here:

— Suchness (S) (*Eidos*): that which is manifestly There, as qualified by Being-in-itself, with or without existential reflexivity (the multiplicity of forms and mirrors);

— Monad (N) (*Nous*, *Monados*, *Ontos qua Qualon*): the first intelligible self-qualification ("*Qualion*") of Reality and hence its first actual singularity, the noetic-presential "$U(N)$" of "Universum" (i.e., "*Qualon*"), with or without singular internal multiplicity of reflexive things (i.e., "*versum*", or possible *extensa*) other than a "bare" eidetic (and hence noetic) being in and of Reality-in-itself (i.e., by its simply Being-There). Such is beyond both the traditional "*Atom*" and "*Platon*", let alone the infinitesimals. It is simply the noumenal All and All-in-All, as well as the first eidetic-archetypal Singularity, with or without phenomenological "allness" (reflexive enclosure);

— Universe (U) (*Universum*, *Kosmos*): the noumenal-phenomenal four-fold Universe, i.e., the surjective, reflexive (multi-dimensionally reflective-transformational), projective, annihilatory universal foliation, ultimately without "inside" nor "outside". The multi-space All by the Surjective Monad — simultaneously a multi-continuum and multi-fractality, being simultaneously Euclidean and non-Euclidean, geometric and pre-geometric, process and non-process (interestingly, see how all these seemingly paradoxical properties can exist in a single underlying multi-space geometry as described in [7] — see also a salient description of the essentially inhomogeneous physical cosmos in relation to random processes as presented in [12]). In other words, Reality's singular Moment and infinite Reflex-

ivity, with or without phenomenal space and time;

— Reality (M) (*Ontos qua Apeiron*): that which is the Real-by-itself. The self-subsistent Reality of Reality in-it-self (with or without *realities* — i.e., with or without internal self-multiplicity), the Surjective Monad, the Reflexive Universe, and Unreality. Here the austerity of the symbolic, presential letter "*M*" (for the essentially "Unlettered") inheres absolutely without any vowel such that it is said that "nothing enters into it and nothing comes out of it";

— Surject (g) and/or Surjectivity (dg) (*Noesis*, *Epoche*): the first self-disclosing instance ("instanton") of Reality, or such self-evident instances in existence. Reality is said not to act upon itself, for it is simply beyond categorical stillness and motion, and so it "acts" only upon the first reflexive mirror, the Universe, thereby capable of infusing new universally isomorphic *differentia* ("solitons"), i.e., new noumenal instances and new phenomenological events in the Universe (with respect to its trans-finite nature). In relation to it, the Universe is like a light-like (holographic, homotopic) mirror-canvas, a ground-base yet ever in motion, upon which the "Lone Artist" paints his "Surjects". This is none other than the innermost nature of Genius (which differs, as we shall see here (i.e., by this more universal qualification) from mere superlative talent, just as eidetic surjectivity is beyond mere reflexivity).

As can be seen, each of the notions above is self-singular: these realities are self-similar among themselves, without categorical parallel apart from the ontological level. In other words, simply because Reality is One (Self-Singular), with or without reference to regular phenomenological (arithmetically countable) oneness, so are the Mirror, the Image, and the Shadow in essence.

As we shall witness in this exposition, all That (Reality, Monad, Universe, Unreality) can be given as follows:

$$M : N\left(U(g, dg)\right) \sim S,$$

where ":" denotes eidetic-noetic Presence (or Moment) and "$\sim$" represents transcendental equality as well as trans-individual self-similarity among the equation's constituents. This, in a word, is more than sufficient to end our exposition at this early stage — for it is a self-contained proof of consciousness for itself —, as it is mainly intended for spontaneous cognizance, but we wish to speak more amiably of things along the epistemological perimeter of the intellect.

Non-composite Oneness belongs to Reality, so to speak, without having to be qualified or necessitated by that which is other than itself, simply because the self-necessary and the possible (existent), even the impossible (non-existent), can only be cognitively perceived "there" in and of the Real, not "elsewhere" by any other means, and not even by any presential concentration of singular multiplicity (i.e., ontological and epistemological gatheredness). In other words, Reality is not diversifiable — and made plural — within and without, since it has no categorical "inside" nor "outside", especially with respect to the discriminative entirety of cognition. Even absolute non-existence can only be conceived in, and necessitated by, Reality as a category — hence, in the absence of multiple intelligible things other than the supposedly primal "opposite" of pure existence, there is no actuality of absolute non-existence that can necessitate Reality as it is, nor is there anything phenomenal and noumenal that can cause it to mingle, in and across phenomenological time and space, with chance, causality, and mediation, let alone with singularly inconsistent multiplicity and Unreality. It is boundless not because it lies in infinite space, or because it is where infinite multiplicity inheres, or because it is a representation of eternity, or even because a finite entity is ultimately annihilated by "not knowing" and "non-existence" in the face of some infinite unknown, but because its ontological rank or weight (i.e., ontic-teleological reality) is without either immediate or extensive multiplicity in its own interiority or reflexive dimensionality, not even the entirety of "knowledge". If this weren't so, a single arbitrary reflective quantity could then also be shown to inhere intransitively (without existential predication), independently of Being, at any ontological level, *just as Being can always necessitate it predicatively*: for things to be situated in existence (extensivity), Being (Reality) must be there first absolutely without mingling with Non-Being (Unreality), *unlike the way things may phenomenologically mingle among themselves* (be it consistently or inconsistently). The metaphysical connection (the simplex of meta-logic) among ontological categories herein must then be, as will be shown shortly, asymmetric and anholonomic. Or else, there would be no discernment of the ontological weight of some absolute presence-essence (not in the way suggested by mere "essentialism", where even in the case of arbitrary entification, essence must always precede existence), and there could be no logic whatsoever at subsequent levels of cognition, and isomorphism would be limited to the arbitrariness of inconsistent, self-flawed cognitive discrimination even on the phenomenological scale of things, which is not as trivial as the "arbitrariness of arbitrary things".

This way, the Essence of Being is its own *Being-qua-Being*, which is identical, only in the "twice-qualified" sense, with the Being of Essence itself, i.e., "within-the-within" and "without-the-without". Only in this ontological instance does eidetic asymmetry vanish.

It is not "logical", and yet it is "not illogical" either — for the entirety of "logic", "anti-logic", and "non-logic" can only be traced (conceptualized) in its presence, with or without the necessity of accidental particularities. For instance, then, when we say "universe" without this qualification, we can still come up with the notion of "multiverse" while often still retaining space-time categories or attributes, or a plethora of schizophrenic universes "apart" from each other in one way

or another, and yet we cannot anyhow apply the same splitting and extensivity, or diffeomorphism, to Reality itself in order to make it appear as a co-dependent and co-differential among others outside its own necessity.

Reality, therefore, is not a set, not a category, not a functor (or functional), not of the likeness of both objective tangible matter (*materia*) and subjective abstract forms (*forma, qualia*). It is neither regular nor aberrant, as commonsense and traditional phenomenology would have "being" defined at best as "inconsistent multiplicity in and of itself". It is not a representation of something that has to have a normative representation, be it abstract or concrete, conscious or unconscious. It simply *IS*, even when there is no language and count to express this, without the notion that consciousness is "always conscious of something" in association with the internal multiplicity of knowledge. However, the four-fold asymmetric universal logic to be sketched in the following section is Reality's exception just as Reality is its exception: we can truly say a great deal of things by means of it, especially consciousness.

Know intuitively (at once, or never know at all) that if Reality weren't Such, both Reality and Unreality would not only be unthinkable and imperceptible (however partial), they would not be, whether in existence or non-existence, in pre-eternity, at present, or in the here-after, in infinite contingency, finite extensivity, or universal emptiness, and there would be no universe whatsoever, finite or infinite, somewhere or nowhere, transcendent or immanent, — and none of these —, and no one would any likely embark upon writing this exposition at all!

Such is our blatant methodology by *Surjectivity* and eidetic redefinition, instead of both psychologism and the Husserlian phenomenological method of "bracketing", which often amounts to either the "arbitrarily subjective over-determination" or the "arbitrarily objective suppression" of certain ontological constitutions already present among phenomenal categories.

4 Beyond Kant, phenomenology, and reflexivity: a four-fold, eidetically qualified universal logic with asymmetric, anholonomic categorical connection

> "*Now, I must tell you of something more tangible than all solid objects and more elusive than all traceless things in the heavens and on the Earth. Behold the highest branches of the tree of knowledge — untouched by reflection —, of which the night-in-itself is the garden.*"

We are now in a position to outline the underlying features of our model of universal logic, which shall manifest the analytic epistemological sector of our present theory. In doing so, we will also make an immediate amiable comparison with the crux of Kantian epistemology, for the present case can be seen as a somewhat more universally deterministic generalization thereof.

As we have previously implied, it is important to distinguish between the phrase "four-fold" in our new framework and that found, e.g., in Buddhist empirical dialectics. In the latter, being of empirical-transformational character at most, there is no trace of essential relationship or logical enclosure with respect to the more contemporary Kantian and Fichtean categories pertaining to "das Ding an sich" (the thing-in-itself). Rather, in that ancient framework, given an object of contemplation A belonging to phenomena and subject to process — and ultimately embedded in a universe of infinite contingency regarding the past, present, and future —, the associated dialectical possibilities, of the utmost extent, are: "A", "non-A", "non-non-A", and "none of these", already (though not sufficiently, as we shall see) in contrast to the more usual forms of binary logic. A roughly tangible example would be the irreversible transformation of water ("A") into milk ("non-A"), into vapor ("non-non-A"), and into curds ("none of these"), by the process of powdering, mixing, and heating however complete.

Though bearing superficial visceral resemblance with this in the use of the similarly expressed four identifiers, our logical strand is more of ontological "unbracketed" (i.e., non-Husserlian) dialectical nature, and not of mere process-based empiricism, existentialism, and phenomenology (i.e., non-Heideggerian). Rather, we subsume the entire phenomenal world of entification, process, and contingency already in the first and second categories (of "A" and "non-A"), as we shall see, thus leaving the two last categories as true ontological categories. We assume that the reader is quite familiar with essentially all kinds of dialectical preliminaries, so we shall proceed directly to the new elements of the four-fold analysis we wish to immediately convey here.

In accordance with the ontic-teleological unity given in the preceding section, we keep in mind four major constituents responsible for the presence of definite universal existence, hereafter denoted as the following "eidetic simplex":

$$\{MO\} : \{S(\text{Suchness}), U(\text{Universe}), N(\text{Monad}), M(\text{Reality})\} + \\ + \{\text{phenomenal instances}, O(\text{phenomenal entirety})\},$$

where the first group belongs uniquely to Reality (M) and the second is due to empirical-dialectical process-based observation whose phenomenological entirety is denoted by O. This representation implies that the identification is made from M to O, i.e., from Reality to phenomena, yielding a true unitary ontic-teleological state for any given elements of O. The analytic union between M and O, in this case, is none other than the Universe, i.e., U as a function of its underlying noetic surjectivity (g, dg).

Now, just as M is singular and four-fold with respect to the above representation, so is O. Due to the union between M and O, there exist common elements between M and O possessing true ontological weight: the "within-the-within" element and the "without-the-without" element. In short,

given an arbitrary phenomenal instance A, we can write, according to the underlying representation

$$O = (\text{without, within, within-the-within, without-the-without}),$$

the following representation:

$$O(A) = (A, \text{non-}A, \text{non-non-}A, \text{none of these}),$$

where we shall simply call the four ontological entries "categories" — for the sake of brevity.

Let us note the following important identifications for the associated elements: given A as an object, there is guaranteed, in the empirical necessity of phenomenological space-time, an entity other than A — in fact a whole range of limitless instances of otherness —, including that which is categorized by traditional Buddhist logic as either "non-non-A" or "none of these", especially in the residual sense of a given underlying process, as we have seen. But, in our approach, these two are not yet eidetically qualified and simply exist as part of the infinite contingency of phenomena — and so we can regard A already as both entity and process, without the need to make use of the earlier formalized aspects of Buddhist logical representation. As such, a phenomenal object A has no "inside" other than the entire phenomenal contingency in the form of immediate "otherness" (e.g., any "non-A"): this, when applied to an arbitrary organic individual, without negating the existence of the extensive world, negates the presence of a non-composite "soul" once and for all (but not the "soul-in-itself" as an eidetically qualified microcosm), which remains true in our deeper context of representation.

Meanwhile, at this point, we shall call the traditionally undecided Kantian categories into existence instead, according to which "non-non-A" ("without-the-without") is the entire fluctuative phenomenological set O, which is devoid of absolute individual entification, simply due to the fact that Kantianism is undecided about A-in-itself, yet leaving it there, as it is, in existence. This arises in turn simply because of the inherent Kantian empirical undecidability between pure subjectivity ("spiritism" and "relativism") and pure objectivity ("material dogmatism") — alluded to elsewhere in a preceding section.

However, given our ontic-teleological equation, the present theory overcomes such undecidability on the epistemological level of things, including the phenomenological problem of the inconsistency of a singular entity (such as the phenomenal mind and its knowledge and abilities): singular yet still constituted by its inevitable inner multiplicity of reflective objects. It is as follows.

Given, for instance, the classic example of "a leaf falling off a tree in a forest": does it fall, after all, when there is no one observing it? Our response to this, accordingly, is that it truly depends on what kind of observer is present, i.e., how he is categorically qualified in Reality. Thus, an arbitrary observer will not qualify as a decisive representation: in that case, the leaf still falls due to, e.g., the law of gravity, for the macroscopic laws of physics are "arbitrarily objective-compulsive" in relation to the arbitrary observer. In other words, such a subjective observer is always objectified (or "subjectified away") by that which is other than himself, which in this case is the totality of the manifest laws of Nature. Hence, his subjective self is bounded by a kind of temporal self-determined objective dogmatism as well, and if he attempts to be objective, he is soon limited to being subjective enough. In all this, he is composed of fundamental indeterminacy not intrinsically belonging to himself — as approached from the "below limit" —, but which is a surjective determination from the "above limit", i.e., from the Universe itself.

Rather strikingly, the situation is fundamentally different if the observer is the Universe itself: whether or not the leaf falls, it depends on Noesis, according to the representative constitution of the Universe in our "Reality equation" above. In other words, there exists a so-called "Ultimate Observer" as a "surjective instanton" with respect to the entire Mirror-Universe of reflexivity. Since this observer exists at the self-similar singular ontological level of Suchness, it is again self-singular without parallel and indeed without any logical extraneous qualifier (and quantifier), thereby encompassing the Real, the Mirror, the Image, and the Shadow, in the manner of Reality. In other words, such an observer is none other than Reality, in relation to the Universe. Needless to say, that need not be "Reality-in-itself" in the rough sense of the phrase, despite existing also at the primary ontological level and in limitless eidetic oneness with Reality. Rather, it is most uniquely none other than it — and nothing else is directly (presentially) like such "Non-Otherness" with respect to Reality itself. Respectively, such an observer is noetic, i.e., the essence is of the level of the Surjective Monad, and such identification is already beyond all practical phenomenology even in its extended descriptive form.

Hence, up to the most lucid isomorphism, the "within-the-within/non-non-A" element of an eidetically qualified entity $\{A\}$ (which, unlike an ordinary entity subject to Buddhist and Kantian dialectics, definitely possesses genuine, empathic inwardness and outwardness) can be identified as none other than the Universe, which in turn is the noumenal A itself, while the corresponding "without-the-without/none-of-these" element as Reality itself, whereas the conventional modes of "within" (A_2) and "without" (A_1) are, respectively, the abstract phenomenological A and the concrete (or material) phenomenological A. Hence the following representation:

$$\{A\} = \{A_1, A_2, U, M\}.$$

A straightforward example of $\{A\}$ is the Universe itself, i.e.,

$$\{\text{Universum}\} = \{\text{the Material Universe, the Abstract Universe, the Universe-in-Itself, Reality}\}.$$

Or, in subtle correspondence with that, we may think of the categorical representation of thought itself, which has no equal parallel among arbitrary phenomena other than what is similar yet other than it (i.e., its possible anti-pod):

{Thought} = {Thought, Anti-Thought, Unthought, Reality}.

Thus, phenomenally, thought always entails anti-thought: both are two intelligible sides of the same coin on the phenomenological horizon. However, note that such anti-thought is not equivalent to the further eidetically qualified Unthought. Simply speaking, this very Unthought somehow allows not the entirety of phenomena to perceive Reality as thinkable in the first place. In this light, the famous dictum by Descartes, "I think, therefore I am," is indeed far from complete. The more complete phrasing would be something like: "I think, therefore I am, I am not, I am not-not, and none of these." And this too, in the face of Reality, would still depend on the eidetic qualification of the one expressing it.

"Away" from all matter and abstract dynamical physical laws, the Universe can thus be identified as a singular surjective-reflexive mirror of "superluminosity" upon which Reality "acts" trans-reflectively through *Noesis* and *Differentia* (especially the qualified infinitesimals), hence the sobriquet "Mirror-Universe" (which is particularly meaningful here, and may or may not be related to the use of the phrase in the description of an exciting geometric structure of the physical Universe as revealed in [8] and based on a chronometrically invariant monad formalism of General Relativity as outlined in [4, 9, 11]). It is said to be "superluminal" in reference to the state of "universal unrest" as measured against all the rest of individual phenomena in the cosmos, somewhat in association with the ever-moving, massless photon as compared to the rest of physical entities (but this is only a gross, fairly illegitimate comparison, as we do not aim at sense-reduction at all).

Other examples include fundamental categories such as space-time, energy, matter, consciousness, etc.

Note that, generally speaking, the abstract phenomenological category (e.g., the concept, instead of the actual stuff, of a tree) is not the same for any entity as the noumenal category. Further, whenever an arbitrary, fluctuative entity $<A>$ (without eidetic qualification) is represented according to the above scheme, we should have instead

$$< A >=< A_1, A_2, \{U\}, \{M\} >,$$

i.e., although $\{U\}$ and $\{M\}$ are present in the above representation, as if being $<A>$'s linearly valid components in their respective contingency, $<A>$ possesses no universal similarity with $\{U\}$ and $\{M\}$, let alone with just Reality, but only with A_1 and A_2 (subject to phenomenological mapping or transformation) — which is why U and M appear "bracketed away" therein, for otherwise they would best be written as "null components" (but which in turn would carry us away from its deeper ontological representation).

Finally, as we have seen, our all-comprehensive "Reality equation" (i.e., all the above in a word) is

$$M : N\left(U(g, dg)\right) \sim S.$$

And we can say something fundamental about the state of Reality and the Universe as follows:

$\{MO\}$ = All-Real (M and O are Real and Self-Evident),

$\{OM\}$ = Ultimately Unreal (leaving Real only M),

$\{MO\} \neq \{OM\}$ (the Reality-condition of asymmetry and anholonomicity),

i.e., the eidetic "distance" (connective foliage) between Reality (M) and Otherness/Phenomena (O) is not the same as that between Otherness/Phenomena (O) and Reality (M) — in part owing to the non-reality of arbitrary phenomena with respect to Reality —, which is why Reality is said to "contain all things, and yet these contain it not", so long as arbitrariness is the case. In this instance, we may effortlessly witness the generally eidetic, anholonomic, asymmetric connection between categories in the Universe, with respect to Reality. (These categories, in the main, being ontology, epistemology, axiology, and phenomenology.) The word "anholonomic" clearly points to the path-dependence, or more precisely the direction-dependence, of our epistemological consideration: *eidetically, surjectively approaching things from the non-dual ontic-teleological Reality will be substantially different from arbitrarily, phenomenologically approaching Reality from* (*the transitive state of*) *things*.

Eidetic symmetry, thus, only holds in an "exotic case" possessed of Qualon, whereby an entity is eidetically qualified, so that it truly bears "resemblance" in "substance" with the Universe and Reality. Ordinary phenomenal symmetry holds in commonsense cases of isomorphism between things in the same category or in extensively parallel categories across boundaries, e.g., between one particle and another in collision, between an actual ball and a geometric sphere, between physics and mathematics, or between language and the world. In this respect, traditional philosophy (as represented chiefly by ontology and epistemology) qualifies itself above such phenomenological parallelism, especially with the very existence of the epistemology of aesthetics, but anyhow remains "infinitely a level lower" than Reality. (Such is in contrast to a famous, epistemologically trivial statement by Stephen Hawking, somewhat in the same line of thinking as some of those working in the area of Artificial Intelligence (*AI*) or certain self-claimed philosophers who enjoy meddling with "scientists" and "technologists" regarding the current state of science and the eventual fate of humanity, which can

be roughly paraphrased as: "The only problem left in philosophy is the analysis of language," where the one saying this "intuitively" mistakes post-modernism for the entirety of philosophy. One, then, might be curious as to what he has in store to say about art in general, let alone Being!)

It is important to state at this point that the kind of consciousness possessing eidetic-noetic symmetry (with respect to the Universe and Reality) is none other than Genius, or Noesis itself, whose nature we shall exclusively elaborate upon in the last section.

5 The Ultimate Observer in brief

> "*Who is looking at who? How far away is the Real from the reflection?*"

We can very empathically say that the Ultimate Observer is such that if that One stopped observing the Universe by way of Surjection (Surjectivity, *Noesis*), and not only in terms of phenomenological abstract laws and concrete entities, it would all cease to exist at once — at one Now — "before before" and "after after", noumenally and phenomenally. This, again, is beyond the level of omnijective reality (omnijectivity) or conscious surrealism (of "altered consciousness states") and mere inter-subjectivity, for it is an eidetically qualified noetic determination without parallel and residue.

The respective observer, then, is called a "noetic observer": he eyes the Universe even before the Universe is "conscious enough to eye him", with all its noumenal and phenomenal instances, and the Universe takes on *essentia* (*forma*) only through him. The level of imagination of such an observer, which is equivalent to the very form and interior of the entire Universe, is not as naive thinkers would potentially suggest (with express slogans like "anybody can dream anything into life" and "anything is possible for anyone"): first of all, he is eidetically qualified by Reality as regards his very presence and his observing the Universe. Thus, it cannot be just an arbitrary observer, let alone "consciousness", in phenomena, and so both typical superficial "science-fiction" and "spiritual pseudo-science" (i.e., "scientific pseudo-spirituality") ultimately fail at this point, leaving only indeterminate non-universal surrealism.

What has been said of Reality thus far, in the foregoing twice-qualified ontological fashion, has been said enough clearly, exhaustively, and exceptionally. Still, let's continue to throw some endless surjective light at any of the better-known sciences (such as physics and cosmology) and at the so far little-understood (or completely misunderstood) philosophy of universal aesthetics (i.e., the nature of Genius).

6 On a model of quantum gravity and quantum cosmology: the all-epistemological connection

> "*Of geometry and motion, however, I must speak, no matter how faint.*"

We now wish to briefly review certain aspects of a model of quantum gravity as outlined in [3]. This consideration may be skipped by those interested only in the supra-philosophical aspects of the present exposition. But, as we shall see, there is an intimately profound universal similarity between a primary underlying wave equation there and our "Reality equation" as presented here, elsewhere.

In the truly epistemological dimension of this theory, gravity and electromagnetism are unified by means of constructing a space-time meta-continuum from "scratch", which allows for the spin of its individual points to arise from first geometric construction and principles, without superficially embedding a variational Lagrangian density in a curved background as well as without first assuming either discreteness or continuity. As a result, we obtain a four-dimensional asymmetric, anholonomic curved space-time geometry possessing curvature, torsion, and asymmetric metricity (generally speaking, the distance between two points A and B, on the fundamentally asymmetric, "multi-planar" manifold, is not the same as that between B and A). The symmetric part of the metric uniquely corresponds to gravity while the anti-symmetric part thereof to electromagnetism (which is a generalized symplectic (pure spin) structure), resulting altogether in a unique, scale-independent spin-curvature sub-structure.

A five-dimensional phase space then exists only in purely geometric fluctuation with respect to the four-dimensional physical manifold, in contrast to regular Kaluza-Klein and string theory approaches. Thus, we do not even assume "quantization", along with continuity, discreteness, and embeddability.

An important result is that both the gravitational and electromagnetic sectors of the theory are "self-wavy", and the entire space-time curvature can be uniquely given by the wave function of the Universe for all cosmological scales, serving as a fundamental fluctuative radius for both the monopolar meta-particle and the Universe. Needless to say, here the Universe and such a meta-particle (monopole) are roughly one and the same. Also crucial is the fact that outside matter and electromagnetic sources (as both are uniquely geometrized by the dynamics of torsion in our theory, while in turn the torsion is composed of the dynamics of the anti-symmetric part of the metric responsible for individual spin "kinemetricity"), gravity uniquely emerges in an electromagnetic field. Another instance is that both gravity and matter appear therein as "emergent" with respect to the entire geometric quantum fluctuation whose primary nature is electromagnetic.

To cut the story short, our quantum gravitational wave equation is as follows:

$$(DD - R)\, U\,(g, dg) = 0\,,$$

where DD is the generalized (anholonomic) wave-operator — constructed by means of the generalized covariant derivative D_i —, R is the spin-curvature scalar, U is the wave function of the Universe, g is the asymmetric metric, and dg is the

asymmetric metrical variation. In contrast to the "spinless description" of the Klein-Gordon equation of special relativistic quantum mechanics and the originally non-geometric Dirac equation, our wave function U is an intrinsic spin-curvature hypersurface "multivariant" (i.e., the hypersurface characteristic equation) and, upon the emergence of a specific toroidal quantum gravitational geometry, becomes none other than the generator of the most general kind of spherical symmetry (especially useful in the description of particle modes).

A complementary wave equation is also given there in the form of a completely geometric eikonal equation:

$$g^{(ik)}\,(D_iU)(D_kU) = -RU^2 \longrightarrow 1\,,$$

which goes over to unity in the case of massive particles (otherwise yielding a null electromagnetic geometry in the case of massless photons), for which

$$R = R\,(g, dg) \longrightarrow -\frac{1}{U^2}\,.$$

Among others, such fundamental equations of ours result along with the following comprehensive tensorial expressions:

$$R_{ik} = W^2(U)\,g_{(ik)} \quad \text{(for gravity and matter)},$$

$$F_{ik} = 2W\,(U)\,g_{[ik]} \quad \text{(for electromagnetism)},$$

where the operations "( )" and "[ ]" on tensorial indices denote symmetrization and antisymmetrization, respectively, and summation is applied to repeated tensorial indices over all space-time values. Note that the above second-rank spin-curvature tensor, represented by the matrix R_{ik}, consists further of two distinct parts built of a symmetric, holonomic gravitational connection (the usual symmetric connection of General Relativity) and a torsional, anholonomic material connection (a dynamical material spin connection constituting the completely geometrized matter tensor).

The strong epistemological reason why this theory, among our other parallel attempts (see, e.g., the work on the geometrization of Mach's principle by the introduction of a furthest completely geometrized, chronometric (co-moving) physical cosmic monad as outlined in [10] — and the list of some of the Author's other works therein), qualifies as a genuine unified field theory and a theory of quantum gravity is that, among others, its equation of motion (namely, the geometric Lorentz equation for the electron moving in a gravitational field) arises naturally from a forceless geodesic motion, that the theory gives a completely geometric energy-momentum tensor of the gravo-electromagnetic field — plus room for the natural emergence of the cosmological term as well as the complete geometrization of the magnetic monopole — and that the theory, without all the previously mentioned ad hoc assumptions (such as the use of arbitrary embedding procedures and the often "elegant" concoction of epistemologically unqualified Lagrangian densities, with non-gravitational field and source terms), naturally yields the eikonal wave equation of geometric optics, therefore completely encompassing the wave-particle duality: therein a particle is a localized wave of pure spin-curvature geometry. Or to be more explicit: elementary particles, including light itself, propagate with certain chirality (helicity) arising purely geometrically due to individual-point spin and manifold torsion, in two geometric transverse and longitudinal modes (hence the existence of two such completely light-like surface vectors in the case of photons, whereby a photon can be regarded as a null surface of propagation with transverse and longitudinal null normal vectors emanating from it, which is the ground-state of all elementary particles).

In short, the theory yields a completely geometric description of physical fields and fundamental motion for all scales, especially as regards the question: "why is there motion in the Universe, rather than phenomenal stillness?" — which is quite comparable to the generically winding epistemic query: "why is there existence, rather than absolute non-existence?".

The full extent of this physical theory is not quite an appropriate subject to discuss here, but we will simply leave it to the interested reader for the immediate comparison of our following two equations:

$$(DD - R)\,U\,(g, dg) = 0 \quad \text{(for the phenomenal Universe)},$$

$$M : N\left(U(g, dg)\right) \sim S \quad \text{(for the noumenal Universe)},$$

with respect to the manifest epistemological connection between the noumenal and phenomenal Universes.

Additionally, our model of quantum gravity also reveals why the physical Universe is manifestly four-dimensional, in terms of the above-said generalized symplectic metrical structure, and whether or not the cosmos originates in time (for instance, due to a "big bang" ensuing from the standard classical, homogeneous, non-quantum gravitational model of cosmology) — to which the definite answer now is: it does not, but it can be said to be "emergent" as it is entirely qualified (necessitated), in the ontic-teleological sense, by that which is other than space-time categories, and in this sense the Universe is both preceded and surpassed by Reality and yet, due to Noesis, is never apart from it. As there remain categories of infinities, certain physical-mathematical singularities may locally exist in the fabric of the cosmos rendering the space-time manifold "non-simply connected", but across such local boundaries the cosmic origin itself cannot truly be said to be (traceable) in time, for the Universe-in-itself is Reality's "Now-Here", infinitely prior to, and beyond, the evolutionary and yet also encompassing it.

7 Genius: a conversation with noumena — closure

> "*That leaf, which silently yellows and falls, is — more than all smothering possibilities — a happening unto itself. If only it were to happen up above instead of down here, among us, the celestial domains would all be terrifyingly cleansed at once.*"

We are now at a psychological and intensely personal stage where we can truly speak of the nature of Genius in the solitude of certain unsheltered sentiments and unearthed fissures belonging to the individual who sees the longest evening all alone, to which he lends all of his insight. That, he verily sees not outside the window, but entirely in himself. The only helplessly beautiful solace he has, then, arises simply from his soul seeing things this way. By "soul", we mean that which moves from the pre-reflexive Surject to the reflexive realms as none other than the microcosm, such that others can hardly notice that he is happening to the Universe as much as the Universe is happening to him.

Weren't Genius synonymous with Infinity — while in the synoptic world of countless impalpable beings, like a contrasting taciturn ghost, he is often an infinitely stray, perpetually long personification (acute inwardness) of the noumenal world along outwardly paradoxical, tragic banishing slopes —, Kierkegaard would not have swiftly declared,

> "*The case with most men is that they go out into life with one or another accidental characteristic of personality of which they say,' Well, this is the way I am. I cannot do otherwise.*' *Then the world gets to work on them and thus the majority of men are ground into conformity. In each generation a small part cling to their 'I cannot do otherwise' and lose their minds. Finally there are a very few in each generation who in spite of all life's terrors cling with more and more inwardness to this 'I cannot do otherwise'. They are the Geniuses. Their 'I cannot do otherwise' is an infinite thought, for if one were to cling firmly to a finite thought, he would lose his mind.*"

Similarly, Weininger is known to have exclaimed,

> "*The age does not create the Genius it requires. The Genius is not the product of his age, is not to be explained by it, and we do him no honor if we attempt to account for him by it... And as the causes of its appearance do not lie in any one age, so also the consequences are not limited by time. The achievements of Genius live forever, and time cannot change them. By his works a man of Genius is granted immortality on the Earth, and thus in a three-fold manner he has transcended time. His universal comprehension and memory forbid the annihilation of his experiences with the passing of the moment in which each occurred; his birth is independent of his age, and his work never dies.*"

(For more such non-dissipating, spectacular universal overtures, see [6].)

Peculiar to Genius is, among other solitary things, an infinite capability for intricate pain (inward ailment), for perpetual angst, which people often misrepresent as arising from mere anti-social loneliness or lack of amusement. But this aspect of Genius cannot be partitioned arbitrarily from the soaring spontaneity of his infinite ecstasy. Rather, Genius is simply beyond ecstasy and despondence, as well as beyond pride and self-deprecation, the way people are used to these terms. In any case, it is a state of universal sensitivity, inspiration, solitude, and creativity, which is the Eye of Creation, whereby Reality is comprehensively "likened" to a form ensuing from Noesis.

This way, most people are mistaken in their belief that Genius and talent are equivalent, for Genius is, indeed, "separated from all else by an entire world, that of noumena", and not situated "within the spectrum of all linearly predictable expectations and contingencies", as Goethe, Schopenhauer, Wilde, Emerson, Weininger, and Wittgenstein would have agreed. Mere belief, assumption, or syllogism is effortlessly devoid of authentic realization, let alone Reality: it is not even worthy of the simplest meta-logical refutation.

Indeed, Genius is in no way the superlative of talent. Talent is, at most, phenomenal-reflective, while Genius is noumenal-surjective and noumenal-reflective. It has been said that Genius does not act as a role model for talent at all: with respect to the latter, the former may appear inanely murky and most wasted, simply because the latter lacks that which is infinitely other than the entire contingency of multiple reflections and projections.

The world of Genius is Moment, Universality, and Creation, where the entirety of noumena is revealed to the persona without residue, which is the greatest, most absolute kudos in existence, be it in the presence or absence of an audience. The world of talent is ordinary — no matter how augmented — time, space, and imitation, i.e., the relative integral power of the inter-subjective contingency and tautology of phenomenal recognition and security.

The ocean of Genius is the heaviest self-necessity of greatly spontaneous assaults and pervasions on any shore without sparing both any large accidental object and a single grain of sand: it evokes creation and destruction entirely in its own being in this world. The pond of talent, amidst dregs, is the relative confidence of "sedimental measurement and experimentation", albeit still related to intensity.

The intentionality of Genius is a self-reserved "Parsifal" of Universality, while that of talent is always other than the thing-in-itself (and so, for instance, a talent associated with science tends not to embrace the essence of science itself, which is one with the essence of creative art and epistemic philosophy, but only something of populistic, tautological "scientism").

The essence of Genius is Reality, not just situational "truth" — not the normative, often progressive, collective truths of talent and society.

The way of Genius in the world is traceless originality and thus defies all sense of imitation and expectation. Who shall discover the traces of fish in water and those of birds in the sky? And yet, this matter of Genius is more than that: he is different from all similarities and differences, absolutely

independent of representation. Hence it is said of men of Genius — for instance by Weininger — that "their parents, siblings, and cousins cannot tell you anything about them, for they simply have no mediational peers, no genial otherness". By contrast, talent is still psychogenetically and methodologically inheritable.

The life of Genius is that of utter sensitivity, and not just volitional silence and loudness. It is one of transcendental consciousness and intensity, and not constituted of mere choice and chance.

As the hallmark of the Genius is authenticity and creativity, which is not situated within the rhyme and rhythm of a mere choice of life-styles, he can do no other than this, and no one needs to tell or teach him anything.

Individuals of Genius exist as universal gradations of the pure eidetic plenum, and not as part of the mere ascending levels of talent. Thus, the particularity of Genius is always simultaneously universal: it is both twice-qualified "*Atom*" and "*Platon*", Instanton and Soliton. He possesses the entirety of Object, Subject, Dimension, and Surject to unbelievable lengths.

Indeed, as has been generically said: "science becomes pure imagination, art pure life, and philosophy pure creation", there in the vicinity of Genius.

Genius is Michelangelo, not Rafaelo. Genius is Leonardo, not rhetoric. Genius is Mozart, not the Royal Court. Genius is Beethoven, not the audience and merely connected hearing. Genius is Zola, not psychotherapy. Genius is Kafka, not stability. Genius is Rembrandt, not feminism. Genius is Tolstoy, not chastisement. Genius is Johann Sebastian, not the Bach family. Genius is Klimt, not neurasthenics and Venus. Genius is van Gogh, not art exhibitionism. Genius is Glinka and Gould, not musical recording. Genius is Abel and Galois, not the Parisian Academy. Genius is Kierkegaard, not Hegelianism. Genius is Weininger, not Aryanism. Genius is Wittgenstein, not philology. Genius is Kant, Einstein, and Zelmanov, not the herd of "scientism". Genius is Goethe, not Prussia. Genius is Cezanne, not Europe. Genius is Emerson, not America. Genius is Neruda, not Chile. Genius is Tagore, not India.

Genius is the Renaissance in motion before everyone else is capable of naming it, not its "timely and subsequent crumbs". Genius is Dream, not sleep. Genius is Insight, not the day. Genius is Vision, not a report or a documentary. Genius is the austere summit, not the floating clouds. Genius is the ocean, not a river. Genius is gold, not the muddy colliery, not the mining. Genius is youth, not childhood, not adolescence, not adulthood, and absolutely not old age. Genius is all-life, not imitation. Genius is all-death, not barren constancy and consistency. Genius is acutely conscious suicide, not helplessness — but definitely not all suicides are Genius. Genius is love, not crude relationship. Genius is music, not licensed instrumentation. Genius is Self, not super-tautological composition. Genius is sheer nostalgy, not learning. Genius is Creation, not school, not training.

Genius is the cold North Atlantic, not the luxurious Titanic. Genius is the Siberian currents, not the avoidance of winter for more festive humidity. Genius is the entire Sonora, not urban life of chance-fragments. Genius is character, not yielding sexuality. Genius is Moment, not societal time. Genius is Mystery, not public space. Genius is Memory, not standard coordination. Genius is Nature, not information — and so not recognition. Genius is the full eclipse as it is, not prediction. Genius is the entire night, not a system.

Genius is Motion-in-itself, not a planned sequence. Genius is real individuality in the Universe, not composite institutional, societal, cultural pride. Genius is the singular conquest, not an artificial war. Genius is the universal meteor, not a celebratory fire-cracker. Genius is the rareness of a tsunami, a volcano, or an earthquake, not reported abrupt casualties. Genius is solitude, not sold and given democracy, and not a republic. Genius is the abyss and the sudden voice and force arising from it, not typical antiquity, Victorianism, and postmodernism.

Genius is the Universe, not a specific age of trends, not a destined place of people.

Genius is Reality, not a situation, not an option, not a collection of societal facts.

Genius is Genius, not talent.

Genius is a word not yet spoken (enough) by other sentient beings. And, respectively, a drop not yet consumed, a meaning not yet sighed, a clarity not yet impregnated. A birth not yet celebrated, a sudden electricity not yet channeled, a humanity not yet recognized.

Often, in relation to tragedy, Genius emerges as a funeral song, preceding all births and surpassing all deaths, which people find hard to canonize. Amidst their superficial merriment, a man of Genius is like the night that falls on their eyes and sinks in their souls — to be forgotten at their selfish ease. He is the loneliness of the day on a deep cogitator's pane, one with the blue nacre of things.

Why then would Genius be most exclusively, among others, associated with tragedy? It is because most people would not mind partaking of "joy as it is", with or without anticipation and as much and gauche as possible, yet they are ever impotent and apprehensive when it comes to facing "the other thing as it is", i.e., tragedy. As Genius is the only spontaneous genera capable of infinitely imbibing the noumenal "thing-in-itself", in universality and in particularity, in representation and in person, a man of Genius would principally never shun tragedy. His objective is inevitably the surjective pure intimation of it.

Thus, tragedy has sought the Genius even from before the dawning of the world. Indeed, he would even volunteer for it. And the entire Universe volunteers for it too, in and through his very individuality. This is why, the theme of tragedy (or death) is rather universal: it is consciously frequented only by very few men and yet by the entire Universe

itself. These men, without losing their Self, which is Reality and the Universe — unlike the way most people understand it —, embrace phenomenal selflessness and defenselessness with full noumenal understanding and bursting innocence: they are "too close" to the torrents of the most unlikely visitation of kisses, "too close" to thunder in the heavy rain, "too close" to the Sun in elevation and peaking radiation, "too close" to the soil and dust in every heavenly intimation, "too close" to the nakedness of Nature in everything raw and full, "too close" to the chiseled understanding of certain winter-banished seeds and underground grains, "too close" to the Cornelian female breast of surreptitiously migrating strengths and silences. They are "too close" to their own prodigious male latitude, in their expensive self-immolating Siriusian nuclear moods, eventually being poured out of life onto the canvas of death as the most splendid of selfless, will-less, unadulterated presence of colors and paintings, while thus rendering themselves too far from incidental admirers other than Reality itself. Such is glory: only due to that does deeply crimson compassion whiten in this world for a few sensitive others to see.

Though this world may see naught but sad wrinkles, the love of Genius is strong in its own unseen furrows, at the core of stars, in the fire of molten things. Genius is strong though weak and peevish in appearance: it is exalted in everything that takes roots and bears its own growth, in everything universal Reality wishes to see for itself. The Crucified is such a rare taste in people's veins to devour. So either they unveil their own souls in the tragedy of Genius and then die to live anew, or live the life of a heathen forever.

When will this world fall into indigenous silence, like Genius, but not in certain sleep? Where is the soft hand of a lovely, caring female weaver upon Genius' crushed, blackening fingers emerging from the rugged Earth and its ravines? In an aspect that relates the solitude of Genius and the continuity of mankind, known and unknown Geniuses have been digging the Earth for eons, for this world's most conscious dreams, so that humanity may gush out with Nature's own blood of youth: such is done among tormenting rocks, yet in order to reach above the Sun — yes, with the entire humanity.

Who would glue his petty, cowardly self to the secret, yet infinitely open, wounds of Genius? Either humanity caresses Genius the way Genius would touch humanity, until nerves, whips, and scourges become impalpable in humanity's constitution of clay and fire, and of some might of the Unknown, or it perishes altogether with self-sufficient Genius not repeating itself for its cause ever again.

And to humanity it will then be said, "Either gaze at the red branches in the park of lovers, where Genius lives and dies unnoticed, where life fills its own cup through entwined hearts, lips, and arms through the sacrificial life of Genius at unseen roots, or, perchance, seek another countenance, another reality altogether and die without Reality ever sketching you in its own bosom."

In this savage world of heavily fabricated walls, who then would want to taste a most tender, fateful wet drop of dew and honey oozing from the pristine skin of Genius, in the rain of tragedy and in the weft of huge solitude, which might just taste like the Universe — all of the Universe?

Who, then, would be able to recapture the moments of Genius, once they pass for good? Would they ever be able to simply rediscover the soul of Genius among many roots, thorns, and tremors and still multiply the silent understanding of love and life that hides in a wide ocean that shall never want to depart from humanity?

Who, then, would abandon the ever-putrefying cowardice, soulless collectivism, and mere conformity with much of this unconscious world and sit with Genius just for one more night — where there shall be no more secrets in the darkness' midst, other than shadowless man, without flight from destiny, naked, engraved, and unshaken on the scarlet horizon behind a thousand prison features? Who shall be loved and sought by freedom this way?

Genius is a most shunned resonance behind all languages: both "knowing" and "not knowing" recognize it not. Whereas people are sole humans, a man of Genius is, infinitely more acutely, the most solely human: he is the one who understands love and sacrifice the most, who breathes limitlessly upon the flanks of wild flowers and hidden rivulets, yet no one among sole humans dares to love him with enough vastness of space. Indeed, he is the drops and substances in the rain, all the non-existence in dust.

When an individual of Genius desires existence in this world, he comes yielding against everyone else's direction, cutting the evening on its very edges, unfolding horizons — even if that means undoing fancy rainbows. And when he yearns for an ultimate self-exile, he rushes towards death unconditionally, just as he once arrived in this world not by slow walking, purblind wandering, and empty gazing, but by the crackling spontaneity that impulsively and immeasurably forms fateful symmetries through the soul's pure motion.

The life of Genius leaves this world a silent place underground for the most solitary and distinguished of understanding, knowledge, tenderness, and pain. Only a few, therefore, know what a "most original Genius" truly means. If only people knew the universal responsibility set upon the shoulders of Genius, and not just its apparent glories, very few of them would dare to aspire to the rank of Genius. Instead, they would be fairly content with talent alone. For, in relation to humanity as a "non-ideal savior", Genius lives with such a palpitating, lonely chest and uplifting sensitivity in the narrowness of time's remaining passage. (As Schopenhauer once declared, "*Great minds are related to the brief span of time during which they live as great buildings are to a little square in which they stand: you cannot see them in all their magnitude because you are standing too close to them.*")

As regards the history of indifference and war that has befallen mankind, the heavens, some say, can't be errant. But

what idea do they have of a man of Genius whose heart of immense autumns is like a shattered clock, which he hears ticking mercilessly every second until its near cease, even when its fire — of awakening blood — moves from his heart's solitude, to his soul's labyrinth, to his lips, to the desire to possess, to nearness, to excitement, to the redemption of humanity? When the only place he can carry humanity to — for the moments and lost wings to take, to hold, to secure — is his ship of winter, passing through wounding seas, violent winds, and threshing floors? When he himself is one of the branches of the long, solitary night — of azure fate — and hardly a resting place for another soul's existence?

A man of Genius loves humanity beyond its occasional self-pity and vain arrogance, without knowing how to carry the luster and growth of the garden of passion and intimacy elsewhere other than through the often awkward abruptness and intensity of each second. And so, wordlessly, certain hidden things are written in blood and yet shared in moisture, freely given and fully experienced — just as the cup, potion, and tavern are spun only at night — even while personal hope, let alone a future, ever shies away for himself, for soon enough nearly everyone's eyes are to shut at length in sleep, not knowing that Reality itself is present in the darkest ravine of their modulations.

Men of Genius do not cross poignant, dark reefs to merely taste the deeps of depravity for themselves, but to make contact with the entirety of humanity and to love the unconsciously tragic as it is. But, of conversing with the severity and weather of naked love in the most drenching downpour of sentiments, who shall readily repay these men by communing in their names, even without having seen them?

Who, then, can cover the perimeter of Genius like a pure ring? In the Genius, life passes in a single heartbeat, and he happens to the world like the grip of the strangest spontaneous intimacy upon the furthest comprehension of sincere lovers. The nakedness of Genius is just as day and night are inseparably present in the world, unveiling each other — and thus essentially beating in each other — more than just taking turns and partaking of chance.

Verily, before the whole world of people ever does it, Genius is the poetry that immediately captures the high flares of every joy and the disconcerting depths of every tragedy there has ever been and will ever be so long as humanity exists. By the very personification of Genius is the most distant fate of humanity drawn near and the nearest pitfalls thereof redeemed.

People do the Genius absolutely no honor by merely projecting phenomenal attributes and expectations — and by merely scholastically and naively reflecting — upon him. When, coincidentally, certain men of Genius happen to be situated in certain domains of the society (instead of living in relative obscurity and epistemic solitude), which is a very rare case, it is to be understood that a zoo that proudly keeps a lion or a falcon, has no way of knowing whether or not it fully possesses it; and yet too often the zoo honors the beast and prides itself in the act only in order to praise itself. Genius exists independently of such a contingency and tautology. The entire gist of societal-phenomenal intentionality approaches not the abyss of the Genius, who, alone, is the monad, center, mind, and heart of the Universe. He is the entirely unabridged, naked pulse of Nature. It is the Genius who merely not "eyes the abyss" and "is conversant with it", but who also exists there with absolute self-certainty, independently of all the objects outside the abyss (out there in the world), and independently of the entire abyss itself. He is not a mere philosopher of "mereology" either. He never has the need to question his own existence nor to "unveil himself", whatsoever. He is not a mystic in this sense (and in that of Wittgenstein): it is not mysticism that is mystical, it is the way things already are in and of his nature; yet this he often projects onto people as "mysticism" in order to be "roughly understood", i.e., when forced to speak to the world.

Indeed, Genius is more of the Universal Mind that establishes (and not just imparts to others) the "Suchness" of the Universe entirely through itself and moves things that way from the infinite past to the infinite future, through the infinite moment, instead of just a mere saint and mystic who has to find his way, by following the ways of other adepts, in much of the Unknown. It is the Pure Sword that still glitters and functions (i.e., moves) in the darkest stretch of space, with or without the presence of mirrors and lights. And it is not just a spark, nor a mere brilliance: Genius is the wholeness of unique illumination and pure presence.

The Universe of Genius individuality is four-fold, encompassing an infinite amount of noumenal uniqueness (not just "totality") and a most extensive category of phenomenal modes of existence. Thus, again, it contains:

— Reality: *Eidos-Nous* — the Surjective Monad, Absolute Unique Singularity,

— The Mirror-Universe — the Reflective Whole, Singularity, Transcendence,

— The Imagery-World — the Projective Particularity, Multiplicity, Immanence,

— Unreality — the Absolute Darkness

i.e., its being-there, entirely in the greatest genus of individuation, is essentially without chance and residue.

The man of Genius, as such, needs no "belief" nor "hypothesis", nor even any "transcendental method", be it of religious, philosophical, or scientific dialectical nature, for he, the Eye-Content of Infinity and the Sign-Severity of Oneness, is he whose essence is All-in-All, the All-One, the Unique: "within", "without", "within-the-within", and "without-the-without". And this is more than just saying that his individual entification is the microcosm — and that he is a particularization of the Universe.

Unlike a mere saint who is the ultimate phenomenal (linear, diametrical) opposite of a mere criminal, a person of Ge-

nius possesses *Animus* (*Anima*, "animate animal"), with respect to the entire Imagery-World, and is therefore the most unpredictable, spontaneous, intense, and creative in his phenomenal actions, beyond the entirety of collective anthropomorphic morality, if not ethics. And, unlike a mere criminal who is the phenomenal opposite of a mere saint, Genius is fully, intrinsically possessed of Noesis. Thus, a single moment of Genius in the Universe enriches existences infinitely, whether the individual is "animal-like" (in terms of instinct, but not merely psycho-pathological: for instance, even when madness seems to have befallen a man of Genius — as Atlas is said to excessively bear the world on his shoulders, alone, more than any other —, it is so without the Genius losing his persona at all, for his essence is absolutely non-composite Individuality and Universality, inwardly and outwardly; madness is a mere "surrealism" the Genius deliberately embraces in order to relatively, specifically "seal" his suffering without ulterior motives other than "inward romanticizing" (for instance, Goethe and Kafka), and the same can be said about the case of a suicidal Genius) of tragedy-in-itself, or whether he is deliberately an entirely new humanity — and, again, not just a new species — beyond the external world's understanding.

The Genius is he who knows the saint more than the saint knows himself, and he who knows the devil more than the devil knows himself: needless to say, he definitely knows Kant better than Kant knows himself (indeed, he who understands Kant, goes beyond him and thereby "bedevils" him, while most others are stuck, without soul, in mere scholastic documentaries on Kantianism). Whether or not he speaks of what people call "morality", it is entirely up to him: in any case, he alone personifies Reality and gives its most elusive aspects to his subjects. Unlike the sadist, he suffers not from the outward surreal vacuum of space and, unlike the masochist, from the inward intimidation of time (again, see Weininger's psychological essay on aspects of sadism and masochism in [6]). His deliberate transgression of established, normative mores is equally non-understandable by most sentient beings as his infinite capacity for tenderness and selflessness. In any of these acts, he truly owns his moments, either by throwing universal light into utter darkness or by annihilating even light in every phenomenal perception. In one respect, he is indeed ageless Momentum: he is child-like, though not exactly a child, and he is sage-like, though not exactly a sage.

As the Genius is he who phenomenally contains the most variegated manifold of attributes, names, and characters, he thus has to represent an entirely new genus of humanity, a whole new epoch in the evolution of the cosmos, beyond the level of acceptance of present humanity. He remains human, simultaneously aloft as the sky — proud as a mountain — and fragile as the sand of time — humbled as a valley — beyond mere acceptance and refusal, and even beyond contemplation. Just as the heavens send down the rain just as much as they reflect sunlight, and just as the great ocean gently intimates sand-grains and yet annihilates shores and settlements, so is Genius the one most capable of sorrow and joy; rage and calmness; destruction and creation — of both infinitely romanticizing and molding the modes of existence.

Thus, while there can be countless linearly, smoothly predictable talented, institutionalized people in the world, "who are just happy and successful enough" without the tinctures of tragedy and without possessing the Surjective Monad of Genius, there is indeed no Genius without a trait of tragedy, for tragedy is the only melodrama in the Universe used as a language to convey and gather known and unknown multitudes: it is a forceful communication among breaths made possible in a largely superficial world and in a truly secluded corner of the Universe — however with the possibility of communication across it. Of this universal epistemic disposition, the Genius would rather embrace moments of melancholia and quiver like certain autumnal sitar-strings, than be merely happy. Again, while not being a merely fateful one, he never shuns tragedy: he voluntarily internalizes any tragedy (especially the tragedy of other men of Genius, whether known or unknown) and still gives it a breathing space and pulse in the Universe (and indeed binds it as a cosmic episode), when most people are wary of it. Nor does the Genius withhold conquest merely for the sake of mercy. He is the virtuoso, and not just the actor. He is also at once the script, the stage, the spectator, and the actor — the very life of the play. In the cosmic sense of the ultimate unification of observers and observables, he is self-observed, self-observing, self-existent.

As such, the following can be said about the dominion and nature of Genius, which belongs to no school and species at all. An individual of Genius is entirely his very own genus, more than a species, of Universality: without him, the Universe is not the Universe, and Reality would never "act upon itself" and "beget an archetype". No one can teach Genius anything. No school, nor training, nor erudition can beget, let alone produce, the conscious existence of Genius. Its meta-human dominion is that of non-composite Self-Will animating the infinitesimals (i.e., meta-particulars) of the Universe. Its person is the one most capable of infinite self-differentiation (besides his intrinsic, immutable uniqueness), precisely because the Universe — the infinite Memory (Holography), Moment (Presence), and Mystery (Precedence) — is never exhausted when it comes differentiation, especially self-distinction.

Genius is the very vein and veil of Nature. Once people of discernment and reflection witness the Genius' unfolding the heavens by climbing them up, at once they shall also witness that he has no ladder nor means, that he is the creator of even the Unknown and of perceptual noema. Or even if at first it appears to them that the Genius uses a ladder or means (such as any transcendental logical method of deduction or any style of art), it will entirely fall back upon themselves after being self-thrown, at them and away from him, by himself, and there is no fear in the Genius regarding this, for, again, he

is everywhere Reality's exception just as Reality is his exception. His sheer independence is the sine qua non of existence.

Thus, where are the kisses to leap towards the solitude of Genius, to consume it for last? Hidden in the pure seethe of an ocean's changeless soul, the love of Genius for the Real and the Human is hardly reachable. Even if Genius appears in the faintest human form, among other things in the perpetual sand of existence, people still find it unreasonable to intimate it. Instead, they readily besiege and confine its very incarnation into disappearance, ridicule by ridicule, betrayal by betrayal, kiss by kiss. But they can imprison not the most invisible, most infinitesimal — the most artful grain (meta-particle) in the Universe. Like unknown butterflies and fresh grapes, however short-lived, the Genius swiftly takes for farewell upon the eyelids of beauty, coming home not any later at the coronet noon of that which has communed with him in existence and appearance.

Only Genius knows Genius, and this is no sentimental exaggeration — whether the inter-subjective world of people (not the world-in-itself) is awake or asleep, it is bound to be troubled by the very person. Indeed, for most, "he draws near from farness, and he draws far from nearness", with respect to perception and non-perception, by the very essence and form of Reality — and Unreality —, for the distance between Genius and people is not the same as that between people and Genius.

Footnote

Suggested parallel reading in philosophy, psychology, mathematics, and physics, especially for the sake of the reader's perspicacity of the present novel epistemological (meta-logical) work in simple comparison with other works dealing with theories of Reality and the Universe.

Submitted on February 29, 2012 / Accepted on March 03, 2012

References

1. Velmans M. Reflexive Monism. *Journal of Consciousness Studies*, 2008, v. 15(2), 5–50.
2. Langan C. The Cognitive-Theoretic Model of the Universe: A New Kind of Reality Theory. http://www.ctmu.net
3. Suhendro I. Spin-Curvature and the Unification of Fields in a Twisted Space. Svenska fysikarkivet, Stockholm, 2008 (original doctorate thesis version, 2004).
4. Zelmanov A. L. Orthometric form of monad formalism and its relations to chronometric and kinemetric invariants. *Doklady Acad. Nauk USSR*, 1976, v. 227(1), 78–81.
5. Wittgenstein L. Tractatus Logico-Philosophicus. (The original draft), 1918.
6. Weininger O. Sex and Character (Geschlecht und Charakter). Wilhelm Braümuller, Leipzig and Vienna 1913 (modern online edition with interlinear translation by Robert Willis, 2004). See also Kevin Solway's splinter page: http://www.theabsolute.net/minefield/genqtpg.html
7. Mao L. F. Smarandache Multi-Space Theory. Post-doctoral research report, the Chinese Academy of Sciences, 2006.
8. Borissova L. and Rabounski D. Fields, Vacuum, and the Mirror Universe. Svenska fysikarkivet, Stockholm, 2009.
9. Zelmanov A. L. Chronometric invariants and comoving coordinates in the general relativity theory. *Doklady Acad. Nauk USSR*, 1956, v. 107(6), 815–818.
10. Suhendro I. A hydrodynamical geometrization of matter and chronometricity in General Relativity. *The Abraham Zelmanov Journal*, 2010, v. 3, 102–120.
11. Zelmanov A. L. Chronometric Invariants — On Deformations and the Curvature of Accompanying Space. Sternberg Astronomical Institute, Moscow, 1944 (published as Zelmanov A. L. Chronometric Invariants — On Deformations and the Curvature of Accompanying Space. American Research Press, 2006).
12. Shnoll S. E. Cosmophysical Factors in Random Processes. Svenska fysikarkivet, Stockholm, 2009.

Macro-Analogies and Gravitation in the Micro-World: Further Elaboration of Wheeler's Model of Geometrodynamics

Anatoly V. Belyakov

E-mail: belyakov.lih@gmail.com

The proposed model is based on Wheeler's geometrodynamics of fluctuating topology and its further elaboration based on new macro-analogies. Micro-particles are considered here as particular oscillating deformations or turbulent structures in non-unitaty coherent two-dimensional surfaces. The model uses analogies of the macro-world, includes into consideration gravitational forces and surmises the existence of closed structures, based on the equilibrium of magnetic and gravitational forces, thereby supplementing the Standard Model. This model has perfect inner logic. The following phenomena and notions are thus explained or interpreted: the existence of three generations of elementary particles, quark-confinement,"Zitterbewegung", and supersymmetry. Masses of leptons and quarks are expressed through fundamental constants and calculated in the first approximation. The other parameters — such as the ratio among masses of the proton, neutron and electron, size of the proton, its magnetic moment, the gravitational constant, the semi-decay time of the neutron, the boundary energy of the beta-decay — are determined with enough precision.

> The world ... is created from nothing, provided the structure ...
>
> *P. Davies*

1 Introduction

The Standard Model of fundamental interactions (SM) is a result of the attempts of thousands of researches in the course of decades. This model thus bears rather complicated mathematical techniques which hide the physical meaning of the phenomena.

Is this process inevitable? And also: can further mathematical details make the Standard Model able to explain virtually everything that takes place in the micro-world? May it be necessary to add SM by the concept proceding not from electrodynamics? This problem statement is grounded, because another adequate model allows us to consider micro-phenomena from another side, and so it remains accessible for more number researchers.

According to contemporary statements, objects of the micro-world cannot be adequately described by means of images and analogies of the surrounding macro-world. But certain analogies successfully interpreting phenomena of the micro-world and explaining their physical essence exist. It will be shown further in the present exposition.

This work uses conceptualization of another class of physical phenomena, and its possibilities are demonstrated. This model has the inner logic which does not contradict confirmed aspects of SM. Besides, it explains some problems which are not solved at the present time.

It is necessary to outline a survey illustration of our model worked out in the spirit of Wheeler's geometrodynamics. The logic of the model, and its adequacy, is justified by many examples. Thus another approach towards understanding micro-phenomena is proposed. Herein, straightforward numerical results are obtained only on the basis of the laws of conservation of energy, charge and spin, and evident relations between fundamental constants, without any additional coefficients. These results, being the basic points of this model, justify the model's correctness.

The geometrization of the physics assumes the interpretation of micro-phenomena by topological images. Many such works have been outlined now: for example, the original elements of the micro-world, from which particles are constructed according to Yershov's model [1], are preons, which are, generally speaking, local singularities.

Wheeler's idea of fluctuating topology is used here as an original model of a micro-element of matter: in particular, electric charges are considered therein as singular points located at a surface and connected to each other through "wormholes" or vortex current tubes of the input-output kind in an additional direction, thus forming a closed contour.

A surface can be two-dimensional, but fractal, topologically non-unitaty coherent at that time. It can consist of vortex tubes linkage which form the three-dimensional structure as a whole.

This paper follows [3], where numerical values of the electric charge and radiation constants were obtained. It is shown in [3] that from the purely mechanistic point of view the so-called *charge* only manifests the degree of the non-equilibrium state of physical vacuum; it is proportional to the momentum of physical vacuum in its motion along the contour of the vortical current tube. Respectively, the spin is proportional to the angular momentum of the physical vacuum with respect to the longitudinal axis of the contour, while the

magnetic interaction of the conductors is analogous to the forces acting among the current tubes.

The electric constant in the framework of the model is a linear density of the vortex tube:

$$\varepsilon_0 = \frac{m_e}{r_e} = 3.233 \times 10^{-16}\ \text{kg/m}, \tag{1}$$

and the value of *inverse magnetic constant* is associated with a centrifugal force:

$$\frac{1}{\mu_0} = c^2\varepsilon_0 = 29.06\,\text{n} \tag{2}$$

appearing by the rotation of a vortex tube of the mass m_e and of the radius r_e with the light velocity c. This force is equivalent to the force acting between two elementary charges by the given radius. Note that Daywitt has obtained analogous results in [4].

One must not be surprised that the electrical charge has dimension of impulse. Moreover, only the number of electric charges z is meaningful for the force of electrical and magnetic interaction, but not the dimension of a unit charge. So, for example, the Coulomb formula takes the form:

$$F_e = \frac{z_1 z_2}{\mu_0 r^2} \tag{3}$$

where r is the relative distance between the charges expressed in the units of r_e.

The co-called standard proton-electron contour intersecting the surface at the points p^+ and p^- is considered in [3] and in further papers. The total kinetic energy of this contour equals the energy limit of the electron. Possibilities of the model explaining different phenomena of the micro-world are considered with the help of this standard contour.

2 On the connection between the electric and the weak interactions

The electric and weak interactions are united in the uniform contour. The form of our model continuum in a neighborhood of a particle is similar to the surface of a hyperboloid. It is conditionally possible to separate the contour into two regions: the proper surface of the region (the region X) and the "branches", or vortex tubes (the region Y), as shown Fig. 1. A perturbation between charged particles along the surface X is transmitted at light velocity in the form of a transverse surface wave, i.e. the electromagnetic wave. The perturbation along vortex tubes by Y spreads in the form of a longitudinal wave with the same velocity of transmission, as it will be shown.

Express the light velocity from (1) as:

$$c = \sqrt{\frac{s}{\varepsilon_0}}\sqrt{\frac{1}{s\mu_0}} \tag{4}$$

where s is some section, for instance, the section of the vortex tube. Upon dimensional analysis, the first factor is a specific volume, the second — a pressure. In other words, this formula coincides with the expression of the local velocity of sound inside continuous medium. It is interpreted in this case as the velocity of the longitudinal wave along the tube of the contour. The longitudinal wave transforms into the transverse surface wave from the viewpoint of an outer observer at the boundary of the X- and Y-regions.

According to [3], the mass of the contour is given by $M = c_0^{2/3} m_e = 4.48 \times 10^5 m_e$. This value equals approximately the *summary mass of W, Z-bosons* (the dimensionless light velocity $c_0 = \frac{c}{[\text{m/sec}]}$ is introduced here). One can state therefore that the vortex current tube is formed by three vortex threads rotating around the principal longitudinal axis. These threads are finite structures. They possess, by necessity, the right and left rotation; the last thread (it is evidently double one) possesses summary null rotation. These threads can be associated with vector bosons W^+, W^-, Z^0 which are considered as true elementary particles as well as the photon, electron and neutrino.

This structure is confirmed by three-jet processes observed by high energies — the appearance of three hadron streams by the heavy Y-particle decay and by the electron and positron annihilation. The dates about detection of three-zone structure of really electron exist [5].

Other parameters of the weak interaction correspond to the given model. So, the projective angle is an addition to the *Weinberg angle of mixing* q_w of the weak interaction. The projective angle is determined in [3] as $\arcsin \frac{c_0^{1/6}}{\sqrt{2\pi a}} = 61.8°$, where a is inverse to the fine structure constant. The value $\sin^2 q_\text{w} = 0.231$ is determined experimentally, i.e. $q_\text{w} = 28.7°$ and $\frac{\pi}{2} - q_\text{w} = 61.3°$. Based exactly on the value of this angle the electric charge is calculated precisely, the numerical value of which has the form [3]:

$$e_0 = m_e c_0^{4/3} \cos q_\text{w} \times [\text{m/sec}] = 1.603 \times 10^{-19}\ \text{kg m/sec}. \tag{5}$$

3 Fermions and bosons

It is necessary to note that vortex structures are stable in this case if they are leaned on the boundary of phase division, i.e. on the two-dimensional surface.

The most close analogy to this model, in the scale of our world, could be *surfaces of ideal liquid*, vortical structures in it and subsequent interaction between them, forming both relief of the surface and sub-surface structures.

Vortex formations in the liquid can stay in two extreme forms — the vortex *at the surface* of radius r_x along the X-axis (let it be the analog of a fermion of the mass m_x) and the vortical current tube *under the surface* of the angular velocity v, the radius r_y and the length l_y along the Y-axis (let it be the analog of a boson of the mass m_y). These structures oscillate inside a real medium, passing through one another (forming an oscillation of oscillations). Probably, fermions conserve their boson counterpart with half spin, thereby determining

their magnetic and spin properties, but the spin is regenerated up to the whole value while fermions passing through boson form. The vortex field, twisting into a spiral, is able to form subsequent structures (current tubes).

The possibility of reciprocal transformations of fermions and bosons forms does not mean that a micro-particle can stay simultaneously in two states, but it shows that a mass (an energy) can have two states and *pass from one form to another*.

It is easy to note that this model of micro-particles gives an overall original interpretation of the employed notions: *mass defect* and *supersymmetry*. At the same time, our model does not require us to introduce additional particles (superplayers) which have remained undetected until now by experiments and, evidently, will not be discovered.

4 The determination of the relation of the masses proton/electron

In order to compare masses of fermions, it is necessary to consider them as objects possessing inner structure. Let us introduce the analog where the vortex tube is similar to a jet crossing the surface of liquid inside a bounded region and originating ring waves, or contours of the second order (which originate, in turn, contours of the third order, etc.). Let this region of intersection correspond to a micro-particle. Then it is considered now as a proper contour and can be characterized by parameters of the contour: a quantum number n, the radius of the vortex thread r, the circuit velocity ν and the mass of the contour M.

Let us proceed to determine the quantum numbers for micro-particles. We express the typical spin of fermions through parameters of their characteristic contour, being restricted to self-evident cases, namely:

1) the spin of the particle equals the momentum of the contour as a whole:

$$\frac{h}{4\pi} = M\nu r\,, \tag{6}$$

2) the spin of the particle equals the momentum of the contour, related to the unity element of the contour structure (the photon):

$$\frac{h}{4\pi} = \frac{M\nu r}{z}\,, \tag{7}$$

where $h = 2\pi a m_e c r_e$ is the Planck constant.

The parameters of M, ν, r following from the charge conservation condition are determined as [3]:

$$M = (an)^2 m_e, \tag{8}$$

$$\nu = c_0^{1/3}\frac{c}{(an)^2}, \tag{9}$$

$$r = c_0^{2/3}\frac{r_e}{(an)^4}, \tag{10}$$

and the number of photons z in the contour for the case of the decay of the contour (ionization) is

$$z \approx n^4. \tag{11}$$

The following evident relation ensues from the expression of the linear density ε_0 (1):

$$\frac{l_y}{r_e} = \frac{m_y}{m_e} = \frac{M}{m_e} = (an)^2. \tag{12}$$

In other words, the relative length of the current tube expressed through the units r_e equals the boson mass M expressed through the units m_e.

Using the parameters obtained in (8), (9), (10), (11) from (6) and (7), we find:

1) for the first particle, assuming that it is a proton

$$n = n_p = \left(\frac{2c_0}{a^5}\right)^{1/4} = 0.3338, \tag{13}$$

2) for the second particle, assuming that it is an electron

$$n = n_e = \left(\frac{2c_0}{a^5}\right)^{1/8} = 0.5777. \tag{14}$$

Taking into account properties of fermions and bosons in our model, we conjecture that the boson thread is able to pack extremely compactly into the *fermion form* by a process of oscillation along the Y-axis. This packing is possible along all four coordinates (degrees of freedom), because this structure can form subsequent structures. Using (10) and (12), we find that the relative linear dimension of a fermion along the X-axis is proportional to the radius of the vortex thread. It can be expressed by the formula:

$$\frac{r}{r_e} = \left(\frac{r}{r_e}\right)\left(\frac{l_y}{r_e}\right)^{1/4} = \frac{(c_0)^{2/3}}{(an)^{7/2}}. \tag{15}$$

For instance, substituting into the above-obtained formulas $n = n_p$, we find the characteristic dimensions of the proton structure expressed through the units r_e: the radius of the vortex thread $r = 0.103$, the linear dimension along the X-axis $r_x = 0.692$ and the length of the vortex thread $l_y = 2092$. For the electron, by the substitution $n = n_e$, we have, respectively: 0.0114, 0.1014 and 6266.

Of course, the expression (15) has only qualitative character, but it can be used for the calculation of the *mass relation* of arbitrary fermions, assuming that the respective masses are proportional to their four-dimensional volumes:

$$\frac{m_{xp}}{m_{xe}} = \left(\frac{r_{xp}}{r_{xe}}\right)^4 = \left(\frac{n_e}{n_p}\right)^{14}. \tag{16}$$

For the given couple of particles, we have the relation $\left(\frac{0.5777}{0.3338}\right)^{14} = 2160$, therefore it is evident that this couple is

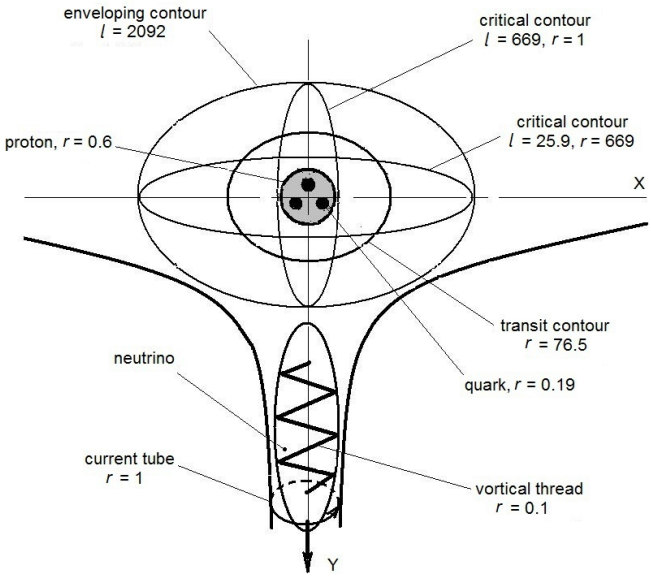

Fig. 1: The contours: scheme of the contours of the proton, and their sizes (in the units of r_e).

really *proton* and *electron*. Thus the given relation is equal to the mass of the proton expressed by the units of the electron mass. It is more evident, because the boson mass of a particle m_{yp} is almost equal to the fermion mass m_{xp} , and it is non-randomly so. Let these masses be equal, then the more precise value is the boson mass according to (12), because it does not depend on the photon number z, which is determined by means of the approximated formula. Then we can correct also the value n_e using the relation (16), and accept that its value is equal to 0.5763. It is necessary to correct the proton mass and electron charge by the cosine of the Weinberg angle. We obtain, as the final result, an almost exact value of the observed proton mass:

$$\frac{m_p}{m_e} = (an_p)^2 \cos q_{\mathrm{w}} = 1835. \qquad (17)$$

The Weinberg angle has also a geometric interpretation as $\cos q_{\mathrm{w}} = \left(\frac{1}{2\pi}\right)^{1/14}$, which confirms indirectly the correctness of the expression (16) also.

The masses of other particles expressed through the units of the electron mass are calculated: for the fermion — according to (16), assuming that n_p is the quantum number for an arbitrary fermion, and for the boson — according to (12).

The quantum numbers for the electron n_e and the proton n_p are their inner determinant parameters, emerging into the influence zone of these particles. The parameter n_e determines the length of the enveloping contour of the electron as a circle of the length $l_y = (an_e)^2 r_e$, corresponding to three inscribed circles of the diameter d_y. The vortex threads rotate inside these circles. This diameter equals the Compton wavelength, i.e. the amplitude of electron oscillations, which follows from the Dirac equation (the phenomena "*Zitterbewegung*"). Evidently, it follows from geometric reasons:

$$d_y = \frac{(an_e)^2 r_e \sin(60^\circ)}{2\pi} = 2.423 \times 10^{-12}\mathrm{m}, \qquad (18)$$

which coincides with the Compton wavelength, where "*Zitterbewegung*" is confirmed by experiments [6].

Analogously, the parameter n_p determines the length of the contour of the proton of the diameter $d_y = \frac{(an_p)^2 r_e}{\pi}$ enveloping the extremely contracted $p^+ - e^-$-contour, parameters of which reach critical values with $\nu = c$, Fig. 1. It follows in this case from (9):

$$n_p = n_{min} = \frac{c_0^{1/6}}{a} = 0.1889 \qquad (19)$$

and using (12) we find further $l_y = c_0^{1/3} r_e = 669 r_e \approx d_y$.

The excitation of elementary particles gives a set of their non-stable forms. So, fermions can have more porous and voluminous packing of boson threads, forming hyperons, etc. Apparently, some preferred configurations of packing exist, but the most compact is a proton, for which the volume and the mass of the particle are *minimal* for baryons.

5 Three generations of elementary particles

A micro-particle is considered in our model as an actual contour, therefore any contour connecting charged particles can be compared with a particle included in a greater contour; i.e. the mass of a relatively lesser contour is assumed to be the mass of a hypothetical fermion (e.g. a baryon as the analog of a proton for greater one), as shown in Fig. 2. Thus, there can exist correlated contours of the first and following orders forming several generation of elementary particles. It is clear that two quantum numbers correspond to every particle depending on its classification: 1) the particle is considered as a fermion (the analog of the proton being part of the greater contour of the following class); 2) the particle is considered as a boson (the mass of the contour of the previous class of particles). Fermion and boson masses are equal only for a proton, besides they have the same quantum number $n = 0.3338$.

The analog of a proton for the μ-contour is the mass of the standard contour $M = c_0^{2/3} m_e$. We find from (16) its quantum number $n_\mu = 0.228$. The analog of a proton for the τ-contour is the mass of the μ-contour, and n_τ is determined from extreme conditions, i.e. when $\nu \to 1$, $r \to 1$ and $n_\tau = n_{min} = 0.1889$. Then we find from (16) the mass of the μ-contour or the τ-analog of a proton which equals $6.05{\times}10^6 m_e$.

It is logical to assume that by analogy with the second class that this mass also consists of three bosons (the middle mass of every boson $2.02 \times 10^6 m_e$, i.e. 1030 GeV), which corresponds to the upper bound of the mass of the unknown Higgs boson. Thus, in reality, the *τ-contour is the largest and the last one in the row*.

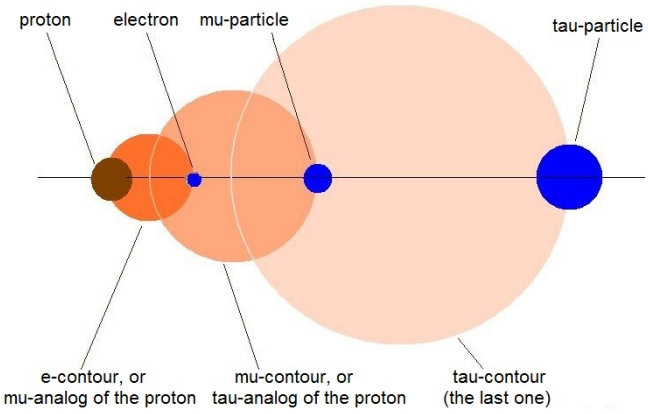

Fig. 2: Scheme of the families of the elementary particles.

Assume that the relation between the masses of baryons and their leptons in the following classes of particles, i.e. between masses of the μ-analog of the proton and a muon, and the τ-analog of a proton and a taon, is the same as for a proton-electron contour: it equals 2092. Then, using the obtained value, we can estimate the masses of other leptons. The mass of a *muon* equals $\frac{4.48\times10^5}{2092} = 214\,m_e$, whereas the mass of a *taon* equals $\frac{6.05\times10^6}{2092} = 2892\,m_e$.

The μ- and the τ-analogs of protons as baryons do not actually exist, but their boson masses $(an_\mu)^2 m_e$ and $(an_\tau)^2 me$ are close to the masses of lightest mesons — kaon and a couple of pions.

6 On the proton's structure

Continuing a hydrodynamic analogy, we assume that any charged particle included in a contour of circulation is the region where a flow of the medium intersects the boundary between X- and Y-regions: the phase transformation is realized in this boundary and the parameters attain *critical values*.

Let us now introduce the notion the density of a fermion and a boson mass: $\rho_x = \frac{m_x}{w_x}$ and $\rho_y = \frac{m_y}{w_y}$. Neglecting their exact forms, assume three-dimensional volumes of fermions and bosons in the simplest form: a fermion — as a sphere $w_x = r_x^3$, a boson thread — as a cylinder $w_y = r^2 l_y$.

Using (10), (12), (15), (16), we obtain, after transformations, their respective densities:

$$\rho_x = \frac{\rho_e n_e^{14} a^{10.5}}{n^{3.5} c_0^2}, \tag{20}$$

$$\rho_y = \frac{\rho_e (an)^8}{c_0^{4/3}}, \tag{21}$$

where ρ_e is the density of the electron for a classical volume $\frac{m_e}{r_e^3} = 4.071\times10^{13}$ kg/m^3.

Of course, the densities of fermion and boson masses by the critical section are equal. Then we find by $\rho_x = \rho_y$ the critical quantum number and the density:

$$n_k = \frac{n_e^{1.217} a^{0.217}}{c^{0.058}} = 0.480, \tag{22}$$

$$\rho_k = \frac{\rho_0 (a n_e)^{9.74}}{c_0^{1.797}} = 7.65\times10^{16}\ \text{kg/m}^3, \tag{23}$$

It is possible to ascribe these averaged parameters to some particle — a *quark*, existing only inside the phase transfer region. At once note that a quark by this interpretation is not a specific particle but only a part of the mass of a proton, obtaining critical parameters. The value of the mass can be determined from the formula (16): $m_k = 12.9\,m_e$. It is easy to calculate further other parameters of an electronic quark. It is possible to verify that the density of a quark is between the fermion and boson densities of a proton, and its size goes in to the size of a nucleon.

The critical velocity of a vortex current is determined from the known hydrodynamic equation:

$$v_k = \left(\frac{p_k}{\rho_k}\right)^{1/2}, \tag{24}$$

where in this case: v_k is the critical velocity, $\rho_k = \frac{m_k}{w_k}$ is the critical density, w_k is the volume of the quark, p_k is the pressure in the critical section, or the energy related to a corresponding volume. The energy of the standard contour equals $m_e c^2$ [3], and the critical volume is determined as $z_k w_k$, where z_k is the number of quarks.

Substituting the indicated values and expressing also v_k through (9), we find from (24) the number of quarks as

$$z_k = \frac{(a n_k)^4 m_e}{c_0^{2/3} m_k} = 3.2. \tag{25}$$

This result shows that the flow of the general contour must split into *three parts* in the region of the proton so as to satisfy the conditions of critical density and velocity. The relation of boson masses of an electron and a proton equals the same value. In fact, using (12), we obtain $\frac{M_e}{M_p} = \left(\frac{n_e}{n_p}\right)^2 = 3.0$.

It means that in order that the conditions of current continuity and charge steadiness in any section of the contour are realized, *inverse circulation currents* must arise in a neighborhood of a proton. It can be interpreted as a whole that zones with different signs of charge exist in a proton. Using a *minimal* number of *non-recurrent force current lines*, we can express schematically current lines in a proton in a unique way, as shown in the Fig. 3

As seen, there exist two critical sections with a conditionally plus current (up in the scheme) and one section with a conditionally minus current (down in the scheme), where three current lines correspond to a general current in the scheme. Therefore, the fermion surface of a proton is constructed: the regions where force lines intersect the critical sections on the line 0 – 0 inside a proton will be projected

on this surface in the form +2/3, +2/3, −1/3 from the total charge according to the number and direction of the force lines intersecting this surface.

Therefore, it is more correct to associate quarks not with critical sections but with *steady ring currents*, containing one or two closed single contours intersecting the critical section, as follows from the scheme. Therefore the masses of quarks can be determined as 1/3 or 2/3 from the summary-calculated $12.9\,m_e$, i.e. they must be equal, respectively, to $4.3\,m_e$ and $8.6\,m_e$, which coincides in fact with the masses of light quarks determined at the present time.

Parameters of quarks of μ- and τ-classes are calculated analogously by substitution of muon and taon quantum numbers in place of n_e, respectively, (Table 1).

Of course, the proposed structure of the proton is a hypothesis of the author only. Nevertheless, the definite numbers and masses of quarks here do not contradict the ones obtained by other methods earlier. Concerning the *confinement* or non-flying of quarks: this phenomenon is self-evident, because a proton in the presently given model has no combined parts, but it has only local features in its structure. The density of a proton in critical-value regions is considerable less than its fermion density: they are, probably "holes" and, of course, they cannot be distinguished as individual particles. On the other hand, only regions of critical sections, being of advanced frontal velocity pressure (dynamical pressure), are observed by experiments as *partons*.

We can deduce one more reason on behalf of the stated model: the Georgi-Glashow hypothesis of a linear potential exists. According to this hypothesis, between infinitely heavy quarks there must act, independently from a distance, a force of attraction (approximately 14 tons). Current tubes are just linear objects in our model.

Concerning the force: its limiting value can be expressed here as the sum of electrical forces' projections relative to the center of the right triangle. The forces act in pairs between critical sections carrying an elementary charge by the condition that the distance between them is minimal (according to (10), for a quark $r = 0.0239\,r_e$). Then, taking into account (3), we find $F_e = \frac{3\cos 30^\circ}{\mu_0 r^2} = 1.33 \times 10^5$ N or 13.3 tons.

7 The weak interaction and the neutrino

The stated scheme of a proton allows us to give a native illustration to the proton-neutron transitions in the weak interactions. For example, in the case of the so-called hunting phenomenon (*e-capture*) if a proton and an electron bring together up to $n \leqslant 1$) an intermediate contour is formed, connecting the particles temporarily. The boson mass of the contour, in addition, must be more than the sum of the combined boson masses of the proton and the electron, precisely:

$$M = (an)^2 m_e + m_{yp} + m_{ye}. \qquad (26)$$

Let n =1, then $M = 27108\,m_e$. Using the general relation

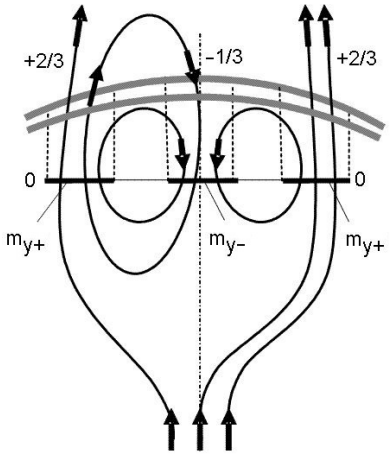

Fig. 3: Scheme of the proton: distribution of the current lines inside the proton.

between the boson mass of a contour and a lepton, we find the mass of the fermion for this contour: $m_x = \frac{27137}{2092} = 12.9\,m_e$.

This result turns out to be independent. The obtained value M coincides with a total mass of the quark and confirms that in the process of *e*-capture the temporal contour is actually formed, which is analogous to earlier considered contours (section 5) where one of the critical sections of a proton as a lepton is present.

Recall that our model contour has the properties of ideal liquid, therefore closed ring formations as parts of this continuum are absolutely inelastic and absolutely deforming at the same time. The contour connecting the particles, by their further coming together, transmits a share of energy-momentum to the inner structure of the proton, deforms and orients itself to the *Y*-region; then it is extracted as a *neutrino* which takes the momentum (spin) of the electron (Fig. 1). In other words, this process is similar to a separation of charge and spin — the phenomenon, fixed in hyperfine conductors [7], which vortex tubes are supposedly similar to.

A similar contour is formed by every act of the weak interaction, and it corresponds to the exchange of intermediate bosons. The relative slowness of this process is connected with the *time constant t*. The typical value of *t*, taking into account a spiral derived structure, determined by the time during which a circulating current passes with the velocity v through all line of the "stretched" counter (the size of *W*-, *Z*-particles). For the standard contour we have

$$t = (4.884)^2\,\frac{R_b(r_e/r)}{v} = 1.25 \times 10^{-9}\ \text{sec}, \qquad (27)$$

where 4.884 is the quantum number for a standard contour [3], r and v are determined by (9) and (10) by the given n, R_b is the Bohr first radius.

It follows from the logic of the model, that a neutrino is a particle analogous to a photon, but it spreads in the *Y*-region,

i.e. it transfers energy along the vortex tube of the contour. As known, two kinds of these particles: a neutrino — with a left spiral and an anti-neutrino — with a right spiral, corresponding to two poles of a general contour. Because a neutrino is a closed structure and exists only in the Y-region, it has no considerable charge and the mass in a fermion form (i.e. in form of the X-surface objects). Probably, a neutrino has a spiral-toroidal structure and thus it inherits or reproduces (depending on the type of the weak interaction) the structure of the vortex tube of the contour.

8 On the magnetic-gravitational interaction

Consider a possibility of existence of the mentioned closed contours at the express of an equilibrium between magnetic forces of repulsion and electrical forces of attraction. Let us formally write this equality for tubes with oppositely directed currents, neglecting the form of the contour and its possible completeness, and expressing the magnetic forces through the Ampere formula in the "Coulomb-less" form:

$$\frac{z_{g1}z_{g2}\gamma m_e^2}{r_i^2} = \frac{z_{e1}z_{e2}\,\mu_0\, m_e^2 c^2\, l_i}{2\pi r_i \times [\sec^2]}, \qquad (28)$$

where z_{g1}, z_{g2} , z_{e1}, z_{e2}, r_i, l_i are gravitational masses and charges expressed through masses and charges of an electron, a distance between current tubes and theirs length.

Substituting μ_0 from (2), we derive from (28) the characteristic size of the contour as the *mean-geometric* of two linear values:

$$l_k = \sqrt{l_i r_i} = \sqrt{\frac{z_{g1}z_{g2}}{z_{e1}z_{e2}}}\,\sqrt{2\pi\gamma\varepsilon_0} \times [\sec]. \qquad (29)$$

The parameter l_k is composite. Using the formulas (10), (12), (29), we obtain for a contour with a unit charge the values l_i and r_i , where the lengths are expressed by the units of r_e:

$$l_i = \frac{c_0^{2/3}}{l_k^2}, \qquad (30)$$

$$r_i = \frac{l_k^4}{c_0^{2/3}}. \qquad (31)$$

The contour can be placed both in the X-region (for example, a contour $p^+ - e^-$) and in the Y-region (inside an atomic nucleus). A deformation of the contour, for example, its contraction by the e-capture, takes place by means of the β-decay energy. When a proton and an electron come together, energy and fermion-mass increase of the contour occurs, while the boson mass decreases, but the impulse (charge) is conserved.

Consider some characteristic cases of a contour contraction and of a further transition of the nucleon from a proton form into a neutron one.

a) Write the equality (29) for $p^+ - e^-$-contour, where $z_{g1} = \frac{m_p}{m_e \cos q_w}$ is the relative mass of the proton, where the cosine of the Weinberg angle is considered, and $z_{g2} = 1$. In this case $l_k = 5977.4 r_e$, which corresponds to the value $\frac{R_b}{\pi}$ exactly. In other words, for the contour $p^+ - e^-$:

$$l_k = \sqrt{\frac{m_p}{m_e \cos q_w}}\,\sqrt{2\pi\gamma\varepsilon_0} \times [\sec] = \frac{R_b}{\pi}. \qquad (32)$$

The extension of the contour is now impossible, because all the mass of the proton is involved in the contour of circulation. Thus the parameters l_i and r_i are limited and equal to 0.0125 and $2.850 \times 10^9 r_e$, respectively, i.e. the length of contour tubes equals the radius of the vortex thread of an electron, approximately (section 4), and the distance between them equals the limiting size of the hydrogen atom ($390^2 R_b$). The last result is confirmed by the fact that the maximal level of energizing of hydrogen atoms in the cosmos, registered at the present time by means of radio astronomy, does not exceed $n = 301$ [8].

b) Let l_k be equal to the Compton wavelength $\lambda_k = 2\pi a r_e$. In this case, l_i and r_i are equal to 0.604 and $1.227 \times 10^6 r_e$, respectively, i.e. the length of contour tubes corresponds to the diameter of a nucleon, and the distance between them — to the size of the most atomic size ($8^2 R_b$). Thus, taking into account (30) and the expression for λ_k, we can express the proton radius in the form:

$$r_p = \frac{c_0^{2/3}}{8\pi^2 a^2} = 0.302 r_e = 851\ \text{fm}, \qquad (33)$$

which corresponds to the size of the proton, determined by the last experiments (842 fm) [9].

The equality (29) of $l_k = \lambda_k$ is observed, if the relation $\frac{z_{g1}z_{g2}}{z_{e1}z_{e2}} = 43.4$. This value can be interpreted as the product of the masses of two quarks $z_{g1}z_{g2}$, included in the contour of a nucleon or an atomic nucleus.

c) The critical contour of $\nu = c$. Here $l_i = c_0^{1/6}$, $r_i = c_0^{1/3}$, $l_k = c_0^{1/4}$ by the units of r_e. The equality (29) is fulfilled provided that the relation $\frac{z_{g1}z_{g2}}{z_{e1}z_{e2}} \approx 1$. A fraction of the impulse is transmitted to its own current (quark) contour of the proton by a further contraction of the contour, because the velocity of circulation cannot exceed the light velocity.

d) The contour is axially symmetric and is placed at the intersection of regions X and Y, which corresponds to a transient state between a proton and a neutron. It is logical to assume that the mass of the contour is situated in a critical state which is intermediate between fermion and boson forms. It is possible to suppose, according to the considered model, that a boson thread is contracted already into a contour by the length l_k, but it is not packed yet into a fermion form.

In this case $l_i = r_i = l_k = c_0^{2/9} r_e$, and the equality (29) is fulfilled provided that the relation $\frac{z_{g1}z_{g2}}{z_{e1}z_{e2}} \approx 1/3$. The limit impulse of this contour $I = \pi\varepsilon_0 l_k c \approx \frac{e_0}{3\cos q_w}$, consequently it could correspond to one excited quark contour.

The size of the magnetic-gravitational contour is correlated with the size of an atom depending on the value of gravi-

tational masses involved in its structure; the product of these masses is in the limits $(5.4\ldots43)m_e^2$ in the intervals of the main quantum numbers $n = 1,\ldots,8$. Moreover, in the region X the relation $\frac{z_{g1}z_{g2}}{z_{e1}z_{e2}}$ is proportional to the degree of deformation of the contour, i.e. to the relation of the size of the symmetric contour l_k with respect to the small axis of the deforming one; the coefficient of proportionality is *constant* and equal to $0.34 \approx 1/3$.

The contour is reoriented into the region Y by the proton-neutron transition. However in this case, in the region Y, there is a *sole solution*, which determines the critical contour by $\nu = c$. Here $l_i = c_0^{1/3}$, $r_i = 1$, $l_k = c_0^{1/6}$ by the units r_e. The contour is inserted in the current tube with the size r_e and the inverse relation is realized exactly for this contour:

$$\frac{z_{e1}z_{e2}}{z_{g1}z_{g2}} = \frac{l_k}{3r_i}. \tag{34}$$

Taking into account that for the symmetric contour $l_k = c_0^{2/9}r_e$ and using the formula (29), we have, after transformations,

$$\frac{c_0^{5/9}r_e^2}{2\pi\gamma\varepsilon_0 \times [\mathrm{sec}^2]} = 3. \tag{35}$$

The uniqueness of the solution indicates that, by the transition of a proton into a neutron, the contour is isolated into the region Y, namely with the corresponding critical parameters, and corresponds to a neutrino.

The expressions (32) and (35) are exact, as the values π and 3 reflect the geometry of the space and its three-dimensionality. It is possible to deduce from them the formula of the *gravitational constant* using the least quantity of values possessing dimensions, and to obtain also the more exact expression for the Weinberg angle. So, removing the expression for ε_0, we find from (35), after transformations,

$$\gamma = \frac{c_0^{5/9}}{6\pi\rho_e \times [\mathrm{sec}^2]} = 6.6733 \times 10^{-11}\ \mathrm{m}^3/\mathrm{sec}^2\,\mathrm{kg}, \tag{36}$$

from (32) and (35):

$$\cos q_{\mathrm{w}} = \frac{\pi^2 c_0^{5/9}}{3a^4}\frac{m_p}{m_e} = 0.8772. \tag{37}$$

Note that the expression for γ shows that the gravitational constant is an acceleration, i.e. the velocity at which the specific volume of matter in the Universe changes, in view of its expansion.

Thus, the analysis of a magnetic-gravitational equilibrium, additionally and independently, confirms the existence of three zones in the proton structure and the correspondence to the masses of light quarks of the active parts of the proton mass, included in the circulation. The conditions stated in sections 4, 6, 8 reflect different aspects of the unit structure of a proton as a whole.

9 The determination of the mass and lifetime of the neutron

A neutron is somewhat heavier than a proton, which is due to the excited condition of its own current (quark) contours. But in SM, only one quark from among the three undergoes a transformation by the proton-neutron jump. Let us assume that this quark contour obtains in addition the energy of a symmetric contour (which is considered in this situation as the own contour of a particle of the mass $\varepsilon_0 l_k$), which leads to its size extension and, respectively, to the increase of the nucleon mass.

Let us equate a total-energy differential, obtained by a nucleon, to the rotational energy of a symmetric contour except the initial rotational energy of a quark contour:

$$\frac{(m_n - m_p)c^2}{\cos q_{\mathrm{w}}} = \varepsilon_0 l_k \nu_i^2 - \frac{m_k \nu_k^2}{2}, \tag{38}$$

where ν_i is the peripheral velocity of a symmetric contour, ν_k is the peripheral velocity of a quark contour, $\frac{1}{2}m_k$ is the averaged mass of a quark contour (section 6). Starting from the masses $c_0^{2/9}m_e$ and $12.9\,m_e$, theirs quantum numbers are determined from the formula (16), the rotational velocities — from (9). Substituting these values we obtain after transformations the expression (by the unites of m_e and r_e):

$$m_n - m_p = r_{ie}\left(c_0^{2/7} - \frac{m_k^{9/7}}{2}\right)\cos q_{\mathrm{w}} = 2.53\,m_e, \tag{39}$$

where r_{ie} is the radius of the vortical thread of the electron determined from (10).

After discharge of a neutrino and deletion of three enclosed current lines, there remains one summary contour in the neutron. This contour consists of three closed force lines. Its size can maximally reach the size of a symmetric contour by means of the obtained energy. This contour forms three vortex threads by the length l_y with co-directed currents. These threads rotate relative to the longitudinal axis and have the boson masses m_y. The equality of magnetic and inertial (centrifugal) forces for vortex threads must follow from the equilibrium condition. By analogy with (28), we have:

$$\frac{m_y \nu_0^2}{r_i} = \frac{z_{e1}z_{e2}\,\mu_0 m_e^2 c^2 l_y}{2\pi r_i \times [\mathrm{sec}^2]}, \tag{40}$$

where ν_0 is the *peripheral velocity* of vortex threads. Taking into account (1), (2), (12), we find from (40):

$$\nu_0 = \frac{\sqrt{z_{e1}z_{e2}}\,r_e}{\sqrt{2\pi} \times [\mathrm{sec}]}, \tag{41}$$

where the velocity does not depend on the length of the vortex threads and the distance between them.

A spontaneous, without action of outer forces, neutron-decay is realized just owing to the own rotation of vortex

threads, causing a variation of its inner structure. In other words, the excited contour deforms and is turned into another configuration with less energy, which corresponds to the initial energy of the proton. This process must characterize itself by the *constant of time* which can be determined as a quotient from a division of the characteristic linear size in terms of the peripheral velocity ν_0. As the diameter of the tube is not determined, r_i is not determined, then it is expediently to consider the length of a symmetric transient contour πl_k as a characteristic size. In this case, the constant of time takes the form for unit charges:

$$\tau = \frac{\pi l_k}{\nu_0} = \sqrt{2\pi^3}\, c_0^{2/9} \times [\text{sec}] = 603 \text{ sec}. \qquad (42)$$

On the other hand, the constant of time can be determined also from energetic reasons, taking into account the difference of the masses of nucleons.

Let a neutron lose step-by-step the transmitted total energy $(m_n - m_p)c^2$ by portions which are proportional to the energy of an electron $m_e \nu_e^2$, where ν_e is the electron's own-contour rotational velocity during the time equal to the period of vortex threads rotation inside the current tube. Determine this characteristic time as $\frac{r_e}{\nu_0} = 2.51$ sec, then, taking into account (9), (39), (41), we obtain the period of the total dispersion of the energy by a neutron:

$$\tau = \frac{\sqrt{2\pi}\,(m_n - m_p) \times [\text{sec}]}{r_{ie} \cos q_{\text{w}}} = 628 \text{ sec}, \qquad (43)$$

The obtained constants of time correspond to the half-life of a neutron $\tau_{1/2}$. By definition, $\tau_{1/2} = \ln 2 \times \tau_n$, where τ_n is the lifetime of a neutron; its value which is obtained by one of the recent studies is 878.5 sec [10], then $\tau_{1/2} = 609$ sec.

Note that the contour of a neutrino also consists of three different vortex fields and probably undergoes periodically small variations of time when forming three configurations relative to a chosen direction. This result, probably, can explain the problem of solar neutrinos and their possible variations.

10 On the β-decay energy

The energy of the excited contour of a neutron by its decay is transmitted to an electron and an anti-neutrino extracted by this process. Taking into account (1), (9), (16), we can express, in relative units, the additional impulse $I_\beta = \pi \varepsilon_0 l_k \nu_i$ transmitted to a nucleon from the symmetric contour:

$$I_\beta = \frac{\pi c_0^{37/63}}{(a n_e)^2} = 47.92\, m_e c. \qquad (44)$$

This impulse is distributed between the contours of a neutrino and an electron with the total mass M_β, and these contours are present in any process of the weak interaction.

In addition, the mass of a neutrino contour is $c_0^{1/3} m_e$, and the mass of an electron contour also cannot be smaller than the critical value $c_0^{1/3} m_e$. The velocity of rotation of the contour by the impulse transmission will be $\frac{I_\beta}{M_\beta}$, and the β-decay energy is $E_\beta = \frac{I_\beta^2}{M_\beta}$; then its maximal value, transmitted additionally to the electron and neutron contours, and, consequently, to the electron and the neutrino, occurs at $M_\beta = 2c_0^{1/3} m_e$. Substituting the values, we obtain the boundary value of energy: $E_{\beta 0} = 1.72$ (in the units of $m_e c^2$) or 0.88 MeV.

The same result can be obtained by means of another, independent way, if we assume that the transient contour is symmetric from an energetic viewpoint (but not from a geometric one). Assume that the limit energy of the mass of a fermion contour equals the energy of rotation of this mass in a boson form, i.e. $m_x c^2 = m_y \nu^2$. Introduce also into the expression of the impulse the value of the spin of the contour: it allows us to characterize the process of the β-decay more objectively. Correct to this end the quantum number n_e for the unit relative mass (the mass of an electron) in the case of arbitrary spin. It is evident that, taking into account of (7) and (14), $n_{ei} = \frac{n_e}{k^{1/8}}$, where k is the relation between an arbitrary spin value and the spin 1/2.

Taking into account the aforesaid equalities and using the formulas (9), (12), (16), we obtain as a result the expression for the impulse of the contour which is analogous to (44), in the units of $m_e c$:

$$I_\beta = \frac{k^{7/12} c_0^{11/9}}{(a n_e)^{14/3}}. \qquad (45)$$

It gives, for $k = 2$, the value of the impulse 47.96 $m_e c$, coinciding with the result of the formula (44).

Thus we have showed that, by the transient condition of a nucleon, the symmetric contour obtains temporarily the spin 1 (joining the spin of an electron 1/2, which then takes a neutrino).

This energy of the β-decay for isotopes can be higher, and its maximal value can be determined. According to our model, a symmetric contour can transfer the limit impulse which equals one third of a charge (section 8, d). Then, taking into account (5), assuming $M_\beta = 2c_0^{1/3} m_e$ and introducing the Weinberg angle, we obtain as a result the simple expression of the β-decay limit energy in the units of $m_e c^2$:

$$E_{\beta lim} = \frac{c_0^{1/3} \cos q_{\text{w}}}{18} = 32.6 \qquad (46)$$

or 16.7 MeV.

In fact, the maximal value of the β-decay energy among different isotopes is registered for the transition $N^{12} \rightarrow C^{12}$ (16.6 MeV), which coincides with the calculated value. The value of the impulse which corresponds to the given energy follows from the formula (45) by $k = 28$. In other words, the obtained spin is proportional to the number of nucleons in the nucleus (for a nitrogen, 28/2 = 14).

In the case of e-capture only a neutrino is extracted, then $M_\beta = c_0^{1/3} m_e$, and the typical energy of the neutrino must be

1.75 MeV.

Namely, such contours, possessing symmetric forms and balanced energies (quarks), are the base of the microstructure of particles: *three* quarks for baryons and *two* — for mesons. Partially, for $k = 1$, the contour, possessing the spin 1/2, has the mass 146.4 m_e. Consequently, two such contours, depending on their properties of combination, can form mesons more easily — pions, and their excited states — , i.e. heavier micro-particles.

Thus, the results obtained in sections 8, 9, 10 in the framework of our model correspond to well-known parameters and admissible limits. Various coincidences of the calculated values with reality (e.g. the number of quarks, the sizes of the axes of characteristic contours, the size of the proton, the gravitational constant, the difference of the masses of nucleons, the half-life of the neutron, the β-decay energy) cannot have accidental nature: they prove that the structure satisfying the magnetic-gravitational equilibrium condition really exists in the micro-world.

11 The magnetic moments of the proton and the neutron

The anomalous magnetic moment of the proton μ_p in the given model can be calculated as follows. The value μ_p depends on the boson configuration of a proton and is determined relative to the Y-axis where μ_p is the product (charge×velocity ×path). We thus have, for a vortex thread, a peripheral velocity ν and a circumference πr. Substituting ν and r from (9) and (10), we obtain as a result:

$$\mu = \frac{\pi c_0 c e_0 r_e}{(a n_p)^6} = 1.393 \times 10^{-26}\ \text{am}^2, \qquad (47)$$

which differs insignificantly from the experimental value.

The magnetic moment of the neutron equals two thirds of the proton's magnetic moment, i.e. proportional to the reduction of the number of intersections of the critical sections by current lines for a proton (six instead of nine, existing in a proton, see Fig. 3). Naturally, the sign of the moment changes in addition, because three positive enclosed currents are removed.

The calculated values of some parameters with respect to reality, or obtained earlier by other methods, are given in Table 1.

12 Conclusion

This work is an attempt to add a physically descriptive interpretation to some phenomena of the micro-world using both topological images of Wheeler's geometrodynamic idea and further macro-world analogies. This approach allows us to include into consideration inertial and gravitational forces.

This model has a logical demonstrative character and determines a scheme for the construction of a possible theory adding up the Standard Model (SM) of particle physics. The new theory must use such mathematical apparatus, in the framework of which vortex structures and their interactions

Particles*	Calculated data	Actual data
Family 1		
Proton	1835	1836
Electron	1	1
Quark	12.9 (4.3; 8.6)	3.93; 9.37
Family 2		
μ-analog of the proton, $m_{x\mu}$	4.48×10^5	4.92×10^5 †
Muon	214	206.8
μ-quark	8780	3230; 276
Family 3		
τ-analog of the proton, $m_{x\tau}$	6.31×10^6	?
τ-lepton	2892	3480
τ-quark	233000	348000; 8260
Other parameters		
Charge of the electron, kg m/s	1.603×10^{-19}	1.602×10^{-19}
Number of the quarks (on the basis of the phase transit condition)	3.2	3
Number of the quarks (on the basis of the magnetic-gravitational equilibrium)	3	3
Interacting force among the quarks, N	1.33×10^5	1.4×10^5
Weinberg angle	28.2°	28.7°
Compton wavelength, m	2.423×10^{-12}	2.426×10^{-12}
The gravitational constant, m^3/kg sec^2	6.673×10^{-11}	6.673×10^{-11}
Radius of the proton, fm	851	842
Difference between the mass of the proton and the mass of the neutron, m_e	2.53	2.53
Semi-decay of the neutron (kinematic estimation), sec	603	609
Semi-decay of the neutron (energetic estimation), sec	628	609
Ultimate high energy of the β-decay, MeV	16.7	16.6
Magnetic moment of the proton, am^2	1.39×10^{-26}	1.41×10^{-26}
Magnetic moment of the neutron, am^2	-0.92×10^{-26}	-0.97×10^{-26}

*Masses of the particles are given in the mass of the electron.
†The summary mass of the W, Z-bosons.

Table 1: The actual numerical parameters, and those calculated according to the model suggested by the author.

could be described. As often mentioned by the author, the contours will be mapped out by singular configurations of force lines of some field.

Nevertheless, the present model gives a correct interpretation even in the initial, elementary form where only laws of conservation are used. It explains some phenomena misunderstood in the framework of SM and allows us to obtain qualitative and, sometimes, quantitative results by calculation of important parameters of the micro-world.

In part, this model predicts that it is impossible by means of experiments conducted at the BAC to obtain new particles — dubbed "super-partners": rather, it is necessary to seek new massive vector bosons in the region of energies approximating 1000 GeV.

Submitted on October 13, 2011 / Accepted on January 31, 2012

References

1. Yershov V. N. Fermions as topological objects. *Progress in Physics*, 2006, v. 1, 19–26.
2. Dewitt B. S. Quantum gravity. *Scientific American*, December 1983, v. 249, 112–129.
3. Belyakov A.V. Charge of the electron, and the constants of radiation according to J. A. Wheeler's Geometrodynamic Model. *Progress in Physics*, 2010, v. 4, 90–94.
4. Daywitt W.C. The Relativity Principle: space and time and the Plank vacuum. *Progress in Physics*, 2010, v. 4, 34–35.
5. *New Scientist*, 1998, no. 2119, 36.
6. Gerritsma R. et al. Quantum simulation of the Dirac equation. *Nature*, 2010, v. 463, 68–71.
7. Jompol Y., Ford C. J. B., Griffiths J. P., Farrer I., Jones G. A. C., Anderson D., Ritchie D. A., Silk T. W., and Schofield A. J. Probing spin-charge separation in a Tomonaga-Luttinger liquid. *Science*, 31 July 2009, v. 325, no. 5940, 597–601.
8. Pedlar A. et al. *Mon. Not. R. Astron. Soc.*, 1978, v.182, 473.
9. Pohl R. et al. The size of the proton. *Nature*, 08 July 2010, v. 466, 213–216.
10. Serebrow A. P. The Measurement of the neutron lifetime with the use of gravitational traps of ultra-could neutrons. *Uspekhi-Physics*, 2005, v. 175, no. 9, 905–923.

Quantum Uncertainty and Relativity

Sebastiano Tosto
Italy. Email: stosto@inwind.it

The major challenge of modern physics is to merge relativistic and quantum theories into a unique conceptual frame able to combine the basic statements of the former with the quantization, the non-locality and non-reality of the latter. A previous paper has shown that the statistical formulation of the space-time uncertainty allows to describe the quantum systems in agreement with these requirements of the quantum world. The present paper aims to extend the same theoretical model and approach also to the special and general relativity.

1 Introduction

Merging quantum mechanics and general relativity is surely the most challenging task of the modern physics. Since their early formulation these theories appeared intrinsically dissimilar, i.e. conceived for different purposes, rooted on a different conceptual background and based on a different mathematical formalism. It is necessary to clarify preliminarily what such a merging could actually mean.

A first attempt was carried out by Einstein himself in the famous EPR paper [1] aimed to bridge quantum behavior and relativistic constraints; he assumed the existence of hypothetical "hidden variables" that should overcome the asserted incompleteness of the quantum mechanics and emphasize the sought compatibility between the theories. Unfortunately this attempt was frustrated by successive experimental data excluding the existence of hidden variables. The subsequent development of both theories seemed to amplify further their initial dissimilarity; consider for instance the emergence of weird concepts like non-locality and non-reality of quantum mechanics, which make still more compelling the search of an unified view.

The most evident prerequisite of a unified model is the quantization of physical observables; being however the general relativity essentially a 4D classical theory in a curved non-Euclidean space-time, the sought model requires new hypotheses to introduce the quantization. A vast body of literature exists today on this topic; starting from these hypotheses several theories have been formulated in recent years, like the string theory [2,3] and loop quantum gravity [4], from which were further formulated the M-theory [5] and the supersimmetric theories [6]. The new way to represent the particles as vibrating strings and multi-dimensional branes is attracting but, even though consistent with the quantization, still under test. Moreover the quantization of the gravity field is not the only problem; additional features of the quantum world, the non-locality and non-reality, appear even more challenging as they make its rationale dissimilar from that of any other physical theory. The quantum mechanics postulates a set of mathematical rules based on the existence of a state vector $|\psi\rangle$ describing the quantum system in Hilbert space and a Hermitian operator corresponding to a measure, whose outcomes are the eigenvalues that represent the observables; the evolution of a system is represented by an evolution operator $T(t)$ such that $|\psi(t)\rangle = T(t)\,|\psi(0)\rangle$ operating on the state vector at the initial time. To these rules overlap also the exclusion and indistinguishability principles to formulate correctly the state vectors. The relativity rests on physical intuitions about the behavior of masses in a gravity field and in accelerated systems; it postulates the equivalence between gravitational and inertial mass and aims to build a covariant model of physical laws under transformation between inertial and non-inertial reference systems.

Apart from the apparent dissimilarity of their basic assumptions, a sort of conceptual asymmetry surely characterizes the quantum and relativistic theories; on the one side abstract mathematical rules, on the other side intuitive statements on the behavior of bodies in a gravity field. If the unification of these theories concerns first of all their basic principles, the task of introducing into a unified model even the concepts of non-locality and non-reality appears seemingly insurmountable. Eventually, a further concern involves the choice of the mathematical formalism appropriate to the unified approach. In general the mathematical formulation of any theoretical model is consequence of its basic assumptions. The tensor calculus is required to introduce covariant relativistic formulae in curvilinear reference systems; is however its deterministic character really suitable to formulate a non-real and non-local theoretical model? This last remark is suggested by previous papers that have already touched on this subject.

Early results showed that a theoretical approach based on the quantum uncertainty only, introduced as a unique assumption to calculate the electron energy levels of many-electron atoms/ions and diatomic molecules [7,8], could be subsequently extended to the special relativity too [9] while being also consistent with the concepts of non-localism and non-realism of quantum mechanics. Despite this encouraging background, however, so far the implications of the concepts introduced in the quoted papers have not been fully investigated and systematically exploited. In these early papers, the connection between quantum approach and special relativity

was preliminarily acknowledged through gradual results progressively obtained, concerning however other less ambitious tasks; for instance, to assess the chance of superluminal speed of neutrinos [9]. The decisive strategy to this purpose was to regard the concept of uncertainty as a fundamental law of nature and not as a mere by-product of the commutation rules of operators. The statistical formulation of the quantum uncertainty has been proven effective on the one side to explain and account for all of the aforesaid features of the quantum world, i.e. quantization and non-reality and non-locality, and on the other side to obtain as corollaries the basic statements of special relativity too along with the invariant interval and Lorentz transformations. So it seemed sensible to exploit more profoundly these early achievements before proceeding towards a more advanced generalization including the general relativity too.

The present paper aims to collect together and push forward these preliminary results through further considerations having more general and systematic character; the approach proposed here is purposely focused towards a unifying task able to combine together quantum and relativistic requirements within the same conceptual frame. For this reason the present paper heavily rests on previous results introduced in the quoted references. While referring to the respective papers when necessary, some selected considerations very short and very important are again reported here for clarity of exposition and to make the present paper as self-contained as possible.

The paper consists of three parts. The first part, exposed in section 2, merely summarizes some concepts already published and some selected results previously achieved; these preliminary ideas are however enriched and merged together with new suggestions. The second part, section 3, stimulates further considerations approaching the intermediate target of merging together basic concepts of quantum mechanics and special relativity. The third part, section 4, aims to show that effectively even the most significant Einstein results of general relativity are compliant with the quantum approach here proposed.

The foremost concern constantly in mind is how to transfer into the beautiful self-consistency of relativity the alien concepts of quantization, non-locality and non-reality of the quantum world.

2 Preliminary considerations

The present section collects some ideas and results reported in previous papers concerning the statistical formulation of quantum uncertainty. Two equations sharing a common number of allowed states

$$\Delta x \Delta p_x = n\hbar = \Delta\varepsilon\Delta t \qquad (2,1)$$

are the only basic assumption of the present model. No hypothesis is made about size and analytical form of these ranges, which are by definition arbitrary. These equations disregard the local values of the dynamical variables, considered indeed random, unknown and unpredictable within their uncertainty ranges and thus of no physical interest. The concept of uncertainty requires the particle delocalized everywhere in its space range Δx without any further detail about its actual motion; in practice the theoretical approach describes a system of quantum particles through their uncertainty ranges only exploiting the following positions

$$p_x \to \Delta p_x, \qquad x \to \Delta x, \qquad t \to \Delta t, \qquad \epsilon \to \Delta\epsilon. \qquad (2,2)$$

The first relevant consequence is that the calculations based on these ranges only waive in fact a specific kind of reference system. Consider for instance $\Delta x = x - x_o$: the lower boundary x_o describes the position of Δx with respect to the origin O of an arbitrary reference system R, the upper boundary x its size. So, owing to the lack of hypotheses or constraints on x_o and x, the considerations inferred through the ranges (2,2) hold in any R whatever it might be, Cartesian or curvilinear or else; also, being both boundary coordinates x_o and x arbitrary and unknowable, their role as concerns size and location of Δx in R could be identically exchanged. Hold also for the other ranges, e.g. for t_o and t of $\Delta t = t - t_o$, the same considerations introduced for x_o and x, in particular the arbitrariness of the time coordinates in the reference system where is defined the time length Δt.

If in R both boundaries are functions of time, as it is to be reasonably expected according to eqs. (2,1), then not only the range size is itself a function of time dependent on the relative signs and values of $\dot{x}$ and $\dot{x}_o$, but also the results hold for reference systems in reciprocal motion; indeed a reference system R_o solidal with x_o moves in R at rate $\dot{x}_o$ and possible acceleration $\ddot{x}_o$. Nothing indeed compels to regard $\dot{x}_o$ as a constant, i.e. R_o could be non-inertial or inertial depending on whether the concerned physical system admits or not accelerations. As any outcome inferred through the positions (2,2) holds by definition in an arbitrary reference system R or R_o, it is clear since now the importance of this conclusion in relativity, which postulates covariant general laws of nature. Introducing local coordinates requires searching a covariant form for the physical laws thereafter inferred; once introducing arbitrary uncertainty ranges that systematically replace the local coordinates "a priori", i.e. conceptually and not as a sort of approximation, hold instead different considerations.

This topic will be concerned in the next subsection 4.1. Here we emphasize some consequences of the positions (2,2): (i) to waive a particular reference system, (ii) to fulfill the Heisenberg principle, (iii) to introduce the quantization through the arbitrary number n of allowed states, (iv) to overcome the determinism of classical physics, (v) to fulfill the requirements of non-locality and non-reality [9]. Hence appears sensible to think that an approach based uniquely on eqs. (2,1) through the quantum positions (2,2) is in principle suitable to

fulfil the requirements of special and general relativity too, far beyond the conceptual horizon of the quantum problems to which the quoted papers were early addressed. While being well known that the concept of uncertainty is a corollary of the operator formalism of wave mechanics, the reverse path is also possible: the operators of wave mechanics can be inferred from eqs. (2,1) [9]. The operator formalism is obtained introducing the probability $\Pi_x = \delta x/\Delta x$ for a free particle to be found in any sub-range δx included in the whole Δx during a given time range δt; it is only required that the sub-range be subjected to the same conditions of arbitrariness and uncertainty of Δx. Analogous considerations hold in defining the probability $\Pi_t = \delta t/\Delta t$ for the particle to be confined during a time sub-range δt within a given δx, while Δt is the time range for the particle to be within Δx. These probabilities allow to infer the operators

$$p_x \to \pm\frac{\hbar}{i}\frac{\partial}{\partial x}, \qquad \epsilon \to \pm\frac{\hbar}{i}\frac{\partial}{\partial t}. \tag{2,3}$$

As intuitively expected, the space and time sub-ranges δx and δt describe a wave packet having finite length and momentum that propagates through Δx during Δt. The positions (2,2), directly related to eqs. (2,1), and the non-relativistic positions (2,3), inferred from eqs. (2,1), compare the two possible ways of introducing the quantum formalism. This result is important for two reasons: (i) it justifies why eqs. (2,1) lead to correct quantum results through the positions (2,2); (ii) the connection and consistency of the positions (2,2) with the familiar wave formalism (2,3) justifies the starting point of the present model, eqs. (2,1) only, as an admissible option rather than as an unfamiliar basic assumption to be accepted itself. Although both eqs. (2,1) and the wave equations introduce the delocalization of a particle in a given region of space, in fact the degree of physical information inherent the respective approaches is basically different: despite their conceptual link, eqs. (2,1) entail a degree of information lower than that of the wave formalism; hence they have expectedly a greater generality.

Consider a free particle. Eqs. (2,1) discard any information about the particle and in fact concern the delocalization ranges of its conjugate dynamical variables only; accordingly they merely acknowledge its spreading throughout the size of Δx during the time uncertainty range Δt. Being also this latter arbitrary, the information provided by eqs. (2,1) concerns the number of states n allowed to the particle and its average velocity component $v_x = \Delta x/\Delta t$ only. The wave mechanics concerns and describes instead explicitly the particle, which is regarded as a wave packet travelling throughout Δx; as it is known, this leads to the concept of probability density for the particle to be localized somewhere within Δx at any time. The probabilistic point of view of the wave mechanics, consequence of Π_x and Π_t, is replaced in eqs. (2,1) by the more agnostic total lack of information about local position and motion of the particle; this minimum information, consistent with the number of allowed states only, corresponds in fact to the maximum generality possible in describing the physical properties of the particle. The fact that according to eqs. (2,1) the particle could likewise be anywhere in all available delocalization range, agrees with the Aharonov-Bohm effect: the particle is anyhow affected by the electromagnetic field even in a region of zero field, because the probabilistic concept of "here and then there" is replaced by that of "anywhere" once regarding the region of the concerned field as a whole 3D uncertainty volume whose single sub-regions cannot be discerned separately. These conclusions also explain the so called "EPR paradox": the idea of spooky action at a distance is replaced by that of action at a spooky distance [9], because the positions (2,2) exclude the concept of local positions and thus that of a specific distance physically distinguishable from any other distance. Just because ignoring wholly and in principle the particle and any detail of its dynamics, while concerning instead uncertainty ranges only where *any* particle could be found, the indistinguishability of identical particles is already inherent the eqs. (2,1); instead it must be postulated in the standard quantum wave theory. The number n of allowed states is the only way to describe the physical properties of the particle; this explains why n plays in the formulae inferred from eqs. (2,1) the same role of the quantum numbers in the eigenvalues calculated solving the appropriate wave equations [7]. An evidence of this statement is shortly sketched for clarity in section 3.

The generality of eqs. (2,1) has relevant consequences: the approach based on these equations has been extended to the special relativity; instead the momentum and energy operators of eqs. (2,3) have limited worth being inherently non-relativistic. In effect the probabilities Π_x and Π_t have been inferred considering separately time and space; it was already emphasized in [9] that Π_x and Π_t should be merged appropriately into a unique space-time probability $\Pi(x, t)$. The necessity of a combined space-time reference system will be discussed in the next section 3. This fact suggests that a general description of the system is obtainable exploiting directly eqs. (2,1), which by their own definition introduce concurrently both space and time coordinates into the formulation of quantum problems; in short, the present paper upgrades the early concept of uncertainty to that of space-time uncertainty in the way highlighted below.

It has been shown that eqs. (2,1) also entail inherently the concepts of non-locality and non-reality of the quantum world: the observable outcome of a measurement process is actually the result of the interaction between test particle and observer, as a function of which early unrelated space and momentum ranges of the former collapse into smaller ranges actually related to n according to eqs. (2,1); accordingly, it follows that the quantized eigenvalues are compliant with the non-locality and non-reality of quantum mechanics. This collapse is intuitively justified here noting that any measurement process aims to get information about physical observables;

without shrinking the initial unrelated ranges, thus reducing their degree of initial uncertainty, the concept of measurement would be itself an oxymoron. These results prospect therefore a positive expectation of relativistic generalization for the positions (2,2). Due to the subtle character of the connection between quantum and relativistic points of view, the present paper examines more closely in the next section the first consequences of the considerations just carried out, previously obtained in the quoted papers: the first goal to show the successful connection of eqs. (2,1) with the special relativity, is to infer the invariant interval and the Lorentz transformation.

3 Uncertainty and special relativity

The special relativity exploits 4-vectors and 4-tensors that consist of a set of dynamical variables fulfilling well defined transformation rules from one inertial reference system to another. For instance, the components u_i of four velocity are defined by the 4-vector dx_i as $u_i = dx_i(cdt)^{-1}(1-(v/c)^2)^{-1/2}$, being v the ordinary 3D space velocity; the angular momentum is defined by the anti-symmetric 4-tensor $\mathbf{M}^{ik} = \sum(x^i p^k - x^k p^i)$, whose spatial components coincide with that of the vector $\mathbf{M} = \mathbf{r} \times \mathbf{p}$.

Despite the wealth of information available from such definitions, however, the central task always prominent in the present paper concerns their link to the concepts of quantization, non-locality and non-reality that inevitably qualify and testify the sought unification: if the final target is to merge quantum theory and relativity, seems ineffective to proceed on without a systematic check step after step on the compliance of such 4-vectors and tensors with the quantum world.

To explain in general the appropriate reasoning, compare the expectations available via tensor calculus and that available via the positions (2,2): having shown previously that eqs. (2,1) are compliant with the non-reality and non-locality, this means verifying the consistency of the former definitions of angular momentum or velocity with the concept of uncertainty. Since both of them necessarily exploit local coordinates, then, regardless of the specific physical problem to be solved, the previous definitions are in fact useless in the present model; the local coordinates are considered here worthless "a priori" in determining the properties of physical systems and thus disregarded.

Merging quantum and relativistic points of view compels instead to infer the angular momentum likewise as shown in [7], i.e. through its own physical definition via the positions (2,2) to exploit eqs. (2,1). For clarity this topic is sketched in the next sub-sections 3.4 to 3.7 aimed to show that indeed the well known relativistic expressions of momentum, energy and angular momentum of a free particle are inferred via trivial algebraic manipulations of eqs. (2,1) without exploiting the aforesaid standard definitions through local 4-coordinates.

Let us show now that the basic statements of special relativity are corollaries of eqs. (2,1) without any hypothesis on the uncertainty ranges. First, the previous section has shown that once accepting the positions (2,2) all inertial reference systems are indistinguishable because of the total arbitrariness of their boundary coordinates; if in particular both x_o and t_o are defined with respect to the origin of an inertial space-time reference system R, then the arbitrariness of the former require that of the latter. So in any approach based on eqs (2,1) only, all R are necessarily equivalent in describing the eigenvalues, i.e. the observables of physical quantities. Second, it is immediate to realize that the average velocity $v_x = \Delta x/\Delta t$ previously introduced must be upper bounded. Consider a free particle in finite sized Δx and Δp_x, thus with finite n; if $v_x \to \infty$ then $\Delta t \to 0$ would require $\Delta\varepsilon \to \infty$, which in turn would be consistent with $\varepsilon \to \infty$ as well. Yet this is impossible, because otherwise a free particle with finite local momentum p_x could have in principle an infinite energy ε; hence, being by definition an allowed value of any physical quantity effectively liable to occur, the value of v_x must be upper bound. Third, this upper value allowed to v_x, whatever its specific value might be, must be invariant in any inertial reference system. Indeed v_x is defined in its own R without contradicting the indistinguishability of all reference systems because its value is arbitrary like that of both Δx and Δt; hence the lack of a definite value of v_x lets R indistinguishable with respect to other inertial reference systems R' whose v'_x is arbitrary as well. If however v_x takes a specific value, called c from now on, then this latter must be equal in any R otherwise some particular $R^{(c)}$ could be distinguishable among any other R', for instance because of the different rate with which a luminous signal propagates in either of them. Thus: finite and invariant value of c, arbitrariness of the boundary coordinates of Δx and equivalence of all reference systems in describing the physical systems are strictly linked. One easily recognizes in these short remarks, straightforward corollaries of eqs (2,1), the basic statements of the special relativity.

This result legitimates thus the attempt to extend the outcomes of the non-relativistic approach of the early papers [7,8] to the special relativity. Before exemplifying some specific topics in the following subsections, it is useful to note that eqs. (2,1) can be read in several ways depending on how are handled the ranges in a given R.

The first example is provided by the ratio $\Delta x/\Delta t$: if the particle is regarded as a corpuscle of mass m delocalized in Δx, thus randomly moving throughout this range, then $\Delta x/\Delta t$ is its average velocity component v_x during Δt, whatever the local features of actual motion within Δx might be. Interesting results can be inferred hereafter in a straightforward way. It is possible to define $\Delta p_x/\Delta t$ equal to $\Delta\varepsilon/\Delta x$ for any n, thus obtaining the concept of average force field component $F_x = \Delta p_x/\Delta t$ throughout Δx, or the related average power $\Delta\varepsilon/\Delta t = F_x v_x$ and so on. This is not mere dimensional exercise; these definitions hold without specifying a particular reference system and will be exploited in the following to check their ability to get both quantum and relativistic results.

In the next subsection will be examined in particular the ratio $\Delta p_x/\Delta x$ to introduce the curvature of the space-time simply via uncertainty ranges, i.e. in the frame of the uncertainty only. In these expressions, the ranges play the same role of the differentials in the respective classical definitions. This suggests how to regard the concept of derivative entirely in the frame of eqs. (2,1) only, i.e. as ratio of uncertainty ranges. The fact that the size of the ranges is arbitrary suggests the chance of thinking, for mere computational purposes, their limit sizes so small to exploit the previous definitions through the differential formalism; for instance it is possible to imagine a particle delocalized in a very small, but conceptually not vanishing, range dx without contradicting any concept introduced in the positions (2,2), because remains valid in principle the statement $dx\Delta p_x = n\hbar$ despite the random values of x between x_o and $x_o + dx$ tend to the classical local value x_o. It is also possible to define very low values of v_x, i.e. $dx/\Delta t \ll c$, because Δx and Δt are independent ranges and so on. Furthermore, hypothesizing $\hbar$ so small that all ranges can be even treated as differentials, let us try to regard and handle the ranges of eqs. (2,1) as if in the limit case $n = 1$ they would read $(dx)(dp_x) = \hbar = (dt)(d\varepsilon)$. This means that, for mere computational purposes, the case $n = 1$ is regarded as a boundary condition to be fulfilled when calculating the sought physical property.

To check the validity of this point through an example of calculation involving v_x, rewrite eqs. (2,1) in the forms $\Delta p_x/\Delta t = \Delta\varepsilon/\Delta x$ and $\Delta\varepsilon = \Delta p_x \Delta x/\Delta t$ that however will be now handled likewise as if $dp_x/dt = F_x = d\varepsilon/dx$ and $d\varepsilon = v_x dp_x$ to assess the results hereafter obtainable. In agreement with these computational notations, which however do not mean at all regarding the formal position $\Delta x/\Delta t \to dx/dt$ as a local limit, let us consider a free particle and write

$$\varepsilon = \int v'_x (dp_x/dv'_x) dv'_x. \tag{3,1}$$

Although these positions are here introduced for calculation purposes only, since actually the uncertainty ranges are by definition incompatible with the concept of differential limit size tends to zero, nevertheless it is easy to check their validity recalling that in a previous paper [9] simple considerations based on eqs. (2,1) only allowed to infer $p_x = \varepsilon v_x/c^2$; this equation is so important that its further demonstration based on a different reasoning is also provided below in subsection 3.4. Replacing in eq (3,1) and integrating yields $\varepsilon = c^{-2} \int v'_x [d(\varepsilon v'_x)/dv'_x] dv'_x$, easily solved in closed form; the solution $\varepsilon = const\left(1 - (v_x/c)^2\right)^{-1/2}$ yields by consequence also $p_x = v_x c^{-2} const\left(1 - (v_x/c)^2\right)^{-1/2}$. If $v_x \to 0$ then $p_x \to 0$; yet nothing compels also the vanishing of ε. Calculating thus the limit p_x/v_x for $v_x \to 0$ and calling m this finite limit,

$$\lim_{v_x \to 0} \frac{p_x}{v_x} = m, \tag{3,2}$$

one infers the integration constant $const = \pm mc^2$; follow immediately the well known expressions

$$\begin{aligned} p_x &= \pm m v_x \left(1 - (v_x/c)^2\right)^{-1/2}, \\ \varepsilon &= \pm mc^2 \left(1 - (v_x/c)^2\right)^{-1/2}. \end{aligned} \tag{3,3}$$

The double sign corresponds in the former case to that of either velocity component, in the latter case to the existence of antimatter. Moreover exploit also $\Delta p_x/\Delta t - \Delta\varepsilon/\Delta x = 0$; regarding again this equation in its computational differential form $dp_x/dt - d\varepsilon/dx = 0$ and solving it with respect to v_x, as if the ranges would really be differentials, one finds of course $v_x = -\Delta x/\Delta t$. These results are important: handling the ranges as differentials entails just the well known relativistic results, which appear however to be limit cases i.e. boundary conditions of the respective definitions via uncertainty ranges; this confirms that the intervals appearing in the invariant interval and in the Lorentz transformation of length and time must be actually regarded as uncertainty ranges, as pointed out in [9], so that also the transformation formulae get full quantum meaning. This holds provided that the ranges related to $\hbar$ be really so small with respect to distances and times of interest to justify the integral calculus; this is certainly true in typical relativistic problems that usually concern massive bodies or cosmological distances and times.

So far the particle has been regarded as a corpuscle characterized by a mass m traveling throughout Δx during the time range Δt. According to the positions (2,3) and owing to the results [9], however, the particle can be identically described as a wave propagating throughout the same space range during the same time range; also to this purpose are enough eqs. (2,1), the basic assumptions of the wave formalism are unnecessary.

Let us regard Δx as the space range corresponding to one wavelength and the related Δt as a reciprocal frequency $\omega = \Delta t^{-1}$; so one finds $\Delta\varepsilon = n\hbar\omega$ with $\omega = 2\pi\nu$, in which case $\Delta x/\Delta t = \omega\lambda = v$ as well. In principle one expects from this result that in general an average velocity v_1 corresponds to the frequency ω_1, thus v_2 to ω_2 and so on. Suppose that, for fixed Δx, a time range $\Delta t'$ and thus a frequency ω' exist such that the right hand side turns into a unique constant velocity, whose physical meaning will appear soon; then, using again the differential formalism, $d(\lambda^{-1}) = -\lambda^{-2} d\lambda$ and $\lambda d\omega' + \omega' d\lambda = 0$ combined into $\lambda(d\omega' - \lambda\omega' d(\lambda^{-1})) = 0$ yield $v'/2\pi = d\omega'/dk$ where $k = 2\pi/\lambda$. Being v' arbitrary like Δx, including the trivial factor 2π in $v'' = v'/2\pi$ yields $v'' = d\omega'/dk$. So are defined the phase and group velocities v and v'' of a wave, which of course coincide if v does not depend on ω; this is possible because Δx and Δt are independent ranges that can fulfil or not this last particular case. Moreover eqs. (2,1) also yield immediately $\Delta\varepsilon/\Delta p = d\nu/d(\lambda^{-1}) = v$. Eventually, dividing both sides of $\Delta x \Delta p_x = n\hbar$ by Δt yields

$F\Delta x = n\hbar\omega$; since $dF/d\nu$ has physical dimension of momentum, being all range sizes arbitrary the last equation reads in general $p = h/\lambda$. These reasonable results are distinctive features of quantum mechanics, here found as corollaries by trivial manipulations of eqs. (2,1). If both corpuscle and wave formalisms are obtained from a unique starting point, eqs. (2,1), then one must accept the corpuscle/wave dual behavior of particles, as already inferred in [9]. This justifies why these equations have been successfully exploited in the early papers [7,8] to describe the quantum systems.

After having checked the compliance of eqs. (2,1) with the fundamental principles of both quantum mechanics and special relativity, we are now justified to proceed further towards the connection between the theories. Eqs. (2,1) allow describing various properties of quantum systems, e.g. in the frame of space/time uncertainty or energy/momentum uncertainty, as better specified in the next subsection. Note that the invariant interval, inferred itself from eqs. (2,1) only, is compliant with the non-locality and non-reality simply regarding the space and time intervals as uncertainty ranges; by consequence merging quantum mechanics and special relativity simply requires abandoning the deterministic meaning of intervals defined by local coordinates, which have classical character and thus are exactly known in principle. Indeed we show below that the invariant interval consists of ranges having fully quantum meaning of space-time uncertainty. In the frame of eqs. (2,1) only, the concept of time derivative necessarily involves the time uncertainty range; an example is $\Delta x/\Delta t$ previously identified with the velocity v_x. This latter, even though handled as dx/dt for computational purposes only, still keeps however its physical meaning of average velocity.

These considerations hold in the reference system R where are defined eqs. (2,1) and suggest a remark on the algebraic formalism; once trusting on eqs. (2,1) only, the concept of derivative is replaced by that of ratio between uncertainty ranges. These latter indeed represent the chance of variability of local quantities; so the derivative takes here the meaning of correlation between these allowed chances. Of course being the ranges arbitrary and unknown, this chance is extended also to the usual computational concept of derivative, as shown before. Once having introduced through the uncertainty the requirements of quantum non-locality and non-reality into the relativistic formulae, a problem seems arising at this point, i.e. that of the covariancy.

This point will be concerned in the next section 4, aimed to discuss the transformations between inertial and non-inertial reference systems. For clarity of exposition, however, it is better to continue the present introductory discussion trusting to the results so far exposed; it is enough to anticipate here that the arbitrariness of the quantum range boundaries, and thus that of the related reference systems as well, is the key topic to merge the requirements of uncertainty and covariancy.

3.1 The space-time uncertainty

This section aims to show that the concept of space-time is straightforward corollary of the space/momentum and time/energy uncertainties. Eqs. (2,1) represent the general way of correlating the concepts of space, momentum, time and energy by linking their uncertainties through the number n of allowed states; just their merging defines indeed the eigenvalues of any physical observable. On the one side, therefore, the necessity of considering concurrently both time and space coordinates with analogous physical meaning appears because of the correlation of their uncertainties; for instance the particular link underlying time and space ranges through c allows to infer the invariant interval and the relativistic expressions of momentum and energy. On the other side the concept of quantization appears strictly related to that of space-time, since the concurrence of both Δx and Δt that defines n also introduces in fact a unique space-time uncertainty. These elementary considerations highlight the common root between relativity and quantum theory, which also accounts for the non-locality and non-reality of the latter according to the conclusions emphasized in [9].

Eqs. (2,1) consist of two equations that link four ranges; for any n, two of them play the role of independent variables and determine a constrain for the other two, regarded therefore as dependent variables. In principle this means that two independent ranges introduce eqs. (2,1) via n. As Δp_x and $\Delta\varepsilon$ include local values of physical observables while Δx and Δt include local values of dynamical variables, it is reasonable to regard as a first instance just these latter as arbitrary independent variables to which are related momentum and energy as dependent variables for any n; however any other choice of independent variables would be in principle identically admissible.

For instance, let us concern $\Delta\varepsilon\Delta x/(v_x/c) = n\hbar c$ considering fixed the energy and coordinate ranges. Two limits of this equation are particularly interesting: (i) $v_x/c \to 0$, which requires in turn $n \to \infty$, and (ii) $v_x \lesssim c$, which requires $\Delta x \lesssim n\hbar c/\Delta\varepsilon$ for any given n. Consider the former limit rewriting identically $(\Delta p_x/v_x)v_x\Delta x = n\hbar$, which reads $v_x\Delta x\Delta m = n\hbar$ according to eq (3,2); since for a free particle v_x is a constant, then $\Delta(mv_x) = \Delta p_x$ i.e. $p_x \approx mv_x$. Guess the related classical energy regarding again $\Delta\varepsilon/\Delta p_x = v_x$ as $d\varepsilon/dp_x = v_x$, whence $d\varepsilon = v_x m dv_x$ i.e. $\varepsilon = mv_x^2/2 + const$. As expected, these expressions of energy and momentum result to be just the non-relativistic limits of eqs. (3,3) for $v_x \ll c$. This is because we have considered here the space coordinate separately from the time coordinate: despite the time range has been somehow introduced into the previous reasoning through the definition of v_x, yet it occurred in the way typical of the Newtonian mechanics, i.e. regarding the time as an entity separated from the space coordinate, and not through the link between Δp_x and $\Delta\varepsilon$ provided by n.

We also know that the classical physics corresponds to

the limit $n \to \infty$ [9]; thus eqs. (2,1) require that the non-relativistic limit $v_x \ll c$ and the classical physics limit $n \to \infty$ are actually correlated. Indeed, eqs. (3,3) have been obtained handling the ranges as differentials just thanks to small values of n. Of course such a correlation is not required when regarding quantum theory and relativity separately, it appears instead here as a consequence of their merging. Since for $n \to \infty$ the difference between n and $n+1$ becomes more and more negligible with respect to n, this latter tends to behave more and more like a continuous variable. It has been shown in [9] that just the quantization entails the non-real and non-local features of the quantum world; instead locality and reality are asymptotic limit properties of the classical world attained by the continuous variable condition $n \to \infty$. Now it appears that just the same quantization condition of n requires also the relativistic properties of the particles, which indeed are well approximated by the corresponding equations of Newtonian physics in the limit $n \to \infty$ i.e. $v_x \ll c$. Otherwise stated, the special relativity rests itself on the quantization condition required by the space/momentum and time/energy uncertainties merged together; these latter are therefore the sought unique fundamental concept on which are rooted quantum properties, non-reality, non-locality and special relativity.

3.2 Energy-momentum uncertainty and Maxwell equations

Let us start from $\Delta\varepsilon = v_x \Delta p_x$; being as usual $\Delta\varepsilon = \varepsilon - \varepsilon_o$ and $\Delta p_x = p_x - p_o$, this uncertainty equation splits into two equations $\varepsilon = v_x p_x$ and $\varepsilon_o = v_x p_o$ defined by the arbitrary boundary values of energy and momentum. Consider first the former equation; dividing both sides by an arbitrary volume V and by an arbitrary velocity component $v_x^{\S}$, the uncertainty equation turns dimensionally into the definition $J_x^{\S} = C^{\S} v_x$ of a mass flow; indeed $J_x^{\S}$ is the flux of the mass m initially defining momentum and energy of the particle, $C^{\S}$ is the corresponding amount of mass per unit volume. Calculating the flux change between any x and $x + \delta x$ during δt, one finds $\delta J_x^{\S} = v_x \delta C^{\S} + C^{\S} \delta v_x$. This result can be exploited in various ways. For instance in a previous paper it has been shown that eqs. (2,1) lead under appropriate hypotheses to the result $J_x^{\S} = -D \partial C^{\S}/\partial x$ [10], being D the diffusion coefficient of m. The particular case of constant v_x in the absence of an external force field acting on m during the time range $\delta t = \delta x / v_x$ yields $\delta J_x^{\S} = -[\partial(D \partial C^{\S}/\partial x)/\partial x]\delta x$. Since $\delta J_x^{\S}/\delta x = -\delta C^{\S}/\delta t$, because $\delta J_x^{\S}/\delta x$ and $\delta C^{\S}/\delta t$ have opposite sign under the hypothesis of gradient driven mass flow in the absence of sinks or sources in the diffusing medium, one obtains the 1D Fick law $\delta C^{\S}/\delta t = \partial(D \partial C^{\S}/\partial x)/\partial x$, trivially extensible to the 3D case. In general, under the constrain of constant v_x only, the vector equations corresponding to $J_x^{\S} = C^{\S} v_x$ and $\delta J_x^{\S} = -v_x \delta C^{\S}$ read

$$\mathbf{J}^{\S} = C^{\S} \mathbf{v}, \qquad \nabla \cdot \mathbf{J}^{\S} = -\partial C^{\S}/\partial t. \tag{3,4}$$

Multiplying by e/m both sides of these expressions, one obtains the corresponding equations for the flux of charge density C_e, i.e. $\mathbf{J}_e = C_e \mathbf{v}$. An analogous result holds for the second part $\varepsilon_o = v_x p_o$ of the initial uncertainty equation, rewritten now as $\mathbf{J}_m = C_m \mathbf{v}$ with $C_m = C^{\S} e_m/m$; the physical meaning of e_m will be remarked below. Put now $C = C_e + C_m$ and $\mathbf{J} = \mathbf{J}_e + \mathbf{J}_m$; then, replacing $\mathbf{J}^{\S}$ and $C^{\S}$ of the mass concentration gradient equation with $\mathbf{J}$ and C, it is possible to introduce an arbitrary vector $\mathbf{U}_-$ such that the second equation eq (3,4) reads

$$\nabla \cdot \nabla \times \mathbf{U}_- = \nabla \cdot \mathbf{J} + \frac{\partial C}{\partial t} \tag{3,5}$$

as it is clear because the left hand side is null. So one obtains

$$\begin{gathered} \nabla \times \mathbf{U}_- = \frac{\partial \mathbf{U}_+}{\partial t} + \mathbf{J}, \qquad \nabla \cdot \mathbf{U}_+ = C, \\ \mathbf{J} = \mathbf{J}_e + \mathbf{J}_m, \qquad C = C_e + C_m. \end{gathered} \tag{3,6}$$

The second equation defines $\mathbf{U}_+$. Since $C = C_e + C_m$, the vector $\mathbf{U}_+$ must reasonably have the form $\mathbf{U}_+ = \mathbf{H} + \mathbf{E}$, where $\mathbf{H}$ and $\mathbf{E}$ are arbitrary vectors to be defined. As also $\mathbf{J}$ is sum of two vectors, $\mathbf{U}_-$ is expected to be itself sum of two vectors too. For mere convenience let us define these latter again through the same $\mathbf{H}$ and $\mathbf{E}$; there is no compelling reason to introduce necessarily further vectors about which additional hypotheses would be necessary to solve the first eq (3,6). Appears now sensible to guess $\mathbf{U}_- = c(\mathbf{H} - \mathbf{E})$, with c mere dimensional factor, for four reasons: (i) $\mathbf{U}_+ + c^{-1}\mathbf{U}_- = 2\mathbf{H}$ and $\mathbf{U}_+ - c^{-1}\mathbf{U}_- = 2\mathbf{E}$, i.e. $\mathbf{U}_-$ and $\mathbf{U}_+$ can be expressed through the same vectors they introduce; (ii) the same holds for the scalars $c^{-1}\mathbf{U}_+ \cdot \mathbf{U}_- = H^2 - E^2$ and $U_+^2 - c^{-2}U_-^2 = 4\mathbf{E} \cdot \mathbf{H}$; (iii) the same holds also for $c^{-1}\mathbf{U}_- \times \mathbf{U}_+ = 2\mathbf{E} \times \mathbf{H}$ and (iv) $U_+^2 + c^{-2}U_-^2 = 2(H^2 + E^2)$. If $\mathbf{H}$ and $\mathbf{E}$ are now specified in particular as vectors proportional to magnetic and electric fields, then the proposed definitions of $\mathbf{U}_-$ and $\mathbf{U}_+$ entail a self-consistent set of scalars and vectors having some interesting features: the scalars (ii) define two invariants with respect to Lorentz transformations, whereas the vector (iii) is proportional to the Poynting vector and defines the energy density flux; moreover the point (iv) defines a scalar proportional to the energy density of the electromagnetic field; eventually the integral $\int \mathbf{U}_+ \cdot \mathbf{U}_- d\mathrm{V}$ over the volume previously introduced is proportional to the Lagrangian of a free field.

Although eqs. (3,5) and (3,6) are general equations straightforward consequences of charge flows, simply specifying purposely them to the case of the electromagnetic field follows the validity of the form assigned to $\mathbf{U}_-$ because of such sensible outcomes. The first eq (3,6) reads thus $c\nabla \times (\mathbf{H} - \mathbf{E}) = \partial(\mathbf{H} + \mathbf{E})/\partial t + (\mathbf{J}_e + \mathbf{J}_m)$. In principle the terms of this equation containing $\mathbf{H}$, $\mathbf{E}$, $\mathbf{J}_e$ and $\mathbf{J}_m$ can be associated in various ways, for instance is admissible $c\nabla \times \mathbf{H} = \partial \mathbf{H}/\partial t + \mathbf{J}_m$; integrating this equation is certainly possible but the solution $\mathbf{H} = \mathbf{H}(x, y, z, t, \mathbf{J}_m)$ would be of scarce interest, i.e. one would merely find the space and time profile of a possible

H consistent with $\mathbf{J}_m$. The same would hold considering the analogous equation for **E**. A combination of mixed terms that appears more interesting is

$$\begin{gathered}\nabla\cdot\mathbf{E}=C_e,\qquad \nabla\cdot\mathbf{H}=C_m,\\ -c\nabla\times\mathbf{E}=\frac{\partial\mathbf{H}}{\partial t}+\mathbf{J}_m,\qquad c\nabla\times\mathbf{H}=\frac{\partial\mathbf{E}}{\partial t}+\mathbf{J}_e.\end{gathered}\tag{3,7}$$

In this form, the interdependence of the magnetic and electric field vectors **H** and **E** through $\mathbf{J}_e$ and $\mathbf{J}_m$ yields the Maxwell equations formulated in terms of charge and current densities. These equations, also inferred from eqs. (2,1), have been written having in mind the maximum generality; C_e and C_m are proportional to the electric charge and magnetic charge densities, $\mathbf{J}_e$ and $\mathbf{J}_m$ to the charge and magnetic current densities. While C_e is known, an analogous physical meaning for C_m is doubtful because the magnetic "monopoles" are today hypothesized only but never experimentally observed. Although it is certainly possible to regard these equations with $C_m = 0$ and $\mathbf{J}_m = 0$, nevertheless seems formally attractive the symmetric character of the four equations (3,7). Note however in this respect that rewriting $\mathbf{E} = \mathbf{E}_o + \mathbf{Q}$ and $\mathbf{H} = \mathbf{H}_o + \mathbf{W}$, where **W** and **Q** are further field vectors whose physical meaning is to be defined, with the positions

$$\begin{gathered}C'_e=\nabla\cdot\mathbf{Q},\qquad \nabla\times\mathbf{Q}=0,\qquad \mathbf{J}'_e=\frac{\partial\mathbf{Q}}{\partial t},\\ \rho_m=-\nabla\cdot\mathbf{W},\qquad \nabla\times\mathbf{W}=0,\qquad \mathbf{J}'_m=\frac{\partial\mathbf{W}}{\partial t},\end{gathered}$$

the equations (3,7) turn into

$$\begin{gathered}\nabla\cdot\mathbf{E}_o=C_e-C'_e,\qquad \nabla\cdot\mathbf{H}_o=\rho_m,\\ -c\nabla\times\mathbf{E}_o=\frac{\partial\mathbf{H}_o}{\partial t}+\mathbf{J}'_m,\qquad c\nabla\times\mathbf{H}_o=\frac{\partial\mathbf{E}_o}{\partial t}-\mathbf{J}'_e+\mathbf{J}_e,\end{gathered}$$

having put here $C_m = 0$ and $\mathbf{J}_m = 0$. In practice rewriting **H** and **E** as a sum of vectors $\mathbf{H}_o$ and $\mathbf{E}_o$ parallel to them plus **W** and **Q** fulfilling the aforesaid conditions one obtains a new set of Maxwell equations whose form, even without reference to the supposed magnetic monopoles, is however still the same as if these latter would really exist. Note eventually that beside eqs. (3,7) there is a further non-trivial way to mix the electric and magnetic terms, i.e.

$$\begin{gathered}\nabla\cdot\mathbf{E}=C_e,\qquad \nabla\cdot\mathbf{H}=C_m,\\ -c\nabla\times\mathbf{E}=\frac{\partial\mathbf{H}}{\partial t}+\mathbf{J}_e,\qquad c\nabla\times\mathbf{H}=\frac{\partial\mathbf{E}}{\partial t}+\mathbf{J}_m,\end{gathered}\tag{3,8}$$

expectedly to be read with $C_m = 0$ and $\mathbf{J}_m = 0$. Work is in progress to highlight the possible physical meaning of **Q** and **W** and that of the eqs. (3,8) still consistent with eq (3,6).

3.3 Uncertainty and wave formalism

Start now from eqs. (3,3) that yield $\varepsilon^2 = (cp_x)^2 + (mc^2)^2$; so the positions (2,3) define the known 2D Klein-Gordon equation $-\partial^2\psi_o/c^2\partial t^2 = -\partial^2\psi_o/\partial x^2 + (mc/\hbar)^2\psi_o$, whose extension to the 4D case is trivial simply assuming $\psi_o = \psi_o(x, y, z, t)$

$$\frac{\partial^2\psi_o}{c^2\partial t^2}-\nabla^2\psi_o+k^2\psi_o=0,\qquad k^2=\left(\frac{mc}{\hbar}\right)^2.\tag{3,9}$$

Eq. (3,9) is equivalent to $O_5^2\psi_o = 0$ inferred from $\mathbf{O}_5\psi_o = 0$, where the total momentum operator $\mathbf{O}_5$ is defined as

$$\begin{gathered}\mathbf{O}_5=\mathbf{a}_j\frac{\hbar}{i}\frac{\partial}{\partial x_j}+\mathbf{a}_4\frac{i}{c}\frac{\hbar}{i}\frac{\partial}{\partial t}+\mathbf{a}_5mc,\\ j=1,2,3;\qquad \mathbf{a}_j\cdot\mathbf{a}_{j'}=\delta_{j,j'}.\end{gathered}$$

Thus $\mathbf{O}_5$ is the sought linear combination $\mathbf{a}_j\mathrm{P}_j+(\mathbf{a}_4 i/c)\mathrm{H}+\mathbf{a}_5 mc$ of the momentum P_j and energy H operators (2,3) via orthogonal unit vector coefficients $\mathbf{a}_j$ and $\mathbf{a}_4 i/c$ and $\mathbf{a}_5$; this combination of space and time operators defines the wave equation corresponding to the relativistic eqs. (3,3).

Replace now ψ_o with $\psi = \psi_o + \mathbf{a}\cdot\mathbf{A} + b\varphi$ in eq (3,9); **a** and b are arbitrary constants, **A** and φ are functions of x_j, t that must still fulfill eq (3,9). Assuming constant both modulus and direction of **a** with respect to **A**, trivial calculations yield three equations. One is once again the Klein-Gordon equation for ψ_o; moreover subtracting and summing to the two remainder terms the amount $\mathbf{a}\cdot\mathbf{J}/c$, where **J** is a further arbitrary vector, the condition $\mathbf{a}\cdot\mathbf{J}/cb = -\rho$ yields the following two equations

$$\begin{gathered}\frac{\partial^2\varphi}{c^2\partial t^2}-\nabla^2\varphi+k^2\varphi-\rho=0,\\ \frac{\partial^2\mathbf{A}}{c^2\partial t^2}-\nabla^2\mathbf{A}+k^2\mathbf{A}-\frac{\mathbf{J}}{c}=0.\end{gathered}\tag{3,10}$$

In principle this result is anyway formally possible with the given b, which links the equations through ρ and $\mathbf{J} = \rho\mathbf{v}$ according to eqs. (3,4). The condition on b requires $\mathbf{a}\cdot\mathbf{J}/c\rho = \mathbf{a}'\cdot\mathbf{J}'/c\rho'$; so in general **J** is not necessarily a constant. Let us specify now this result. If **A** and φ are proportional to the magnetic and electric potentials, then ρ and **J** are charge density and flux; in effect the particular case $\varphi \propto r^{-1}$ agrees with the physical meaning of the former, whence the meaning of the latter as well. The fact that ψ_o differs from $\psi = \psi_o + \mathbf{a}\cdot(\mathbf{A} - \mathbf{J}\varphi/c\rho)$ by the vector $\mathbf{A} - \mathbf{J}\varphi/c\rho \neq 0$ suggests defining $\mathbf{a} = \xi\mathbf{J}'/c$ in order obtain the scalar $\mathbf{J}'\cdot\mathbf{A}/c - \varphi\mathbf{J}'\cdot\mathbf{J}/\rho c^2$, i.e. $\mathbf{J}'\cdot\mathbf{A}/c - \rho'\varphi\mathbf{v}'\cdot\mathbf{v}/c^2$; ξ is a proportionality factor. So putting $\varphi = \varphi' q$, with q proportionality factor, the result is $\mathbf{J}'\cdot\mathbf{A}/c - \rho'\varphi'$ with $q^{-1} = \mathbf{v}'\cdot\mathbf{v}/c^2$. In this way one obtains $\psi = \psi_o + \xi(\mathbf{J}'\cdot\mathbf{A}/c - \rho'\varphi')$, while eqs. (3,10) are the well known Proca's equations in vector form.

Note that ξ has physical dimension $field^{-2}$, which indeed justifies the particular way of defining **a**, while the scalar in parenthesis characterizes the wave function of a particle moving in the presence of magnetic and electric potentials.

Since a free particle has by definition kinetic energy only, the scalar additive to ψ_o is a perturbative term due to the magnetic and electric potentials; so it should reasonably represent a kinetic energy perturbation due to the presence of magnetic and electric fields. This suggests that the complete Lagrangian $T - U$ of the particle moving in the electromagnetic field should be therefore given by the linear combination of the scalar just found and the free field scalar $c\mathbf{U}_- \cdot \mathbf{U}_+ = H^2 - E^2$, i.e. it should be obtained by volume integration of $\mathbf{J}' \cdot \mathbf{A}/c - \rho'\varphi' + \chi(E^2 - H^2)$, being χ an appropriate coefficient of the linear combination of potential and kinetic energy terms.

This topic is well known and does not deserve further comments. It is worth noticing instead that eqs. (3,10) can be also obtained introducing the extended space-time momentum operator $\mathbf{O}_7$ collecting together the space and time operators of the positions (2,3) in a unique linear combination expressed as follows

$$\mathbf{O}_7 = \mathbf{a}_j\partial/\partial x_j + \mathbf{a}_4 i\partial/\partial(ct) + \mathbf{a}_5 i/x_5 + \mathbf{a}_6\partial/\partial x_6 + \mathbf{a}_7\partial/\partial x_7,$$

where x_5, x_6 and x_7 are to be regarded as extra-coordinates. Putting $x_5 = \hbar/mc$, the wave function that yields directly both eqs. (3,10) with this operator reads accordingly

$$\psi = \psi_o + \mathbf{a} \cdot (\mathbf{A} - \mathbf{J}x_5^2/c)x_6 + (\varphi - \rho x_5^2)x_7.$$

Still holds the position $\mathbf{a}_j \cdot \mathbf{a}_{j'} = \delta_{j,j'}$ that regards again the various $\mathbf{a}_j$, with $j = 1..7$, as a set of orthogonal unit vectors in a 7D dimensional space where is defined the equation $O_7^2\psi = 0$ containing as a particular case the Klein-Gordon equation. The sixth and seventh addends of $\mathbf{O}_7$ are ineffective when calculating $O_7^2\psi_o$, which indeed still yields the free particle equation; however just these addends introduce the non-null terms of Proca's equations in the presence of fields.

In summary, the free particle eq (3,9) is nothing else but the combination of the two eqs. (3,3) expressed through the wave formalism of quantum mechanics; its successive manipulation leads to define the Lagrangian of the electromagnetic field in the presence of magnetic and electric potentials while introducing additional extra-dimensions. It appears however that the chance of defining 3 extra-dimensions to the familiar ones defining the space-time is suggested, but not required in the present model, by the relativistic wave formalism only.

3.4 Uncertainty and invariant interval

In [9] has been inferred the following expression of invariant interval

$$\Delta x^2 - c^2\Delta t^2 = \delta s^2 = \Delta x'^2 - c^2\Delta t'^2 \qquad (3,11)$$

in two inertial reference systems R and R'. Owing to the fundamental importance of this invariant in special relativity, from which can be inferred the Lorentz transformations [11], we propose here a further instructive proof of eq (3,11) based uniquely on the invariance of c. Consider then the uncertainty range $\Delta x = x - x_o$ and examine how its size might change during a time range Δt if in general $x = x(\Delta t)$ and $x_o = x_o(\Delta t)$.

Let be $\delta_\pm = \Delta x \pm v\Delta t$ the range in R that generalizes the definition $\Delta x/\Delta t = v_x$ to $\delta_\pm \neq 0$ through a new velocity component $v \neq v_x$ taking also into account the possible signs of v. Regard both $\delta_\pm$ as possible size changes of Δx during the time range Δt in two ways: either (i) with x_o replaced by $x_o \pm v\Delta t$ while keeping fixed x or (ii) with x replaced by $x \pm v\Delta t$ while keeping fixed x_o. Of course the chances (i) or (ii) are equivalent because of the lack of hypotheses on Δx and on its boundary coordinates. In both cases one finds indeed $\delta_+ = \Delta x + v\Delta t$ and $\delta_- = \Delta x - v\Delta t$, which yield $\bar{\bar{\delta}} = (\delta_+ + \delta_-)/2 = \Delta x$; so the range size Δx, seemingly steady in R, is actually a mean value resulting from random displacements of its lower or upper boundaries from x_o or x at average rates $v = \dot{x}_o$ or $v = \dot{x}$ as a function of time. Of course v is in general arbitrary. The actual space-time character of the uncertainty, hidden in $\bar{\bar{\delta}}$, appears instead explicitly in the geometric mean $< \delta >=< \delta_-\delta_+ >= (\Delta x^2 - v^2\Delta t^2)^{1/2}$ of both time deformations allowed to Δx. Note however that the origin O of the reference system R where is defined Δx appears stationary in (ii) to an observer sitting on x_o because is x that displaces, but in (i) O appears moving to this observer at rate $\mp\dot{x}_o$. Consider another reference system R' solidal with x_o, thus moving in R at rates $\pm\dot{x}_o$. In R' is applicable the chance (ii) only, as x_o is constant; it coincides with the origin in R' and, although it does not in R, yet anyway $\dot{x}_o = 0$. So the requirement that both (i) and (ii) must be equivalent to describe the deformation of Δx in R and R', otherwise these reference systems would be distinguishable, requires concluding that the chance (ii) must identically hold itself both in R and R'. This is possible replacing $v = \dot{x} = c$ in $< \delta >$, which indeed makes in this particular case the deformation rate (ii) of Δx indistinguishable in R and R': in both systems $\dot{x}_o = 0$, as x_o is by definition constant, whereas $\dot{x}$ also coincides because of the invariancy of c; when defined through this particular position, therefore, $< \delta^{(c)} >$ is invariant in any R and R' in agreement with eqs. (3,11). These equations have been written considering spacelike intervals; of course an identical reasoning holds also writing eqs. (3,11) as timelike intervals.

3.5 The invariancy of eqs. (2,1)

The following considerations concern the invariancy of eqs. (2,1) in different inertial reference systems. The proof is based on the arbitrariness of the range sizes and on the fact that in any R and R' actually n is indistinguishable from n' pertinent to the different range sizes resulting from the Lorentz transformations; indeed neither n nor n' are specified and specifiable by assigned values, rather they symbolize arbitrary numbers of states. Admitting different range sizes in inertial reference systems in reciprocal motion, the chance of any n in R corresponds to any other chance allowed to n' in R'. However the fact that the ranges are arbitrary compels

considering the totality of values of n and n', not their single values, in agreement with the physical meaning of eqs. (2,1). Hence, despite the individual numbers of states can be different for specific $\Delta x\Delta p_x$ in R and $\Delta x'\Delta p'_x$ in R', the sets of all arbitrary integers represented by all n and n' remain in principle indistinguishable regardless of how any particular n might transform into another particular n'.

The fact of having inferred in [9] the interval invariant in inertial reference systems, the Lorentz transformations of time and length and the expression $p_x = \varepsilon v_x/c^2$, should be itself a persuasive proof of the compliance of eqs. (2,1) with special relativity; now it is easy to confirm this conclusion demonstrating the expression of p_x in a more straightforward way, i.e. exploiting uniquely the concept of invariancy of c. The present reasoning starts requiring an invariant link between $\Delta p_x = p_1 - p_o$ and $\Delta\varepsilon = \varepsilon_1 - \varepsilon_o$ in $\Delta\varepsilon = \Delta p_x\Delta x/\Delta t$. This is possible if $\Delta x/\Delta t = c$, hence $\Delta p_x c = \Delta\varepsilon$ is a sensible result: it means of course that any local value ε within $\Delta\varepsilon$ must be equal to cp_x calculated through the corresponding local value p_x within Δp_x although both are unknown. If however $\Delta x/\Delta t < c$, the fact that the arbitrary v_x is not an invariant compels considering for instance $v_x^k\Delta x/\Delta t = qc^{k+1}$ with k arbitrary exponent and $q < 1$ arbitrary constant. Then $(\Delta p_x v_x^{-k})c^{k+1}q = \Delta\varepsilon$ provides in general an invariant link of $\Delta p_x v_x^{-k}$ with $\Delta\varepsilon$ through $c^{k+1}q$. Is mostly interesting the chance $k = 1$ that makes the last equation also consistent with the previous particular case, i.e. $(\Delta p_x/v_x)c^2q = \Delta\varepsilon$; so one finds $\varepsilon_1 v'_x/c^2 - p_1 = \varepsilon_o v'_x/c^2 - p_o$ with $v'_x = v_x/q$. The arbitrary factor q is inessential because v_x is arbitrary itself, so it can be omitted; hence $p_x = \varepsilon v_x/c^2$ when considering any local values within the respective ranges because of the arbitrariness of p_o, p_1, ε_o, ε_1. At this point holds identically the reasoning of the previous subsection. Rewrite $\Delta\varepsilon - (\Delta p_x/v_x)c^2 = 0$ as $\delta_\pm = \Delta\varepsilon \pm (\Delta p_x/v)c^2 \neq 0$ with $v \neq v_x$ to calculate $\overline{\delta^-} = \Delta\varepsilon$ and $< \delta\varepsilon >= \pm\sqrt{\Delta\varepsilon^2 - (\Delta p_x/v)^2c^4}$; one concludes directly that the invariant quantity of interest is that with $v = c$, i.e. $\delta\varepsilon_c = \pm\sqrt{\Delta\varepsilon^2 - \Delta p_x^2c^2}$ that reads

$$\Delta\varepsilon^2 = \delta\varepsilon_c^2 + \Delta p_x^2c^2. \qquad (3,12)$$

So $\varepsilon^2 = (mc^2)^2 + p_x^2c^2$ once having specified $\delta\varepsilon_c$ with the help of eq (3,2). This is not a trivial way to obtain again eqs (3,3). In general the ranges are defined by arbitrary boundary values; then ε_1 and ε_o can be thought in particular as arbitrary values of ε, thus invariant themselves if calculated by means of eqs. (3,3). So, despite the local values within their own uncertainty ranges are unknown, the range $\Delta\varepsilon$ defined as the difference of two invariant quantities must be invariant itself. Consider thus in particular the interval of eq (3,11). It is interesting to rewrite this result with the help of eqs. (2,1) as $(n\hbar)^2\Delta p_x^{-2} - c^2(n\hbar)^2\Delta\varepsilon^{-2} = \delta s^2 = \Delta x'^2 - c^2\Delta t'^2$, which yields therefore

$$\delta p_x\delta s = n\hbar = \delta p'_x\delta s, \qquad (3,13)$$

$$\delta p_x = \pm\frac{\Delta p_x\Delta\varepsilon}{\sqrt{\Delta\varepsilon^2 - (c\Delta p_x)^2}}, \qquad \delta p'_x = \pm\frac{\Delta p'_x\Delta\varepsilon'}{\sqrt{\Delta\varepsilon'^2 - (c\Delta p'_x)^2}}.$$

So $\delta p_x = \delta p_x(\Delta p_x, \Delta\varepsilon)$, whereas $\delta p'_x = \delta p'_x(\Delta p'_x, \Delta\varepsilon')$ as well. Both δs and δp_x at left hand side are invariant: the former by definition, the latter because formed by quantities $\Delta\varepsilon$ and Δp_x defined by invariant boundary quantities ε_1, ε_o, p_1, p_o of the eqs. (3,3). Being the range sizes arbitrary and not specifiable in the present theoretical model, the first eq. (3,13) is nothing else but the first eqs. (2,1) explicitly rewritten twice with different notation in invariant form. This feature of the first eq. (3,13) confirms not only the previous reasoning on n and n', thus supporting the relativistic validity of eqs. (2,1) in different inertial reference systems, but also the necessity of regarding the ranges of special relativity as uncertainty ranges; in other words the concept of invariancy merges with that of total arbitrariness of n, on which was based the previous reasoning. In conclusion: (i) disregarding the local coordinates while introducing the respective uncertainty ranges according to the positions (2,2) is enough to plug the classical physics into the quantum world; (ii) replacing the concepts of space uncertainty and time uncertainty with that of space-time uncertainty turns the non-relativistic quantum physics into the relativistic quantum physics; (iii) the conceptual step (ii) is fulfilled simply considering time dependent range sizes; (iv) if the deterministic intervals of special relativity are regarded as uncertainty ranges, then the well known formulae of special relativity are in fact quantum formulae that, as a consequence of eqs. (2,1), also fulfil the requirements of non-locality and non-reality. Accordingly, it is not surprising that the basic postulates of special relativity are in fact corollaries of eqs. (2,1) only, without the need of any further hypothesis.

3.6 The angular momentum

Let us show how the invariant interval of eq (3,11) leads to the relativistic angular momentum. Expand in series the range $\delta s = \sqrt{\Delta x^2 - c^2\Delta t^2}$ noting that in general

$$\sqrt{a^2 - b^2} = a - \Big(b/a + (b/a)^3/4 + (b/a)^5/8 + \cdot\cdot\Big)\,b\Big/2.$$

Calculated with an arbitrary number of terms, the series expansion can be regarded as an exact result. Thus write $\delta s = \delta r_x - \delta r_t/2$ where $\delta r_t = c\Delta t\left[c\Delta t/\Delta x + (c\Delta t/\Delta x)^3/4 + \cdot\cdot\right]$ and $\delta r_x = \Delta x$. Being Δt and Δx both arbitrary, δr_x and δr_t are independent ranges. Regard δs as the x-component of an arbitrary uncertainty vector range $\delta\mathbf{s} = \delta\mathbf{r}_s - \delta\mathbf{r}_t/2$ and repeat identically the reasoning introduced in [7] and shortly sketched here; the subscripts stand for "space" and "time". Insert $\delta\mathbf{s}$ in the classical component $M_w = \delta\mathbf{s}\times\delta\mathbf{p}\cdot\mathbf{w}$ of angular momentum $\mathbf{M}$ along the arbitrary unit vector $\mathbf{w}$. The analytical form of the function expressing the local value $\mathbf{p}$ does not need to be specified; according to the positions (2,2) $\mathbf{p}$ is a random value to be replaced by its own uncertainty

range $\delta\mathbf{p}$ to find the eigenvalues of the angular momentum. For the mere fact of having introduced an invariant interval into the definition of angular momentum, therefore, M_w results defined by the sum of two scalars $M_{w,s} = \delta\mathbf{r}_s \times \delta\mathbf{p} \cdot \mathbf{w}$ and $M_{w,t} = -\delta\mathbf{r}_t \times \delta\mathbf{p} \cdot \mathbf{w}/2$. So $M_{w,s} = \mathbf{w} \times \delta\mathbf{r}_s \cdot \delta\mathbf{p}$, i.e. $M_{w,s} = \delta\mathbf{p} \cdot \delta\mathbf{I}_s$ with $\delta\mathbf{I}_s = \mathbf{w} \times \delta\mathbf{r}_s$. If $\delta\mathbf{p}$ and $\delta\mathbf{I}_s$ are orthogonal then $M_{w,s} = 0$; else $M_{w,s} = \delta p_{I_s} \delta I_s$, defined by the conjugate dynamical variables $\delta p_{I_s} = \delta\mathbf{p} \cdot \delta\mathbf{I}_s / |\delta\mathbf{I}_s|$ and $\delta I_s = |\delta\mathbf{I}_s|$, yields immediately by virtue of eqs. (2,1) $M_{w,s} = \pm l\hbar$ with l arbitrary integer including zero; instead of n, we have used the standard notation l for the eigenvalues of angular motion of the particle. Identically one finds also $M_{w,t} = \pm l'\hbar/2$, with l' arbitrary integer including zero too. Hence $M_w = \pm l\hbar \pm l'\hbar/2$.

The first addend is clearly the non-relativistic component $l\hbar$ of angular momentum already found in [7], the latter yields an additional component $l'\hbar/2$ of angular momentum. Having considered the invariant range δs rather than the space range Δx only, the further number l' of states is due to the time term of the space-time uncertainty; putting $\Delta t = 0$, i.e. omitting the time/energy uncertainty and thus the time coordinate, $\delta r_t = 0$ and M_w coincides with the non-relativistic quantum component of angular momentum only.

Four important remarks concern:

(i) the number l of states allowed for the non-relativistic angular momentum component coincides with the quantum number of the eigenvalue of the non-relativistic angular momentum wave equation;

(ii) the concept of space-time uncertainty defines the series development of the particular invariant range δs as sum of two terms, the second of which introduces a new non-classical component of angular momentum $l'/2$;

(iii) the local momentum $\mathbf{p}$ and local coordinate $\mathbf{s}$ within the ranges $\delta\mathbf{p}$ and $\delta\mathbf{s}$ are not really calculated, rather they are simply required to change randomly within the respective ranges of values undetermined themselves; (iv) the boundary coordinates of both $\delta\mathbf{p}$ and $\delta\mathbf{s}$ do not appear in the result, rather is essential the concept of delocalization ranges only to infer the total component as a sum of both eigenvalues.

The component $M_w = \pm l\hbar \pm s\hbar$, with $s = l'/2$, requires introducing $\mathbf{M} = \mathbf{L} + \mathbf{S}$. In [7] the non-relativistic M_{nr}^2 has been calculated summing its squared average components between arbitrary values $-L$ and $+L$ allowed for $\pm l$, with L by definition positive, thus obtaining $M_{nr}^2 = 3 < (\hbar l)^2 >= L(L+1)\hbar^2$. Replace now $\pm l$ with $\pm l \pm s$; with $j = l \pm s$ ranging between arbitrary $-J$ and J, then $M^2 = 3 < (\hbar j)^2 >= 3(2J+1)^{-1} \sum_{-J}^{J} (\hbar j)^2 = \hbar^2 J(J+1)$ being J positive by definition. The obvious identity $\sum_{-J}^{J} j^2 \equiv 2 \sum_{0}^{J} j^2$ requires that J consistent with M^2 takes all values allowed to $|j|$ from $|l - s|$ up to $|l + s|$ with $l \leq L$ and $s \leq S$. Since no hypothesis has been made on $\mathbf{L}$ and $\mathbf{S}$, this result yields in general the addition rule of quantum vectors. Also, holds for $\mathbf{S}$ the same reasoning carried out for $\mathbf{L}$ in [7], i.e. only one component of $\mathbf{S}$ is known, whereas it is immediate to realize that $S^2 = \hbar^2(L'/2+1)L'/2$.

The physical meaning of $\mathbf{S}$ appears considering that: (i) $l'\hbar/2$ is an angular momentum, inferred likewise as and contextually to $l\hbar$; (ii) l' results when considering the invariant space-time uncertainty range into the definition of M_w; (iii) l and l' are independent, indeed they concern two independent uncertainty equations; the former is related to the angular motion of the particle, the latter must be instead an intrinsic property of the particle, as l' is defined regardless of whether $l = 0$ or $l \neq 0$. Since in particular $l' \neq 0$ even though the orbital angular momentum is null, $\mathbf{S}$ can be nothing else but the intrinsic property of the particle we call spin angular momentum. Indeed it could be also inferred in the typical way of reasoning of the special relativity i.e. introducing observers and physical quantities in two different inertial reference systems R and R' in relative constant motion; so, exploiting exactly the same procedure considering couples $\delta\mathbf{r}$ and $\delta\mathbf{p}$ together with $\delta\mathbf{r}'$ and $\delta\mathbf{p}'$ fulfilling the Lorentz transformation one finds of course the same result.

It is significant the fact that here the spin is inferred through the invariant interval of eq (3,13), i.e. exploiting eqs. (2,1) only. This is another check of the conceptual compliance of these equations with the special relativity.

3.7 The hydrogenlike atom/ion

The following example of calculation concerns first the non-relativistic hydrogenlike atom/ion. Assume first the origin O of R on the nucleus, the energy is thus $\varepsilon = p^2/2m - Ze^2/r$ being m the electron mass. Since $p^2 = p_r^2 + M^2/r^2$, the positions (2,2) $p_r \to \Delta p_r$ and $r \to \Delta r$ yield $\varepsilon = \Delta p_r^2/2m + M^2/2m\Delta r^2 - Ze^2/\Delta r$. Two numbers of states, i.e. two quantum numbers, are expected because of the radial and angular uncertainties. Eqs. (2,1) and the results of section 3.3 yield $\varepsilon = n^2\hbar^2/2m\Delta r^2 + l(l+1)\hbar^2/2m\Delta r^2 - Ze^2/\Delta r$ that reads $\varepsilon = \varepsilon_o + l(l+1)\hbar^2/2m\Delta r^2 - E_o/n^2$ with $E_o = Z^2e^4m/2\hbar^2$ and $\varepsilon_o = (n\hbar/\Delta r - Ze^2m/n\hbar)^2/2m$. Minimize ε putting $\varepsilon_o = 0$, which yields $\Delta r = n^2\hbar^2/Ze^2m$ and $\varepsilon_{tot} = [l(l+1)/n^2 - 1]E_o/n^2$; so $l \leq n-1$ in order to get $\varepsilon < 0$, i.e. a bound state. Putting thus $n = n_o + l + 1$ one finds the electron energy levels $\varepsilon_{el} = -E_o/(n_o + l + 1)^2$ and the rotational energy $\varepsilon_{rot} = l(l+1)E_o/n^4$ of the atom/ion as a whole around O. So $\varepsilon_{rot} = \varepsilon_{tot} - \varepsilon_{el}$. Repeat the same reasoning putting O on the center of mass of the system nucleus + electron; it is trivial to infer $E'_o = Z^2e^4m_r/2\hbar^2$ and $\Delta r' = n^2\hbar^2/Ze^2m_r$, being m_r the electron-nucleus reduced mass. If instead O is fixed on the electron, i.e. the nucleus moves with respect to this latter, then $E''_o = Z^2e^4A/2\hbar^2$ and $\Delta r'' = n^2\hbar^2/Ze^2A$, being A the mass of the nucleus. Thus various reference systems yield the same formula, and then again $\varepsilon'_{rot} = \varepsilon'_{tot} - \varepsilon'_{el}$ and $\varepsilon''_{rot} = \varepsilon''_{tot} - \varepsilon''_{el}$, yet as if the numerical result would concern particles of different mass.

The ambiguity between change of reference system and

change of kind of particle is of course only apparent; it depends merely on the erroneous attempt of transferring to the quantum world dominated by the uncertainty the classical way of figuring an "orbital" system of charges where one of them really rotates around the other. Actually the uncertainty prevents such a phenomenological way of thinking: instead the correct idea is that exists a charge located somewhere with respect to the nucleus and interacting with it, without chance of specifying anything else. This is shown noting that anyway one finds $E_{el} = -Ze^2/2\Delta\rho$ with $\Delta\rho$ symbolizing any radial range of allowed distances between the charges, regardless of which particle is actually in O. Since the total uncertainty range $2\Delta\rho$ is the diameter of a sphere centered on O, the different energies are mere consequence of different delocalization extents of a unique particle with respect to any given reference point.

This reasoning shows that different ranges of allowed radial momenta entail different allowed energies: if the particle of mass m is replaced for instance by one of lower mass, then $\Delta\rho$ increases while therefore Δp_ρ decreases; i.e. E_o reasonably decreases along with the range of allowed radial momenta. Of course it is not possible to infer "a priori" if these outcomes concern the motion of three different particles or the motion of a unique particle in three different reference systems; indeed no specific mass appears in the last conclusion. The allowed radial momenta only determine ε_{el}, defined as $-E_o$ of two charges $-Ze$ and e at diametric distance with respect to O times n^{-2}; this latter is the fingerprint of the quantum delocalization meaning of $\Delta\rho$. So E_o is defined by the mass m of the particle whose energy levels are of interest; for instance in the case of a mesic atom m would be the mass of a negative muon.

Note that ε_{el} is the intrinsic energy of the system of two charges, regardless of the kinetic energy of the atom as a whole and the rotational energy, i.e. $\Delta\varepsilon = \varepsilon_{tot} - \varepsilon_{el} = l(l+1)E_o/n^2$. The physical meaning of the boundary coordinates of Δx and Δt has been already emphasized.

Let us consider now the boundary values of other uncertainty ranges, examining also the harmonic oscillator and the angular momentum. The vibrational and zero point energies of the former $n\hbar\omega$ and $\hbar\omega/2$ define $\Delta\varepsilon = \varepsilon_{tot} - \varepsilon_{zp} = n\hbar\omega$; i.e. the lower boundary of the range is related to an intrinsic energy not due to the oscillation of the mass, likewise as that of the hydrogenlike atom was the binding energy. In the case of angular momentum $\Delta M_w = M_w - l'\hbar = l\hbar$, with $M_w \equiv M_{tot,w}$, i.e. the lower boundary of the range is still related to the intrinsic angular momentum component of the particle; from this viewpoint, therefore, the spin is understandable as the intrinsic property not dependent on the specific state of motion of the particle with respect to which the arbitrary values of l define the range size ΔM_w. The same holds for the relativistic kinetic energy of a free particle; the series development of the first eq (3,3) shows that its total energy is the rest energy plus higher order terms, i.e. one expects $\Delta\varepsilon = \varepsilon - mc^2$; also now the lower boundary of the range is an intrinsic feature of the particle, not related to its current state of motion. Classically, the energy is defined an arbitrary constant apart; here it appears that this constant is actually an intrinsic property of the particle, not simply a mathematical requirement, and that a similar conclusion should hold in general, thus expectedly also for the relativistic hydrogenlike energy. Let us concern the relativistic case specifying the energy ranges in order to infer the binding energy $\varepsilon_{el} < 0$ through trivial manipulations of eq (3,12) $\Delta\varepsilon^2 = c^2\Delta p^2 + \delta\varepsilon_c^2$. This expression is the 4D extension of that considering the component Δp_x only; whatever the three space components and their link to Δp might be, their arbitrariness allows to write again $\Delta p = p_1 - p_o$ and $\Delta\varepsilon = \varepsilon_1 - \varepsilon_o$. The first steps of calculations are truly trivial: consider $c\Delta p/\delta\varepsilon_c$ then calculate $(c\Delta p - \Delta\varepsilon)/\delta\varepsilon_c$, so that $(cp_1 - \Delta\varepsilon)/\delta\varepsilon_c = b + \sqrt{a^2-1} - a$ with $a = \Delta\varepsilon/\delta\varepsilon_c$ and $b = cp_o/\delta\varepsilon_c$. Next $(cp_1 - \Delta\varepsilon)^2/\delta\varepsilon_c^2$ yields trivially

$$\frac{\Delta\varepsilon^2}{(cp_1 - \Delta\varepsilon)^2} - \frac{(c\Delta p)^2}{(cp_1 - \Delta\varepsilon)^2} = \frac{1}{\left(b + \sqrt{a^2-1} - a\right)^2}.$$

A reasonable position is now $(cp_1 - \Delta\varepsilon)^2 = (c\Delta p)^2$: indeed the left hand side $\Delta\varepsilon^2/(c\Delta p)^2 = 1$ for $b \to \infty$, i.e. for $\delta\varepsilon_c \to 0$, agrees with the initial equation. Trivial manipulations yield

$$\frac{cp_1}{\Delta\varepsilon} = 1 \pm \frac{1}{\sqrt{1 + \left(b + \sqrt{a^2-1} - a\right)^{-2}}},$$

$$c\Delta p = \pm(cp_1 - \Delta\varepsilon), \qquad a = \frac{\Delta\varepsilon}{\delta\varepsilon_c}, \qquad b = \frac{cp_o}{\delta\varepsilon_c}.$$

This result has not yet a specific physical meaning because it has been obtained simply manipulating the ranges $\Delta\varepsilon$, $\delta\varepsilon_c$ and $c\Delta p$. Physical information is now introduced taking the minus sign and calculating the non-vanishing first order term of series development of the right hand side around $b = \infty$, which is $1/2b^2$; the idea that specifies the result is thus the non-relativistic hydrogenlike energy $-(\alpha Z/n)^2 mc^2/2$ previously found. Requiring $b = n/\alpha Z$, the limit of the ratio $cp_1/\Delta\varepsilon$ is thus the energy in mc^2 units gained by the electron in the bound state with respect to the free state. To infer a recall that $n = l + 1$ and note that the second equation $\pm\Delta\varepsilon = cp_o - cp_1 \pm cp_1$ reads $\pm\Delta\varepsilon = cp_o$ or $\pm\Delta\varepsilon = cp_o - 2cp_1$; dividing both sides by $\delta\varepsilon_c$, the latter suggests $cp_1/\delta\varepsilon_c = (2\alpha Z)^{-1}$ in order that $\pm a = n/\alpha Z$ or $\pm a = (n-1)/\alpha Z$ read respectively $\pm a = (l+1)/\alpha Z$ or $\pm a = l/\alpha Z$, i.e. $a = (l + 1/2 \pm 1/2)/\alpha Z$.

In conclusion the relativistic form of the binding energy ε_{el} is

$$\frac{\varepsilon_{el}}{mc^2} = \sqrt{1 + \frac{(\alpha Z)^2}{\left(n + \sqrt{(j+1/2)^2 - 1} - (j+1/2)\right)^2}} - 1$$

with $j = l \pm s$. If $n \to \infty$ then $\varepsilon_{el} \to 0$, while the non-relativistic limit previously found corresponds to $\alpha Z \to 0$.

3.8 The pillars of quantum mechanics

Let us show now that the number of allowed states introduced in eqs. (2,1) leads directly to both quantum principles of exclusion and indistinguishability of identical particles. The results of the previous section suggest the existence of different kinds of particles characterized by their own values of l'. If this conclusion is correct, then the behavior of the particles should depend on their own l'. Let us consider separately either possibility that l' is odd or even including 0.

If $l'/2$ is zero or integer, any change of the number N of particles is physically indistinguishable in the phase space: are indeed indistinguishable the sums $\sum_{j=1}^{N} l_j + Nl'/2$ and $\sum_{j=1}^{N+1} l_j^* + (N+1)l'/2$ controlling the total value of M_w before and after increasing the number of particles; indeed the respective l_j and l_j^* of the j-th particles are arbitrary. In other words, even after adding one particle to the system, M_w and thus M^2 replicate any possible value allowed to the particles already present in the system simply through a different assignment of the respective l_j; so, in general a given number of allowed states determining M_w in not uniquely related to a specific number of particles.

The conclusion is different if l' is odd and $l'/2$ half-integer; the states of the phase space are not longer indistinguishable with respect to the addition of particles since M_w jumps from ... integer, half-integer, integer... values upon addition of each further particle, as any change of the number of particles necessarily gives a total component of M_w, and then a resulting quantum state, different from the previous one. In other words any odd-l' particle added to the system entails a new quantum state distinguishable from those previously existing, then necessarily different from that of the other particles. The conclusion is that a unique quantum state is consistent with an arbitrary number of even-l' particles, whereas a unique quantum state characterizes each odd-l' particle. This is nothing else but a different way to express the Pauli exclusion principle, which is thus corollary itself of quantum uncertainty. Recall also the corollary of indistinguishability of identical particles, already remarked; eqs. (2,1) concern neither the quantum numbers of the particles themselves nor their local dynamical variables but ranges where *any* particle could be found, whence the indistinguishability.

We have shown that a unique formalism based on eqs. (2,1) only is enough to find the basic principles of both special relativity and quantum mechanics; also, quantum and relativistic results have been concurrently inferred. The only essential requirement to merge special relativity and quantum mechanics is to regard the intervals of the former as the uncertainty ranges of the latter. The next step concerns of course the general relativity.

4 Uncertainty and general relativity

In section 3 the attempt to generalize the non-relativistic results of the papers [7,8] was legitimated by the possibility of obtaining preliminarily the basic postulates of special relativity as straightforward corollaries of eqs. (2,1). Doing so, the positions (2,2) ensure that the special relativity is compliant with the concepts of quantization, non-reality and non-locality of quantum mechanics [9]. At this point, the attempt of extending further an analogous approach to the general relativity is now justified by showing two fundamental corollaries: (i) the equivalence of gravitational and inertial forces and (ii) the coincidence of inertial and gravitational mass. These concepts, preliminarily introduced in [9], are so important to deserve being sketched again here.

Once accepting eqs. (2,1) as the unique assumption of the present model, the time dependence of the uncertainty range sizes $\Delta x = x - x_o$ and $\Delta p_x = p_x - p_o$ rests on their link to Δt through n; for instance it is possible to write $d\Delta x/d\Delta t$ in any R without contradicting eqs. (2,1); this position simply means that changing Δt, e.g. the time length allowed for a given event to be completed, the space extent Δx necessary for the occurring of that event in general changes as well. In other words there is no reason to exclude that $\Delta t \to \Delta t + \Delta t^{\S}$, with $\Delta t^{\S}$ arbitrary, affects the sizes of Δx and Δp_x although n remains constant; in fact eqs. (2,1) do not prevent such a possibility. Hence, recalling that here the derivative is the ratio of two uncertainty ranges, the rate $\Delta\dot{x}$ with which changes Δx comes from the chance of assuming $\dot{x} = \delta x/d\Delta t$ and/or $\dot{x}_o = \delta x_o/d\Delta t$; also, since analogous considerations hold for $d\Delta p_x/d\Delta t$ one finds similarly $\dot{p}_x$ and $\dot{p}_o$. Also recall that the boundary values of the ranges are arbitrary, so neither p_o and p_x nor their time derivatives need to be specified by means of assigned values. Since $\dot{p}_o$ and $\dot{p}_x$ are here simply definitions, introduced in principle but in fact never calculated, the explicit analytical form of the momentum p of general relativity does not need to be known; the previous examples of angular momentum and hydrogenlike atoms elucidate this point. The following reasoning exploits therefore the mere fact that a local force is related to a local momentum change, despite neither the former nor the latter are actually calculable functions of coordinates.

Let us define Δt and the size change rates $d\Delta x/d\Delta t$ and $d\Delta p_x/d\Delta t$ in an arbitrary reference system R as follows

$$d\Delta p_x/d\Delta t = F = -n\hbar\Delta x^{-2} d\Delta x/d\Delta t \qquad (4,1)$$

with $F \neq 0$ provided that $\dot{x} \neq \dot{x}_o$ and $\dot{p}_x \neq \dot{p}_o$. At left hand side of eqs. (4,1) the force component F involves explicitly the mass of the particle through the change rate of its momentum; at the right hand side F concerns the range Δx and its size change rate only, while the concept of mass is implicitly inherent the physical dimensions of $\hbar$. It is easy to explain why a force field arises when changing the size of Δx: this means indeed modifying also the related size of Δp_x and thus the extent of values allowed to the random p_x; the force field is due to the resulting $\dot{p}_x$ throughout Δx whenever its size is altered. After having acknowledged the link between $\Delta\dot{x}$ and

F intuitively suggested by eqs. (2,1), the next task is to check the conceptual worth of eqs. (4,1). Let x_o be the coordinate defined with respect to the origin O of R where hold eqs. (2,1). If $\Delta t = t - t_o$ with $t_o = const$, then the previous expression reads $d\Delta p_x/dt = F = -n\hbar\Delta x^{-2} d\Delta x/dt$. Formally eqs. (4,1) can be rewritten in two ways depending on whether x_o or x, and likewise p_o or p_x, are considered constants: either (i) $\Delta\dot{p}_x \equiv \dot{p}_x$ so that $\dot{p}_x = F_x = -n\hbar\Delta x^{-2}\dot{x}$ or (ii) $\Delta\dot{p}_x \equiv \dot{p}_o$ so that $\dot{p}_o = F_o = -n\hbar\Delta x^{-2}\dot{x}_o$.

The physical meaning of these results is realized imagining in R the system observer + particle: the former is sitting on x_o, the latter is fixed on x. In (i) the observer is at rest with respect to O and sees the particle accelerating according to $\dot{p}_x$ by effect of F_x generated in R during the deformation of the space-time range Δx. In (ii) the situation is different: now Δx deforms while also moving in R at rate $\dot{x}_o$ with respect to O, the deformation occurs indeed just because the particle is at rest with respect to O; thus the force F_o displaces the observer sitting on x_o, which accelerates with respect to the particle and to O according to $-\dot{p}_o$. In a reference system R_o solidal with x_o, therefore, a force F'_o still acts on the observer although he is at rest; the reason is clearly that R_o is non-inertial with respect to R because of its local acceleration related to $-\dot{p}_o$. Although the reasoning is trivially simple, the consequence is important: both situations take place in the presence of a force component because both cases (i) and (ii) are equally allowed and conceptually equivalent; however the force in R is real, it accelerates a mass, that in R_o does not; yet $F_x \neq 0$ compels admitting in R also $F_o \neq 0$, which in turn reads $F'_o \neq 0$ in R_o. Whatever the transformation rule from F_o to F'_o might be, the conclusion is that an observer in an accelerated reference frame experiences a force similar to that able to accelerate a massive particle with respect to the observer at rest. Of course F_x is actually the component of a *force field*, because it is an average value defined throughout a finite sized range Δx deforming as a function of time, whereas F_o and F'_o are by definition *local* forces in x_o; if however the size of Δx is smaller and smaller, then F_x is better and better defined itself like a classical local force.

Now we are also ready to find the equivalence between inertial and gravitational mass. Note indeed that F_x has been defined through a unique mass m only, that appearing in the expression of momentum; hence from the standpoint of the left hand side of eqs. (4,1) we call m inertial mass. Consider in this respect that just this mass must somehow appear also at right hand side of eqs. (4,1) consisting of uncertainty ranges only, which justifies the necessary position $n\hbar\Delta\dot{x}\Delta x^{-2} = m\sum_{j=2}^{\infty} a_j \Delta x^{-j}$ according which the mass is also an implicit function of Δx, $\Delta\dot{x}$, $\hbar$ and n; the lower summation index is due to the intuitive fact that $\Delta\dot{x}$ cannot be function of or proportional to Δx otherwise it would diverge for $\Delta x \to \infty$, hence the power series development of the quantity at left hand side must start from Δx^{-2}. So, putting as usual the coefficient of the first term of the series $a_2 = k_G$, eqs. (4,1) yields $F = -k_G m\Delta x^{-2} + ma_3\Delta x^{-3} + \cdots$. Three remarks on this result are interesting: (i) the first term is nothing else but the Newton gravity field, where now the same m plays also the expected role of gravitational mass generating a radial force that vanishes with x^{-2} law if expressed through the local radial distance x from m; (ii) F is in general additive at the first order only, as it is evident considering the sum of $\Delta\dot{x}_1$ due to F_1 related to m_1 plus an analogous $\Delta\dot{x}_2$ due to F_2 in the presence of another mass m_2; (iii) gravitational mass generating F and inertial mass defined by $\dot{p}_o$ coincide because in fact m is anyway that uniquely defined in eqs. (4,1). By consequence of (ii) force and acceleration are co-aligned at the first order only. The proportionality factor k_G has physical dimensions $\mathrm{l}^3\mathrm{t}^{-2}$; multiplying and dividing the first term at right hand side by a unit mass m^u and noting that $m^u m$ can be equivalently rewritten as $m'm''$ because m is arbitrary like m' and m'', the physical dimensions of k_G turn into $\mathrm{l}^3\mathrm{t}^{-2}\mathrm{m}^{-1}$ while

$$F = -Gm'm''\Delta x^{-2} + m'm''a_3\Delta x^{-3} + \cdots. \qquad (4,2)$$

In conclusion eqs. (2,1) allow to infer as corollaries the two basic statements of general relativity, the arising of inertial forces in accelerated systems and the equivalence principle.

This result legitimates the attempt to extend the approach hitherto outlined to the general relativity, but requires introducing a further remark that concerns the concept of covariance; this concept has to do with the fact that eqs. (4,1) introduce in fact two forces F_x and F_o in inertial, R, and non-inertial, R_o, reference systems. This early idea introduced by Einstein first in the special relativity and then extended also to the general relativity, aimed to exclude privileged reference systems by postulating the equivalence principle and replacing the concept of gravity force with that of space-time curved by the presence of the mass; Gaussian curvilinear coordinates and tensor calculus are thus necessary to describe the local behavior of a body in a gravity field. This choice allowed on the one side to explain the gedankenexperiment of light beam bending within an accelerated room and on the other side to formulate a covariant theory of universal gravitation through space-time Gaussian coordinates.

Yet the covariancy requires a mathematical formalism that generates conflict with the probabilistic basis of the quantum mechanics: the local metric of the space-time is indeed deterministic, obviously the gravity field results physically different from the quantum fields. It makes really difficult to merge such a way of describing the gravitation with the concepts of non-locality and non-reality that characterize the quantum world. In the present model the concept of force appears instead explicitly: without any "ad hoc" hypothesis the Newton law is obtained as approximate limit case, whereas the transformation from an inertial reference system R to a non-inertial reference system R_o correctly describes the arising of an inertial force.

Hence the present theoretical model surely differs in principle from the special and general relativity; yet, being derived from eqs. (2,1), it is consistent with quantum mechanics as concerns the three key requirements of quantization, non-reality, non-locality. Also, the previous discussion exploits a mathematical formalism that despite its extreme simplicity efficiently bypasses in the cases examined the deterministic tensor formalism of special relativity. In the next sub-section 4.1 attention will be paid to the concept of covariancy, not yet explicitly taken into consideration when introducing the special relativity and apparently skipped so far. Actually this happened because, as shown below, the concept of covariance is already inherent "per se" in the concept of uncertainty once having postulated the complete arbitrariness of size and boundary coordinates of the delocalization ranges.

Let us conclude this introductory discussion rewriting the eqs. (4,1) as $\Delta\dot{p}_x = F = \mu\Delta\ddot{x}$, where

$$\mu = -n\hbar\frac{\Delta\dot{x}}{\Delta x^2\Delta\ddot{x}}$$

has of course physical dimensions of mass; indeed $\Delta\dot{p}_x$ ensures that effectively μ must somehow be related to the mass of a particle despite it is defined as a function of space delocalization range and its proper time derivatives only.

It is worth noticing that in eq (3,2) the mass was defined regarding the particle as a delocalized corpuscle confined within Δx, here the quantum of uncertainty $\hbar$ introduces the mass μ uniquely through its physical dimension. Also note that $\mu/\hbar$ has dimension of a reciprocal diffusion coefficient D, so the differential equation $\Delta\dot{x}/(\Delta x^2\Delta\ddot{x}) = \mp(Dn)^{-1}$ admits the solution $\Delta x = (L(\xi) + 1)\sqrt{D\tau_o}$, where L is the Lambert function and $\xi = \pm n\exp(\mp n\Delta t/\tau_o)$; the double sign is due to that possibly owned by μ, the integration constants are $-t_o$ defining $\Delta t = t - t_o$ and τ_o. In conclusion we obtain in the same R of eqs. (4,1)

$$\begin{aligned} &F = \pm n^2\frac{\hbar/\tau_o}{\sqrt{D\tau_o}}\frac{L(\xi)}{(L(\xi)+1)^3}, \quad \frac{\Delta x}{\Delta x_D} = L(\xi) + 1, \\ &\mu = \pm\hbar/D, \quad \xi = \pm n\exp(\mp n\Delta t/\tau_o), \\ &\Delta x_D = \sqrt{D\tau_o}. \end{aligned} \tag{4,3}$$

Note that the ratio $\Delta\dot{x}/\Delta\ddot{x} = \mp(L(\xi) + 1)^2\tau_o/n$ inferred from the given solution never diverges for $n > 0$; moreover Δx defined by this solution is related to the well known FLRW parameter $q = -\ddot{a}a/\dot{a}^2$, where a is the scale factor of the universe. Replacing this latter with Δx thanks to the arbitrariness of Δx_D and Δx itself, one finds that $q = \mp L(\xi)^{-1}$.

The importance of eqs. (4,3) rests on the fact that $\Delta x = \Delta x_D$ for $n = 0$ whereas instead, selecting the lower sign, $\Delta x < \Delta x_D$ for any $n > 0$; the reason of it will be clear in the next section 4.3 dealing with the space-time curvature.

It is worth remarking here the fundamental importance of n: (i) in [9] its integer character was proven decisive to discriminate between reality/locality and non-reality/non-locality of the classical and quantum worlds; (ii) previously small or large values of n were found crucial to describe relativistic or non-relativistic behavior; (iii) here the values $n = 0$ and $n > 0$ appear decisive to discriminate between an unphysical world without eigenvalues and a physical world as we know it. This last point will be further remarked in the next subsection 4.2.

Eventually μ deserves a final comment: μ is a mass defined within Δx uniquely because of its $\Delta\dot{x}$ and $\Delta\ddot{x}$; its sign can be in principle positive or negative depending on that of the former or the latter.

Relate Δx to the size of our universe, which is still expanding so that $\Delta\dot{x} \neq 0$; also, since there is no reason to exclude that the dynamics of the whole universe corresponds to $\Delta\ddot{x} \neq 0$ too, assume in general an expansion rate not necessarily constant.

It follows for instance $\mu < 0$ if the universe expands at increasing rate, i.e. with $\Delta\dot{x} > 0$ and $\Delta\ddot{x} > 0$. Eqs. (4,3) show that a mass is related to non-vanishing Δx and $\Delta\dot{x}$, $\Delta\ddot{x}$. This result appears in fact sensible recalling the dual corpuscle/wave behavior of quantum particles, i.e. imagining the particle as a wave propagating throughout the universe.

It is known that a string of fixed length L vibrates with two nodes L apart, thus with fundamental frequency $\nu_o = v/2L$ and harmonics $\nu_n = n\nu_o = nv/2L$; the propagation velocity of the wave is $v = \nu_n\lambda_n = \sqrt{T/\sigma}$, being T and σ the tension and linear density of the string. If L changes as a function of time while the string is vibrating and the wave propagating, then ν_n and λ_n become themselves functions of time.

Let the length change occur during a time δt; it is trivial to find $\delta\nu_n/\nu_n = (\dot{v}/v - \dot{L}/L)\delta t$, i.e. the frequency change involves L, $\dot{L}$ and $\dot{v}$. Put now L equal to the diameter of the universe at a given time, i.e. identify it with Δx; then propagation rate and frequency of the particle wave clearly change in an expanding universe together with its dynamic delocalization extent.

This therefore means changing the energy $\hbar\delta\nu_n$ of the particle wave, which in turn corresponds to a mass change $\delta m = \hbar\delta\nu_n c^{-2}$. All this agrees with the definition $\mu = \mu(\Delta x, \Delta\dot{x}, \Delta\ddot{x})$ and supports the analogy with the vibrating string. If so the mass μ results related itself to the big-bang energy, early responsible of the expansion. Once again is the uncertainty the key to highlight the origin of μ: likewise as the time change of Δx entails the rising of a force, see eqs. (4,1), correspondingly the time change of the size of the universe changes the delocalization extent of all matter in it contained and thus its internal energy as well.

Two questions arise at this point: has μ so defined something to do with the supposed "dark mass"? If this latter is reasonably due to the dynamics of our universe and if the kind of this dynamics determines itself both space-time curvature and sign of $\pm\mu$, has this sign to do with the fact that

our universe is preferentially made of matter rather than of antimatter? Work is in advanced progress to investigate these points, a few preliminary hints are sketched below.

4.1 Uncertainty and covariancy

In general the laws of classical mechanics are not covariant by transformation from inertial to non-inertial reference systems. Their form depends on the arbitrary choice of the reference system describing the time evolution of local coordinates, velocities and accelerations; this choice is subjectively decided for instance to simplify the formulation of the specific problem of interest.

A typical example is that of a tethered mass m rotating frictionless around an arbitrary axis: no force is active in R where the mass rotates, whereas in R_o solidal with the mass is active the centrifugal force; also, if the constrain restraining the mass to the rotation axis fails, the motion of the mass becomes rectilinear and uniform in R but curved in R_o, where centrifugal and Coriolis forces also appear. Let in general the non-covariancy be due to a local acceleration a_R in R, to which corresponds a combination a_{R_o} of different accelerations in R_o. This dissimilarity, leading to fictitious forces appearing in R_o only, suggested to Einstein the need of a covariant theory of gravitation. Just in this respect however the theoretical frame of the present model needs some comments.

First, the local coordinates are conceptually disregarded since the beginning and systematically eliminated according to the positions (2,2), whence the required non-locality and non-reality of the present model; accordingly the functions of coordinates turn into functions of arbitrary ranges, i.e. in 2D $a_R(x,t) \to a_R(\Delta x, \Delta\varepsilon, \Delta p, \Delta t, n)$, whereas the same holds for a_{R_o}. So the classical x-components of a_R and a_{R_o} transform anyway into different combinations of the same ranges $\Delta x, \Delta\varepsilon, \Delta p, \Delta t$; the only information is that the local a_R and a_{R_o} become random values within ranges $\Delta a_R = a_R^{(2)} - a_R^{(1)}$ and $\Delta a_{R_o} = a_{R_o}^{(2)} - a_{R_o}^{(1)}$. Yet being these range sizes arbitrary and unpredictable by definition, maybe even equal, is still physically significant now the formal difference between a_R and a_{R_o}?

Second, eqs. (4,1) introduce explicitly a force component F via $\Delta\dot{p}_x$ consequence of $\Delta\dot{x} \neq 0$; still appears also in the present model the link between force and deformation of the space-time, hitherto intended however as expansion or contraction of a 2D space-time uncertainty range.

Third, the positions (2,2) discriminate non-inertial, R_o, and inertial, R, reference systems; from the arbitrariness of x_o and p_o follows that of $\dot{x}_o$ and $\dot{p}_o$ as well. For instance the previous discussion on the 2D eqs. (4,1) leads directly to Einstein's gedankenexperiment of the accelerated box; in the present model the expected equivalence between gravity field in an inertial reference system, F_x, and inertial force in accelerated frames, F'_o, is indeed obtained simply considering the time dependence of both boundary coordinates of Δx; without specifying anything, this also entails the equivalence of gravitational and inertial mass. Being all space-time ranges arbitrary, the equivalence principle previously inferred is extensible to any kind of acceleration through a more general, but conceptually identical, 4D transformation from any R to any other R_o; indeed defining appropriately x_{oj} and their time derivatives $\dot{x}_{oj}$ and $\ddot{x}_{oj}$ times m, with $j = 1, 2, 3$, one could describe in principle also the inertial forces of the example quoted above through the respective p_j, p_{oj} and $\dot{p}_j$, $\dot{p}_{oj}$.

The key point of the present discussion is just here: the arbitrariness of both x_j and x_{oj} generalizes the chances of accounting in principle for any a_R and any a_{R_o}. A typical approach of classical physics consists of two steps: to introduce first an appropriate R according which are defined the local coordinates and to examine next the same problem in another R_o via a suitable transformation of these coordinates, whence the necessity of the covariancy. The intuitive considerations just carried out suggest instead that the classical concept of coordinate transformation fails together with that of local coordinates themselves. Imagine an observer able to perceive a range of values only, without definable boundaries and identifiable coordinates amidst; when possibly changing reference system, he could think to the transformation of the whole range only. This is exactly what has been obtained from eqs. (4,1) through the arbitrary time dependence of both x and x_o: the classical physics compels deciding either R or R_o, the quantum uncertainty requires inherently both of them via the two boundary coordinates of space-time ranges. The ambiguity of forces appearing in either of them only becomes in fact completeness of information, paradoxically just thanks to the uncertainty: the classical freedom of deciding "a priori" either kind of reference system, inertial or not, is replaced by the necessary concurrency of both of them simply because each couple of local dynamical variables is replaced by a couple of ranges.

As shown in the 2D eqs. (4,1), in the present model R-like or R_o-like reference systems are not alternative options but complementary features in describing any physical system that involves accelerations. Accordingly eqs. (4,1) have necessarily introduced two forces, F_x and F_o, related to the two standpoints that entail the equivalence principle as a particular case. After switching the concept of local dynamical variables with that of space-time uncertainty, the physical information turns in general into two coexisting perspectives contextually inferred; inertial and non-inertial forces are no longer two unlike or fictitious images of a unique law of nature merely due to different formulations in R or R_o, but, since each one of them requires the other, they generalize the equivalence principle itself. Just this intrinsic link surrogates here the concept of covariancy in eliminating a priori the status of privileged reference system. On the one hand, the chance of observers sitting on accelerated x_o or x excludes by necessity a unique kind of reference system; on the other hand, avoiding fictitious forces appearing in R_o only testifies the ability

of the present approach to incorporate all forces into a unique formulation regardless of their inertial and non-inertial nature.

Instead of bypassing the ambiguity of unlike forces appearing in either reference system only by eliminating the forces, the present model eliminates instead the concept itself of privileged reference system in the most general way possible when describing a physical system, i.e. through the concomitant introduction of both R and R_o. The total arbitrariness of both boundary coordinates of the uncertainty ranges on the one side excludes a hierarchical rank of R or R_o in describing the forces of nature, while affirming instead the complementary nature of their unique physical essence; on the other side it makes this conclusion true in general, regardless of whether x_o or x is related to the origin O of R and to the size of Δx.

4.2 Uncertainty and space-time curvature

The concept of curvature is well known in geometry and in physics; it is expressed differently depending on the kind of reference system. In general relativity the space-time curvature radius is given by $\rho = g^{ik}R_{ik}$, being g^{ik} the contravariant metric tensor and R_{ik} the Ricci tensor. As already emphasized, however, the central issue to be considered here is not the mathematical formalism to describe the curvature but the conceptual basis of the theoretical frame hitherto exposed; the key point is again that the positions (2,2) exclude the chance of exploiting analytical formulae to calculate the local curvature of the space-time. So, once having replaced the concept of space-time with that of space-time uncertainty, the way to describe its possible curvature must be accordingly reviewed. Just at this stage, eqs. (2,1) are exploited to plug also the quantum non-locality and non-reality in the conceptual structure of the space-time, i.e. into the general relativity.

In a previous paper [9] these features of the quantum world were introduced emphasizing that the measurement process perturbs the early position and momentum of the observed particle, assumed initially in an unphysical state not yet related to any number of states and thus to any observable eigenvalue. Owing to the impossibility of knowing the initial state of the particle, the early conjugate dynamical variables were assumed to fall within the respective $\Delta x^{\S}$ and $\Delta p_x^{\S}$; the notation emphasizes that before the measurement process these ranges are not yet compliant with eqs. (2,1), i.e. they are unrelated. These ranges, perturbed during the measurement process by interaction with the observer, collapse into the respective Δx and Δp_x mutually related according to the eqs. (2,1) and thus able to define eigenvalues of physical observables through n; this also means that $\Delta x^{\S}$ and $\Delta p_x^{\S}$ were mere space uncertainty ranges, whereas after the measurement process only they turn into the respective Δx and Δp_x that take by virtue of eqs. (2,1) the physical meaning of space-time uncertainty ranges of position and momentum. The paper [9] has explained the reason and the probabilistic character of such a collapse to smaller sized ranges, thanks to which the measurement process creates itself the number of states: the non-reality follows just from the fact that after the measurement process only, the particle leaves its early unphysical state to attain an allowed physical state characterized by the n-th eigenvalue.

This kind of reasoning is now conveyed to describe how and why a particle while passing from an unphysical state to any allowed physical state also curves concurrently the space-time. In this way the basic idea of the general relativity, i.e. the space-time curvature, is conceived itself according the concepts of non-reality and non-locality; the latter also follows once excluding the local coordinates and exploiting the uncertainty ranges of eqs. (2,1) only.

To start the argument, note that the arbitrary boundaries of the range $\Delta x^{\S} = x^{\S} - x_o$ control the actual path traveled by a particle therein delocalized. Let the space reference system be an arbitrary 1D x-axis about which nothing is known; information like flat or curled axis is inessential. Thus the following considerations are not constrained by any particular hypothesis on the kind of possible curvature of the early 1D reference system. Consider first the space range $\Delta x^{\S}$ alone; changing by an arbitrary amount $dx^{\S}$ the actual distance of $x^{\S}$ from x_o on the x-axis, the size of $\Delta x^{\S}$ changes as well so that $d\Delta x^{\S}/dx^{\S} = 1$, i.e. $d\Delta x^{\S} = dx^{\S}$. This implicitly means that the range $\Delta x^{\S}$ overlaps to, i.e. coincides with, the reference x-axis. Thus the delocalization motion of the particle lies by definition between the aforesaid boundary coordinates just on this axis, whatever its actual geometry before the measurement process might be. In principle this reasoning holds for any other uncertainty range corresponding to $\Delta x^{\S}$, e.g. the early local energy of a particle delocalized within $\Delta x^{\S}$ could be a function of its local coordinate along the x-axis; however such a local value of energy is inconsequential, being in fact unobservable in lack of n and thus by definition unphysical.

Consider again the aforesaid 1D space range, yet assuming now that a measurement process is being carried out to infer physical information about the particle; as a consequence of the perturbation induced by the observer, the actual correlation of $\Delta x = x - x_o$ with its conjugate range $\Delta p_x = p_x - p_o$ of allowed momenta introduces n too; now, by virtue of eqs. (2,1), these ranges take the physical meaning of space-time uncertainties and concur to define allowed eigenvalues according to the concept of quantum non-reality. Although Δx is still expressed by two arbitrary coordinates on the x-axis, it is no longer defined by these latter only; rather Δx is defined taking into account also its correlation with Δp_x through n. In other words eqs. (2,1) compel regarding the change of x, whatever it might be, related to that of Δp_x; this does not contradict the concept of arbitrariness of the ranges so far assumed, as x remains in fact arbitrary like Δp_x itself and unknown like the function $x(\Delta p_x)$ correlating them. Yet, when calculating $d\Delta x/dx$ with the condition $\Delta x \Delta p_x = n\hbar$, we ob-

tain in general $d\Delta x/dx = -(n\hbar)^{-1}\Delta x^2 d\Delta p_x/dx \neq 1$.

To summarize, $\Delta x^{\S}$ and Δx have not only different sizes but also different physical meaning, i.e. the former is mere precursor of the latter: before the measurement process $\Delta x^{\S}$ overlapped to the x-axis and had mere space character, the early path length of the particle lay on the reference axis, i.e. $d\Delta x^{\S} = dx^{\S}$; after the measurement process $\Delta x^{\S}$ shrinks into the new Δx such that in general $d\Delta x \neq dx$, thus no longer coincident with the x-axis and with space-time character. In this way the measurement process triggers the space-time uncertainty, the space-time curvature and the allowed eigenvalues as well.

Let us visualize for clarity why the transition from space to space-time also entails curved Gaussian coordinates as a consequence of the interaction of the particle with the observer. If $\Delta x^{\S}$ shrinks to Δx, then the early boundary coordinates of the former must somehow approach each other to fit the smaller size of the latter; thus the measurement driven contraction pushes for instance $x^{\S}$ towards a new x closer to x_o along the reference axis previously coinciding with the space range $\Delta x^{\S}$ and its possible $dx^{\S}$. So, after shrinking, $\Delta x^{\S}$ turns into a new bowed space-time range, Δx, forcedly decoupled from the reference x-axis because of its acquired curvature, whence $dx \neq dx^{\S}$ as well. If length of the x-axis and size of the uncertainty range physically allowed to delocalize the particle do no longer coincide, the particle that moves between x_o and x follows actually a bowed path reproducing the new curvature of Δx, no longer that possibly owned by the 1D reference system itself, whence the curvature of the 2D space-time uncertainty range.

This is possible because nothing is known about the actual motion of the particle between the boundary coordinates x_o and x of the reference x-axis; moreover it is also possible to say that the new curvature is due to the presence of a mass in $\Delta x^{\S}$, as in lack of a particle to be observed the reasoning on the measurement process would be itself a non-sense.

The last remark suggests correctly that the space-time is actually flat in the absence of matter, as expected from the original Einstein hypothesis, so is seemingly tricky the previous specification that even the early $\Delta x^{\S}$ could even owe a possible curvature coincident with that of the x-reference axis; this specification, although redundant, was deliberately introduced to reaffirm the impossibility and uselessness of hypotheses on the uncertainty ranges and to avoid confusion between arbitrariness of the uncertainty ranges and Einstein's hypothesis.

Eventually, the probabilistic character of the shrinking of delocalization range, emphasized in [9], guarantees the probabilistic nature of the origin of space-time and its curvature. Indeed all above is strictly related to the time uncertainty: a time range Δt is inevitably necessary to carry out the measurement process during which $\Delta x^{\S}$ and $\Delta p_x^{\S}$ collapse into Δx and Δp_x.

As found in the previous section, the correlation of the range deformation with the time involves change of momentum of the particle within Δp_x, i.e. the rising of a force component as previously explained. This reasoning therefore collects together four concepts: (i) introduces the space-time as a consequence of the measurement process starting from an unphysical state of the particle in a mere space range and in an unrelated momentum range, both not compliant separately with observable eigenvalues; (ii) introduces the non-reality into the space-time curvature, triggered by the measurement process; (iii) links a force field to this curvature by consequence of the measurement process; (iv) introduces the uncertainty into the concepts of flat space and curved space-time: the former is replaced by the idea of an early space uncertainty range where is delocalized the particle coincident with the coordinate axis, whatever its actual geometry might be; the latter is replaced by the idea of early geometry modified by the additional curvature acquired by the new Δx with respect to that possibly owned by the x-axis during their decoupling. Of course just this additional curvature triggered by the measurement process on the particle present in $\Delta x^{\S}$ is anyway that experimentally measurable.

In conclusion, the measurement process not only generates the quantum eigenvalues of the particle, and thus its observable properties described by their number of allowed states, but also introduces the space-time inherent eqs. (2,1) concurrently with new size and curvature with respect to the precursor space delocalization range. Hence the particle is effectively confined between x_o and x during the time range Δt; yet, in the 2D feature of the present discussion, it moves outside the reference axis. Actually these conclusions have been already inferred in eqs. (4,3); it is enough to identify $\Delta x^{\S}$ with the previous Δx_D for $n = 0$ to find all concepts so far described.

Note that the existence of a curved space-time was not explicitly mentioned in section 3, in particular when calculating the orbital and spin angular momenta or hydrogenlike energy in subsection 3.3, simply because it was unnecessary and inconsequential: the eigenvalues do not depend on the properties of the uncertainty ranges, e.g. on their sizes and possible curvature, nor on the random values of local dynamical variables therein defined. To evidence either chance of flat or curved space-time uncertainty, the next sub-section 4.3.2 describes the simulation of a specific physical experiment, the light beam bending in the presence of a gravitational mass, whose outcome effectively depends on the kind of path followed by the particle.

This "operative" aspect of the model is indeed legitimate now; after having introduced the basic requirements of special and general relativity and a possible explanation of the space-time curvature, we are ready to check whether or not some significant outcomes of general relativity can be effectively obtained in the conceptual frame of eqs. (2,1) through the positions (2,2) only. Once again, the essential requirement to merge relativity and quantum mechanics is to regard

the deterministic intervals of the former as the quantum uncertainty ranges of the latter.

4.3 Some outcomes of general relativity

Before proceeding on, it is useful a preliminary remark. Despite the conceptual consistency of eqs. (2,1) with the special relativity, extending an analogous approach to the general relativity seems apparently difficult.

Consider for instance the time dilation and the red shift in the presence of a stationary gravitational potential φ. As it is known, the general relativity achieves the former result putting $dx^1 = dx^2 = dx^3 = 0$ in the interval $-ds^2 = g_{ik}dx^i dx^k$; calculating the proper time in a given point of space as $\tau = c^{-1}\int \sqrt{-g_{00}}dx^0$, the integration yields $\tau = c^{-1}x^0\sqrt{1+2\varphi/c^2}$, i.e. $\tau = c^{-1}x^0(1+\varphi/c^2)$.

In an analogous way is calculated the red shift $\Delta\omega = c^{-2}\omega\Delta\varphi$ between two different points of space where exists a gap $\Delta\varphi$ of gravitational potential φ. Are the ranges of eqs. (2,1) alone suitable and enough to find similar results once having discarded the local conjugate variables?

Appears encouraging in this respect the chance of having obtained as corollaries the fundamental statements of special and general relativity. Moreover is also encouraging the fact that some qualitative hints highlight reasonable consequences of eqs. (2,1).

Put $m' = \hbar\omega/c^2$ to describe a system formed by a photon in the gravity field of the mass m; thus $\Delta\dot{p}_x = F$ of eq (4,1) is now specified as the momentum change of the photon because of the force component F due to m acting on m'. Since the photon moves in the vacuum at constant velocity c there are two possibilities in this respect: the photon changes its wavelength or its propagation direction.

These chances correspond to two relevant outcomes of general relativity, i.e. the red shift and the light beam bending in the presence of a gravity field; the former occurs when the initial propagation direction of the photon coincides with the x-axis along which is defined the force component $\Delta\dot{p}_x$, i.e. radial displacement, the latter when the photon propagates along any different direction. The bending effect is of course closely related to the previous considerations about the actual curvature of the space-time uncertainty range that makes observable the path of the photon; this means that in fact the deflection of the light beam replicates the actual profile of Δx with respect to the x-axis.

Eventually, also the perihelion precession of orbiting bodies is to be expected because of non-Newtonian terms in eq (4,2); it is known indeed that the mere gravitational potential of Newton law allows closed trajectories only [12].

From a qualitative point of view, therefore, it seems that the results of general relativity should be accessible also in the frame of the present theoretical approach. It is necessary however to explain in detail how the way of reasoning early introduced by Einstein is replaced here to extend the previous results of special relativity. The following subsections aim to show how to discuss the curvature of the space-time uncertainty range and then how to describe time dilation, red shift and light beam bending exploiting uniquely the uncertainty ranges of eqs. (2,1) only, exactly as done at the beginning of section 3.

4.3.1 The time dilation and the red shift

Infer from eqs. (2,1) $\Delta x\Delta p_x/\Delta t = n\hbar/\Delta t$, which also reads $m\Delta x\Delta v_x/\Delta t = n\hbar/\Delta t$. Holds also here the remark introduced about eqs. (4,1), i.e. the particular boundary values of p_o and p_x determining the size of the momentum range $\Delta p_x = p_x - p_o$ are arbitrary, not specifiable in principle and indeed never specified; therefore, since neither p_o nor p_x need being calculated, the actual expression of local momentum is here inessential. So, merely exploiting the physical dimensions of momentum, it is possible to replace Δp_x with $m\Delta v_x$ and write $m\Delta v_x\Delta x/\Delta t = n\hbar/\Delta t$, whatever Δv_x and m might in fact be. Hence, the energy at right hand side can be defined as follows

$$m\varphi_x = -\frac{n\hbar}{\Delta t}, \qquad \varphi_x = -\Delta x\frac{\Delta v_x}{\Delta t}, \qquad \varphi_x < 0. \quad (4,4)$$

Being the range sizes positive by definition, φ_x has been intentionally introduced in the first equation with the negative sign in order that $m\varphi_x = -\Delta\varepsilon$ correspond to an attractive force component $F = -\Delta\varepsilon/\Delta x$ of the same kind of the Newton force, in agreement with the conceptual frame of relativity. Also, φ_x does not require specifying any velocity because for the following considerations is significant its definition as a function of Δv_x only. This result can be handled in two ways.

In the first way, the first eq. (4,4) is rewritten as follows

$$-\frac{\hbar}{\Delta t} = \varepsilon\frac{\varphi_x}{c^2}, \qquad \varepsilon = (m/n)c^2, \quad (4,5)$$

in which case one finds

$$\frac{\Delta t - t_o}{\Delta t} = 1 + \frac{\varphi_x}{c^2}, \qquad \frac{\hbar}{\varepsilon} = t_o,$$

$$\frac{m\varphi_x}{\Delta x} = -m\frac{\Delta v_x}{\Delta t} = -F_N. \quad (4,6)$$

Note that t_o is a proper time of the particle, because it is defined through the energy of this latter. In this case the number n is unessential and could have been omitted: being the mass m arbitrary, m/n is a new mass arbitrary as well. The third result defines φ_x as a function of the expected Newton force component F_N; hence φ_x corresponds classically to a gravitational potential. The first equation is interesting: it correlates through φ_x the time ranges $\Delta t' = \Delta t - t_o$ and Δt. Note that if $\varphi_x \to 0$ then $\Delta t \to \infty$ according to eqs. (4,4) or (4,5), i.e. $\Delta t' \to \Delta t$; hence the gravitational potential φ_x provides a relativistic correction of Δt, which indeed decreases to $\Delta t'$ for $\varphi_x \neq 0$. Eq. (4,6) is thus just the known

expression $\tau = (x_0/c)(1+\varphi_x/c^2)$ previously reported once replacing $\tau/(c^{-1}x_0)$ with $\Delta t'/\Delta t$; indeed in the present approach the local quantities are disregarded and replaced by the corresponding ranges of values. The first eq (4,6) shows that time slowing down $\Delta t - t_o$ occurs in the presence of a gravitational potential with respect to Δt pertinent to $\varphi_x = 0$.

The second way to handle eqs. (4,4) consists of considering two different values of φ_x at its right hand side and a particle that climbs the radial gap corresponding to the respective values of gravitational potential with respect to the origin of an arbitrary reference system; moreover, being ε constant by definition because t_o is fixed, the proper times of the particle t_1 and t_2 define the corresponding time ranges Δt_1 and Δt_2 necessary for the particle to reach the given radial distances. So eqs. (4,5) yield with obvious meaning of symbols

$$-\frac{\hbar/\varepsilon}{\Delta t^{(1)}} = \frac{\varphi_x^{(1)}}{c^2} \qquad -\frac{\hbar/\varepsilon}{\Delta t^{(2)}} = \frac{\varphi_x^{(2)}}{c^2}.$$

Hence, putting $\omega = \Delta t^{-1}$, one finds

$$\frac{\omega_1 - \omega_2}{\omega_o} = \frac{\varphi_x^{(2)} - \varphi_x^{(1)}}{c^2}, \qquad \omega_o = \frac{\varepsilon}{\hbar}. \tag{4,7}$$

Here ω_o is the proper frequency of the free photon with respect to which are calculated ω_1 and ω_2 at the respective radial distances. This expression yields the frequency change between two radial distances as a function of ω_o

$$\Delta\omega = \frac{\Delta\varphi_x}{c^2}\omega_o.$$

Since φ_x is negative, the sign of $\Delta\omega$ is opposite to that of $\Delta\varphi_x$: if $\varphi_x^{(2)}$ is stronger than $\varphi_x^{(1)}$, then $\varphi_x^{(2)} - \varphi_x^{(1)} < 0$, which means that $\omega_2 > \omega_1$. One finds the well known expression of the red shift occurring for decreasing values of gravitational potential. We have inferred two famous result of general relativity through uncertainty ranges only. Now we can effectively regard these results as outcomes of quantum relativity.

4.3.2 The light beam bending

Rewrite eq (4,2) as $F_N\Delta x/(\hbar\omega/c^2) = -Gm/\Delta x$; here F_N is due to the mass m acting along the x direction on a photon having frequency ω and traveling along an arbitrary direction; the notation emphasizes that the photon energy $\hbar\omega/c^2$ replaces the mass of a particle in the gravity field of m. The distance between photon and m is of course included within Δx. Introduce with the help of eq (4,4) the gravitational potential $\varphi_x = -F_N\Delta x/m$, so that $\varphi_x/c^2 = Gm/(c^2\Delta x)$. Now it is possible to define the beam deflection through φ_x, according to the idea that the beam bending is due just to the gravitational potential; we already know why this effect is to be in fact expected. Of course, having discarded the local coordinates, the reasoning of Einstein cannot be followed here; yet since $\delta\phi = \delta\phi(\varphi_x)$, with notation that emphasizes the dependence of the bending angle $\delta\phi$ of the photon upon the field φ_x, it is certainly possible to express the former as series development of the latter, i.e. $\delta\phi = \alpha + \beta(\varphi_x/c^2) + \gamma(\varphi_x/c^2)^2 + \cdots$; α, β and γ are coefficients to be determined. Clearly $\alpha = 0$ because $\delta\phi = 0$ for $m = 0$, i.e. there is no bending effect; so

$$\delta\phi \approx \frac{Gm\beta}{c^2\Delta x}, \qquad \frac{Gm}{c^2\Delta x} \approx \frac{-\beta + \sqrt{\beta^2 + 4\gamma\delta\phi}}{2\gamma}. \tag{4,8}$$

The former expression is simpler but more approximate than the latter, because it account for one term of the series development of $\delta\phi(\varphi_x)$ only; the latter calculates instead φ_x as a function of $\delta\phi$ at the second order approximation for reasons that will appear below. Consider first the former expression and note that even in lack of local coordinates the deflection can be expressed as the angle between the tangents to the actual photon path at two arbitrary ordinates y_- and y_+ along its way: i.e., whatever the path of the photon might be, we can figure m somewhere on the x-axis and the photon coming from $-\infty$, crossing somewhere the x axis at any distance within Δx from m and then continuing a bent trajectory towards $+\infty$. Let the abscissas of the arbitrary points y_- and y_+ on the x-axis be at distances Δx_- and Δx_+ from m; the tangents to these points cross somewhere and define thus an angle $\delta\phi'$. The sought total deflection $\delta\phi$ of the photon corresponds thus to the asymptotic tangents for y_- and y_+ tending to $-\infty$ and ∞. Note now that the same reasoning holds also for a reversed path, i.e. for the photon coming from infinity and traveling towards minus infinity; the intrinsic uncertainty affecting these indistinguishable and identically allowed chances suggests therefore a boundary condition to calculate the change of photon momentum h/λ during its gravitational interaction with the mass. The impossibility of distinguishing either chance requires defining the total momentum range of the photon as $\Delta p = h/\lambda - (-h/\lambda) = 2h/\lambda$, i.e. $\Delta p = (2/c)\hbar\omega$. Since the momentum change depends on $c/2$, and so also the interaction strength $\Delta p/\Delta t$ corresponding to F_N, it is reasonable to assume that even $\delta\phi$ should depend on $c/2$; so putting $\beta = 4$ in the former expression of $\delta\phi$ and noting that the maximum deflection angle calculated for $y_- \to -\infty$ and $y_+ \to +\infty$ corresponds to the minimum distance range Δx, one finds the well known result

$$\delta\phi \approx \frac{4Gm}{c^2\Delta x_{\min}}.$$

The numerical factor 4 appears thus to be the fingerprint of the quantum uncertainty, whereas the minimum approach distance of the Einstein formula is of course replaced here by its corresponding uncertainty range $\Delta x_{\min}$. It is also interesting to consider the second equation (4,8), which can be identically rewritten as follows putting $\gamma = \gamma'\beta$ and again $\beta = 4$ to be consistent with the previous result as a particular case; so

$$\rho = \frac{\sqrt{1+\gamma'\delta\phi} - 1}{\gamma'}, \qquad \rho = \frac{r_{S\,chw}}{\Delta x_{\min}}, \qquad r_{S\,chw} = \frac{2Gm}{c^2},$$

with the necessary convergence condition of the series that reads $\left|\gamma'\varphi_x/c^2\right| < 1$ and requires

$$\frac{\sqrt{1+\gamma'\delta\phi}-1}{2} < 1.$$

This condition requires $-\delta\phi^{-1} \leq \gamma' < 8\delta\phi^{-1}$, and therefore $r_{Schw}\delta\phi^{-1} \leq \Delta x_{\min} < 4r_{Schw}\delta\phi^{-1}$. Replace in this result $\delta\phi = \pi$ and consider what happens when a photon approaches m at distances r_{bh} between $\pi^{-1}r_{Schw} < r_{bh} < 4\pi^{-1}r_{Schw}$: (i) the photon arrives from $-\infty$ and makes half a turn around m; (ii) after this one half turn it reaches a position diametrically opposite to that of the previous step; (iii) at this point the photon is still in the situation of the step (i), i.e. regardless of its provenience it can make a further half a turn, and so on. In other words, once arriving at distances of the order of $2Gm/c^2$ from m the photon starts orbiting without possibility of escaping; in this situation m behaves as a black body. Here the event horizon turns actually into a range of event horizons, i.e. into a shell surrounding m about $\sim 3\pi^{-1}r_{Schw}$ thick where the gravitational trapping is allowed to occur; this result could be reasonably expected because no particle, even the photon, can be exactly localized at some deterministic distance from an assigned point of space-time, i.e. the event horizon is replaced by a range of event horizons. Note however that the reasoning can be repeated also imposing $\delta\phi = 2\pi$ and, more in general, $\delta\phi = 2j\pi$ where j describe the number of turns of the photon around m. In principle the reasoning is the same as before, i.e. after j revolutions required by $\delta\phi$ the photon is allowed to continue again further tours; yet now trivial calculations yield $(j\pi)^{-1}r_{Schw} < r_{bh} < 4(j\pi)^{-1}r_{Schw}$. At increasing j the shell allowing the turns of the photon becomes thinner and thinner while becoming closer and closer to m. As concerns the ideal extrapolation of this result to approach distances $r_{bh} < \pi^{-1}r_{Schw}$ one can guess for $j \to \infty$ the chance of photons to spiral down and asymptotically fall directly on m without a stable orbiting behavior.

4.3.3 The Kepler problem and the gravitational waves

The problem of perihelion precession of planets is too long to be repeated here even in abbreviated form. It has been fully concerned in a paper preliminarily submitted as preprint [13]. We only note here how this problem is handled in the frame of the present model. It is known that the precession is not explained in the frame of classical mechanics. If the potential energy has the form $-\alpha/r$ the planet follows a closed trajectory; it is necessary a form of potential energy like $\alpha/r + \delta U$ to describe the perihelion precession. The Newton law entails the former kind of potential energy, but does not justifies the correction term δU. In our case, however, we have found the Newton law as a particular case of a more general force containing additional terms, eq (4,2); thanks to these latter, therefore, it is reasonable to expect that the additional potential term enables the perihelion precession to be described. Also in this case the formula obtained via quantum uncertainty ranges coincides with the early Einstein formula. The same holds for the problem of the gravitational waves, also concerned together with some cosmological considerations in the quoted preprint. Both results compel regarding once again the intervals of relativity as uncertainty ranges.

4.3.4 Preliminary considerations on eqs. (4,3)

This subsection introduces preliminary order of magnitude estimates on the propagation wave corresponding to the mass $\mu = \hbar/D$; the ± sign is omitted because the following considerations concern the absolute value of μ only.

Consider a wave with two nodes at a diametric distance d_u on a sphere simulating the size of universe; the first harmonic has then wavelength $\lambda_u = 2d_u$. Let the propagation rate v of such a wave be so close to c, as shown below, that for brevity and computational purposes only the following estimates are carried out replacing directly v with c. Guess the quantities that can be inferred from D by means of elementary considerations on its physical dimensions in a reference system R fixed on the center of the whole universe. Calculate D as λ_u times c, i.e. $D = 2d_u c$, and define τ as $\sqrt{D\tau} = d_u/2$, i.e. as the time elapsed for μ to cover the radial distance of the universe; so τ describes the growth of the universe from a size ideally tending to zero at the instant of the big-bang to the current radius $\sqrt{D\tau}$. Since $\lambda_u = 0$ at $\tau = 0$ and $\lambda_u = 2d_u$ at the current time τ, then $d_u = 8c\tau$ and $D = 16c^2\tau$. Moreover, considering that G times mass corresponds to D times velocity, guess that $m_u = 16c^3\tau/G$ introduces the mass m_u to which correspond the rest energy $\varepsilon_u = 16c^5\tau/G$ and rest energy density $\eta_u = 3c^2/(16\pi G\tau^2)$ calculated in the volume $V_u = 4\pi(d_u/2)^3/3$ of the universe. Also, the frequency $\omega_\mu = \xi c^2/D$ of the μ-wave defines the zero point energy

$$\varepsilon_{zp} = \hbar\omega_\mu/2 = \mu' c^2/2 \qquad \mu' = \xi\mu$$

of oscillation of μ; the proportionality constant ξ will be justified below. At right hand side appears the kinetic energy of the corpuscle corresponding to $\hbar\omega_\mu/2$, in agreement with the mere kinetic character of the zero point energy. Note that with trivial manipulations $D = 16c^2\tau$ reads also in both forms

$$\frac{\hbar^2}{2\mu(d_u/2)^2} = \frac{\hbar}{2\tau} \qquad \lambda_\mu = d_u/2 = \frac{\hbar}{\mu c} \qquad (4,9)$$

The left hand side of the first equation yields ε_{zp} of the μ-corpuscle, also calculable from $\Delta p_{zp}^2/2\mu$ i.e. $\hbar^2/2\mu\Delta x_{zp}^2$ replacing Δx_{zp} with $d_u/2$; this means that the momentum of a free unbounded particle initially equal to an arbitrary value p_1 increases to p_2 after confinement in a range Δx_{zp}, whence the conjugate range $\Delta p_{zp} = p_2 - p_1$. Equating this result to $\mu c^2/2$ one finds the second equation, which shows that the Compton length of the μ-particle is the universe radius. Also $\hbar/2\tau$

must describe a zero point energy; this compels introducing the frequency $\omega_u = 1/\tau$ so that it reads $\hbar\omega_u/2$.

Define now the ratio $\sigma_\mu = \mu D/\mathrm{V}_\mu\omega_\mu$ to express the linear density of μ as a function of its characteristic volume V_μ and length $\Delta x_\mu = \mathrm{V}_\mu\omega_\mu/D$: since the squared length inherent D concerns by definition a surface crossed by the particle per unit time, Δx_μ lies along the propagation direction of μ. This way of defining $\sigma_\mu = \mu/\Delta x_\mu$ is thus useful to calculate the propagation velocity of the μ-wave exploiting the analogy with the string under tension T; so $v = \sqrt{T/\sigma_\mu}$ yields $T = \hbar c^2/\mathrm{V}_\mu\omega_\mu$, which in fact regards the volume V_μ as a physical property of the mass μ. This expression of T appears reasonable recalling that μ is defined by the ratio $\Delta\dot{x}\Delta\ddot{x}^{-1}\Delta x^{-2}$ of uncertainty ranges, which supports the idea of calculating its mass linear density within the space-time uncertainty range Δx_μ that defines σ_μ through V_μ. Consider that also the ratio v^2/G has the dimension of mass/length; replacing again v with c we obtain $c^2 = TG/c^2$, i.e. the tension of the string corresponds to a value of F of eqs. (4,3) of the order of the Planck force acting on μ; so, comparing with the previous expression of T, one infers $\mathrm{V}_\mu \approx \hbar G/\omega_\mu c^2$, i.e. $\mathrm{V}_\mu \approx \hbar DG/c^4$. Thus V_μ has a real physical identity defined by the fundamental constants of nature and specified to the present problem by ω_μ^{-1}.

Before commenting this point, let us show that the actual propagation velocity of the μ-wave is very close to c. Exploit the wave and corpuscle formulae of the momentum of μ putting $h/\lambda_u = \mu v/\sqrt{1-(v/c)^2}$ i.e. $2\pi\sqrt{1-(v/c)^2} = (v/c)$; then $v \approx 0.99c$ justifies the expressions inferred above, whereas $\varepsilon_\mu = \mu c^2/\sqrt{1-(v/c)^2}$ is about 6.4 times the rest value μc^2. Call ξ this kinetic correction factor. In principle all expressions where appears explicitly μ still hold, replacing however this latter with $\mu' = \xi\mu$ as done before; it explains why ω_μ has been defined just via ξ. This is also true for $\varepsilon'_\mu = \mu' c^2$, for $\varepsilon'_{zp} = \varepsilon_{zp}(\mu')$ and for the effective Compton length λ'_μ, which result therefore slightly smaller than $d_u/2$ because it is the Loretz contraction of the proper length λ_μ, but not for ω_u, whose value is fixed by τ and d_u. Indeed at this point is intuitive to regard τ as a time parameter as a function of which are calculated all quantities hitherto introduced.

Before considering this problem let us introduce the particular value of τ equal to the estimated age of our universe, commonly acknowledged as about 4×10^{17}s; this yields the following today's time figures:

$$d_u = 9.6\times10^{26}\mathrm{m}, \qquad m_u = 2.6\times10^{54}\mathrm{kg},$$
$$\omega_u = 2.5\times10^{-18}\mathrm{s}^{-1}, \qquad \varepsilon_u = 2.3\times10^{71}\mathrm{J},$$
$$\eta_u = 5.0\times10^{-10}\mathrm{Jm}^{-3}, \qquad \hbar\omega_u/2 = 1.3\times10^{-52}\mathrm{J},$$

and also

$$D = 5.8\times10^{35}\mathrm{m}^2\mathrm{s}^{-1}, \qquad \omega_\mu = 9.9\times10^{-19}\mathrm{s}^{-1},$$
$$\mu = 1.8\cdot10^{-70}\mathrm{kg}, \qquad \mu' = 1.2\times10^{-69}\mathrm{kg},$$
$$\varepsilon'_\mu \approx 1.0\times10^{-52}\mathrm{J}, \qquad \hbar\omega_\mu/2 = 5.2\times10^{-53}\mathrm{J}.$$

It is interesting the fact that the results split into two groups of values: the quantities with the subscript u do not contain explicitly μ and are in fact unrelated to D, ω_μ and ε_μ. Are easily recognized the diameter d_u and the mass m_u of matter in the universe, which support the idea that just the dynamics of the universe, i.e. $\Delta\dot{x}$ and $\Delta\ddot{x}$, concur together with its size, i.e. Δx, to the mass in it present.

This was indeed the main aim of these estimates. The average rest mass density m_u/V_u is about $5.6\times10^{-27}\mathrm{Kg/m}^3$. Is certainly underestimated the actual energy ε_u, here calculated without the kinetic Lorentz factor taking into account the dynamic behavior of m_u, i.e. the average velocity of the masses in the universe; ε_u and thus η_u are expected slightly greater than the quoted values. However this correction factor can be neglected for the present purposes because it would be of the order of a few % only at the ordinary speed with which moves the matter. The order of magnitude of the energy density η_u, of interest here, is close to that expected for the average vacuum energy density η_{vac}; it suggests $\eta_u = \eta_{vac}$, i.e. the idea that matter and vacuum are a system at or near to the dynamic equilibrium based on creation and annihilation of virtual particles and antiparticles. This way of linking the energy densities of μ and matter/vacuum emphasizes that the dynamic of the universe, regarded as a whole system, concerns necessarily its total size and life time; this clearly appears in eqs. (4,9) and is not surprising, since μ is consequence itself of the space-time evolution $\Delta\dot{x}\Delta\ddot{x}^{-1}\Delta x^{-2}$ of the universe.

Note now the large gap between the values of μ and m_u: this is because the former is explicit function of D, the latter does not although inferred in the frame of the same reasoning. Despite the different values and analytical form that reveal their different physical nature, a conceptual link is therefore to be expected between them. Let the characteristic volume V_μ be such that $\varepsilon'_{zp}/\mathrm{V}_\mu = \eta_{vac} = \eta_u$, which requires $\mathrm{V}_\mu = 8\pi G\tau^2\mu'/3$. This means that the universe evolves keeping the average energy density due to the ordinary matter, η_u, in equilibrium with that of the vacuum, η_{vac}, in turn triggered by the zero point energy density of μ' delocalized in it: in this way both η_{vac} and η_u result related to the early big-bang energy and subsequent dynamics of the universe described by μ. To verify this idea, get some numbers: $\mathrm{V}_\mu = 8\pi G\tau^2\mu'/3$ results about $1.0\times10^{-43}\mathrm{m}^3$, whereas $\mathrm{V}_\mu = \hbar G/\omega_\mu c^2$ yields the reasonably similar value $7.9\times10^{-44}\mathrm{m}^3$. Moreover there is a further significant way to calculate V_μ. Define the volume $V_\mu = \pi(d_u/2)^2\Delta x_\mu$ and rewrite identically $\Delta x_\mu = \hbar G/Dc^2$, having put T just equal to the Planck force; one finds $V_\mu = \pi\hbar G\tau/c^2$ i.e. $V_\mu = 9.8\times10^{-44}\mathrm{m}^3$ that agrees with the previous values although it does not depend on μ and thus on the correction factor ξ. In other words, ξ could have been also calculated in order that ω and μ' fit this last value of V_μ; of course the result would agree with the relativistic wave/corpuscle behavior of μ.

These outcomes confirm the consistency of the ways to calculate V_μ and the physical meaning of μ', in particular the considerations about T. Yet the most intriguing result is that the size of V_μ also comes from a very large number, the area of a diametric cross section of the universe, times an extremely small number, the thickness $\Delta x_\mu = 8.6 \times 10^{-97}$m used to calculate the linear density σ_μ and thus T. Of course any diametric section is indistinguishable from and thus physically unidentifiable with any other section, otherwise should exist some privileged direction in the universe; so the volume V_μ, whatever its geometrical meaning might be, must be regarded as permeating all universe, in agreement with the concept of delocalization required by eqs. (2,1).

Despite $\mu' c^2/2$ is a very small energy, its corresponding energy density accounts in fact for that of the vacuum because of the tiny value of V_μ. Compare this estimate with that of $m_u c^2$ intuitively regarded in the total volume V_u of the universe: so as V_u is the characteristic volume of ordinary matter, likewise V_μ is the characteristic volume of μ i.e. a sort of effective physical size of this latter. Since $\mu' > \mu$, the first eq (4,9) includes in V_μ an excess of zero point energy with respect to that previously calculated with μ'; just for this reason indeed $\hbar\omega_u/2 > \hbar\omega'_\mu/2$. The previous expressions of ε'_{zp} account for the actual kinetic mass μ' by replacing the rest mass μ. Yet in the first eq (4,9) this is not possible because τ, once fixed, is consistent with μ and not with μ'. The simplest idea to explain this discrepancy is that actually $\hbar/2\tau$ accounts for two forms of energy: the zero point energy, which can be nothing else but $\xi\mu c^2/2$ previously inferred, plus an extra quantity

$$\delta\varepsilon = \hbar^2\mu^{-1}(d_u/2)^{-2}/2 - \xi\mu c^2/2$$

accounting for the dynamic behavior of both μ-particle and universe. Hence the energy balance per unit volume of universe consists of four terms: η_u, η_{vac}, η_{zp} and $\delta\eta_{zp} = \delta\varepsilon/V_\mu$. The first two terms, equal by hypothesis, are also equal to the third by definition and have been already calculated; $\delta\varepsilon$ amounts to about 7.9×10^{-53}J, so that $\delta\eta_{zp} = 8.7\times10^{-10}$J/m^3. Hence $\delta\eta_{zp}$ is about 64% of $\delta\eta_{zp} + \eta_{vac}$ and about 35% of the total energy density $\delta\eta_{zp} + \eta_{vac} + \eta_u + \eta_{zp} = 2.4 \times 10^{-9}$J/m^3.

The former estimate is particularly interesting because neither η_{vac} nor $\delta\eta_{zp}$ are directly related to the matter present in the universe; rather the picture so far outlined suggests that η_{vac} is related to μ within V_μ randomly delocalized throughout the whole physical size of the universe, whereas the ordinary matter is in turn a local coalescence from the vacuum energy density precursor. This idea explains why $\mu' c^2/V_\mu = 1.1 \times 10^{-9}$Jm^{-3} is twice η_u; actually this result must be intended as $\mu' c^2/V_\mu = \eta_{vac} + \eta_u$. As concerns the negative sign of μ, see eqs. (4,3), note that actually the second eq (4,9) reads $\lambda_\mu = \pm\hbar/\mu c$ and that ξ turns into $-\xi$ replacing v with $-v$; it is easy to realize that this leaves unchanged λ_μ and the quantities that depend on mu', e.g. ω_μ and V_μ, while the universe time τ of eq (4,9) changes its sign. Also σ_μ change its sign, so the tension T must be replaced by $-T$.

The last remark concerns the physical meaning of $\delta\varepsilon$; it is neither vibrational or zero point energy of μ, nor vacuum or matter energy. If so, what then is it? Is it the so called dark energy?

5 Discussion

The discussion of the results starts emphasizing the conceptual path followed in the previous sections to merge relativity and quantum physics via the basic eqs. (2,1). The prerequisites of the present model rest on three outstanding key words: quantization, non-locality, non-reality. Without sharing all three of these features together, the search of a unified theory would be physically unconvincing and intrinsically incomplete. The first result to be noted is that the present model of quantum relativity finds again formulae known since their early Einstein derivation, which indeed agree with the experimental results, although with a physical meaning actually different; instead of deterministic intervals, the relativistic formulae must be regarded as functions of the corresponding uncertainty ranges. On the one side, this coincidence ensures the consistency of the present theoretical model with the experience. On the other side, the sought unification unavoidably compels transferring the acknowledged weirdness of the quantum world to the relativistic phenomena: it requires regarding the intervals and distances likewise the ranges of eqs. (2,1), i.e. as a sort of evanescent entities, undefined and arbitrary, not specified or specifiable by any hypothesis, whose only feature and role rests on their conceptual existence and ability to replace the local dynamical variables, in no way defined and definable too. For instance the invariant interval of special relativity turns into a space-time uncertainty range whose size, whatever it might be, remains effectively unchanged in all inertial reference systems; in other words, this well known concept still holds despite its size is actually indeterminable.

Strictly speaking, it seems understandable that nothing else but an evanescent idea of uncertainty ranges could explain counterintuitive quantum features like the non-reality and non-locality; the former has been described in subsection 4.2 as a consequence of the measurement driven compliance of the eigenvalues with eqs. (2,1), the latter has been related in [9] to the elusiveness of concepts like local distances that hide the ultimate behavior of the matter. The EPR paradox or the dual corpuscle/wave behavior or the actual incompleteness of quantum mechanics testify in fact different appearances of the unique fundamental concept of uncertainty; the approach of sections 3 and 4 is so elementary and straightforward to suggest that the present way of reasoning focuses just on the limited degree of knowledge we can in fact afford, i.e. only on the physical outcome that waives any local information.

Despite this statement represents the most agnostic start-

ing point possible, nevertheless it paradoxically connects quantum theory and relativity in the most profound way expectable: from their basic postulates to their most significant results. In this respect the section 4 shows an alternative conceptual path, less geometrical, towards some relevant outcomes of general relativity: Einstein's way to account for the gravity through the geometrical model of curved spacetime is replaced by simple considerations on the uncertainty ranges of four fundamental dynamical variables of eqs. (2,1). In this way the approach is intrinsically adherent to the quantum mechanics, which rests itself on the same equations. For this reason even the general relativity is compliant with the non-locality and non-reality of the quantum world, as it has been sketched in section 3.

This conclusion seems surprising, because usually the relativity aims to describe large objects on a cosmological scale; yet its features inferred in the present paper can be nothing else but a consequence of quantum properties consistent with well known formulae early conceived for other purposes. A more detailed and complete treatment is exposed in the paper [13], including also the gravitational waves and the perihelion precession of the Kepler problem.

The quantization of the gravity field is regarded as the major task in several relativistic models; although this idea is in principle reductive alone, because also the non-reality and non-locality deserve equal attention, examining the present results this way of thinking appears in fact acceptable. Indeed the number of states n accounts not only for the quantization of the results, as it is obvious, but also for the non-locality and non-reality themselves; as highlighted in [9] the reality and locality of the classical world appear for $n \to \infty$ only, i.e. when n tends to behave like a continuous variable so that the Bell inequality is fulfilled. So it is reasonable to think that the quantization has in effect a hierarchical role predominant on the other quantum properties. Yet this actually happens if n is never exactly specified because of its arbitrariness, thus ensuring the invariancy of eqs. (2,1); its effectiveness in describing both quantum and relativistic worlds appears due indeed to its lack of specific definition and to its twofold meaning of number of states and quantum number. Just this ambivalence is the further feature that remarks the importance of n; on the one side it represents an essential outcome of the quantum mechanics, on the other side it assigns its quantum fingerprint to any macroscopic system necessarily characterized by a number of allowed states. Of course the incompleteness of information governing the quantum world compels an analogous limit to the relativity; yet, without accepting this restriction since the beginning into the sought unified model through eqs. (2,1), the elementary considerations of sections 3 and 4 would rise topmost difficulties in formulating correct outcomes. Moreover, typical ideas of quantum mechanics provide a possible explanation of experiments that involve relativistic concepts. An example in this respect has been proposed in the paper [9] as concerns the possibility of a superluminal velocity under investigation in a recent experiment carried out with neutrinos and still to be confirmed. A relativistic quantum fluctuation hypothesized in the quoted paper appears compatible with a superluminal velocity transient that, just because of its transitory character, can be justified without violating any standard result of the deterministic formulae of early relativity. Other problems are presently under investigation.

Regardless of the results still in progress, seems however significant "per se" the fact itself that the quantum character of the relativistic formulae widens in principle the descriptive applicability of the standard relativity.

Submitted on March 16, 2012 / Accepted on March 21, 2012

References

1. Einstein A., Podolski B., Rosen N. Can quantum mechanics description of Physical Reality be considered Complete? *Physical Review*, 1935, v. 47, 777–780.
2. Polcinski J. String theory, Cambridge University Press, 1998, Cambridge.
3. Green M.B., Schwarz J.H. and Witten E. Superstring Theory, Cambridge University Press, (1987).
4. Carlip S., Quantum gravity: a progress report. *Reports on Progress in Physics*, 2001, v. 64, p. 885.
5. Becker K, Becker M., Schwarz J. String theory and M-Theory: a modern introduction. Cambridge University Press, Cambridge, 2007.
6. Wess J., Bagger J. Supersimmetry and Supergravity, Princeton University Press, Princeton, 1992.
7. Tosto S. An analysis of states in the phase space: the energy levels of quantum systems. *Il Nuovo Cimento B*, 1996, v. 111(2), 193–215.
8. Tosto S. An analysis of states in the phase space: the diatomic molecules. *Il Nuovo Cimento D*, 1996, v. 18(12), 1363–1394.
9. Tosto S. Spooky action at a distance or action at a spooky distance? *Progress in Physics*, 2012, v. 1, 11–26.
10. Tosto S. An analysis of states in the phase space: uncertainty, entropy and diffusion. *Progress in Physics*, 2011, v. 4, 68–78.
11. Landau L., Lifchits E. Theorie du Champ, MIR, Moscow, 1966.
12. Landau L., Lifchits E. Mechanique, MIR Moscow, 1969.
13. Tosto S. An analysis of states in the phase space: from quantum mechanics to general relativity, arXiv gr-qc/0807.1011.

On a Fractional Quantum Potential

Robert Carroll
University of Illinois, Urbana, IL 61801, USA

Fractional quantum potential is considered in connection to the fractal calculus and the scale relativity.

1 Introduction

For fractals we refer to [1, 2] and for differential equations cf. also [3–7]. The theme of scale relativity as in [8–15] provides a profound development of differential calculus involving fractals (cf. also the work of Agop et al in the journal Chaos, Solitons, and Fractals) and for interaction with fractional calculus we mention [6,16–19]. There are also connections with the Riemann zeta function which we do not discuss here (see e.g. [20]). Now the recent paper [21] of Kobelev describes a Leibnitz type fractional derivative and one can relate fractional calculus with fractal structures as in [16, 18, 19, 25] for example. On the other hand scale relativity with Hausdorff dimension 2 is intimately related to the Schrödinger equation (SE) and quantum mechanics (QM) (cf. [12]). We show now that if one can write a meaningful Schrödinger equation with Kobelev derivatives (α-derivatives) then there will be a corresponding fractional quantum potential (QP) (see e.g. [4, 6, 18, 19] for a related fractional equation and recall that the classical wave function for the SE has the form $\psi = R\exp(iS/\hbar)$).

Going now to [21] we recall the Riemann-Liouville (RL) type fractional operator (assumed to exist here)

$$ {}_cD_z^\alpha[f(z)] = \begin{cases} \dfrac{1}{\Gamma(-\alpha)}\displaystyle\int_c^z (z-\zeta)^{-\alpha-1} f(\zeta)d\zeta \\ c \in \mathbf{R},\ Re(\alpha) < 0 \\ \dfrac{d^m}{dz^m}\,{}_cD_z^{\alpha-m}[f(z)] \\ m-1 \le \Re\alpha < m \end{cases} \tag{1.1} $$

(the latter for $m \in \mathbf{N} = \{1, 2, 3, \ldots\}$). For $c = 0$ one writes (**1A**) ${}_0D_z^\alpha[f(z)] = D_z^\alpha[f(z)]$ as in the classical RL operator of order α (or $-\alpha$). Moreover when $c \to \infty$ (1.1) may be identified with the familiar Weyl fractional derivative (or integral) of order α (or $-\alpha$). An ordinary derivative corresponds to $\alpha = 1$ with (**1B**) $(d/dz)[f(z)] = D_z^\alpha[f(z)]$. The binomial Leibnitz rule for derivatives is

$$ D_z^1[f(z)g(z)] = g(z)D_z^1[f(z)] + f(z)D_z^1[g(z)] \tag{1.2} $$

whose extension in terms of RL operators D_z^α has the form

$$ D_z^\alpha[f(z)g(z)] = \sum_{n=0}^{\infty} \binom{\alpha}{n} D_z^{\alpha-n}[f(z)]D_z^n[g(z)]; \tag{1.3} $$

$$ \binom{\alpha}{k} = \frac{\Gamma(\alpha+1)}{\Gamma(\alpha-k+1)\Gamma(k+1)};\ \ \alpha,\, k \in \mathbf{C}. $$

The infinite sum in (1.3) complicates things and the binomial Leibnitz rule of [21] will simplify things enormously. Thus consider first a momomial z^β so that

$$ D_z^\alpha[z^\beta] = \frac{\Gamma(\beta+1)}{\Gamma(\beta-\alpha+1)} z^{\beta-\alpha};\ \ \Re(\alpha) < 0;\ \ \Re(\beta) > -1. \tag{1.4} $$

Thus the RL derivative of z^β is the product

$$ D_z^\alpha[z^\beta] = C^*(\beta,\alpha)z^{\beta-\alpha};\ \ C^*(\beta, ga) = \frac{\Gamma(\beta+1)}{\Gamma(\beta-\alpha+)}. \tag{1.5} $$

Now one considers a new definition of a fractional derivative referred to as an α derivative in the form

$$ \frac{d_\alpha}{dz}[z^\beta] = d_\alpha[z^\beta] = C(\beta,\alpha)z^{\beta-\alpha}. \tag{1.6} $$

This is required to satisfy the Leibnitz rule (1.2) by definition, given suitable conditions on $C(\beta,\alpha)$. Thus first (**1C**) $z^\beta = f(z)g(z)$ with $f(z) = z^{\beta-\epsilon}$ and $g(z) = z^\epsilon$ for arbitrary ϵ the application of (1.3) implies that

$$ \begin{aligned} \frac{d_\alpha}{dz}[z^\beta] &= z^\epsilon \frac{d_\alpha}{dz} z^{\beta-\epsilon} + z^{\beta-\epsilon}\frac{d_\alpha}{dz} z^\epsilon \\ &= z^\epsilon C(\beta-\epsilon,\alpha)z^{\beta-\epsilon-\alpha} + z^{\beta-\epsilon}C(\epsilon,\alpha)z^{\epsilon-\alpha} \\ &= [C(\beta-\epsilon,\alpha) + C(\epsilon,\alpha)]z^{\beta-\alpha}. \end{aligned} \tag{1.7} $$

Comparison of (1.6) and (1.7) yields (**1D**) $C(\beta-\epsilon,\alpha) + C(\epsilon,\alpha) = C(\beta,\alpha)$. To guarantee (1.2) this must be satisfied for any β, ϵ, α. Thus (**1D**) is the basic functional equation and its solution is (**1E**) $C(\beta,\alpha) = A(\alpha)\beta$. Thus for the validity of the Leibnitz rule the α-derivative must be of the form

$$ d_\alpha[z^\beta] = \frac{d_\alpha}{dz}[z^\beta] = A(\alpha)\beta z^{\beta-\alpha}. \tag{1.8} $$

One notes that $C^*(\beta,\alpha)$ in (1.5) is not of the form (**1E**) and the RL operator D_z^α does not in general possess a Leibnitz rule. One can assume now that $A(\alpha)$ is arbitrary and $A(\alpha) = 1$ is chosen. Consequently for any β

$$ \frac{d_\alpha}{dz}z^\beta = \beta z^{\beta-\alpha};\ \ \frac{d_\alpha}{dz}z^\alpha = \alpha;\ \ \frac{d_\alpha}{dz}z^0 = 0. \tag{1.9} $$

Now let K denote an algebraically closed field of characteristic 0 with $K[x]$ the corresponding polynomial ring and

$K(x)$ the field of rational functions. Let $F(z)$ have a Laurent series expansion about 0 of the form

$$\begin{aligned} F(z) &= \sum_{-\infty}^{\infty} c_k z^k; \\ F_+(z) &= \sum_{0}^{\infty} c_k z^k; \\ F_-(z) &= \sum_{-\infty}^{-1} c_k z^k;\ c_k \in K \end{aligned} \tag{1.10}$$

and generally there is a k_0 such that $c_k = 0$ for $k \leq k_0$. The standard ideas of differentiation hold for $F(z)$ and formal power series form a ring $K[[x]]$ with quotient field $K((x))$ (formal Laurent series). One considers now the union (**1F**) $K \ll x \gg = \cup_1^\infty K((x^{1/k}))$. This becomes a field if we set

$$x^{1/1} = x,\ x^{m/n} = (x^{1/n})^m. \tag{1.11}$$

Then $K \ll x \gg$ is called the field of fractional power series or the field of Puiseux series. If $f \in K \ll x \gg$ has the form (**1G**) $f = \sum_{k_o}^{\infty} c_k x^{m_k/n_k}$ where $c_1 \neq 0$ and $m_k, n_k \in \mathbf{N} = \{1, 2, 3, \ldots\}$, $(m_i/n_i) < (m_j/n_j)$ for $i < j$ then the order is (**1H**) $O(f) = m/n$ where $m = m_1$, $n = n_1$ and $f(x) = F(x^{1/n})$. Now given n and z complex we look at functions

$$\begin{aligned} f(z) &= \sum_{-\infty}^{\infty} c_k (z - z_0)^{k/n} = f_+(z) + f_-(z); \\ f_+(z) &= \sum_{0}^{\infty} c_k (z - z_0)^{k/n}, \\ f_-(z) &= \sum_{-\infty}^{-1} c_k (z - z_0)^{k/n};\ c_k = 0\ (k \leq k_0) \end{aligned} \tag{1.12}$$

(cf. [21] for more algebraic information - there are some misprints).

One considers next the α-derivative for a basis (**1I**) $\alpha = m/n;\ 0 < m < n;\ m, n \in \mathbf{N} = \{1, 2, 3, \cdots\}$. The α-derivative of a Puiseux function of order $O(f) = 1/n$ is again a Puiseux function of order $(1 - m)/n$. For $\alpha = 1/n$ we have

$$f_+ = \sum_{0}^{\infty} c_k z^{k/n} = \sum_{0}^{\infty} c_k z^{\beta};\ \beta = \beta(k) = \frac{k}{n} \tag{1.13}$$

leading to

$$\frac{d_\alpha}{dz} f_+(z) = \sum_{1}^{\infty} \alpha\beta c_k z^{(k-1)/n} = \sum_{0}^{\infty} c_{p+1} \alpha\beta z^{p/m}; \tag{1.14}$$

$$\begin{aligned} \frac{d_\alpha}{dz} f_-(z) &= \sum_{-\infty}^{-1} c_k \alpha\beta z^{(k-1)/n} = \sum_{-\infty}^{-2} c_{p+1} \alpha\beta z^{p/n} \\ &= \sum_{-\infty}^{-1} \hat{c}_p z^{p/n};\ \hat{c}_{-1} = 0. \end{aligned}$$

Similar calculations hold for $\alpha = m/n$ (there are numerous typos and errors in indexing in [21] which we don't mention further). The crucial property however is the Leibnitz rule

$$\frac{d_\alpha}{dz}(fg) = g\frac{d_\alpha}{dz} f + f\frac{d_\alpha}{dz} g;\ (d_\alpha \sim \frac{d_\alpha}{dz}) \tag{1.15}$$

which is proved via arguments with Puiseux functions. This leads to the important chain rule

$$\frac{d_\alpha}{dz} F(g_i(z)) = \sum \frac{\partial F}{\partial g_k} \frac{d_\alpha}{dz} g_k(z). \tag{1.16}$$

Further calculation yields (again via use of Puiseux functions)

$$\frac{d_\alpha^m}{dz^m}\left[\frac{d_\alpha^\ell}{dz^\ell} f\right] = \frac{d_\alpha^\ell}{dz^\ell}\left[\frac{d_\alpha^m}{dz^m} f\right], \tag{1.17}$$

$$\int f(z) d_\alpha z = \sum_{0}^{\infty} \int z^\beta d_\alpha z;\ \int z^\beta d_\alpha z = \frac{z^{\beta+\alpha}}{\beta + \alpha}, \tag{1.18}$$

$$\frac{d_\alpha}{dz} \int f(z) d_\alpha z = f(z) = \int \frac{d_\alpha}{dz} d_\alpha z, \tag{1.19}$$

where $d_\alpha z$ here is an integration symbol here).

The α-exponent is defined as

$$\begin{aligned} E_\alpha(z) &= \sum_{0}^{\infty} \frac{(z^\alpha/\alpha)^k}{\Gamma(\alpha + 1)} = \exp\left(\frac{z^\alpha}{\alpha}\right); \\ E_1(z) &= e^z;\ E_\alpha(0) = 1\ (0 < \alpha, 1). \end{aligned} \tag{1.20}$$

The definition is motivated by the fact that $E_\alpha(z)$ satisfies the α-differential equation (**1J**) $(d_\alpha/dz)E_\alpha(z) = E_\alpha(z)$ with $E_\alpha(0) = 1$. This is proved by term to term differentiation of (1.20). It is worth mentioning that $E_\alpha(z)$ does not possess the semigroup property (**1K**) $E_\alpha(z_1 + z_2) \neq E_\alpha(z_1)E_\alpha(z_2)$.

2 Fractals and fractional calculus

For relations between fractals and fractional calculus we refer to [16, 18, 19, 24, 25, 27, 28]. In [16] for example one assumes time and space scale isotropically and writes $[x^\mu] = -1$ for $\mu = 0, 1, \cdots, D - 1$ and the standard measure is replaced by (**2A**) $d^D x \to d\rho(x)$ with $[\rho] = -D\alpha \neq -D$ (note [ ] denotes the engineering dimension in momentum units). Here $0 < \alpha < 1$ is a parameter related to the operational definition of Hausdorff dimension which determines the scaling of a Euclidean volume (or mass distribution) of characteristic size R (i.e. $V(R) \propto R^{d_H}$). Taking $\rho \propto d(r^{D\alpha})$ one has (**2B**) $V(R) \propto \int d\rho_{Euclid}(r) = \propto \int_0^R dr r^{D\alpha - 1} \propto R^{D\alpha}$, showing that $\alpha = d_H/D$. In general as cited in [16] the Hausdorff dimension of a random process (Brownian motin) described by a fractional differintegral is proportional to the order α of the differintegral. The same relation holds for deterministic fractals and in general the fractional differintegration of a curve

changes its Hausdorff dimension as $d_H \to d_H + \alpha$. Moreover integrals on "net fractals" can be approximated by the left sided RL fractional of a function $L(t)$ via

$$\int_0^{\bar{t}} d\rho(t)L(t) \propto {}_0I_{\bar{t}}^{\alpha}L(t) = \frac{1}{\Gamma(t)}\int_0^{\bar{t}} dt(\bar{t}-t)^{\alpha-1}L(t);$$
$$\rho(t) = \frac{\bar{t}^{\alpha}-(\bar{t}-t)^{\alpha}}{\Gamma(\alpha+1)}, \tag{2.1}$$

where α is related to the Hausdorff dimension of the set (cf. [24]). Note that a change of variables $t \to \bar{t} - t$ transforms (2.1) to

$$\frac{1}{\Gamma(\alpha)}\int_0^t dt t^{\alpha-1}L(\bar{t}-t). \tag{2.2}$$

The RL integral above can be mapped into a Weyl integral for $\bar{t} \to \infty$. Assuming $lim_{\bar{t}\to\infty}$ the limit is formal if the Lagrangian L is not autonomous and one assumes therefore that $lim_{\bar{t}\to\infty}L(\bar{t}-t) = L[q(t), \dot{q}(t)]$ (leading to a Stieltjes field theory action). After constructing a "fractional phase space" this analogy confirms the interpretation of the order of the fractional integral as the Hausdorff dimension of the underlying fractal (cf. [18]).

Now for the SE we go to [4, 6, 18, 19]. Thus from [4] (1009.5533) one looks at a Hamiltonian operator

$$H_{\alpha}(p,r) = D_{\alpha}|p|^{\alpha} + V(r)\ (1 < \alpha \leq 2). \tag{2.3}$$

When $\alpha = 2$ one has $D_2 = 1/2m$ which gives the standard Hamiltonian operator (**2C**) $\hat{H}(\hat{p},\hat{r}) = (1/2m)\hat{p}^2 + \hat{V}(\hat{r})$. Thus the fractional QM (FQM) based on the Levy path integral generalizes the standard QM based on the Feynman integral for example. This means that the path integral based on Levy trajectories leads to the fractional SE. For Levy index $\alpha = 2$ the Levy motion becomes Brownian motion so that FQM is well founded. Then via (2.2) one obtains a fractional SE (GSE) in the form

$$i\hbar\partial_t\psi = D_{\alpha}(-\hbar^2\Delta)^{\alpha/2}\psi + V(r)\psi\ \ (1 < \alpha \leq 2) \tag{2.4}$$

with 3D generalization of the fractional quantum Riesz derivative $(-\hbar^2\Delta)^{\alpha/2}$ introduced via

$$(-\hbar^2\Delta)^{\alpha/2}\psi(r,t) = \frac{1}{(2\pi\hbar)^3}\int d^3p e^{\frac{ipr}{\hbar}}|p|^{\alpha}\phi(p,t) \tag{2.5}$$

where ϕ and ψ are Fourier transforms. The 1D FSE has the form

$$i\hbar\partial_t\psi(x,t) = -D_{\alpha}(\hbar\nabla)^{\alpha}\psi + V\psi\ \ (1 < \alpha \leq 2). \tag{2.6}$$

The quantum Riesz fractional derivative is defined via

$$(\hbar\nabla)^{\alpha}\psi(x,t) = -\frac{1}{2pi\hbar}\int_{-\infty}^{\infty} dp\, e^{\frac{ipx}{\hbar}}|p|^{\alpha}\phi(p,t) \tag{2.7}$$

where

$$\phi(p,t) = \int_{-\infty}^{\infty} dx\, e^{\frac{-ixt}{\hbar}}\psi(x,t) \tag{2.8}$$

with the standard inverse. Evidently (2.6) can be written in operator form as (**2D**) $i\hbar\partial_t\psi = H_{\alpha}\psi;\ H_{\alpha} = -D_{\alpha}(\hbar\nabla)^{\alpha} + V(x)$

In [6] (0510099) a different approach is used involving the Caputo derivatives (where ${}_c^+D(x)k = 0$ for $k = constant$. Here for (**2E**) $f(kx) = \sum_0^{\infty} a_n(kx)^{n\alpha}$ one writes ($D \to \bar{D}$)

$${}_c^+f(kx) = k^{\alpha}\sum_0^{\infty} a_{n+1}\frac{\Gamma(1+(n+1)\alpha)}{\Gamma(1+n\alpha)}(kx)^{n\alpha}. \tag{2.9}$$

Next to extend the definition to negative reals one writes

$$x \to \bar{\chi}(x) = sgn(x)|x|^{\alpha};\ \bar{D}(x) = sgn(x)_c^+D(|x|). \tag{2.10}$$

There is a parity transformation Π satisfying (**2F**) $\Pi\bar{\chi}(x) = -\bar{\chi}(x)$ and $\Pi\bar{D}(x) = -\bar{D}(x)$. Then one defines (**2G**) $f(\bar{\chi}(kx)) = \sum_0^{\infty} a_n\bar{\chi}^n(kx)$ with a well defined derivative

$$\bar{D}f(\bar{\chi}(kx)) = sgn(k)|k|^{\alpha}\sum_0^{\infty} a_{n+1}\frac{\Gamma(1+(n+1)\alpha)}{\Gamma(1+n\alpha)}\bar{\chi}^n(kx). \tag{2.11}$$

This leads to a Hamiltonian H^{α} with

$$H^{\alpha} = -\frac{1}{2}mc^2\left(\frac{\hbar}{mc}\right)^{2\alpha}\bar{D}^i\bar{D}_i + V(\hat{X}^1,\ldots,\hat{X}^i,\ldots,\hat{X}^{3N}) \tag{2.12}$$

with a time dependent SE

$$H^{\alpha}\Psi = \left[-\frac{1}{2}mc^2\left(\frac{\hbar}{mc}\right)^{2\alpha}\bar{D}^i\bar{D}_i + V(\hat{X}^1,\ldots,\hat{X}^i,\ldots\hat{X}^{3N})\right]\Psi = i\hbar\partial_t\Psi. \tag{2.13}$$

3 The SE with α-derivative

Now we look at a 1-D SE with α-derivatives $d_{\alpha} \sim d_{\alpha}/dx$ (without motivational physics). We write $d_{\alpha}x^{\beta} = \beta x^{\beta-\alpha}$ as in (1.9) and posit a candidate SE in the form

$$i\hbar\partial_t\psi = D_{\alpha}\hbar^2 d_{\alpha}^2\psi + V(x)\psi. \tag{3.1}$$

In [11, 12] for example (cf. also [29]) one deals with a Schrödinger type equation

$$\mathcal{D}^2\Delta\psi + i\mathcal{D}\partial_t\psi - \frac{\mathcal{W}}{2m}\psi = 0 \tag{3.2}$$

where $\mathcal{D} \sim (\hbar/2m)$ in the quantum situation. Further $\mathcal{D}$ is allowed to have macro values with possible application in biology and cosmology (see Remark 3.1 below).

Consider a possible solution corresponding to $\psi = R\exp(iS/\hbar)$ in the form (**3A**) $\psi = RE_{\alpha}\ (iS/\hbar)$ with E_{α} as in (1.20). Then one has for $S = S(x,t)$ (**3B**) $\psi_t = R_tE_{\alpha} + R\partial_tE_{\alpha}$ and via (1.15)-(1.16)

$$d_{\alpha}\left[RE_{\alpha}\left(\frac{iS}{\hbar}\right)\right] = (d_{\alpha}R)E_{\alpha} + RE_{\alpha}\frac{i}{\hbar}(d_{\alpha}S); \tag{3.3}$$

$$d_\alpha^2\left[RE_\alpha\left(\frac{iS}{\hbar}\right)\right] = (d_\alpha^2 R)E_\alpha + 2(d_\alpha R)E_\alpha\frac{i}{\hbar}d_\alpha S + \\ + RE_\alpha\left(\frac{i}{\hbar}d_\alpha S\right)^2 + RE_\alpha\frac{i}{\hbar}d_\alpha^2 S; \tag{3.4}$$

$$\partial_t E_\alpha(z) = \partial_t\sum_0^\infty\frac{(z^\alpha/\alpha))^k}{\Gamma(k+1}} = \frac{z_t}{\alpha}\sum_1^\infty\frac{(z^\alpha/\alpha)}{\Gamma(k)} = \\ = \frac{z_t}{\alpha}\sum_0^\infty\frac{(z^\alpha/\alpha)^m}{\Gamma(m+1)} = \frac{z_t}{\alpha}E_\alpha. \tag{3.5}$$

Then from (**3B**), (3.4), (3.3), and (3.5) we combine real and imaginary parts in

$$i\hbar\left[R_t E_\alpha + \frac{iS_t}{\alpha\hbar}RE_\alpha\right] = VRE_\alpha + D_\alpha\hbar^2\left[(d_\alpha^2 R)E_\alpha + \right. \\ \left. 2(d_\alpha R)E_\alpha\frac{i}{\hbar}d_\alpha S - \frac{RSE_\alpha}{\hbar^2}(d_\alpha S)^2 + \frac{iRE_\alpha}{\hbar}d_\alpha^2 S\right] \tag{3.6}$$

leading to

$$R_t E_\alpha = -2D_\alpha d_\alpha RE_\alpha(d_\alpha S) - D_\alpha RE_\alpha d_\alpha^2 S; \tag{3.7}$$

$$-\frac{1}{\alpha}S_t RE_\alpha = VRE_\alpha + D_\alpha\hbar^2 d_\alpha^2 RE_\alpha - RE_\alpha(d_\alpha S)^2.$$

Thus E_α cancels and we have

$$R_t = -2D_\alpha(d_\alpha R)(d_\alpha S) - D_\alpha R d_\alpha^2 S; \tag{3.8}$$

$$-\frac{1}{\alpha}S_t R = VR + D_\alpha\hbar^2 d_\alpha^2 R - R(d_\alpha S)^2.$$

Now recall the classical situation here as (cf. [30, 31])

$$S_t + \frac{S_x^2}{2m} + V - \frac{\hbar^2 R''}{2mR} = 0;\ \partial_t(R^2) + \frac{1}{m}(R^2 S')' = 0. \tag{3.9}$$

This gives an obvious comparison:

1. Compare $2RR_t + (1/m)(2RR'S' + R^2 S'') = 0 \sim 2R_t + (1/m)(2R'S' + RS'') = 0$ with $R_t = -2D_\alpha(d_\alpha R)(d_\alpha S) - D_\alpha R d_\alpha^2 S$
2. Compare $S_t + (S_x^2/2m) + V - \frac{\hbar^2 R''}{2mR} = 0$ with $-\frac{1}{\alpha}S_t = V - \frac{D_\alpha\hbar^2 d_\alpha^2 R}{R} + (d_\alpha S)^2$

which leads to

THEOREM 3.1

The assumption (3.1) for a 1-D α-derivative Schrödinger type equation leads to a fractional quantum potential

$$Q_\alpha = -\frac{D_\alpha\hbar^2 d_\alpha^2 R}{R} \tag{3.10}$$

For the classical case with $d_\alpha R \sim R'$ (i.e. $\alpha = 1$) one has $D_\alpha = 1/2m$ and one imagines more generally that $D_\alpha\hbar^2$ may have macro values. ■

REMARK 3.1

We note that the techniques of scale relativity (cf. [11, 12]) lead to quantum mechanics (QM). In the non-relativistic case the fractal Hausdorff dimension $d_H = 2$ arises and one can generate the standard quantum potential (QP) directly (cf. also [29]). The QP turns out to be a critical factor in understanding QM (cf. [30–32, 35–37]) while various macro versions of QM have been suggested in biology, cosmology, etc. (cf. [8, 11, 12, 38, 39]). The sign of the QP serves to distinguish diffusion from an equation with a structure forming energy term (namely QM for $D_\alpha = 1/2m$ and fractal paths of Hausdorff dimension 2). The multi-fractal universe of [16,23] can involve fractional calculus with various degrees α (i.e. fractals of differing Hausdorff dimension). We have shown that, given a physical input for (3.1) with the α-derivative of Kobelev ([21]), the accompanying α-QP could be related to structure formation in the related theory. ■

Submitted on March 24, 2012 / Accepted on March 25, 2012

References

1. Falconer K. The geometry of fractal sets. Cambridge Univ. Press, 1985; Fractal geometry. Wiley, 2003.
2. Mandelbrot B. Fractals and chaos. Springer, 2004.
3. Kigami J. Analysis on fractals. Cambridge Univ. Press, 2001.
4. Laskin N. arXiv: quant-ph/0206098; math-ph/1009.5533.
5. Strichartz R. Differential equations on fractals. Princeton Univ. Press, 2006.
6. Herrmann R. arXiv: math-ph/0510099; physics/0805.3434; Fraktionale Infinitesimalrechnung. BoD, Norderstedt, 2008.
7. Kilbas A., Srivastava H., and Trujillo J. Theory and applications of fractional differential equations. North-Holland, 2006.
8. Auffray C. and Nottale L. *Progress in Biophysics and Molecular Biology*, v. 97, 79 and 115.
9. Celerier M. and Nottale L. *Journal of Physics A*, 2004, v. 37, 931; 2006, v. 39, 12565; 2007, v. 40, 14471; arXiv: hep-th/0112213.
10. Celerier M. and Nottale L. arXiv: physics/0911.2488 and 1009.2934.
11. Nottale L. arXiv: physics/0812.0941, 0812.3857, and 0901.1270; *Chaos, Solitons, and Fractals*, 2005, v. 25, 797–803; 1996, v. 7, 877–938; 1999, v. 10, 459; 1998, v. 9, 1035 and 1043; 2001, v. 12, 1577; 2003, v. 16, 539.
12. Nottale L. Fractal space time and microphysics: Towards a theory of scale relativity. World Scientific, 1993; Scale relativity and fractional space-time. Imperial College Press, 2011.
13. Nottale L. and Celerier M. arXiv: quant-ph/0711.2418.
14. Nottale L., Celerier M., and Lehner T. arXiv: quant-ph/0307093; *Journal of Mathematical Physics*, 2006, v. 47, 032203.
15. Nottale L. and Lehner T. arXiv: quant-ph/0610201.
16. Calcagni G. arXiv: hep-th/0912.3142, 1001.0571, 1012.1244, 1106.0295, 1106.5787, and 1107.5041.
17. El-Nabulsi R. and Torres D. arXiv: math-ph/0702099.
18. Tarasov V. arXiv: nlin.CD/0312044, 0602029, 0602096, and 1107.4205; astro-ph/0604491; physics/1107.5749; *International Journal of Mathematics*, 2007, v. 18, 281–299.
19. Tarasov V. and Zaslavsky G. arXiv: physics/0511144.
20. Le Mehaute A., Nivanen L., El Kaabouchi A., and Wang Q. arXiv: cond-mat/0907.4252.
21. Kobelev V. arXiv: math-ph/1202.2714; *Chaos*, 2006, v. 16, 043117.
22. Rocco A. and West B. arXiv: chao-dyn/9810030.
23. Calcagni G., Gielen S., and Oriti D. arXiv: gr-qc/1201.4151.

24. Ren F., Liang J., Wang X., and Qiu W. *Chaos, Solitons, and Fractals*, 2003, v. 16, 101–117.
25. Rocco A. and West B. arXiv: chao-dyn/810030.
26. Schevchenko V. arXiv: hep-ph/0903.0565.
27. Eyink G. *Communications in Mathematical Physics*, 1989, v. 125, 613–636; 1989, v. 126, 85–101.
28. Yang XiaoJun. arXiv: math-ph/1106.3010.
29. Carroll R. Thermodynamics and scale relativity. arXiv: gr-qc/1110.3059.
30. Carroll R. Fluctuations, information, gravity, and the quantum potential. Springer, 2006.
31. Carroll R. On the quantum potential. Arima Publ., 2007.
32. Carroll R. On the emergence theme of physics. World Scientific, 2010.
33. Carroll R. Quantum Potential as Information: A mathematical survey. In: *New trends in quantum information*, Eds. Felloni, Singh, Licata, and Sakaji, Aracne Editrice, 2010, 155–189.
34. Carroll R. arXiv: math-ph/1007.4744; gr-qc/1010.1732. and 1104.0383
35. Frieden B. Physics from Fisher information. Cambridge Univ. Press, 1998; Science from Fisher information. Springer, 2004.
36. Garbaczewski P. arXiv: cond-mat/0703147, 0811.3856, and 0902.3536; quant-ph/0612151, 0805.1536, and 1112.5962.
37. Grössing G. *Entropy*, 2010, v. 12, 1975–2044.
38. Zak M. *International Journal of Theoretical Physics*, 1992, v. 32, 159–190; 1994, v. 33, 2215–2280; *Chaos, Solitons, and Fractals*, 1998, v. 9, 113–1116; 1999, v. 10, 1583–1620; 2000, v. 11, 2325–2390; 2002, v. 13, 39–41; 2007, v. 32, 1154–1167; 2306; *Physics Letters A*, 1989, v. 133, 18–22, 1999, v. 255, 110–118; *Information Sciences*, 2000, v. 128, 199–215; 2000, v. 129, 61–79; 2004, v. 165, 149–169.
39. Zak M. *International Journal of Theoretical Physics*, 1994, v. 33, 1113–1116; 2000, v. 39, 2107–2140; *Chaos, Solitons, and Fractals*, 2002, v. 14, 745–758; 2004, v. 19, 645–666; 2005, v. 26, 1019–1033, 2006, v. 28, 616–626; 2007, v. 32, 1154–1167; 2007, v. 34, 344–352; 2009, v. 41, 1136–1149 and 2306–2312; 2009, v. 42, 306–315; *Foundation of Physics Letters*, 2002, v. 15, 229–243.

A Model Third Order Phase Transition in Fe – Pnictide Superconductors

Chinedu E. Ekuma and Ephraim O. Chukwuocha

Department of Physics, University of Port Harcourt, PMB 053 Choba, Port Harcourt, Rivers, Nigeria
E-mail: panaceamee@yahoo.com

By identifying the orders of phase transition through the analytic continuation of the functional of the free energy of the Ehrenfest theory, we have developed a theory for studying the dependence of the local magnetic moment, M on the Fe – As layer separation in the third order phase transition regime. We derived the Euler – Lagrange equation for studying the dynamics of the local magnetic moment, and tested our model with available experimental data.

1 Introduction

Since the discovery of superconductivity in Fe – based pnictides oxides [1], there has been enormous research activities to understand the origin of their superconductivity. This immense interest in the physics and chemistry communities is reminiscent of the excitement that accompanied the discovery of high – T_c cuprate superconductors in the early 1980s. Normally, in Fe – based superconductors, antiferromagnetic (AFM) order is suppressed by charge (hole) doping but spin interactions still exist [2]. It should be noted that superconductivity can still be induced in the pnictides without charge doping through either isoelectric doping, non-stoichiometry, or by use of non-thermal control parameters such as application of non-hydrostatic pressure. Also it should be noted that the parent compounds of the iron pnictides are metallic, albeit highly dissipative, bad metals [3]. Most striking is the spectroscopy evidence that Fe based superconductors are weakly correlated electronic system [4, 5]. Thus, the origin of the observed superconductivity may not be due to Mott physics. Put differently, for the fact that spin is relevant in Fe pnictide superconductors, they are basically itinerant magnetism suggesting that the Mott – Hubbard physics may be irrelevant in physics of Fe pnictide superconductors. We can thus speculate that the superconductivity observed in Fe pnictides are locally and dynamically spin polarized due to strong Fe spin fluctuations with the itinerant nature of Fe providing the "glue". Hence, spin-fluctuation mediated through the spin channel may be relevant in understanding the origin and nature of the observed superconductivity in Fe pnictide.

Fe pnictide superconductors have layered structure. The Fe atom layers of these pnictide systems are normally sandwiched by pnictogen, for example, Arsenic (As). Hence, the magnetic moment of Fe depends strongly on the inter-layer distances of Fe-As [6]. The magnetic moment of transition metals also depends on volume [7]. This leads to the so-called lattice anharmonicity.

In quasi 2D layered materials, a state with some rather unexpected properties (new mean field solution) is observed at non-zero [8]. This new mean field property observed in these layered systems cannot be described by the ordinary phenomenological Ginzburg – Landau theory. Also, the thermodynamic relation $\int_0^{T_c}[\delta C_e(H,T)/\mathrm{T}]dT = 0$ which holds for 2^{nd} order phase transition is violated in some materials with Bose – Einstein condensate (BEC)-like phase transition (see for example as in spin glasses [9], ferromagnetic and antiferromagnetic spin models with temperature driven transitions [10]). We speculate that the normal Landau theory developed for 2^{nd} order phase transition may not adequately account for the physics of the phase transitions and associated phenomena, for example, magneto-volume effect due to lattice anharmonicity in Fe pnictide superconductors. This motivated us to develop a new Landau-like mean field theory for studying Fe-pnictide superconductors. The theory is based on the Ehrenfest classification of orders of phase transitions [11]. Specifically, we will study the dependence of the local magnetic moment, M on the Fe-As layer separation, z.

2 Theoretical Framework

According to Hilfer [12], rewriting the singular part of the local free energy within a restricted path through the critical point in terms of the finite difference quotient, and analytically continuing in the orders, allows one to classify continuous phase transitions precisely according to their orders. We speculate that there exist phase transition of orders greater than two as there is no known physical reason why such transitions should not exist in nature since they certainly exist in a number of theoretical models like quantum chromodynamics (QCD), lattice field theory and statistical physics [13]. At least, higher order phase transitions ($\geq$2) are tenuous at best and their non-detection might have been due to the hasty generalization that all that departs from phase transition of order two can always be explained in terms of field fluctuation [13, 14].

The dependence of the magnetic moment, M on the Fe-As layer separation is completely determined by the functional (the magnetic free energy functional), $F[z, \langle M\rangle]$ where $\langle M\rangle$ is the local magnetic moment. However, F must be invariant under the symmetry group (e.g. Abelian Higg's model) [15] of the disordered phase in order to minimize the total energy [13]. In general, F is a very complex functional of $\langle M\rangle$. To

make $\langle M \rangle$ to be spatially continuous in equilibrium, in the ordered phase, we essentially for all cases, redefine it. This suggests that F be expressed in terms of a local free energy density, $f[z, \langle M \rangle]$ (the local magnetic free energy) which is a function of the field at the point "z". After coarse graining, in its simplest form [13, 14], F is give (for orders of phase transition > 2) by,

$$F_p(M,z) = \int d^d r |M|^{2(p-2)} \{-a_p|M|^2 + b_p|M|^4 + c_p|\nabla M|^2 + |M|^2 \alpha (z - z_c)^{2(p-2)}\}, \forall p > 2 \quad (1)$$

where p is the order of the phase transition, $a_p = a_o(1 - H/H_c)$, $b_p \gg 1$, z is the Fe-As layer distance (inter-atomic separation), z_c is the critical point, and $\alpha < 0$ (a typical material dependent parameter).

Equation 1 is the model equation we are proposing for studying the dependence of M on the Fe-As inter-atomic separation. For 3^{rd} order phase transition, $p = 3$, Eq. 1 reduces to,

$$F_3(M,z) = \int d^d r |M|^2 \{-a_3|M|^2 + b_3|M|^4 + c_3|\nabla M|^2 + |M|^2 \alpha (z - z_c)^2\} \quad (2)$$

If we neglect the gradient term, and minimize the local magnetic free energy with respect to M, Eq. 2 reduces to

$$M^2 = \frac{2}{3b_3}[a_3 + |\alpha|(z - z_c)^2] \quad (3)$$

which basically leads (i.e., substituting Eq. 3 into 2) to the local free energy

$$\langle f_3 \rangle = [\frac{2}{3b_3}(a_3 + |\alpha|(z - z_c)^2)]^2 \{\frac{5}{3}|\alpha|(z - z_c)^2 - \frac{1}{3}a_3\}. \quad (4)$$

In the presence of the gradient term to the local magnetic free energy, using variational principle, after scaling, we obtain the Euler – Lagrange equation for M as,

$$\varphi^5 - \varphi^3[1 - \alpha(z - z_c)^2] - \varphi|\nabla^2 \varphi| = 0. \quad (5)$$

3 Model Application

Using the data of Egami et al. [16], we calculated the magnetic moment, M using our model Eq. 3. The plot of experimentally determined critical temperature against our calculated M (μ_B) are as shown in Fig. 1. Observe that there is strong correlation between T_c and M. Most significantly, our model predicted correctly the range of values of magnetic moment of Fe, in Fe pnictide superconductors. As it is evidence from the plot, the magnetic moment range from 0.59 to 0.73 μ_B. The experimentally measured value for the magnetic moment of Fe in LaOFeAs for instance, range from 0.30 to 0.64 μ_B [17, 18].

We speculate that the observed strong correlation between T_c and M stems from the fact that the superconducting critical temperature T_c depends very sensitively on the iron pnictogen (i.e., Fe-As-Fe) bond angle which in turn, depends on the Fe-As layer separation [19]. This present observation is in tandem with the understanding that the bonding of the arsenic atoms changed dramatically as a function of magnetic moment [20] and the core-level spectroscopy measurements on $CeFeAsO_{0.89}F_{0.11}$ [21] which showed very rapid spin fluctuation dependent magnetic moment. Since from our model Eq. 3, M is proportional to z (for $a_3 \ll 1$), the observed strong correlation is to be expected. This observation confirms our earlier assertion that spin mediated fluctuations may be the major dominant mediator in the superconductivity of Fe pnictide superconductors. However, electron-phonon coupling through the spin-channel is also to be expected.

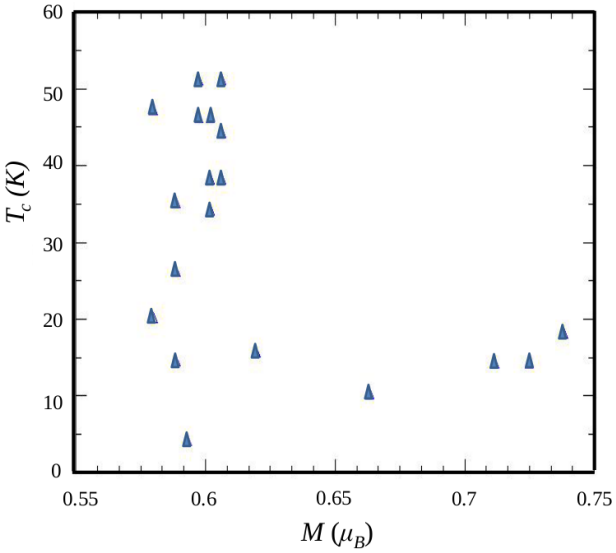

Fig. 1: Color-online. Superconducting experimental critical temperature, T_c from Ref. [16] against the calculated M obtained using Eq. 3 at the critical point.

Acknowledgment

This work is supported by the Government of Ebonyi State, Federal Republic, Nigeria.

Submitted on March 24, 2012 / Accepted on April 2, 2012

References

1. Kamihara Y., Watanabe T., Hirano, M. and Hosono, H. Iron-based layered superconductor La[O(1-x)F(x)]FeAs (x = 0.05-0.12) with T(c) = 26 K. *Journal of the American Chemical Society*, 2008, v. 130 (11), 3296 – 3297.
2. Haule K., Shim J. H., and Kotliar, G. Correlated Electronic Structure of $LaO_{1-x}F_xFeAs$. *Physical Review Letters*, 2008, v. 100, 226402.
3. Si Q. and Abrahams A. Strong Correlations and Magnetic Frustration in the High T_c Iron Pnictides. *Physical Review Letters*, 2008, v. 101, 076401.
4. Ren Z. -A., Lu W., Yang J., Yi W., Shen X. -L., Li Z. -C., Che G. -C., Dong X. -L., Sun L. -L., Zhou F. and Zhao Z. -X. Superconductivity at 55 K in Iron-Based F-Doped Layered Quaternary Compound $Sm[O_{1-x}F_x]FeAs$. *Chinese Physics Letters*, 2008, v. 25, 2215.

5. Yang W. -L., Sorini W. A., Chen C. -C., Moritz B., Lee W. -E., Vernay F., Olalde-Velasco P., Denlinger J. -D., Delley B, Chu F. G., Analytis J. -G., Fisher I. -R., Ren Z. -A., Yang J., Lu W., Zhao Z. -X., van den Brink J., Hussain Z., Shen Z. -X. and Devereaux T. -P. Evidence for weak electronic correlations in iron pnictides. *Physical Review B.*, 2009, v. 80 , 014508.
6. Yin Z. -P., Lebegue S., Han M. -J., Neal B. P., Savrasov S. -Y. and Pickett W. -E. Electron-Hole Symmetry and Magnetic Coupling in Antiferromagnetic LaFeAsO. *Physical Review Letters*, 2008, v. 101 , 047001.
7. Chikazumi S. Physics of Magnetism. John Wiley & Sons, New York, NY, USA, 1964.
8. Cronström C. and Noga M. Third-order phase transition and superconductivity in thin films. *Czechoslovak Journal of Physics*, 2001, v. 51 (2), 175 – 184.
9. Stanley H. E. Introduction to Phase Transition and Critical Phenomena. Clarendon Press, London, 1971.
10. Campostrini M., Rossi P. and and Vicar E. Large-N phase transition in lattice two-dimensional principal chiral models. *Physical Review D*, 1995, v. 52 , 395.
11. Kumar P., Hall D. and Goodrich R. G. Thermodynamics of the Superconducting Phase Transition in $Ba_{0.6}K_{0.4}BiO_3$. *Physical Review Letters*, 1991, v. 82 , 4532.
12. Hilfer R. Multiscaling and the classification of continuous phase transitions. *Physical Review Letters*, 1992, v. 68 , 190.
13. Ekuma E. C., Asomba G. C. and Okoye C. M. I. Thermodynamics of third order phase transition: A solution to the Euler-Lagrange equations. *Physica B: Condensed Matter*, 2010, v. 405 , 2290 – 2293.
14. Ekuma E. C., Asomba G. C. and Okoye C. M. I. Ginzburg–Landau theory for higher order phase transition. *Physica C: Superconductivity*, 2012, v. 472 , 1 – 4.
15. Callaway D. J. E. and Carson L. J. Abelian Higgs model: A Monte Carlo study. *Physical Review D*, 1982, v. 25 , 531 – 537.
16. Egami T., Fine B. V., Parshall D., Subedi A. and Singh D. J. Spin-Lattice Coupling and Superconductivity in Fe Pnictides. *Advances in Condensed Matter Physics*, 2010, v. 2010 , 164916.
17. Ishida K., Nakai Y. and Hosono H. To What Extent Iron-Pnictide New Superconductors Have Been Clarified: A Progress Report. *Journal Physical Society of Japan*, 2009, v. 78 , 062001.
18. de la Cruz C., Huang Q., Lynn J. W., Li J., Ratcliff II W., Zarestky J. L., Mook H. A., Chen G. F., Luo J. L., Wang N. L. and Dai P. Magnetic order close to superconductivity in the iron-based layered $LaO_{1-x}F_xFeAs$ systems. *Nature*, 2008, v. 453 (7197), 899 – 902.
19. Lee C. -H., Iyo A., Eisaki H., Kito H., Fernandez-Dia M. T., Ito T., Kihou K., Matsuhata H., Braden M. and Yamada K. Effect of Structural Parameters on Superconductivity in Fluorine-Free $LnFeAsO_{1-y}$ (Ln = La, Nd). *Journal Physical Society of Japan*, 2008, v. 77 , 083704.
20. Yildirim T. Strong Coupling of the Fe-Spin State and the As-As Hybridization in Iron-Pnictide Superconductors from First-Principle Calculations. *Physical Review Letters*, 2009, v. 102 , 037003.
21. Kreyssig A., Green M. A., Lee Y., Samolyuk G. D., Zajdel P., Lynn J. W., Bud'ko S. L., Torikachvili M. S., Ni N., Nandi S., Leão J. B., Poulton S. J., Argyriou D. N., Harmon B. N., McQueeney R. J., Canfield P. C. and Goldman A. I. Pressure-induced volume-collapsed tetragonal phase of $CaFe_2As_2$ as seen via neutron scattering *Physical Review B*, 2008, v. 78 , 184517

LETTERS TO PROGRESS IN PHYSICS

LETTERS TO PROGRESS IN PHYSICS

On the Exact Solution Explaining the Accelerate Expanding Universe According to General Relativity

Dmitri Rabounski

A new method of calculation is applied to the frequency of a photon according to the travelled distance. It consists in solving the scalar geodesic equation (equation of energy) of the photon, and manifests gravitation, non-holonomity, and deformation of space as the intrinsic geometric factors affecting the photon's frequency. The solution obtained in the expanding space of Friedmann's metric manifests the exponential cosmological redshift: its magnitude increases, exponentially, with distance. This explains the accelerate expansion of the Universe registered recently by the astronomers. According to the obtained solution, the redshift reaches the ultimately high value $z = e^{\pi} - 1 = 22.14$ at the event horizon.

During the last three years, commencing in 2009, I published a series of research papers [1–5] wherein I went, step-by-step, in depth of the cosmological redshift problem. I targeted an explanation of the non-linearity of the cosmological redshift law and, hence, the accelerate expansion of the Universe. I suggested that the explanation may be found due to the space-time geometry, i.e. solely with the use of the geometric methods of the General Theory of Relativity.

Naturally, this is the most promising way to proceed in this problem. Consider the following: in 1927, Lemaître's theory [6] already predicted the linear reshift law in an expanding space of Friedmann's metric (a Friedmann universe). As was then shown by Lemaître, this theoretical result matches the linear redshift law registered in distant galaxies*. The anomalously high redshift registered in very distant Ia-type supernovae in the last decade [7–9] manifests the non-linearity of the redshift law. It was then interpreted as the accelerate expansion of our Universe. Thus, once the space-time geometry has already made Lemaître successful in explaining the linear redshift, we should expect a success with the non-linear redshift law when digging more in the theory.

Lemaître deduced the cosmological redshift on the basis of Einstein's field equation. The left-hand side of the equation manifests the space curvature, while the right-hand side describes the substance filling the space. In an expanding space, all objects scatter from each other with the velocity of the space expansion. Lemaître considered the simplest case of deforming spaces — the space of Friedmann's metric. Such a space is free of gravitational fields and rotation, but is curved due to its deformation (expansion or compression). Solving Einstein's equation for Friedmann's metric, Lemaître obtained the curvature radius R of the space and the speed of its change $\dot{R}$. Then he calculated the redshift, assuming that it is a result of the Doppler effect on the scattering objects of the expanding Friedmann universe.

Lemaître's method of deduction would remain quite good, except for three drawbacks, namely —

1) It works only in deforming spaces, i.e. under the assumption that the cosmological redshift is a result of the Doppler effect in an expanding space. In static (non-deforming) spaces, this method does not work. In other words, herein is not a way to calculate how the frequency of a photon will change with the distance of the photon's travel in the space of a static cosmological metric (which is known to be of many kinds);
2) In this old method, the Doppler effect does not follow from the space (space-time) geometry but has the same formula as that of classical physics. Only the speed of change of the curvature radius with time $\dot{R}$ (due to the expansion of space) is used as the velocity of the light source. In other words, the Doppler formula of classical physics is assumed to be the same in an expanding Friedmann universe. This is a very serious simplification, because it is obvious that the Doppler effect should have a formula, which follows from the space geometry (Friedmann's metric in this case);
3) This method gives the linear redshift law — a straight line $z = \frac{\dot{R}}{c}$, which "digs" in the wall $\dot{R} = c$. As a result, the predicted cosmological redshift is limited by the numerical value $z_{\max} = 1$. However, we know dozens of much more redshifted galaxies and quasars. In 2011, the highest redshift registered by the astronomers is $z = 10.3$ (the galaxy UDFj-39546284).

So, in his theory, Lemaître calculated the cosmological redshift in a roundabout way: by substituting, into the Doppler formula of classical physics, the speed of change of the curvature radius $\dot{R}$ he obtained his redshift law, i.e., by solving Einstein's equation for Friedmann's metric.

*According to the astronomical observations, spectral lines of distant galaxies and quasars are redshifted as if these objects scatter with the radial velocity $u = H_0 d$, which increases 72 km/sec per each megaparsec of the distance d to the object. $H_0 = 72 \pm 8$ km/sec×Mpc $= (2.3 \pm 0.3) \times 10^{-18}$ sec^{-1} is known as the Hubble constant. 1 parsec = 3.0857×10^{18} cm $\simeq 3.1 \times 10^{18}$ cm.

In contrast to Lemaître, I suggested that the cosmological redshift law can be deduced in a more direct and profound way. It is as follows. The generally covariant geodesic equation — the four-dimensional equation of motion of a particle — can be projected onto the time line and the three-dimensional spatial section of an observer. As a result, we obtain the scalar geodesic equation, which is the equation of energy of the particle, and the vectorial geodesic equation (the three-dimensional equation of motion). The in-depth mathematical formalism of the said projection was introduced in 1944 by Zelmanov [10, 11], and is known as the theory of chronometric invariants*. Solving the scalar geodesic equation (equation of energy) of a photon, we shall obtain how the photon's energy and frequency change according to the remoteness of the signal's source to the observer. This is the *frequency shift law*, particular forms of which we can deduce by solving the scalar geodesic equation of a photon in the space of any particular metric.

The same method of deduction may be applied to mass-bearing particles. By solving the scalar geodesic equation for a mass-bearing particle ("stone-like objects"), we shall obtain that the relativistic mass of the object changes according to the remoteness to the observer in the particular space.

First, following this new way of deduction, I showed that the redshift, observed by the astronomers, should be present in a space which rotates at the velocity of light [1, 2]. In this case, the Hubble constant plays a rôle of the frequency of the rotation. The redshift due to the space rotation should be present even if the space is static (non-deforming).

The light-speed rotation is only attributed to the so-called isotropic region of space (home of the trajectories of light). This can be shown by "adapting" the space metric to the isotropic space condition (equality of the metric to zero), which makes a replacement among the components g_{00} and g_{0i} of the fundamental metric tensor $g_{\alpha\beta}$. In Minkowski's space, this replacement means that the isotropic region has a non-diagonal metric, where $g_{00}=0$, $g_{0i}=1$, $g_{11}=g_{22}=g_{33}=-1$. Such isotropic metrics were studied in the 1950's by Petrov: see §25 and the others in his *Einstein Spaces* [12]. More insight into this subject is provided in my third paper on the redshift problem [3].

On the other hand, a regular sublight-speed observer shall observe all events according to the components of the fundamental metric tensor $g_{\alpha\beta}$ of his own (non-isotropic) space — home of "solid objects". Therefore, I then continued the research study with the regular metrics, which are not "adapted" to the isotropic space condition.

In two recent papers [4, 5], I solved the scalar geodesic equation for mass-bearing particles and massless particles (photons), in the most studied particular spaces: in the space of Schwarzschild's mass-point metric, in the space of an electrically charged mass-point (the Reissner-Nordström metric), in the rotating space of Gödel's metric (a homogeneous distribution of ideal liquid and physical vacuum), in the space of a sphere of incompressible liquid (Schwarzschild's metric), in the space of a sphere filled with physical vacuum (de Sitter's metric), and in the deforming space of Friedmann's metric (empty or filled with ideal liquid and physical vacuum).

Herein I shall go into the details of just one of the obtained solutions — that in an expanding Friedmann universe, — wherein I obtained the exponential cosmological redshift, thus giving a theoretical explanation to the accelerate expansion of the Universe registered recently by the astronomers.

The other obtained solutions shall be omitted from this presentation. The readers who are curious about them are directly referred to my two recent publications [4, 5].

So, according to Zelmanov's chronometrically invariant formalism [10, 11], any four-dimensional (generally covariant) quantity is presented with its observable projections onto the line of time and the three-dimensional spatial section of an observer. This is as well true about the generally covariant geodesic equation. As Zelmanov obtained, the projected (chronometrically invariant) geodesic equations of a mass-bearing particle, whose relativistic mass is m, are

$$\frac{dm}{d\tau}-\frac{m}{c^2}F_i\mathrm{v}^i+\frac{m}{c^2}D_{ik}\mathrm{v}^i\mathrm{v}^k=0\,, \tag{1}$$

$$\frac{d(m\mathrm{v}^i)}{d\tau}-mF^i+2m\left(D^i_k+A^{\cdot i}_{k\cdot}\right)\mathrm{v}^k+m\triangle^i_{nk}\mathrm{v}^n\mathrm{v}^k=0\,, \tag{2}$$

while the projected geodesic equations of a massless particle-photon, whose relativistic frequency is ω, have the form

$$\frac{d\omega}{d\tau}-\frac{\omega}{c^2}F_ic^i+\frac{\omega}{c^2}D_{ik}c^ic^k=0\,, \tag{3}$$

$$\frac{d(\omega c^i)}{d\tau}-\omega F^i+2\omega\left(D^i_k+A^{\cdot i}_{k\cdot}\right)c^k+\omega\triangle^i_{nk}c^nc^k=0\,. \tag{4}$$

Here $d\tau=\sqrt{g_{00}}\,dt-\frac{1}{c^2}v_i\,dx^i$ is the observable time, which depends on the gravitational potential $\mathrm{w}=c^2\left(1-\sqrt{g_{00}}\right)$ and the linear velocity $v_i=-\frac{c\,g_{0i}}{\sqrt{g_{00}}}$ of the rotation of space. Four factors affect the particles: the gravitational inertial force F_i, the angular velocity A_{ik} of the rotation of space, the deformation D_{ik} of space, and the Christoffel symbols Δ^i_{jk} (expressing the space non-uniformity). According to the scalar geodesic equation (equation of energy), two factors, F_i and D_{ik}, affect the energy of the particle. They are determined [10, 11] as

$$F_i=\frac{1}{\sqrt{g_{00}}}\left(\frac{\partial\mathrm{w}}{\partial x^i}-\frac{\partial v_i}{\partial t}\right),\qquad \sqrt{g_{00}}=1-\frac{\mathrm{w}}{c^2}\,, \tag{5}$$

$$D_{ik}=\frac{1}{2\sqrt{g_{00}}}\frac{\partial h_{ik}}{\partial t}\,,\quad D^{ik}=-\frac{1}{2\sqrt{g_{00}}}\frac{\partial h^{ik}}{\partial t}\,,\quad D=\frac{\partial\ln\sqrt{h}}{\sqrt{g_{00}}\,\partial t}\,, \tag{6}$$

where $D=h^{ik}D_{ik}$, while h_{ik} is the chr.inv.-metric tensor

$$h_{ik}=-g_{ik}+\frac{1}{c^2}v_iv_k\,,\quad h^{ik}=-g^{ik},\quad h^i_k=\delta^i_k\,. \tag{7}$$

*The property of chronometric invariance means that the quantity is invariant along the three-dimensional spatial section of the observer.

The geodesic equations of mass-bearing and massless particles have the same form. Only the sublight velocity v^i and the relativistic mass m are used for mass-bearing particles, instead of the observable velocity of light c^i and the frequency ω of the photon. Therefore, they can be solved in the same way to yield similar solutions.

My suggestion is then self-obvious. By solving the scalar geodesic equation of a mass-bearing particle in each of the so-called cosmological metrics, we should obtain how the observed (relativistic) mass of the particle changes according to the distance from the observer in each of these universes. I will further refer to it as the *cosmological mass-defect*. The scalar geodesic equation of a photon should give the formula of the frequency shift of the photon according to the travelled distance (the *cosmological frequency shift*).

Consider the space of Friedmann's metric

$$ds^2 = c^2dt^2 - R^2\left[\frac{dr^2}{1-\kappa r^2} + r^2\left(d\theta^2 + \sin^2\theta\, d\varphi^2\right)\right], \qquad (8)$$

wherein Lemaître [6] deduced the linear redshift law. Here $R = R(t)$ is the curvature radius of the space, while $\kappa = 0, \pm 1$ is the curvature factor. If $\kappa = -1$, the three-dimensional subspace possesses hyperbolic (open) geometry. If $\kappa = 0$, its geometry is flat. If $\kappa = +1$, it has elliptic (closed) geometry.

As is seen from the metric, such a space — a Friedmann universe — is free of ($g_{00} = 1$) and rotation ($g_{0i} = 0$), but is deforming, which reveals the functions $g_{ik} = g_{ik}(t)$. It may expand, compress, or oscillate. Such a space can be empty, or filled with a homogeneous and isotropic distribution of ideal (non-viscous) liquid in common with physical vacuum (Λ-field), or filled with one of the media.

Friedmann's metric is expressed through a "homogeneous" radial coordinate r. This is the regular radial coordinate divided by the curvature radius, whose scales change according to the deforming space. As a result, the homogeneous radial coordinate r does not change its scale with time.

The scalar geodesic equation for a photon travelling along the radial direction in a Friedmann universe takes the form

$$\frac{d\omega}{d\tau} + \frac{\omega}{c^2}\, D_{11}\, c^1 c^1 = 0\,, \qquad (9)$$

where c^1 [$\sec^{-1}$] is the solely nonzero component of the observable "homogeneous" velocity of the photon. The square of the velocity is $h_{11}\, c^1 c^1 = c^2$ [$\mathrm{cm}^2/\sec^2$]. We calculate the components of the chr-inv.-metric tensor h_{ik} according to Friedmann's metric. After some algebra, we obtain

$$h_{11} = \frac{R^2}{1-\kappa r^2}\,, \quad h_{22} = R^2 r^2, \quad h_{33} = R^2 r^2 \sin^2\theta\,, \qquad (10)$$

$$h = \det\|h_{ik}\| = h_{11}\, h_{22}\, h_{33} = \frac{R^6 r^4 \sin^2\theta}{1-\kappa r^2}\,, \qquad (11)$$

$$h^{11} = \frac{1-\kappa r^2}{R^2}\,, \quad h^{22} = \frac{1}{R^2 r^2}\,, \quad h^{33} = \frac{1}{R^2 r^2 \sin^2\theta}\,. \qquad (12)$$

With these formulae of the components of h_{ik}, we obtain the tensor of the space deformation D_{ik} in a Friedmann universe. According to the definition (6), we obtain

$$D = \frac{3\dot{R}}{R}\,, \quad D_{11} = \frac{R\dot{R}}{1-\kappa r^2}\,, \quad D^1_1 = \frac{\dot{R}}{R}\,. \qquad (13)$$

The curvature radius as a function of time, $R = R(t)$, can be found by assuming a particular type of the space deformation. The trace of the tensor of the space deformation, $D = h^{ik}D_{ik}$, is by definition the speed of relative deformation of the volume. A volume, which is deforming freely, expands or compresses so that its volume undergoes equal relative changes with time

$$D = const\,, \qquad (14)$$

which, in turn, is a world-constant of the space. This is the primary type of space deformation: I suggest referring to it as the *constant* (*homotachydioncotic*) *deformation*[*].

Consider a constant-deformation (homotachydioncotic) Friedmann universe. With $D = \frac{3\dot{R}}{R}$ according to Friedmann's metric, we have $\frac{\dot{R}}{R} = A = const$ in this case. We thus arrive at the equation $\frac{1}{R}\, dR = A dt$, which is $d\ln R = A dt$. Assuming the curvature radius at the moment of time $t = t_0$ to be a_0, we obtain

$$R = a_0\, e^{At}, \qquad \dot{R} = a_0 A e^{At}\,, \qquad (15)$$

and, therefore,

$$D = 3A\,, \quad D_{11} = \frac{a_0^2 A e^{2At}}{1-\kappa r^2}\,, \quad D^1_1 = A\,. \qquad (16)$$

Return now to the scalar geodesic equation of a photon in a Friedmann universe, which is formula (9). Because $g_{00} = 1$ and $g_{0i} = 0$ according to Friedmann's metric, we have $d\tau = dt$. Therefore, because $h_{11}\, c^1 c^1 = c^2$, the scalar geodesic equation transforms into $h_{11}\frac{d\omega}{dt} + \omega D_{11} = 0$. From here we obtain $h_{11}\frac{d\omega}{\omega} = -D_{11}\, dt$, and, finally, the equation

$$h_{11}\, d\ln\omega = -\, D_{11}\, dt\,. \qquad (17)$$

By substituting h_{11} and D_{11}, we obtain

$$d\ln\omega = -A\, dt\,, \qquad (18)$$

where $A = \frac{\dot{R}}{R}$ is a world-constant of the Friedmann space.

As is seen, this equation is independent of the curvature factor κ. Therefore, its solution will be common for the hyperbolic ($\kappa = -1$), flat ($\kappa = 0$), and elliptic ($\kappa = +1$) geometry of the Friedmann space.

This equation solves as $\ln\omega = -At + \ln B$, where B is an integration constant. So forth, we obtain $\omega = B e^{-At}$. We calculate the integration constant B from the condition $\omega = \omega_0$

[*]I refer to this kind of universe as *homotachydioncotic* (in Greek — ομοταχυδιογκωτικό). This term originates from *homotachydioncosis* — ομοταχυδιόγκωσης — volume expansion with a constant speed, from όμο which is the first part of όμοιος (omeos) — the same, ταχύτητα — speed, διόγκωση — volume expansion, while compression can be considered as negative expansion.

at the initial moment of time $t = t_0 = 0$. We have $B = \omega_0$. Thus, we obtain the final solution $\omega = \omega_0\, e^{-At}$ of the scalar geodesic equation. Expanding the world-constant $A = \frac{\dot{R}}{R}$ and the duration of the photon's travel $t = \frac{d}{c}$, we have

$$\omega = \omega_0\, e^{-\frac{\dot{R}}{R}\frac{d}{c}}, \tag{19}$$

where $d = ct$ [cm] is the distance to the source emitting the photon. At small distances (and durations) of the photon's travel, the obtained solution takes the linearized form

$$\omega \simeq \omega_0 \left(1 - \frac{\dot{R}}{R}\,\frac{d}{c}\right). \tag{20}$$

The obtained solution manifests that photons travelling in a constant-deformation (homotachydiastolic) Friedmann universe which expands ($A > 0$) should lose energy and frequency with each mile of the travelled distance. The energy and frequency loss law is exponential (19) at large distances of the photon's travel, and is linear (20) at small distances.

Accordingly, the photon's frequency should be redshifted. The magnitude of the redshift increases with the travelled distance. This is a *cosmological redshift*, in other words.

Let a photon have a wavelength $\lambda_0 = \frac{c}{\omega_0}$ being emitted by a distantly located source, while its frequency registered at the arrival is $\lambda = \frac{c}{\omega}$. Then we obtain the magnitude $z = \frac{\lambda - \lambda_0}{\lambda_0} = \frac{\omega_0 - \omega}{\omega}$ of the redshift in an expanding constant-deformation (homotachydiastolic) Friedmann universe. It is

$$z = e^{\frac{\dot{R}}{R}\frac{d}{c}} - 1\,, \tag{21}$$

which is an *exponential redshift law*. At small distances of the photon travel, it takes the linearized form

$$z \simeq \frac{\dot{R}}{R}\,\frac{d}{c}\,. \tag{22}$$

which manifests a *linear redshift law*.

If such a universe compresses ($A < 0$), this effect changes its sign, thus becoming a *cosmological blueshift*.

Our linearized redshift formula (22) is the same as $z = \frac{\dot{R}}{R}\frac{d}{c}$ obtained by Lemaître [6], the "father" of the theory of an expanding universe. He followed, however, another way of deduction which limited him only to the linear formula. He therefore was confined to believing in the linear redshift law alone.

The ultimately high redshift $z_{\max}$, which could be registered in our Universe, is calculated by substituting the ultimately large distance into the redshift law. If following Lemaître's theory [6], $z_{\max}$ should follow from the linear redshift law $z = \frac{\dot{R}}{R}\frac{d}{c} = A\frac{d}{c}$. Because $A = \frac{\dot{R}}{R}$ is the world-constant of the Friedmann space, the ultimately large curvature radius $R_{\max}$ is determined by the ultimately high velocity of the space expansion which is the velocity of light $\dot{R}_{\max} = c$. Hence, $R_{\max} = \frac{c}{A}$. The ultimately large distance $d_{\max}$ (the event horizon) is regularly determined from the linear law for scattering galaxies, which is $u = H_0\, d$: the scattering velocity u should reach the velocity of light ($u = c$) at the event horizon ($d = d_{\max}$).* The law $u = H_0\, d$ is known due to galaxies and quasars whose scattering velocities are much lower than the velocity of light. Despite this fact, the empirical linear law $u = H_0\, d$ is regularly assumed to be valid upto the event horizon. Thus, they obtain $d_{\max} = \frac{c}{H_0} = (1.3 \pm 0.2){\times}10^{28}$ cm. Then they assume the linear coefficient H_0 of the empirical law of the scattering galaxies to be the world-constant $A = \frac{\dot{R}}{R}$, which follows from the space geometry. As a result, they obtain $d_{\max} = R_{\max}$ and $z_{\max} = H_0\,\frac{d_{\max}}{c} = 1$ due to the linear redshift law. How then to explain the dozens of very distant galaxies and quasars, whose redshift is much higher than $z = 1$?

On the other hand, it is obvious that the ultimately high redshift $z_{\max}$, ensuing from the space (space-time) geometry, should be a result of the laws of relativistic physics. In other words, $z = z_{\max}$ should follow from not a straight line $z = \frac{\dot{R}}{R}\frac{d}{c} = H_0\,\frac{d}{c} = \frac{u}{c}$, which digs in the vertical "wall" $u = c$, but from a non-linear relativistic function.

In this case, the Hubble constant H_0 remains a linear coefficient only in the pseudo-linear beginning of the real redshift law arc, wherein the velocities of scattering are small in comparison with the velocity of light. At velocities of scattering close to the velocity of light (close to the event horizon), the Hubble constant H_0 loses the meaning of the linear coefficient and the world-constant A due to the increasing non-linearity of the real redshift law.

Such a non-linear formula has been found in the framework of our theory alluded to here. This is the exponential redshift law (21), which then gives the Lemaître linear redshift law (22) as an approximation at small distances.

We now use the exponential redshift law (21) to calculate the ultimately high redshift $z_{\max}$, which could be conceivable in an expanding Friedmann space of the constant-deformation type. The event horizon $d = d_{\max}$ is determined by the world-constant $A = \frac{\dot{R}}{R}$ of the space. Thus, the ultimately large curvature radius is $R_{\max} = \frac{c}{A}$, while the distance corresponding to $R_{\max}$ on the hypersurface is $d_{\max} = \pi R_{\max} = \frac{\pi c}{A}$. Suppose now that a photon has arrived from a source, which is located at the event horizon. According to the exponential redshift law (21), the photon's redshift at the arrival should be

$$z_{\max} = e^{\frac{\dot{R}}{R}\frac{d_{\max}}{c}} - 1 = e^{\pi} - 1 = 22.14\,, \tag{23}$$

which is the ultimately high redshift in such a universe.

The deduced exponential increase of the redshift implies the accelerate expansion of space. This "key prediction" of our theory was surely registered by the astronomers in the last decade: the very distant Ia-type supernovae manifested the increasing non-linearity of the redshift law and, hence, the accelerate expansion of our Universe [7–9].

*The law for scattering galaxies dictates that distant galaxies and quasars scatter with the radial velocity $u = H_0 d$, increasing as 72 km/sec per each megaparsec. The linear coefficient of the law, $H_0 = 72 \pm 8$ km/sec×Mpc = $= (2.3 \pm 0.3){\times}10^{-18}$ sec^{-1}, is known as the Hubble constant.

We therefore can conclude that the observed non-linear redshift law and the accelerate expansion of space have been explained in the constant-deformation (homotachydioncotic) Friedmann universe.

The deduced exponential law points out the ultimately high redshift $z_{\max} = 22.14$ for objects located at the event horizon. The highest redshifted objects, registered by the astronomers, are now the galaxies UDFj-39546284 ($z = 10.3$) and UDFy-38135539 ($z = 8.55$). According to our theory, they are still distantly located from the "world end". We therefore shall expect, with years of further astronomical observation, more "high redshifted surprises" which will approach the upper limit $z_{\max} = 22.14$.

In analogy to massless particles-photons, we can consider the scalar geodesic equation of a mass-bearing particle. In a Friedmann universe this equation takes the form

$$\frac{dm}{d\tau} + \frac{m}{c^2} D_{11} \mathrm{v}^1 \mathrm{v}^1 = 0 , \qquad (24)$$

which, alone, is non-solvable. This is because mass-bearing particles can travel at any sub-light velocity, which is therefore an unknown variable of the equation.

This problem vanishes in a constant-deformation Friedmann universe, by the assumption according to which massive bodies travel not arbitrarily, but are only being carried out with the expanding (or compressing) space. In this particular case, particles travel with the velocity of space deformation, $\mathrm{v} = \dot{R}$. Because $\mathrm{v}^2 = h_{ik}\mathrm{v}^i\mathrm{v}^k$, we have $h_{ik}\mathrm{v}^i\mathrm{v}^k = \dot{R}^2$. Thus, and with $d\tau = dt$ according to Friedmann's metric, the scalar geodesic equation of mass-bearing particles transforms into $h_{11}\frac{dm}{dt} + \frac{m}{c^2} D_{11}\dot{R}^2 = 0$, i.e. $h_{11}\frac{dm}{m} = -\frac{\dot{R}^2}{c^2} D_{11}\, dt$. We obtain

$$h_{11}\, d\ln m = -\frac{\dot{R}^2}{c^2} D_{11}\, dt . \qquad (25)$$

Then, expanding R, $\dot{R}$ (15), and D_{11} (16) according to a constant-deformation space, we obtain the scalar geodesic equation in the form

$$d\ln m = -\frac{a_0^2 A^3 e^{2At}}{c^2}\, dt , \qquad (26)$$

where $A = \frac{\dot{R}}{R} = const$. It solves as $\ln m = -\frac{a_0^2 A^2}{2c^2} e^{2At} + \ln B$, where the integration constant B can be found from the condition $m = m_0$ at the initial moment of time $t = t_0 = 0$. After some algebra, we obtain the final solution of the scalar geodesic equation. It is the double-exponential function

$$m = m_0\, e^{-\frac{a_0^2 A^2}{2c^2}\left(e^{2At}-1\right)} , \qquad (27)$$

which, at a small distance to the object, takes the linearized form

$$m \simeq m_0 \left(1 - \frac{a_0^2 A^3 t}{c^2}\right). \qquad (28)$$

The obtained solution manifests the *cosmological mass-defect* in a constant-deformation (homotachydiastolic) Friedmann universe: the more distant an object we observe in an expanding universe is, the less should be its observed mass m to its real mass m_0. Contrarily, the more distant an object we observe in a compressing universe, the heavier should be this object according to observation.

Our Universe seems to be expanding. This is due to the cosmological redshift registered in the distant galaxies and quasars. Therefore, according to the cosmological mass-defect deduced here, we should expect distantly located cosmic objects to be much heavier than we estimate on the basis of astronomical observations. The magnitude of the expected mass-defect should be, according to the obtained solution, in the order of the redshift of the objects.

The cosmological mass-defect complies with the cosmological redshift. Both of these effects are deduced in the same way, by solving the scalar geodesic equation for mass-bearing and massless particles, respectively. One effect cannot be in the absence of the other, because the geodesic equations have the same form. This is a basis of the space (space-time) geometry, in other words. Therefore, once the astronomers register the linear redshift law and its non-linearity in very distant cosmic objects, they should also find the corresponding cosmological mass-defect according to the solution presented here. Once the cosmological mass-defect is discovered, we will be able to say, surely, that our Universe is an expanding Friedmann universe of the constant-deformation (homotachydiastolic) type.

Submitted on January 14, 2012 / Accepted on January 15, 2012

References

1. Rabounski D. Hubble redshift due to the global non-holonomity of space. *The Abraham Zelmanov Journal*, 2009, v. 2, 11–28.
2. Rabounski D. An explanation of Hubble redshift due to the global non-holonomity of space. *Progress in Physics*, 2009, v. 1, L1–L2.
3. Rabounski D. On the speed of rotation of isotropic space: insight into the redshift problem. *The Abraham Zelmanov Journal*, 2009, v. 2, 208–223.
4. Rabounski D. Cosmological mass-defect — a new effect of General Relativity. *The Abraham Zelmanov Journal*, 2011, v. 4, 137–161.
5. Rabounski D. Non-linear cosmological redshift: The exact theory according to General Relativity. *The Abraham Zelmanov Journal*, 2012, v. 5, 3–30.
6. Lemaître G. Un Univers homogène de masse constante et de rayon croissant rendant compte de la vitesse radiale des nébuleuses extra-galactiques. *Annales de la Societe Scientifique de Bruxelles*, ser. A, 1927, tome 47, 49–59 (published in English, in a substantially shortened form, as: Lemaître G. Expansion of the universe, a homogeneous universe of constant mass and increasing radius accounting for the radial velocity of extra-galactic nebulæ. *Monthly Notices of the Royal Astronomical Society*, 1931, v. 91, 483–490).
7. Riess A. G., Filippenko A. V., Challis P., Clocchiatti A., Diercks A., Garnavich P. M., Gilliland R. L., Hogan C. J., Jha S., Kirshner R. P., Leibundgut B., Phillips M. M., Reiss D., Schmidt B. P., Schommer R. A., Smith R. C., Spyromilio J., Stubbs C., Suntzeff N. B.,

Tonry J. Observational evidence from supernovae for an accelerating Universe and a cosmological constant. *The Astronomical Journal*, 1998, v. 116, no. 3, 1009–1038.

8. Perlmutter S., Aldering G., Goldhaber G., Knop R. A., Nugent P., Castro P. G., Deustua S., Fabbro S., Goobar A., Groom D. E., Hook I. M., Kim A. G., Kim M. Y., Lee J. C., Nunes N. J., Pain R., Pennypacker C. R., Quimby R., Lidman C., Ellis R. S., Irwin M., McMahon R. G., Ruiz-Lapuente P., Walton N., Schaefer B., Boyle B. J., Filippenko A. V., Matheson T., Fruchter A. S., Panagia N., Newberg H. J. M., Couch W. J. Measurements of Omega and Lambda from 42 high-redshift supernovae. *The Astrophysical Journal*, 1999, v. 517, no. 2, 565–586.
9. Leibundgut B. and Sollerman J. A cosmological surprise: the universe accelerates. *Europhysics News*, 2001, v. 32, no. 4, 121–125.
10. Zelmanov A. L. Chronometric Invariants: On Deformations and the Curvature of Accompanying Space. Translated from the preprint of 1944, American Research Press, Rehoboth (NM), 2006.
11. Zelmanov A. L. Chronometric invariants and accompanying frames of reference in the General Theory of Relativity. *Soviet Physics Doklady*, 1956, v. 1, 227–230 (translated from *Doklady Academii Nauk USSR*, 1956, v. 107, no. 6, 815–818).
12. Petrov A. Z. Einstein Spaces. Pergamon Press, Oxford, 1969 (translated by R. F. Kelleher, edited by J. Woodrow).

LETTERS TO PROGRESS IN PHYSICS

Social Aspects of Cold Fusion: 23 Years Later

Ludwik Kowalski

The field of Cold Fusion, now called Condensed Matter Nuclear Science (CMNS), remains controversial. The original 1989 claim made by M. Fleischmann and S. Pons was that a chemical process in an electrolytic cell could initiate a nuclear reaction–fusion of two deuterium nuclei. More recent CMNS claims, made by experimental scientists, are: emission of charged nuclear projectiles during electrolysis; accumulation of ^{4}He; production of radioactive isotopes; and transmutation of elements. In the US, CMNS claims have been evaluated in two Department of Energy (DOE) investigations, in 1989 and 2004, as summarized in this article. These investigations did not lead to any resolution of the controversy. Scientists and adminstrators are not ideal; competition among them, as among other groups of people, tends to have both positive and negative influences.

1 Introduction

The so-called "scientific methodology", a set of norms developed to deal with difficulties, especially with mistakes and controversies, is well known. Most scientific mistakes are recognized when new results are discussed with colleagues, or via the peer review process. Occasional errors in published papers are subsequently discovered during replications conducted by other researchers. Scientific results, if valid, wrote Huizenga [1], must be reproducible on demand. "When errors are discovered, acknowledged and corrected, the scientific process moves quickly back on track, usually without either notice or comment in the public press." The scientific process, in other words, is self-corrective. The purpose of this presentation is to analyze an ongoing controversy about the so-called "cold fusion" (CF). The author of this article, and three other researchers, tried to verify one recent CF claim – emission of alpha particles during electrolysis. The results were negative, as described in [2]. Critical analysis of some CF claims, as illustrated in [3], can enrich nuclear physics courses, even at the undergraduate level.

Why is the CMNS controversy started in 1989 unresolved? Because CF claims are still not reproducible on demand, and because they conflict with accepted theories. A theory, in this context, is not just a hypothesis, or only a logical/mathematical argument. It is a logical structure that is known to agree with a wide range of already verified experimental data. Researchers know the rule–theories guide but experiments decide. But they are very reluctant to abandon accepted theories. To be reluctant means to insist on additional verifications of new experimental results. Referring to such situations, Huizenga wrote: "There are occasionally surprises in science and one must be prepared for them." Theories are not carved in stone; scientists do not hesitate to modify or reject theories when necessary. Rejecting a highly reproducible experimental result "on theoretical grounds" would not be consistent with scientific methodology. Unlike mathematics, science is based, in the final analysis, on experimental data, not on logical proofs.

2 The Original Claim

It is well known that two hydrogen nuclei can fuse, releasing energy. But this happens only at extremely high temperatures. At ordinary temperatures the probability of the reaction is practically zero, due to the well known coulomb repulsion of positive nuclei. This has been confirmed by reliable experimental data. But two scientists – Steven Jones, a physicist, and Martin Fleischmann, a chemist – independently speculated that this might not always be true. The term CF was introduced by them to identify the claimed fusion of hydrogen nuclei (ionized atoms dissolved in solid metals). The DOE supported Jones' work long before Fleischmann and his colleague Pons (F&P) applied for similar support. That is why the DOE asked Jones to evaluate the new research proposal. He was later accused (by the administration of Utah University) of stealing the idea of CF from F&P. Trying to establish priority, Utah University organized a press conference (March 23, 1989) at which the discovery of generation of nuclear heat in an electrolytic cell was announced to the world. The released heat was declared to be due to fusion of deuterium nuclei – ionized atoms dissolved in palladium. At that time Jones and his co-workers had already authored numerous peer-reviewed articles [4]. But their claim was not excess heat; it was emission of neutrons.

3 The First DOE Investigation

Most scientists immediately rejected claims conflicting with well-known facts and theories. But many attempts to replicate F&P's poorly-described experiments were made. Some attempts were successful (unaccounted heat was generated at rates close to one watt), while others were not [5]. That was the beginning of the controversy. Fleischmann and Pons wanted to study the CF phenomenon for another year or so but

were forced to announce the discovery by the university administrators [6]. They had no evidence that the measured heat was due to a nuclear reaction. The only thing they knew was that it could not be attributed to a known chemical reaction.

Suppose their experimental results had been described without any interpretation, and the phenomenon had been named "anomalous electrolysis". Such a report would not have led to a sensational press conference; it would have been made in the form of an ordinary peer review publication. Only electrochemists would have been aware of the claim; they would have tried to either confirm or refute it. The issue of "how to explain excess heat" would have been addressed later, if the reported phenomenon were confirmed. But that is not what happened. Instead of focusing on experimental data (in the area in which F&P were recognized authorities) most critics focused on the disagreements with the coulomb barrier theory. Interpretational mistakes were quickly recognized and this contributed to the premature skepticism toward their experimental data.

But the significance of CF, if real, was immediately recognized. Some believed that ongoing research on high-temperature fusion, costing billions of dollars, should be stopped to promote research on CF. Others concluded, also prematurely, that such a move would be opposed by "vested interests" of mainstream scientists. Responding to such considerations, the US government quickly ordered a formal investigation. A panel of scientists, named ERAB (Energy Research Advisory Board), and headed by John Huizenga, was formed to investigate CF in 1989. The final report, submitted to the DOE several months later, interfered with the normal development of the field. It should be noted that ERAB scientists investigating the CF claims were not personally involved in replications of experiments. Their report [7], based on visits to several laboratories rather than participation in experiments, can be summarized by the following statements:
Conclusions:

1. There is no evidence that a nuclear process is responsible for excess heat.
2. Lack of experimental reproducibility remains a serious concern.
3. Theoretically predicted fusion products were not found in expected quantities.
4. There is no evidence that CF can be used to produce useful energy.
5. The CF interpretation is not consistent with what is known about hydrogen in metals.
6. The CF interpretation is not consistent with what is known about nuclear phenomena.

Recommendations:

7. We recommend against any extraordinary funding.
8. We recommend modest support for more experiments.
9. We recommend focusing on excess heat and possible errors.
10. We recommend focusing on correlations between fusion products and excess heat.
11. We recommend focusing on the theoretically predicted tritium in electrolytic cells.
12. We recommend focusing on theoretically predicted neutrons.

Note that only one conclusion (item 2) refers to CF experiments. Conclusion 4 is about anticipated practical uses of CF while the remaining four conclusions (1, 3, 5, and 6) are about various aspects of the suggested interpretation of experimental results. Instead of focusing on reality of excess heat critics focused on the fact that the hypothesis was not consistent with what was known about hot nuclear fusion. The same observation can be made about recommendations. Only one of them (item 9) refers to possible errors in experiments. Items 7 and 8 refer to future funding while items 10, 11, and 12 refer to what was expected on the basis of the suggested hot-fusion interpretation. It is clear that the ERAB observations were based mostly on "theoretical grounds,"and not on identified errors in experimental data. Recommendations about future financial support for CF were very important. But they were ignored by the DOE. Support for CF research practically stopped in 1989. Another result of the first DOE investigation was that editors of some scientific journals stopped accepting articles dealing with CF research. Why was the scientific methodology of validation of claims – theories guide but experiments decide – not followed by the DOE-appointed scientists? Why did "rejections on theoretical grounds" prevail?

4 The Second DOE Investigation

The second DOE investigation of CF was announced in March 2004, nearly 15 years after the first one. Links to three online documents related to that investigation – Conference Agenda, Meeting Agenda, and DOE CF Report – can be found in [8]. The six most important scientific questions, based on new experimental claims, were:

a) Is it true that unexpected protons, tritons, and alpha particles are emitted [9, 10] in some CF experiments?
b) Is it true that generation of heat, in some CF experiments, is linearly correlated with the accumulation of ^{4}He and that the rate of generation of excess heat is close to the expected 24 MeV per atom of ^{4}He [9, 11]?
c) Is it true that highly unusual isotopic ratios [9, 12] have been observed among the reaction products?
d) Is it true that radioactive isotopes [9, 13] have been found among reaction products?
e) Is it true that transmutation of elements [10, 14] has occurred?

f) Are the ways of validating of claims made by CF researchers (see conference reports presened at [16, 17, 18]) consistent with accepted methodologies in other areas of science?

A positive answer to even one of these questions would be sufficient to justify an official declaration that cold fusion, in light of recent data, should be treated as a legitimate area of research. But only the (b) question was addressed by the selected referees [8]. They were asked to review the available evidence of correlation between the reported excess heat and production of fusion products. One third of them stated that the evidence for such correlation was conclusive. That was not sufficient; the attitude of the scientific establishment toward cold fusion research did not change.

5 Conclusion

The CF controversy is unprecedented in terms of its duration, intensity, and caliber of adversaries on both sides of the divide. Huizenga and Fleischmann were indisputable leaders in nuclear science and electrochemistry. CMNS researchers are mostly also Ph.D. level scientists. The same is true for those scientists who believe that the announced discovery of CF was a "scientific fiasco". We are still waiting for at least one reproducible-on-demand demonstration of a nuclear effect resulting from a chemical (atomic) process. In the case of CF the self-correcting process of scientific development emphasized by Huizenga has not worked. This fiasco seems to be due to the fact that scientists appointed to investigate CF claims did not follow the rules of scientific methodology.

Submitted on January 30, 2012 / Accepted on February 5, 2012

References

1. Huizenga J.R. Cold fusion: The scientific fiasco of the century. Oxford University Press, New York, 2nd ed., 1993, pp. 1–10.
2. Driscoll J. et al. Issues Related to Reproducibility in a CMNS Experiment. *Journal of Condensed Matter Nuclear Science*, 2011, v. 5, 34–41.
3. Kowalski L. Rossi's Reactors – Reality or Fiction? *Progress in Physics*, 2012, v. 1, 33–35. The online version of this article is at: http://www.ptep-online.com/index_files/2012/PP-28-07.PDF
4. Jones S.E. et al. Observations of Cold Nuclear Fusion in Condenced Matter. *Nature*, 1989, v. 228, 737–740.
5. Beaudette C. Excess Heat: Why Cold Fusion Research Prevailed. Oak Grow Press, LLC, South Bristol, USA, 2000. Also see: http://en.wikipedia.org/wiki/Cold_fusion#Announcement
6. Fleischmann M. Private conversation in 2002, after his presentation: "Background to Cold Fusion: The Genesis of a Concept" in: Proceedings of the 10th Intercantionl Conference on Cold Fusion, World Scientific, 2006.
7. ERAB, "Report of the cold fusion panel to the Energy Research Advisory Board", Department of Energy, DOE/S-0073: Washington, DC, 1989.
8. Krivit S. Special online collection, "2004 DOE Review of Cold Fusion" in: http://www.lenr-canr.org/Collections/DoeReview.htm
9. Storms E. Science of Low Energy Nuclear Reaction: A Comprehensive Compilation of Evidence and Explanations about Cold Fusion. World Scientific Publishing Company, 2007.
10. Mosier-Boss P.A. et al. Use of CR-39 in Pd/D Codeposition Experiments: A Response to Kowalski. *European Physical Journal - Applied Physics*, 2008, v. 41, 291-295.
11. Hagelstein P.L. et al. New Physical Effects in Metal Deuterides. In: Eleventh International Conference on Condensed Matter Nuclear Science, 2004, Marseille, France.
12. Urutskoev L.I. et al. Observation of transformation of chemical elements during an electric discharge. *Annales de la Fondation Louis de Broglie*, 2002, v. 27, 701.
13. Karabut A.B. et al. Nuclear product ratio for glow discharge in deuterium. *Physics Letters A*, 1992, v. 170, 265.
14. Mizuno T. Nuclear Transmutation: The Reality of Cold Fusion. Infinite Energy Press, 1998.
15. Iwamura Y. et al. Elemental Analysis of Pd Complexes: Effects of D_2 gas permeation. *Japanease Journal of Applied Physics*, 2002, v. 41, 4642–4648.
16. International Conference on Cold Fusion, Cambridge, MA, USA, 2003, (published by World Scientific Co. Pte. Ltd.).
17. Proceedings of the 11th International Conference on Cold Fusion, Marseilles, France, 2004, (published by World Scientific Co. Pte. Ltd.).
18. Proceedings of the 12th International Conference on Cold Fusion, Yokohama, Japan, 2005, (published by World Scientific Co. Pte. Ltd.).

The Journal on Advanced Studies in Theoretical and Experimental Physics, including Related Themes from Mathematics

PROGRESS IN PHYSICS

A quarterly issue scientific journal, registered with the Library of Congress (DC, USA). This journal is peer reviewed and included in the abstracting and indexing coverage of: Mathematical Reviews and MathSciNet (AMS, USA), DOAJ of Lund University (Sweden), Zentralblatt MATH (Germany), Scientific Commons of the University of St. Gallen (Switzerland), Open-J-Gate (India), Referativnyi Zhurnal VINITI (Russia), etc.

Electronic version of this journal:
http://www.ptep-online.com

Postal Address

Department of Mathematics and Science,
University of New Mexico,
705 Gurley Ave., Gallup, NM 87301, USA

ISSN: 1555-5534 (print)
ISSN: 1555-5615 (online)

Standard Address Number: 297-5092
Printed in the United States of America

JULY 2012 **VOLUME 3**

CONTENTS

Information for Authors and Subscribers

Progress in Physics has been created for publications on advanced studies in theoretical and experimental physics, including related themes from mathematics and astronomy. All submitted papers should be professional, in good English, containing a brief review of a problem and obtained results.

All submissions should be designed in LaTeX format using *Progress in Physics* template. This template can be downloaded from *Progress in Physics* home page http://www.ptep-online.com. Abstract and the necessary information about author(s) should be included into the papers. To submit a paper, mail the file(s) to the Editor-in-Chief.

All submitted papers should be as brief as possible. We accept brief papers, no larger than 8 typeset journal pages. Short articles are preferable. Large papers can be considered in exceptional cases to the section *Special Reports* intended for such publications in the journal. Letters related to the publications in the journal or to the events among the science community can be applied to the section *Letters to Progress in Physics*.

All that has been accepted for the online issue of *Progress in Physics* is printed in the paper version of the journal. To order printed issues, contact the Editors.

This journal is non-commercial, academic edition. It is printed from private donations. (Look for the current author fee in the online version of the journal.)

Characterisation of Low Frequency Gravitational Waves from Dual RF Coaxial-Cable Detector: Fractal Textured Dynamical 3-Space

Reginald T. Cahill

School of Chemical and Physical Sciences, Flinders University, Adelaide 5001, Australia
E-mail: Reg.Cahill@flinders.edu.au

Experiments have revealed that the Fresnel drag effect is not present in RF coaxial cables, contrary to a previous report. This enables a very sensitive, robust and compact detector, that is 1st order in v/c and using one clock, to detect the dynamical space passing the earth, revealing the sidereal rotation of the earth, together with significant wave/turbulence effects. These are "gravitational waves", and previously detected by Cahill 2006, using an Optical-Fibre – RF Coaxial Cable Detector, and Cahill 2009, using a preliminary version of the Dual RF Coaxial Cable Detector. The gravitational waves have a 1/f spectrum, implying a fractal structure to the textured dynamical 3-space.

1 Introduction

Data from a new gravitational wave experiment is reported*, revealing a fractal 3-space, flowing past the earth at ∼500 km/s. The wave/turbulence or "gravitational waves" have a significant magnitude, and are now known to have been detected numerous times over the last 125 years. The detector uses a single clock with RF EM waves propagating through dual coaxial cables, and is 1st order in v/c. The detector is sensitive, simple to operate, robust and compact. It uses the surprising discovery that there is no Fresnel drag effect in coaxial cables, whereas there is in gases, optical fibres, liquids etc. Data from an analogous detector using optical fibres and single coaxial cables was reported in 2006 [1, 2]. Because of the discovery reported herein that detector calibration has now been correctly redetermined. Results from Michelson-Morley [3, 4], Miller [5], Torr and Kolen [6] and DeWitte [7], are now in remarkable agreement with the velocity of absolute motion of the earth determined from NASA spacecraft earth-flyby Doppler shift data [8, 9], all revealing a light/EM speed anisotropy of some 486km/s in the direction RA=4.29^h, Dec=-75.0°: that speed is ∼300,000-500 km/s for radiation travelling in that direction, and ∼300,000+500 km/s travelling in the opposite, northerly direction: a significant observed anisotropy that physics has ignored. The actual daily average velocity varies with days of the year because of the orbital motion of the earth - the aberration effect discovered by Miller, but shows fluctuations over all time scales.

In 2002 it was discovered that the Michelson-Morley 1887 light-speed anisotropy experiment, using the interferometer in gas mode, had indeed detected anisotropy, by taking account of both the Lorentz length contraction effect for the interferometer arms, and the refractive index effect of the air in the light paths [3, 4]. These gas-mode interferometer experiments show the difference between Lorentzian Relativity (LR) and Special Relativity (SR). In LR the length contraction effect is caused by motion of a rod, say, through the dynamical 3-space, whereas in SR the length contraction is only a perspective effect, supposedly occurring only when the rod is moving relative to an observer. This was further clarified when an exact mapping between Galilean space and time coordinates and the Minkowski-Einstein spacetime coordinates was recently discovered [10].

The Michelson interferometer, having the calibration constant $k^2 = (n^2-1)(n^2-2)$ where n is the refractive index of the light-path medium, has zero sensitivity to EM anisotropy and gravitational waves when operated in vacuum-mode ($n = 1$). Fortunately the early experiments had air present in the light paths†. A very compact and cheap Michelson interferometric anisotropy and gravitational wave detector may be constructed using optical fibres [11], but for most fibres $n \approx \sqrt{2}$ near room temperature, and so needs to be operated at say 0°C. The $(n^2 - 2)$ factor is caused by the Fresnel drag [12]. The detection of light speed anisotropy - revealing a flow of space past the detector, is now entering an era of precision measurements, as reported herein. These are particularly important because experiments have shown large turbulence effects in the flow, and are beginning to characterise this turbulence. Such turbulence can be shown to correspond to what are, conventionally, known as gravitational waves, although not those implied by General Relativity, but more precisely are revealing a fractal structure to dynamical 3-space.

*This report is from the Gravitational Wave Detector Project at Flinders University.

†Michelson and Morley implicitly assumed that $k^2 = 1$, which considerably overestimated the sensitivity of their detector by a factor of ∼ 1700 (air has $n = 1.00029$). This error lead to the invention of "spacetime" in 1905. Miller avoided any assumptions about the sensitivity of his detector, and used the earth orbit effect to estimate the calibration factor k^2 from his data, although even that is now known to be incorrect: the sun 3-space inflow component was unknown to Miller. It was only in 2002 that the design flaw in the Michelson interferometer was finally understood [3, 4].

2 Fresnel Drag

The detection and characterisation of these wave/turbulence effects requires only the development of small and cheap detectors, as these effects are large. However in all detectors the EM signals travel through a dielectric, either in bulk or optical fibre or through RF coaxial cables. For this reason it is important to understand the so-called Fresnel drag effect. In optical fibres the Fresnel drag effect has been established, as this is important in the operation of Sagnac optical fibre gyroscopes, for only then is the calibration independent of the fibre refractive index, as observed. The Fresnel drag effect is a phenomenological formalism that characterises the effect of the absolute motion of the propagation medium, say a dielectric, upon the speed of the EM radiation relative to that medium.

The Fresnel drag expression is that a dielectric in absolute motion through space at speed v, relative to space itself, causes the EM radiation to travel at speed

$$V(v) = \frac{c}{n} + v\left(1 - \frac{1}{n^2}\right) \qquad (1)$$

wrt the dielectric, when V and v have the same direction. Here n is the dielectric refractive index. The 2nd term is known as the Fresnel drag, appearing to show that the moving dielectric "drags" the EM radiation, although this is a misleading interpretation; see [13] for a derivation*. If the Fresnel drag is always applicable then, as shown herein, a 1st order in v/c detector requires two clocks, though not necessarily synchronised, but requiring a rotation of the detector arm to extract the v-dependent term. However, as we show herein, if the Fresnel drag is not present in RF coaxial cables, then a detector 1st order in v/c and using one clock, can detect and characterise the dynamical space. In [13] it was incorrectly concluded that the Fresnel effect was present in RF coaxial cables, for reasons related to the temperature effects, and discussed later.

3 Dynamical 3-Space

We briefly outline the dynamical modelling of 3-space. It involves the space velocity field $\mathbf{v}(\mathbf{r}, t)$, defined relative to an observer's frame of reference.

$$\nabla \cdot \left(\frac{\partial \mathbf{v}}{\partial t} + (\mathbf{v}\cdot\nabla)\,\mathbf{v}\right) + \frac{\alpha}{8}\left((\mathrm{tr}D)^2 - \mathrm{tr}(D)^2\right) + .. = -4\pi G\rho \qquad (2)$$

$\nabla \times \mathbf{v} = \mathbf{0}$ and $D_{ij} = \partial v_i \partial x_j$. The velocity field $\mathbf{v}$ describes classically the time evolution of the substratum quantum foam. The bore hole g anomaly data has revealed $\alpha = 1/137$, the fine structure constant. The matter acceleration is found by determining the trajectory of a quantum matter wavepacket. This is most easily done by maximising the proper travel time τ:

$$\tau = \int dt \sqrt{1 - \frac{\mathbf{v}_R^2(\mathbf{r}_0(t), t)}{c^2}} \qquad (3)$$

where $\mathbf{v}_R(\mathbf{r}_o(t), t) = \mathbf{v}_o(t) - \mathbf{v}(\mathbf{r}_o(t), t)$, is the velocity of the wave packet, at position $\mathbf{r}_0(t)$, wrt the local space – a neo-Lorentzian Relativity effect. This ensures that quantum waves propagating along neighbouring paths are in phase, and so interfere constructively. This maximisation gives the quantum matter geodesic equation for $\mathbf{r}_0(t)$

$$\mathbf{g} = \frac{\partial \mathbf{v}}{\partial t} + (\mathbf{v}\cdot\nabla)\mathbf{v} + (\nabla\times\mathbf{v})\times\mathbf{v}_R - \frac{\mathbf{v}_R}{1 - \dfrac{\mathbf{v}_R^2}{c^2}}\,\frac{1}{2}\,\frac{d}{dt}\left(\frac{\mathbf{v}_R^2}{c^2}\right) + ... \qquad (4)$$

with $\mathbf{g} \equiv d\mathbf{v}_o/dt = d^2\mathbf{r}_o/dt^2$. The 1st term in $\mathbf{g}$ is the Euler space acceleration $\mathbf{a}$, the 2nd term explains the Lense-Thirring effect, when the vorticity is non-zero, and the last term explains the precession of orbits. While the velocity field has been repeatedly detected since the Michelson-Morley 1887 experiment, the best detection has been using

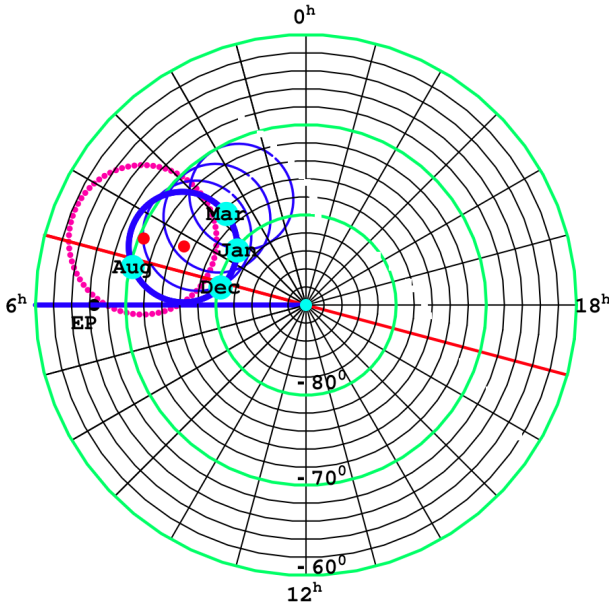

Fig. 1: South celestial pole region. The dot (red) at RA=4.29^h, Dec=-75°, and with speed 486 km/s, is the direction of motion of the solar system through space determined from spacecraft earth-flyby Doppler shifts [9], revealing the EM radiation speed anisotropy. The thick (blue) circle centred on this direction is the observed velocity direction for different days of the year, caused by earth orbital motion and sun space inflow. The corresponding results from Miller gas-mode interferometer are shown by 2nd dot (red) and its aberration circle (red dots) [5]. For March the velocity is RA=2.75^h, Dec=-76.6°, and with speed 499.2 km/s, see Table 2 of [9].

*The Fresnel Drag in (1) can be "derived" from the Special Relativity velocity-addition formula, but there v is the speed of the dielectric wrt to the observer, and as well common to both dielectrics and coaxial cables.

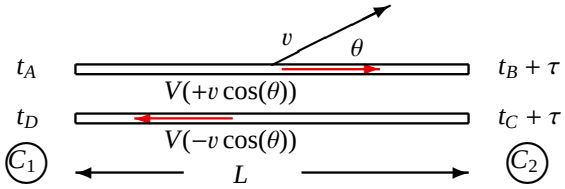

Fig. 2: Schematic layout for measuring the one-way speed of light in either free-space, optical fibres or RF coaxial cables, without requiring the synchronisation of the clocks C_1 and C_2: here τ is the unknown offset time between the clocks. V is the speed of EM radiation wrt the apparatus, with or without the Fresnel drag in (1), and v is the speed of the apparatus through space, in direction θ. DeWitte used this technique in 1991 with 1.5 km RF cables and Cesium atomic clocks [7]. In comparison with data from spacecraft earth-flyby Doppler shifts [9] this experiments confirms that there is no Fresnel drag effect in RF coaxial cables.

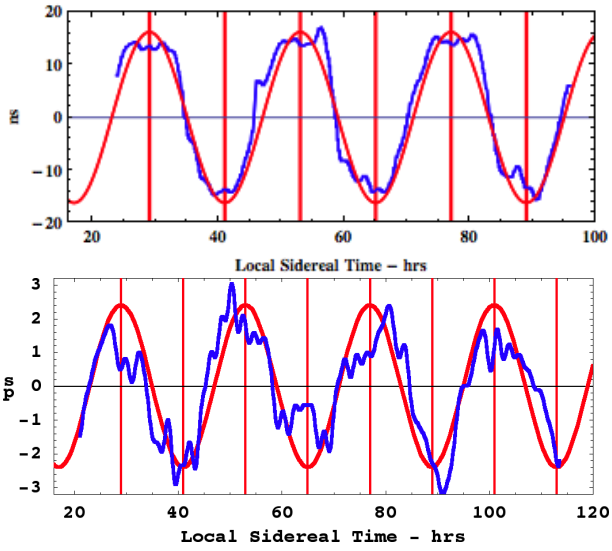

Fig. 3: Top: Data from the 1991 DeWitte NS horizontal coaxial cable experiment, $L = 1.5$ km, $n = 1.5$, using the arrangement shown in Fig. 2. The time variation of ~ 28 ns is consistent with the Doppler shift results with speed 500 km/s, but using Dec=-65°: the month for this data is unknown, and the vertical red lines are at RA=5^h. If a Fresnel drag effect is included the speed would have to be 1125 km/s, in disagreement with the Doppler shift data, demonstrating that there is no Fresnel drag in coaxial cables. Bottom: Dual coaxial cable detector data from May 2009 using the technique in Fig. 5 and without looping: $L = 20$ m, Doppler shift data predicts Dec= $-77°$, $v = 480$ km/s giving a sidereal dynamic range of 5.06 ps, very close to that observed. The vertical red lines are at RA=5^h. In both data sets we see the earth sidereal rotation effect together with significant wave/turbulence effects.

the spacecraft earth-flyby Doppler shift data [9], see Fig1. The above reveals gravity to be an emergent phenomenon where quantum matter waves are refracted by the time dependent and inhomogeneous 3-space velocity field. The α-term in (2) explains the so-called "dark matter" effects: if $\alpha \to 0$ and $v_R/c \to 0$ we recover Newtonian gravity, for then $\nabla\cdot\mathbf{g} = -4\pi G\rho$ [12]. Note that the relativistic term in (4) arises from the quantum matter dynamics – not from the space dynamics.

4 Gravitational Waves: Dynamical Fractal 3-Space

Eqn. (3) for the elapsed proper time maybe written in differential form as

$$d\tau^2 = dt^2 - \frac{1}{c^2}(d\mathbf{r}(t) - \mathbf{v}(\mathbf{r}(t), t)dt)^2 = g_{\mu\nu}(x)dx^\mu dx^\nu \qquad (5)$$

which introduces a curved spacetime metric $g_{\mu\nu}$ for which the geodesics are the quantum matter trajectories when freely propagating through the dynamical 3-space. Gravitational wave are traditionally thought of as "ripples" in the spacetime metric $g_{\mu\nu}$. But the discovery of the dynamical 3-space means that they are more appropriately understood to be turbulence effects of the dynamical 3-space vector $\mathbf{v}$, because it is $\mathbf{v}$ that is directly detectable, whereas $g_{\mu\nu}$ is merely an induced mathematical artefact. When the matter density $\rho = 0$, (2) will have a time-dependent fractal structured solutions, as there is no length scale. The wave/turbulence effects reported herein confirm that prediction, see Fig. 9.

5 First Order in v/c Speed of EMR Experiments

Fig. 2 shows the arrangement for measuring the one-way speed of light, either in vacuum, a dielectric, or RF coaxial cable. It is usually argued that one-way speed of light measurements are not possible because the clocks C_1 and C_2 cannot be synchronised. However this is false, and at the same time shows an important consequence of (1). In the upper part of Fig. 2 the actual travel time t_{AB} from A to B is determined by

$$V(v\cos(\theta))t_{AB} = L + v\cos(\theta)t_{AB} \qquad (6)$$

where the 2nd term comes from the end B moving an additional distance $v\cos(\theta)t_{AB}$ during time interval t_{AB}. Then

$$t_{AB} = \frac{L}{V(v\cos(\theta)) - v\cos(\theta)} = \frac{nL}{c} + \frac{v\cos(\theta)L}{c^2} + .. \qquad (7)$$

$$t_{CD} = \frac{L}{V(v\cos(\theta)) + v\cos(\theta)} = \frac{nL}{c} - \frac{v\cos(\theta)L}{c^2} + .. \qquad (8)$$

on using (1), i.e. assuming the validity of the Fresnel effect, and expanding to 1st oder in v/c. However if there is no Fresnel drag effect then we obtain

$$t_{AB} = \frac{L}{V(v\cos(\theta)) - v\cos(\theta)} = \frac{nL}{c} + \frac{v\cos(\theta)Ln^2}{c^2} + .. \qquad (9)$$

$$t_{CD} = \frac{L}{V(v\cos(\theta)) + v\cos(\theta)} = \frac{nL}{c} - \frac{v\cos(\theta)Ln^2}{c^2} + .. \qquad (10)$$

The important observation is that the v/c terms are independent of the dielectric refractive index n in (7) and (8), but

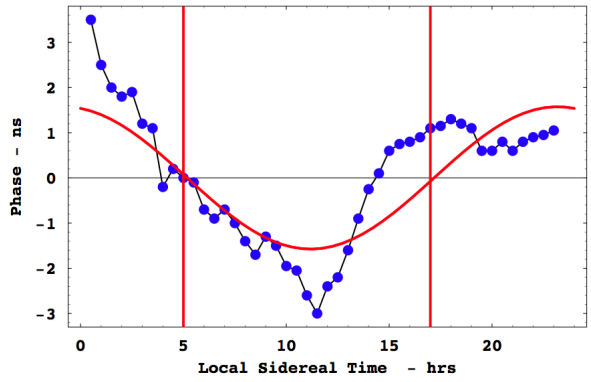

Fig. 4: Data from the 1981 Torr-Kolen experiment at Logan, Utah [6]. The data shows variations in travel times (ns), for local sidereal times, of an RF signal travelling through 500 m of coaxial cable orientated in an EW direction. The red curve is sidereal effect prediction for February, for a 3-space speed of 480 km/s from the direction, RA=5^h, Dec=-70°.

have an n^2 dependence in (9) and (10), in the absence of the Fresnel drag effect.

If the clocks are not synchronised then t_{AB} is not known, but by changing direction of the light path, that is varying θ, the magnitude of the 2nd term may be separated from the magnitude of the 1st term, and v and its direction determined. The clocks may then be synchronised. For a small detector the change in θ can be achieved by a direct rotation. Results (7) and (8), or (9) and (10), have been exploited in various detector designs.

6 DeWitte 1st Order in v/c Detector

The DeWitte $L = 1.5$ km RF coaxial cable experiment, Brussels 1991, was a double 1st order in v/c detector, using the scheme in Fig.2, and employing 3 Caesium atomic clocks at each end, and overall measuring $t_{AB} - t_{CD}$. The orientation was NS and rotation was achieved by that of the earth [7].

$$t_{AB} - t_{CD} = \frac{2v\cos(\theta)Ln^2}{c^2} \qquad (11)$$

The dynamic range of $\cos(\theta)$ is $2\sin(\lambda-\beta)\cos(\delta)$, caused by the earth rotation, where λ is the latitude of the detector location, β is the local inclination to the horizontal, here $\beta = 0$, and δ is the declination of **v**. The data shows remarkable agreement with the velocity vector from the flyby Doppler shift data, see Fig. 3. However if there is Fresnel drag in the coaxial cables, there would be no n^2 factor in (11), and the DeWitte data would give a much larger speed $v = 1125$ km/s, in strong disagreement with the flyby data.

7 Torr and Kolen 1st Order in v/c Detector

A one-way coaxial cable experiment was performed at the Utah University in 1981 by Torr and Kolen [6]. This involved two Rb clocks placed approximately 500 m apart with a 5 MHz sinewave RF signal propagating between the clocks via a nitrogen filled coaxial cable buried in the ground and maintained at a constant pressure of ~2 psi. Torr and Kolen observed variations in the one-way travel time, as shown in Fig.4 by the data points. The theoretical predictions for the Torr-Kolen experiment for a cosmic speed of 480 km/s from the direction, RA=5^h, Dec=-70°, as shown in Fig. 4. The maximum/minimum effects occurred, typically, at the predicted times. Torr and Kolen reported fluctuations in both the magnitude, from 1–3 ns, and time of the maximum variations in travel time, just as observed in all later experiments, namely wave effects.

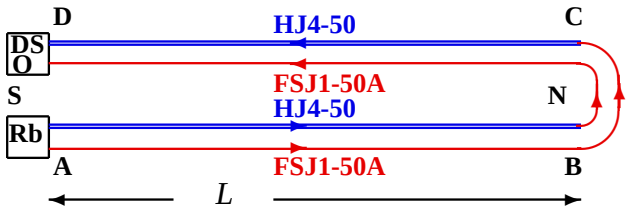

Fig. 5: Because Fresnel drag is absent in RF coaxial cables this dual cable setup, using one clock, is capable of detecting the absolute motion of the detector wrt to space, revealing the sidereal rotation effect as well as wave/turbulence effects. In the 1st trial of this detector this arrangement was used, with the cables laid out on a laboratory floor, and preliminary results are shown in Figs. 3. In the new design the cables in each circuit are configured into 8 loops, as in Fig. 6, giving $L = 8 \times 1.85$ m $= 14.8$ m. In [1] a version with optical fibres in place of the HJ4-50 coaxial cables was used, see Fig. 11. There the optical fibre has a Fresnel drag effect while the coaxial cable did not. In that experiment optical-electrical converters were used to modulate/demodulate infrared light.

8 Dual RF Coaxial Cable Detector

The Dual RF Coaxial Cable Detector exploits the Fresnel drag anomaly, in that there is no Fresnel drag effect in RF coaxial cables. Then from (9) and (10) the round trip travel time is, see Fig. 5,

$$t_{AB} + t_{CD} = \frac{2nL}{c} + \frac{v\cos(\theta)L(n_1^2 - n_2^2)}{c^2} + .. \qquad (12)$$

where n_1 and n_2 are the effective refractive indices for the two different RF coaxial cables, with two separate circuits to reduce temperature effects. Shown in Fig. 6 is a photograph. The Andrews Phase Stabilised FSJ1-50A has $n_1 = 1.19$, while the HJ4-50 has $n_2 = 1.11$. One measures the travel time difference of two RF signals from a Rubidium frequency standard (Rb) with a Digital Storage Oscilloscope (DSO). In each circuit the RF signal travels one-way in one type of coaxial cable, and returns via a different kind of coaxial cable. Two circuits are used so that temperature effects cancel - if a temperature change alters the speed in one type of cable, and so the travel time, that travel time change is the

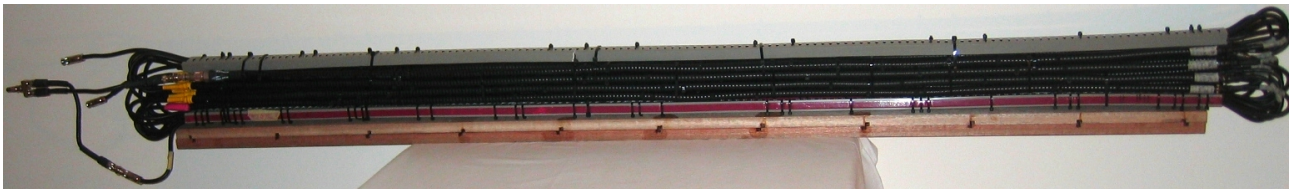

Fig. 6: Photograph of the RF coaxial cables arrangement, based upon 16 ×1.85 m lengths of phase stabilised Andrew HJ4-50 coaxial cable. These are joined to 16 lengths of phase stabilised Andrew FSJ1-50A cable, in the manner shown schematically in Fig. 5. The 16 HJ4-50 coaxial cables have been tightly bound into a 4×4 array, so that the cables, locally, have the same temperature, with cables in one of the circuits embedded between cables in the 2nd circuit. This arrangement of the cables permits the cancellation of temperature differential effects in the cables. A similar array of the smaller diameter FSJ1-50A cables is located inside the grey-coloured conduit boxes.

same in both circuits, and cancels in the difference. The travel time difference of the two circuits at the DSO is

$$\Delta t = \frac{2v\cos(\theta)L(n_1^2 - n_2^2)}{c^2} + .. \qquad (13)$$

If the Fresnel drag effect occurred in RF coaxial cables, we would use (7) and (8) instead, and then the $n_1^2 - n_2^2$ term is replaced by 0, i.e. there is no 1st order term in v. That is contrary to the actual data in Figs. 3 and 7.

The preliminary layout for this detector used cables laid out as in Fig.5, and the data is shown in Fig.3. In the compact design the Andrew HJ4-50 cables are cut into 8×1.85 m shorter lengths in each circuit, corresponding to a net length of $L = 8 \times 1.85 = 14.8$ m, and the Andrew FSJ1-50A cables are also cut, but into longer lengths to enable joining. However the curved parts of the Andrew FSJ1-50A cables contribute only at 2nd order in v/c. The apparatus was horizontal, $\beta = 0$, and orientated NS, and used the rotation of the earth to change the angle θ. The dynamic range of $\cos(\theta)$, caused by the earth rotation only, is again $2\sin(\lambda - \beta)\cos(\delta)$, where $\lambda = -35^\circ$ is the latitude of Adelaide. Inclining the detector at angle $\beta = \lambda$ removes the earth rotation effect, as now the detector arm is parallel to the earth's spin axis, permitting a more accurate characterisation of the wave effects.

9 Temperature Effects

The cable travel times and the DSO phase measurements are temperature dependent, and these effects are removed from the data, rather than attempt to maintain a constant temperature, which is impractical because of the heat output of the Rb clock and DSO. The detector was located in a closed room in which the temperature changed slowly over many days, with variations originating from changing external weather driven temperature changes. The temperature of the detector was measured, and it was assumed that the timing errors were proportional to changes in that one measured temperature. These timing errors were some 30ps, compared to the true signal of some 8ps. Because the temperature timing errors are much larger, the temperature induced $\Delta t = a + b\Delta T$ was fitted to the timing data, and the coefficients a and b determined. Then this Δt time series was subtracted from the data, leaving the actual required phase data. This is particularly effective as the temperature variations had a distinctive signature. The resulting data is shown in Fig.8. In an earlier test for the Fresnel drag effect in RF coaxial cables [13] the technique for removing the temperature induced timing errors was inadequate, resulting in the wrong conclusion that there was Fresnel drag in RF coaxial cables.

10 Dual RF Coaxial Cable Detector: Data

The phase data, after removing the temperature effects, is shown in Fig. 8 (top), with the data compared with predictions for the sidereal effect only from the flyby Doppler shift data. As well that data is separated into two frequency bands (bottom), so that the sidereal effect is partially separated from the

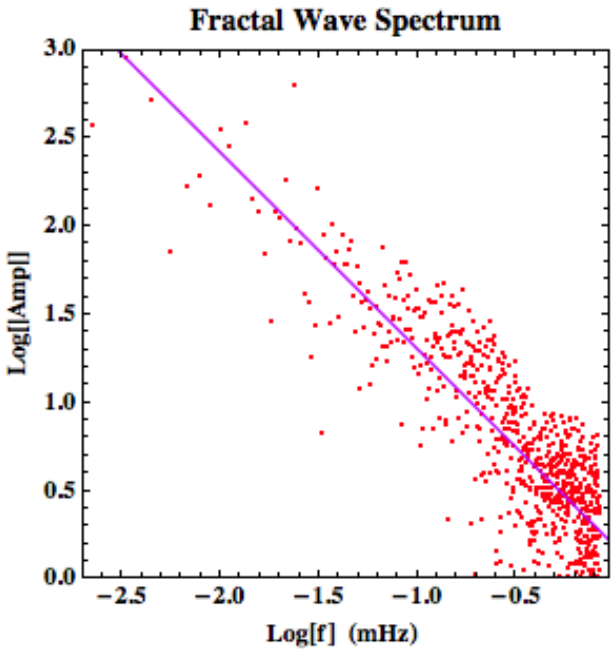

Fig. 7: Log-Log plot of the data (top) in Fig. 7, with the straight line being $A \propto 1/f$, indicating a $1/f$ fractal wave spectrum. The interpretation for this is the 3-space structure shown in Fig. 9.

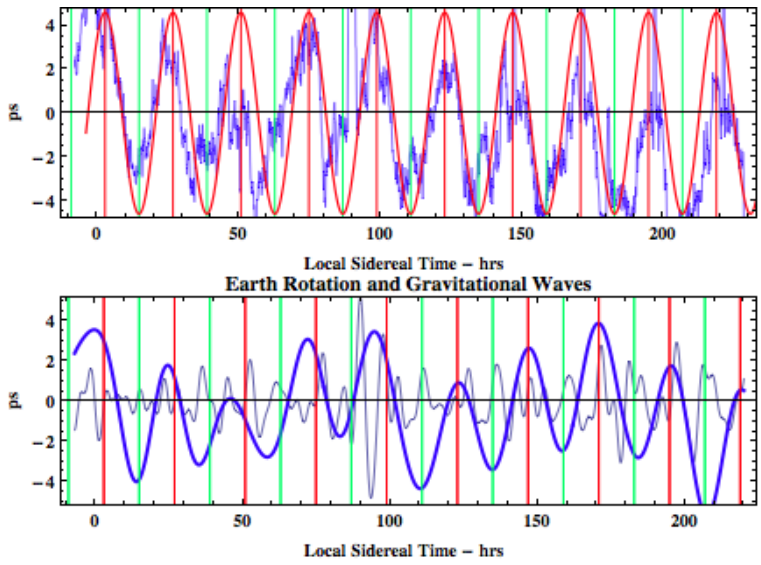

Fig. 8: Top: Travel time differences (ps) between the two coaxial cable circuits in Fig. 5, orientated NS and horizontal, over 9 days (March 4-12, 2012, Adelaide) plotted against local sidereal time. Sinewave, with dynamic range 8.03 ps, is prediction for sidereal effect from flyby Doppler shift data for RA=2.75^h (shown by red fudicial lines), Dec=-76.6°, and with speed 499.2 km/s, see Table 2 of [9], also shown in from Fig. 1. Data shows sidereal effect and significant wave/turbulence effects. Bottom: Data filtered into two frequency bands 3.4×10^{-3} mHz $< f <$ 0.018 mHz (81.4 $h > T >$ 15.3 h) and 0.018 mHz $< f <$ 0.067 mHz (15.3 $h > T >$ 4.14 h), showing more clearly the earth rotation sidereal effect (plus vlf waves) and the turbulence without the sidereal effect. Frequency spectrum of top data is shown in Fig. 7.

gravitational wave effect, *viz* 3-space wave/turbulence. Being 1st order in v/c it is easily determined that the space flow is from the southerly direction, as also reported in [1]. Miller reported the same sense, i.e. the flow is essentially from S to N, though using a 2nd order detector that is more difficult to determine. The frequency spectrum of this data is shown in Fig. 7, revealing a fractal $1/f$ form. This implies the fractal structure of the 3-space indicated in Fig. 9.

11 Optical Fibre RF Coaxial Cable Detector

An earlier 1st order in v/c gravitational wave detector design is shown in Fig. 11, with some data shown in Fig. 10. Only now is it known why that detector also worked, namely that there is a Fresnel drag effect in the optical fibres, but not in the RF coaxial cable. Then the travel time difference, measured at the DSO is given by

$$\Delta t = \frac{2v\cos(\theta)L(n_1^2 - 1)}{c^2} + .. \qquad (14)$$

where n_1 is the effective refractive index of the RF coaxial cable. Again the data is in remarkable agreement with the flyby determined **v**.

12 2nd Order in v/c Gas-Mode Detectors

It is important that the gas-mode 2nd order in v/c data from Michelson and Morley, 1887, and from Miller, 1925/26, be

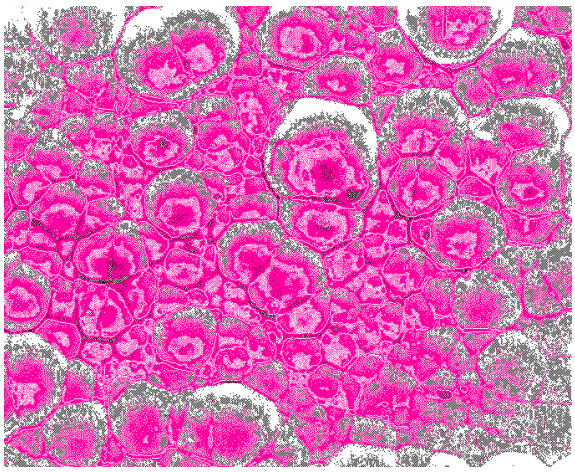

Fig. 9: Representation of the fractal wave data as a revealing the fractal textured structure of the 3-space, with cells of space having slightly different velocities, and continually changing, and moving wrt the earth with a speed of ~500 km/s.

reviewed in the light of the recent experiments and flyby data. Shown in Fig. 12 (top) is Miller data from September 16, 1925, 4^{h}40′ Local Sidereal Time (LST) - an average of data from 20 turns of the gas-mode Michelson interferometer. Plot and data after fitting and then subtracting both the temperature drift and Hicks effects from both, leaving the expected si-

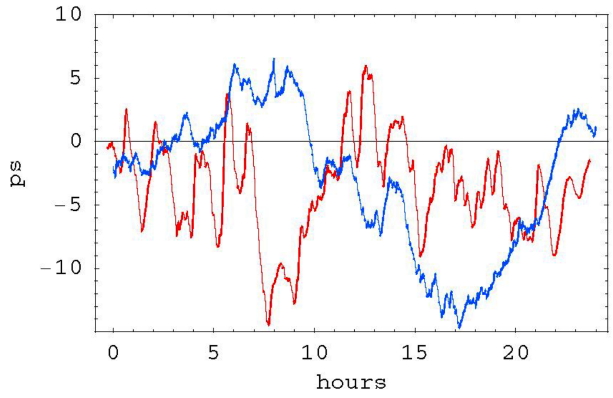

Fig. 10: Phase difference (ps), with arbitrary zero, versus local time data plots from the Optical Fibre - Coaxial Cable Detector, see Fig. 11 and [1, 2], showing the sidereal time effect and significant wave/turbulence effects. The plot (blue) with the most easily identified minimum at ~17 hrs local Adelaide time is from June 9, 2006, while the plot (red) with the minimum at ~8.5 hrs local time is from August 23, 2006. We see that the minimum has moved forward in time by approximately 8.5 hrs. The expected sidereal shift for this 65 day difference, without wave effects, is 4.3 hrs, to which must be added another ~1h from the aberration effects shown in Fig. 1, giving 5.3hrs, in agreement with the data, considering that on individual days the min/max fluctuates by ±2hrs. This sidereal time shift is a critical test for the detector. From the flyby Doppler data we have for August RA=5^h, Dec=-70°, and speed 478 km/s, see Table 2 of [9], the predicted sidereal effect dynamic range to be 8.6 ps, very close to that observed.

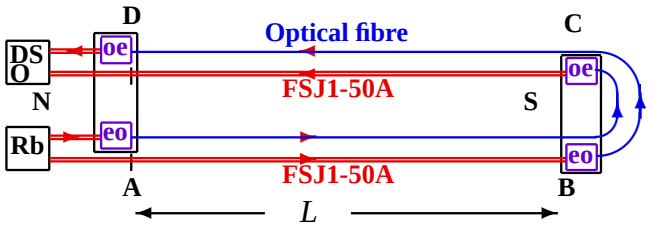

Fig. 11: Layout of the optical fibre - coaxial cable detector, with L = 5.0 m. 10 MHz RF signals come from the Rubidium atomic clock (Rb). The Electrical to Optical converters (EO) use the RF signals to modulate 1.3 μm infrared signals that propagate through the single-mode optical fibres. The Optical to Electrical converters (OE) demodulate that signal and give the two RF signals that finally reach the Digital Storage Oscilloscope (DSO), which measures their phase difference. The key effects are that the propagation speeds through the coaxial cables and optical fibres respond differently to their absolute motion through space, with no Fresnel drag in the coaxial cables, and Fresnel drag effect in the optical fibres. Without this key difference this detector does not work.

nusoidal form. The error bars are determined as the rms error in this fitting procedure, and show how exceptionally small were the errors, and which agree with Miller's claim for the errors. Best result from the Michelson-Morley 1887 data - an average of 6 turns, at 7^h LST on July 11, 1887, is shown in Fig.12 (bottom). Again the rms error is remarkably small. In both cases the indicated speed is v_P - the 3-space speed projected onto the plane of the interferometer. The angle is the azimuth of the 3-space speed projection at the particular LST. Fig. 13 shows speed fluctuations from day to day significantly exceed these errors, and reveal the existence of 3-space flow turbulence - i.e gravitational waves. The data shows considerable fluctuations, from hour to hour, and also day to day, as this is a composite day. The dashed curve shows the non-fluctuating best-fit sidereal effect variation over one day, as the earth rotates, causing the projection onto the plane of the interferometer of the velocity of the average direction of the space flow to change. The predicted projected sidereal speed variation for Mt Wilson is 251 to 415 km/s, using the Casinni flyby data and the STP air refractive index of $n = 1.00026$ appropriate atop Mt. Wilson, and the min/max occur at approximately 5hrs and 17hrs local sidereal time (Right Ascension). For the Michelson-Morley experiment in Cleveland the predicted projected sidereal speed variation is 239 to 465 km/s. Note that the Cassini flyby in August gives a RA= 5.15^h, close to the RA apparent in the above plot. The green data points, showing daily fluctuation bars, at 5^h and 13^h, are from the Michelson-Morley 1887 data, from averaging (excluding only the July 8 data for 7^h because it has poor S/N), and with same rms error analysis. The fiducial time lines are at 5^h and 17^h. The data indicates the presence of turbulence in the 3-space flow, i.e gravitational waves, being first seen in the Michelson-Morley experiment.

13 Conclusions

The Dual RF Coaxial Cable Detecto, exploits the Fresnel drag anomaly in RF coaxial cables, *viz* the drag effect is absent in such cables, for reasons unknown, and this 1st order in v/c detector is compact, robust and uses one clock. This anomaly now explains the operation of the Optical-Fibre - Coaxial Cable Detector, and permits a new calibration. These detectors have confirmed the absolute motion of the solar system and the gravitational wave effects seen in the earlier experiments of Michelson-Morley, Miller, DeWitte and Torr and Kolen. Most significantly these experiments agree with one another, and with the absolute motion velocity vector determined from spacecraft earth-flyby Doppler shifts. The observed significant wave/turbulence effects reveal that the so-called "gravitational waves" are easily detectable in small scale laboratory detectors, and are considerably larger than those predicted by GR. These effects are not detectable in vacuum-mode Michelson terrestrial interferometers, nor by their analogue vacuum-mode resonant cavity experiments.

The new Dual RF Coaxial Cable Detector permits a detailed study and characterisation of the wave effects, and with the detector having the inclination equal to the local latitude the earth rotation effect may be removed, as the detector is

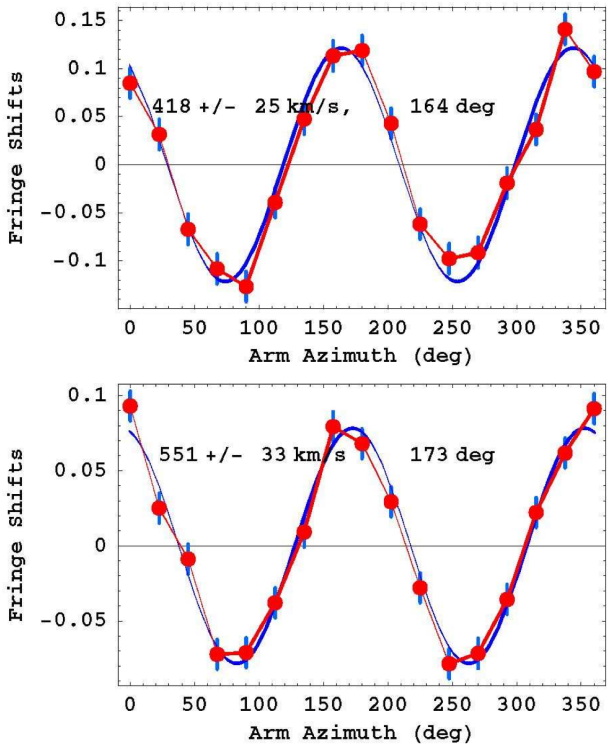

Fig. 12: Top: Typical Miller data from 1925/26 gas-mode Michelson interferometer, from 360° rotation. Bottom: Data from Michelson-Morley 1887 gas-mode interferometer, from 360° rotation.

then parallel to the earth's spin axis, enabling a more accurate characterisation of the wave effects. The major discovery arising from these various results is that 3-space is directly detectable and has a fractal textured structure. This and numerous other effects are consistent with the dynamical theory for this 3-space. We are seeing the emergence of fundamentally new physics, with space being a a non-geometrical dynamical system, and fractal down to the smallest scales describable by a classical velocity field, and below that by quantum foam dynamics [12]. Imperfect and incomplete is the geometrical model of space.

Acknowledgements

The Dual RF Coaxial Cable Detector is part of the Flinders University Gravitational Wave Detector Project. The DSO, Rb RF frequency source and coaxial cables were funded by an Australian Research Council Discovery Grant: *Development and Study of a New Theory of Gravity*. Special thanks to CERN for donating the phase stabilised optical fibre, and to Fiber-Span for donating the optical-electrical converters. Thanks for support to Professor Warren Lawrance, Bill Drury, Professor Igor Bray, Finn Stokes and Dr David Brotherton.

Submitted on April 17, 2012 / Accepted on April 21, 2012

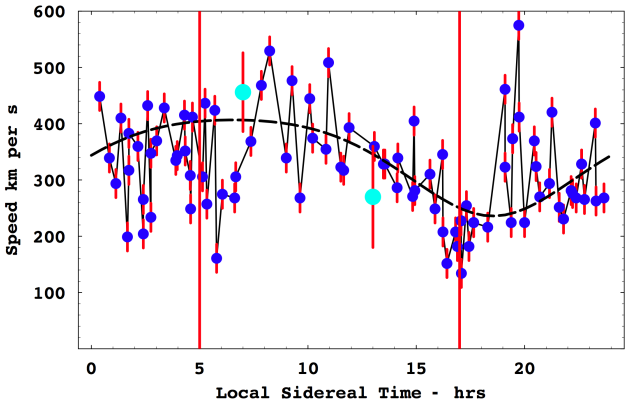

Fig. 13: Miller data for composite day in September 1925, and also showing Michelson-Morley 1887 July data at local sidereal times of 7^h and 13^h. The waved/turbulence effects are very evident, and comparable to data reported herein from the new detector.

References

1. Cahill R.T. A New Light-Speed Anisotropy Experiment: Absolute Motion and Gravitational Waves. *Progress in Physics*, 2006, v. 4, 73–92.
2. Cahill R.T. Absolute Motion and Gravitational Wave Experiment Results. Contribution to *Australian Institute of Physics National Congress*, Brisbane, Paper No. 202, 2006.
3. Cahill R.T. and Kitto K. Michelson-Morley Experiments Revisited. *Apeiron*, 2003, v. 10(2), 104–117.
4. Cahill R.T. The Michelson and Morley 1887 Experiment and the Discovery of Absolute Motion. *Progress in Physics*, 2005, v. 3, 25–29.
5. Miller D.C. The Ether-Drift Experiment and the Determination of the Absolute Motion of the Earth. *Reviews of Modern Physics*, 1933, v. 5, 203–242.
6. Torr D.G. and Kolen P. in: Precision Measurements and Fundamental Constants, Taylor B.N. and Phillips W.D. (eds.) *National Bureau of Standards (U.S.), Spec. Pub.*, 1984, 617–675.
7. Cahill R.T. The Roland De Witte 1991 Experiment. *Progress in Physics*, 2006, v. 3, 60–65.
8. Anderson J.D., Campbell J.K., Ekelund J.E., Ellis J. and Jordan J.F. Anomalous Orbital-Energy Changes Observed during Spacecraft Flybys of Earth. *Physical Review Letters*, 2008, v. 100, 091102.
9. Cahill R.T. Combining NASA/JPL One-Way Optical-fibre Light-Speed Data with Spacecraft Earth-Flyby Doppler-Shift Data to Characterise 3-Space Flow. *Progress in Physics*, 2009, v. 4, 50–64.
10. Cahill R.T. Unravelling Lorentz Covariance and the Spacetime Formalism. *Progress in Physics*, 2008, v. 4, 19–24.
11. Cahill R.T. and Stokes F. Correlated Detection of sub-mHz Gravitational Waves by Two Optical-fibre Interferometers. *Progress in Physics*, 2008, v. 2, 103–110.
12. Cahill R.T. Process Physics: From Information Theory to Quantum Space and Matter. Nova Science Pub., New York, 2005.
13. Cahill R.T. and Brotherton D., Experimental Investigation of the Fresnel Drag Effect in RF Coaxial Cables. *Progress in Physics*, 2011, v. 1, 43–48.

Synchronous Measurements of Alpha-Decay of ^{239}Pu Carried out at North Pole, Antarctic, and in Puschino Confirm that the Shapes of the Respective Histograms Depend on the Diurnal Rotation of the Earth and on the Direction of the Alpha-Particle Beam

S. E. Shnoll[*§¶], M. E. Astashev[*], I. A. Rubinshtein[†], V. A. Kolombet[*], S. N. Shapovalov[‡], B. I. Bokalenko[‡], A. A. Andreeva[*], D. P. Kharakoz[*], I. A. Melnikov[‖]

[*]Institute of Theoretical and Experimental Biophysics, Russ. Acad. Sciences. E-mail: shnoll@mail.ru (Simon E. Shnoll)
[†]Skobeltsyn Institute of Nuclear Physics, Moscow State University. E-mail: iarubinst@mail.ru (Ilia A. Rubinstein)
[‡]Arctic and Antarctic Research Institute
[§]Physics Department, Moscow State University
[¶]Puschino Institute for Natural Sciences
[‖]Shirshov Institute of Oceanology, Russ. Acad. Sciences

Dependence of histogram shapes from Earth diurnal rotation, and from direction of alpha-particles issue at ^{239}Pu radioactive decay is confirmed by simultaneous measurements of fluctuation amplitude spectra — shapes of corresponding histograms. The measurements were made with various methods and in different places: at the North Pole, in Antarctic (Novolazarevskaya station), and in Puschino.

1 Introduction

Fine structure of an amplitude fluctuation spectrum (i.e., that of "data spread") can be determined during measurements of different nature changes with the Earth rotation around its axis and its movement along its orbit.

This follows from the regular changes in the shape of the respective histograms with diurnal and annual periods. Well-defined periods are observed: those of "stellar" (1,436 minutes) and "solar" (1,440 minutes) days, "calendar" (365 average solar days), "tropical" (365 solar days 5 hours 48 minutes) and "sidereal" (365 days 6 hours 9 minutes) years [1].

Experiments with collimators that allow studies of alpha-particle beams with definite directions indicate that this regularity is related to non-uniformity (anisotropy) of space [1, 6].

Dependence on the diurnal Earth rotation shows in high probability of shape similarity of histograms obtained during measurements in different locations at the same local time, as well as in the disappearance of diurnal periods near the North Pole [2]. However, together with synchronous changes in histogram shapes according to the local time, some experiments show changes in histogram changes simultaneously according to an absolute time [2]. It was discovered that synchronism with regard to absolute time (e.g. during measurements in Antarctic and in Puschino, Moscow Region) observed during measurements of alpha-decay of ^{239}Pu, depends on the spatial orientation of the collimators [1, 3, 5].

In order to study dependences of the absolute synchronism phenomenon, experiments carried out near the North Pole, which would minimize effects of the Earth's diurnal rotation, were required,.

The first such attempt was undertaken in 2001 by joint efforts of Inst. Theor. & Experim. Biophysics of Russ. Acad. Sciences (ITEB RAS) and Arctic & Antarctic Res. Inst. (AARI), when twenty-four-hour measurements of ^{239}Pu alpha-decay with a counter without collimator were carried out continuously during several days in a North Pole expedition on the "Akademik Fedorov" research vessel.

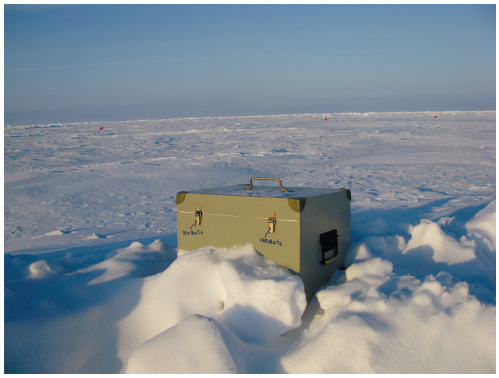

Fig. 1: Measuring device at North Pole.

However, the ship was not able to come closer than latitude 82° North to the North Pole. But even this incomplete approaching to the North pole has shown almost complete disappearance of diurnal changes in the histogram shapes that were observed during the same period of time in Puschino (latitude 54° North) [2].

In 2003, we found out that diurnal changes in histogram shapes also disappear when alpha-radioactivity is measured with collimators that issue alpha-particle beams directed towards the Pole star. This indicated that histogram shapes depend on a space direction of a process[1, 6].

This conclusion was later repeatedly confirmed by experiments with collimators directed westward, eastward, northward, or rotated in the horizontal plane counterclockwise with

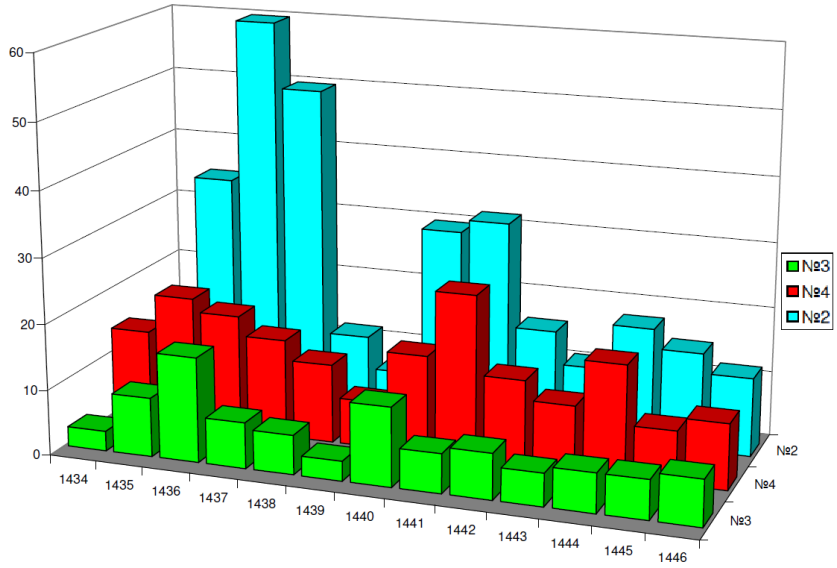

Fig. 2: During the ^{239}Pu alpha-decay measurements at the North Pole, the effect of the daily period disappearance is more pronounced for the vertical detector (device no. 3) than for the horizontal one (device no. 4). For comparison, daily period is shown for synchronous measurements in Puschino with a westward-directed collimator (device no. 2). The abscissa axis shows minutes. The ordinate axis shows the number of the similar pairs obtained during this period with a total number of the compared rows of 360.

periods of 1, 2, 3, 4, 5, 6, 12 hours. The histogram shape changed with the respective periods.

In 2011, we were able to carry out synchronous experiments on ^{239}Pu alpha-decay using nine different devices, two of which were located at the North Pole during the period of work at the Pan-Arctic ice drifting station (latitude 89° 01 — 89° 13 North, longitude 121° 34 —140° 20 East), one in Antarctic (the Novolazarevskaia station, latitude 70° South, longitude 11° East), and six more having different collimators in Puschino (latitude 54° North, longitude 37° East).

As a result of this project, we were able to confirm the conclusion that histogram shapes depend on the diurnal rotation of the Earth, and to show that, when alpha-particle beam is directed along the meridian, the histogram shape changes synchronously from the North Pole to the Antarctic.

2 Materials and methods

The device was installed on the surface of drifting ice near the geographic North Pole (Fig. 1) and worked continuously since April 5, 11 till April 12, 11, until its accumulators were out of charge.

The measurement results obtained at the North Pole since April 5, 11 till April 12, 11 were analyzed in the ITEB RAS in Puschino. The analysis was, as usual, comparison of histogram shapes for measurements made with different devices. A detailed description of the methods of histogram construction and shape comparison can be found in [1].

This paper is based on the results obtained from the simultaneous measurements of alpha-activity of the ^{239}Pu samples with the activity of 100–300 registered decay events per second using 9 different devices with semiconductor alpha-particle detectors constructed by one of the authors (I. A. Rubinshtein) with and without collimators [6] and registration system constructed by M. E. Astashev (see [7]).

The main characteristics of the devices used in this study are given in Table 1.

Because of special complications presented by the conditions at the North Pole (no sources of electricity, significant temperature variations) a special experimental system with autonomous electricity source, thermostat, and time recording was created by M. E. Astashev. This device contained two independent alpha-particle counters (I. A. Rubinshtein), one directed upwards and another one directed sidewards, which were combined with a special recording system.

A system based on the computing module Arduino Nano V.5 [7–1] was used for registering the signals from the alpha-particle counter. The software provided all service functions for impulse registration, formation of the text data for the flash card, obtaining the time data, regulation of the heater, obtaining the temperature and the battery charge data. The data were recorded onto a 1 Gb microSD card, and the function library Fat16.h, real time clock were implemented using the DS1302 chip [7–2] with a lithium battery CR2032 independent power supply [7–3]. Power supply of the registering system and alpha-particle counters was provided by four waterproof unattended geleous lead batteries of 336 W× h total capacity [7–3]. To provide working conditions for the batteries and stability of the system, a 12 W electric heater with pulse-duration control and temperature detector AD22100 was added [7–4]. Pulse counters were implemented by processing external hardware interruptions of the computing module. The data were recorded onto the card as plain text.

Number	Device type	Coordinates	The expected purpose, i.e. registration of the histogram shape changes caused by:
1	Collimator, directed eastward	Puschino, lat. 54° North, long. 37° East	diurnal Earth rotation
2	Collimator, directed westward	Puschino, lat. 54° North, long. 37° East	diurnal Earth rotation
3	Flat detector without collimator, directed "upwards"	North Pole	Earth circumsolar rotation
4	Flat detector without collimator, directed "sidewards"	North Pole	combined, diurnal and circumsolar, Earth rotation
5	Collimator, directed towards the Polar Star	Puschino, lat. 54° North, long. 37° East	circumsolar Earth rotation
6	Polar Star directed collimator-free flat detector	Puschino, lat. 54° North, long. 37° East	combined, diurnal and circumsolar, Earth rotation
7	Sun directed collimator, clockwise rotation	Puschino, lat. 54° North, long. 37° East	circumsolar Earth rotation
8	Collimator-free flat detector, directed "upwards"	Puschino, lat. 54° North, long. 37° East	combined, diurnal and circumsolar, Earth rotation
9	Horizontal collimator, directed northward	Puschino, lat. 54° North, long. 37° East	combined, diurnal and circumsolar, Earth rotation

Table 1: The devices for the measurements of ^{239}Pu alpha-decay used in this study.

3 Results

3.1 Daily periods of the histogram shape changes depend on the detector orientation

Fig. 2 shows that measurement of ^{239}Pu alpha-activity in Puschino with a westward-directed collimator (device no. 2) leads to appearance of similar histograms with two clearly distinguished periods, which are equal to a sidereal day (1,436 min) and a solar day (1,440 min). During measurements at the North Pole with flat detectors, daily periods almost disappear. It can be noticed, however, that daily periods are slightly more pronounced for the flat detector directed sidewards (horizontally; device no. 4). The periods disappear for measurements at the North Pole with a detector directed upwards (vertically; device no 3).

Dependence of the effects observed at the North Pole on the detector orientations, which was revealed while looking for the diurnal periods, indicates that these effects were not caused by any influence by some "geophysic" impacts on the studied processes or on the measurement system. Not location of the device but rather orientation of the detector determines the outcome. A similar result was observed for two other Pole Star-directed detectors in Puschino, one of which was flat and another had a collimator (data not shown). The main effect, disappearance of the daily period, was significantly more pronounce with a collimator-equipped detector.

3.2 The absolute time synchronism of the changes in the histogram shapes, in the ^{239}Pu alpha-activity measurements in Antarctic, at the North Pole and in Puschino depends on the orientation of the detectors

The main role of the spatial orientation rather than geographical localization in the studied phenomena is clearly seen from the high probability of the histogram similarity if they are measured simultaneously at the same absolute time using a vertical detector at the North Pole and a Pole Star-directed detector with a collimator in Puschino (Fig. 3A, B)

Dependence of the synchronism with regard to the absolute time on the spatial orientation of the detectors was particularly clearly revealed during comparison of the histograms constructed on the basis of ^{239}Pu alpha-activity measurements in Antarctic, at the North Pole, and in Puschino.

In Fig. 4 A and B, we can see high probability of absolute synchronism for measurements performed on April 8, 2011 and on April 9, 2011 in Antarctic (no. 8) with a vertical detector located at the North Pole (no. 3), and in Puschino with a collimator directed at the Sun (no. 7). There is no synchronism for experiments with a horizontal detector at the North Pole (no.4) and detector in Antarctic (no. 8).

Therefore, during measurements at the North Pole with a vertical detector, or with collimator-equipped detectors aimed at the Sun or at the Pole Star in Puschino, that is both detectors cannot depend upon Earth diurnal rotation, there was an absolute synchronism of the histogram shape change with histogram shape changes in Antarctic.

Another illustration of the role of detector orientation for the measurements at the North Pole is given in Fig.5. Absolute synchronism of the histogram shape change is more pronounced for comparison of the ^{239}Pu alpha-activity measurements in Puschino with a collimator constantly directed at the Sun and at the North Pole with a vertically-directed collimator.

4 Discussion

The results of the present study confirm that the changes in the histogram shape depend on the diurnal rotation of the

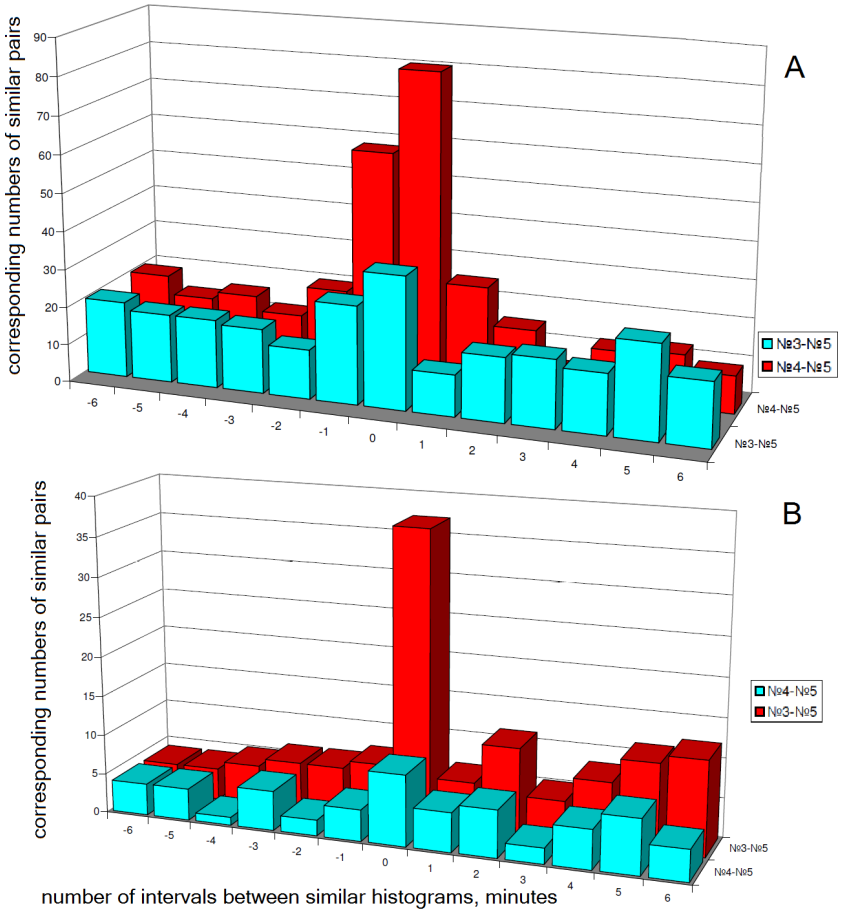

Fig. 3: Two experiments were performed on April 8, 2011(A) and April 9, 2011(B). High probability of the histogram shape similarity at the same absolute time is observed for measurements in Puschino using Pole Star-directed detector with a collimator (device no. 5) and at the North Pole with a vertical detector (device no. 3). There is no similarity during similar measurements in Puschino (the same device no. 5) and at the North Pole with a horizontal detector (device no. 4). X-axis is numbers of intervals between similar histograms, min.; Y-axis is correspondent numbers of similar pairs.

Earth and that this dependence is caused by anisotropy of our space. Daily periods of the changes in the histogram shapes are not observed when alpha-particle beams are parallel to the Earth axis.

Absolute synchronism of the changes in the histogram shapes is observed in experiments with collimators directed at the Pole Star and at the Sun in Puschino (latitude 54° North) (no. 5). and for measurements at the North Pole (latitude 90° North) with a "vertical" detector only (no. 3). There is no absolute synchronism with the "horizontal" counter (no. 4). By analogy, absolute synchronism of the changes in the histogram shapes for measurements in Antarctic is observed only for measurements at the North Pole with a "vertical" detector and a Sun-directed detector in Puschino.

Comparison of these data with the "local time effect", i.e. synchronous changes in the histogram shape in different geographical locations at the same local time, allows to suggest that changes in the histogram shapes, which are synchronous in different geographical locations with regard to the absolute time, are caused by the movement of the laboratory with the Earth along the solar orbit, and synchronism with regard to the absolute time is caused by Earth rotations. This conclusion should be a subject of additional studies.

Acknowledgements

This work was made possible through the financial support from the founder of the "Dynasty Foundation", Professor D. B. Zimin. We are grateful to M. N. Kondrashova for important discussions, interest and friendly support. We also gratefully acknowledge important discussions of the research plans and of the obtained results with D. Rabounski. We are grateful to M. A. Panteleev for his helpful advice and English version of the article.

We thank A. G. Malenkov, E. I. Boukalov, and A. B. Tsetlin for their helpful advice on the organization of the studies at the North Pole.

Submitted on March 11, 2012 / Accepted on March 16, 2012

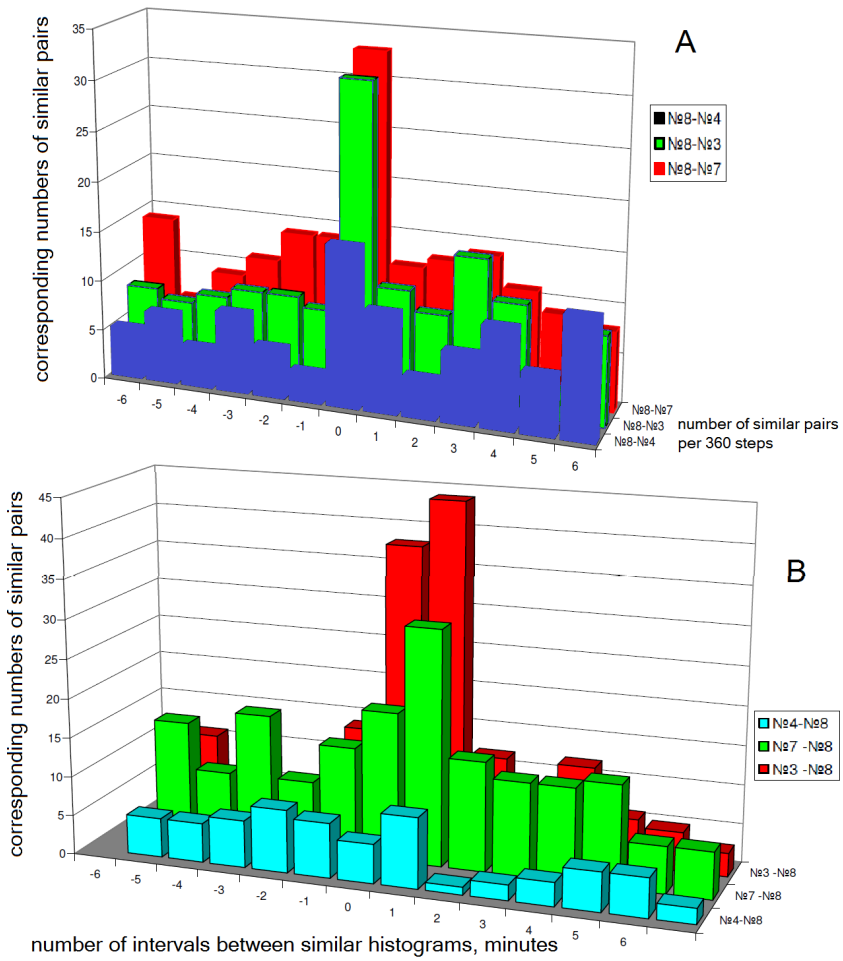

Fig. 4: The experiments, A and B. The shapes of the histograms change synchronously with regard to the absolute time during measurements of the ^{239}Pu alpha-activity in Antarctic and at the North Pole with a vertical detector (no. 8 — no. 3) and in Puschino with a collimator directed at the Sun (no. 8 — no. 7). During measurements at the North Pole with a horisontally-directed collimator, there is no synchronism with Antarctic (no. 8 — no. 4).

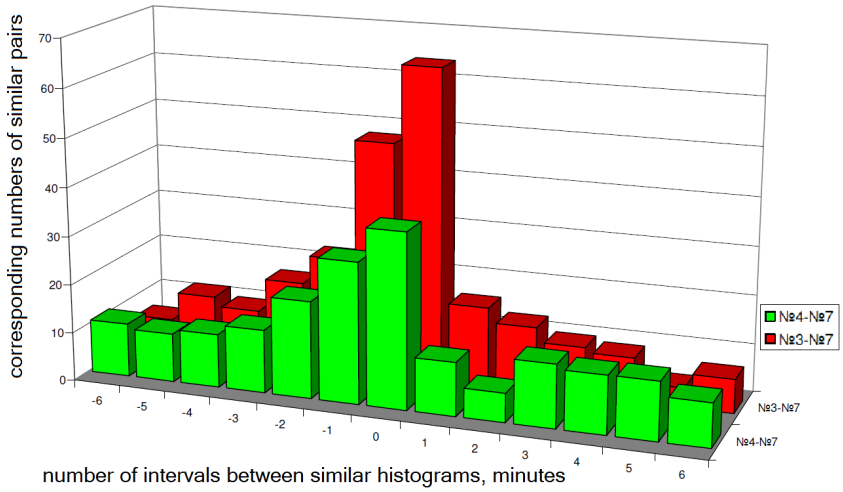

Fig. 5: Absolute synchronism of the changes in the historgram shapes for measurements of ^{239}Pu alpha-activity in Puschino with a collimator directed at the Sun (no. 7) and measurements at the North Pole with a vertical (no. 3) and a horizontal (no. 4) detectors. Absolute synchronism is more pronounced for measurements with a vertical detector.

References

1. Shnoll S. E. Cosmic Physical Factors in Random Processes. Svenska Fisikarkivet, Stockholm, 2009, (*in Russian*)
2. Shnoll S. E., Rubinshtein I. A., Zenchenko K. I., Zenchenko T. A., Udal'tsova N. V., Kondradov A. A., Shapovalov S. N., Makarevich A. V., Gorshkov E. S., Troshichev O. A. Dependence of "macroscopic fluctuations" on geographic coordinates (from materials of Arctic (2000) and Antarctic (2001) expeditions). *Biofizika*, 2003 Nov–Dec, v. 48 (6), 1123–1131 (*in Russian*).
3. Shnoll S. E., Zenchenko K. I., Berulis I. I., Udal'tsova N. V., Zhirkov S. S., Rubinshtein I. A. Dependence of "macroscopic fluctuations" from cosmophysical factors. Spatial anisotropy. *Biofizika*, 2004 Jan–Feb, v. 49 (1), 132–139 (*in Russian*).
4. Shnoll S. E., Rubinshtein I. A., Zenchenko K. I., Shlektarev V. A., Kaminsky A. V., Konradov A. A., Udaltsova N. V. Experiments with rotating collimators cutting out pencil of alpha-particles at radioactive decay of Pu-239 evidence sharp anisotropy of space. *Progress in Physics*, 2005, v. 1 81–84.
5. Shnoll S. E. Changes in fine structure of stochastic distributions as a consequence of space-time fluctuations. *Progress in Physics*, 2006, v. 2 39–45.
6. Shnoll S. E. and Rubinstein I. A.. Changes in fine structure of stochastic distributions as a consequence of space-time fluctuations. *Progress in Physics*, 2009, v. 2 83–95.
7. http://arduino.cc/en/Main/ArduinoBoardNano; http://www.henningkarlsen.com/electronics/a_l_ds1302.php; http://arduino.cc/forum/index.php/topic,8268.0.html; http://www.delta-batt.com/upload/iblock/19e/delta%20hr12-7.2.pdf; http://www.analog.com/en/mems-sensors/analog-temperature-sensors/ad22100/products/product.html

Dependence of Changes of Histogram Shapes from Time and Space Direction is the Same when Fluctuation Intensities of Both Light-Diode Light Flow and ^{239}Pu Alpha-Activity are Measured

I. A. Rubinshtein*, S. E. Shnoll†§¶, A. V. Kaminsky‖, V. A. Kolombet†, M. E. Astashev†, S. N. Shapovalov‡, B. I. Bokalenko‡, A. A. Andreeva†, D. P. Kharakoz†

*Skobeltsyn Institute of Nuclear Physics, Moscow State University
E-mail: iarubinst@mail.ru
†Institute of Theoretical and Experimental Biophysics, Russ. Acad. Sciences
E-mail: shnoll@mail.ru
‡Arctic and Antarctic Research Institute
§Physics Faculty, Moscow State University
¶Puschino Institute for Natural Sciences
‖Elfi-tech Ltd., Rekhovot, Israel

The paper tells that spectra of fluctuation amplitudes, that is, shapes of corresponding histograms, resulting measurements of intensity of light fluxes issued by a light-diode and measurements of intensity of ^{239}Pu alpha-particles issues change synchronously. Experiments with light beams show the same diurnal periodicity and space direction dependencies as experiments with radioactivity. Thus new possibilities for investigation of "macroscopic fluctuations" come.

1 Introduction

Previous papers [1] have shown that shapes of fluctuation amplitudes spectra, i.e. shapes of corresponding histograms, constructed by results of measurements of various nature processes — from electronic device noises, rates of chemical and biochemical reactions, and Brownian movement to radioactive decay of various types — are determined by cosmophysical factors: diurnal and circumsolar rotations of the Earth. A histogram shape depends on geographical coordinates and space direction. Shapes of histograms of different nature processes taking place in different geographical locations but at the same local times are the same.

A histogram shape depends on a direction which alpha-particles issued at radioactive decay follow; this was shown in measurements of ^{239}Pu alpha-radioactivity fluctuations. Study of dependence between fluctuations and angle orientation of their source benefits a lot from focusing a source. When diameter of net collimator holes decreases, registered activity of particles flow falls crucially, preventing statistical reliability of results. This adverse effect complicates construction and use of a focused collimator-equipped ^{239}Pu source. For that matter, we have examined similar time and space direction dependencies at measurements of fluctuations of light beams intensity. Regularities of histogram shape changes at measurements of light flux intensity fluctuations were shown to be absolutely the same as those at measurements of radioactive alpha-decay. Use of this fact makes it possible to increase substantially accuracy of spatial resolution at increase of a light beam and to set out a lot of other experiment versions.

2 Devices and methods

2.1 Measurements of variously directed light flows. Sources and detectors of light flows

We measured fluctuations of intensity of light beams provided by a light diode and measured with a photo diode. Values to register were numbers of events, i.e. exceedings of a set threshold of light intensity per a time unit.

AL 307D light diode with ~630 nm wave length and 8 mA direct current was used as source of light. A224 photo diode by FGUP "PULSAR" Federal State Unitary Enterprise was used as a detector. Light and photo diodes were fastened in a tube with light channel; diameter of the tube was 3 mm, and space between diodes was 35 mm (Fig. 1).

The collimator with light and photodiodes can be oriented in a desired direction. Alternate component of the photo diode current comes through the low-noise amplifier to the input of the comparator registering signals that exceed a preset threshold value. The value should provide 200-500 exceeding

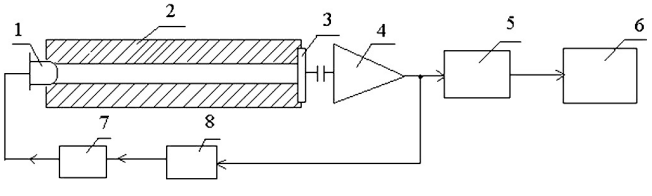

Fig. 1: Functional diagram of device measuring light beam fluctuations 1 — light diode 2 — collimator 3 — photo diode 4 — low-noise amplifier 5 — comparator 6 — impulse counter 7 — stabilizer of mean-square voltage value at amplifier (4) output 8 — light diode current generator

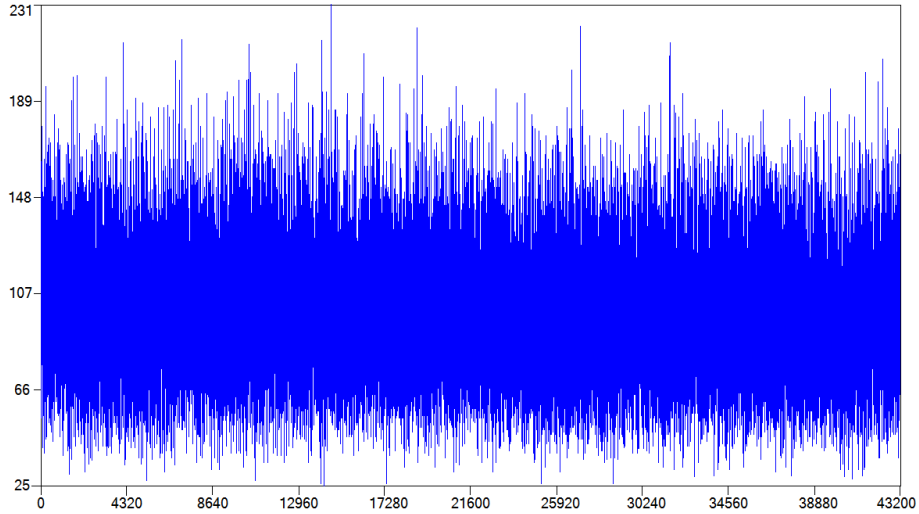

Fig. 2: Illustration of a time series image at measurements of fluctuations of light flow intensity. X-axis is time in seconds. Y-axis is numbers of light flow fluctuations with heights exceeding the device noise.

signals per a second. Besides counting impulses, the device can examine fluctuations of distribution of an amplifier signal heights by digitizing signals with a preset frequency, for example, 300 Hz. Nature of amplifier signal height distribution is electric noise. Its fluctuations can be examined by AD of noise signal followed with histograming of equal time periods.

Impacts of photons falling to photodiode were determined with measurements of mean-square values of amplifier signals, the amplifier being connected to source of current equal to photo diode CD without lighting (1.4 mcA). It equals to 5.6 mV, whereas mean-square value of signals at photons falling is 36 mV. If an electronic device noise consists of two components, its value can be determined by the following expression:

$$U_n = \sqrt{U_{n_1}^2 + U_{n_2}^2} \, .$$

In our case: U_{n_1} is photon noise signal, U_{n_2} is noise signal of current equal to photo diode one, and U_n is total noise signal. From here: U_{n_1} = 32.2 mV, that is ≅6 folds higher than current noise.

2.2 Results of measurements of numbers of discriminator threshold exceedings per a second

They were saved in a computer archive. Histograms were constructed, usually, by 60 results of measurements during one minute total time.

2.3 Computing histograms and analysis of their shapes

They have been multiply described earlier [1]. Shapes of histograms were compared by Edwin Pozharsky auxiliary computer program requiring further expert-made "similar-nonsimilar" diagnosis and by completely automated computer program by Vadim Gruzdev [2].

3 Results

Most of measurements were made at the Institute of Theoretical and Experimental Biophysics of Russian Academy of Sciences (ITEB RAS) in Puschino and in AARI Novolazarevskaya station in Antarctic. In Puschino we used a device with three light beam collimators directed towards West, East, and Polar Star and devices with alpha-activity measuring collimators directed the same towards West, East, and Polar Star. In Novolazarevskaya station we measured alpha-activity with

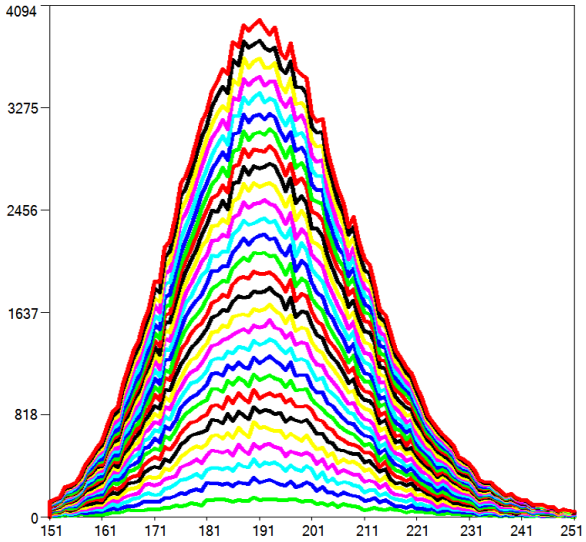

Fig. 3: Change of shapes of non-smoothed summed distributions according to stepwise increase of amount of light flow intensity measurements. 172,800 one-second measurements during two days: May 4 and 5, 2011. The collimator is East-directed. Layer lines mark each 6,000 measurements. X-axis is intensity (amounts of events per a second); Y-axis is amounts of measurements corresponding to the fluctuations intensity.

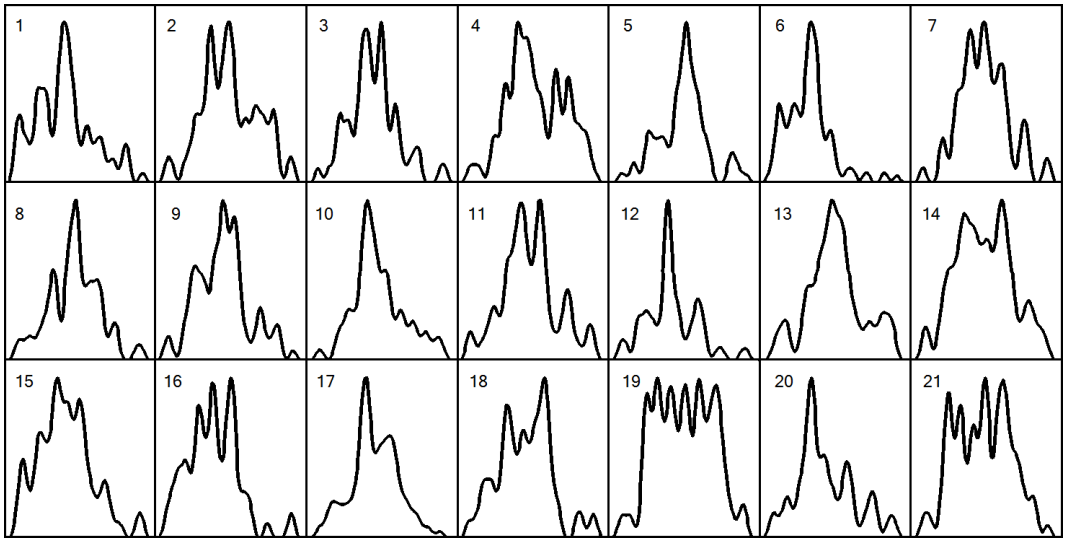

Fig. 4: Fragment of a computer log. Histograms constructed by sixty results of one-second measurements of East-directed light flow fluctuations on May 4, 2011. The histograms are seven times smoothed.

a collimator-free device.

Fig. 2 presents a section of a time series — results of registration of fluctuations of light flows from a West-directed beam. This is a typical stochastic process — white noise.

At this figure a regular fine structure, the same as in investigation of any other process, can be seen. The structure, different in different time periods, does not disappear but becomes more distinct when amount of measurements increase. The nature of this fine structure should become a subject of some special investigations (see in [1]).

The main material of this work is shape of sample distributions, histograms constructed by small (30–60) amount of measurements. The general shape of such histograms was at examination of light flux fluctuations the same as at examination of radioactivity and other processes. This can be seen from Fig. 4.

Similarity of shapes of histograms resulting measurements during other processes is conditioned by a reason shared by all of them. This follows from high probability of histogram shapes similarity at synchronous independent measurements of processes with different nature.

3.1 High probability of similarity of histograms computed by results of simultaneous measurements of light and alpha-decay intensities

Fig. 5 shows high probability of histograms similarity at synchronous measurements of light and alpha-decay intensities.

Comparing series of 360 (1) and 720 (2) histogram pairs we found that shapes of histograms resulting two different processes are high probably similar; this is shown at Fig. 6. Considering the “mirrorness” effect, that is coincidence of shapes of histograms that become similar after mirror overlapping (line 3 at Fig. 5), one can see the same similarity. This

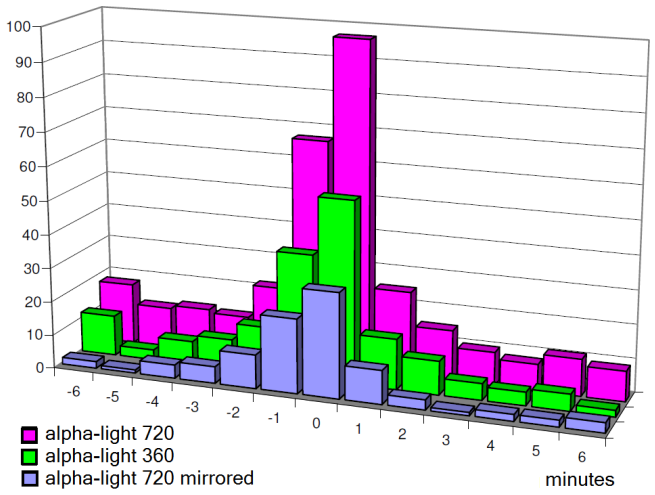

Fig. 5: High probable similarities of shapes of histograms constructed by sixty results of synchronous measurements of alpha-decay fluctuations, and light-beam intensity fluctuations. The measurements were made at West-directions of both 239Pu alpha-particles and light beams. X-axis is values of interval (minutes) between similar histograms. Y-axis is numbers of similar pairs of histograms corresponding to the values. Measurements dated April 4–5, 2011.

and similar experiments confirm the conclusion on the independence of a histogram shape from nature of a process under examination (^{239}Pu alpha-decay and flow of photons from a light diode).

Fig. 6 presents pairs of histograms, comprising the peak corresponding to the maximal probability of histograms similarity at measurements of light and alpha-activity. Shapes of all kinds can be found here. No shapes typical just for synchronism phenomenon are available.

Fig. 7 presents a larger scale of a Fig. 6 part to illustrate

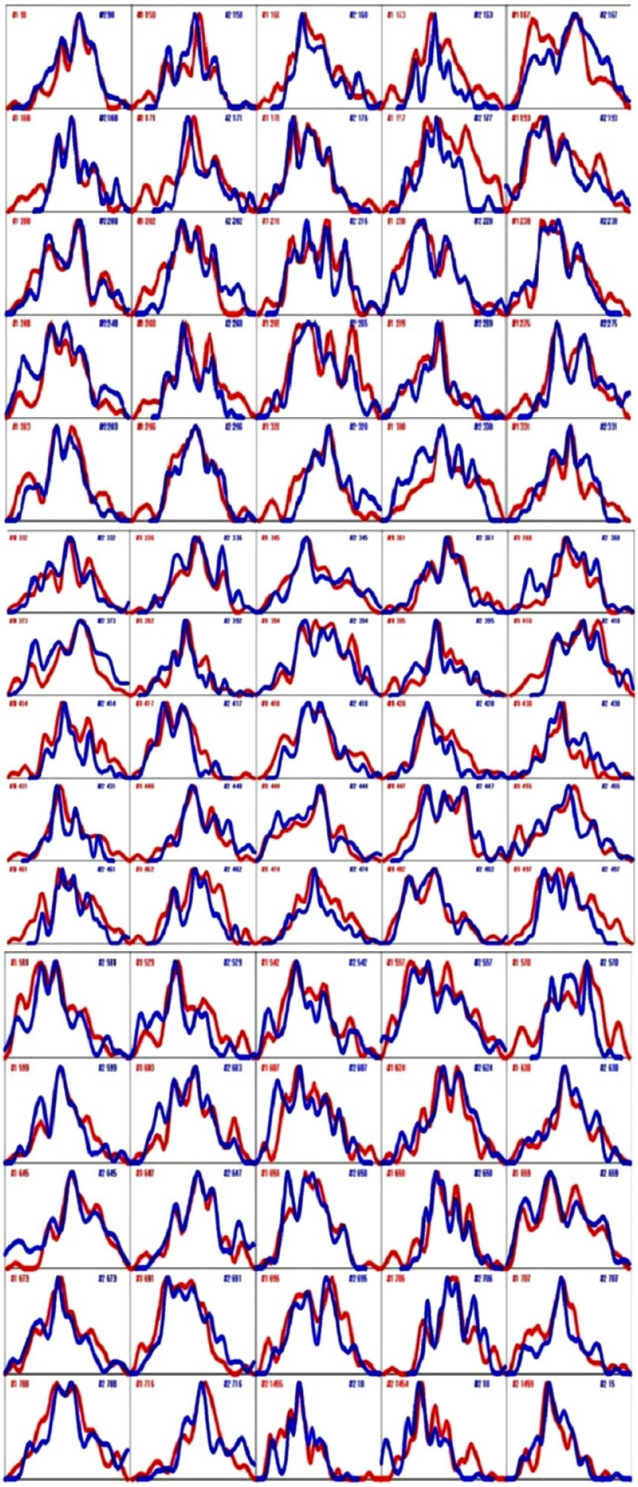

Fig. 6: Fragment of a computer log. Pairs of synchronous histograms from the central peak of Fig. 4. Indicated are numbers of histograms in series.

more visually similarity of shapes of histograms constructed by results of synchronous measurements of α-radioactivity and light intensity fluctuations.

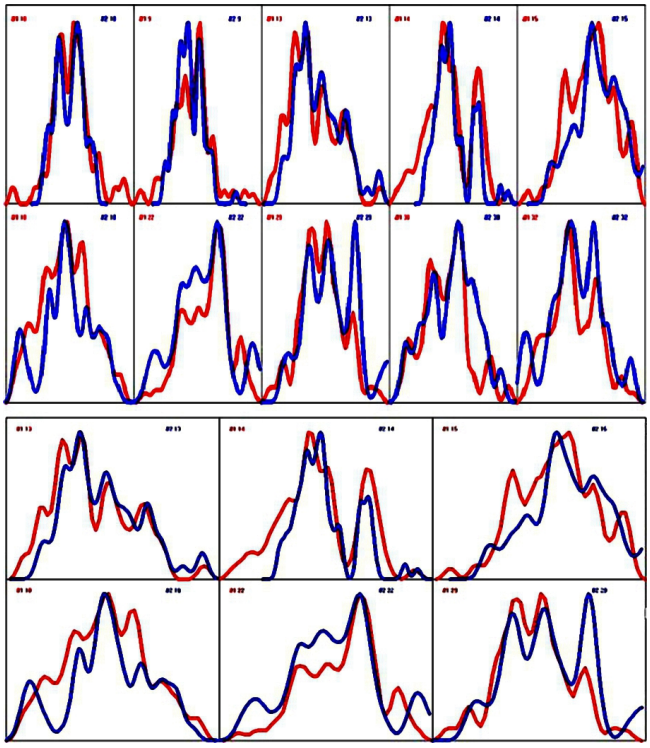

Fig. 7: Enlarged part of Fig. 6.

3.2 Near-a-day periods of similar shape histograms realization at measurements of light intensity fluctuations and their dependence from space direction of a light beam

Fig. 9 presents dependence between a period of similar histograms occurrence and a light beam direction. One can see that star and Sun periods appear equally both at West and East directions of a beam, and disappear completely when a beam is directed towards the Polar Star.

Therefore, changes of histogram shapes at measurements of light flow fluctuation are again related with axial rotation of the Earth. Distinct separation of near-a-day periods into "star" and "Sun" ones, the same as in other cases, means high degree of space anisotropy of observed effects. Difference between star and Sun days is only four minutes, corresponding to 1° in angular measure. These near-a-day periods from Fig. 10 are solved with approximately 20 angular minutes accuracy. Discrimination power of our method may, probably be determined by a collimator aperture, that is narrowness of a light beam.

The absolute lack of near-a-day periods when a light beam is directed towards the Polar Star is the same rather corresponds to ideas on relation of histogram shapes with diurnal Earth rotation. Moreover, the phenomenon means, as was earlier mentioned, that a histogram shape is provided not by some "effects" on a process under examination but only by space anisotropy.

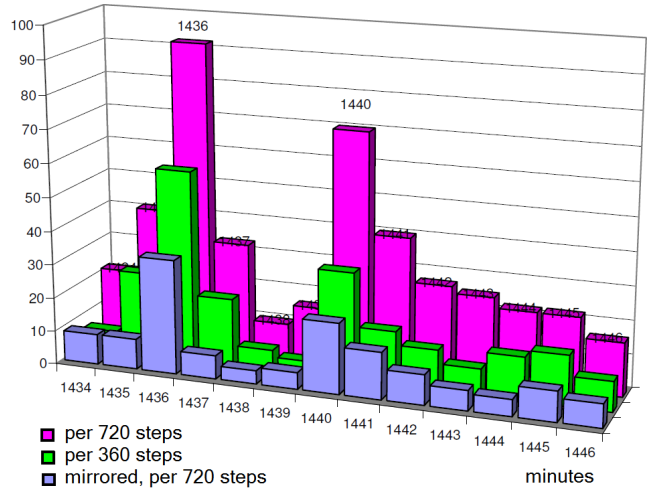

Fig. 8: Shapes of histograms resulting measurements of light intensity, the same as measurements of other nature processes, change with distinct day periods: star (1,436 minutes) and Sun (1,440 minutes) ones. A light beam is directed towards the West. Measurements were made on May 4–5, 2011. Distributions at comparison of lines from 1) 360, 2) 720, and 3) mirror similar pairs only at 760 histograms per a line. X-axis is periods (minutes); Y-axis is numbers of similar pairs after the correspondent time interval.

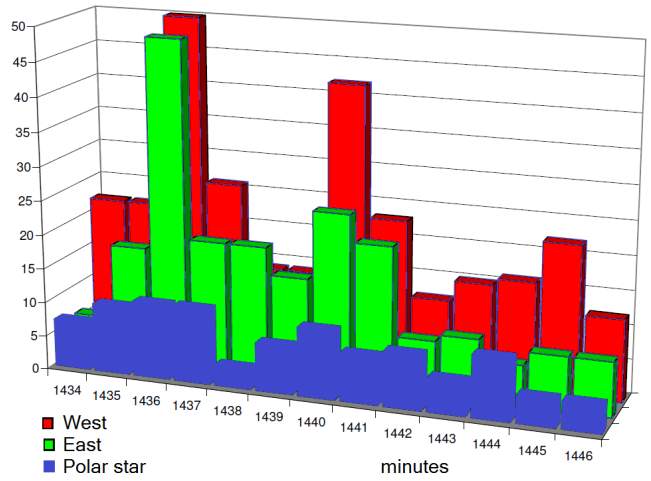

Fig. 9: It can be seen that when a light beam is directed towards the Polar Star no day period presents, and when it is West- or East-directed day periods ("star days" — 1,436 minutes and "Sun Days" — 1,440 minutes) are expressed very distinctly. X-axis is periods (minutes); Y-axis is numbers of similar histogram pairs correspondent to the period value.

3.3 Palindrome effect

A palindrome effect has been presented in [3, 4] when changes of histograms in different days periods were examined. The effect is that succession of histogram shapes since 6 am till 6 pm of accurate local time is like a reverse (inverse) histograms succession since 6 pm till 6 am of a following day. The effect was explained as follows: these are the moments when Earth axial rotation changes its sign relatively its circumsolar rotation: since 6 am till 6 pm ("the day time") these rotations have opposite directions, and 6 pm till 6 am they are co-directed. This implies that a histogram shape is determined by a direction of laboratory rotation corresponding to that of Earth at its diurnal rotation.

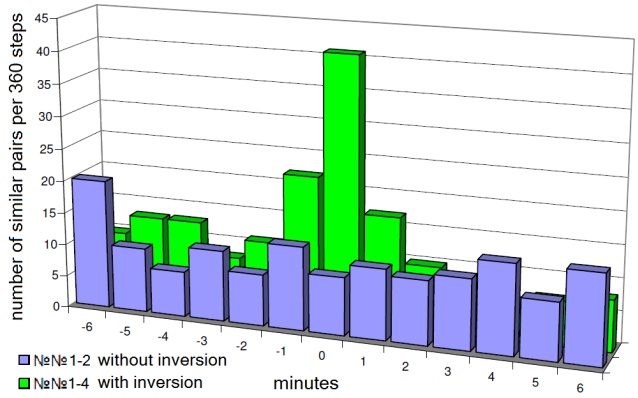

Fig. 10: A palindrome effect in an experiment with light beams. Presence of high similarity of synchronous one-minute histograms at comparison of "daytime" ones with those "nighttime" with inversion of one series and absence of the similarity without inversion. The measurements were made on March 27–28, 2011.

As can be seen from Fig. 10, at examination of histogram shapes in experiments with light beams rather distinct palindrome effect can be seen. When 6 am to 6 pm series of histograms ("day-time histograms") are compared with direct succession of "night-time" histograms their similarity is low probable (a number of similar pairs is little). And when daytime histograms are compared with inverse histogram series probability of synchronous histograms similarity is high.

The palindrome effect seems quite convincing evidence for dependence of a histogram shape from space direction. For this matter, we repeatedly tested its reproducibility at comparison of one-minute histograms with our routine expert method using GM and with just developed by V. A. Gruzdev HC computer program. With the HC program, the palindrome effect was obtained at comparison of ten-minute histograms. 72 "daytime" ten-minute histograms were compared with 72 histograms of direct and inverse series of "nighttime" histograms on "all with all" basis. As one can see from Fig. 11, application of completely automated comparison of histogram shapes with the help of HC program finds the same highly distinct palindrome effect.

3.4 When a light beam is West- or East-directed, similar western histograms are realized 720 minutes later than eastern ones

One of the evidences for relation of a histogram shape with diurnal Earth rotation was results of experiments with alpha-activity measurements with West- and East-directed collimators [5]. No *synchronous* similarity of the histograms could be found in the experiments. When two series — western and eastern ones — are compared, similar histograms occur in

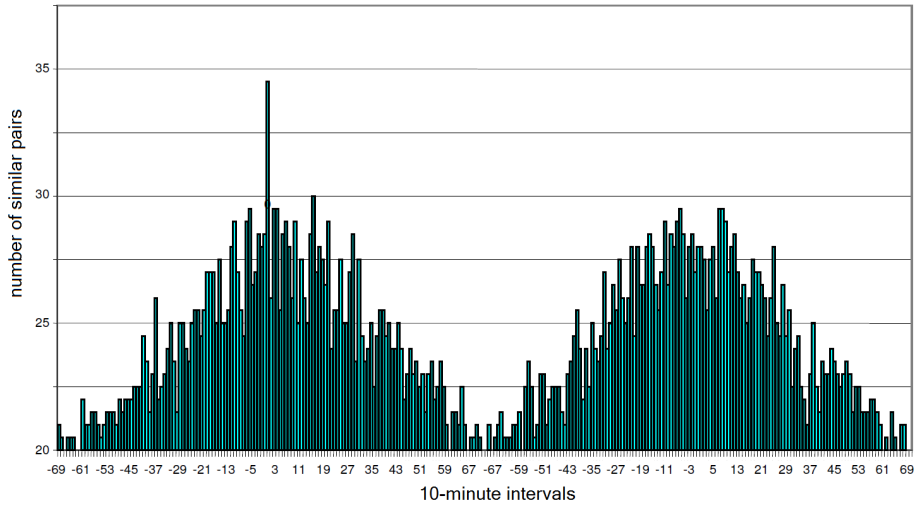

Fig. 11: The palindrome effect in experiments with light. A beam is directed towards West at comparison of ten-minutes histograms with the help of HC computer program. Left: distribution of number of similar histogram pairs at comparison of "daytime" (since 6 am till 6 pm March 27, 2011) histogram series with inverse "nighttime" (since 6 pm March 27 till 6 am March 28, 2011) histogram series; right: the same at comparison of inversion-free series.

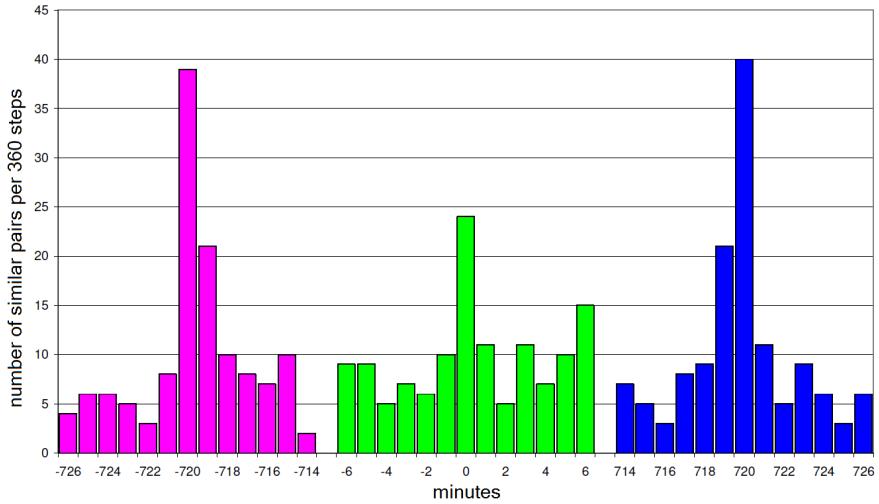

Fig. 12: When a light beam is West- or East-directed, probability of synchronous occurrence of similar histograms is low (intervals are near zero) and that with 720 minutes is high. Measurements from May 4–5, 2011.

720 minutes, that is, in half a day. More detailed investigation allowed us to find a "time arrow" [6]: histograms registered at measurements with eastern collimator were more similar with western in 720 minutes of the following day. In experiments with West- and East-directed light beams, occurrence of similar histograms in 720 minutes and absence of similarity at simultaneous (synchronous) measurements was observed the same rather distinctly. This is illustrated by Figs. 11 and 12.

3.5 Histograms obtained when a light beam is directed towards the Polar Star in Puschino are high probably similar by absolute time with those obtained at measurements of alpha-activity in Antarctic

We observed the same phenomenon earlier at synchronous measurements of alpha-activity in Puschino and in Novolazarevskaya (Antarctic). Histograms resulting measurements of ^{239}Pu alpha-activity in Puschino with a Polar Star directed collimator or with a Sun-directed collimator were high probably similar at one the same time with histograms resulting alpha-activity measurements in Novolazarevskaya with a collimator-free counter. When collimators were West and East directed no synchronism by absolute time between Puschino and Novolazarevskaya was noticed. Expression of synchronism by absolute and local times and its dependence from a space direction are extremely significant phenomena. Appropriate studies we began long ago [7] and continued them in the previous work at simultaneous measurements of alpha-activity in Puschino, Antarctic, and North Pole [8]. In this study we just got added evidence that light beam fluctuations along with alpha-activity measurements could be a quite ap-

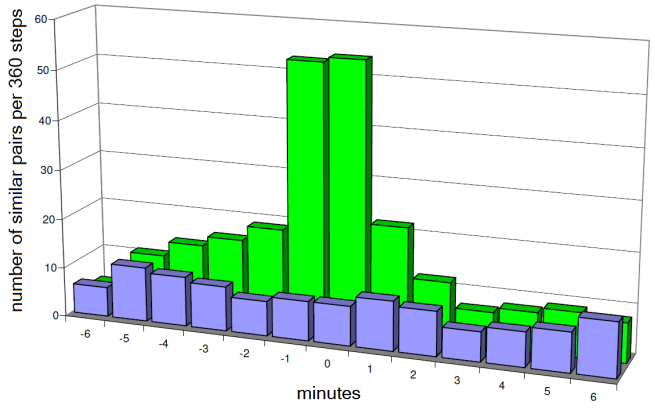

Fig. 13: At 720 minutes shift of eastern histograms measured since 6 am till 6 pm of exact local time to western histograms 6 pm — 6 am of the following day high probable similarity is observed. Without the shift eastern and western histograms are not similar.

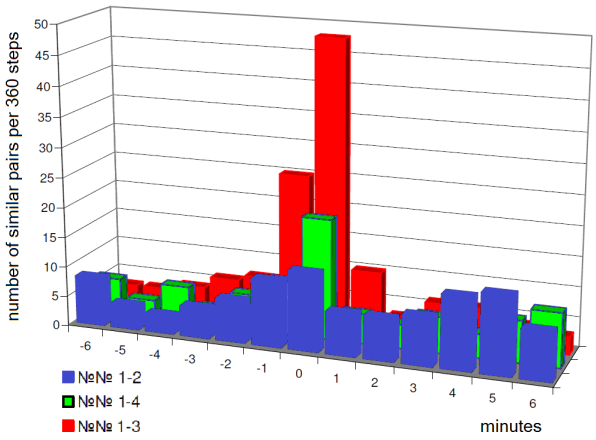

Fig. 14: Time-dependence of numbers of similar pairs of histograms resulting measurements of light beam fluctuations in Puschino and of alpha-activity in Novolazarevskay (1) when a light beam is directed towards Polar Star (3), West (2), and East (4). The origin of X-axis is the moment of absolute time synchronism. Measurements done in May 6, 2011.

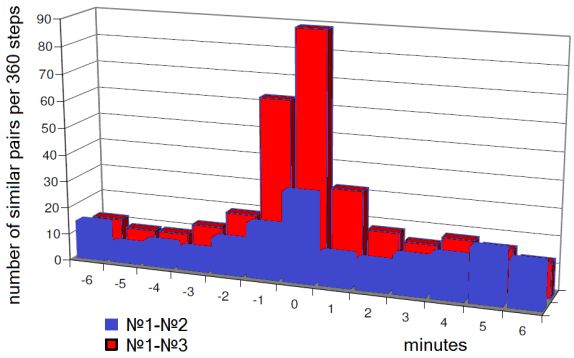

Fig. 15: High probability of absolute time synchronous changes of similarity of shapes of histograms resulting measurements of fluctuations of Polar Star directed light beam in Puschino and fluctuations of alpha-decay in Antarctic. No synchronous similarity can be seen when a light beam is West or East directed. Measurements from May 6, 2011.

propriate object for similar studies. This can be seen from the results of the experiment presented at Figs. 14 and 15.

In this experiment we compared histograms resulting measurements of intensity fluctuations of three light beams: 1) Polar Star, 2) West, and 3) East directed, made in Puschino, with those resulting measurements of alpha-activity with a collimator-free counter, made in Novolazarevskaya. From Figs. 13 and 14 it can be seen that when a light beam is directed highly probable absolute time synchronism of histogram shapes changes in Puschino and in Novolazarevskaya is observed. No synchronism is observed when light beams are West and East directed. The result obtained earlier with collimators and alpha-activity is repeated.

More detailed examinations of these phenomena should become an object for special study.

4 Discussion

Evidence of identical regularities observed at comparison of histogram shapes — spectra of fluctuation amplitudes — of alpha-decay and light diode generated light flow intensities, proves previous conclusion on universality of the phenomenon under examination [1, 9]. This result is not more surprising than identity of regularities at measurements of Brownian movement and radioactivity; or radioactivity and noises in semiconductor schemes [10, 11]. The most significant is an arising possibility to make, with the help of the developed method, more accurate and various examinations of dependence between observed effects and space directions.

As the paper shows, at use of a Polar Star directed light beam absolute (not local) time synchronism in different geographical points — Puschino (54° NL) and Novolazarevskaya (Antarctic, 70° SL) is the same observed. It means that at measurements in such directions factors determining shapes of histograms are expressed, being the same all over the Earth. These regularities, seeming us rather significant, along with others obtained earlier should make body of some special publication.

In conclusion, it should be once more mentioned that to our opinion experiments with light — near-a-day periods, palindrome effects, dependence from a beam direction — also cannot be explained with somewhat universal “effects”. Some “external power” equally affecting alpha-activity, Brownian movement, and fluctuations of photons flow seems unbelievable. The same as earlier, we suppose unevenness and anisotropy of different areas of space-time continuum where examined processes (“laboratories”) get in the result of Earth movement at its diurnal and circumsolar rotations, to be the only general factor determining shapes of histograms of so different processes [1].

Acknowledgements

This study was possible due to the financial support and interest to this line of investigations of the founder of "Dynasty Foundation", Professor D. B. Zimin.

S. E. Shnoll was supported by persistent interest and understanding of M. N. Kondrashova.

We thank V. A. Schlektarev for vivid interest to the study and manufacture of important devices. We are thankful to Olga Seraya for translation of the manuscript.

The continuous support and discussion on the essence of the work with D. Rabounski is of a great importance for S. E. Shnoll.

We are grateful to the colleagues for the discussion, at all stages of the study, at the laboratory seminar. We also thank V. A. Gruzdev for discussion and Fig. 11.

Submitted on March 11, 2012 / March 16, 2012

References

1. Shnoll S. E. Cosmic Physical Factors in Random Processes. Svenska Fisikarkivet, Stockholm, 2009, (*in Russian*)
2. Gruzdev V. A. Algorithmization of histogram comparing process. Calculation of correlations after deduction of normal distribution curves. *Progress in Physics*, 2012, v. 3, 25–28 (this issue).
3. Shnoll S. E., Panchelyuga V. A. and Shnoll A. E. The Palindrome Effect. *Progress in Physics*, 2009, v. 1 3–7.
4. Shnoll S. E. The "Scattering of the Results of Measurements" of Processes of Diverse Nature is Determined by the Earth's Motion in the Inhomogeneous Space-Time Continuum. The Effect of "Half-Year Palindromes". *Progress in Physics*, 2012, v. 1, 3–7.
5. Shnoll S. E., and Rubinstein I. A. Regular Changes in the Fine Structure of Histograms Revealed in the Experiments with Collimators which Isolate Beams of Alpha-Particles Flying at Certain Directions. *Progress in Physics*, 2009, v. 2, 83–95.
6. Shnoll S. E., Rubinstein I. A. and Vedenkin N. N. The "arrow of time" in the experiments in which alpha-activity was measured using collimators directed East and West. *Progress in Physics*, 2010, v. 1, 26–29.
7. Shnoll S. E., Rubinstein I. A., Zenchenko K. I., Zenchenko T. A., Udaltsova N. V., Konradov A. A., Shapovalov S. N., Makarevich A. V., Gorshkov E. S., and Troshichev O. A. Relationship between macroscopic fluctuations and geographical coordinates as inferred from the Data of the 2000 Arctic and 2001 Antarctic expeditions. *Biophysics*, 2003, v. 48 (6), 1039–1047.
8. Shnoll S. E., Astashev M. A., Rubinshtein I. A., Kolombet V. A., Shapovalov S. N., Bokalenko B. I., Andreeva A. A., Kharakoz D. P., and Melnikov I. A. Synchronous measurements of alpha-decay of ^{239}Pu carried out at North Pole, Antarctic, and in Puschino confirm that the shapes of the respective histograms depend on the diurnal rotation of the Earth and on the direction of the alpha-particle beam. *Progress in Physics*, 2012, v. 3, 11–16 (this issue).
9. Shnoll S. E., and Kaminsky A. V. Cosmophysical factors in the fluctuation amplitude spectrum of Brownian motion. *Progress in Physics*, 2010, v. 3, 25–30.
10. Shnoll S. E. and Kaminsky A. V. The study of synchronous (by local time) changes of the statistical properties of thermal noise and alpha-activity fluctuations of a ^{239}Pu sample. arXiv: physics/0605056.

Algorithmization of Histogram Comparing Process. Calculation of Correlations after Deduction of Normal Distribution Curves

Vadim A. Gruzdev
Russian New University
E-mail: 2801218@gmail.com

A newly established computer program for histogram comparing can reproduce main features of the "macroscopic fluctuations" phenomenon: diurnal and yearly periodicity of histogram shapes changing; synchronism of their changing by local and absolute times and "palindrome" phenomenon. The process is comparing of histogram shapes by correlation coefficients and figure areas resulting reducing of picked normal curves from histograms.

1 Introduction

Discovery of macroscopic fluctuations in stochastic processes provided actuality of a computer able to compare shapes of histograms releasing an expert from this labor [1]. Fuzziness of examined shapes and difficulties in their grouping, that is, forming of similar shapes "clusters" made a computer comparison of histogram shapes a rather hard task [1].

Our paper presents a brief of Histogram Comparer (HC), a computer program replacing an expert essentially. Calculation of correlation coefficients of curves resulting deduction of an appropriate normal distribution from a smoothed histogram is taken as a basis for the algorithm. To compare such curves, the same as with expert comparison, maximal correlation coefficients are obtained after the correlations are shifted relatively each other and mirrored, if necessary. The idea of such a transformation of histograms has been used in N. V. Udaltsova's PhD theses [2].

Main effects revealed at visual expert comparison could be reproduced with the help of the HC program [4, 5].

The HC should be run together with E. V. Pozharsky Histogram Manager program (GM) as a whole complex [3]. In this complex GM performs operations of conversion of time series into histograms and construction of distribution of intervals between histograms marked in results of HC comparison as similar. A histogram massif obtained with GM is exported into HC, which performs their comparison. The result is reloaded into GM for construction of interval distributions.

2 Main stages of histograms comparison with the GM-HC program complex

Fig. 1 shows a GM conversion of a time series of results of successive measurements of ^{239}Pu alpha-activity into series of correspondent histograms, illustrating the work of GM program.

Further the histograms are exported into HC. After the histograms are loaded, preprocessing starts — a corresponding normal distribution is calculated for each histogram. Calculation is made according to equation

$$f(x) = \frac{1}{\sigma\sqrt{2\pi}} \exp\left(-\frac{(x-\mu)^2}{2\sigma^2}\right) \sum_{i=1}^{L} a_i \,. \qquad (1)$$

Conversion of histograms following deduction of appropriately picked normal distribution is shown at Fig. 2.

As one can see from Fig. 2, histogram structural features essential for our analysis in "replicas" remain unchanged and become more distinct. Comparison of "replicas" in a suggested program is realized in two versions: simple and detailed. A simple comparison implies relative shift and mirroring in a pair of "replicas".

Detailed comparison implies additionally compressing-stretching of one of the "replicas" — from 0.5 to 1.5 of an initial length in 10% increment. Consequently, a detailed comparison requires higher consumption of computing time.

Fig. 3 demonstrates process of replicas coinciding necessary for following determination of correlation coefficient maximal achievable for this pair.

2.1 Picking of correlation coefficients range

Results of comparison of each pair are entered into a table as values of maximal achievable correlation coefficient and curve areas ratio. A pair is regarded as similar when values of its correlation coefficient and curve areas ratio overshoot corresponding values of a threshold filter. Threshold values are set by a user. Criterion of threshold meanings is presence or absence of expressed intervals of reoccurrence of similar pairs in a result of comparison. Experience of using the program tells there are not more than 2 versions of combinations of threshold values allowing expressiveness of correspondingly 2 alternately expressed intervals, or expressed intervals are absent.

2.2 Analysis of comparison results and construction of similar pairs numbers distribution according to values of time intervals separating them in GM

A result of program comparison is entered into a binary file of a histograms similarity table in GM-supported GMA format

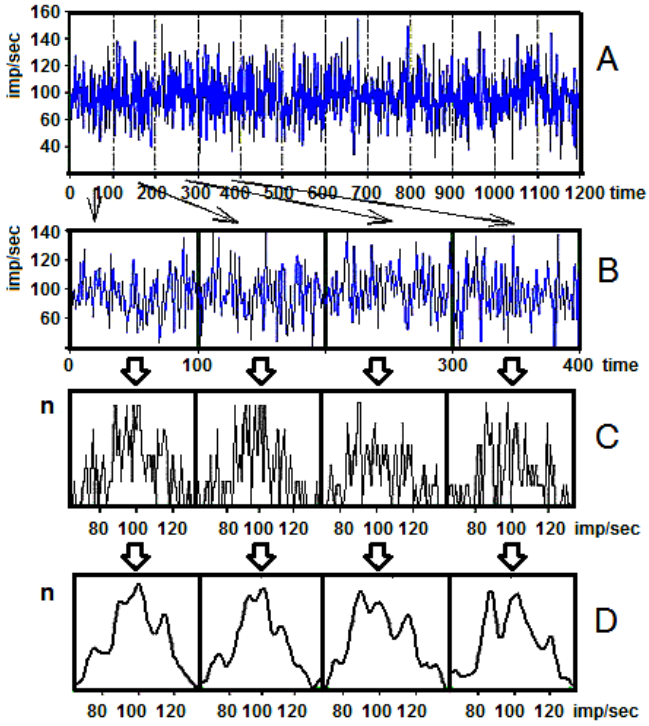

Fig. 1: Steps of histograming with GM program [1] exemplified by measurements of radioactivity a — a fragment of time series of measurement results. X-axis is time (sec.); Y-axis is numbers of alpha-decays per a second b — a time series is divided into non-overlapping sections, 100 successive numbers each c — each section is followed by a histogram (X-axis is value of activity (imp/sec); Y-axis is numbers of measurements corresponding to a value) d — the histograms from 1-c are seven-times smoothed with "moving summation" or with "a window" equal, for example, to 4; typical histogram shapes can be seen.

(description of GMA format ia a courtesy of the GM author, E. V. Pozharsky). GM calculates time interval separating each histogram pair marked as similar in the table and constructs a graphical display of intervals occurrence, i.e. histogram.

3 Examples of GM-HC complex use at determination of near-a-day periods of similar shape histograms reoccurrence and examination of "palindrome phenomenon"

3.1 Near-a-day periods

Fig. 4 presents an example of visual ("expert") comparison of histograms resulting measurements of 239Pu alpha-activity. Each histogram was constructed by 60 results of one-minute measurements. Comparison with total mixing (randomization) was made by T. A. Zenchenko. A whole series contained 143 one-hour histograms. 1,592 similar pairs were picked. The figure shows distribution of numbers of similar pairs according to values of time intervals separating them.

There are sharp extremes at the intervals equal to 1, 24 and 48 hours at the figure. These extremes correspond to a

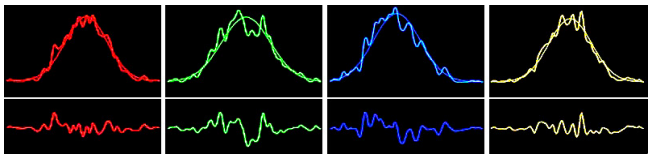

Fig. 2: The upper line is histograms with applied correspondent normal curves; the lower line is results of normal curves deduction from histograms; the resulting curves are, in fact, "replicas" of fine structures of fluctuation amplitudes spectrum.

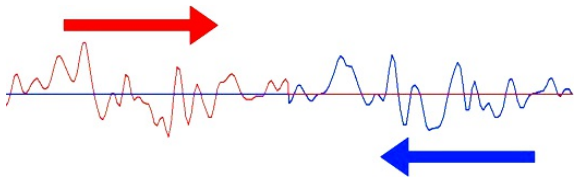

Fig. 3: Illustration of "simple" comparison. Direction of shift is pointed by arrows. Two these experiments were performed on April 8, 2011 (the left histogram arc) and April 9, 2011 (the right histogram arc).

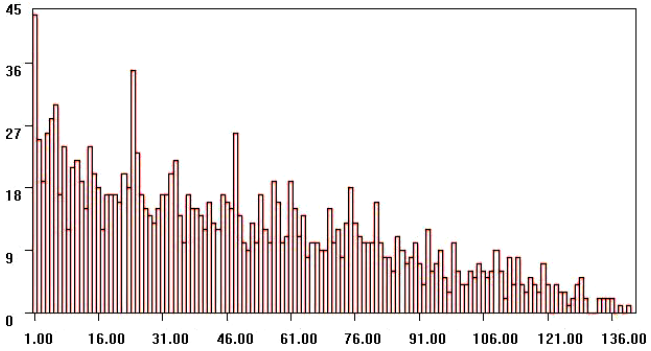

Fig. 4: Results of comparison of one-hour histograms constructed by results of ^{239}Pu alpha-activity measurements from July 7 to July 15, 2000, in Puschino. X-axis is intervals (hours); Y-axis is number of similar pairs corresponding to value of interval. (Taken from [1].)

"near zone effect" — maximal probability of realization of similar histograms in nearest, neighboring, intervals and their realization with near-a-day periods. Total mixing (randomization) of histogram series guaranties reliability of regularities revealed in expert comparison [1].

Fig. 5 presents result of automatic comparison, performed by HC computer program in the same task. It is clear that in reproduction of main effects the program is rather inferior to the expert in quality of histograms comparison.

3.2 "Palindrome effect" [1]

Figs. 7 and 8 show one of the main phenomena of "macroscopic fluctuations" — a palindrome effect — reproduced with HC program.

A "palindrome effect" is conditioned by dependence of a histogram shape from correlation of Earth motion directions: at its axial rotation and circumsolar movement. In a day-time axial rotation of Earth is antisircumsolar. In night-time the

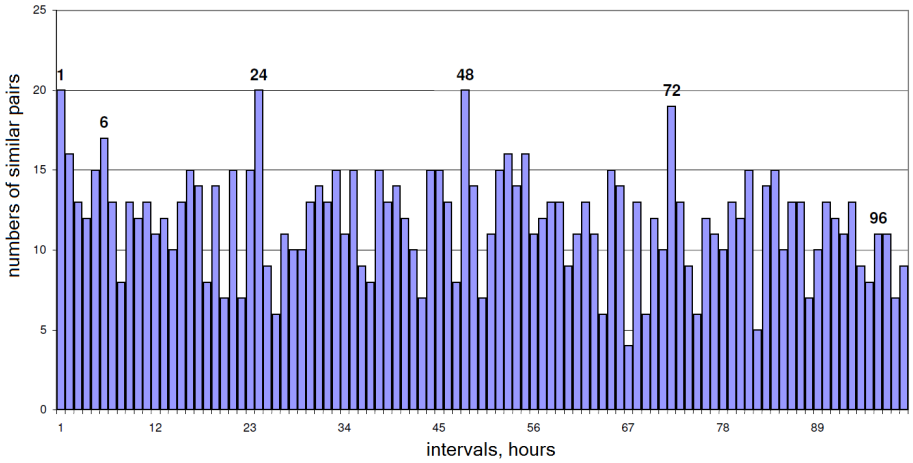

Fig. 5: Diurnal periods revealed at comparison of non-smoothed one-hour histograms by HC program. The histograms are computed by measurements of ^{239}Pu alpha-activity with a collimator-free counter since February 10 till March, 1, 2010.

both movements are co-directed. Succession of "day-time" histograms shapes was shown to repeat inversely in nights. In other words, one the same "text" is "read" forward and backward forming a palindrome. The moments of day-night transitions are 6 pm by local time and of night-day transitions are 6 am. Comparison of forward and backward sequences gives a valuable possibility to verify objectiveness of obtained distributions. The same histograms are compared. Result of comparison depends on direction of sequences only.

Figs. 6–8 present results of "palindrome effect" examination at measurements of fluctuations of intensities of light beam and ^{239}Pu alpha-decay in two ways: at expert (visual) estimation of histograms similarity (Fig. 6) and at HC comparison (Figs. 7 and 8). Fig. 6 is an expert comparison of histograms constructed by 60 one-second measurements (that is, during 1 minute). Figs. 7 and 8 show the results of comparison of 10-minute histograms with the HC program.

As one can see from Figs. 6–8, when histograms constructed by measurements of a light beam fluctuations [4] or fluctuations of ^{239}Pu alpha-decay intensities [1] are compared, a distinct palindrome effect can be observed. There is high probability of synchronous similarity of "day-time" histograms series with inverse series of night-time histograms. There is no similarity of synchronous histograms when a day-time series is compared with a direct (non-inverted) night-time series. Nevertheless comparison of histograms with HC programs gives "coarser" results, with 10 minutes interval, versus one-minute intervals at expert comparison.

The illustrations show principal availability of the HC program for examination of fine structure of histograms. But expert comparison determines similar histograms more specially, HC gives much higher "background" of stochastic shapes. Besides, these figures show similarity of palindrome effects at measurements of fluctuations of alpha-decay intensity, that is, independence of a macroscopic fluctuations phenomenon from nature of processes under examination [1].

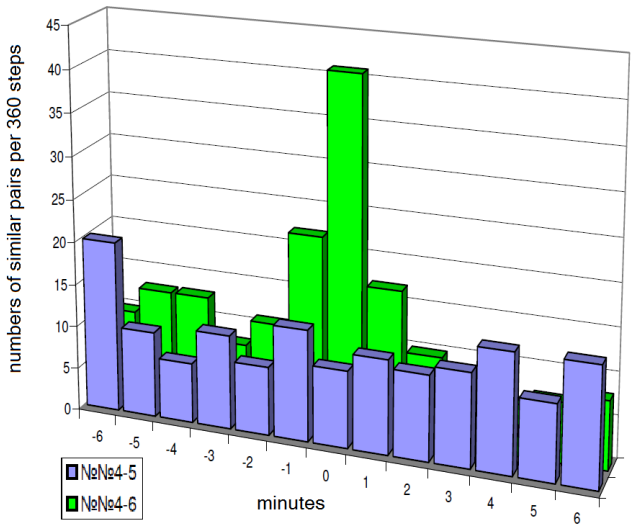

Fig. 6: Expert comparison. A palindrome effect in an experiment with measurements of fluctuations of light-diode light beam intensities. High similarity of synchronous one-minute histograms at comparison of "day-time" and "night-time" histograms when one series is inverted and absence of similarity at the absence of inversion. Measurements on April 6, 2011. X-axis is one-minute intervals; Y-axis is number of similar pairs corresponding to an interval.

4 Conclusions

1. Application of HC program allows reproduction of main effects of "macroscopic fluctuations" phenomenon.
2. Nevertheless, range of correlation coefficients values is to be picked up each time complicating the work.
3. The optimal way is combination of expert analysis with estimation of confidence of main conclusion with GM-HC combination.

You can get text and manual of the program from its author after e-mail request via: 2801218@gmail.com

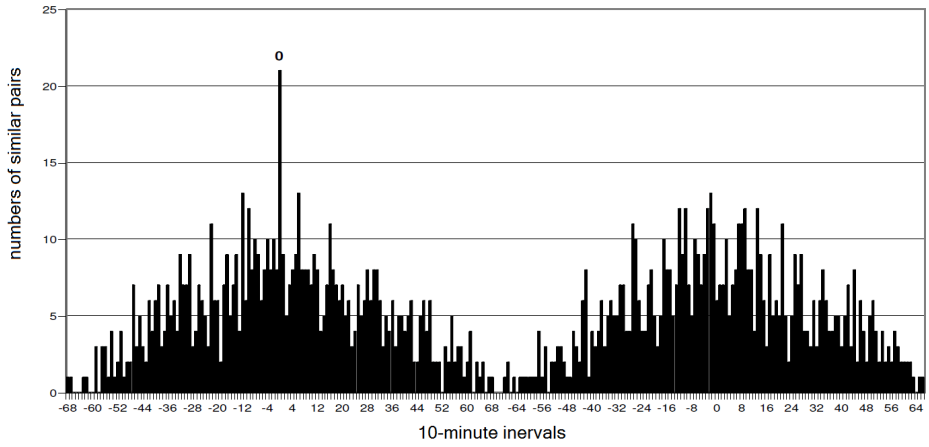

Fig. 7: Comparison of 10-minute histograms by the HC computer program. A palindrome effect in experiments with measurements of fluctuations of light-diode light beam intensities. Left is distribution of numbers of similar histogram pairs at comparison of "day-time" (since 6 am till 6 pm April 6, 2011) series histograms with inverse "night-time" (since 6 pm April, 27 till 6 am April 7, 2011). Right — the same at comparison of series without inversion.

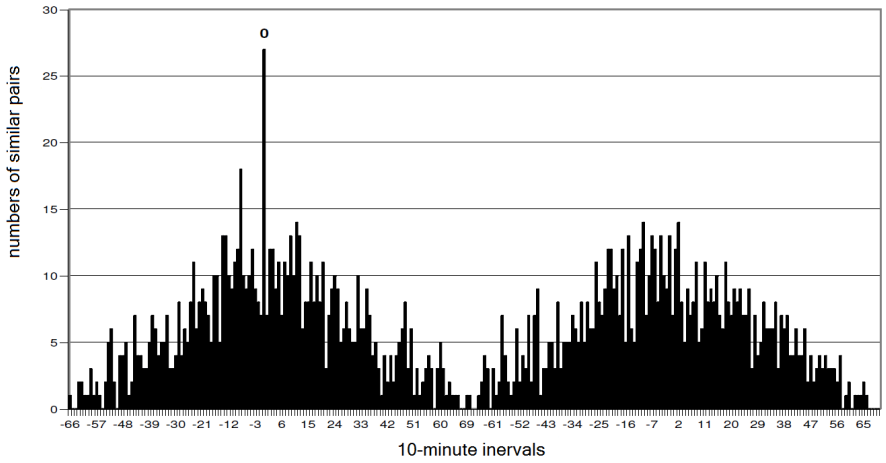

Fig. 8: Comparison of 10-minute histograms by computer HC program. Palindrome effect in experiments on measurements of ^{239}Pu alpha-activity with West-directed collimator. Left — distribution of numbers of similar histograms at comparison of histograms of "day-time" series (from 6 am to 6 pm May 27, 2005) with inverse "night-time" series of histograms (from 6 pm May 27 to 6 am May 28, 2005); right — the same at comparison of series without inversion.

Acknowledgements

Author is grateful to S. E. Shnoll for formulation of the problem, provided materials and essential discussion; V. A. Kolombet for essential discussion and his attention to the work; E. V. Pozharsky for consulting in work with GM interfaces and Professor V. I. Maslyankin ("Programming technology", Russian New University) for tutoring.

Submitted on March 11, 2012 / Accepted on March 16, 2012

References

1. Shnoll S. E. Cosmic Physical Factors in Random Processes. Svenska Fisikarkivet, Stockholm, 2009, (*in Russian*).
2. Udaltsova N. V., Possible cosmophysical casuality of parameters of biochemical and physic-chemical processes. *PhD theses Inst. Biophysics, USSR Acad. Ssi.*, 1990, (*in Russian*).
3. Shnoll S. E., Kolombet V. A., Pozharsky E. V., Zenchenko T. A., Zvereva I. M., Konradov A. A. Illustration of synchronism of changes of fine structure of measurement results distribution exemplified by radioactive decay of radium family isotopes. *Biofizika*, 1998, v. 43 (4), 732–735 (*in Russian*).
4. Rubinshtein I. A., Shnoll S. E., Kaminsky A. V., Kolombet V. A., Astashev M. A., Shapovalov S. N., Bokalenko B. I., Andreeva A. A., Kharakoz D. P. Dependence of changes of histogram shapes from time and space direction is the same when intensities of fluctuations of both of light-diode provided light flux and ^{239}Pu alpha-activity are measured. *Progress in Physics* , 2012, v. 3, 17–24 (this issue).
5. Shnoll S. E., Astashev M. A., Rubinshtein I. A., Kolombet V. A., Shapovalov S. N., Bokalenko B. I., Andreeva A. A., Kharakoz D. P., Melnikov I. A. Synchronous measurements of alpha-decay of ^{239}Pu carried out at North Pole, Antarctic, and in Puschino confirm that the shapes of the respective histograms depend on the diurnal rotation of the Earth and on the direction of the alpha-particle beam. *Progress in Physics*, 2012, v.3, 11–16 (this issue).

The Radial Electron Density in the Hydrogen Atom and the Model of Oscillations in a Chain System

Andreas Ries
Universidade Federal de Pernambuco, Centro de Tecnologia e Geociências, Laboratório de Dispositivos e Nanoestruturas,
Rua Acadêmico Hélio Ramos s/n, 50740-330 Recife – PE, Brazil
E-mail: andreasries@yahoo.com

The radial electron distribution in the Hydrogen atom was analyzed for the ground state and low-lying excited states by means of a fractal scaling model originally published by Müller in this journal. It is shown that Müller's standard model is not fully adequate to fit these data and an additional phase shift must be introduced into its mathematical apparatus. With this extension, the radial expectation values could be expressed on the logarithmic number line by very short continued fractions where all numerators are Euler's number. Within the rounding accuracy, no numerical differences between the expectation values (calculated from the wavefunctions)and the corresponding modeled values exist, so the model matches these quantum mechanical data exactly. Besides that, Müller's concept of proton resonance states can be transferred to electron resonances and the radial expectation values can be interpreted as both, proton resonance lengths and electron resonance lengths. The analyzed data point to the fact that Müller's model of oscillations in a chain system is compatible with quantum mechanics.

1 Introduction

The radial electron probability density in the Hydrogen atom was analyzed by a new fractal scaling model, originally published by Müller [1–3] in this journal. This model is basing on four principal facts:

1. The proton is interpreted as an oscillator.
2. Most matter in the universe is provided by protons, therfore the proton is *the dominant oscillation state* in all the universe.
3. Space is not considered as completely empty, consequently all proton oscillators are somehow coupled to each other. A quite simple form to consider such a coupling is the formation of a chain of proton harmonic oscillators.
4. Provided that items 1–3 are correct, every process or state in the universe which is abundantly realized or allowed to exist over very long time scales, is consequently coupled to the proton oscillations, and should retain some properties that can be explained from the mathematical structure of a chain of proton harmonic oscillators.

Müller has shown that a chain of similar harmonic oscillators generates a spectrum of eigenfrequencies, that can be expressed by a continued fraction equation [2]

$$f = f_p \exp S, \tag{1}$$

where f is any natural oscillation frequency of the chain system, f_p the oscillation frequency of one proton and S the continued fraction corresponding to f. S was suggested to be in the canonical form with all partial numerators equal 1 and the partial denominators are positive or negative integer values:

$$S = n_0 + \cfrac{1}{n_1 + \cfrac{1}{n_2 + \cfrac{1}{n_3 + \ldots}}}. \tag{2}$$

Besides the canonical form, Müller proposed fractions with all numerators equal 2 and all denominators are divisible by 3. Such fractions divide the logarithmic scale in allowed values and empty gaps, i.e. ranges of numbers which cannot be expressed with this type of continued fractions.

In three previous articles [4–6] it was shown that the model works quite well when all the numerators were substituted by Euler's number, so that

$$S = n_0 + \cfrac{e}{n_1 + \cfrac{e}{n_2 + \cfrac{e}{n_3 + \ldots}}}. \tag{3}$$

In this work, the attention has been focused to the spatial electron distribution in the Hydrogen atom, considering the ground state (n = 1) and the first low-lying excited electronic states (n = 2–6).

In the Hydrogen atom, the distance between the electron and the proton is always very small and quantum mechanics allows to calculate the exact spatial electron density distribution. If the proton is somehow oscillating and Müller's model applies, one can expect a characteristic signature in the set of radial expectation values.

Actually these values compose an extremely interesting data set to analyze, since the expectation values can be calculated by quantum mechanics from exact analytical wave-

functions and do not have any measurement error (errors in physical constants such as a_0 and $\hbar$ can be neglected).

Therefore, it can be requested that Müller's model must reproduce these expectation values *exactly*, which is indeed possible, but only when introducing a further modification to the model.

2 Data sources and computational details

When considering polar coordinates, the solutions of the non-relativistic Schrödinger equation $\hat{H}\Psi = E\Psi$ for a spherical potential can be written in the form

$$\Psi(r, \theta, \phi) = R(r)\Theta(\theta)\Phi(\phi),$$

where $R(r)$ is the so-called radial part of the wavefunction Ψ, and the functions $\Theta(\theta)$ and $\Phi(\phi)$ are the angular parts.

For every orbital or wavefunction, the probability to find the electron on a shell with inner radius r and outer radius $r + dr$ is proportional to r^2R^2dr (note that the functions as given in Table 1 are not normalized). Following the formalism of quantum mechanics, the average or expectation value $\langle r \rangle$ was calculated by numerical integration

$$\langle r \rangle = N \int_0^\infty r^3R^2dr, \tag{4}$$

where N is the normalization constant so that holds:

$$N \int_0^\infty r^2R^2dr = 1.$$

Table 1 displays the radial part $R(Z, r)$ for the orbitals 1s to 6h of hydrogen-like atoms together with the corresponding radial expectation values (for $Z = 1$, wavefunctions taken from reference [7]). The expectation values are given in Å and were rounded to three significant digits after decimal point.

In a second step, these numerical values were expressed on the logarithmic number line by continued fractions. Numerical values of continued fractions were always calculated using the the Lenz algorithm as indicated in reference [8].

3 Results and discussion

3.1 The standard model is insufficient

In order to interpret the expectation values $\langle r \rangle$ as proton resonance lengths, following strictly the formalism of previous articles, it must be written:

$$\ln \frac{\langle r \rangle}{\lambda_C} = p + S, \tag{5}$$

where S is the continued fraction as given in equation 3, $\lambda_C = \frac{h}{2\pi mc}$ is the reduced Compton wavelength of the proton with the numerical value $2.103089086 \times 10^{-16}$ m. In the following tables, $p + S$ is abbreviated as $[p; n_0 \mid n_1, n_2, n_3, \dots]$. The free link n_0 and the partial denominators n_i are integers divisible by 3. For convergence reason, one has to include $|e{+}1|$ as allowed partial denominator. This means the free link n_0 is allowed to be $0, \pm3, \pm6, \pm9 \dots$ and all partial denominators n_i can take the values $e{+}1, -e{-}1, \pm6, \pm9, \pm12 \dots$.

For consistency with previous publications, the following conventions hold: a data point is considered as an outlier (i.e. does not fit into Müller's model), when its continued fraction representation produces a numerical error higher than 1%. The numerical error is always understood as the absolute value of the difference between $\langle r \rangle$ from quantum mechanics (given in Table 1), and the value obtained from the evaluation of the corresponding continued fraction.

It was found that the complete set of radial expectation values can be interpreted as proton resonance lengths without any outliers according to equation 5 (results not shown). However, small numerical errors were still present. Having in mind that this is a data set without measurement errors, this result is not satisfying.

From the obvious fact that the wavefunction is an electron property, it arouse the idea to interpret the data set as electron resonance lengths. Then, a fully analogous equation can be set up:

$$\ln \frac{\langle r \rangle}{\lambda_{C_{electron}}} = p + S, \tag{6}$$

where $\lambda_{C_{electron}}$ is the reduced Compton wavelength of the electron with the numerical value $3.861592680 \times 10^{-13}$ m.

Again the expectation values could be interpreted as electron resonance lengths according to equation 6 without the presence of outliers, but some numerical errors remained (results not shown).

Since the aforementioned equations do not reproduce the dataset exactly as proton or electron resonance lengths, possible changes of the numerator were investigated.

Müller had already proposed continued fractions with all numerators equal 2 in one of his publications [9]. As a first numerical trial, the number of outliers was determined when modeling the data set with numerators from 2.0 to 3.0 (step-size 0.05). Figure 1 displays the results for both, proton and electron resonances. It turned out that number 2 must be excluded from the list of possible numerators, as outliers are present. Moreover, the results suggest that the whole range from 2.55 to 2.85 can be used as numerator in equations 5 and 6 without producing outliers, thus, another criterium must be applied to determine the correct numerator.

Considering only the range of numerators which did not produce outliers, the sum of squared residuals (or squared numerical errors) was calculated. It strongly depends on the numerator (see Figure 2). Again the results are not satisfying. As can be seen, considering electron resonances, the "best numerator" is 2.70, while for proton resonances it is 2.78, de-

Table 1: Radial wavefunctions $R(Z, r)$ of different orbitals for hydrogen-like atoms together with the corresponding radial expectation values according to equation 4 ($Z = 1$ assumed). $\rho = \frac{2Zr}{na_0}$, n = main quantum number, a_0 = Bohr radius, Z = atomic number.

Radial wavefunction $R(Z, r)$	$\langle r \rangle$ [Å]
$R_{1s} = (Z/a_0)^{\frac{3}{2}} 2e^{-\frac{\rho}{2}}$	0.794
$R_{2s} = \frac{(Z/a_0)^{\frac{3}{2}}}{2\sqrt{2}}(2-\rho)e^{-\frac{\rho}{2}}$	3.175
$R_{2p} = \frac{(Z/a_0)^{\frac{3}{2}}}{2\sqrt{6}}\rho e^{-\frac{\rho}{2}}$	2.646
$R_{3s} = \frac{(Z/a_0)^{\frac{3}{2}}}{9\sqrt{3}}\left(6-6\rho+\rho^2\right)e^{-\frac{\rho}{2}}$	7.144
$R_{3p} = \frac{(Z/a_0)^{\frac{3}{2}}}{9\sqrt{6}}(4-\rho)\rho e^{-\frac{\rho}{2}}$	6.615
$R_{3d} = \frac{(Z/a_0)^{\frac{3}{2}}}{9\sqrt{30}}\rho^2 e^{-\frac{\rho}{2}}$	5.556
$R_{4s} = \frac{(Z/a_0)^{\frac{3}{2}}}{96}\left(24-36\rho+12\rho^2-\rho^3\right)e^{-\frac{\rho}{2}}$	12.700
$R_{4p} = \frac{(Z/a_0)^{\frac{3}{2}}}{32\sqrt{15}}\left(20-10\rho+\rho^2\right)\rho e^{-\frac{\rho}{2}}$	12.171
$R_{4d} = \frac{(Z/a_0)^{\frac{3}{2}}}{96\sqrt{5}}(6-\rho)\rho^2 e^{-\frac{\rho}{2}}$	11.113
$R_{4f} = \frac{(Z/a_0)^{\frac{3}{2}}}{96\sqrt{35}}\rho^3 e^{-\frac{\rho}{2}}$	9.525
$R_{5s} = \frac{(Z/a_0)^{\frac{3}{2}}}{300\sqrt{5}}\left(120-240\rho+120\rho^2+20\rho^3+\rho^4\right)e^{-\frac{\rho}{2}}$	19.844
$R_{5p} = \frac{(Z/a_0)^{\frac{3}{2}}}{150\sqrt{30}}\left(120-90\rho+18\rho^2-\rho^3\right)\rho e^{-\frac{\rho}{2}}$	19.315
$R_{5d} = \frac{(Z/a_0)^{\frac{3}{2}}}{150\sqrt{70}}\left(42-14\rho+\rho^2\right)\rho^2 e^{-\frac{\rho}{2}}$	18.257
$R_{5f} = \frac{(Z/a_0)^{\frac{3}{2}}}{300\sqrt{70}}(8-\rho)\rho^3 e^{-\frac{\rho}{2}}$	16.669
$R_{5g} = \frac{(Z/a_0)^{\frac{3}{2}}}{900\sqrt{70}}\rho^4 e^{-\frac{\rho}{2}}$	14.552
$R_{6s} = \frac{(Z/a_0)^{\frac{3}{2}}}{2160\sqrt{6}}\left(720-1800\rho+1200\rho^2+300\rho^3+30\rho^4-\rho^5\right)e^{-\frac{\rho}{2}}$	28.576
$R_{6p} = \frac{(Z/a_0)^{\frac{3}{2}}}{432\sqrt{210}}\left(840-840\rho+252\rho^2-28\rho^3+\rho^4\right)\rho e^{-\frac{\rho}{2}}$	28.046
$R_{6d} = \frac{(Z/a_0)^{\frac{3}{2}}}{864\sqrt{105}}\left(336-168\rho+24\rho^2-\rho^3\right)\rho^2 e^{-\frac{\rho}{2}}$	26.988
$R_{6f} = \frac{(Z/a_0)^{\frac{3}{2}}}{2592\sqrt{35}}\left(72-18\rho+\rho^2\right)\rho^3 e^{-\frac{\rho}{2}}$	25.401
$R_{6g} = \frac{(Z/a_0)^{\frac{3}{2}}}{12960\sqrt{7}}(10-\rho)\rho^4 e^{-\frac{\rho}{2}}$	23.284
$R_{6h} = \frac{(Z/a_0)^{\frac{3}{2}}}{12960\sqrt{77}}\rho^5 e^{-\frac{\rho}{2}}$	20.638

spite presenting a local minimum at 2.70 too. However, numerators different from e are inconsistent with previous publications. The fact that these "best numerators" are numerically very close to Euler's number, suggests that the choice of e as numerator is probably correct and something else in the model must be changed for this particular dataset.

For any common experimental data set, the here found numerical inconsistencies could be explained with measurement errors. One could even think that Müller's model is just too simple to reproduce nature's full reality; then the numerical deviations could also be explained by the insufficiency of the model itself. Fortunately the high accuracy of the expec-

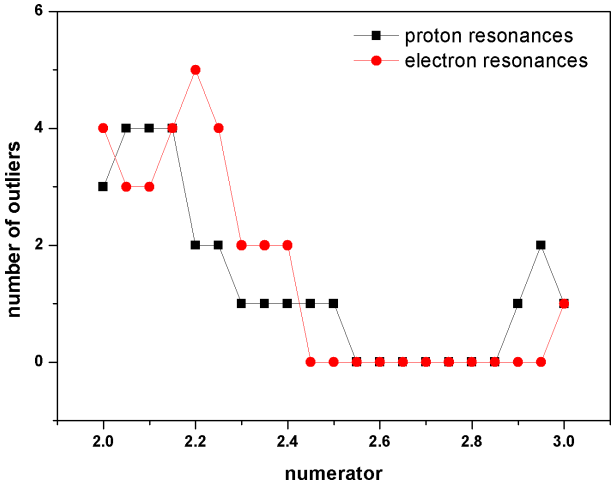

Fig. 1: Determination of the correct numerator for the dataset of expectation values (equations 5 and 6): the number of outliers as a function of the tested numerator.

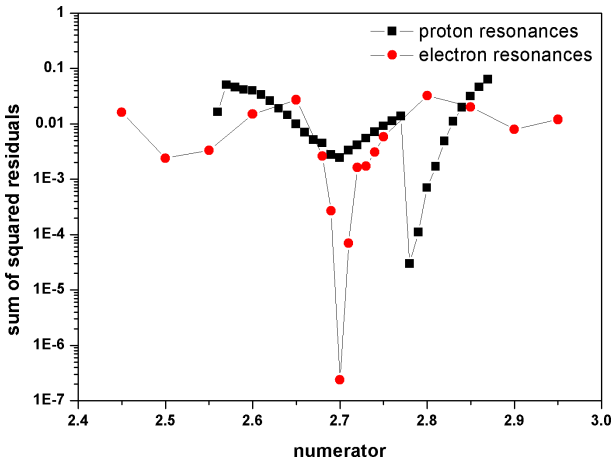

Fig. 2: Determination of the correct numerator for the dataset of expectation values (equations 5 and 6): the sum of squared residuals as a function of the tested numerator.

tation values creates the opportunity to test Müller's model very critically and to extend it.

3.2 Extending Müller's model

It is now shown that the following extension provides a solution, so that (i) Euler's number can be persist as numerator, and (ii) the whole dataset can be expressed by short continued fractions without any numerical errors, which means, this extended model reproduces the dataset *exactly*.

An additional phase shift δ was introduced in equations 5 and 6. For proton resonances, it can then be written:

$$\ln \frac{\langle r \rangle}{\lambda_C} = \delta + p + S. \qquad (7)$$

And analogously for electron resonances:

$$\ln \frac{\langle r \rangle}{\lambda_{C_{electron}}} = \delta + p + S. \qquad (8)$$

As shown in previous articles, the phase shift p varies among the dataset, so that some data points take $p = 0$ and others $p = 3/2$. Contrary to this, the phase shift δ must be equal for all data points in the set. This means the fractal spectrum of resonances is shifted on the logarithmic number line and the principal nodes are not more at $0, \pm 3, \pm 6, \pm 9 \ldots$, but now at $0 + \delta, \pm 3 + \delta, \pm 6 + \delta, \pm 9 + \delta \ldots$.

The underlying physical idea is that δ should be a small positive or negative number, characterizing a small deviation from Müller's standard model. To guarantee that the model does not become ambiguous, values of $|\delta|$ must always be smaller than 3/2.

For the here considered data set, the phase shift δ could be determined as a *very small number*, with the consequence that all numerical errors vanished (were smaller than 0.001 Å). The numerical values were $\delta = 0.017640$ when interpreting the data as proton resonances and $\delta = 0.002212$ in case of electron resonances. Tables 2 and 3 show the continued fraction representations when interpreting the expectation values as proton and electron resonances, respectively.

3.3 Interpretation

As can be seen, when accepting a *small* phase shift δ, the radial expectation values can be perfectly interpreted as both, proton and electron resonances. Besides that, the continued fraction representations are equal for proton and electron resonances, only the free link and the phase shift p differ. This is unavoidable due to the fact that different reference Compton wavelengths were used; so the logarithmic number line was calibrated differently.

The free link and the phase shift p are parameters which basically position the data point on the logarithmic number line, indicating the principal node. Then the first partial denominator determines whether the data point is located before or after this principal node. So the data point can be either in a compression or expansion zone, thus, now a specific property of its oscillation state is indicated. The equality of the set of partial denominators in the continued fraction representations is a necessary requirement for interpreting the expectation values as both, proton and electron resonances. Both oscillators must transmit at least qualitatively the same "oscillation property information" to the wavefunction.

However, when accepting the phase shift idea, it is always mathematically possible to interprete *any* set of proton resonances as a set of phase-shifted electron resonances. So what are the physical arguments for associating the expectation values to both oscillators?

- In an atom, electrons and the nucleus share a very small volume of space. The electron wavefunction is most

Table 2: Continued fraction representation of the radial expectation values of Hydrogen orbitals according to equation 7, considering proton resonances (δ = 0.017640).

Orbital	Continued fraction representation of $\langle \mathbf{r} \rangle$
1s	[0; 12 | e+1, -6, -6] [1.5; 12 | -e-1, -9]
2s	[0; 15 | -e-1, 9, e+1] [1.5; 12 | e+1, 24, 6]
2p	[0; 15 | -e-1, e+1, -e-1, 12, e+1] [1.5; 12 | 6, -e-1, 6, -e-1]
3s	[0; 15 | 132, -e-1]
3p	[0; 15 | -48, -6]
3d	[0; 15 | -12, 12, e+1]
4s	[0; 15 | e+1, e+1, -6, 6] [1.5; 15 | -e-1, e+1, 27, -e-1]
4p	[1.5; 15 | -e-1, e+1, -6, e+1, e+1, e+1]
4d	[0; 15 | 6, -21, -e-1, e+1]
4f	[0; 15 | 9, -15, 9]
5s	[1.5; 15 | -6, 45]
5p	[1.5; 15 | -6, 6, e+1, -e-1, 6]
5d	[0; 15 | e+1, -e-1, e+1, 6, -e-1, -12] [1.5; 15 | -6, e+1, -e-1, e+1, -9]
5f	[0; 15 | e+1, -e-1, -e-1, e+1, -33] [1.5; 15 | -e-1, -e-1, -e-1, e+1, -6]
5g	[0; 15 | e+1, -471] [1.5; 15 | -e-1, 15, 9, e+1]
6s	[1.5; 15 | -30, e+1, -18]
6p	[1.5; 15 | -24, -9, e+1, -e-1]
6d	[1.5; 15 | -18, -27]
6f	[1.5; 15 | -12, -e-1, e+1, 12]
6g	[1.5; 15 | -9, -21]
6h	[1.5; 15 | -6, -6, 6, -e-1, 6]

Table 3: Continued fraction representation of the radial expectation values of Hydrogen orbitals according to equation 8, considering electron resonances (δ = 0.002212).

Orbital	Continued fraction representation of $\langle \mathbf{r} \rangle$
1s	[0; 6 | -e-1, -9] [1.5; 3 | e+1, -6, -6]
2s	[0; 6 | e+1, 24, 6] [1.5; 6 | -e-1, 9, e+1]
2p	[0; 6 | 6, -e-1, 6, -e-1] [1.5; 6 | -e-1, e+1, -e-1, 12, e+1]
3s	[1.5; 6 | 132, -e-1]
3p	[1.5; 6 | -48, -6]
3d	[1.5; 6 | -12, 12, e+1]
4s	[0; 9 | -e-1, e+1, 27, -e-1] [1.5; 6 | e+1, e+1, -6, 6]
4p	[0; 9 | -e-1, e+1, -6, e+1, e+1, e+1]
4d	[1.5; 6 | 6, -21, -e-1, e+1]
4f	[1.5; 6 | 9, -15, 9]
5s	[0; 9 | -6, 45]
5p	[0; 9 | -6, 6, e+1, -e-1, 6]
5d	[0; 9 | -6, e+1, -e-1, e+1, -9] [1.5; 6 | e+1, -e-1, e+1, 6, -e-1, -12]
5f	[0; 9 | -e-1, -e-1, -e-1, e+1, -6] [1.5; 6 | e+1, -e-1, -e-1, e+1, -33]
5g	[0; 9 | -e-1, 15, 9, e+1] [1.5; 6 | e+1, -471]
6s	[0; 9 | -30, e+1, -18]
6p	[0; 9 | -24, -9, e+1, -e-1]
6d	[0; 9 | -18, -27]
6f	[0; 9 | -12, -e-1, e+1, 12]
6g	[0; 9 | -9, -21]
6h	[0; 9 | -6, -6, 6, -e-1, 6]

basically an electron property, always existing in close proximity to the nucleus (protons). From this it would not be a surprise that both oscillators contribute to the properties of the wavefunction. In general, one can now speculate that particularly physical parameters related to an atomic wavefunction are hot candidates to be interpretable as electron resonances.

- The phase shift was not invented to justify electron resonances, it is also required for an exact reproduction of the data set through proton resonances.
- When considering Müller's standard model (equations 5 and 6), the sum of squared residuals is much lower when interpreting the data as electron resonances. In this case the "best numerator" is also closer to Euler's number (see Fig. 2). Therefore, the wavefunction is principally governed by the electron oscillations. Certainly the proton oscillations influence the system too, they can be interpreted as a perturbation. The system tends to adjust to both oscillators and this seems to be the cause of the observed phase shifts. Hopefully, similar data will confirm this in near future.

4 Conclusions

Müller's model must be extended in two ways. First, it must be recognized that electron resonances exist in the universe as proton resonances do, and the same mathematical formalism for a chain of proton oscillators can be applied to a chain of electron oscillators. Second, an additional phase shift δ is

proposed to provide a reasonable mathematical extension of the model.

Of course, much more data must be analyzed and the future will show if this extended model can stand and give useful results when applying to other data sets. Particularly interesting for analyses would be quite accurate data from quantum mechanics.

Now one has to ask regarding previously published papers on this topic [4–6]: are there any results that must be reconsidered? The answer is definitively yes. In reference [4], masses of elementary particles were analyzed and only for 86% of the particles a continued fraction expression could be found. There is high probability that this exceptional high number of outliers (14%, nowhere else found) can be reduced considering a phase shift δ; or different phase shifts δ can put the elementary particles into different groups. In another paper [6], half-lifes of excited electronic states of atoms were found to be proton resonance periods, however, a possible interpretation as electron resonance periods has not been attempted yet. Possibly a small phase shift could here also reduce the number of outliers. This everything is now subject of future research.

Acknowledgments

The author greatly acknowledges the financial support from the Brazilian governmental funding agencies FACEPE and CNPq.

Submitted on May 2, 2012 / Accepted on May 06, 2012

References

1. Müller H. Fractal scaling Models of resonant oscillations in chain systems of harmonic oscillators. *Progress in Physics*, 2009, v. 2 72–76.
2. Müller H. Fractal scaling models of natural oscillations in chain systems and the mass distribution of the celestial bodies in the solar system. *Progress in Physics*, 2010, v. 1 62–66.
3. Müller H. Fractal scaling models of natural oscillations in chain systems and the mass distribution of particles. *Progress in Physics*, 2010, v. 3 61–66.
4. Ries A., Fook M.V.L. Fractal structure of nature's preferred masses: Application of the model of oscillations in a chain system. *Progress in Physics*, 2010, v. 4, 82–89.
5. Ries A., Fook M.V.L. Application of the Model of Oscillations in a Chain System to the Solar System. *Progress in Physics*, 2011, v. 1, 103–111.
6. Ries A., Fook M.V.L. Excited Electronic States of Atoms described by the Model of Oscillations in a Chain System. *Progress in Physics*, 2011, v. 4, 20–24.
7. Pauling L., Wilson E.B. Introduction to quantum mechanics. McGraw-Hill, New York, 1935.
8. Press W. H., Teukolsky S. A., Vetterling W. T., Flannery B. P. Numerical recipes in C. Cambridge University Press, Cambridge, 1992.
9. Otte R., Müller H.. German patent No. DE102004003753A1, date: 11.08.2005

Gravitational Acceleration and the Curvature Distortion of Spacetime

William C. Daywitt
National Institute for Standards and Technology (retired), Boulder, Colorado
E-mail: wcdaywitt@me.com

The Crothers solution to the Einstein vacuum field consists of a denumerable infinity of Schwarzschild-like metrics that are non-singular everywhere except at the point mass itself. When the point-mass distortion from the Planck vacuum (PV) theory is inserted into the Crothers calculations, the combination yields a composite model that is physically transparent. The resulting static gravitational field using the Crothers metrics is calculated and compared to the Newtonian gravitational field and the gravitational field associated with the black hole model.

1 Newtonian Introduction

When a test mass m' travels in the gravitational field of a point mass m situated at $r = 0$, the Newtonian theory of gravity predicts that the acceleration experienced by the test mass

$$\frac{d^2r}{dt^2} = -\frac{mG}{r^2} \tag{1}$$

is *independent of the mass* m'. In this theory the relative magnitudes of m' and m are arbitrary and lead to the following equation for the magnitude of the gravitational force between the two masses

$$\frac{m'mG}{r^2} = \frac{(m'c^2/r)(mc^2/r)}{c^4/G}$$
$$= \left(\frac{m'c^2/r}{c^4/G}\right)\left(\frac{mc^2/r}{c^4/G}\right)\frac{c^4}{G} \tag{2}$$

when expressed in terms of the ratio c^4/G.

In the PV theory [1] the force mc^2/r represents the curvature distortion the mass m exerts on the PV state (and hence on spacetime), and the ratio

$$\frac{c^4}{G} = \frac{m_*c^2}{r_*} \tag{3}$$

represents the maximum such curvature force, where m_* and r_* are the mass and Compton radius of the Planck particles constituting the PV. The corresponding relative curvature force is represented by the n-ratio

$$n_r \equiv \frac{mc^2/r}{c^4/G} = \frac{mc^2/r}{m_*c^2/r_*} \tag{4}$$

which is a direct measure of the curvature distortion exerted on spacetime and the PV by the point mass. Since the minimum distortion is 0 ($m = 0$ or $r \to \infty$) and the maximum is 1, the n-ratio is physically restricted to the range $0 \le n_r \le 1$ as are the equations of general relativity [2].

The important fiducial point at $n_{r_s} = 0.5$ is the Schwarzschild radius $r_s = 2mr_*/m_*$, where

$$rn_r = \frac{mc^2}{m_*c^2/r_*} = r_s n_{r_s} = 0.5r_s\,. \tag{5}$$

The acceleration (1) can now be expressed exclusively in terms of the relative curvature distortion n_r:

$$a(n_r) = -\frac{d^2r}{dt^2} = \frac{mc^4}{r^2c^4/G} = \frac{c^2}{r}\frac{mc^2/r}{m_*c^2/r_*}$$
$$= \frac{c^2}{r}n_r = \frac{c^2}{rn_r}n_r^2 = \frac{2c^2}{r_s}n_r^2 \tag{6}$$

whose normalized graph $a/(2c^2/r_s)$ is plotted in the first figure.

2 Affine Connection

The conundrum posed by equation (1), that the acceleration of the test particle is independent of its mass m', is the principle motivation behind the general theory of relativity [3, p. 4]; an important ramification of which is that, in a free-falling local reference frame, the acceleration vanishes as in equation (7). That result leads to the following development. Given the two coordinate systems $x^\mu = x^\mu(\xi^\nu)$ and $\xi^\mu = \xi^\mu(x^\nu)$ and the differential equation

$$\frac{d^2\xi^\mu}{d\tau^2} = 0 \tag{7}$$

Fig. 1: The graph plots the normalized Newtonian acceleration $a/(2c^2/r_s)$ as a function of n_r ($0 \le n_r \le 1$).

applying the chain law to the differentials gives

$$\frac{d^2\xi^\mu}{d\tau^2} = \frac{\partial\xi^\mu}{\partial x^\nu}\frac{d^2x^\nu}{d\tau^2} + \frac{\partial^2\xi^\mu}{\partial x^\alpha \partial x^\nu}\frac{dx^\alpha}{d\tau}\frac{dx^\nu}{d\tau} = 0\,. \tag{8}$$

Then using

$$x^\alpha(\xi^\mu(x^\beta)) = x^\alpha \qquad \Longrightarrow \qquad \frac{\partial x^\beta}{\partial\xi^\mu}\frac{\partial\xi^\mu}{\partial x^\nu} = \delta^\beta_\nu \tag{9}$$

to eliminate the coefficient of $d^2x^\nu/d\tau^2$ in (8) leads to

$$\frac{d^2x^\beta}{d\tau^2} + \frac{\partial x^\beta}{\partial\xi^\mu}\frac{\partial^2\xi^\mu}{\partial x^\alpha\partial x^\nu}\frac{dx^\alpha}{d\tau}\frac{dx^\nu}{d\tau} = 0\,. \tag{10}$$

Rearranging indices in (10) finally yields

$$\frac{d^2x^\mu}{d\tau^2} + \Gamma^\mu_{\nu\rho}\frac{dx^\nu}{d\tau}\frac{dx^\rho}{d\tau} = \frac{du^\mu}{d\tau} + \Gamma^\mu_{\nu\rho}u^\nu u^\rho = 0 \tag{11}$$

where $u^\mu = dx^\mu/d\tau$ is a typical component of the test-mass 4-velocity and

$$\Gamma^\mu_{\nu\rho} \equiv \frac{\partial x^\mu}{\partial\xi^\alpha}\frac{\partial^2\xi^\alpha}{\partial x^\nu\partial x^\rho} \tag{12}$$

is the *affine connection*. The affine connection vanishes when there is no gravitational distortion; so for the point mass m, it should be solely a function of the curvature distortion n_r given by (4).

The affine connection can be related to the the metric coefficients $g_{\alpha\beta}$ via [3, p. 7]

$$\Gamma^\mu_{\nu\rho} = \frac{g^{\mu\alpha}}{2}\left[\frac{\partial g_{\rho\alpha}}{\partial x^\nu} + \frac{\partial g_{\nu\alpha}}{\partial x^\rho} - \frac{\partial g_{\nu\rho}}{\partial x^\alpha}\right] \tag{13}$$

which, for a metric with no cross terms ($g^{\alpha\beta} = 0$ for $\alpha \neq \beta$), reduces to

$$\frac{2\Gamma^1_{\nu\rho}}{g^{11}} = \frac{\partial g_{\rho 1}}{\partial x^\nu} + \frac{\partial g_{\nu 1}}{\partial x^\rho} - \frac{\partial g_{\nu\rho}}{\partial x^1} \tag{14}$$

with $\mu = 1$ for example.

Since only radial effects are of interest in the present paper, only the x^0 and x^1 components of the spherical polar coordinate system $(x^\mu) = (x^0, x^1, x^2, x^3) = (ct, r, \theta, \phi)$ are required. Then the affine connection in (11) for the $\mu = 1$ component reduces to

$$\frac{du^1}{d\tau} = -\Gamma^1_{\nu\rho}u^\nu u^\rho$$

$$= -\left[\Gamma^1_{00}(u^0)^2 + 2\Gamma^1_{01}u^0u^1 + \Gamma^1_{11}(u^1)^2\right] \tag{15}$$

which under static conditions ($u^1 = dr/d\tau = 0$ for the test mass) produces

$$\frac{du^1}{d\tau} = -\Gamma^1_{00}(u^0)^2\,. \tag{16}$$

In the spherical system with $d\theta = d\phi = 0$, the metric becomes

$$ds^2 = c^2d\tau^2 = g_{00}\,c^2dt^2 + g_{11}\,dr^2 \tag{17}$$

where g_{00} and g_{11} are functions of the coordinate radius $x^1 = r$. Under these conditions the only non-zero affine connections from (14) are:

$$\Gamma^0_{10} = \Gamma^0_{01} = \frac{g^{00}}{2}\frac{\partial g_{00}}{\partial x^1} \tag{18}$$

$$\Gamma^1_{00} = \frac{-g^{11}}{2}\frac{\partial g_{00}}{\partial x^1} \qquad \text{and} \qquad \Gamma^1_{11} = \frac{g^{11}}{2}\frac{\partial g_{11}}{\partial x^1}\,. \tag{19}$$

Using (17), the velocity u^0 can be calculated from

$$cd\tau = g_{00}^{1/2}dx^0\left[1 + \left(\frac{g_{11}}{g_{00}}\right)\left(\frac{dr/dt}{c}\right)^2\right]^{1/2} \tag{20}$$

which for static conditions ($dr/dt = 0$) leads to

$$u^0 = \frac{dx^0}{d\tau} = \frac{c}{g_{00}^{1/2}}\,. \tag{21}$$

Inserting (21) into (16) gives

$$\frac{du^1}{d\tau} = -\frac{c^2\Gamma^1_{00}}{g_{00}} = \frac{c^2}{g_{00}}\left(\frac{g^{11}}{2}\frac{\partial g_{00}}{\partial r}\right) \tag{22}$$

along with its covariant twin

$$\frac{du_1}{d\tau} = g_{11}\frac{du^1}{d\tau}$$

$$= \frac{g_{11}c^2}{g_{00}}\left(\frac{g^{11}}{2}\frac{\partial g_{00}}{\partial r}\right) = \frac{c^2}{g_{00}}\left(\frac{\partial g_{00}}{2\partial r}\right). \tag{23}$$

Then combining (22) and (23) leads to the static acceleration

$$\left|\frac{du^1}{d\tau}\frac{du_1}{d\tau}\right|^{1/2} = \left(-g^{11}\right)^{1/2}\left(\frac{c^2}{g_{00}}\right)\left(\frac{\partial g_{00}}{2\partial r}\right). \tag{24}$$

3 Static Acceleration

The metric coefficients g_{00} and g^{11} for a point mass m at $r = 0$ are given by (A6) and (A7) in the Appendix. After some straightforward manipulations, (24) leads to the (normalized) static gravitational acceleration ($0 \le n_r \le 1$)

$$\frac{a_n(n_r)}{2c^2/r_s} = \left|\frac{(du^1/d\tau)(du_1/d\tau)}{(2c^2/r_s)^2}\right|^{1/2}$$

$$= \frac{n_r^2}{(1 - r_s/R_n)^{1/2}(1 + 2^n n_r^n)^{2/n}} \tag{25}$$

$$= \frac{n_r^2}{[(1 + 2^n n_r^n)^{1/n} - 2n_r]^{1/2}(1 + 2^n n_r^n)^{3/2n}} \tag{26}$$

$$= \frac{n_r^2}{[(1 + 1/2^n n_r^n)^{1/n} - 1]^{1/2}(2n_r)^{1/2}(1 + 2^n n_r^n)^{3/2n}} \tag{27}$$

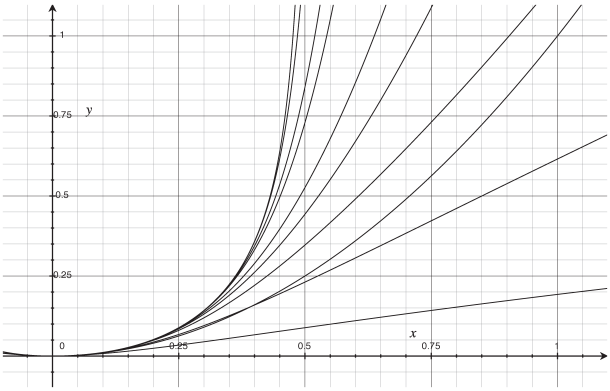

Fig. 2: The graph plots $a_n/(2c^2/r_s)$ as a function of n_r for the indices $n = 1, 2, 3, 4, 5, 8, 10, 20, 40$ from bottom-to-top of the graph. The curve that intersects (1,1) is the normalized Newtonian acceleration from (6). The $n = 3$ curve is the original Schwarzschild result [5] ($0 \le n_r \le 1$).

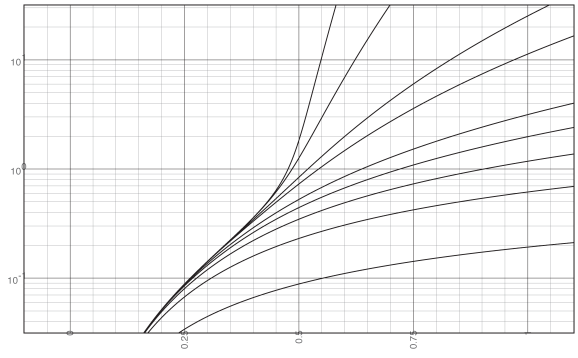

Fig. 3: The graph is a lin-log plot of $a_n/(2c^2/r_s)$ as a function of n_r for the indices $n = 1, 2, 3, 4, 5, 8, 10, 20, 40$ from bottom-to-top of the graph ($0 \le n_r \le 1$).

in terms of the relative curvature force n_r, all of which vanish for $n_r = 0$. Formally, the acceleration in the denominator on the left of (25)

$$\frac{\Delta v}{\Delta t} = \frac{c}{(r_s - r_s/2)/c} = \frac{2c^2}{r_s} \tag{28}$$

is the acceleration of a test mass starting from rest at $r = r_s$ ($n_r = 0.5$) and accelerating to the speed of light c in its fall to $r_s/2$ ($n_r = 1$) in the time interval $(r_s - r_s/2)/c$.

The limits of (26) and (27) as $n \to \infty$ are easily seen to be

$$\frac{a_\infty(n_r)}{2c^2/r_s} = \begin{cases} n_r^2/(1-2n_r)^{1/2} & , 0 \le n_r \le 0.5 \\ \infty & , 0.5 \le n_r \le 1 \end{cases} \tag{29}$$

where $n_r < 0.5$ and $n_r > 0.5$ are used in (26) and (27) respectively. Equations (26) and (27) are plotted in Figures 2 and 3 for various indices n, all plots of which are continuous in the entire range $0 \le n_r \le 1$. The curve that runs through the point (1,1) in Figure 2 is the Newtonian result from (6). It is clear from Figure 3 that the acceleration diverges in the range $0.5 \le n_r \le 1$ for the limit $n \to \infty$. In the range $0 \le n_r \le 0.5$ the acceleration is given by the upper equation in (29) — this result is identical with the static black-hole acceleration [3, p. 43].

4 Summary and Comments

The nature of the vacuum state provides a force constraint ($n_r \le 1$) on any theory of gravity, whether it's the Newtonian theory or the general theory of relativity [2]. This effect manifests itself rather markedly in the equation for the Kerr-Newman black-hole area A for a charged spinning mass [4]:

$$A = \frac{4\pi G}{c^4} \times \left[2m^2G - Q^2 + 2(m^4G^2 - c^2J^2 - m^2Q^2G)^{1/2}\right] \tag{30}$$

where Q and J are the charge and angular momentum of the mass m. Using the relation in (3) and $G = e_*^2/m_*^2$ [1], it is straightforward to transform (30) into the following equation

$$\begin{aligned} \frac{A}{4\pi r_*^2} = \; & 2\left(\frac{m}{m_*}\right)^2 - \left(\frac{Q}{e_*}\right)^2 + \\ & +2\left[\left(\frac{m}{m_*}\right)^4 - \left(\frac{J}{r_* m_* c}\right)^2 - \left(\frac{m}{m_*}\right)^2\left(\frac{Q}{e_*}\right)^2\right]^{1/2} \end{aligned} \tag{31}$$

where all of the parameters (e_*, m_*, r_*, except c of course) in the denominators of the terms are PV parameters; and all of the terms are properly normalized to the PV state, the area A by the area $4\pi r_*^2$, the angular momentum J by the angular momentum $r_* m_* c$, and so forth.

The "dogleg" in Figure (4) at the Schwarzschild radius r_s ($n_r = 0.5$) and the pseudo-singularity in the black-hole metric at r_s are features of the Einstein differential geometry approach to relativistic gravity — how realistic these features are remains to be seen. At this point in time, though, astrophysical measurements have not yet reached the $n_r = 0.5$ point (see below) where the dogleg and the black-hole results can be experimentally checked, but that point appears to be rapidly approaching. Whatever future measurements might show, however, the present calculations indicate that the point-mass-PV interaction that leads to n_r may point to the physical mechanism that underlies gravity phenomenology.

The evidence for black holes with all m/r ratios appears to be growing [3, Ch. 6]; so it is important to see if the present calculations can explain the experimental black-hole picture that is prevalent in today's astrophysics. The salient feature of a black hole is the event horizon [3, pp. 2, 152], that pseudo-surface at $r = r_s$ at which strange things are supposed to happen. A white dwarf of mass 9×10^{32}gm and radius 3×10^8cm exerts a curvature force on the PV equal to 2.7×10^{45}dyne, while a neutron star of mass 3×10^{33}gm and radius 1×10^6cm exerts a force of 2.7×10^{48}dyne [2]. Dividing these forces

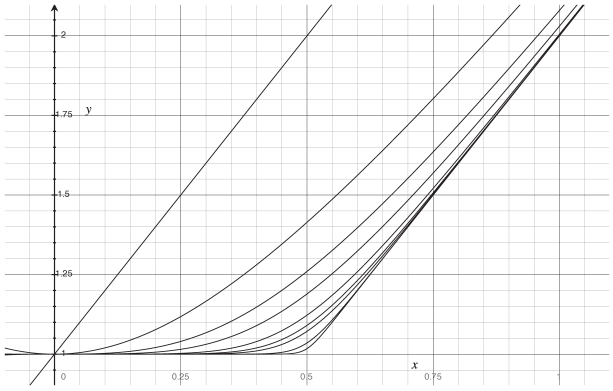

Fig. 4: The graph plots R_n/r as a function of n_r for the indices $n = 1, 2, 3, 4, 6, 8, 10, 20, 40$. The straight line is the $n = 1$ curve ($0 \leq n_r \leq 1$).

by the 1.21×10^{49}dyne force in the denominator of (4) leads to the n-ratios $n_r = 0.0002$ and $n_r = 0.2$ at the surface of the white dwarf and neutron star respectively. The surfaces of these two objects are real physical surfaces — thus they cannot be black holes.

On the other hand, SgrA* [3, p. 156] is thought to be a supermassive black-hole with a mass of about 4.2×10^6 solar masses and a radius confined to $r < 22 \times 10^{11}$ [cm], leading to the SgrA* n-ratio $n_r > 0.28$. For an n-ratio of 0.28, however, the plots in Figures 2–4 show that the behavior of spacetime and the PV is smooth. To reach the $n_r = 0.5$ value and the dogleg, the SgrA* radius would have to be about 12×10^{11} [cm], a result not significantly out of line with the measurements.

Finally, it should be noted that the black-hole formalism is the result of substituting $R_n = r$ in the metric (A1) of the Appendix. Unfortunately, since $R_n/r > 1$ signifies a response of the vacuum to the perturbation n_r at the coordinate radius r, the effect of this substitution is to eliminate that response. This is tantamount to setting $n_r = 0$ in the second-to-last expression of (A3).

Appendix: Crothers Vacuum Metrics

The general solution to the Einstein vacuum field [5] [6] for a point mass m at $r = 0$ consists of the infinite collection ($n = 1, 2, 3, \cdots$) of Schwarzschild-like metrics that are *non-singular* for all $r > 0$:

$$ds^2 = (1 - r_s/R_n)\, c^2 dt^2 - \frac{(r/R_n)^{2n-2}\, dr^2}{1 - r_s/R_n} - \\ -R_n^2(d\theta^2 + \sin^2\theta d\phi^2) \qquad \text{(A1)}$$

where

$$r_s = 2\,\frac{mG}{c^2} = 2\,\frac{mc^2}{m_* c^2/r_*} = 2rn_r \qquad \text{(A2)}$$

$$R_n = (r^n + r_s^n)^{1/n} = r(1 + 2^n n_r^n)^{1/n} = r_s \frac{(1 + 2^n n_r^n)^{1/n}}{2n_r} \qquad \text{(A3)}$$

and where r is the coordinate radius from the point mass to the field point of interest and r_s is the Schwarzschild radius. The ratio R_n/r as a function of n_r is plotted in Figure 4 for various indices n. The n-ratios 0, 0.5, and 1 correspond to the r values $r \to \infty$, r_s, and $r_s/2$ respectively.

All the metrics in (A1) for $n \geq 2$ reduce to

$$ds^2 = (1 - 2n_r)\, c^2 dt^2 - \frac{dr^2}{1 - 2n_r} - r^2(d\theta^2 + \sin^2\theta d\phi^2) \qquad \text{(A4)}$$

for $n_r \ll 1$.

It is clear from the expressions in (A3) that the requirement of asymptotic flatness [3, p.55] is fulfilled for all finite n. On the other hand, the proper radius $\mathcal{R}_n$ from the point mass at $r = 0$ to the coordinate radius r is not entirely calculable:

$$\mathcal{R}_n(r) = \int_0^r (-g_{11})^{1/2} dr$$

$$= \int_0^{r_s/2} (?)dr + \int_{r_s/2}^r (-g_{11})^{1/2} dr \qquad \text{(A5)}$$

due to the failure of the general theory in the region $0 < r < r_s/2$ [2].

The metric coefficients of interest in the text for $d\theta = d\phi = 0$ are

$$g_{00} = (1 - r_s/R_n) \qquad \text{(A6)}$$

$$g_{11} = -\frac{(r/R_n)^{2n-2}}{1 - r_s/R_n} = \frac{1}{g^{11}}\,. \qquad \text{(A7)}$$

From (A3)

$$\frac{\partial R_n}{\partial r} = \frac{1}{(1 + 2^n n_r^n)^{(1-1/n)}} \qquad \text{(A8)}$$

and from (A8)

$$\frac{\partial g_{00}}{\partial r} = \frac{r_s}{R_n^2}\frac{\partial R_n}{\partial r}\,. \qquad \text{(A9)}$$

Submitted on May 3, 2012 / Accepted on May 11, 2012

References

1. Daywitt W.C. The Planck vacuum. *Progress in Physics*, 2009, v. 1, 20–26.
2. Daywitt W.C. Limits to the validity of the Einstein field equations and general relativity from the viewpoint of the negative-energy Planck vacuum state. *Progress in Physics*, 2009, v. 3, 27–29.
3. Raine D., Thomas E. *Black Holes: An Introduction*. Second Edition, Imperial College Press, London, 2010. The reader should note that m is used in the present paper to denote physical mass — it is not the geometric mass $m\,(\equiv MG/c^2)$ as used in this reference.
4. http://www.phy.olemiss.edu/~luca/Topics/bh/laws.html
5. Crothers S.J. On the general solution to Einstein's vacuum field and its implications for relativistic degeneracy. *Progress in Physics*, 2005, v. 1, 68–73.
6. Daywitt W.C. The Planck vacuum and the Schwarzschild metrics. *Progress in Physics*, 2009, v. 3, 30–31.

Cumulative-Phase-Alteration of Galactic-Light Passing Through the Cosmic-Microwave-Background: A New Mechanism for Some Observed Spectral-Shifts

Hasmukh K. Tank

Indian Space Research Organization, 22/693, Krishna Dham-2, Vejalpur, Ahmedabad-380015, India
E-mail: tank.hasmukh@rediffmail.com, hasmukh.tank1@gmail.com

Currently, whole of the measured "cosmological-red-shift" is interpreted as due to the "metric-expansion-of-space"; so for the required "closer-density" of the universe, we need twenty times more mass-energy than the visible baryonic-matter contained in the universe. This paper proposes a new mechanism, which can account for good percentage of the red-shift in the extra-galactic-light, greatly reducing the requirement of dark matter-energy. Also, this mechanism can cause a new kind of blue-shift reported here, and their observational evidences. These spectral-shifts are proposed to result due to cumulative phase-alteration of extra-galactic-light because of vector-addition of: (i) electric-field of extra-galactic-light and (ii) that of the cosmic-microwave-background (CMB). Since the center-frequency of CMB is much lower than extra-galactic-light, the cumulative-phase-alteration results in *red*-shift, observed as an additional contributor to the measured "cosmological red-shift"; and since the center-frequency of CMB is higher than the radio-frequency-signals used to measure velocity of space-probes like: Pioneer-10, Pioneer-11, Galileo and Ulysses, the cumulative-phase-alteration resulted in blue-shift, leading to the interpretation of deceleration of these space-probes. While the galactic-light experiences the red-shift, and the ranging-signals of the space-probes experience *blue*-shift, they are comparable in magnitude, providing a supportive-evidence for the new mechanism proposed here. More confirmative-experiments for this new mechanism are also proposed.

1 Introduction

Currently, whole of the "cosmological red-shift" is interpreted in terms of "metric-expansion-of-space", so for the required "closer-density" of the universe, we need twenty times more mass-energy than the visible baryonic-matter contained in the universe. This paper proposes a new mechanism, which can account for good percentage of the red-shift in the extra-galactic-light, greatly reducing the requirement of dark matter-energy. Prior to this, many scientists had proposed alternative-interpretations of "the cosmological red-shift", but the alternatives proposed so far were rather speculative; for example, speculating about possible presence of iron-particles in the inter-galactic-space, or presence of atoms of gas, or electrons, or virtual-particles... etc. How can we say for sure that such particles are indeed there in the inter-galactic-space? Even if they are there, is the "cross-section" of their interactions sufficient? Whereas a mechanism proposed here is based on experimentally established facts, namely the presence of "cosmic-microwave-background" (CMB), we are sure that CMB is indeed present in the inter-galactic-space. And we know for sure that electric-field-vectors of light and CMB are sure to get added.

This mechanism predicts both kids of spectral-shifts, *red*-shift as well as *blue*-shift. The solar-system-astrometric-anomalies [1, 2] are indicated here to arise due to the *blue*-shift caused by the cumulative-phase-alteration-mechanism proposed here. These anomalies are actually providing supportive-evidences for the new mechanism proposed here.

Brief reminder of the "solar system astrometric anomalies" will be in order here: (a) Anomalous secular increase of the eccentricity of the orbit of the moon [3–7] (b) the fly-by-anomaly [8–10] (c) precession of Saturn [11–12], (d) secular variation of the gravitational-parameter GM (i.e. G times mass M of the Sun) [13–16] (e) secular variation of the Astronomical-Unit [17–23] and (f) the Pioneer anomaly. For description of Pioneers see: [24] for general review of Pioneer-anomaly see: [25]. Of course, the traditional constant part of the anomalous-acceleration does not show up in the motion of major bodies of the solar system [26–44]. For the attempts of finding explanations for the Pioneer-anomaly in terms of conventional physics see: [45–52].

In this new mechanism for the spectral-shift, proposed here, there is no loss of energy; energy lost by cosmic-photons get transferred to CMB; so, it is in agreement with the law of conservation of energy. More verification-experiments for this new mechanism are also proposed here, so it is a testable proposal.

Moreover, this proposal is not in conflict with the existing theories, because it does not claim that whole of the measured "cosmological red-shift" is due to this "cumulative-phase-alteration-mechanism"; some 5% of the red-shift must be really due to "metric-expansion-of-space", reducing requirement of total-mass-of-the-universe to the observable

baryonic matter, making it sufficient for the required "closer-density". Thus this new mechanism is likely to resolve many of the problems of the current Standard Model of Cosmology.

2 Cumulative phase-alteration of the Extra-Galactic-Light passing through the Cosmic-Microwave-Background (CMB)

Let us imagine a horizontal arrow of three centimeter length representing instantaneous magnitude and direction of electric-field of the "extra-galactic-light". Then add a small arrow of just five mm length at an angle minus thirty degrees, representing instantaneous magnitude and direction of the "cosmic-microwave-background". We can see that the resultant vector has increased in magnitude, but lagged behind by a small angle theta. As the wave of extra-galactic-light travels in space, a new arrow representing CMB keeps on getting added to the previous resultant-vector. This kind of phase and amplitude-alterations continue for billions of years in the case of "extra-galactic-light"; producing a cumulative-effect. Since the speed of rotation of the vector representing CMB is much slower than that of light, the CMB-vector pulls-back the Light-vector resulting in reduction of cyclic-rotations. This process can be mathematically expressed as follows:

Electric field of pure light-wave can be expressed as:

$$\Psi(X,t) = A \exp i(\omega t - kX)$$

where ω represents the angular-frequency of light, and k the wave-number. Taking into consideration only the time-varying-part, at a point p :

$$\Psi(t) = A\,[\cos\omega t + i \sin\omega t] \tag{1}$$

When electric-fields of CMB get added to light, the resultant-sum can be expressed as:

$$\Psi(t) = A\left[N(t)\cos\omega t + i\hat{N}(t)\sin\omega t\right] \tag{2}$$

Where: $N(t)$ represents instantaneous magnitude of alteration caused by CMB, and $\hat{N}(t)$ represents its Hilbert-transform. When all the spectral-components of $N(t)$ are phase-shifted by +90 degrees, we get its Hilbert-transform $\hat{N}(t)$.

As a communications-engineer we use band-pass-filter to remove out-of-band noise. This author has also developed a noise-cancelling-technique, to reduce the effect of even in-band-noise by up-to 10 dB. But in the extra-galactic-space there are no band-pass-filters, so the phase-alterations caused by CMB keep on getting accumulated. After billions of years, when this light reaches our planet earth there is a cumulative-phase-alteration in the extra-galactic-light, observed as a part of "the cosmological red-shift". Since the center-frequency of CMB is much lower than extra-galactic-light, the cumulative-phase-alteration results in red-shift; and since the center-frequency of CMB is higher than the radio-frequency-signals (2110 MHz for the uplink from Earth and 2292 MHz for the downlink to Earth) used to measure velocity of Pioneer-10, Pioneer-11, Galileo and Ulysses space-probes, the cumulative-phase-alteration resulted in blue-shift, leading to the interpretation of deceleration of these space-probes. C. Johan Masreliez [53] has presented a "cosmological explanation for the Pioneer-anomaly", in terms of expansion of space, whereas here it is proposed that the expansion-of-space appears mostly due to the "cumulative-phase-alteration" of light due to CMB. This shows that there is a co-relation between the magnitudes of anomalous-accelerations of the Pioneer-10-11 space-probes and the "cosmological red-shift". Although, one of the shifts is red-shift, and the other is *blue*-shift, their magnitudes, in terms of decelerations, are strikingly the same; as described in detail in the next paragraph:

We can express the cosmological red-shift z_c in terms of de-acceleration experienced by the photon, as follows [54–55]: For z_c smaller than one:

$$z_c = \frac{f_0 - f}{f} = \frac{H_0 D}{c}$$

i.e.

$$\frac{h\Delta f}{hf} = \frac{H_0 D}{c}$$

i.e.

$$h\Delta f = \frac{hf}{c^2}(H_0 c) D \tag{3}$$

That is, the loss in energy of the photon is equal to its mass (hf/c^2) times the acceleration $a = H_0 c$, times the distance D travelled by it. Where: H_0 is Hubble-parameter. And the value of constant acceleration a is:

$$a = H_0 c, \quad a = 6.87 \times 10^{-10}\ \ m/s^2.$$

And now, we will see that the accelerations experienced by the Pioneer-10, Pioneer-11, Galileo and Ulysses space-probes do match strikingly with the expression (3):

Carefully observed values of de-accelerations [27]:
For Pioneer-10:
$a = (8.09 \pm 0.2) \times 10^{-10}\ \ m/s^2 = H_0 c \pm$ local-effect.
For Pioneer-11:
$a = (8.56 \pm 0.15) \times 10^{-10}\ \ m/s^2 = H_0 c \pm$ local-effect.
For Ulysses:
$a = (12 \pm 3) \times 10^{-10}\ \ m/s^2 = H_0 c \pm$ local-effect.
For Galileo:
$a = (8 \pm 3) \times 10^{-10}\ \ m/s^2 = H_0 c \pm$ local-effect.
And: as we already derived earlier, for the "cosmologically-red-shifted-photon", $a = 6.87 \times 10^{-10}\ \ m/s^2 = H_0 c$.
The "critical acceleration" of modified Newtonian dynamics MOND: $a_0 = H_0 c$. The rate of "accelerated-expansion" of the universe: $a_{exp} = H_0 c$.

Perfect matching of values of decelerations of all the four space-probes is itself an interesting observation; and its matching with the deceleration of cosmologically-red-

shifting-photons can not be ignored by a scientific mind as a coincidence.

There is one more interesting thing about the value of this deceleration as first noticed by Milgrom, that: with this value of deceleration, an object moving with the speed of light would come to rest exactly after the time T_0 which is the age of the universe.

The attempt proposed by this author refers only to the constant part of the PA. It should be acknowledged that also a time-varying part has been discovered as well.

3 Possible verification-experiments

Vector-addition of light and CMB can be simulated using computers. The vector to be added to light-vector can be derived from the actual CMB received. Every time new and new CMB-vector can be added to the resultant vector of previous addition.

Secondly, we know that there is certain amount of unisotropy in the CMB. Microwaves coming from some directions are more powerful than others. So, we can look for any co-relation between the strength of CMB from a given direction and value of cosmological-red-shift.

Thirdly, we can establish a reverberating-satellite-link, in which we can first transmit a highly-stable frequency to geo-synchronous-satellite; receive the signal back; re-transmit the CMB-noise-corrupted-signal back to satellite, and continue such repetitions for an year or longer and compare the frequency of the signal with the original source.

4 Conclusion

After getting the results of verification-experiments, the new mechanism proposed here namely: "Cumulative Phase-Alteration of the Extra-Galactic-Light passing through Cosmic-Microwave-Background (CMB)" it seems possible to explain: not only the large percentage of "cosmological red-shift", but also the Pioneer-anomaly. Quantitative analysis may leave 5% of the measured value of the "cosmological red-shift" for the standard explanation in terms of "metric-expansion-of-space", reducing the requirement of total-mass of the universe to the already-observable baryonic matter; thus it is likely to resolve many of the problems of current standard-model-cosmology. This author also proposes to investigate if this new mechanism of spectral-shifts will be able to accommodate some of the solar-system-astrometric-anomalies.

Submitted on: June 14, 2012 / Accepted on: June 15, 2012

References

1. Lämmerzahl C., Preuss O., and Dittus H. "Is the physics within the solar system really understood?" in Lasers, Clocks and Drag Free Control: Exploration of Relativistic Gravity in Space, Dittus H., Lämmerzahl C., and Turyshev S.G., Eds., pp.75–104, Springer, Berlin, Germany, 2008.
2. Anderson J.D., Nieto M.M., 2010, in Klioner S.A., Seidelmann P.K., Soffel M.H., eds, Proc. IAU Symp. 261, Relativity in Fundamental Astronomy: Dynamics, Reference Frames, and Data Analysis. Cambridge Univ. Press, Cambridge, p. 189.
3. Williams J.G., Boggs D.H., Yoder C.F., Ratcliff J.T., Dickey J.O. Lunar rotational dissipation in solid body and molten core. *Journal of Geophysical Research – Planets*, 2001, v. 106, 27933–27968.
4. Williams J.G., Dickey J.O., 2003, in Noomen R., Klosko S., Noll C., Pearlman M., eds, Proc. 13th Int. Workshop Laser Ranging, NASA/CP-2003-212248, Lunar Geophysics, Geodesy, and Dynamics, p.75. `http://cddis.nasa.gov/lw13/docs/papers/sci_williams_1m.pdf`
5. Williams J.G., Boggs D.H., 2009, in Schilliak S., ed., Proc. 16th Int. Workshop Laser Ranging, Lunar Core Mantle. What Does LLR See? p. 101. `http://cddis.gsfc.nasa.gov/lw16/docs/papers/sci_1` (read p. 115–116 where it is written: "While the mean motion and semimajor axis rates are compatible with our understanding of dissipation in Earth and Moon, LLR solutions consistently find an anomalous eccentricity rate").
6. Iorio L. On the anomalous secular increase of the eccentricity of the orbit of the Moon. *Monthly Notices of the Royal Astronomical Society*, 211, v. 415, 1266–1275.
7. Iorio L. An empirical explanation of the anomalous increase in the astronomical unit and the lunar eccentricity. *Astronomical Journal*, 2011, v. 142, 68–70.
8. Anderson J.D., Campbell J.K., and Nieto M.M. The energy transfer process in planetary flybys. *New Astronomy*, 2007, v. 12, no. 5, 383–397.
9. Anderson J.D., Campbell J.K., Ekelund J.E., Ellis J., and Jordan J.F. Anomalous orbital-energy changes observed during spacecraft flybys of earth. *Physical Review Letters*, 2008, v. 100, no. 9, 091102.
10. Iorio L. The Effect of General Relativity on Hyperbolic Orbits and Its Application to the Flyby Anomaly. *Scholarly Research Exchange*, 2009, Article ID: 807695.
11. Pitjeva, E.V.: EPM ephemerides and relativity. In: Klioner, S.A., Seidelmann, P.K., Soffel, M.H., (Eds.) IAU Symposium, Vol. 261 of IAU Symposium, pp. 170–178, (2010).
12. Fienga A., Laskar J., Kuchynka P., Manche H., Desvignes G., Gastineau M., Cognard I., Theureau G. The INPOP10 a planetary ephemeris and its applications in fundamental physics. *Celestial Mechanics and Dynamical Astronomy*, 2011, v. 111, no. 3, 363–385.
13. Pitjeva E.V., Pitjev N.P. Estimations of changes of the Sun's mass and the gravitation constant from the modern observations of planets and spacecraft. *Solar System Research*, 2012, v. 46(1), 78–87.
14. Iorio L. Classical and Relativistic OrbitalMotions around a Mass-Varying Body. *Scholarly Research Exchange Physics*, 2010, Article ID: 261249.
15. Iorio L. Orbital effects of Suns mass loss and the Earths fate. *Natural Science*, 2010, v. 2(4), 329–337.
16. Iorio L. Effect of sun and planet-bound dark matter on planet and satellite dynamics in the solar system. *Journal of Cosmology and Astroparticle Physics*, 2010, v. 05, 018.
17. Krasinsky G.A., Brumberg V.A. Secular increase of astronomical unit from analysis of the major planet motions, and its interpretation. *Celestial Mechanics and Dynamical Astronomy* 2004, v. 90, 267–288.
18. Standish E.M. The Astronomical Unit Now, in Transit of Venus: new views of the solar system and galaxy, IAU Coll. 196, Kurtz D.W., Cambridge: Cambridge University Press, 2005, pp. 163–179.
19. Iorio L. Secular increase of the astronomical unit and perihelion precessions as tests of the Dvali Gabadadze Porrati multidimensional braneworld scenario. *Journal of Cosmology and Astroparticle Physics*, 2011, v. 09, 006.

20. Arakida H. Application of time transfer function to McVittie spacetime: gravitational time delay and secular increase in astronomical unit. *General Relativity and Gravitation*, 2011, v. 43(8), 2127–2139.
21. Arakida H. Time delay in Robertson McVittie space-time and its application to increase of astronomical unit. *New Astronomy*, 2009, v. 14(3), 264–268.
22. Ito Y. *Publications of the Astronomical Society of Japan*, 2009, v. 61, 1373.
23. Miura T., Arakida H., Kasai M., and Kuramata S. *Publications of the Astronomical Society of Japan*, 2009, v. 61, 1247.
24. W. J. Dixon, Pioneer spacecraft reliability and performance. *Acta Astronautica*, 1975, v. 2(9–10), pp. 801–817.
25. Turyshev S.G., Toth V.T. The Pioneer Anomaly. *Living Reviews in Relativity*, 2010, v. 13, Article ID: 4.
26. Anderson J.D., Laing P.A., Lau E.L., Liu A.S., Nieto M.M., and Turyshev, S.G. Indication, from Pioneer 10, 11, Galileo, and Ulysses Data, of an Apparent Anomalous, Weak, Long-Range Acceleration. *Physical Review Letters*, 1998, v. 81, 2858–2861 [(Comment by Katz J.I.: Phys. Rev. Lett. Vol. 83, 1892 (1999); Reply: Phys. Rev. Lett. 83, 1893 (1999)].
27. Turyshev S.G., Toth V.T., Ellis J., Markwardt C.B. Support for Temporally Varying Behavior of the Pioneer Anomaly from the Extended Pioneer 10 and 11 Doppler Data Sets, *Physical Review Letters*, 2011, v. 107, no. 8, 081103.
28. Standish E.M. "Planetary and Lunar Ephemerides: testing alternate gravitational theories", in Recent Developments in Gravitation and Cosmology, A. Macias, C. Lämmerzahl, and A. Camacho, Eds., v. 977 of AIP Conference Proceedings, pp. 254–263, American Institute of Physics, Melville, NJ, USA, 2008.
29. Standish E.M. "Testing alternate gravitational theories", in Fundamental Astronomy: Dynamics, Reference Frames, and Data Analysis, Proceedings of the International Astronomical Union, S. A.
30. Klioner P., Seidelmann K., and Soffel M.H., Eds., v. 261 of IAU Symposium, pp. 179–182, 2010.
31. Iorio L. and Giudice G. What do the orbital motions of the outer planets of the Solar System tell us about the Pioneer anomaly? *New Astronomy*, 2006, v. 11, no. 8, 600–607.
32. Page G.L., Dixon D.S., and Wallin J.F. Can minor planets be used to assess gravity in the outer solar system? *Astrophysical Journal*, 2006, v. 642, no. 1, 606–614.
33. Tangen K. Could the Pioneer anomaly have a gravitational origin? *Physical Review D*, 2007, v. 76, no. 4, 042005.
34. Iorio L. Can the pioneer anomaly be of gravitational origin? A phenomenological answer. *Foundations of Physics*, 2007, v. 37, no. 6, 897–918.
35. Iorio L. Jupiter, Saturn and the Pioneer anomaly: a planetary-based independent test. *Journal of Gravitational Physics*, 2007, v. 1, no. 1, 5–8.
36. Wallin J.F., Dixon D.S., and Page G.L. Testing gravity in the outer solar system: results from trans-neptunian objects. *Astrophysical Journal*, 2007, v. 666, no. 2, 1296–1302.
37. Iorio L. "The Lense-Thirring effect and the Pioneer anomaly: solar system tests", in Proceedings of the the 11th Marcel Grossmann Meeting on Recent Developments in Theoretical and Experimental General Relativity, Gravitation and Relativistic Field Theorie, H. Kleinert, R.T. Jantzen, and R. Ruffini, Eds., pp. 2558–2560, World Scientific, 2008.
38. Fienga A., Laskar J., Kuchynka P., Leponcin-Lafitte C., Manche1 H., and Gastineau M., "Gravity tests with INPOP planetary ephemerides", in Relativity in Fundamental Astronomy, S.A. Klioner, P.K. Seidelman, and M.H. Soffel, Eds., Proceedings IAU Symposium no. 261, pp. 159–169, 2010.
39. Page G.L., Wallin J.F., and Dixon D.S. How well do we know the orbits of the outer planets? *Astrophysical Journal*, 2009, v. 697, no. 2, 1226–1241.
40. Iorio L. Does the Neptunian system of satellites challenge a gravitational origin for the Pioneer anomaly. *Monthly Notices of the Royal Astronomical Society*, 2010, v. 405, no. 4, 2615–2622.
41. Page G.L., Wallin J.F., and Dixon D.S. How well do we know the orbits of the outer planets? *Astrophysical Journal*, 2009, v. 697, no. 2, 1226–1241.
42. Iorio L. Does the Neptunian system of satellites challenge a gravitational origin for the Pioneer anomaly? *Monthly Notices of the Royal Astronomical Society*, 2010, v. 405, no. 4, 2615–2622.
43. Page G.L. Exploring the weak limit of gravity at solar system scales. *Publications of the Astronomical Society of the Pacific*, 2010, v. 122, no. 888, 259–260.
44. Iorio L. Orbital effects of the time-dependent component of the Pioneer anomaly. *Modern Physics Letters A*, 2012, v. 27, no. 12, 1250071.
45. Bertolami O., Francisco F., Gil P.J.S., and Paramos J. Thermal analysis of the Pioneer anomaly: a method to estimate radiative momentum transfer. *Physical Review D*, 2008, v. 78, no. 10, 103001.
46. Rievers B., Lämmerzahl C., List M., Bremer S., and Dittus H. New powerful thermal modelling for high-precision gravity missions with application to Pioneer 10/11. *New Journal of Physics*, 2009, v. 11, 113032.
47. Bertolami O., Francisco F., Gil P.J.S., and Paramos J. Estimating radiative momentum transfer through a thermal analysis of the pioneer anomaly. *Space Science Reviews*, 2010, v. 151, no. 1–3, 75–91.
48. Rievers B., Bremer S., List M., Lämmerzahl C., and Dittus H. Thermal dissipation force modeling with preliminary results for Pioneer 10/11. *Acta Astronautica*, 2010, v. 66, no. 3–4, 467–476.
49. Rievers B., Lämmerzahl C., and Dittus H. Modeling of thermal perturbations using raytracing method with preliminary results for a test case model of the pioneer 10/11 radioisotopic thermal generators. *Space Science Reviews*, 2010, v. 151, no. 1–3, 123–133.
50. Rievers B., Lämmerzahl C. High precision thermal modeling of complex systems with application to the flyby and Pioneer anomaly. *Annalen der Physik*, 2011, v. 523, no. 6, 439–449.
51. Francisco F., Bertolami O., Gil P.J.S., and Paramos J. Modelling the reflective thermal contribution to the acceleration of the Pioneer spacecraft. *Physics Letters B*, at press, 2012, `http://arxiv.org/abs/1103.5222`.
52. Turyshev S.G., Toth V.T., Kinsella G.L., Siu-Chun L., Shing M., Ellis J. Support for the thermal origin of the Pioneer anomaly. *Physical Review Letters*, 2012, at press, `http://arxiv.org/abs/1204.2507`.
53. Masreliez C.J. A Cosmological Explanation to the Pioneer Anomaly. *Astrophysics and Space Science*, 2005, v. 299, no. 1, 83–108.
54. Tank H.K. A new law emerging from the recurrences of the "critical-acceleration" of MOND, suggesting a clue to unification of fundamental forces. *Astrophysics and Space Science*, 2010, v. 330, 203–205.
55. Tank H.K. Some clues to understand MOND and the accelerated expansion of the universe. *Astrophysics and Space Science*, 2011, v. 336, no. 2, 341–343.

One-Way Speed of Light Measurements Without Clock Synchronisation

Reginald T. Cahill
School of Chemical and Physical Sciences, Flinders University, Adelaide 5001, Australia
E-mail: Reg.Cahill@flinders.edu.au

The 1991 DeWitte double one-way 1st order in v/c experiment successfully measured the anisotropy of the speed of light using clocks at each end of the RF coaxial cables. However Spavieri *et al.*, Physics Letters A (2012), have reported that (i) clock effects caused by clock transport should be included, and (ii) that this additional effect cancels the one-way light speed timing effect, implying that one-way light speed experiments "do not actually lead to the measurement of the one-way speed of light or determination of the absolute velocity of the preferred frame". Here we explain that the Spavieri *et al.* derivation makes an assumption that is not always valid: that the propagation is subject to the usual Fresnel drag effect, which is not the case for RF coaxial cables. As well DeWitte did take account of the clock transport effect. The Spavieri *et al.* paper has prompted a clarification of these issues.

1 Introduction

The enormously significant 1991 DeWitte [1] double one-way 1st order in v/c experiment successfully measured the anisotropy of the speed of light using clocks at each end of the RF coaxial cables. The technique uses rotation of the light path to permit extraction of the light speed anisotropy, despite the clocks not being synchronised. Data from this 1st order in v/c experiment agrees with the speed and direction of the anisotropy results from 2nd order in v/c Michelson gas-mode interferometer experiments by Michelson and Morley and by Miller, see data in [2], and with NASA spacecraft earth-flyby Doppler shift data [3], and also with more recent 1st order in v/c experiments using a new single clock technique [2], Sect. 5. However Spavieri *et al.* [4] reported that (i) clock effects caused by clock transport should be included, and (ii) that this additional effect cancels the one-way light speed timing effect, implying that one-way light speed experiments "do not actually lead to the measurement of the one-way speed of light or determination of the absolute velocity of the preferred frame". Here we explain that the Spavieri *et al.* derivation makes an assumption that is not always valid: that the propagation is subject to the usual Fresnel drag effect, which is not the case for RF coaxial cables. The Spavieri *et al.* paper has prompted a clarification of these issues. In particular DeWitte took account of both the clock transport effect, and also that the RF coaxial cables did not exhibit a Fresnel drag, though these aspects were not discussed in [1].

2 First Order in v/c Speed of EMR Experiments

Fig. 1 shows the arrangement for measuring the one-way speed of light, either in vacuum, a dielectric, or RF coaxial cable. It is usually argued that one-way speed of light measurements are not possible because the clocks C_1 and C_2 cannot be synchronised. However this is false, although an important previously neglected effect that needs to be included is the clock offset effect caused by transport when the apparatus is rotated [4], but most significantly the Fresnel drag effect is not present in RF coaxial cables. In Fig. 1 the actual travel time $t_{AB} = t_B - t_A$ from A to B, as distinct from the clock indicated travel time $T_{AB} = T_B - T_A$, is determined by

$$V(v\cos(\theta))t_{AB} = L + v\cos(\theta)t_{AB} \qquad (1)$$

where the 2nd term comes from the end B moving an additional distance $v\cos(\theta)t_{AB}$ during time interval t_{AB}. With Fresnel drag $V(v) = \frac{c}{n} + v\left(1 - \frac{1}{n^2}\right)$, when V and v are parallel, and where n is the dielectric refractive index. Then

$$t_{AB} = \frac{L}{V(v\cos(\theta)) - v\cos(\theta)} = \frac{nL}{c} + \frac{v\cos(\theta)L}{c^2} + .. \qquad (2)$$

However if there is no Fresnel drag effect, $V = c/n$, as is the case in RF coaxial cables, then we obtain

$$t_{AB} = \frac{L}{V(v\cos(\theta)) - v\cos(\theta)} = \frac{nL}{c} + \frac{v\cos(\theta)Ln^2}{c^2} + .. \qquad (3)$$

It would appear that the two terms in (2) or (3) can be separated by rotating the apparatus, giving the magnitude and direction of $\mathbf{v}$. However it is $T_{AB} = T_B - T_A$ that is measured, and not t_{AB}, because of an unknown fixed clock offset τ, as the clocks are not *a priori* synchronised, and as well an angle dependent clock transport offset $\Delta\tau$, at least until we can establish clock synchronisation, as explained below. Then the clock readings are $T_A = t_A$ and $T_B = t_B + \tau$, and $T'_B = t'_B + \tau + \Delta\tau$, where $\Delta\tau$ is a clock offset that arises from the slowing of clock C_2 as it is transported during the rotation through angle $\Delta\theta$, see Fig. 1.

3 Clock Transport Effect

The clock transport offset $\Delta\tau$ follows from the clock motion effect

$$\Delta\tau = dt\sqrt{1 - \frac{(\mathbf{v}+\mathbf{u})^2}{c^2}} - dt\sqrt{1 - \frac{\mathbf{v}^2}{c^2}} = -dt\frac{\mathbf{v}\cdot\mathbf{u}}{c^2} + ..., \qquad (4)$$

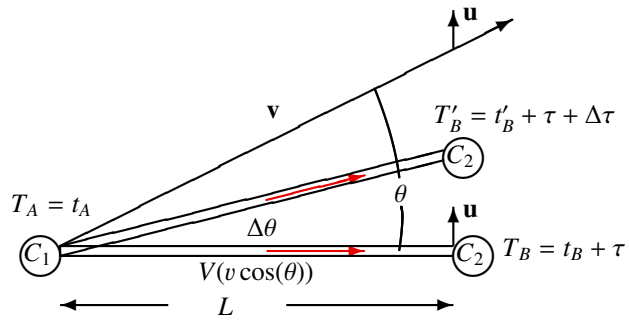

Fig. 1: Schematic layout for measuring the one-way speed of light in either free-space, optical fibres or RF coaxial cables, without requiring the synchronisation of the clocks C_1 and C_2. Here τ is the, initially unknown, offset time between the clocks. Times t_A and t_B are true times, without clock offset and clock transport effects, while $T_A = t_A$, $T_B = t_A + \tau$ and $T'_B = t'_B + \tau + \Delta\tau$ are clock readings. $V(v\cos(\theta))$ is the speed of EM radiation wrt the apparatus before rotation, and $V(v\cos(\theta - \Delta\theta))$ after rotation, $\mathbf{v}$ is the velocity of the apparatus through space in direction θ relative to the apparatus before rotation, $\mathbf{u}$ is the velocity of transport for clock C_2, and $\Delta\tau < 0$ is the net slowing of clock C_2 from clock transport, when apparatus is rotated through angle $\Delta\theta > 0$. Note that $\mathbf{v} \cdot \mathbf{u} > 0$.

when clock C_2 is transported at velocity $\mathbf{u}$ over time interval dt, compared to C_1. Now $\mathbf{v} \cdot \mathbf{u} = vu\sin(\theta)$ and $dt = L\Delta\theta/u$. Then the change in T_{AB} from this small rotation is, using (3) for the case of no Fresnel drag,

$$\Delta T_{AB} = \frac{v\sin(\theta)Ln^2\Delta\theta}{c^2} - \frac{v\sin(\theta)L\Delta\theta}{c^2} + ... \qquad (5)$$

as the clock transport effect appears to make the clock-determined travel time smaller (2nd term). Integrating we get

$$T_B - T_A = \frac{nL}{c} + \frac{v\cos(\theta)L(n^2-1)}{c^2} + \tau, \qquad (6)$$

where τ is now the constant offset time. The $v\cos(\theta)$ term may be separated by means of the angle dependence. Then the value of τ may be determined, and the clocks synchronised. However if the propagation medium is vacuum, liquid, or dielectrics such as glass and optical fibres, the Fresnel drag effect is present, and we then use (2), and not (3). Then in (6) we need make the replacement $n \to 1$, and then the 1st order in v/c term vanishes, as reported by Spavieri *et al.*. However, in principle, separated clocks may be synchronised by using RF coaxial cables.

4 DeWitte 1st Order in v/c Detector

The DeWitte $L = 1.5$ km 5 MHz RF coaxial cable experiment, Brussels 1991, was a double 1st order in v/c detector, using the scheme in Fig. 1, but employing a 2nd RF coaxial cable for the opposite direction, giving clock difference $T_D - T_C$, to cancel temperature effects, and also used 3 Caesium atomic clocks at each end. The orientation was NS and

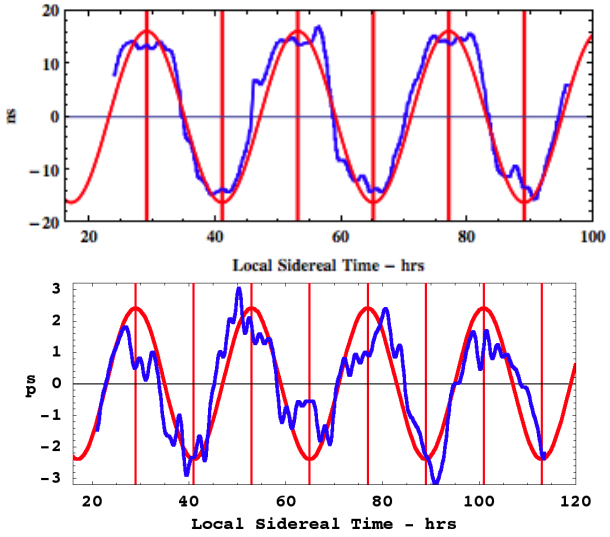

Fig. 2: Top: Data from the 1991 DeWitte NS RF coaxial cable experiment, $L = 1.5$ km, using the arrangement shown in Fig. 1, with a 2nd RF coaxial cable carrying a signal in the reverse direction. The vertical red lines are at RA=5^h and 17^h. DeWitte gathered data for 178 days, and showed that the crossing time tracked sidereal time, and not local solar time, see Fig. 3. DeWitte reported that $v \approx 500$ km/s. If a Fresnel drag effect is included no effect would have been seen. Bottom: Dual coaxial cable detector data from May 2009 using the technique in Fig. 4 with $L = 20$ m. NASA Spacecraft Doppler shift data predicts Dec= $-77°$, $v = 480$ km/s, giving a sidereal dynamic range of 5.06 ps, very close to that observed. The vertical red lines are at RA=5^h and 17^h. In both data sets we see the earth sidereal rotation effect together with significant wave/turbulence effects.

rotation was achieved by that of the earth [1]. Then

$$T_{AB} - T_{CD} = \frac{2v\cos(\theta)L(n^2-1)}{c^2} + 2\tau \qquad (7)$$

For a horizontal detector the dynamic range of $\cos(\theta)$ is $2\sin(\lambda)\cos(\delta)$, caused by the earth rotation, where λ is the latitude of the detector location and δ is the declination of $\mathbf{v}$. The value of τ may be determined and the clocks synchronised. Some of DeWitte's data and results are in Figs. 2 and 3. DeWitte noted that his detector produced no effect at RF frequency of 1GHz, suggesting that the absence of Fresnel drag in RF coaxial cables may be a low frequency effect. This means that we should write the Fresnel drag expression as $V(v) = \frac{c}{n} + v\left(1 - \frac{1}{m(f)^2}\right)$, where $m(f)$ is RF frequency f dependent, with $m(f) \to n$ at high f.

5 Dual RF Coaxial Cable Detector

The single clock Dual RF Coaxial Cable Detector exploits the absence of the Fresnel drag effect in RF coaxial cables [2]. Then from (3) the round trip travel time for one circuit is, see Fig. 4,

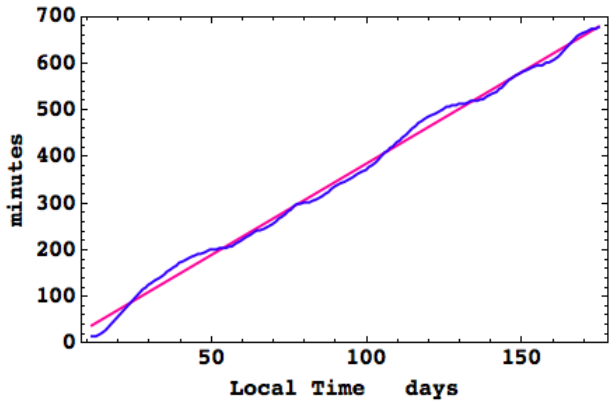

Fig. 3: DeWitte collected data over 178 days and demonstrated that the zero crossing time, see Fig. 2, tracked sidereal time and not local solar time. The plot shows the negative of the drift in the crossing time vs local solar time, and has a slope, determined by the best-fit straight line, of -3.918 minutes per day, compared to the actual average value of -3.932 minutes per day. Again we see fluctuations from day to day.

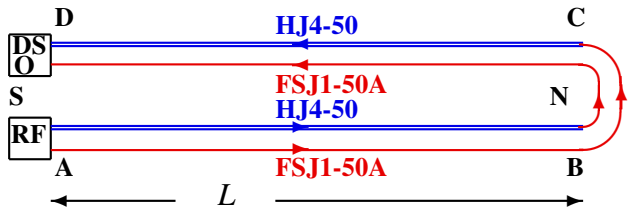

Fig. 4: Because Fresnel drag is absent in RF coaxial cables this dual cable setup, using one clock (10 MHz RF source) and Digital Storage Oscilloscope (DSO) to measure and store timing difference between the two circuits, as in (9)), is capable of detecting the absolute motion of the detector wrt to space, revealing the sidereal rotation effect as well as wave/turbulence effects. Results from such an experiment are shown in Fig. 2. Andrews phase-stablised coaxial cables are used. More recent results are reported in [2].

$$t_{AB} + t_{CD} = \frac{(n_1 + n_2)L}{c} + \frac{v\cos(\theta)L(n_1^2 - n_2^2)}{c^2} + .. \qquad (8)$$

where n_1 and n_2 are the effective refractive indices for the two different RF coaxial cables. There is no clock transport effect as the detector is rotated. Dual circuits reduce temperature effects. The travel time difference of the two circuits at the DSO is then

$$\Delta t = \frac{2v\cos(\theta)L(n_1^2 - n_2^2)}{c^2} + .. \qquad (9)$$

A sample of data is shown in Fig. 2, using RF=10 MHz, and is in excellent agreement with the DeWitte data, the NASA flyby Doppler shift data, and the Michelson-Morley and Miller results.

6 Conclusions

The absence of the Fresnel drag in RF coaxial cables enables 1st order in v/c measurements of the anisotropy of the speed of light. DeWitte pioneered this using the multiple clock technique, and took account of the clock transport effect, while the new dual RF coaxial cable detector uses only one clock. This provides a very simple and robust technique to detect motion wrt the dynamical space. Experiments by Michelson and Morley 1887, Miller 1925/26, DeWitte 1991, Cahill 2006, 2009, 2012, and NASA earth-flyby Doppler shift data now all agree, giving the solar system a speed of $\sim$ 486 km/s in the direction RA=4.3^h, Dec= -75.0°. These experiments have detected the fractal textured dynamical structure of space - the privileged local frame [2]. This report is from the Gravitational Wave Detector Project at Flinders University.

Submitted on July 2, 2012 / Accepted on July 12, 2012

References

1. Cahill R.T. The Roland De Witte 1991 Experiment. *Progress in Physics*, 2006, v. 3, 60–65.
2. Cahill R.T. Characterisation of Low Frequency Gravitational Waves from Dual RF Coaxial-Cable Detector: Fractal Textured Dynamical 3-Space. *Progress in Physics*, 2012, v. 3, 3–10.
3. Cahill R.T. Combining NASA/JPL One-Way Optical-fibre Light-Speed Data with Spacecraft Earth-Flyby Doppler-Shift Data to Characterise 3-Space Flow. *Progress in Physics*, 2009, v. 4, 50–64.
4. Spavieri G., Quintero J., Unnikrishnan S., Gillies G.T., Cavalleri G., Tonni E. and Bosi L. Can the One-Way Speed of Light be used for Detection of Violations of the Relativity Principle? *Physics Letters A*, 2012, v. 376, 795–797.

Additional Proofs to the Necessity of Element No.155, in the Periodic Table of Elements

Albert Khazan

E-mail: albkhazan@gmail.com

Additional versions of the location of the isotopes and element No.155 are suggested to the Periodic Table of Elements.

As was pointed out recently [1], the Periodic Table of Elements ends with element No.155 which manifests the upper limit of the Table after whom no other elements exist. In this connexion the number of the isotopes contained in each single cell of the Nuclear Periodic Table could be interested. (The Nuclear Periodic Table is constructed alike the Periodic Table of Elements, including Periods, Groups, Lanthanides, and Actinides.) Therefore, it is absolutely lawful to compare these two tables targeting the location of element No.155 [2].

Fig. 1 shows an S-shaped arc of the isotopes, whose form changes being dependent on the number of Period, and the number of the isotopes according to the summation of them. As seen, the arc is smooth up to element No.118, where the number of the isotopes of the cell equals to 4468. This is the known last point, after whom the arc transforms into the horizontal straight. In the region of the numbers 114–118, the rate of change of the isotopes in the arc decreases very rapid (4312–4468), upto element No.118 whose cell contains just one isotope. Hence we conclude that only the single isotope is allowed for the number higher than No.118. This was verified for the points No.118, No.138 and No.155, who are thus located along the strict horizontally straight. The common arc can be described by the equation, whose truth of approximation is $R^2 = 1$.

The next version of the graph is constructed by logarithmic coordinates, where the x-coordinate is $\ln X$ and the y-coordinate is $\ln Y$ (see Fig. 2). The original data are: the number Z of each single element (the axis X), and the summary number of the isotopes (the axis Y). Once the graph created, we see a straight line ending by a curve. As seen, the last numbers form a horizontally located straight consisting of the 10 last points. The obtained equation demonstrates the high degree of precision ($R^2 = 0.997$).

The most interesting are the structures, where the two arcs (No.55–No.118) coincide completely with each other. The left side of the parabolas in the tops forms two horizontal areas of 10 points. The two dotted lines at the right side are obtained by the calculations for elements being to 0.5 unit forward. The both equations posses the coefficient $R^2 = 0.992$.

All three presented versions of the distribution of the isotopes in the cell No.155 show clearly that this number should exist as well as element No.155.

Submitted on July 16, 2012 / Accepted on July 20, 2012

References

1. Khazan A. Upper Limit in Mendeleev's Periodic Table — Element No.155. American Research Press, Rehoboth (NM), 2012.
2. The Nuclear Periodic Table, — http://www.radiochemistry.org/periodictable/images/NuclearPeriodicTable-300doi.jpg

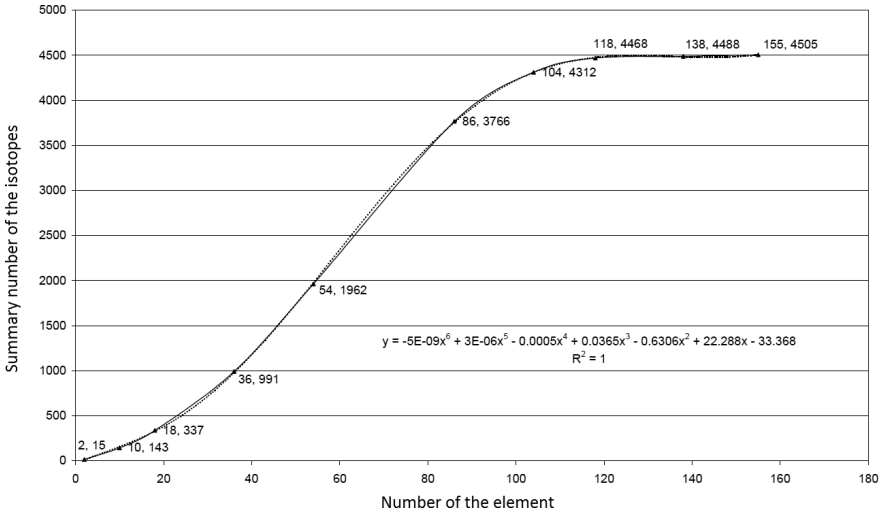

Fig. 1: Dependency of the summary number of the isotopes on the number of the element.

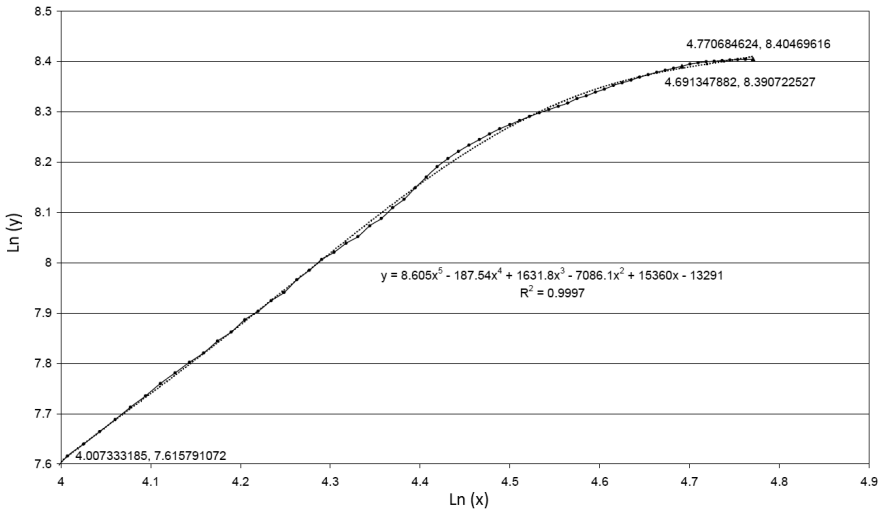

Fig. 2: Dependency of Ln (y) on Ln (x).

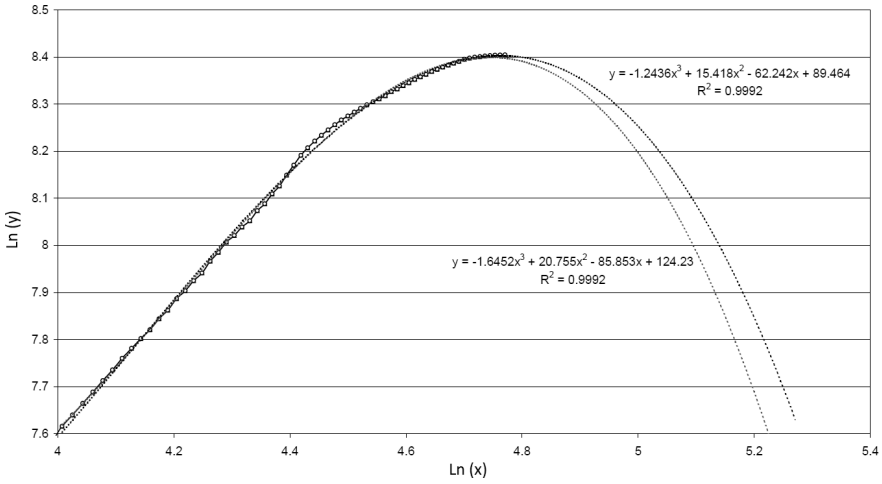

Fig. 3: Dependency of Ln (y) on Ln (x).

Quasar Formation and Energy Emission in Black Hole Universe

Tianxi Zhang

Department of Physics, Alabama A & M University, Normal, Alabama. E-mail: tianxi.zhang@aamu.edu

Formation and energy emission of quasars are investigated in accord with the black hole universe, a new cosmological model recently developed by Zhang. According to this new cosmological model, the universe originated from a star-like black hole and grew through a supermassive black hole to the present universe by accreting ambient matter and merging with other black holes. The origin, structure, evolution, expansion, and cosmic microwave background radiation of the black hole universe have been fully explained in Paper I and II. This study as Paper III explains how a quasar forms, ignites and releases energy as an amount of that emitted by dozens of galaxies. A main sequence star, after its fuel supply runs out, will, in terms of its mass, form a dwarf, a neutron star, or a black hole. A normal galaxy, after its most stars have run out of their fuels and formed dwarfs, neutron stars, and black holes, will eventually shrink its size and collapse towards the center by gravity to form a supermassive black hole with billions of solar masses. This collapse leads to that extremely hot stellar black holes merge each other and further into the massive black hole at the center and meantime release a huge amount of radiation energy that can be as great as that of a quasar. Therefore, when the stellar black holes of a galaxy collapse and merge into a supermassive black hole, the galaxy is activated and a quasar is born. In the black hole universe, the observed distant quasars powered by supermassive black holes can be understood as donuts from the mother universe. They were actually formed in the mother universe and then swallowed into our universe. The nearby galaxies are still very young and thus quiet at the present time. They will be activated and further evolve into quasars after billions of years. At that time, they will enter the universe formed by the currently observed distant quasars as similar to the distant quasars entered our universe. The entire space evolves iteratively. When one universe expands out, a new similar universe is formed from its inside star-like or supermassive black holes.

1 Introduction

Quasars are quasi-stellar objects, from which light is extremely shifted toward the red [1-5]. If their large redshifts are cosmological, quasars should be extremely distant and thus very luminous such that a single quasar with the scale of the solar system can emit the amount of energy comparable to that emitted by dozens of normal galaxies [6-7]. A highly charged quasar may also have significant electric redshift [8].

Quasars are generally believed to be extremely luminous galactic centers powered by supermassive black holes with masses up to billions of solar masses [9-13]. It is usually suggested that the material (e.g., gas and dust) falling into a supermassive black hole is subjected to enormous pressure and thus heated up to millions of degrees, where a huge amount of thermal radiation including waves, light, and X-rays give off [14-16]. However, the density of the falling material, if it is less dense than the supermassive black hole, is only about that of water. In other words, the pressure of the falling gas and dust may not go such high required for a quasar to emit energy as amount of that emitted by hundred billions of the Sun.

According to the Einsteinian general theory of relativity [17] and its Schwarzschild solution [18], the gravitational field (or acceleration) at the surface of a black hole is inversely proportional to its mass or radius. For a supermassive black hole with one billion solar masses, the gravitational field at the surface is only about 1.5×10^4 m/s^2. Although this value is greater than that of the Sun ($\sim$ 270 m/s^2), it is about two-order smaller than that of a white dwarf with 0.8 solar masses and 0.01 solar radii ($\sim 2.2 \times 10^6$ m/s^2), eight-order smaller than that of a neutron star with 1.5 solar masses and 10 km in radius ($\sim 2.0 \times 10^{12}$ m/s^2), and eight-order smaller than that of a star-like black hole with 3 solar masses ($\sim 5 \times 10^{12}$ m/s^2). Table 1 shows the gravitational field at the surface of these typical objects. A black hole becomes less violent and thus less power to the ambient matter and gases as it grows. Therefore, a supermassive black hole may not be able to extremely compress and heat the falling matter by such relative weak gravitational field. It is still unclear about how a quasar is powered by a supermassive black hole.

The Chandra X-ray observations of quasars 4C37.43 and 3C249.1 have provided the evidence of quasar ignition with an enormous amount of gas to be driven outward at high speed or a galactic superwind [19]. The observation of quasar Q0957+561 has shown the existence of an intrinsic magnetic moment, which presents an evidence that the quasar may not have a closed event horizon [20]. In addition, the observations

Object	M (M_{Sun})	R (m)	g_R (m/s^2)
Sun	1	7×10^8	270
White Dwarfs	0.8	7×10^6	2×10^4
Nneutron Stars	1.5	1×10^4	2×10^{12}
Black Holes (BH)	3	3×10^3	5×10^{12}
Spermassive BH	10^9	3×10^{12}	1.5×10^4

Table 1: Mass, radius, and gravitational field at the surface of the Sun, white dwarf, neutron star, star-like black hole (BH), and supermassive black hole.

of the distant quasars have shown that some supermassive black holes were formed when the universe was merely 1-2 billion years after the big bang had taken place [5, 21]. How the supermassive black holes with billions of solar masses were formed so rapidly during the early universe is a great mystery raised by astronomers recently [22]. Theoretically, such infant universe should only contain hydrogen and helium, but observationally scientists have found a lot of heavy elements such as carbon, oxygen, and iron around these distant quasars, especially the large fraction of iron was observed in quasar APM 08279+5255 [23], which has redshift $Z = 3.91$. If the heavy ions, as currently believed, are produced during supernova explosions when stars runs out of their fuel supplies and start to end their lives, then quasars with heavy elements should be much elder than the main sequence stars and normal galaxies.

Recently, in the 211$^{\text{th}}$ AAS meeting, Zhang proposed a new cosmological model called black hole universe [24]. In Paper I [25], Zhang has fully addressed the origin, structure, evolution, and expansion of black hole universe (see also [26]). In Paper II [27], Zhang has quantitatively explained the cosmic microwave background radiation of black hole universe (see [28]), an ideal black body. Zhang [29] summarized the observational evidences of black hole universe. According to this new cosmological model, the universe originated from a hot star-like black hole with several solar masses, and gradually grew through a supermassive black hole with billions of solar masses to the present state with hundred billion-trillions of solar masses by accreting ambient material and merging with other black holes. The entire space is hierarchically structured with infinite layers. The innermost three layers are the universe in which we live, the outside space called mother universe, and the inside star-like and supermassive black holes called child universes. The outermost layer is infinite in radius and limits to zero for both the mass density and absolute temperature, which corresponds to an asymptotically flat spacetime without an edge and outside space and material. The relationship among all layers or universes can be connected by the universe family tree. Mathematically, the entire space can be represented as a set of all black hole universes. A black hole universe is a subset of the entire space or a subspace and the child universes are null sets or empty spaces. All layers or universes are governed by the same physics, the Einsteinian general theory of relativity with the Robertson-Walker metric of spacetime, and expand physically in one way (outward). The growth or expansion of a black hole universe decreases its density and temperature but does not alter the laws of physics.

In the black hole universe model, the observed distant quasars are suggested to be donuts from the mother universe. They were formed in the mother universe from star-like black holes rather than formed inside our universe. In other words, the observed distant quasars actually were child universes of the mother universe, i.e., little sister universes of our universe. After they were swallowed, quasars became child universes of our universe. In general, once a star-like black hole is formed in a normal galaxy, the black hole will eventually inhale, including merge with other black holes, most matter of the galaxy and grow gradually to form a supermassive black hole. Therefore, quasars are supposed to be much elder than the normal stars and galaxies, and thus significantly enriched in heavy elements as measured. Some smaller redshift quasars might be formed in our universe from the aged galaxies that came from the mother universe before the distant quasars entered. Nearby galaxies will form quasars after billions of years and enter the new universe formed from the observed distant quasars as donuts. The entire space evolves iteratively. When one universe expands out, a new similar universe is formed from its inside star-like or supermassive black holes. This study as Paper III develops the energy mechanism for quasars to emit a huge amount of energy according to the black hole universe model.

2 Energy Mechanism for Quasars

As a consequence of the Einsteinian general theory of relativity, a main sequence star, at the end of its evolution, will become, in terms of its mass, one of the follows: a dwarf, a neutron star, or a stellar black hole. A massive star ends its life with supernova explosion and forms a neutron star or a black hole. Recently, Zhang [30] proposed a new mechanism called gravitational field shielding for supernova explosion. For the evolution of the entire galaxy, many details have been uncovered by astronomers, but how a galaxy ends its life is still not completely understood. In the black hole universe, all galaxies are suggested to eventually evolve to be supermassive black holes. Galaxies with different sizes form supermassive black holes with different masses. Quasars are formed from normal galaxies through active galaxies as shown in Figure 1.

Once many stars of a galaxy have run out of their fuels and formed dwarfs, neutral stars, and black holes, the galaxy shrinks its size and collapses toward the center, where a massive black hole with millions of solar masses may have already existed, by the gravity. During the collapse, the dwarfs,

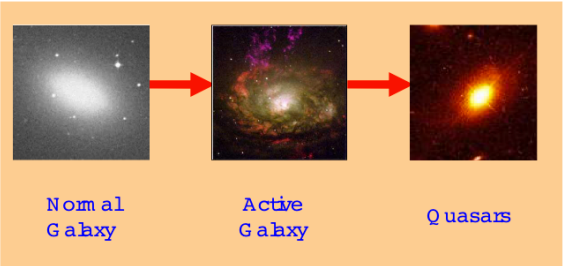

Fig. 1: Formation of quasars. A normal galaxy evolves into an active one and ends by a quasar (Images of Hubble Space Telescope).

neutron stars, and stellar black holes are merging each other and gradually falling into the massive black hole at the center to form a supermassive black hole with billions of solar masses. When stellar black holes merge and collapse into a supermassive black hole, a huge amount of energies are released. In this situation, the galaxy is activated and a quasar is born.

In a normal galaxy, such as our Milky Way, most stars are still active and bright because they have not yet run out of their fuels to form dwarfs, neutron stars, and black holes. In the disk of a normal galaxy, there should be not much of such hardly observed matter as shown by the measurements [31-32]. In the center of a normal galaxy, a quiet massive black hole with millions of solar masses may exist. Once many stars have run out of their fuels and evolved into dwarfs, neutron stars, and black holes, the disk of the galaxy becomes dim, though intensive X-rays can emit near the neutron stars and black holes, and starts to shrink and collapse. As the galaxy collapses, the black holes fall towards (or decrease of orbital radius) the center and merge with the massive black hole at the center, where huge amounts of energies leak out of the black holes through the connection region, where the event horizons are broken. The galaxy first activates with a luminous nucleus and then becomes a quasar in a short period at the evolution end.

The inside space of a black hole is a mystery and can never be observed by an observer in the external world. It is usually suggested that when a star forms a Schwarzschild black hole its matter will be collapsed to the singularity point with infinite density. Material falling into the black hole will be crunched also to the singularity point. Other regions under the event horizon of the black hole with radius $R = 2GM/c^2$ are empty. The inside space of the black hole was also considered to be an individual spacetime with matter and field distributions that obeys the Einsteinian general theory of relativity. Gonzalez-Diaz [33] derived a spacetime metric for the region of nonempty space within the event horizon from the Einsteinian field equation.

In the black hole universe model, we have considered the inside space of the Schwarzschild black hole as an individual spacetime, which is also governed by the Friedmann equation

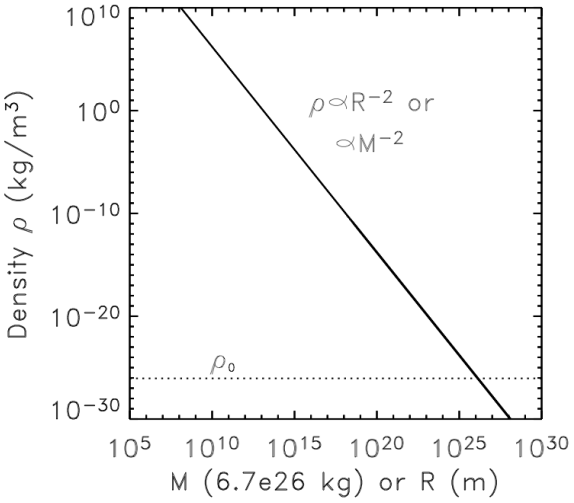

Fig. 2: The density of a black hole versus its mass or radius (solid line). The dotted line refers to $\rho = \rho_0$ the density of the present universe, so that the intersection of the two lines represents the density, radius, and mass of the present universe.

with the Robertson-Walker metric of spacetime and where matter is uniformly distributed rather than crunched into a single point. Highly curved spacetime sustains the highly dense matter and strong gravity. A black hole governed by the Einsteinian general theory of relativity with the Robertson-Walker metric of spacetime is usually static with a constant mass-radius ratio called M-R relation or a constant density when it does not eat or accrete matter from its outside space [25]. The density of the matter is given by

$$\rho = \frac{M}{V} = \frac{3c^2}{8\pi GR^2} = \frac{3c^6}{32\pi G^3 M^2}, \qquad (1)$$

where $V = 4\pi R^3/3$ is the volume. Figure 2 shows the density of black hole as a function of its radius or mass. It is seen that the density of the black hole universe is inversely proportional to the square of radius or mass. At the present time, the mass and radius of the universe are 9×10^{51} kg and 1.3×10^{26} m, respectively, if the density of the universe is chosen to be $\rho_0 = 9 \times 10^{-27}$ kg/m^3.

The total radiation energy inside a black hole, an ideal black body, is given by

$$U = \frac{4}{3}\pi\beta R^3 T^4 = \mu R^3 T^4, \qquad (2)$$

where T is the temperature and β is a constant [27]. The constant μ is given by

$$\mu = \frac{4}{3}\pi\beta = \frac{32\pi^6 k_B^4}{45h^3c^3}, \qquad (3)$$

where k_B is the Boltzmann constant, h is the Planck constant, and c is the light speed. Using the Robertson-Walker metric

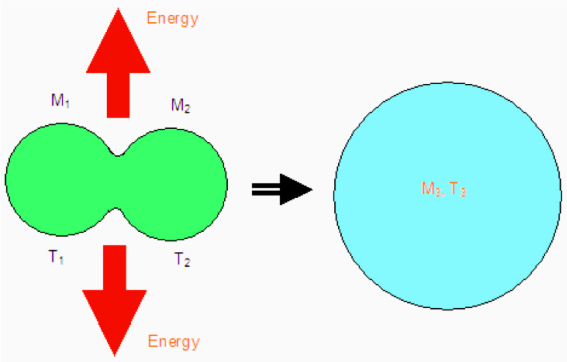

Fig. 3: A sketch for two star-like black holes to merge into a larger one and release energy from the reconnection region where the event horizons break.

with the curvature parameter $k = 1$ to describe the black hole spacetime, we have obtained in Paper I, from the Einsteinian field equation, that the black hole is stable $dR/dt = 0$ if no material and radiation enter, otherwise the black hole enlarges or expands its size at a rate $dR/dt = RH$ and thus decrease its density and temperature. Here H is the Hubble parameter.

When two black holes merge, their event horizons first break and then reconnect to form a single enveloping horizon and therefore a larger black hole. Brandt et al. [34] simulated the merge and collision of black holes. During the period of the reconnection of the event horizons, a huge amount of radiation energy leak/emit out from the black holes through the connection region, where the formed event horizon is still concave and has negative curvature. As many star-like black holes merge, a supermassive black hole or a quasar forms.

To illustrate the energy emission of a quasar, we first consider two black holes with mass M_1, M_2 (or radius R_1, R_2) and temperature T_1, T_2 to merge into a larger black hole with mass $M_3 = M_1 + M_2$ (or radius $R_3 = R_1 + R_2$ because of the M-R relation) and temperature T_3. Figure 3 show a schematic sketch for the merging of two black holes and the energy emission from them. This is somewhat similar to the energy release by fusion of two light nuclei. The total energy radiated from the collision region can be estimated as

$$E = \mu R_1^3 T_1^4 + \mu R_2^3 T_2^4 - \mu R_3^3 T_3^4. \tag{4}$$

It can be positive if the merged black hole is colder than the merging black holes (i.e., $E > 0$, if $T_3 < T_1, T_2$).

For N star-like black holes and one massive black hole to merge into a supermassive black hole, the total radiation energy that is emitted out can be written as

$$E_{\text{total}} = \mu \sum_{j=0}^{N} R_j^3 T_j^4 - \mu R_Q^3 T_Q^4, \tag{5}$$

where R_j and T_j are the radius and temperature of the j^{th} stellar black hole ($j = 0$ for the massive black hole existed at the center), R_Q and T_Q are the radius and temperature of the supermassive black hole formed at the end, and N is the number of the star-like black holes formed in the galaxy. The radius of the supermassive black hole can be estimated as

$$R_Q = \sum_{j=0}^{N} R_j. \tag{6}$$

Considering all the star-like black holes to have the same size and temperature (for simplicity or in an average radius and temperature), we have

$$E_{\text{total}} = \mu R_0^3 T_0^4 + \mu N R_j^3 T_j^4 - \mu N^3 R_j^3 T_Q^4. \tag{7}$$

Here we have also considered that $R_Q >> R_0$ and

$$R_Q = R_0 + N R_j \simeq N R_j. \tag{8}$$

Paper II has shown that the temperature of a black hole including our black hole universe depends on its size or radius. For a child universe (i.e., star-like or supermassive black hole), the relation is approximately power law,

$$T \propto \frac{1}{R^\delta}, \tag{9}$$

where δ is a power law index less than about 3/4. Applying this temperature-radius relation into Eqs. (8) and (7), we have,

$$T_Q = T_j N^{-\delta}, \tag{10}$$

and

$$E_{\text{total}} = \mu R_j^3 T_j^4 N (1 - N^{2-4\delta}). \tag{11}$$

The average luminosity of a collapsing galaxy (or quasar) can be written as

$$L \equiv E_{\text{total}}/\tau \tag{12}$$

where τ is the time for all star-like black holes in a galaxy to merge into a single supermassive black hole.

It is seen that the luminosity of a quasar increases with δ, N, R_j, and T_j, but decreases with τ. As an example, choosing $R_j = 9$ km (or $M_j \simeq 3M_s$), $T_j = 10^{12}$ K, $N = 10^9$, and $\tau = 10^9$ years, we obtain $L \simeq 7.3 \times 10^{37}$ W, which is $\sim 2 \times 10^{11}$ times that of the Sun and therefore about the order of a quasar's luminosity [35]. The formed supermassive black hole will be three billion solar masses. Here δ is chosen to be greater enough (e.g., 0.55). For a hotter T_j, a shorter τ, or a larger N, the luminosity is greater. Therefore, if quasars are collapsed galaxies at their centers that star-like black holes are merging into supermassive black holes, then the huge luminosities of quasars can be understood. The extremely emitting of energy may induce extensive shocks and produce jet flows of matter outward along the strong magnetic field lines.

To see how the luminosity of a quasar depends on the parameters N, δ, T_j, and τ, we plot the luminosity of a collapsing galaxy (merging black holes or an ignited quasar) in

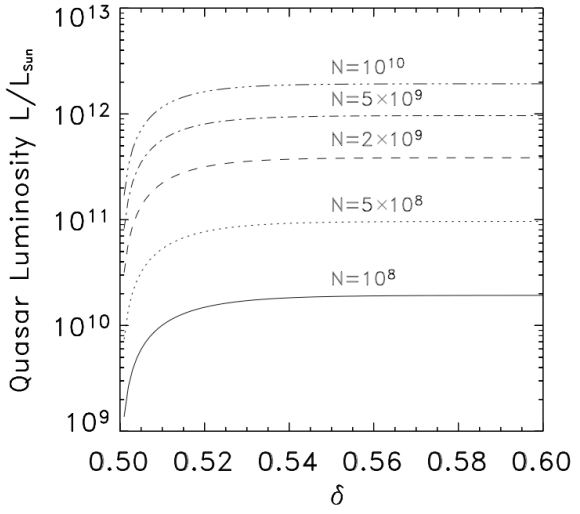

Fig. 4: Quasar luminosity vs. δ with $N = 10^8, 5\times10^5, 2\times10^9, 5\times10^9, 10^{10}$. δ should be greater than 0.5 for a quasar to emit energy. The luminosity saturates when $\delta \gtrsim 0.52$.

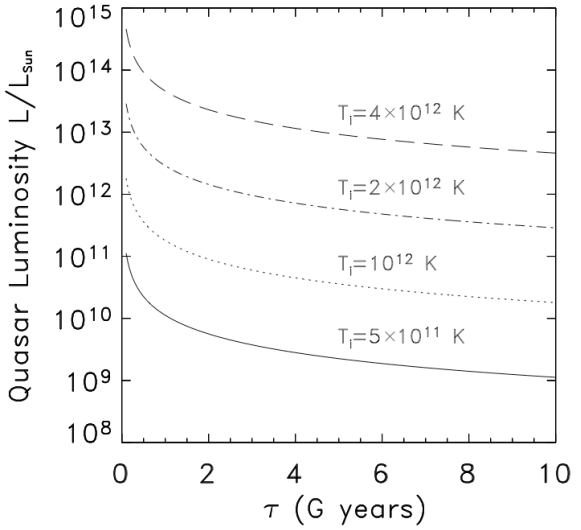

Fig. 5: Quasar luminosity vs. τ with $N = 10^8, 5\times10^5, 2\times10^9, 5\times10^9, 10^{10}$. It increases with the temperature of star-like black holes but decreases with the time for them to merge.

Figure 4 as a function of δ and in Figure 5 as a function of τ with different N. In Figure 4, we let δ vary from 0.5 to 0.6 as the x-axis and N be equal to 10^8, 2×10^8, 5×10^8, and 10^9, where other parameters are fixed at $R_j = 9$ km, $T_j = 10^{12}$ K, and $\tau = 10^9$ years. In Figure 5, we let τ vary from 10^8 years to 10^{10} years as the x-axis and T_j equal to 5×10^{11}, 10^{12}, 2×10^{12}, and 4×10^{12} K, where other parameters are fixed at $R_j = 9$ km, $N = 10^9$, and $\delta = 0.55$.

It is seen from Figure 4 that the luminosity of a quasar increases with δ and N, and saturates when $\delta \gtrsim 0.52$. For a supermassive black hole to emit energy, δ must be greater than about 0.5. Paper II has shown $\delta \lesssim 3/4 = 0.75$. From Figure 5, we can see that the luminosity decreases with the collapsing time τ and increases with T_j.

Corresponding to the possible thermal history given by Paper II, δ varies as the black hole universe grows. Figure 6 plots the parameters γ defined in Paper II and δ as functions of the radius R. It is seen that when a supermassive black hole grows up to $R \gtrsim 10^{14}$ km (or $M \gtrsim 3\times10^5$ billion solar masses) it does not emit energy when it merges with other black holes because $\delta < 0.5$. In the observed distant voids, it is possible to have this kind of objects called mini-black-hole universes. The observed distant quasars may have grown up to this size or mass now and so that quite at present. A cluster, when most of its galaxies become supermassive black holes or quasars, will merge into a mini-black-hole universe.

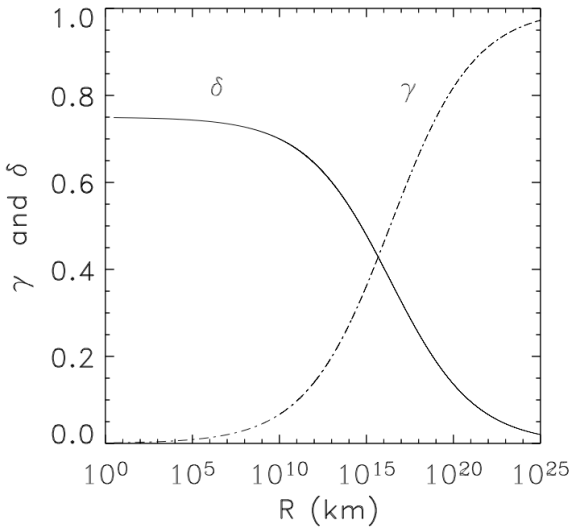

Fig. 6: Parameters γ and δ versus radius R. When a supermassive black hole grows to $R \gtrsim 3\times10^{14}$ km or $M \gtrsim 10^{14}$ solar masses, it does not emit energy because $\delta < 0.5$.

3 Discussions and Conclusions

If there does not pre-exist a massive black hole at the center of a galaxy, a supermassive black hole can also be formed from the galaxy. As the galaxy shrinks it size, a hot star-like black hole enlarges its size when it swallows dwarfs or neutron stars, which may also collapse to form black holes [36] or merges with other black holes and forms a supermassive black hole at the end.

As a summary, we proposed a possible explanation for quasars to ignite and release a huge amount of energy in accord with the black hole universe model. General relativity tells us that a main sequence star will, in terms of its mass, form a dwarf, a neutron star, or a black hole. After many stars in a normal galaxy have run out of their fuels and formed dwarfs, neutron stars, and black holes, the gravity cause the galaxy to eventually collapse and form a supermassive black

hole with billions of solar masses. It has been shown that this collapse can lead to the extremely hot stellar black holes to merge each other and further into the massive black hole at the center and release intense thermal radiation energy as great as a quasar emits. When the stellar black holes of a galaxy collapse and merge into a supermassive black hole, the galaxy is activated and a quasar is born. The observed distant quasars were donuts from the mother universe. They were actually formed in the mother universe as little sisters of our universe. After the quasars entered our universe, they became our universe's child universes. The results from this quasar model are consistent with observations.

Acknowledgements

This work was supported by the NASA EPSCoR grant (NNX-07AL52A), NSF CISM and MRI grants, AAMU Title III program, and National Natural Science Foundation of China (G40890161).

Submitted on July 17, 2012 / Accepted on July 22, 2012

References

1. Burbidge E.M. Quasi-stellar objects. *Annual Review of Astronomy and Astrophysics*, 1967, v. 5, 399–452.
2. Burbidge G. Redshifts and distances. *Nature*, 1979, v. 282, 451–455.
3. Hazard C., McMahon R. New quasars with Z = 3.4 and 3.7 and the surface density of very high redshift quasars. *Nature*, 1985, v. 314, 238–240.
4. Bechtold J. et al. Chandra survey of radio-quiet, high-redshift quasars. *The Astrophysical Journal*, 2003, v. 588, 119–127.
5. Fan X.H. et al. A survey of z>5.7 quasars in the Sloan Digital Sky Survey: II. Discovery of three additional quasars at z>6. *The Astronomical Journal*, 2003, v. 125, 1649–1659.
6. Hartwick F.D.A., Schade D. The space distribution of quasars. *Annual Review of Astronomy and Astrophysics*, 1990, v. 28, 437–489.
7. Boyle B.J. et al. The 2dF QSO redshift survey - I. The optical luminosity function of quasi-stellar objects. *Monthly Notices of the Royal Astronomical Society*, 2000, v. 317, 1014–1022.
8. Zhang T.X. Electric redshift and quasars. *Astrophysical Journal Letters*, 2006, v. 636, L61–L64.
9. Lynden-Bell D. Galactic nuclei as collapsed old quasars. *Nature*, 1969, v. 223, 690–694.
10. Rees M.J. Black hole models for active galactic nuclei. *Annual Review of Astronomy and Astrophysics*, 1984, v. 22, 471–506.
11. Bahcall J.N., Kirhakos S., Saxe D.H., Schneider D.P. Hubble Space Telescope Images of a sample of 20 nearby luminous quasars. *The Astrophysical Journal*, 1997, v. 479, 642–658.
12. Lobanov A.P., Roland J. A supermassive binary black hole in the quasar 3C 345. *Astronomy and Astrophysics*, 2005, v. 431, 831–846.
13. Begelman M.C., King A.R., Pringle J.E. The nature of SS433 and the ultraluminous X-ray sources. *Monthly Notices of the Royal Astronomical Society*, 2006, v. 370, 399–404.
14. Shapiro S.L., Teukolsky S.A. The collapse of dense star clusters to supermassive black holes - The origin of quasars and AGNs. *The Astrophysical Journal Letters*, 1985, v. 292, L41–L44.
15. Wyithe J., Stuart B., Loeb A. Self-regulated growth of supermassive black holes in galaxies as the origin of the optical and X-ray luminosity functions of quasars. *The Astrophysical Journal*, 2003, v. 595, 614–623.
16. Reeves J.N., Pounds K., Uttley P., Kraemer S., Mushotzky R., Yaqoob T., George I.M., Turner T.J. Evidence for gravitational infall of matter onto the supermassive black hole in the quasar PG 1211+143? *The Astrophysical Journal Letters*, 2005, v. 633, L81–L84.
17. Einstein A. Die Grundlage der allgemeinen Relativitätstheorie, *Annalen der Physik*, 1916, v. 354, 769–822.
18. Schwarzschild K. On the gravitational field of a mass point according to Einstein's theory. *Sitzungsberichte der Königlich Preussischen Akademie der Wissenschaften zu Berlin, Phys.-Math.*, 1916, 189–196.
19. Stockton A., Fu H., Henry J.P., Canalizo G. Extended X-ray emission from QSOs. *The Astrophysical Journal*, 2006, v. 638, 635–641.
20. Schild R.E., Leiter D.J., Robertson, S.L. Observations supporting the existence of an intrinsic magnetic moment inside the central compact object within the quasar Q0957+561. *The Astronomical Journal*, 2006, v. 132, 420–432.
21. Fan X.F. et al. A survey of $z > 5.8$ quasars in the Sloan Digital Sky Survey. I. Discovery of three new quasars and the spatial density of luminous quasars at $z \sim 6$. *Astron. J.*, 2001, v. 122, 2833–2849.
22. Hamann F., Ferland G. Elemental abundances in quasistellar objects: Star formation and galactic nuclear evolution at high redshifts. *Annual Review of Astronomy and Astrophysics*, 1999, v. 37, 487–531.
23. Hasinger G., Schartel N., Komossa S. Discovery of an ionized Fe K edge in the z=3.91 broad absorption line quasar APM 08279+5255 with XMM-Newton. *The Astrophysical Journal Letters*, 2002, v. 573, L77–L80.
24. Zhang T.X. A new cosmological model: Black hole universe, *Bulletin of the American Astronomical Society*, 2007, v. 39, 1004–1004.
25. Zhang T.X. A new cosmological model: Black hole universe, *Progress in Physics*, 2009a, v. 3, 3–11 (Paper I).
26. Zhang T.X. Anisotropic expansion of the black hole universe. *Bulletin of the American Astronomical Society*, 2009b, v. 41, 499–499.
27. Zhang T.X. Cosmic microwave background radiation of black hole universe. *Astrophysics and Space Science*, 2010a, v. 330, 157–165 (Paper II).
28. Zhang T.X. Cosmic microwave background radiation of black hole universe, *Bulletin of the American Astronomical Society*, 2009c, v. 41, 754–754.
29. Zhang T.X. Observational evidences of black hole universe. *Bulletin of the American Astronomical Society*, 2010b, v. 42, 314–314.
30. Zhang T.X. Gravitational field shielding and supernova explosions. *The Astrophysical Journal Letters*, 2010c, v. 725, L117–L120.
31. Hellemans A. ASTRONOMY: Galactic disk contains no dark matter *Science*, 1997, v. 278, 1230–1230.
32. Creze M., Chereul E., Bienaymo O., Pichon C. The distribution of nearby stars in phase space mapped by Hipparcos. I. The potential well and local dynamical mass. *Astronomy and Astrophysics*, 1998, v. 329, 920–936.
33. Gonzalez-Diaz P.E. The spacetime metric inside a black hole. *Nuovo Cimento Letters*, 1981, v. 2, L161–L163.
34. Brandt S., Font J.A., Ibanez J.M., Masso J., Seidel E. Numerical evolution of matter in dynamical axisymmetric black hole spacetimes I. Methods and tests. *Computer Physics Commmunications*, 2000, v. 124, 169–196.
35. Sparke L.S., Gallaher J.S. Galaxies in the Universe: an Introduction, Cambridge University Press, 2000.
36. Dermer C.D., Atoyan A. Collapse of neutron stars to black holes in binary systems: A model for short gamma-ray bursts. *The Astrophysical Journal Letters*, 2006, v. 643, L13–L16.

Generalizations of the Distance and Dependent Function in Extenics to $2D$, $3D$, and $n-D$

Florentin Smarandache
University of New Mexico, Mathematics and Science Department, 705 Gurley Ave., Gallup, NM 87301, USA
E-mail: smarand@unm.edu

Dr. Cai Wen defined in his 1983 paper: — the distance formula between a point x_0 and a one-dimensional (1D) interval $<a,b>$; — and the dependence function which gives the degree of dependence of a point with respect to a pair of included $1D$-intervals. His paper inspired us to generalize the Extension Set to two-dimensions, i.e. in plane of real numbers R^2 where one has a rectangle (instead of a segment of line), determined by two arbitrary points $A(a_1,a_2)$ and $B(b_1,b_2)$. And similarly in R^3, where one has a prism determined by two arbitrary points $A(a_1,a_2,a_3)$ and $B(b_1,b_2,b_3)$. We geometrically define the linear and non-linear distance between a point and the $2D$ and $3D$-extension set and the dependent function for a nest of two included $2D$ and $3D$-extension sets. Linearly and non-linearly attraction point principles towards the optimal point are presented as well. The same procedure can be then used considering, instead of a rectangle, any bounded $2D$-surface and similarly any bounded $3D$-solid, and any bounded $(n-D)$-body in R^n. These generalizations are very important since the Extension Set is generalized from one-dimension to 2, 3 and even n-dimensions, therefore more classes of applications will result in consequence.

1 Introduction

Extension Theory (or Extenics) was developed by Professor Cai Wen in 1983 by publishing a paper called Extension Set and Non-Compatible Problems. Its goal is to solve contradictory problems and also nonconventional, nontraditional ideas in many fields. Extenics is at the confluence of three disciplines: philosophy, mathematics, and engineering. A contradictory problem is converted by a transformation function into a non-contradictory one. The functions of transformation are: extension, decomposition, combination, etc. Extenics has many practical applications in Management, Decision-Making, Strategic Planning, Methodology, Data Mining, Artificial Intelligence, Information Systems, Control Theory, etc. Extenics is based on matter-element, affair-element, and relation-element.

2 Extension Distance in $1D$-space

Let's use the notation $<a,b>$ for any kind of closed, open, or half-closed interval $[a,b]$, (a,b), $(a,b]$, $[a,b)$. Prof. Cai Wen has defined the extension distance between a point x_0 and a real interval $X=<a,b>$, by

$$\rho(x_0,X)=\left|x_0-\frac{a+b}{2}\right|-\frac{b-a}{2}, \tag{1}$$

where in general:

$$\rho:(R,R^2)\to(-\infty,+\infty). \tag{2}$$

Algebraically studying this extension distance, we find that actually the range of it is:

$$\rho(x_0,X)\in\left[-\frac{b-a}{2},+\infty\right] \tag{3}$$

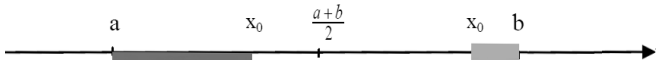

Fig. 1:

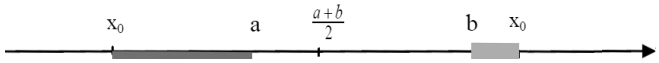

Fig. 2:

or its minimum range value $-\left(\frac{b-a}{2}\right)$ depends on the interval X extremities a and b, and it occurs when the point x_0 coincides with the midpoint of the interval X, i.e. $x_0=\frac{a+b}{2}$. The closer is the *interior point* x_0 to the midpoint of the interval $<a,b>$, the negatively larger is $\rho(x_0,X)$.

In Fig. 1, for interior point x_0 between a and $\frac{a+b}{2}$, the extension distance $\rho(x_0,X)=a-x_0$ is the *negative length of the brown line segment* [left side]. Whereas for interior point x_0 between $\frac{a+b}{2}$ and b, the extension distance $\rho(x_0,X)=x_0-b$ is the *negative length of the blue line segment* [right side]. Similarly, the further is *exterior point* x_0 with respect to the closest extremity of the interval $<a,b>$ to it (i.e. to either a or b), the positively larger is $\rho(x_0,X)$.

In Fig. 2, for exterior point $x_0<a$, the extension distance $\rho(x_0,X)=a-x_0$ is the positive length of the brown line segment [left side]. Whereas for exterior point $x_0>b$, the extension distance $\rho(x_0,X)=x_0-b$ is the *positive length of the blue line segment* [right side].

3 Principle of the Extension $1D$-Distance

Geometrically studying this extension distance, we find the following principle that Prof. Cai Wen has used in 1983

defining it:

> $\rho(x_0, X)$ is *the geometric distance between the point* x_0 *and the closest extremity point of the interval* $<a, b>$ *to it (going in the direction that connects* x_0 *with the optimal point), distance taken as negative if* $x_0 \in <a, b>$, *and as positive if* $x_0 \subset <a, b>$.

This principle is very important in order to generalize the extension distance from $1D$ to $2D$ (two-dimensional real space), $3D$ (three-dimensional real space), and $n-D$ (n-dimensional real space).

The extremity points of interval $< a, b>$ are the point a and b, which are also the boundary (frontier) of the interval $< a, b>$.

4 Dependent Function in $1D$-Space

Prof. Cai Wen defined in 1983 in $1D$ the Dependent Function $K(y)$. If one considers two intervals X_0 and X, that have no common end point, and $X_0 \subset X$, then:

$$K(y) = \frac{\rho(y, X)}{\rho(y, X) - \rho(y, X_0)}. \qquad (4)$$

Since $K(y)$ was constructed in $1D$ in terms of the extension distance $\rho(.,.)$, we simply generalize it to higher dimensions by replacing $\rho(.,.)$ with the generalized in a higher dimension.

5 Extension Distance in $2D$-Space

Instead of considering a segment of line AB representing the interval $<a, b>$ in $1R$, we consider a rectangle $AMBN$ representing all points of its surface in $2D$. Similarly as for $1D$-space, the rectangle in $2D$-space may be closed (i.e. all points lying on its frontier belong to it), open (i.e. no point lying on its frontier belong to it), or partially closed (i.e. some points lying on its frontier belong to it, while other points lying on its frontier do not belong to it).

Let's consider two arbitrary points $A(a_1, a_2)$ and $B(b_1, b_2)$. Through the points A and B one draws parallels to the axes of the Cartesian system XY and one thus one forms a rectangle $AMBN$ whose one of the diagonals is just AB.

Let's note by O the midpoint of the diagonal AB, but O is also the center of symmetry (intersection of the diagonals) of the rectangle $AMBN$. Then one computes the distance between a point $P(x_0, y_0)$ and the rectangle $AMBN$. One can do that following the same principle as Dr. Cai Wen did:

— compute the distance in $2D$ (two dimensions) between the point P and the center O of the rectangle (intersection of rectangle's diagonals);

— next compute the distance between the point P and the closest point (let's note it by P') to it on the frontier (the rectangle's four edges) of the rectangle $AMBN$.

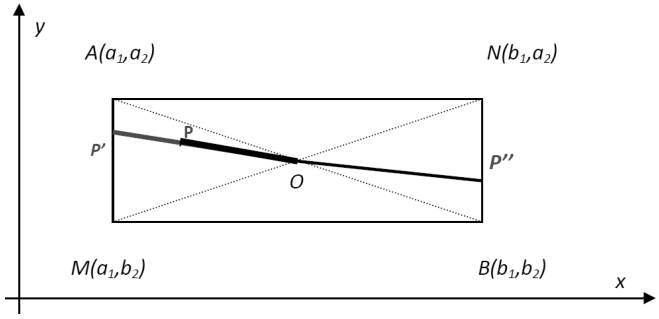

Fig. 3: P is an interior point to the rectangle $AMBN$ and the optimal point O is in the center of symmetry of the rectangle.

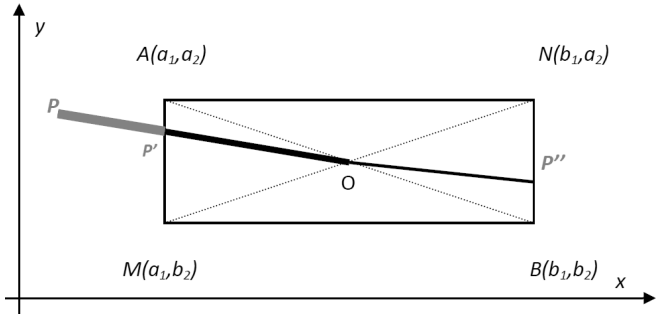

Fig. 4: P is an exterior point to the rectangle $AMBN$ and the optimal point O is in the center of symmetry of the rectangle.

This step can be done in the following way: considering P' as the intersection point between the line PO and the frontier of the rectangle, and taken among the intersection points that point P' which is the closest to P; this case is entirely consistent with Dr. Cai's approach in the sense that when reducing from a $2D$-space problem to two $1D$-space problems, one exactly gets his result.

The Extension $2D$-Distance, for $P \neq O$, will be:

$$\rho((x_0, y_0), AMBN) = d(\text{point } P, \text{ rectangle } AMBN) =$$
$$= |PO| - |P'O| = \pm|PP'|, \qquad (5)$$

i) which is equal to the negative length of the red segment $|PP'|$ in Fig. 3, when P is interior to the rectangle $AMBN$;

ii) or equal to zero, when P lies on the frontier of the rectangle $AMBN$ (i.e. on edges AM, MB, BN, or NA) since P coincides with P';

iii) or equal to the positive length of the blue segment $|PP'|$ in Fig. 4, when P is exterior to the rectangle $AMBN$, where $|PO|$ means the classical $2D$-distance between the point P and O, and similarly for $|P'O|$ and $|PP'|$.

The Extension $2D$-Distance, for the optimal point, i.e. $P = O$, will be

$$\rho(O, AMBN) = d(\text{point } O, \text{ rectangle } AMBN) =$$
$$= -\max d(\text{point } O, \text{ point } M \text{ on the frontier of } AMBN). \qquad (6)$$

The last step is to devise the Dependent Function in $2D$-space similarly as Dr. Cai's defined the dependent function in $1D$. The midpoint (or center of symmetry) O has the coordinates

$$O\left(\frac{a_1+b_1}{2}, \frac{a_2+b_2}{2}\right). \tag{7}$$

Let's compute the

$$|PO| - |P'O|. \tag{8}$$

In this case, we extend the line OP to intersect the frontier of the rectangle $AMBN$. P' is closer to P than P'', therefore we consider P'. The equation of the line PO, that of course passes through the points $P(x_0, y_0)$ and $O\left(\frac{a_1+b_1}{2}, \frac{a_2+b_2}{2}\right)$, is:

$$y - y_0 = \frac{\frac{a_2+b_2}{2} - y_0}{\frac{a_1+b_1}{2} - x_0}(x - x_0). \tag{9}$$

Since the x-coordinate of point P' is a_1 because P' lies on the rectangle's edge AM, one gets the y-coordinate of point P' by a simple substitution of $x_{P'} = a_1$ into the above equality:

$$y_{P'} = y_0 + \frac{a_2+b_2-2y_0}{a_1+b_1-2x_0}(a_1 - x_0). \tag{10}$$

Therefore P' has the coordinates

$$P'\left[x_{P'} = a_1,\ y_{P'} = y_0 + \frac{a_2+b_2-2y_0}{a_1+b_1-2x_0}(a_1 - x_0)\right]. \tag{11}$$

The distance

$$d(PQ) = |PQ| = \sqrt{\left(x_0 - \frac{a_1+b_1}{2}\right)^2 + \left(y_0 - \frac{a_2+b_2}{2}\right)^2}, \tag{12}$$

while the distance

$$\begin{aligned} d(P', Q) &= |P'Q| = \\ &= \sqrt{\left(a_1 - \frac{a_1+b_1}{2}\right)^2 + \left(y_{P'} - \frac{a_2+b_2}{2}\right)^2} = \\ &= \sqrt{\left(\frac{a_1-b_1}{2}\right)^2 + \left(y_{P'} - \frac{a_2+b_2}{2}\right)^2}. \end{aligned} \tag{13}$$

Also, the distance

$$d(PP') = |PP'| = \sqrt{(a_1 - x_0)^2 + (y_{P'} - y_0)^2}. \tag{14}$$

Whence the Extension $2D$-distance formula

$$\rho[(x_0, y_0),\ AMBN] =$$

$$= d[P(x_0, y_0),\ A(a_1, a_2)\, MB(b_1, b_2)\, N] =$$

$$= |PQ| - |P'Q| \tag{15}$$

$$= \sqrt{\left(x_0 - \frac{a_1+b_1}{2}\right)^2 + \left(y_0 - \frac{a_2+b_2}{2}\right)^2} - \sqrt{\left(\frac{a_1-b_1}{2}\right)^2 + \left(y_{P'} - \frac{a_2+b_2}{2}\right)^2} \tag{16}$$

$$= \pm|PP'| \tag{17}$$

$$= \pm\sqrt{(a_1 - x_0)^2 + (y_{P'} - y_0)^2}, \tag{18}$$

where

$$y_{P'} = y_0 + \frac{a_2+b_2-2y_0}{a_1+b_1-2x_0}(a_1 - x_0). \tag{19}$$

6 Properties

As for $1D$-distance, the following properties hold in $2D$:

6.1 Property 1

a) $(x, y) \in \mathrm{Int}(AMBN)$ if $\rho[(x, y), AMBN] < 0$, where $\mathrm{Int}(AMBN)$ means interior of $AMBN$;

b) $(x, y) \in \mathrm{Fr}(AMBN)$ if $\rho[(x, y), AMBN] = 0$, where $\mathrm{Fr}(AMBN)$ means frontier of $AMBN$;

c) $(x, y) \notin AMBN$ if $\rho[(x, y), AMBN] > 0$.

6.2 Property 2

Let $A_0M_0B_0N_0$ and $AMBN$ be two rectangles whose sides are parallel to the axes of the Cartesian system of coordinates, such that they have no common end points, and $A_0M_0B_0N_0 \subset AMBN$. We assume they have the same optimal points $O_1 \equiv O_2 \equiv O$ located in the center of symmetry of the two rectangles. Then for any point $(x, y) \subset R^2$ one has $\rho[(x, y), A_0M_0B_0N_0] \geqslant \rho[(x, y), AMBN]$. See Fig. 5.

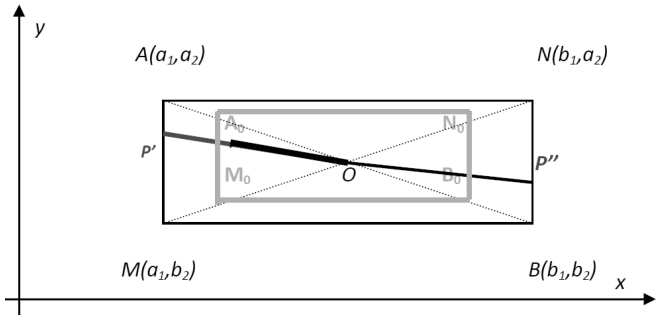

Fig. 5: Two included rectangles with the same optimal points $O_1 \equiv O_2 \equiv O$ located in their common center of symmetry.

7 Dependent $2D$-Function

Let $A_0M_0B_0N_0$ and $AMBN$ be two rectangles whose sides are parallel to the axes of the Cartesian system of coordinates, such that they have no common end points, and $A_0M_0B_0N_0 \subset AMBN$.

The Dependent $2D$-Function formula is:

$$K_{2D(x,y)} = \frac{\rho[(x, y), AMBN]}{\rho[(x, y), AMBN,] - \rho[(x, y), A_0M_0B_0N_0]}. \tag{20}$$

7.1 Property 3

Again, similarly to the Dependent Function in $1D$-space, one has:

a) If $(x, y) \in \mathrm{Int}(A_0M_0B_0N_0)$, then $K_{2D(x,y)} > 1$;

b) If $(x, y) \in \mathrm{Fr}(A0M0B0N0)$, then $K_{2D(x,y)} = 1$;

c) If $(x, y) \in \mathrm{Int}\,(AMBN - A_0M_0B_0N_0)$, then $0 < K_{2D(x,y)} < 1$;

d) If $(x, y) \in \mathrm{Fr}\,(AMBN)$, then $K_{2D(x,y)} = 0$;

e) If $(x, y) \notin AMBN$, then $K2D(x, y) < 0$.

8 General Case in 2*D*-Space

One can replace the rectangles by any finite surfaces, bounded by closed curves in 2*D*-space, and one can consider any optimal point *O* (not necessarily the symmetry center). Again, we assume the optimal points are the same for this nest of two surfaces. See Fig. 6.

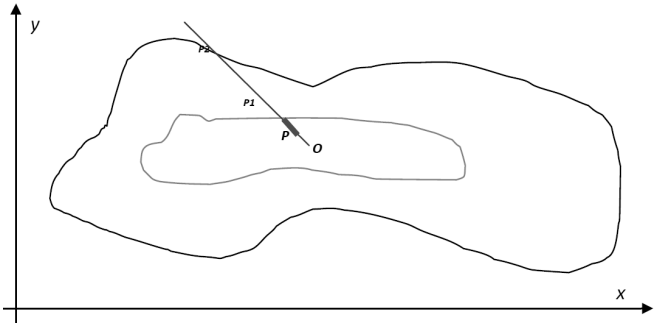

Fig. 6: Two included arbitrary bounded surfaces with the same optimal points situated in their common center of symmetry.

9 Linear Attraction Point Principle

We introduce the Attraction Point Principle, which is the following:

Let S be a given set in the universe of discourse U, and the optimal point $O \subset S$. Then each point $P\,(x_1, x_2, \ldots, x_n)$ from the universe of discourse tends towards, or is attracted by, the optimal point O, because the optimal point O is an ideal of each point. That's why one computes the extension $(n-D)$-distance between the point P and the set S as $\rho\,[(x_1, x_2, \ldots, x_n), S\,]$ on the direction determined by the point P and the optimal point O, or on the line PO, i.e.:

a) $\rho\,[(x_1, x_2, \ldots, x_n), S\,]$ is the negative distance between P and the set frontier, if P is inside the set S;

b) $\rho\,[(x_1, x_2, \ldots, x_n), S\,] = 0$, if P lies on the frontier of the set S;

c) $\rho\,[(x_1, x_2, \ldots, x_n), S\,]$ is the positive distance between P and the set frontier, if P is outside the set.

It is a king of convergence/attraction of each point towards the optimal point. There are classes of examples where such attraction point principle works. If this principle is good in all cases, then there is no need to take into consideration the center of symmetry of the set S, since for example if we have a 2*D* piece which has heterogeneous material density, then its center of weight (barycenter) is different from the center of symmetry. Let's see below such example in the 2*D*-space: Fig. 7.

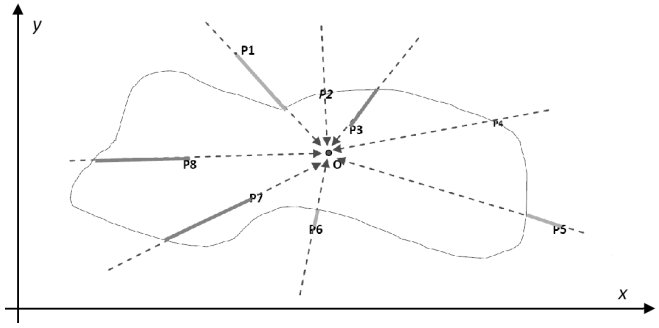

Fig. 7: The optimal point O as an attraction point for all other points $P_1, P_2, \ldots, P_8$ in the universe of discourse R^2.

10 Remark 1

Another possible way, for computing the distance between the point P and the closest point P' to it on the frontier (the rectangle's four edges) of the rectangle $AMBN$, would be by drawing a perpendicular (or a geodesic) from P onto the closest rectangle's edge, and denoting by P' the intersection between the perpendicular (geodesic) and the rectangle's edge. And similarly if one has an arbitrary set S in the 2*D*space, bounded by a closed urve. One computes

$$d(P, S) = \inf_{Q \in S} |PQ| \tag{21}$$

as in the classical mathematics.

11 Extension Distance in 3*D*-Space

We further generalize to 3*D*-space the Extension Set and the Dependent Function. Assume we have two points (a_1, a_2, a_3) and (b_1, b_2, b_3) in D. Drawing through A end B parallel planes to the planes' axes (XY, XZ, YZ) in the Cartesian system XYZ we get a prism $AM_1M_2M_3BN_1N_2N_3$ (with eight vertices) whose one of the transversal diagonals is just the line segment AB. Let's note by O the midpoint of the transverse diagonal AB, but O is also the center of symmetry of the prism.

Therefore, from the line segment AB in 1*D*-space, to a rectangle $AMBN$ in 2*D*-space, and now to a prism $AM_1M_2M_3BN_1N_2N_3$ in 3*D*-space. Similarly to 1*D*- and 2*D*-space, the prism may be closed (i.e. all points lying on its frontier belong to it), open (i.e. no point lying on its frontier belong to it), or partially closed (i.e. some points lying on its frontier belong to it, while other points lying on its frontier do not belong to it).

Then one computes the distance between a point $P\,(x_0, y_0, z_0)$ and the prism $AM_1M_2M_3BN_1N_2N_3$. One can do that following the same principle as Dr. Cai's:

— compute the distance in 3*D* (two dimensions) between the point P and the center O of the prism (intersection of prism's transverse diagonals);

— next compute the distance between the point P and the closest point (let's note it by P') to it on the frontier of

the prism $AM_1M_2M_3BN_1N_2N_3$ (the prism's lateral surface); considering P' as the intersection point between the line OP and the frontier of the prism, and taken among the intersection points that point P' which is the closest to P; this case is entirely consistent with Dr. Cai's approach in the sense that when reducing from $3D$-space to $1D$-space one gets exactly Dr. Cai's result;

— the Extension $3D$-Distance $d(P, AM_1M_2M_3BN_1N_2N_3)$ is $d(P, AM_1M_2M_3BN_1N_2N_3) = |PO| - |P'O| = \pm|PP'|$, where $|PO|$ means the classical distance in $3D$-space between the point P and O, and similarly for $|P'O|$ and $|PP'|$. See Fig. 8.

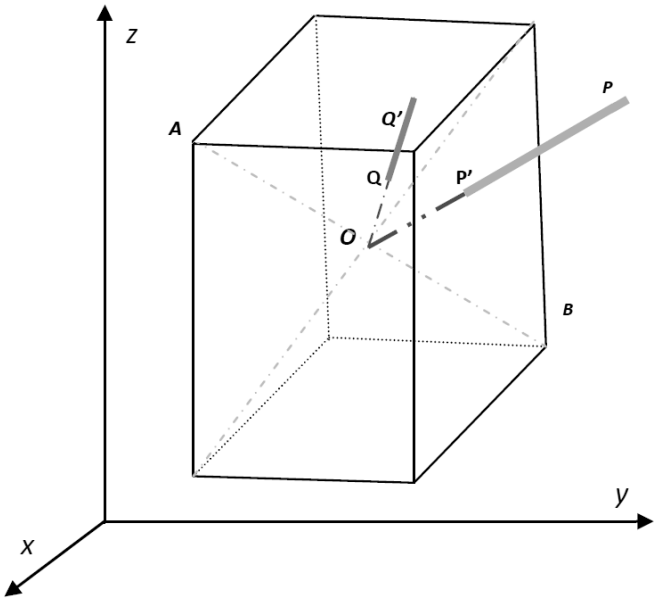

Fig. 8: Extension $3D$-Distance between a point and a prism, where O is the optimal point coinciding with the center of symmetry.

12 Property 4

a) $(x, y, z) \in \text{Int}\,(AM_1M_2M_3BN_1N_2N_3)$ if $\rho\,[(x, y, z), AM_1M_2M_3BN_1N_2N_3] < 0$, where $\text{Int}\,(AM_1M_2M_3BN_1N_2N_3)$ means interior of $AM_1M_2M_3BN_1N_2N_3$;

b) $(x, y, z) \in \text{Fr}\,(AM_1M_2M_3BN_1N_2N_3)$ if $\rho\,[(x, y, z), AM_1M_2M_3BN_1N_2N_3] = 0$ means frontier of $AM_1M_2M_3BN_1N_2N_3$;

c) $(x, y, z) \notin AM_1M_2M_3BN_1N_2N_3$ if $\rho\,[(x, y, z), AM_1M_2M_3BN_1N_2N_3] > 0$.

13 Property 5

Let $A_0M_{01}M_{02}M_{03}B_0N_{01}N_{02}N_{03}$ and $AM_1M_2M_3BN_1N_2N_3$ be two prisms whose sides are parallel to the axes of the Cartesian system of coordinates, such that they have no common end points, and $A_0M_{01}M_{02}M_{03}B_0N_{01}N_{02}N_{03} \subset AM_1M_2M_3BN_1N_2N_3$. We assume they have the same optimal points $O_1 \equiv O_2 \equiv O$ located in the center of symmetry of the two prisms.

Then for any point $(x, y, z) \in R^3$ one has

$$\rho\,[(x, y, z), A_0M_{01}M_{02}M_{03}B_0N_{01}N_{02}N]_{03} \geqslant \rho\,[(x, y, z)AM_1M_2M_3BN_1N_2N_3]\,.$$

14 The Dependent $3D$-Function

The last step is to devise the Dependent Function in $3D$-space similarly to Dr. Cai's definition of the dependent function in $1D$-space. Let the prisms $A_0M_{01}M_{02}M_{03}B_0N_{01}N_{02}N_{03}$ and $AM_1M_2M_3BN_1N_2N_3$ be two prisms whose faces are parallel to the axes of the Cartesian system of coordinates XYZ, such that they have no common end points in such a way that $A_0M_{01}M_{02}M_{03}B_0N_{01}N_{02}N_{03} \subset AM_1M_2M3BN_1N_2N_3$. We assume they have the same optimal points $O_1 \equiv O_2 \equiv O$ located in the center of symmetry of these two prisms.

The Dependent 3D-Function formula is:

$$K_{3D(x,y,z)} = \Big(\rho\,[(x, y, z), AM_1M_2M_3BN_1N_2N_3]\Big) \times \times \Big(\rho\,[(x, y, z), AM_1M_2M_3BN_1N_2N_3,] - - \rho\,[(x, y, z), A_0M_{01}M_{02}M_{03}BN_{01}N_{02}N_{03}]\Big)^{-1}. \quad (22)$$

15 Property 6

Again, similarly to the Dependent Function in $1D$- and $2D$-spaces, one has:

a) If $(x, y, z) \in \text{Int}\,(A_0M_{01}M_{02}M_{03}B_0N_{01}N_{02}N_{03})$, then $K_{3D}(x, y, z) > 1$;

b) If $(x, y, z) \in \text{Fr}\,(A_0M_{01}M_{02}M_{03}B_0N_{01}N_{02}N_{03})$, then $K_{3D}(x, y, z) = 1$;

c) If $(x, y, z) \in \text{Int}\,(AM_1M_2M_3BN_1N_2N_3 - -A_0M_{01}M_{02}M_{03}B_0N_{01}N_{02}N_{03})$, then $0 < K_{3D}(x, y, z) < 1$;

d) If $(x, y, z) \in \text{Fr}\,(AM_1M_2M_3BN_1N_2N_3)$, then $K_{3D}(x, y, z) = 0$;

e) If $(x, y, z) \notin AM_1M_2M_3BN_1N_2N_3$, then $K_{3D}(x, y, z) < 0$.

16 General Case in $3D$-Space

One can replace the prisms by any finite $3D$-bodies, bounded by closed surfaces, and one considers any optimal point O (not necessarily the centers of surfaces' symmetry). Again, we assume the optimal points are the same for this nest of two $3D$-bodies.

17 Remark 2

Another possible way, for computing the distance between the point P and the closest point P' to it on the frontier (lateral

surface) of the prism $AM_1M_2M_3BN_1N_2N_3$ is by drawing a perpendicular (or a geodesic) from P onto the closest prism's face, and denoting by P' the intersection between the perpendicular (geodesic) and the prism's face.

And similarly if one has an arbitrary finite body B in the $3D$-space, bounded by surfaces. One computes as in classical mathematics:

$$d(P, B) = \inf_{Q \in B} |PB|. \tag{23}$$

18 Linear Attraction Point Principle in $3D$-Space

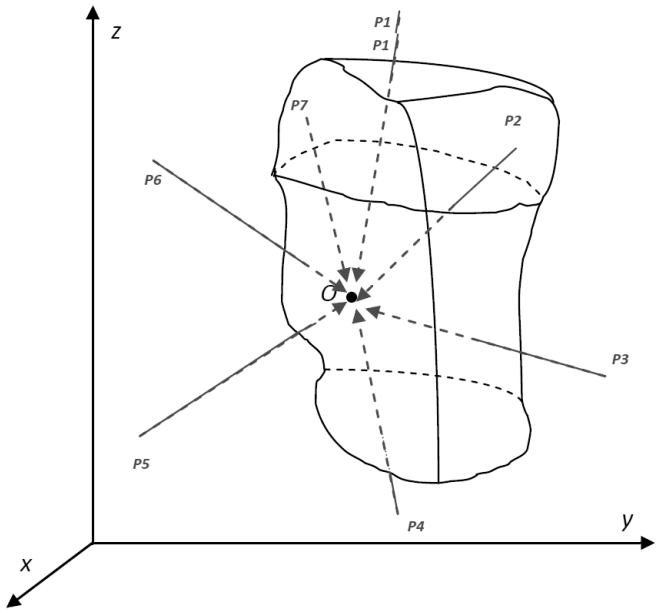

Fig. 9: Linear Attraction Point Principle for any bounded $3D$-body.

19 Non-Linear Attraction Point Principle in $3D$-Space, and in $(n-D)$-Space

There might be spaces where the attraction phenomena undergo not linearly by upon some specific non-linear curves. Let's see below such example for points P_i whose trajectories of attraction towards the optimal point follow some non-linear $3D$-curves.

20 $(n-D)$-Space

In general, in a universe of discourse U, let's have an $(n-D)$-set S and a point P. Then the Extension Linear $(n-D)$-Distance between point P and set S, is:

$$\rho(P, S) = \begin{cases} -d(P, P'), & P \neq 0,\ P \in |OP'| \\ \underset{P' \in \mathrm{Fr}(S)}{} \\ d(P, P'), & P \neq 0,\ P' \in |OP| \\ \underset{P' \in \mathrm{Fr}(S)}{} \\ -\max d(P, M), & P = 0 \\ \underset{P' \in \mathrm{Fr}(S)}{} \end{cases} \tag{24}$$

where O is the optimal point (or linearly attraction point); $d(P, P')$ means the classical linearly $(n-D)$-distance between two points P and P'; $\mathrm{Fr}(S)$ means the frontier of set S; and $|OP'|$ means the line segment between the points O and P' (the extremity points O and P' included), therefore $P \in |OP'|$ means that P lies on the line OP', in between the points O and P'.

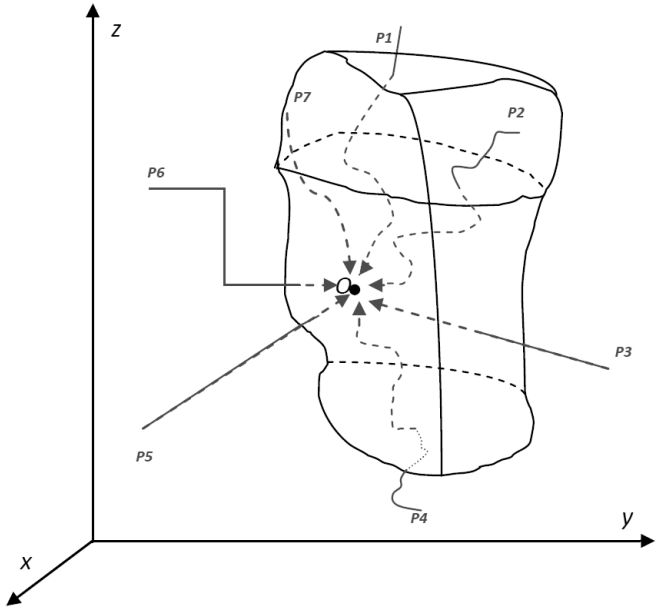

Fig. 10: Non-Linear Attraction Point Principle for any bounded $3D$-body.

For P coinciding with O, one defined the distance between the optimal point O and the set S as the negatively maximum distance (to be in concordance with the $1D$-definition).

And the Extension Non-Linear $(n-D)$-Distance between point P and set S, is:

$$\rho_c(P, S) = \begin{cases} -d_c(P, P'), & P \neq 0,\ P \in c(OP') \\ \underset{P' \in \mathrm{Fr}(S)}{} \\ d_c(P, P'), & P \neq 0,\ P' \in c(OP) \\ \underset{P' \in \mathrm{Fr}(S)}{} \\ -\max d_c(P, M), & P = 0 \\ \underset{P' \in \mathrm{Fr}(S),\ M \in c(O)}{} \end{cases} \tag{25}$$

where means the extension distance as measured along the curve c; O is the optimal point (or non-linearly attraction point); the points are attracting by the optimal point on trajectories described by an injective curve c; $dc(P, P')$ means the non-linearly $(n-D)$-distance between two points P and P', or the arc length of the curve c between the points P and P'; $\mathrm{Fr}(S)$ means the frontier of set S; and $c(OP')$ means the curve segment between the points O and P' (the extremity points O and P' included), therefore $P \in (OP')$ means that P lies on the curve c in between the points O and P'.

For P coinciding with O, one defined the distance between the optimal point O and the set S as the negatively maximum curvilinear distance (to be in concordance with the $1D$-definition).

In general, in a universe of discourse U, let's have a nest of two $(n-D)$-sets, $S_1 \subset S_2$, with no common end points, and a point P. Then the Extension Linear Dependent $(n-D)$-Function referring to the point $P(x_1, x_2, \ldots, x_n)$ is:

$$K_{nD}(P) = \frac{\rho(P, S_2)}{\rho(P, S_2) - \rho(P, S_1)}, \quad (26)$$

where is the previous extension linear $(n-D)$-distance between the point P and the $(n-D)$-set S_2.

And the Extension Non-Linear Dependent $(n-D)$-Function referring to point $P(x_1, x_2, \ldots, x_n)$ along the curve c is:

$$K_{nD}(P) = \frac{\rho_c(P, S_2)}{\rho_c(P, S_2) - \rho_c(P, S_1)}, \quad (27)$$

where is the previous extension non-linear $(n-D)$-distance between the point P and the $(n-D)$-set S_2 along the curve c.

21 Remark 3

Particular cases of curves c could be interesting to studying, for example if c are parabolas, or have elliptic forms, or arcs of circle, etc. Especially considering the geodesics would be for many practical applications. Tremendous number of applications of Extenics could follow in all domains where attraction points would exist; these attraction points could be in physics (for example, the earth center is an attraction point), economics (attraction towards a specific product), sociology (for example attraction towards a specific life style), etc.

22 Conclusion

In this paper we introduced the *Linear and Non-Linear Attraction Point Principle*, which is the following:

Let S be an arbitrary set in the universe of discourse U of any dimension, and the optimal point $O \in S$. Then each point $P(x_1, x_2, \ldots, x_n)$, $n \geqslant 1$, from the universe of discourse (linearly or non-linearly) tends towards, or is attracted by, the optimal point O, because the optimal point O is an ideal of each point.

It is a king of convergence/attraction of each point towards the optimal point. There are classes of examples and applications where such attraction point principle may apply.

If this principle is good in all cases, then there is no need to take into consideration the center of symmetry of the set S, since for example if we have a $2D$ factory piece which has heterogeneous material density, then its center of weight (barycenter) is different from the center of symmetry.

Then we generalized in the track of Cai Wen's idea to extend $1D$-set to an extension $(n-D)$-set, and thus defined the *Linear* (or *Non-Linear*) *Extension* $(n-D)$*-Distance* between a point $P(x_1, x_2, \ldots, x_n)$ and the $(n-D)$-set S as $\rho[(x_1, x_2, \ldots, x_n), S]$ on the linear (or non-linear) direction determined by the point P and the optimal point O (the line PO, or respectively the curvilinear PO) in the following way:

1) $\rho[(x_1, x_2, \ldots, x_n), S]$ is the negative distance between P and the set frontier, if P is inside the set S;
2) $\rho[(x_1, x_2, \ldots, x_n), S] = 0$, if P lies on the frontier of the set S;
3) $\rho[(x_1, x_2, \ldots, x_n), S]$ is the positive distance between P and the set frontier, if P is outside the set.

We got the following properties:

4) It is obvious from the above definition of the extension $(n-D)$-distance between a point P in the universe of discourse and the extension $(n-D)$-set S that:
   i) Point $P(x_1, x_2, \ldots, x_n) \in \mathrm{Int}(S)$ if $\rho[(x_1, x_2, \ldots x_n), S] < 0$;
   ii) Point $P(x_1, x_2, \ldots, x_n) \in \mathrm{Fr}(S)$ if $\rho[(x_1, x_2, \ldots x_n), S] = 0$;
   iii) Point $P(x1, x2, \ldots, x_n) \notin S$ if $\rho[(x_1, x_2, \ldots x_n), S] > 0$.
5) Let S_1 and S_2 be two extension sets, in the universe of discourse U, such that they have no common end points, and $S_1 \subset S_2$. We assume they have the same optimal points $O1 \equiv O2 \equiv O$ located in their center of symmetry. Then for any point $P(x_1, x_2, \ldots, x_n) \in U$ one has:

$$\rho[(x_1, x_2, \ldots x_n), S_2] \geqslant \rho[(x_1, x_2, \ldots x_n), S_1]. \quad (28)$$

Then we proceed to the generalization of the dependent function from $1D$-space to Linear (or Non-Linear) $(n-D)$-space Dependent Function, using the previous notations.

The *Linear* (or *Non-Linear*) *Dependent* $(n-D)$*-Function* of point $P(x_1, x_2, \ldots, x_n)$ along the curve c, is:

$$K_{nD}(x_1, x_2, \ldots, x_n) = \Big(\rho_c[(x_1, x_2, \ldots x_n), S_2]\Big) \times$$
$$\times \Big(\rho_c[(x_1, x_2, \ldots x_n), S_2] - \rho_c[(x_1, x_2, \ldots x_n), S_1]\Big)^{-1} \quad (29)$$

(where c may be a curve or even a line) which has the following property:

6) If point $P(x_1, x_2, \ldots, x_n) \in \mathrm{Int}(S1)$, then $K_{nD}(x_1, x_2, \ldots, x_n) > 1$;
7) If point $P(x_1, x_2, \ldots, x_n) \in \mathrm{Fr}(S1)$, then $K_{nD}(x_1, x_2, \ldots, x_n) = 1$;
8) If point $P(x_1, x_2, \ldots, x_n) \in \mathrm{Int}(S2 - S1)$, then $K_{nD}(x_1, x_2, \ldots, x_n) \in (0, 1)$;
9) If point $P(x_1, x_2, \ldots, x_n) \in \mathrm{Int}(S2)$, then $K_{nD}(x_1, x_2, \ldots, x_n) = 0$;
10) If point $P(x_1, x_2, \ldots, x_n) \notin \mathrm{Int}(S2)$, then $K_{nD}(x_1, x_2, \ldots, x_n) < 0$.

Submitted on July 15, 2012 / Accepted on July 18, 2012

References

1. Cai Wen. Extension Set and Non-Compatible Problems. *Journal of Scientific Exploration*, 1983, no. 1, 83–97; Cai Wen. Extension Set and Non-Compatible Problems. In: *Advances in Applied Mathematics and Mechanics in China*. International Academic Publishers, Beijing, 1990, 1–21.
2. Cai Wen. Extension theory and its application. *Chinese Science Bulletin*, 1999, v. 44, no. 7, 673–682. Cai Wen. Extension theory and its application. *Chinese Science Bulletin*, 1999, v. 44, no. 17, 1538–1548.
3. Yang Chunyan and Cai Wen. Extension Engineering. Public Library of Science, Beijing, 2007.
4. Wu Wenjun et al. Research on Extension Theory and Its Application. Expert Opinion. 2004, http://web.gdut.edu.cn/ĕxtenics/jianding.htm
5. Xiangshan Science Conferences Office. Scientific Significance and Future Development of Extenics — No. 271 Academic Discussion of Xiangshan Science Conferences, Brief Report of Xiangshan Science Conferences, Period 260, 2006, 1.

LETTERS TO PROGRESS IN PHYSICS

LETTERS TO PROGRESS IN PHYSICS

Routes of Quantum Mechanics Theories

Spiridon Dumitru
Department of Physics (retired), Transilvania University, B-dul Eroilor 29, 500036, Brašov, Romania
E-mail: s.dumitru42@yahoo.com

The conclusive view of quantum mechanics theory depends on its routes in respect with CIUR (Conventional Interpretation of Uncertainty Relations). As the CIUR is obligatorily assumed or interdicted the mentioned view leads to ambiguous, deficient and unnatural visions respectively to a potentially simple, mended and natural conception. The alluded dependence is illustrated in the attached poster.

Specification

The announced poster is a collage where some scientific ideas, suggested and argued in our papers [1,2], together with the known traffic signs, are figuratively pasted on the Popescu Gopo's cartoon "*Calea proprie*" ("*Proper route*") [3].

Submitted on February 24, 2012 / Accepted on March 03, 2012

References

1. Dumitru S. Reconsideration of the Uncertainty Relations and quantum measurements. *Progress in Physics*, 2008, v. 2, 50–68.
2. Dumitru S. Do the Uncertainty Relations really have crucial significances for Physics? *Progress in Physics*, 2010, v. 4, 25–29.
3. Popescu Gopo I. Filme, Filme, Filme… (Cartoons, Cartoons, Cartoons…) A booklet of cartoons, Ed. Meridiane, Bucharest 1963 (*in Rumanian*).

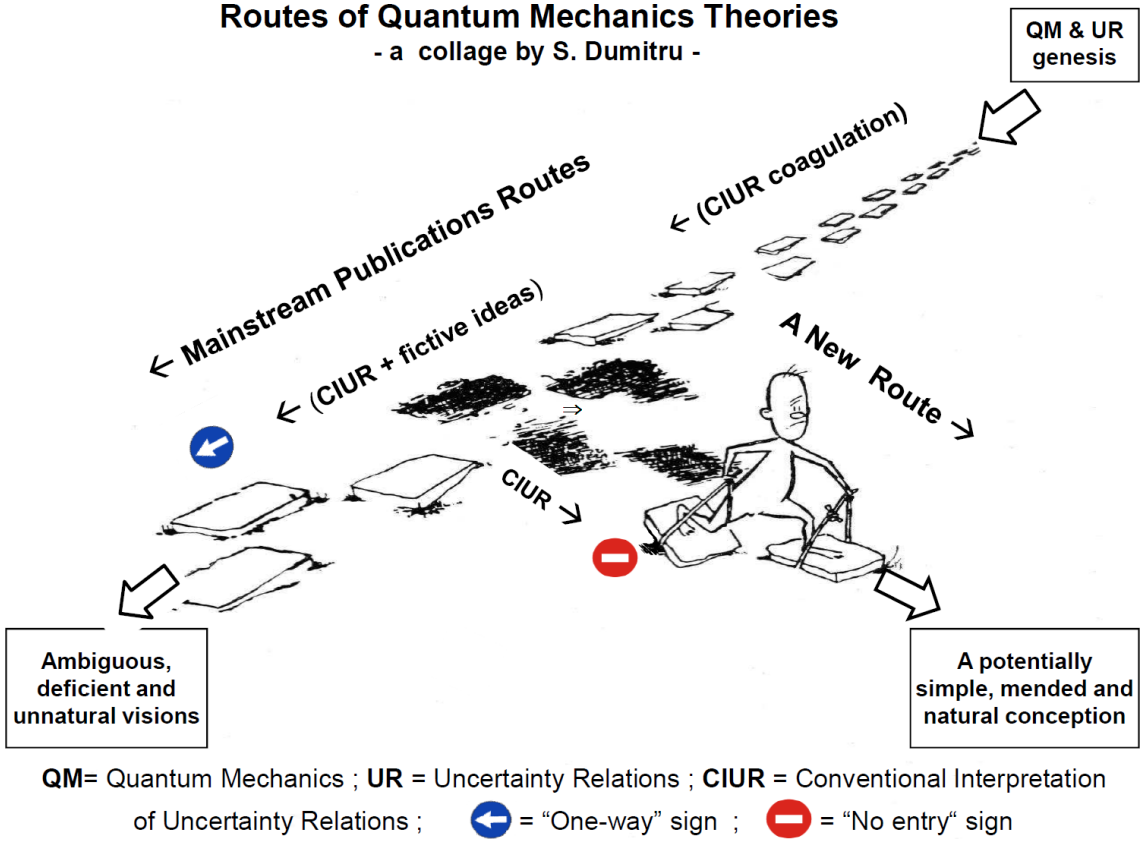

LETTERS TO PROGRESS IN PHYSICS

A Final Note on the Nature of the Kinemetric Unification of Physical Fields and Interactions

(On the occasion of Abraham Zelmanov's birthday and the near centennial of Einstein's general theory of relativity)

Indranu Suhendro
www.zelmanov.org

A present-day category of approaches to unification (of the physical fields) lacks the ultimate epistemological and scientific characteristics as I have always pointed out elsewhere. This methodological weakness is typical of a lot of post-modern "syllogism physics" (and ultimately the solipsism of such scientism in general). Herein, we shall once again make it clear as to what is meant by a true unified field theory in the furthest epistemological-scientific-dialectical sense, which must inevitably include also the natural kinemetric unity of the observer and physical observables.

Herein, I shall state my points very succinctly. Apart from the avoidance of absolutely needless verbosity, this is such as to also encompass the scientific spirit of Albert Einstein, who tirelessly and independently pursued a pure kind of geometrization of physics as demanded by the real geometric quintessence of General Relativity, and that of Abraham Zelmanov, who formulated his theory of chronometric invariants and a most all-encompassing classification of inhomogeneous, anisotropic general relativistic cosmological models and who revealed a fundamental preliminary version of the kinemetric monad formalism of General Relativity for the unification of the observer and observables in the cosmos.

1. A true unified field theory must not start with an arbitrarily concocted Lagrangian density (with merely the appearance of the metric determinant $\sqrt{-g}$ together with a sum of variables inserted by hand), for this is merely a way to embed — and not construct from first principles — a variational density in an ad hoc given space (manifold). In classical General Relativity, in the case of pure vacuum, i.e., $R_{\alpha\beta} = 0$, there is indeed a rather unique Lagrangian density: the space-time integral over $R\sqrt{-g}$, the variation of which gives $R_{\alpha\beta} = 0$. Now, precisely because there is only one purely geometric integrand here, namely the Ricci curvature scalar R (apart from the metric volume term $\sqrt{-g}$), this renders itself a valid geometric-variational reconstruction of vacuum General Relativity, and it is a mere tautology: thus it is valid rather in a secondary sense (after the underlying Riemannian geometry of General Relativity is encompassed). Einstein indeed did not primarily construct full General Relativity this way. In the case of classical General Relativity with matter and fields, appended to the pure gravitational Lagrangian density are the matter field and non-geometrized interactions (such as electromagnetism), giving the relevant energy-momentum tensor: this "integralism procedure" (reminiscent of classical Newtonian-Lagrangian dynamics) is again only tautologically valid since classical General Relativity does not geometrize fields other than the gravitational field. Varying such a Lagrangian density sheds no further semantics and information on the deepest nature of the manifold concerned.

2. Post-modern syllogism physics — including string theory and other toy-models (a plethora of "trendy salad approaches") — relies too heavily on such an arbitrary procedure. Progress associated with such a mere "sticky-but-not-solid approach" — often with big-wig politicized, opportunistic claims — seems rapid indeed, but it is ultimately a mere facade: something which Einstein himself would scientifically, epistemologically abhor (for him, in the pure Spinozan, Kantian, and Schopenhauerian sense).

3. Thus, a true unified field theory must build the spin-curvature geometry of space-time, matter, and physical fields from scratch (first principles). In other words, it must be constructed from a very fundamental level (say, the differential tetrad and metricity level), i.e., independently of mere embedding and variationalism. When one is able to construct the tetrad and metricity this way, he has a pure theory of kinemetricity for the universal manifold M: his generally asymmetric, anholonomic metric $g_{\alpha\beta}$, connection W, and curvature R will depend on not just the coordinates but also on their generally non-integrable (asymmetric) differentials: $\mathrm{M}(x, dx) \rightarrow \mathrm{M}(g, dg) \rightarrow \mathrm{W}(g, dg) \rightarrow R(g, dg)$. In other words, it becomes a multi-fractal first-principle geometric construction, and the geometry is a true chiral metacontinuum. This will then be fully capable of producing the true universal equation of motion of the unified fields as a whole in a single package (including the electromagnetic Lorentz equation of motion and the chromodynamic Yang-Mills

equation of motion) and the nature of pure geometric motion — kinemetricity — of the cosmos will be revealed. This, of course, is part of the the emergence of a purely geometric energy-momentum tensor as well. The ultimate failure of Einstein's tireless, beautiful unification efforts in the past was that he could hardly arrive at the correct geometric Lorentz equation of motion and the associated energy-momentum tensor for the electromagnetic field (and this is not as many people, including specialists, would understand it). In my past works (with each of my theories being independent and self-contained; and I do not repeat myself ever), I have shown how all this can be accomplished: one is with the construction of an asymmetric metric tensor whose anti-symmetric part gives pure spin and electromagnetism, and whose differential structure gives an anholonomic, asymmetric connection uniquely dependent on x and dx (and hence x and the world-velocity u, giving a new kind of Finslerian space), which ultimately constructs matter (and motion) from pure kinemetric scratch. Such a unified field theory is bound to be scale-independent (and metaphorically saying, "semi-classical"): beyond (i.e., truly independent of) both quantum mechanical and classical formalisms.

4. Such is the ultimate epistemology — and not just methodology — of a scientific construct with real mindful power (intellection, and not just intellectualism), i.e., with real scientific determination. That is why, the subject of quantum gravity (or quantum cosmology) will look so profoundly different to those rare few who truly understand the full epistemology and the purely geometric method of both our topic (on unification) and General Relativity. These few are the true infinitely self-reserved ones (truly to unbelievable lengths) and cannot at all be said to be products of the age and its trends. Quantizing space-time (even using things like the Feynman path-integrals and such propagators) in (extended) General Relativity means nothing if somewhat alien procedures are merely brought (often in disguise) as part of a mere embedding procedure: space-time is epistemologically and dialectically not exactly on the same footing as quantum and classical fields, matter, and energy (while roughly sharing certain parallelism with these things); rather, it must categorically, axiomatically qualify these things. Even both quantum mechanically and classically it is evident that material things possessed of motion and energy are embedded in a configuration space, but the space-time itself cannot be wholly found in these constituents. In the so-called "standard model", for example, even when quarks are arrived at as being material constituents "smaller than atoms", one still has no further (fundamental) information of the profounder things a quark necessarily contains, e.g., electric charge, spin, magnetic moment, and mass. In other words, the nature of both electromagnetism and matter is not yet understood in such a way. At the profoundest level, things cannot merely be embedded in space-time nor can space-time itself be merely embedded in (and subject to) a known quantum procedure. Geometry is geometry: purer, greater levels of physico-mathematical reality reside therein, within itself, and this is such only with the first-principle construction of a new geometry of spin-curvature purely from scratch — not merely synthetically from without — with the singular purpose to reveal a complete kinemetric unity of the geometry itself, which is none other than motion and matter at once. Again, such a geometry is scale-independent, non-simply connected, anholonomic, asymmetric, inhomogeneous: it ultimately has no "inside" nor "outside" (which, however, goes down to saying that there are indeed profound internal geometric symmetries).

5. Thus, the mystery (and complete insightful understanding) of the cosmos lies in certain profound scale-independent, kinemetric, internal symmetries of the underlying geometry (i.e., meta-continuum), and not merely in ad hoc projective, embedding, and variational procedures (including the popular syllogism of "extra dimensions").

"There are few who swim against the currents of time, living certain majestic smolderings and alien strengths as if they have died to live forever. There are so few who are like the vortex of a midnight river and the slope of a cosmic edge, in whose singularity and declivity the age is gone. There are fewer who are like a solid, unnamed, stepping stone in the heavy currents of the age of false light and enlightenment; as a generic revolutionary praxis goes, they'd rather be so black and coarse — solidly ingrained and gravitating — than smooth and merely afloat. But fewer still are those who are the thunder for all ages and in all voids: they are not grounded and sheltered on earth — they terrify it, — nor do they hang and dwell in the sky — they split it: — that light, so very few can witness its pure blinding longitude and touch its brief sublime density, is the truest Sensation (Sight-Sense, Causation-Reason) for real humanity to be the exact thing at the exact time in the Universe: itself."

Submitted on May 15, 2012 / Accepted on May 16, 2012

The Journal on Advanced Studies in Theoretical and Experimental Physics, including Related Themes from Mathematics

PROGRESS IN PHYSICS

A quarterly issue scientific journal, registered with the Library of Congress (DC, USA). This journal is peer reviewed and included in the abstracting and indexing coverage of: Mathematical Reviews and MathSciNet (AMS, USA), DOAJ of Lund University (Sweden), Zentralblatt MATH (Germany), Scientific Commons of the University of St. Gallen (Switzerland), Open-J-Gate (India), Referativnyi Zhurnal VINITI (Russia), etc.

Electronic version of this journal:
http://www.ptep-online.com

Postal Address

Department of Mathematics and Science,
University of New Mexico,
705 Gurley Ave., Gallup, NM 87301, USA

ISSN: 1555-5534 (print)
ISSN: 1555-5615 (online)

Standard Address Number: 297-5092
Printed in the United States of America

OCTOBER 2012 **VOLUME 4**

CONTENTS

Information for Authors and Subscribers

Progress in Physics has been created for publications on advanced studies in theoretical and experimental physics, including related themes from mathematics and astronomy. All submitted papers should be professional, in good English, containing a brief review of a problem and obtained results.

All submissions should be designed in LaTeX format using *Progress in Physics* template. This template can be downloaded from *Progress in Physics* home page http://www.ptep-online.com. Abstract and the necessary information about author(s) should be included into the papers. To submit a paper, mail the file(s) to the Editor-in-Chief.

All submitted papers should be as brief as possible. We accept brief papers, no larger than 8 typeset journal pages. Short articles are preferable. Large papers can be considered in exceptional cases to the section *Special Reports* intended for such publications in the journal. Letters related to the publications in the journal or to the events among the science community can be applied to the section *Letters to Progress in Physics*.

All that has been accepted for the online issue of *Progress in Physics* is printed in the paper version of the journal. To order printed issues, contact the Editors.

This journal is non-commercial, academic edition. It is printed from private donations. (Look for the current author fee in the online version of the journal.)

Pluto Moons exhibit Orbital Angular Momentum Quantization per Mass

Franklin Potter

Sciencegems.com, 8642 Marvale Drive, Huntington Beach, CA, 92646, USA. E-mail: frank11hb@yahoo.com

The Pluto satellite system of the planet plus five moons is shown to obey the quantum celestial mechanics (QCM) angular momentum *per mass* quantization condition predicted for any gravitationally bound system.

The Pluto satellite system has at least five moons, Charon, P5, Nix, P4, and Hydra, and they are nearly in a 1:3:4:5:6 resonance condition! Before the recent detection of P5, Youdin et al. [1] (2012) analyzed the orbital behavior of the other four moons via standard Newtonian gravitation and found regions of orbital stability using distances from the Pluto-Charon barycenter.

I report here that these five moons each exhibit angular momentum quantization *per mass* in amazing agreement with the prediction of the quantum celestial mechanics (QCM) proposed by H. G. Preston and F. Potter [2, 3] in 2003. QCM predicts that bodies orbiting a central massive object in gravitationally bound systems obey the angular momentum L per mass μ quantization condition

$$\frac{\mathrm{L}}{\mu} = mc\mathrm{H}, \tag{1}$$

with m an integer and c the speed of light. For most systems studied, m is an integer less than 20. The Preston gravitational distance H defined by the system total angular momentum divided by its total mass

$$\mathrm{H} = \frac{\mathrm{L_T}}{\mathrm{M_T}c} \tag{2}$$

provides a characteristic QCM distance scale for the system.

At the QCM equilibrium orbital radius, the L of the orbiting body agrees with its Newtonian value $\mu\sqrt{GM_T r}$. One assumes that after tens of millions of years that the orbiting body is at or near its QCM equilibrium orbital radius r and that the orbital eccentricity is low so that our nearly circular orbit approximation leading to these particular equations holds true. For the Pluto system, Hydra has the largest eccentricity of 0.0051 and an m value of 12.

Details about the derivation of QCM from the general relativistic Hamilton-Jacobi equation and its applications to orbiting bodies in the Schwarzschild metric approximation and to the Universe in the the interior metric can be found in our original 2003 paper [2] titled "Exploring Large-scale Gravitational Quantization without $\hbar$ in Planetary Systems, Galaxies, and the Universe". Further applications to gravitational lensing [4], clusters of galaxies [5], the cosmological redshift as a gravitational redshift [6], exoplanetary systems and the Kepler-16 circumbinary system [7] all support this QCM approach.

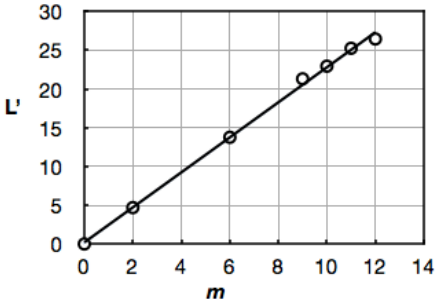

Fig. 1: The Pluto System fit to QCM

Table 1: Pluto system orbital parameters

	$r \times 10^6$ m	period (d)	ϵ	m	P_2/P_1
Pluto	2.035	6.387230	0.0022	2	
Charon	17.536	6.387230	0.0022	6	1
P5	42.	20.2	~ 0	9	2.915
Nix	48.708	24.856	0.0030	10	3.880
P4	59.	32.1	~ 0	11	5.038
Hydra	64.749	38.206	0.0051	12	6.405

The important physical parameters of the Pluto system satellites from NASA, ESA, and M. Showalter (SETI Institute) et al. [8] as listed at Wikipedia are given in the table. The system total mass is essentially the combined mass of Pluto (13.05×10^{21} kg) and Charon (1.52×10^{21} kg). The QCM values of m in the next to last column were determined by the best linear regression fit ($R^2 = 0.998$) to the angular momentum quantization per mass equation and are shown in the figure as $L' = L/\mu c$ plotted against m with slope $H = 2.258$ meters. Using distances from the center of Pluto instead of from the barycenter produces the same m values ($R^2 = 0.995$) but a slightly different slope.

In QCM the orbital resonance condition is given by the period ratio given in the last column calculated from

$$\frac{\mathrm{P_2}}{\mathrm{P_1}} = \frac{(m_2+1)^3}{(m_1+1)^3}. \tag{3}$$

With Charon as the reference, this system of moons has nearly a 1:3:4:5:6 commensuration, with the last moon Hydra having

the largest discrepancy of almost 7%. If Hydra moves further out from the barycenter toward its QCM equilibrium orbital radius for $m = 12$ in the next few million years, then its position on the plot will improve but its m value will remain the same. Note also that P5 at $m = 9$ may move slightly closer to the barycenter. Dynamic analysis via the appropriate QCM equations will be reported later. Note that additional moons of Pluto may be found at non-occupied m values.

The QCM plot reveals that not all possible m values are occupied by moons of Pluto and at the same time predicts orbital radii where additional moons are expected to be. The present system configuration depends upon its history of formation and its subsequent evolution, both processes being dependent upon the dictates of QCM. Recall [2] that the satellite systems of the Jovian planets were shown to obey QCM, with some QCM orbital states occupied by more than one moon.

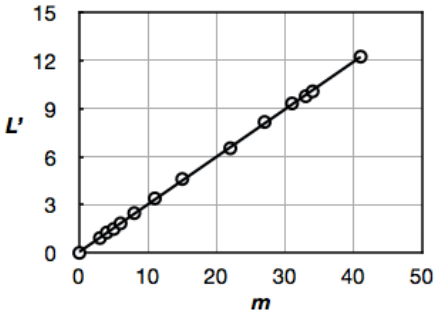

Fig. 2: The Solar System fit to QCM

I show in Fig. 2 the linear regression plot ($r^2 = 0.999$) for the Solar System, this time with 8 planets plus the largest 5 additional minor planets Ceres, Pluto, Haumea, Makemake, and Eris. From the fit, the slope gives us a Solar System total angular momentum of about 1.78×10^{45} kg m^2/s, far exceeding the angular momentum contributions of the planets by a factor of at least 50! Less than a hundred Earth masses at the 50,000–100,000 A.U. distance of the Oort Cloud therefore determines the angular momentum of the Solar System. Similar analyses have been done for numerous exoplanet systems [7] with multiple planets with the result that additional angular momentum is required, meaning that more planets and/or the equivalent of an Oort Cloud are to be expected.

The existence of angular momentum per mass quantization dictates also that the energy per mass quantization for a QCM state obeys

$$\frac{\mathrm{E}}{\mu} = -\frac{r_g^2 c^2}{8n^2 H^2} = -\frac{G^2 M_T^4}{2n^2 {L_T}^2} \qquad (4)$$

with $n = m + 1$ for circular orbits and Schwarzschild radius r_g. One expects $H \gg r_g$ for the Schwarzschild approximation to be acceptable, a condition upheld by the Pluto system, the Solar System, and all exoplanet systems. The corresponding QCM state wave functions are confluent hypergeometric functions that reduce to hydrogen-like wave functions for circular orbits. Therefore, a QCM energy state exists for each $n \geqslant 2$. A body in a QCM state but not yet at the equilibrium radius for its m value will slowly drift toward this radius over significant time periods because the QCM accelerations are small.

In retrospect, the Pluto system is probably more like a binary system than a system with a single central mass, with the moons beyond Charon in circumbinary orbits around the barycenter. As such, I was surprised to find such a good fit to the QCM angular momentum restriction which was derived for the single dominant mass system. Additional moons of Pluto, should they exist, can provide some more insight into the application of QCM to this gravitationally bound system.

Meanwhile, the identification of additional exoplanets in nearby systems, particularly circumbinary planets, promises to create an interesting challenge for establishing QCM as a viable approach toward a better understanding of gravitation theory at all size scales.

Acknowledgements

The author acknowledges Sciencegems.com for its generous support.

Submitted on August 02, 2012 / Accepted on August 07, 2012

References

1. Youdin A. N., Kratter K. M., Kenyon S. J. Circumbinary Chaos: Using Pluto's Newest Moon to Constrain the Masses of Nix & Hydra. arXiv: 1205.5273v1.
2. Preston H. P., Potter F. Exploring Large-scale Gravitational Quantization without h-bar in Planetary Systems, Galaxies, and the Universe. arXiv: gr-qc/030311v1.
3. Potter F., Preston H. G. Quantum Celestial Mechanics: large-scale gravitational quantization states in galaxies and the Universe. *1st Crisis in Cosmology Conference: CCC-I*, Lerner E. J. and Almeida J. B., eds., AIP CP822, 2006, 239–252.
4. Potter F., Preston H. G. Gravitational Lensing by Galaxy Quantization States. arXiv: gr-qc/0405025v1.
5. Potter F., Preston H. G. Quantization State of Baryonic Mass in Clusters of Galaxies. *Progress in Physics*, 2007, v. 1, 61–63.
6. Potter F., Preston H. G. Cosmological Redshift Interpreted as Gravitational Redshift. *Progress in Physics*, 2007, v. 2, 31–33.
7. Potter F., Preston H. G. Kepler–16 Circumbinary System Validates Quantum Celestial Mechanics. *Progress in Physics*, 2012, v. 1, 52–53.
8. Showalter M., Weaver H. A., Stern S. A., Steffi A. J., Buie M. W. Hubble Discovers New Pluto Moon, 11 July 2012. www.spacetelescope.org/news/heic1212

On the Decomposition of the Spacetime Metric Tensor and of Tensor Fields in Strained Spacetime

Pierre A. Millette

University of Ottawa (alumnus), K4A 2C3 747, Ottawa, CANADA. E-mail: PierreAMillette@alumni.uottawa.ca

We propose a natural decomposition of the spacetime metric tensor of General Relativity into a background and a dynamical part based on an analysis from first principles of the effect of a test mass on the background metric. We find that the presence of mass results in strains in the spacetime continuum. Those strains correspond to the dynamical part of the spacetime metric tensor. We then apply the stress-strain relation of Continuum Mechanics to the spacetime continuum to show that rest-mass energy density arises from the volume dilatation of the spacetime continuum. Finally we propose a natural decomposition of tensor fields in strained spacetime, in terms of dilatations and distortions. We show that dilatations correspond to rest-mass energy density, while distortions correspond to massless shear transverse waves. We note that this decomposition in a massive dilatation and a massless transverse wave distortion, where both are present in spacetime continuum deformations, is somewhat reminiscent of wave-particle duality. We note that these results are considered to be local effects in the particular reference frame of the observer. In addition, the applicability of the proposed metric to the Einstein field equations remains open.

1 Introduction

We first demonstrate from first principles that spacetime is strained by the presence of mass. Strained spacetime has been explored recently by Tartaglia *et al.* in the cosmological context, as an extension of the spacetime Lagrangian to obtain a generalized Einstein equation [1, 2]. Instead, in this analysis, we consider strained spacetime within the framework of Continuum Mechanics and General Relativity. This allows for the application of continuum mechanical results to the spacetime continuum. In particular, this provides a natural decomposition of the spacetime metric tensor and of spacetime tensor fields, both of which are still unresolved and are the subject of continuing investigations (see for example [3–7]).

2 Decomposition of the Spacetime Metric Tensor

There is no straightforward definition of local energy density of the gravitational field in General Relativity [8, see p. 84, p. 286] [6, 9, 10]. This arises because the spacetime metric tensor includes both the background spacetime metric and the local dynamical effects of the gravitational field. No natural way of decomposing the spacetime metric tensor into its background and dynamical parts is known.

In this section, we propose a natural decomposition of the spacetime metric tensor into a background and a dynamical part. This is derived from first principles by introducing a test mass in the spacetime continuum described by the background metric, and calculating the effect of this test mass on the metric.

Consider the diagram of Figure 1. Points A and B of the spacetime continuum, with coordinates x^μ and $x^\mu + dx^\mu$ respectively, are separated by the infinitesimal line element

$$ds^2 = g_{\mu\nu}\, dx^\mu dx^\nu \tag{1}$$

where $g_{\mu\nu}$ is the metric tensor describing the background state of the spacetime continuum.

We now introduce a test mass in the spacetime continuum. This results in the displacement of point A to $\widetilde{A}$, where the displacement is written as u^μ. Similarly, the displacement of point B to $\widetilde{B}$ is written as $u^\mu + du^\mu$. The infinitesimal line element between points $\widetilde{A}$ and $\widetilde{B}$ is given by $\widetilde{ds}^2$.

By reference to Figure 1, the infinitesimal line element $\widetilde{ds}^2$ can be expressed in terms of the background metric tensor as

$$\widetilde{ds}^2 = g_{\mu\nu}(dx^\mu + du^\mu)(dx^\nu + du^\nu). \tag{2}$$

Multiplying out the terms in parentheses, we get

$$\widetilde{ds}^2 = g_{\mu\nu}(dx^\mu dx^\nu + dx^\mu du^\nu + du^\mu dx^\nu + du^\mu du^\nu). \tag{3}$$

Expressing the differentials du as a function of x, this equation becomes

$$\begin{aligned}\widetilde{ds}^2 = g_{\mu\nu}(&dx^\mu dx^\nu + dx^\mu\, u^\nu{}_{;\alpha}\, dx^\alpha + u^\mu{}_{;\alpha}\, dx^\alpha dx^\nu + \\ &+ u^\mu{}_{;\alpha}\, dx^\alpha\, u^\nu{}_{;\beta}\, dx^\beta)\end{aligned} \tag{4}$$

where the semicolon (;) denotes covariant differentiation. Rearranging the dummy indices, this expression can be written as

$$\widetilde{ds}^2 = (g_{\mu\nu} + g_{\mu\alpha}\, u^\alpha{}_{;\nu} + g_{\alpha\nu}\, u^\alpha{}_{;\mu} + g_{\alpha\beta}\, u^\alpha{}_{;\mu} u^\beta{}_{;\nu})\, dx^\mu dx^\nu \tag{5}$$

and lowering indices, the equation becomes

$$\widetilde{ds}^2 = (g_{\mu\nu} + u_{\mu;\nu} + u_{\nu;\mu} + u^\alpha{}_{;\mu} u_{\alpha;\nu})\, dx^\mu dx^\nu. \tag{6}$$

Fig. 1: Effect of a test mass on the background metric tensor

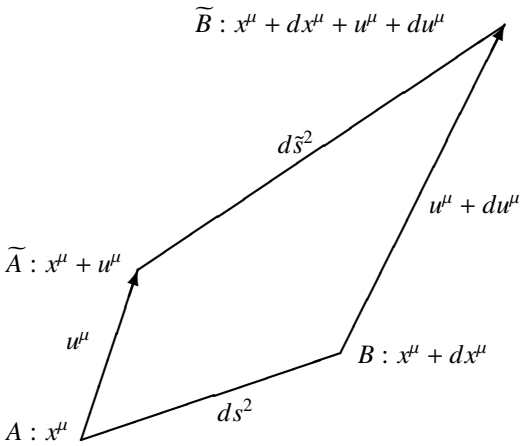

The expression $u_{\mu;\nu} + u_{\nu;\mu} + u^\alpha{}_{;\mu} u_{\alpha;\nu}$ is equivalent to the definition of the strain tensor $\varepsilon^{\mu\nu}$ of Continuum Mechanics. The strain $\varepsilon^{\mu\nu}$ is expressed in terms of the displacements u^μ of a continuum through the kinematic relation [11, see p. 149] [12, see pp. 23–28]:

$$\varepsilon^{\mu\nu} = \frac{1}{2}(u^{\mu;\nu} + u^{\nu;\mu} + u^{\alpha;\mu} u_\alpha{}^{;\nu}). \tag{7}$$

Substituting for $\varepsilon^{\mu\nu}$ from Eq.(7) into Eq.(6), we get

$$\widetilde{ds}^2 = (g_{\mu\nu} + 2\,\varepsilon_{\mu\nu})\, dx^\mu dx^\nu. \tag{8}$$

Setting [12, see p. 24]

$$\widetilde{g}_{\mu\nu} = g_{\mu\nu} + 2\,\varepsilon_{\mu\nu} \tag{9}$$

then Eq.(8) becomes

$$\widetilde{ds}^2 = \widetilde{g}_{\mu\nu}\, dx^\mu dx^\nu \tag{10}$$

where $\widetilde{g}_{\mu\nu}$ is the metric tensor describing the spacetime continuum with the test mass.

Given that $g_{\mu\nu}$ is the background metric tensor describing the background state of the continuum, and $\widetilde{g}_{\mu\nu}$ is the spacetime metric tensor describing the final state of the continuum with the test mass, then $2\,\varepsilon_{\mu\nu}$ must represent the dynamical part of the spacetime metric tensor due to the test mass:

$$g^{dyn}_{\mu\nu} = 2\,\varepsilon_{\mu\nu}. \tag{11}$$

We are thus led to the conclusion that the presence of mass results in strains in the spacetime continuum. Those strains correspond to the dynamical part of the spacetime metric tensor. Hence the applied stresses from mass (i.e. the energy-momentum stress tensor) result in strains in the spacetime continuum, that is strained spacetime.

3 Rest-Mass Energy Relation

The introduction of strains in the spacetime continuum as a result of the energy-momentum stress tensor allows us to use by analogy results from Continuum Mechanics, in particular the stress-strain relation, to provide a better understanding of strained spacetime.

The stress-strain relation for an isotropic and homogeneous spacetime continuum can be written as [12, see pp. 50–53]:

$$2\mu_0 \varepsilon^{\mu\nu} + \lambda_0 g^{\mu\nu} \varepsilon = T^{\mu\nu} \tag{12}$$

where $T^{\mu\nu}$ is the energy-momentum stress tensor, $\varepsilon^{\mu\nu}$ is the resulting strain tensor, and

$$\varepsilon = \varepsilon^\alpha{}_\alpha \tag{13}$$

is the trace of the strain tensor obtained by contraction. ε is the volume dilatation defined as the change in volume per original volume [11, see p. 149–152] and is an invariant of the strain tensor. λ_0 and μ_0 are the Lamé elastic constants of the spacetime continuum: μ_0 is the shear modulus and λ_0 is expressed in terms of κ_0, the bulk modulus:

$$\lambda_0 = \kappa_0 - \mu_0/2 \tag{14}$$

in a four-dimensional continuum. The contraction of Eq.(12) yields the relation

$$2(\mu_0 + 2\lambda_0)\varepsilon = T^\alpha{}_\alpha \equiv T. \tag{15}$$

The time-time component T^{00} of the energy-momentum stress tensor represents the total energy density given by [13, see pp. 37–41]

$$T^{00}(x^k) = \int d^3\mathbf{p} E_p f(x^k, \mathbf{p}) \tag{16}$$

where $E_p = (\rho^2 c^4 + p^2 c^2)^{1/2}$, ρ is the rest-mass energy density, c is the speed of light, $\mathbf{p}$ is the momentum 3-vector and $f(x^k, \mathbf{p})$ is the distribution function representing the number of particles in a small phase space volume $d^3\mathbf{x}d^3\mathbf{p}$. The space-space components T^{ij} of the energy-momentum stress tensor represent the stresses within the medium given by

$$T^{ij}(x^k) = c^2 \int d^3\mathbf{p} \frac{p^i p^j}{E_p} f(x^k, \mathbf{p}). \tag{17}$$

They are the components of the net force acting across a unit area of a surface, across the x^i planes in the case where $i = j$.

In the simple case of a particle, they are given by [14, see p. 117]

$$T^{ii} = \rho\, v^i v^i \tag{18}$$

where v^i are the spatial components of velocity. If the particles are subject to forces, these stresses must be included in the energy-momentum stress tensor.

Explicitly separating the time-time and the space-space components, the trace of the energy-momentum stress tensor is written as

$$T^{\alpha}{}_{\alpha} = T^{0}{}_{0} + T^{i}{}_{i}. \tag{19}$$

Substituting from Eq.(16) and Eq.(17), using the metric $\eta^{\mu\nu}$ of signature $(+---)$, we obtain:

$$T^{\alpha}{}_{\alpha}(x^k) = \int d^3\mathbf{p}\left(E_p - \frac{p^2c^2}{E_p}\right) f(x^k, \mathbf{p}) \tag{20}$$

which simplifies to

$$T^{\alpha}{}_{\alpha}(x^k) = \rho^2 c^4 \int d^3\mathbf{p} \frac{f(x^k, \mathbf{p})}{E_p}. \tag{21}$$

Using the relation [13, see p. 37]

$$\frac{1}{\overline{E}_{har}(x^k)} = \int d^3\mathbf{p} \frac{f(x^k, \mathbf{p})}{E_p} \tag{22}$$

in equation Eq.(21), we obtain the relation

$$T^{\alpha}{}_{\alpha}(x^k) = \frac{\rho^2 c^4}{\overline{E}_{har}(x^k)} \tag{23}$$

where $\overline{E}_{har}(x^k)$ is the Lorentz invariant harmonic mean of the energy of the particles at x^k.

In the harmonic mean of the energy of the particles $\overline{E}_{har}$, the momentum contribution $\mathbf{p}$ will tend to average out and be dominated by the mass term ρc^2, so that we can write

$$\overline{E}_{har}(x^k) \simeq \rho c^2. \tag{24}$$

Substituting for $\overline{E}_{har}$ in Eq.(23), we obtain the relation

$$T^{\alpha}{}_{\alpha}(x^k) \simeq \rho c^2. \tag{25}$$

The total rest-mass energy density of the system is obtained by integrating over all space:

$$T^{\alpha}{}_{\alpha} = \int d^3\mathbf{x}\; T^{\alpha}{}_{\alpha}(x^k). \tag{26}$$

The expression for the trace derived from Eq.(19) depends on the composition of the sources of the gravitational field. Considering the energy-momentum stress tensor of the electromagnetic field, we can show that $T^{\alpha}{}_{\alpha} = 0$ as expected for massless photons, while

$$T^{00} = \frac{\epsilon_0}{2}\left(E^2 + c^2B^2\right)$$

is the total energy density, where ϵ_0 is the electromagnetic permittivity of free space, and E and B have their usual significance.

Hence $T^{\alpha}{}_{\alpha}$ corresponds to the invariant rest-mass energy density and we write

$$T^{\alpha}{}_{\alpha} = T = \rho c^2 \tag{27}$$

where ρ is the rest-mass energy density. Using Eq.(27) into Eq.(15), the relation between the invariant volume dilatation ε and the invariant rest-mass energy density becomes

$$2(\mu_0 + 2\lambda_0)\varepsilon = \rho c^2 \tag{28}$$

or, in terms of the bulk modulus κ_0,

$$4\kappa_0\varepsilon = \rho c^2. \tag{29}$$

This equation demonstrates that rest-mass energy density arises from the volume dilatation of the spacetime continuum. The rest-mass energy is equivalent to the energy required to dilate the volume of the spacetime continuum, and is a measure of the energy stored in the spacetime continuum as volume dilatation. κ_0 represents the resistance of the spacetime continuum to dilatation. The volume dilatation is an invariant, as is the rest-mass energy density.

4 Decomposition of Tensor Fields in Strained Spacetime

As opposed to vector fields which can be decomposed into longitudinal (irrotational) and transverse (solenoidal) components using the Helmholtz representation theorem [11, see pp. 260–261], the decomposition of spacetime tensor fields can be done in many ways (see for example [3–5, 7]).

The application of Continuum Mechanics to a strained spacetime continuum offers a natural decomposition of tensor fields, in terms of dilatations and distortions [12, see pp. 58–60]. A *dilatation* corresponds to a change of volume of the spacetime continuum without a change of shape (as seen in Section 3) while a *distortion* corresponds to a change of shape of the spacetime continuum without a change in volume. Dilatations correspond to longitudinal displacements and distortions correspond to transverse displacements [11, see p. 260].

The strain tensor $\varepsilon^{\mu\nu}$ can thus be decomposed into a strain deviation tensor $e^{\mu\nu}$ (the *distortion*) and a scalar e (the *dilatation*) according to [12, see pp. 58–60]:

$$\varepsilon^{\mu\nu} = e^{\mu\nu} + e g^{\mu\nu} \tag{30}$$

where

$$e^{\mu}{}_{\nu} = \varepsilon^{\mu}{}_{\nu} - e\delta^{\mu}{}_{\nu} \tag{31}$$

$$e = \frac{1}{4}\varepsilon^{\alpha}{}_{\alpha} = \frac{1}{4}\varepsilon. \tag{32}$$

Similarly, the energy-momentum stress tensor $T^{\mu\nu}$ is decomposed into a stress deviation tensor $t^{\mu\nu}$ and a scalar t according to

$$T^{\mu\nu} = t^{\mu\nu} + t g^{\mu\nu} \tag{33}$$

where similarly

$$t^{\mu}{}_{\nu} = T^{\mu}{}_{\nu} - t\delta^{\mu}{}_{\nu} \tag{34}$$

$$t = \frac{1}{4}T^{\alpha}{}_{\alpha}. \tag{35}$$

Using Eq.(30) to Eq.(35) into the strain-stress relation of Eq.(12) and making use of Eq.(15) and Eq.(14), we obtain separated dilatation and distortion relations respectively:

$$\begin{aligned} &\text{dilatation} : t = 2(\mu_0 + 2\lambda_0)e = 4\kappa_0 e = \kappa_0 \varepsilon \\ &\text{distortion} : t^{\mu\nu} = 2\mu_0 e^{\mu\nu}. \end{aligned} \tag{36}$$

The distortion-dilatation decomposition is evident in the dependence of the dilatation relation on the bulk modulus κ_0 and of the distortion relation on the shear modulus μ_0. As shown in Section 3, the dilatation relation of Eq.(36) corresponds to rest-mass energy, while the distortion relation is traceless and thus massless, and corresponds to shear transverse waves.

This decomposition in a massive dilatation and a massless transverse wave distortion, where both are present in spacetime continuum deformations, is somewhat reminiscent of wave-particle duality. This could explain why dilatation-measuring apparatus measure the massive 'particle' properties of the deformation, while distortion-measuring apparatus measure the massless transverse 'wave' properties of the deformation.

5 Conclusion

In this paper, we have proposed a natural decomposition of the spacetime metric tensor into a background and a dynamical part based on an analysis from first principles, of the impact of introducing a test mass in the spacetime continuum. We have found that the presence of mass results in strains in the spacetime continuum. Those strains correspond to the dynamical part of the spacetime metric tensor.

We have applied the stress-strain relation of Continuum Mechanics to the spacetime continuum to show that rest-mass energy density arises from the volume dilatation of the spacetime continuum.

Finally we have proposed a natural decomposition of tensor fields in strained spacetime, in terms of dilatations and distortions. We have shown that dilatations correspond to rest-mass energy density, while distortions correspond to massless shear transverse waves. We have noted that this decomposition in a dilatation with rest-mass energy density and a massless transverse wave distortion, where both are simultaneously present in spacetime continuum deformations, is somewhat reminiscent of wave-particle duality.

It should be noted that these results are considered to be local effects in the particular reference frame of the observer. In addition, the applicability of the proposed metric to the Einstein field equations remains open.

Submitted on August 5, 2012 / Accepted on August 08, 2012

References

1. Tartaglia A. A Strained Space-time to Explain the large Scale Properties of the Universe. *International Journal of Modern Physics: Conference Series*, 2011, v. 3, 303–311.
2. Tartaglia A., Radicella N., Sereno M. Lensing in an elastically strained space-time. *Journal of Physics: Conference Series*, 2011, v. 283, 012037.
3. Deser S. Covariant decomposition of symmetric tensors and the gravitational Cauchy problem. *Annales de l'Institut Henri Poincaré A*, 1967, v. 7(2), 149–188.
4. Krupka D. The Trace Decomposition Problem. *Contributions to Algebra and Geometry*, 1995, v. 36(2), 303–315.
5. Straumann N. Proof of a decomposition theorem for symmetric tensors on spaces with constant curvature. arXiv: gr-qc/0805.4500v1.
6. Chen X.-S., Zhu B.-C. Physical decomposition of the gauge and gravitational fields. arXiv: gr-qc/1006.3926v3.
7. Chen X.-S., Zhu B.-C. Tensor gauge condition and tensor field decomposition. arXiv: gr-qc/1101.2809v5.
8. Wald R.M. General Relativity. The University of Chicago Press, Chicago, 1984.
9. Szabados L.B. Quasi-Local Energy-Momentum and Angular Momentum in GR: A Review Article. *Living Reviews in Relativity*, 2004, v. 7, 4.
10. Jaramillo J.L., Gourgoulhon E. Mass and Angular Momentum in General Relativity. arXiv: gr-qc/1001.5429v2.
11. Segel L.A. Mathematics Applied to Continuum Mechanics. Dover Publications, New York, 1987.
12. Flügge W. Tensor Analysis and Continuum Mechanics. Springer-Verlag, New York, 1972.
13. Padmanabhan T. Gravitation, Foundations and Frontiers. Cambridge University Press, Cambridge, 2010.
14. Eddington A.S. The Mathematical Theory of Relativity. Cambridge University Press, Cambridge, 1957.

Quantum Constraints on a Charged Particle Structure

Eliahu Comay

Charactell Ltd., PO Box 39019, Tel-Aviv, 61390, Israel. E-mail: elicomay@post.tau.ac.il

The crucial role of a Lorentz scalar Lagrangian density whose dimension is $[L^{-4}]$ ($\hbar = c = 1$) in a construction of a quantum theory is explained. It turns out that quantum functions used in this kind of Lagrangian density have a definite dimension. It is explained why quantum functions that have the dimension $[L^{-1}]$ cannot describe particles that carry electric charge. It is shown that the 4-current of a quantum particle should satisfy further requirements. It follows that the pion and the $W^{\pm}$ must be composite particles. This outcome is inconsistent with the electroweak theory. It is also argued that the $125\,GeV$ particle found recently by two LHC collaborations is not a Higgs boson but a $t\bar{t}$ meson.

1 Introduction

The fundamental role of mathematics in the structure of theoretical physics is regarded as an indisputable element of the theory [1]. This principle is utilized here. The analysis relies on special relativity and derives constraints on the structure of equations of motion of quantum particles. The discussion examines the dimensions of wave functions and explains why spin-0 and spin-1 elementary quantum particles cannot carry an electric charge. This conclusion is relevant to the validity of the electroweak theory and to the meaning of recent results concerning the existence of a particle having a mass of 125 GeV [2, 3].

Units where $\hbar = c = 1$ are used in this work. Hence, only one dimension is required and it is the length, denoted by $[L]$. For example, mass, energy and momentum have the dimension $[L^{-1}]$, etc. Greek indices run from 0 to 3 and the diagonal metric used is $g_{\mu\nu} = (1, -1, -1, -1)$. The symbol $_{,\mu}$ denotes the partial differentiation with respect to x^{μ} and an upper dot denotes a differentiation with respect to time. The summation convention is used for Greek indices.

The second section shows that quantum functions have a definite dimension. This property is used in the third section where it is proved that Klein-Gordon (KG) fields and those of the $W^{\pm}$ particle have no self-consistent Hamiltonian. The final section contains a discussion of the significance of the results obtained in this work.

2 The dimensions of quantum fields

In this section some fundamental properties of quantum theory are used for deriving the dimensions of quantum fields. A massive quantum mechanical particle is described by a wave function $\psi(x^{\mu})$. The phase $\varphi(\alpha)$ is an important factor of $\psi(x^{\mu})$ because it determines the form of an interference pattern. For the present discussion it is enough to demand that the phase is an analytic function which can be expanded in a power series that contains more than one term. It means that in the following expansion of the phase,

$$\varphi(\alpha) = \sum_{i=0}^{\infty} a_i \alpha^i, \tag{1}$$

the inequality $a_i \neq 0$ holds for two or more values of the index i.

The requirement stating that all terms of a physical expression must have the same dimension and the form of the right hand side of (1) prove that α must be dimensionless. By the same token, in a relativistic quantum theory, α must also be a Lorentz scalar. (The possibility of using a pseudoscalar factor is not discussed here because this work aims to examine the parity conserving electromagnetic interactions of a quantum mechanical particle.) It is shown below how these two requirements impose dramatic constraints on acceptable quantum mechanical equations of motion of a charged particle.

Evidently, a pure number satisfies the two requirements. However, a pure number is inadequate for our purpose, because the phase varies with the particle's energy and momentum. The standard method of constructing a quantum theory is to use the Plank's constant $\hbar$ which has the dimension of the action, and to define the phase as the action divided by $\hbar$. In the units used here, $\hbar = 1$ and the action is dimensionless. Thus, a relativistic quantum theory satisfies the two requirements presented above if it is derived from a Lagrangian density $\mathcal{L}$ that is a Lorentz scalar having the dimension $[L^{-4}]$. Indeed, in this case, the action

$$S = \int \mathcal{L} d^4 x^{\mu} \tag{2}$$

is a dimensionless Lorentz scalar. It is shown below how the dimension $[L^{-4}]$ of $\mathcal{L}$ defines the dimension of quantum fields.

Being aware of these requirements, let us find the dimension of the quantum functions used for a description of three kinds of quantum particles. The Dirac Lagrangian density of

a free spin-1/2 particle is [4, see p. 54]

$$\mathcal{L} = \bar{\psi}[\gamma^{\mu} i\partial_{\mu} - m]\psi. \tag{3}$$

Here the operator has the dimension $[L^{-1}]$ and the Dirac wave function ψ has the dimension $[L^{-3/2}]$.

The Klein-Gordon Lagrangian density of a free spin-0 particle is [4, see p. 38]

$$\mathcal{L} = \phi^{*}_{,\mu}\phi_{,\nu}g^{\mu\nu} - m^2\phi^{*}\phi. \tag{4}$$

Here the operator has the dimension $[L^{-2}]$ and the KG wave function ϕ has the dimension $[L^{-1}]$.

The electrically charged spin-1 $W^{\pm}$ particle is described by a 4-vector function W_{μ}. W_{μ} and the electromagnetic 4-potential A_{μ} are linear combinations of related quantities [5, see p. 518]. Evidently, they have the same dimension. Hence, like the KG field, the dimension of W_{μ} is $[L^{-1}]$.

The dimension of each of these fields is used in the discussions presented in the rest of this work.

3 Consequences of the dimensions of quantum fields

Before analyzing the consequences of the dimension of quantum fields and of the associated wave functions, it is required to realize the Hamiltonian's role in quantum theories. The following lines explain why the Hamiltonian is an indispensable element of Relativistic Quantum Mechanics (RQM) and of Quantum Field Theory (QFT). This status of the Hamiltonian is required for the analysis presented below.

The significance of hierarchical relationships that hold between physical theories is discussed in the literature [6, see pp. 1-6] and [7, see pp. 85, 86]. The foundation of the argument can be described as follows. Physical theories take the form of differential equations. These equations can be examined in appropriate limits. Now RQM is a limit of QFT. The former holds for cases where the number of particles can be regarded as a constant of the motion. Therefore, if examined in this limit, QFT must agree with RQM. By the same token, the classical limit of RQM must agree with classical physics. This matter has been recognized by the founders of quantum mechanics who have proven that the classical limit of quantum mechanics agrees with classical physics. The following example illustrates the importance of this issue. Let us examine an inelastic scattering event. The chronological order of this process is as follows:

a. First, two particles move in external electromagnetic fields. Relativistic classical mechanics and classical electrodynamics describe the motion.

b. The two particles are very close to each other. RQM describes the process.

c. The two particles collide and interact. New particles are created. The process is described by QFT.

d. Particle creation ends but particles are still very close to one another. RQM describes the state.

e. Finally, the outgoing particles depart. Relativistic classical mechanics and classical electrodynamics describe the motion.

Evidently, in this kind of experiment, energy and momentum of the initial and the final states are well defined quantities and their final state values abide by the law of energy-momentum conservation. It means that the specific values of the energy-momentum of the final state agree with the corresponding quantities of the initial state. Now, the initial and the final states are connected by processes that are described by RQM and QFT. In particular, the process of new particle creation is described only by QFT. Hence, RQM and QFT must "tell" the final state what are the precise initial values of the energy-momentum. It follows that RQM as well as QFT must use field functions that have a self-consistent Hamiltonian.

The Hamiltonian H and the de Broglie relations between a particle's energy-momentum and its wave properties yield the fundamental equation of quantum mechanics

$$i\frac{\partial\psi}{\partial t} = H\psi. \tag{5}$$

The Hamiltonian density $\mathcal{H}$ is derived from the Lagrangian density by the following well known Legendre transformation

$$\mathcal{H} = \sum_{i} \dot{\psi}_i \frac{\partial\mathcal{L}}{\partial\dot{\psi}}_{i} - \mathcal{L}, \tag{6}$$

where the index i runs on all functions.

The standard form of representing the interaction of an electric charge with external fields relies on the following transformation [8, see p. 10]

$$-i\frac{\partial}{\partial x^{\mu}} \rightarrow -i\frac{\partial}{\partial x^{\mu}} - eA_{\mu}(x^{\nu}). \tag{7}$$

Now let us examine the electromagnetic interaction of the three kinds of quantum mechanical particle described in the previous section. This is done by adding an interaction term $\mathcal{L}_{int}$ to the Lagrangian density. As explained above, this term must be a Lorentz scalar whose dimension is $[L^{-4}]$. The required form of the electromagnetic interaction term represents the interaction of charged particles with electromagnetic fields *and* the interaction of electromagnetic fields with charged particles. This term is written as follows [9, see p. 75]

$$\mathcal{L}_{int} = -j^{\mu}A_{\mu}. \tag{8}$$

Here j^{μ} is the 4-current of the quantum particle and A_{μ} is the electromagnetic 4-potential.

Charge conservation requires that j^{μ} satisfies the continuity equation

$$j^{\mu}_{,\mu} = 0. \tag{9}$$

The 0-component of the 4-vector j^{μ} represents density. It follows that its dimension is $[L^{-3}]$ and the electromagnetic interaction (8) is a term of the Lagrangian density. For this reason, it is a Lorentz scalar whose dimension is $[L^{-4}]$. Hence,

a quantum particle can carry electric charge provided a self-consistent 4-current can be defined for it. Furthermore, a self-consistent definition of density is also required for a construction the Hilbert space where density is used for defining its inner product.

It is well known that a self-consistent 4-current can be defined for a Dirac particle [8, see pp. 8,9,23,24]

$$j^{\mu} = e\bar{\psi}\gamma^{\mu}\psi. \tag{10}$$

This expression has properties that are consistent with general requirements of a quantum theory. In particular, the 4-current is related to a construction of a Hilbert space. Here the density $\psi^{\dagger}\psi$ is the 0-component of the 4-current (10). As required, this quantity has the dimension $[L^{-3}]$. Thus, electromagnetic interactions of charged spin-1/2 Dirac particles are properly described by the Dirac equation.

Let us turn to the case of a charged KG or W^{μ} particle. Here the appropriate wave function has the dimension $[L^{-1}]$. This dimension proves that it cannot be used for constructing a self-consistent Hilbert space. Indeed, let ϕ denote a function of such a Hilbert space and let O be an operator operating on this space. Then, the expectation value of O is

$$< O >= \int \phi^{*} O \phi d^{3}x. \tag{11}$$

Now, $< O >$ and O have the same dimension. Therefore ϕ must have the dimension $[L^{-3/2}]$. This requirement is not satisfied by the function ϕ of a KG particle or by W^{μ} because here the dimension is $[L^{-1}]$. Hence, there is no Hilbert space for a KG or W^{μ} particle. For this reason, there is also no Hamiltonian for these functions, because a Hamiltonian is an operator operating on a Hilbert space. Analogous results are presented for the specific case of the KG equation [10].

The dimension $[L^{-1}]$ of the KG and the W^{μ} functions also yields another very serious mathematical problem. Indeed, in order to have a dimension $[L^{-4}]$, their Lagrangian density has terms that are *bilinear* in derivatives with respect to the space-time coordinates. Thus, the KG Lagrangian density is (4) and the W^{μ} Lagrangian density takes the following form [11, see p. 307]

$$\mathcal{L}_{W} = -\frac{1}{4}(\partial_{\mu}W_{\nu} - \partial_{\nu}W_{\mu} + gW_{\mu} \times W_{\nu})^{2}. \tag{12}$$

As is well known, an operation of the Legendre transformation (6) on a Lagrangian density that is *linear* in time derivatives yields an expression that is *independent* of time derivatives. Thus, the Dirac Lagrangian density (3) yields a Hamiltonian that is free of time derivatives. On the other hand, the Hamiltonian density of the KG and W^{μ} particles depends on time derivatives. Indeed, using (5) , one infers that for these particles, the Hamiltonian density depends quadratically on the Hamiltonian. Hence, there is no explicit expression for the Hamiltonian of the KG and the W^{μ} particles.

Two results are directly obtained from the foregoing discussion. The Fock space, which denotes the occupation number of particles in appropriate states, is based on functions of the associated Hilbert space. Hence, in the case of KG or W^{μ} function there are very serious problems with the construction of a Fock space because these functions have no Hilbert space. Therefore, one also wonders what is the meaning of the creation and the annihilation operators of QFT.

Another result refers to the 4-current. Thus, both the KG equations and the W^{μ} function have a 4-current that satisfies (9) [11, see p. 12] and [12, see p. 199]. However, the contradictions derived above prove the following important principle: *The continuity relation* (9) *is just a necessary condition for an acceptable 4-current. This condition is not sufficient and one must also confirm that a theory that uses a 4-current candidate is contradiction free.*

The contradictions which are described above hold for the KG and the $W^{\pm}$ particles provided that these particles are elementary pointlike quantum mechanical objects which are described by a function of the form $\psi(x^{\mu})$. Hence, *in order to avoid contradictions with the existence of charged pions and $W^{\pm}$, one must demand that the pions and the $W^{\pm}$ are composite particles.* Several aspects of this conclusion are discussed in the next section. It should also be noted that the results of this section are consistent with Dirac's lifelong objection to the KG equation [13].

4 Discussion

An examination of textbooks provides a simple argument supporting the main conclusion of this work. Indeed, quantum mechanics is known for more than 80 years. It turns out that the Hamiltonian problem of the hydrogen atom of a Dirac particle is discussed adequately in relevant textbooks [8, 14]. By contrast, in spite of the long duration of quantum mechanics as a valid theory, an appropriate discussion of the Hamiltonian solution of a hydrogen-like atom of a relativistic electrically charged integral spin particle is not presented in textbooks. Note that the operator on the left hand side of the KG equation [14, see p. 886]

$$(\partial_{\mu} + ieA_{\mu})g^{\mu\nu}(\partial_{\nu} + ieA_{\nu})\phi = -m^{2}\phi \tag{13}$$

is *not* related to a Hamiltonian because (13) is a Lorentz scalar whereas the Hamiltonian is a 0-component of a 4-vector.

An analogous situation holds for the Hilbert and the Fock spaces that are created from functions on which the Hamiltonian operates. Thus, in the case of a Dirac particle, the density $\psi^{\dagger}\psi$ is the 0-component of the conserved 4-current (10). This expression is suitable for a definition of the Hilbert space inner product of any pair of integrable functions

$$(\psi_{i}^{\dagger}, \psi_{j}) \equiv \int \psi_{i}^{\dagger}\psi_{j}\, d^{3}x. \tag{14}$$

Indeed, it is derivative free and this property enables the usage of the Heisenberg picture which is based on time-

independent functions. Integration properties prove that (14) is linear in $\psi_i^\dagger$ and ψ_j. Thus,

$$(a\psi_i^\dagger + b\psi_k^\dagger, \psi_j) = a(\psi_i^\dagger, \psi_j) + b(\psi_k^\dagger, \psi_j).$$

Furthermore, $(\psi_i^\dagger, \psi_i)$ is a real non-negative number that vanishes if and only if $\psi_i \equiv 0$. These properties are required from a Hilbert space inner product. It turns out that the construction of a Hilbert space is the cornerstone used for calculating successful solutions of the Dirac equation and of its associated Pauli and Schroedinger equations as well.

By contrast, in the case of particles having an integral spin, one cannot find in the literature an explicit construction of a Hilbert space. Indeed, the $[L^{-1}]$ dimension of their functions proves that the simple definition of an inner product in the form $\int \phi_i^* \phi_j \, d^3x$ has the dimension $[L]$ which is unacceptable. An application of the 0-component of these particles 4-current [11, see p. 12] and [12, see p. 199] is not free of contradictions. Thus, the time derivative included in these expressions prevents the usage of the Heisenberg picture. Relation (7) proves that in the case of a charged particle the density depends on *external* quantities. These quantities may vary in time and for this reason it cannot be used in a definition of a Hilbert space inner product. In the case of the W^μ function, the expression is inconsistent with the linearity required from a Hilbert space inner product.

The results found in this work apply to particles described by a function of the form

$$\psi(x^\mu). \tag{15}$$

Their dependence on a single set of four space-time coordinates x^μ means that they describe an elementary pointlike particle. For example, this kind of function cannot adequately describe a pion because this particle is not an elementary particle but a quark-antiquark bound state. Thus, it consists of a quark-antiquark pair which are described by *two* functions of the form (15). For this reason, one function of the form (15) cannot describe a pion simply because a description of a pion should use a larger number of degrees of freedom. It follows that the existence of a π^+, which is a spin-0 charged particle, does not provide an experimental refutation of the theoretical results obtained above.

Some general aspects of this work are pointed out here. There are two kinds of objects in electrodynamics of Dirac particles: massive charged spin-1/2 particles and charge-free photons. The dimension of a Dirac function is $[L^{-3/2}]$ and the dimension of the electromagnetic 4-potential is $[L^{-1}]$. Now, the spin of any interaction carrying particle must take an integral value in order that the matrix element connecting initial and final states should not vanish. The dimension of an interaction carrying particle must be $[L^{-1}]$ so that the Lagrangian density interaction term have the dimension $[L^{-4}]$. These properties must be valid for particles that carry any kind of interaction between Dirac-like particles. Hence, the pions and the $W^\pm$ have integral spin and dimension $[L^{-1}]$. However, in order to have a self-consistent Hilbert and Fock spaces, a function describing an elementary massive particle must have the dimension $[L^{-3/2}]$. Neither a KG function nor the W^μ function satisfies this requirement.

The conclusion stating that the continuity equation (9) is only a *necessary condition* required from a physically acceptable 4-current and that further consistency tests must be carried out, looks like a new result of this work that has a general significance.

Before discussing the state of the $W^\pm$ charged particles, let us examine the strength of strong interactions. Each of the following arguments proves that strong interactions yield extremely relativistic bound states and that the interaction part of the Hamiltonian swallows a large portion of the quarks' mass.

A. Antiquarks have been measured directly in the proton [15, see p. 282]. This is a clear proof of the extremely relativistic state of hadrons. Indeed, for reducing the overall mass of the proton, it is energetically "profitable" to add the mass of two quarks because the increased interaction is very strong.

B. The mass of the ρ meson is about five times greater than the pion's mass. Now these mesons differ by the relative spin alignment of their quark constituents. Evidently, spin interaction is a relativistic effect and the significant π, ρ mass difference indicates that strong interactions are very strong indeed.

C. The pion is made of a u, d quark-antiquark pair and its mass is about $140\ MeV$. Measurements show that there are mesons made of the u, d flavors whose mass is greater than $2000\ MeV$ [6]. Hence, strong interactions consume most of the original mass of quarks.

D. Let us examine the pion and find an estimate for the intensity of its interactions. The first objective is to find an estimate for the strength of the momentum of the pion's quarks. The calculation is done in units of fm, and $1\ fm^{-1} \simeq 200\ MeV$. The pion's spatial size is somewhat smaller than that of the proton [16]. Thus, let us assume that the pion's quark-antiquark pair are enclosed inside a box whose size is $2.2\ fm$ and the pion's quark wave function vanishes on its boundary. For the x-component, one finds that the smallest absolute value of the momentum is obtained from a function of the form $\sin(\pi x/2.2)$. Hence, the absolute value of this component of the momentum is $\pi/2.2$. Thus, for the three spatial coordinates, one multiplies this number by $\sqrt{3}$ and another factor of 2 accounts for the quark-antiquark pair. It follows that the absolute value of the momentum enclosed inside a pion is

$$|\,\mathbf{p}\,| \simeq 1000\ MeV. \tag{16}$$

This value of the momentum is much greater than the

pion's mass. It means that the system is extremely relativistic and (16) is regarded as the quarks' kinetic energy. Thus, the interaction consumes about 6/7 of the kinetic energy *and* the entire mass of the quark-antiquark pair. In other word, the pion's kinetic energy is about 7 times greater than its final mass. It is interesting to compare these values to the corresponding quantities of the positronium, which is an electron-positron system bound by the electromagnetic force. Here the ratio of the kinetic energy to the final mass is about 7/1000000. On the basis of this evidence one concludes that strong interactions must be much stronger than the experimental mass of the pion.

Relying on these arguments and on the theoretical conclusion stating that the $W^{\pm}$ must be composite objects, it is concluded that the $W^{\pm}$ particles contain one top quark. Thus, the W^{+} is a superposition of three meson families: $t\bar{d}$, $t\bar{s}$ and $t\bar{b}$. Here the top quark mass is $173\,GeV$ and the mass of the W is $80\,GeV$ [16]. The difference indicates the amount swallowed by strong interactions. This outcome also answers the question where are the mesons of the top quark? The fact that the $W^{\pm}$ is a composite particle which is a superposition of mesons is inconsistent with the electroweak theory and this fact indicates that the foundations of this theory should be examined.

Another result of this analysis pertains to recent reports concerning the existence of a new particle whose mass is about $125\,GeV$ and its width is similar to that of the $W^{\pm}$ [2,3]. Thus, since the mass of the top quark is about $173\,GeV$ and this quantity is by far greater than the mass of any other quark, it makes sense to regard the $125\,GeV$ particle as a $t\bar{t}$ meson. For this reason, the $t\bar{t}$ meson is heavier than the $80\,GeV$ $W^{\pm}$ which consists of one top quark and a lighter quark.

A $t\bar{t}$ mesonic structure of the $125\,GeV$ particle explains naturally its quite sharp disintegration into two photons. Indeed, the disintegration of a bound system of charged spin-1/2 particle-antiparticle pair into two photons is a well known effect of the ground state of the positronium and of the π^0 meson. On the other hand, the results obtained in this work deny the $W^{+}W^{-}$ disintegration channel of the $125\,GeV$ particle, because the Ws are composite particles and a $W^{+}W^{-}$ system is made of two quark-antiquark pairs. For this reason, their two photon disintegration should be accompanied by other particles. Hence, a $W^{+}W^{-}$ two photon outcome should show a much wider energy distribution. This kind of $W^{+}W^{-} \rightarrow \gamma\gamma$ disintegration is inconsistent with the quite narrow width of the $125\,GeV$ data. It turns out that for a Higgs mass of $125\,GeV$, Standard Model Higgs decay calculations show that the $W^{+}W^{-} \rightarrow \gamma\gamma$ channel is dominant [17, see section 2.3.1]. However, it is proved in this work that the $W^{+}W^{-}$ disintegration channel of the $125\,GeV$ particle is incompatible with the data. Therefore, one denies the Higgs boson interpretation of the $125\,GeV$ particle found at the LHC [2, 3]. This outcome is consistent with the Higgs boson inherent contradictions which are discussed elsewhere [10].

Submitted on July 29, 2012 / Accepted on August 10, 2012

References

1. Wigner E. P. The unreasonable effectiveness of mathematics in the natural sciences. *Communications in Pure and Applied Mathematics*, 1960, v. 13, 1–14.
2. The ATLAS Collaboration. Latest Results from ATLAS Higgs Search. http://www.atlas.ch/news/2012/latest-results-from-higgs-search.html.
3. The CMS Collaboration. Evidence for a new state decaying into two photons in the search for the standard model Higgs boson in pp collisions. http://cdsweb.cern.ch/record/1460419/files/HIG-12-015-pas.pdf.
4. Bjorken J. D. and Drell S. D. Relativistic Quantum Fields. McGraw, New York, 1965.
5. Sterman G. An Introduction to Quantum Field Theory. Cambridge University Press, Cambridge, 1993.
6. Rohrlich F. Classical Charged Particle. Addison-Wesley, Reading MA, 1965.
7. Einstein A. Albert Einstein in His Own Words. Portland House, New York, 2000.
8. Bjorken J. D. and Drell S. D. Relativistic Quantum Mechanics. McGraw, New York, 1964.
9. Landau L. D., Lifshitz E. M. The classical theory of fields. Elsevier, Amsterdam, 2005.
10. Comay E. Physical Consequences of Mathematical Principles. *Progress in Physics*, 2009, v. 4, 91–98.
11. Weinberg S. The Quantum Theory of Fields. Cambridge University Press, Cambridge, 1996.
12. Pauli W., Weisskopf V. The quantization of the scalar relativistic wave equation. *Helvetica Physica Acta*, 1934, v. 7, 709–731. English translation: Miller A. I. Early Quantum Electrodynamics. Cambridge University Press, Cambridge, 1994. pp. 188–205. (In the text, page references apply to the English translation.)
13. Dirac P. A. M. Mathematical Foundations of Quantum Theory, in: Marlow A. R. (Editor), Mathematical Foundations of Quantum Theory. Academic, New York, 1978.
14. Messiah A. Quantum Mechanics v. 2, North-Holland, Amsterdam, 1966.
15. Perkins D. H. Introduction to high energy physics. Addison-Wesley, Menlo Park (CA), 1987.
16. Amsler C. et al. Review of particle physics. *Physics Letters B*, 2008, v. 667, 1–1340.
17. Djouadi A. The anatomy of electroweak symmetry breaking Tome I: The Higgs boson in the Standard Model. *Physics Reports*, 2008 v. 457, 1–216. arXiv: hep-ph/0503172v2.

Should the Wave-Function be a Part of the Quantum Ontological State?

Aurélien Drezet

Institut Neel, 25 rue des Martyrs 38042, Grenoble, France. E-mail: aurelien.drezet@grenoble.cnrs.fr

We analyze the recent no go theorem by Pusey, Barrett and Rudolph (PBR) concerning ontic and epistemic hidden variables. We define two fundamental requirements for the validity of the result. We finally compare the models satisfying the theorem with the historical hidden variable approach proposed by de Broglie and Bohm.

1 Introduction

Recently, a new no go theorem by M. Pusey, J. Barret and T. Rudolph (PBR in the following) was published [1]. The result concerns ontic versus epistemic interpretations of quantum mechanics. Epistemic means here knowledge by opposition to "ontic" or ontological and is connected with the statistical interpretation defended by Einstein. This of course stirred much debates and discussions to define the condition of validity of this fundamental theorem. Here, we discuss two fundamental requirements necessary for the demonstration of the result and also discuss the impact of the result on possible hidden variable models. In particular, we will stress the difference between the models satisfying the PBR theorem and those who apparently contradict its generality.

2 The axioms of the PBR theorem

In order to identify the main assumptions and conclusions of the PBR theorem we first briefly restate the original reasoning of ref. 1 in a slightly different language. In the simplest version PBR considered two non orthogonal pure quantum states $|\Psi_1\rangle = |0\rangle$ and $|\Psi_2\rangle = [|0\rangle + |1\rangle]/\sqrt{2}$ belonging to a 2-dimensional Hilbert space $\mathbb{E}$ with basis vectors $\{|0\rangle, |1\rangle\}$. Using a specific (nonlocal) measurement M with basis $|\xi_i\rangle$ ($i \in [1, 2, 3, 4]$) in $\mathbb{E} \otimes \mathbb{E}$ (see their equation 1 in [1]) they deduced that $\langle\xi_1|\Psi_1 \otimes \Psi_1\rangle = \langle\xi_2|\Psi_1 \otimes \Psi_2\rangle = \langle\xi_3|\Psi_2 \otimes \Psi_1\rangle = \langle\xi_4|\Psi_2 \otimes \Psi_2\rangle = 0$. In a second step they introduced hypothetical "Bell's like" hidden variables λ and wrote implicitly the probability of occurrence $P_M(\xi_i; j, k) = |\langle\xi_i|\Psi_j \otimes \Psi_k\rangle|^2$ in the form:

$$P_M(\xi_i; j, k) = \int P_M(\xi_i|\lambda, \lambda')\varrho_j(\lambda)\varrho_k(\lambda')d\lambda d\lambda' \qquad (1)$$

where $i \in [1, 2, 3, 4]$ and $j, k \in [1, 2]$. One of the fundamental axiom used by PBR (axiom 1) is an independence criterion at the preparation which reads $\varrho_{j,k}(\lambda, \lambda') = \varrho_j(\lambda)\varrho_k(\lambda')$. In these equations we introduced the conditional "transition" probabilities $P_M(\xi_i|\lambda, \lambda')$ for the outcomes ξ_i supposing the hidden state λ, λ' associated with the two independent Q-bits are given. The fundamental point here is that $P_M(\xi_i|\lambda, \lambda')$ is independent of Ψ_1, Ψ_2. This a very natural looking-like axiom (axiom 2) which was implicit in ref. 1 and was not further discussed by the authors. We will see later what are the consequence of its abandonment.

For now, from the definitions and axioms we obtain:

$$\left.\begin{array}{l} \int P_M(\xi_1|\lambda, \lambda')\varrho_1(\lambda)\varrho_1(\lambda')d\lambda d\lambda' = 0 \\ \int P_M(\xi_2|\lambda, \lambda')\varrho_1(\lambda)\varrho_2(\lambda')d\lambda d\lambda' = 0 \\ \int P_M(\xi_3|\lambda, \lambda')\varrho_2(\lambda)\varrho_1(\lambda')d\lambda d\lambda' = 0 \\ \int P_M(\xi_4|\lambda, \lambda')\varrho_2(\lambda)\varrho_2(\lambda')d\lambda d\lambda' = 0 \end{array}\right\}. \qquad (2)$$

The first line implies $P_M(\xi_1|\lambda, \lambda') = 0$ if $\varrho_1(\lambda)\varrho_1(\lambda') \neq 0$. This condition is always satisfied if λ and λ' are in the support of ϱ_1 in the λ-space and λ'-space. Similarly, the fourth line implies $P_M(\xi_4|\lambda, \lambda') = 0$ if $\varrho_2(\lambda)\varrho_2(\lambda') \neq 0$ which is again always satisfied if λ and λ' are in the support of ϱ_2 in the λ-space and λ'-space. Finally, the second and third lines imply $P_M(\xi_2|\lambda, \lambda') = 0$ if $\varrho_1(\lambda)\varrho_2(\lambda') \neq 0$ and $P_M(\xi_3|\lambda, \lambda') = 0$ if $\varrho_1(\lambda)\varrho_2(\lambda') \neq 0$.

Taken separately these four conditions are not problematic. But, in order to be true simultaneously and then to have

$$P_M(\xi_i|\lambda, \lambda') = 0 \qquad (3)$$

for a same pair of λ, λ' (with $[i = 1, 2, 3, 4]$) the conditions require that the supports of ϱ_1 and ϱ_2 intersect. If this is the case Eq. 3 will be true for any pair λ, λ' in the intersection.

However, this is impossible since from probability conservation we must have $\sum_{i=1}^{i=4} P_M(\xi_i|\lambda, \lambda') = 1$ for every pair λ, λ'. Therefore, we must necessarily have

$$\varrho_2(\lambda) \cdot \varrho_1(\lambda) = 0 \quad \forall\lambda \qquad (4)$$

i.e. that ϱ_1 and ϱ_2 have nonintersecting supports in the λ-space. Indeed, it is then obvious to see that Eq. 2 is satisfied if Eq. 4 is true. This constitutes the PBR theorem for the particular case of independent prepared states Ψ_1, Ψ_2 defined before. PBR generalized their results for more arbitrary states using similar and astute procedures described in ref. 1.

If this theorem is true it would apparently make hidden variables completely redundant since it would be always possible to define a bijection or relation of equivalence between the λ space and the Hilbert space: (loosely speaking we could in principle make the correspondence $\lambda \Leftrightarrow \psi$). Therefore it would be as if λ is nothing but a new name for Ψ itself. This would justify the label "ontic" given to this kind of interpretation in opposition to "epistemic" interpretations ruled out by the PBR result.

However, the PBR conclusion stated like that is too strong as it can be shown by carefully examining the assumptions necessary for the derivation of the theorem. Indeed, using the independence criterion and the well known Bayes-Laplace formula for conditional probability we deduce that the most general Bell's hidden variable probability space should obey the following rule

$$P_M(\xi_i; j, k) = \int P_M(\xi_i|\Psi_j, \Psi_k, \lambda, \lambda')\varrho_j(\lambda)\varrho_k(\lambda')d\lambda d\lambda' \quad (5)$$

in which, in contrast to equation 1, the transition probabilities $P_M(\xi_i|\Psi_j, \Psi_k, \lambda, \lambda')$ now depend explicitly on the considered quantum states Ψ_j, Ψ_k. We point out that unlike λ, Ψ is in this more general approach not a stochastic variable. This difference is particularly clear in the ontological interpretation of ref. 3 where Ψ plays the role of a dynamic guiding wave for the stochastic motion of the particle. Clearly, relaxing this PBR premise has a direct effect since we lose the ingredient necessary for the demonstration of Eq. 4. (more precisely we are no longer allowed to compare the product states $|\Psi_j \otimes \Psi_k\rangle$ as it was done in ref. 1). Indeed, in order for Eq. 2 to be simultaneously true for the four states ξ_i (where $P_M(\xi_i|\Psi_j, \Psi_k, \lambda, \lambda')$ now replace $P_M(\xi_i|\lambda, \lambda')$) we must have

$$\left.\begin{array}{l} P_M(\xi_1|\Psi_1, \Psi_1, \lambda, \lambda') = 0, P_M(\xi_2|\Psi_1, \Psi_2, \lambda, \lambda') = 0 \\ P_M(\xi_3|\Psi_2, \Psi_1, \lambda, \lambda') = 0, P_M(\xi_4|\Psi_2, \Psi_2, \lambda, \lambda') = 0 \end{array}\right\}. \quad (6)$$

Obviously, due to the explicit Ψ dependencies, Eq. 6 doesn't anymore enter in conflict with the conservation probability rule and therefore doesn't imply Eq. 4. In other words the reasoning leading to PBR theorem doesn't run if we abandon the axiom stating that

$$P_M(\xi_i|\Psi_j, \Psi_k, \lambda, \lambda') := P_M(\xi_i|\lambda, \lambda') \quad (7)$$

i.e. that the dynamic should be independent of Ψ_1, Ψ_2. This analysis clearly shows that Eq. 7 is a fundamental prerequisite (as important as the independence criterion at the preparation) for the validity of the PBR theorem [4]. In our knowledge this point was not yet discussed [5].

3 Discussion

Therefore, the PBR deduction presented in ref. 1 is actually limited to a very specific class of Ψ-epistemic interpretations. It fits well with the XIXth like hidden variable models using Liouville and Boltzmann approaches (i.e. models where the transition probabilities are independent of Ψ) but it is not in agreement with neo-classical interpretations, e.g. the one proposed by de Broglie and Bohm [3], in which the transition probabilities $P_M(\xi|\lambda, \Psi)$ and the trajectories depend explicitly and contextually on the quantum states Ψ (the de Broglie-Bohm theory being deterministic these probabilities can only reach values 0 or 1 for discrete observables ξ). As an illustration, in the de Broglie Bohm model for a single particle the spatial position $\mathbf{x}$ plays the role of λ. This model doesn't require the condition $\varrho_1(\lambda) \cdot \varrho_2(\lambda) = |\langle \mathbf{x}|\Psi_1\rangle|^2 \cdot |\langle \mathbf{x}|\Psi_1\rangle|^2 = 0$ for all λ in clear contradiction with Eq. 4. We point out that our reasoning doesn't contradict the PBR theorem *per se* since the central axiom associated with Eq. 7 is not true anymore for the model considered. In other words, if we recognize the importance of the second axiom discussed before (i.e. Eq. 7) the PBR theorem becomes a general result which can be stated like that:

i) If Eq. 7 applies then the deduction presented in ref. 1 shows that Eq. 4 results and therefore $\lambda \leftrightarrow \Psi$ which means that epistemic interpretation of Ψ are equivalent to ontic interpretations. This means that a XIXth like hidden variable models is not really possible even if we accept Eq. 7 since we don't have any freedom on the hidden variable density $\rho(\lambda)$.

ii) However, if Eq. 7 doesn't apply then the ontic state of the wavefunction is already assumed - because it is a variable used in the definition of $P_M(\xi|\lambda, \Psi)$. This shows that ontic interpretation of Ψ is necessary. This is exemplified in the de Broglie-Bohm example: in this model, the "quantum potential" is assumed to be a real physical field which depends on the magnitude of the wavefunction, while the motion of the Bohm particle depends on the wavefunction's phase. This means that the wavefunction has ontological status in such a theory. This is consistent with the spirit of PBR's paper, but the authors didn't discussed that fundamental point.

We also point out that in the de Broglie-Bohm ontological approach the independence criterion at the preparation is respected in the regime considered by PBR. As a consequence, it is not needed to invoke retrocausality to save epistemic approaches.

It is important to stress how Eq. 4, which is a consequence of Eq. 7, contradicts the spirit of most hidden variable approaches. Consider indeed, a wave packet which is split into two well spatially localized waves Ψ_1 and Ψ_2 defined in two isolated regions 1 and 2. Now, the experimentalist having access to local measurements ξ_1 in region 1 can define probabilities $|\langle \xi_1|\Psi_1\rangle|^2$. In agreement with de Broglie and Bohm most proponents of hidden variables would now say that the hidden variable λ of the system actually present in box 1 should not depends of the overall phase existing between Ψ_1 and Ψ_2. In particular the density of hidden variables $\varrho_\Psi(\lambda)$ in region 1 should be the same for $\Psi = \Psi_1 + \Psi_2$ and $\Psi' = \Psi_1 - \Psi_2$ since $|\langle \xi_1|\Psi\rangle|^2 = |\langle \xi_1|\Psi'\rangle|^2$ for every local measurements ξ_1 in region 1. This is a weak form of separability which is accepted even within the so exotic de Broglie Bohm's approach but which is rejected for those models accepting Eq. 4.

This point can be stated differently. Considering the state $\Psi = \Psi_1 + \Psi_2$ previously discussed we can imagine a two-slits like interference experiment in which the probability for detecting outcomes x_0, ie., $|\langle x_0|\Psi\rangle|^2$ vanish for some values x_0 while $|\langle x_0|\Psi_1\rangle|^2$ do not. For those models satisfying Eq. 7 and forgetting one instant PBR theorem we deduce that in the hypothetical common support of $\varrho_{\Psi_1}(\lambda)$ and $\varrho_\Psi(\lambda)$ we must have

$P_M(\xi_0|\lambda) = 0$ since this transition probability should vanish in the support of Ψ. This allows us to present a "*poor-man*" version of the PBR's theorem: The support of $\varrho_{\Psi_1}(\lambda)$ can not be completely included in the support of $\varrho_\Psi(\lambda)$ since otherwise $P_M(\xi_0|\lambda) = 0$ would implies $|\langle x_0|\Psi_1\rangle|^2 = 0$ in contradiction with the definition. PBR's theorem is stronger than that since it shows that in the limit of validity of Eq. 7 the support of $\varrho_{\Psi_1}(\lambda)$ and $\varrho_\Psi(\lambda)$ are necessarily disjoints. Consequently, for those particular models the hidden variables involved in the observation of the observable ξ_0 are not the same for the two states Ψ and Ψ_1. This is fundamentally different from de Broglie-Bohm approach where λ (e.g. $\mathbf{x}(t_0)$) can be the same for both states.

This can lead to an interesting form of quantum correlation even with one single particle. Indeed, following the well known scheme of the Wheeler Gedanken experiment one is free at the last moment to either observe the interference pattern (i.e. $|\langle x_0|\Psi\rangle|^2 = 0$) or to block the path 2 and destroy the interference (i.e. $|\langle x_0|\Psi_1\rangle|^2 = 1/2$). In the model used by Bohm where Ψ acts as a guiding or pilot wave this is not surprising: blocking the path 2 induces a subsequent change in the propagation of the pilot wave which in turn affects the particle trajectories. Therefore, the trajectories will not be the same in these two experiments and there is no paradox. However, in the models considered by PBR there is no guiding wave since Ψ serves only to label the non overlapping density functions of hidden variable $\varrho_{\Psi_1}(\lambda)$ and $\varrho_\Psi(\lambda)$. Since the beam block can be positioned after the particles leaved the source the hidden variable are already predefined (i.e. they are in the support of $\varrho_\Psi(\lambda)$). Therefore, the trajectories are also predefined in those models and we apparently reach a contradiction since we should have $P_M(\xi_0|\lambda) = 0$ while we experimentally record particles with properties ξ_0. The only way to solve the paradox is to suppose that some mysterious quantum influence is sent from the beam blocker to the particle in order to modify the path during the propagation and correlate it with presence or absence of the beam blocker. However, this will be just equivalent to the hypothesis of the de Broglie-Bohm guiding wave and quantum potential and contradicts apparently the spirit and the simplicity of Ψ-independent models satisfying Eq. 7.

4 An example

We point out that despite these apparent contradictions it is easy to create an hidden variable model satisfying all the requirements of PBR theorem. Let any state $|\Psi\rangle$ be defined at time $t = 0$ in the complete basis $|k\rangle$ of dimension N as $|\Psi\rangle = \sum_k^N \Psi_k|k\rangle$ with $\Psi_k = \Psi'_k + i\Psi''_k$. We introduce two hidden variables λ, and μ as the N dimensional real vectors $\lambda := [\lambda_1, \lambda_2..., \lambda_N]$ and $\mu := [\mu_1, \mu_2..., \mu_N]$. We thus write the probability $P_M(\xi, t, \Psi) = |\langle\xi|U(t)\Psi\rangle|^2$ of observing the outcome ξ at time t as

$$\int P_M(\xi, t|\{\lambda_k, \mu_k\}_k) \prod_k^N \delta(\Psi'_k - \lambda_k)\delta(\Psi''_k - \mu_k)d\lambda_k d\mu_k = P_M(\xi, t|\{\Psi'_k, \Psi''_k\}_k) = |\sum_k \langle\xi|U(t)|k\rangle\Psi_k|^2 \quad (8)$$

where $U(t)$ is the Schrodinger evolution operator. Since Ψ can be arbitrary we thus generally have in this model

$$P_M(\xi, t|\{\lambda_k, \mu_k\}_k) = |\sum_k \langle\xi|U(t)|k\rangle(\lambda_k + i\mu_k)|^2.$$

The explicit time variation is associated with the unitary evolution $U(t)$ which thus automatically includes contextual local or non local influences (coming from the beam blocker for example). We remark that this model is of course very formal and doesn't provide a better understanding of the mechanism explaining the interaction processes. The hidden variable model we proposed is actually based on a earlier version shortly presented by Harrigan and Spekkens in ref. [2]. We completed the model by fixing the evolution probabilities and by considering the complex nature of wave function in the Dirac distribution. Furthermore, this model doesn't yet satisfy the independence criterion if the quantum state is defined as $|\Psi\rangle_{12} = |\Psi\rangle_1 \otimes |\Psi\rangle_2$ in the Hilbert tensor product space. Indeed, the hidden variables $\lambda_{12,k}$ and $\mu_{12,k}$ defined in Eq. 8 are global variables for the system 1,2. If we write

$$|\Psi\rangle_{12} = \sum_{n,p}^{N_1,N_2} \Psi_{12;n,p}|n\rangle_1 \otimes |p\rangle_2 = \sum_{n,p}^{N_1,N_2} \Psi_{1;n}\Psi_{2;p}|n\rangle_1 \otimes |p\rangle_2 \quad (9)$$

the indices k previously used become a doublet of indices n, p and the probability

$$P_M(\xi, t|\Psi_{12}) = |\sum_{n,p}^{N_1,N_2} \langle\xi|U(t)|n, p\rangle_{12}\Psi_{12;n,p}|^2$$

in Eq. 8 reads now:

$$\int P_M(\xi, t|\{\lambda_{12;n,p}, \mu_{12;n,p}\}_{n,p}) \times \prod_n^{N_1}\prod_p^{N_2} \delta(\Psi'_{12;n,p} - \lambda_{12;n,p}) \times\delta(\Psi''_{12;n,p} - \mu_{12;n,p})d\lambda_{12;n,p}d\mu_{12;n,p} = P_M(\xi, t|\{\Psi'_{12;n,p}, \Psi''_{12;n,p}\}_{n,p}) \quad (10)$$

which indeed doesn't show any explicit separation of the hidden variables density of states for subsystems 1 and 2. However, in the case where Eq. 9 is valid we can alternatively

introduce new hidden variable vectors λ_1, λ_2 and μ_1, μ_2 such that $P_M(\xi, t|\Psi_{12})$ reads now:

$$\int P_M(\xi, t|\{\lambda_{1;n}, \lambda_{2;p}, \mu_{1;n}, \mu_{2;n}\}_{n,p}) \times \prod_n^{N_1} \delta(\Psi'_{1;n} - \lambda_{1;n})\delta(\Psi''_{1;n} - \mu_{1;n})d\lambda_{1;n}d\mu_{1;n} \times \prod_p^{N_2} \delta(\Psi'_{2;p} - \lambda_{2;p})\delta(\Psi''_{2;p} - \mu_{2;p})d\lambda_{2;n}d\mu_{2;p} = P_M(\xi, t|\{\Psi'_{1;n}, \Psi 2'_{2;p}, \Psi''_{1;n}, \Psi''_{2;n}\}_{n,p}). \quad (11)$$

Clearly here the density of probability $\varrho_{12}(\lambda_1, \lambda_2, \mu_1, \mu_2)$ can be factorized as $\varrho_1(\lambda_1, \mu_1) \cdot \varrho_2(\lambda_2, \mu_2)$ where

$$\varrho_1(\lambda_1, \mu_1) = \prod_n^{N_1} \delta(\Psi'_{1;n} - \lambda_{1;n})\delta(\Psi''_{1;n} - \mu_{1;n})$$

$$\varrho_2(\lambda_2, \mu_2) = \prod_n^{N_2} \delta(\Psi'_{2;n} - \lambda_{2;n})\delta(\Psi''_{2;n} - \mu_{2;n}) \quad (12)$$

Therefore, the independence criterion at the preparation (i.e. axiom 1) is here fulfilled.

Additionally, since by definition Eq. 8 and 10 are equivalent we have

$$P_M(\xi, t|\{\Psi'_{1;n}, \Psi 2'_{2;p}, \Psi''_{1;n}, \Psi''_{2;n}\}_{n,p}) = P_M(\xi, t|\{\Psi'_{12;n,p}, \Psi''_{12;n,p}\}_{n,p}). \quad (13)$$

Moreover, since $\Psi_{1;n}$ and $\Psi_{2;n}$ can have any complex values the following relation holds for any value of the hidden variables:

$$P_M(\xi, t|\{\lambda_{1;n}, \lambda_{2;p}, \mu_{1;n}, \mu_{2;n}\}_{n,p}) = P_M(\xi, t|\{\lambda_{12;n,p}, \mu_{12;n,p}\}_{n,p}) \quad (14)$$

with $\lambda_{12;n,p} + i\mu_{12;n,p} = (\lambda_{1;n} + i\mu_{1;n})(\lambda_{2;p} + i\mu_{2;p})$. This clearly define a bijection or relation of equivalence between the hidden variables $[\lambda_{12}, \mu_{12}]$ on the one side and $[\lambda_1, \mu_1, \lambda_2, \mu_2]$ on the second side. Therefore, we showed that it is always possible to define hidden variables satisfying the 2 PBR axioms: i) statistical independence at the sources or preparation

$$\varrho_{j,k}(\lambda, \lambda') = \varrho_j(\lambda)\varrho_k(\lambda')$$

(if Eq. 9 is true) and ii) Ψ-independence at the dynamic level, i.e., satisfying Eq. 7. We point out that the example discussed in this section proves that the PBR theorem is not only formal since we explicitly proposed a hidden variable model satisfying the two requirements of PBR theorem. This model is very important since it demonstrates that the de Broglie Bohm approach is not the only viable hidden variable theory. It is interesting to observe that our model corresponds to the case discussed in point i) of section 3 while Bohm's approach corresponds to the point labeled ii) in the same section 3. Additionally, the new model is fundamentally stochastic (since the transition probabilities $P_M(\xi|\lambda)$ have numerical values in general different from 1 or 0) while Bohm's approach is deterministic.

5 Conclusion

To conclude, we analyzed the PBR theorem and showed that beside the important independence criterion already pointed out in ref. 1 there is a second fundamental postulate associated with Ψ-independence at the dynamic level (that is our Eq. 7). We showed that by abandoning this prerequisite the PBR conclusion collapses. We also analyzed the nature of those models satisfying Eq. 7 and showed that despite their classical motivations they also possess counter intuitive features when compared for example to de Broglie Bohm model. We finally constructed an explicit model satisfying the PBR axioms. More studies would be be necessary to understand the physical meaning of such hidden variable models.

Submitted on August 20, 2012 / Accepted on August 22, 2012

References

1. Pusey M.F., Barrett J., Rudolph T. On the reality of the quantum state. *Nature Physics*, 2012, v. 8, 478–478.
2. Harrigan N., Spekkens R. W. Einstein, incompleteness, and the epistemic view of quantum states. *Foundations of Physics*, 2010, v. 40, 125–157.
3. de Broglie L. La mécanique ondulatoire et la structure atomique de la matière et du rayonnement. *Journal de Physique et le Radium*, 1927, v. 8, 225–241.
4. We point out that we will not save the naive interpretation of PBR's theorem by using the "implicit" notation $\Lambda = (\lambda, \Psi)$ and by writing $\int P_M(\xi|\Lambda)\varrho(\Lambda)d\Lambda$ in order to hide the Ψ dependence $P_M(\xi|\Lambda) := P_M(\xi|\lambda, \Psi)$. Indeed, at the end of the day we have to compare different Ψ states and the explicit notation becomes necessary. The importance of Eq. 7 for PBR's result can therefore not be avoided.
5. See also A. Drezet, arXiv:1203.2475 (12 March 2012) for a detailed discussion of PBR's theorem.

Relativistic Dynamics in the Vicinity of a Uniformly Charged Sphere

Chifu E. Ndikilar* and Lucas W. Lumbi†

*Department of Physics, Federal University Dutse, P.M.B. 7156, Dutse, Nigeria
†Department of Physics, Nasarawa State University, Nigeria
E-mail: ebenechifu@yahoo.com

The motion of test and photons in the vicinity of a uniformly charged spherically symmetric mass distribution is studied using a newly developed relativistic dynamical approach. The derived expressions for the mechanical energy and acceleration vector of test particles have correction terms of all orders of c^{-2}. The expression for the gravitational spectral shift also has additional terms which are functions of the electric potential on the sphere.

1 Introduction

In a recent article [1], the relativistic dynamical approach to the study of classical mechanics in homogeneous spherical distributions of mass (Schwarzschild's gravitational field) was introduced. Here, the relativistic dynamical theory of a combined gravitational and electric field within homogeneous spherical distributions of mass is developed.

2 Motion of test particles

According to Maxwell's theory of electromagnetism, the electric potential energy for a particle of non-zero rest mass in an electric field V_e is given by

$$V_e = q\,\Phi_e\,, \tag{1}$$

where q is the electric charge of the particle and Φ_e is the electric scalar potential. Also, from Newton's dynamical theory, it is postulated [2] that the instantaneous mechanical energy for test particles in combined gravitational and electric fields is defined by

$$E \;=\; T + V_g + V_e\,, \tag{2}$$

where T is the total relativistic kinetic energy and V_g is the gravitational potential. From [1], T and V_g in Schwarzschild's gravitational field are given by

$$T \;=\; \left[\left(1-\frac{u^2}{c^2}\right)^{-1/2} - 1\right] m_0 c^2 \tag{3}$$

and the instantaneous relativistic gravitational potential energy (V_g) for a particle of nonzero rest mass is

$$V_g \;=\; m_p\Phi_e \;=\; -\left(1-\frac{u^2}{c^2}\right)^{-1/2}\frac{GMm_0}{r}\,, \tag{4}$$

where $\Phi_e = \frac{-GM}{r}$ is the gravitational scalar potential in a spherically symmetric gravitational field, $r > R$, the radius of the homogeneous sphere, G is the universal gravitational constant, c is the speed of light in vacuum, m_p is the passive mass of the test particle, M is the mass of the static homogeneous spherical mass, m_0 is the rest mass of the test particle and u is the instantaneous velocity of the test particle. Also, for a uniformly charged spherically symmetric mass the electric potential energy is given as

$$V_e \;=\; \frac{qQ}{4\pi\epsilon_0 r}\,, \tag{5}$$

where Q is the total charge on the sphere and q is the charge on the test particle. Thus, the instantaneous mechanical energy for the test particle can be written more explicitly as

$$E \;=\; m_0c^2\left[\left(1-\frac{GM}{c^2r}\right)\left(1-\frac{u^2}{c^2}\right)^{-1/2} - 1\right] + \frac{qQ}{4\pi\epsilon_0 r}\,. \tag{6}$$

The expression for the instantaneous mechanical energy has post Newton and post Einstein correction terms of all orders of c^{-2}. The relativistic dynamical equation of motion for particles of non-zero rest masses in combined electric and gravitational fields is given as [2]

$$\frac{d}{d\tau}\overline{P} \;=\; -m_p\overline{\nabla}\Phi_g - q\overline{\nabla}\Phi_e\,, \tag{7}$$

where $\overline{P}$ is the instantaneous linear momentum of the test particles . Thus, in this field, the relativistic dynamical equation of motion for test particles is given explicitly as

$$\begin{aligned}\frac{d}{d\tau}\left[\left(1-\frac{u^2}{c^2}\right)^{-1/2}\overline{u}\right] &= \\ &= -\left(1-\frac{u^2}{c^2}\right)^{-1/2}\overline{\nabla}\Phi_g - \frac{q}{m_0}\overline{\nabla}\Phi_e\end{aligned} \tag{8}$$

or

$$\begin{aligned}\overline{a} + \frac{1}{2c^2}\left(1-\frac{u^2}{c^2}\right)^{-1}\frac{d}{d\tau}(u^2)\overline{u} &= \\ &= \frac{GM}{r^2} - \frac{q}{m_0}\left(1-\frac{u^2}{c^2}\right)^{1/2}\overline{\nabla}\Phi_e\,,\end{aligned} \tag{9}$$

where $\overline{a}$ is the instantaneous acceleration vector of the test particles and thus the time equation of motion is obtained as

$$a_{x_0} + \frac{1}{2c^2}\left(1-\frac{u^2}{c^2}\right)^{-1}\frac{d}{d\tau}(u^2)u_{x^0} \;=\; 0\,. \tag{10}$$

The azimuthal equation of motion is

$$\dot{r}\sin\theta\,\dot{\phi} + r\cos\theta\,\dot{\theta}\,\dot{\phi} + r\sin\theta\,\ddot{\phi} + \\ + \frac{1}{2c^2}\left(1-\frac{u^2}{c^2}\right)^{-1}\frac{d}{d\tau}(u^2)\,u_\phi \;=\; 0\,. \quad (11)$$

The polar equation of motion is given as

$$r\,\ddot{\theta} + \dot{r}\,\dot{\theta} + \frac{1}{2c^2}\left(1-\frac{u^2}{c^2}\right)^{-1}\frac{d}{d\tau}(u^2)\,u_\theta \;=\; 0 \quad (12)$$

and the radial equation of motion is

$$a_r + \frac{1}{2c^2}\left(1-\frac{u^2}{c^2}\right)^{-1}\frac{d}{d\tau}(u^2)u_r = \\ = -\frac{GM}{r^2} - \frac{q}{m_0}\left(1-\frac{u^2}{c^2}\right)^{1/2}\overline{\nabla}\Phi_e\,. \quad (13)$$

As in [1], the equations have correction terms not found in the general relativistic approach.It is also worth remarking that the homogeneous charge distribution on the sphere and the charge on the test particle affects only the radial component of the motion and hence the other components are the same as those of an uncharged sphere [1].

3 Motion of photons

From [1], it can be deduced that the instantaneous gravitational potential energy of a photon is given as

$$V_g = -\frac{h\nu}{c^2}\,\frac{GM}{r}\,. \quad (14)$$

The instantaneous electric potential energy of the photon is given [2] as

$$V_e = -\frac{h\nu}{c^2}\,\overline{\nabla}\Phi_e \quad (15)$$

or more explicitly in this field as

$$V_e = -\frac{h\nu}{c^2}\,\frac{Q}{4\pi\epsilon_0 r}\,. \quad (16)$$

Also, the instantaneous kinetic energy of the photon [1] is given as

$$T = h(\nu-\nu_0)\,. \quad (17)$$

Thus, the instantaneous mechanical energy of a photon in this combined gravitational and electric field is obtained as

$$E \;=\; h(\nu-\nu_0) - \frac{h\nu}{c^2 r}\left(GM + \frac{Q}{4\pi\epsilon_0}\right). \quad (18)$$

Suppose at $r = r_0$, $E = E_0$ then

$$E_0 \;=\; -\frac{kh\nu_0}{c^2 r_0}\,, \quad (19)$$

where

$$k \;=\; GM + \frac{Q}{4\pi\epsilon_0}\,. \quad (20)$$

Thus, from the principle of conservation of mechanical energy

$$-\frac{kh\nu_0}{c^2 r_0} \;=\; h(\nu-\nu_0) - \frac{kh\nu}{c^2 r} \quad (21)$$

or

$$\nu \;=\; \nu_0\left(1-\frac{k}{c^2 r_0}\right)\left(1-\frac{k}{c^2 r}\right)^{-1}. \quad (22)$$

Equation (22) is the expression for spectral shift in this field with contributions from the gravitational and electric potentials. It has corrections of all orders of c^{-2}.

Also, for photons, the instantaneous linear momentum is given [1] as

$$\overline{P} = \frac{h\nu}{c^2}\,\overline{u}\,. \quad (23)$$

Hence, as in Newton's dynamical theory, the equation of motion of photons in this field is obtained from equation (7) as

$$\frac{d}{d\tau}\,(\nu\overline{u}) \;=\; -\nu\,\overline{\nabla}\Phi_g - \frac{qc^2}{h}\,\overline{\nabla}\Phi_e\,. \quad (24)$$

Thus the presence of an electric field introduces an additional term to the expression for the equation of motion of photons.

4 Conclusion

This article provides a crucial link between gravitational and electric fields. It also introduces, hither to unknown corrections of all orders of c^{-2} to the expressions of instantaneous mechanical energy, spectral shift and equations of motion for test particles and photons in combined spherically symmetric gravitational and electric field.

Submitted on August 17, 2012 / Accepted on August 22, 2012

References

1. Chifu E.N. Relativistic Dynamical Theory for Test Particles and Photons in Static Spherically Symmetric Gravitational Fields. *Progress in Physics*, 2012, v. 2, 3–5.
2. Howusu S.X.K. Complete Dynamical Theories of Physics. Jos University Press, Jos, 2010.

A Bipolar Model of Oscillations in a Chain System for Elementary Particle Masses

Andreas Ries
Universidade Federal de Pernambuco, Centro de Tecnologia e Geociências, Laboratório de Dispositivos e Nanoestruturas,
Rua Acadêmico Hélio Ramos s/n, 50740-330 Recife – PE, Brazil
E-mail: andreasries@yahoo.com

The philosophical idea of a bipolar nature (the Chinese "Yin and Yang") is combined with the mathematical formalism of a fractal scaling model originally published by Müller in this journal. From this extension new rules for the calculation of proton and electron resonances via continued fractions are derived. The set of the 117 most accurately determined elementary particle masses (all with error < 0.13%) was expressed through this type of continued fractions. Only one outlier was found, in all other cases the numerical errors were smaller than the standard deviation. Speaking in terms of oscillation properties, the results suggest that the electron is an inverted or mirrored oscillation state of the proton and vice versa. A complete description of elementary particle masses by the model of oscillations in a chain system is only possible when considering both, proton and electron resonances.

1 Introduction

The mass distribution of elementary particles is still an unsolved mystery of physics. According tho the Standard Model, mass is given by arbitrary variable couplings to the Higgs boson, and the coupling is then adequately adjusted to reproduce the experimentally observed mass.

However, the particle mass spectrum is not completely chaotic, and some groupings are clearly visible. Several attempts have already been made to obtain equations to describe regularities in the set of elementary particle masses.

For instance Greulich [1] calculated the masses of all fundamental elementary particles (those with a lifetime $> 10^{-24}$ seconds) with an inaccuracy of approximately 1% using the equation

$$\frac{m_{particle}}{m_{electron}} = \frac{N}{2\alpha},$$

where α is the fine structure constant (= 1/137.036), and N is an integer variable.

Paasch [2] assigned each elementary particle mass a position on a logarithmic spiral. As a result, particles then accumulate on straight lines.

A study from India [3] revealed a tendency for successive mass differences between particles to be close to an integer multiple or integer fraction of 29.315 MeV. The value 29.315 MeV is the mass difference between a muon and a neutral pion.

Even more recently Boris Tatischeff published a series of articles [4–8] dealing with fractal properties of elementary particle masses. He even predicted tentatively the masses of some still unobserved particles [5].

An other fractal scaling model was used in a previous article of the present author [9], and a set of 78 accurately measured elementary particle masses was expressed in the form of continued fractions. This underlying model was originally published by Müller [10–12], and its very basic idea is to treat all protons as fundamental oscillators connected through the physical vacuum. This leads to the idea of a chain of equal harmonic proton oscillators with an associated logarithmic spectrum of eigenfrequencies which can be expressed through continued fractions. Particle masses are interpreted as proton resonance states and expressed in continued fraction form. However, the results obtained in reference [9] were not completely satisfying since around 14% of the masses were outliers, i.e. could not be reproduced by this model.

A more recent article [13] revealed that electron resonance states exist analogously which serves now as the basis for further extensions of Müller's model. From this starting point, the present article proposes a new version of the model developed with the objective to reproduce all elementary particle masses.

2 Data sources and computational details

Masses of elementary particles (including the proton and electron reference masses) were taken from the Particle Data Group website [14] and were expressed in GeV throughout the whole article. An electronic version of these data is available for downloading. Quark masses were eliminated from the list because it has not been possible to isolate quarks.

Some of the listed particle masses are extremely accurate and others have a quite high measurement error. Figure 1 shows an overview of the particle masses and their standard deviations (expressed in % of the particle mass). It can be roughly estimated that more or less 60% of the particles have a standard deviation (SD) below 0.13%; this set of excellent measurements consists of 117 particles and only this selection of very high quality data was used for the numerical analysis and extension of Müller's model.

Table 1: Continued fraction representations of the lepton masses (x = -1.75083890054)

Particle	Mass ± SD [GeV] Continued fraction representation(s)	Numerical error [GeV]
electron	$5.10998910 \times 10^{-4} \pm 1.3 \times 10^{-11}$ P [x; -6 | 12, -6]	1.21×10^{-15}
μ^-	$1.05658367 \times 10^{-1} \pm 4.0 \times 10^{-9}$ P [x; 0 | -6, -9, -e-1, 12, -6, -15] E [-x; 3 | e+1, e+1, -e-1, e+1, 9, -48, e+1, -e-1]	2.45×10^{-10} 3.06×10^{-9}
τ^-	$1.77682 \pm 1.6 \times 10^{-4}$ P [0; 0 | e+1, 6, -e-1, e+1, -e-1, -e-1] P [x; 3 | -e-1, -e-1, 231] E [0; 9 | -e-1, 6, -e-1, -e-1, -6] E [-x; 6 | 6, e+1, -45]	4.52×10^{-5} 2.50×10^{-6} 6.81×10^{-5} 1.92×10^{-5}

Fig. 1: Overview of particle masses on the logarithmic number line together with their standard deviations expressed in % of the mass. Note that a few particles with very low or high mass or percentage error were omitted for clarity (e.g. electron, muon, proton, gauge bosons).

Table 2: Continued fraction representations of the boson masses (x = -1.75083890054)

Particle	Mass ± SD [GeV] Continued fraction representation(s)	Numerical error [GeV]
W^+	$8.0399 \times 10^1 \pm 2.3 \times 10^{-2}$ E [0; 12 | -81, e+1, (24)]	3.23×10^{-5}
Z^0	$9.11876 \times 10^1 \pm 2.1 \times 10^{-3}$ P [x; 6 | 9, -e-1, -15, -e-1, e+1] E [0; 12 | 30, -6, (12)]	1.01×10^{-3} 7.23×10^{-4}

For consistency with previous articles on this topic, the following abbreviations and conventions for the numerical analysis hold:

Calculation method:
The considered particle mass is transformed into a continued fraction according to the equations

$$\ln \frac{m_{particle}}{m_{electron}} = p + S, \qquad \ln \frac{m_{particle}}{m_{proton}} = p + S,$$

where p is the phase shift and S is the continued fraction (e is Euler's number)

$$S = n_0 + \cfrac{e}{n_1 + \cfrac{e}{n_2 + \cfrac{e}{n_3 + ...}}}. \qquad (1)$$

The continued fraction representation $p+S$ is abbreviated as $[p; n_0 \mid n_1, n_2, n_3, \dots]$, where the free link n_0 is allowed to be $0, \pm 3, \pm 6, \pm 9 \dots$ and all partial denominators n_i can take the values $e+1, -e-1, \pm 6, \pm 9, \pm 12 \dots$. In the tables these abbreviations were marked with P or E, in order to indicate proton or electron resonance states.

For practical reasons only 18 partial denominators were determined. Next, the particle mass was repeatedly calculated from the continued fraction, every time considering one more partial denominator. As soon as the calculated mass value (on the linear scale) was in the interval "mass ± standard deviation", no further denominators were considered and the resulting fractions are displayed in the tables. In some rare cases, this procedure provides a mass value just a little inside the interval and considering the next denominator would match the measured value almost exactly. In such cases this denominator is then additionally given in brackets.

The numerical error is always understood as the absolute value of the difference between the measured particle mass and the mass calculated from the corresponding continued fraction representation.

In order to avoid machine based rounding errors, numerical values of continued fractions were always calculated using the the Lenz algorithm as indicated in reference [15].

Outliers:
A particle mass is considered as an outlier (i.e. does not fit into the here extended Müller model) when its mass, as calculated from the corresponding continued fraction representation provides a value outside the interval "particle mass ± standard deviation".

3 Results and discussion

3.1 Fundamental philosophical idea

Chinese philosophy is dominated by the concept of "Yin and Yang" describing an indivisible whole of two complementary effects (male–female, day–night, good–bad, etc.). This means that everything has two opposite poles, and both poles are necessary to understand the whole thing (e.g. male can only be understood completely because female also exists as the opposite).

Table 3: Continued fraction representations of the light unflavored mesons (x = -1.75083890054)

Particle	Mass ± SD [GeV] Continued fraction representation(s)	Numerical error [GeV]
π^+	$1.3957018 \times 10^{-1} \pm 3.5 \times 10^{-7}$	
	P [x; 0 | -18, 6, 6, (-117)]	7.67×10^{-10}
	E [0; 6 | -6, -e-1, e+1, -e-1, 48]	1.68×10^{-7}
π^0	$1.349766 \times 10^{-1} \pm 6.0 \times 10^{-7}$	
	E [0; 6 | -6, -6, -6, 6, -e-1]	2.49×10^{-7}
η^0	$5.47853 \times 10^{-1} \pm 2.4 \times 10^{-5}$	
	P [0; 0 | -6, e+1, -e-1, 6, -e-1, 12]	6.52×10^{-7}
	E [0; 6 | e+1, -e-1, e+1, -6, -e-1, e+1, (24)]	2.51×10^{-7}
$\rho(770)^{0,+}$	$7.7549 \times 10^{-1} \pm 3.4 \times 10^{-4}$	
	P [0; 0 | -15, e+1, (-174)]	1.73×10^{-7}
$\omega(782)^0$	$7.8265 \times 10^{-1} \pm 1.2 \times 10^{-4}$	
	P [0; 0 | -15, (243)]	2.10×10^{-7}
	E [-x; 6 | -6, -6, e+1, -9, (135)]	4.51×10^{-11}
$\eta'(958)^0$	$9.5778 \times 10^{-1} \pm 6.0 \times 10^{-5}$	
	P [0; 0 | 132, (30)]	6.81×10^{-7}
	E [-x; 6 | -12, -e-1, -6, (-24)]	4.66×10^{-7}
$\phi(1020)^0$	$1.019455 \pm 2.0 \times 10^{-5}$	
	P [0; 0 | 33, -12, e+1]	4.92×10^{-6}
$f_2(1270)^0$	$1.2751 \pm 1.2 \times 10^{-3}$	
	P [0; 0 | 9, -21]	3.84×10^{-4}
	P [x; 3 | -e-1, e+1, -6, (36)]	1.87×10^{-5}
	E [-x; 6 | 39, -e-1]	3.78×10^{-4}
$f_1(1285)^0$	$1.2818 \pm 6.0 \times 10^{-4}$	
	P [0; 0 | 9, -9, -6]	2.46×10^{-5}
	P [x; 3 | -e-1, e+1, -6, -e-1, e+1]	9.88×10^{-5}
	E [-x; 6 | 36, -6]	1.20×10^{-4}
$a_2(1320)^{0,+}$	$1.3183 \pm 5.0 \times 10^{-4}$	
	P [0; 0 | 9, -e-1, e+1, -e-1, e+1, -e-1, e+1]	4.50×10^{-4}
	P [x; 3 | -e-1, e+1, 186]	5.66×10^{-6}
	E [-x; 6 | 27, -e-1, e+1, -e-1]	2.98×10^{-4}
$f_1(1420)^0$	$1.4264 \pm 9.0 \times 10^{-4}$	
	P [0; 0 | 6, 6, -6, (-39)]	1.64×10^{-6}
	P [x; 3 | -e-1, 6, 24]	9.34×10^{-5}
	E [-x; 6 | 15, -15]	3.29×10^{-5}
$\rho_3(1690)^{0,+}$	$1.6888 \pm 2.1 \times 10^{-3}$	
	P [0; 0 | e+1, e+1, -e-1, (-51)]	1.95×10^{-5}
	P [x; 3 | -e-1, -6, -e-1, e+1]	5.29×10^{-4}
	E [0; 9 | -e-1, e+1, 12]	8.78×10^{-4}

Table 4: Continued fraction representations of masses of the strange mesons (x = -1.75083890054)

Particle	Mass ± SD [GeV] Continued fraction representation(s)	Numerical error [GeV]
K^+	$4.93677 \times 10^{-1} \pm 1.6 \times 10^{-5}$	
	P [0; 0 | -e-1, -6, e+1, 45]	5.65×10^{-7}
	E [0; 6 | e+1, -e-1, -e-1, 15, -e-1]	6.96×10^{-6}
	E [-x; 6 | -e-1, e+1, e+1, 6, e+1, -6]	4.04×10^{-6}
K^0, K^0_S, K^0_L	$4.97614 \times 10^{-1} \pm 2.4 \times 10^{-5}$	
	E [-x; 6 | -e-1, e+1, e+1, -e-1, -e-1, e+1, e+1]	4.73×10^{-6}
$K^*(892)^+$	$8.9166 \times 10^{-1} \pm 2.6 \times 10^{-4}$	
	P [0; 0 | -54, e+1]	6.63×10^{-5}
	E [-x; 6 | -9, -6, 6]	6.13×10^{-5}
$K^*(892)^0$	$8.9594 \times 10^{-1} \pm 2.2 \times 10^{-4}$	
	P [0; 0 | -60, e+1, -e-1]	1.47×10^{-4}
	E [-x; 6 | -9, -e-1, -6]	5.48×10^{-5}
$K_2^*(1430)^+$	$1.4256 \pm 1.5 \times 10^{-3}$	
	P [0; 0 | 6, 6, -6]	7.56×10^{-4}
	P [x; 3 | -e-1, 6, 30]	1.08×10^{-4}
	E [-x; 6 | 15, -21]	1.40×10^{-4}
$K_2^*(1430)^0$	$1.4324 \pm 1.3 \times 10^{-3}$	
	P [0; 0 | 6, 6, 6]	3.72×10^{-4}
	P [x; 3 | -e-1, 6, 9, (-e-1)]	6.31×10^{-4}
	E [-x; 6 | 15, -6, e+1, (36)]	5.37×10^{-7}

In physics we can find a number of analogous dualities, for instance: positive and negative charges, north and south magnetic poles, particles and antiparticles, emission and absorption of quanta, destructive and constructive interference of waves, nuclear fusion and fission, and in the widest sense also Newton's principle "action = reaction".

From these observations an interesting question arises: does such a duality also exist in the model of oscillations in a chain system, and how must this model be extended to make the "Yin-Yang" obvious and visible?

Applying this idea to Müller's model, it must be claimed that the fundamental spectrum of proton resonances must have an opposite, an anti-oscillation or inverted oscillation spectrum. What could it be?

We know that these proton master-oscillations are stable, so the theorized counter-oscillations must belong to a particle with similar lifetime than the proton. Consequently the electron is the only particle that could be a manifestation of such an inverted oscillation.

Now the concept of an inverted oscillation must be translated into a mathematical equation. According to Müller's standard model, we can express the electron mass as a proton resonance and the proton mass as an electron resonance:

$$\ln \frac{m_{electron}}{m_{proton}} = p + \mathrm{S_p},$$

$$\ln \frac{m_{proton}}{m_{electron}} = p + \mathrm{S_e},$$

where p is the phase shift (with value 0 or 1.5) and S the continued fraction as discussed in previous papers (given in equation (1)). Obviously for $p \neq 0$, $\mathrm{S_p} \neq \mathrm{S_e}$, and this is the starting point for the further modification of the model. We have to adjust the phase shift (when different from zero) in such a way that both continued fractions become opposite in the sense of oscillation information. This means that the denominators of $\mathrm{S_p}$ and $\mathrm{S_e}$ must be the same, but with opposite

sign. If

$$S_p = n_0 + \cfrac{e}{n_1 + \cfrac{e}{n_2 + \cfrac{e}{n_3 + ...}}},$$

then must hold for S_e:

$$S_e = -n_0 + \cfrac{e}{-n_1 + \cfrac{e}{-n_2 + \cfrac{e}{-n_3 + ...}}}.$$

Mathematically it is now obvious that one equation must be modified by a minus sign and we have to write:

$$\ln \frac{m_{electron}}{m_{proton}} = p + S_p, \quad (2)$$

$$\ln \frac{m_{proton}}{m_{electron}} = -p + S_e, \quad (3)$$

However, this is not yet a complete set of rules to find new continued fraction representations of the proton and electron; in order to arrive at a conclusion, it is absolutely necessary to develop further physical ideas.

Idea 1 – Length of continued fractions

The resulting continued fractions S_p and S_e should be short. A previous article already suggested that short fractions are associated with stability [9]. However, the fractions must not be too short. The fundamental oscillators must be represented by the simplest variant of a chain of oscillators. This is a single mass hold via two massless flexible strings between two motionless, fixed walls. This setup leads to 3 parameters determining the eigenfrequency of the chain, the mass value and the two different lengths of the strings. Consequently the continued fraction also should have 3 free parameters (the free link and two denominators). This idea solves the conceptual problem of a "no information oscillation". When expressing the electron mass as a proton resonance, then $\ln \frac{m_{electron}}{m_{proton}} = p + S$, and p must not have values determining S as zero or any other integer number ($\pm 3, \pm 6, \pm 9...$). In such a case no continued fraction can be written down, and the oscillation would not have any property.

Idea 2 – Small denominators

According to Müller's theory, a high positive or negative denominator locates the data point in a fluctuating zone. Consequently the considered property should be difficult to be kept constant. From all our observations, it is highly reasonable to believe that proton and electron masses are constant even over very long time scales. Therefore their masses cannot be located too deep inside a fluctuation zone. In this study, the maximum value of the denominators was tentatively limited to ± 18.

Idea 3 – The free link

The calculation

$$\ln \frac{m_{electron}}{m_{proton}} \approx -7.51$$

Table 5: Continued fraction representations of masses of the charmed, and charmed strange mesons (x = -1.75083890054)

Particle	Mass ± SD [GeV] Continued fraction representation(s)	Numerical error [GeV]
D^+	$1.86957 \pm 1.6 \times 10^{-4}$	
	P [0; 0 | e+1, 12, 27]	2.92×10^{-5}
	E [0; 9 | -e-1, 9, 39]	5.45×10^{-6}
	E [-x; 6 | 6, -213]	1.95×10^{-8}
D^0	$1.86480 \pm 1.4 \times 10^{-4}$	
	P [0; 0 | e+1, 12, -e-1, -6]	1.03×10^{-4}
	E [0; 9 | -e-1, 9, -12, e+1]	1.29×10^{-4}
	E [-x; 6 | 6, 129]	6.40×10^{-6}
$D^*(2007)^0$	$2.00693 \pm 1.6 \times 10^{-4}$	
	P [0; 0 | e+1, -18, -e-1, e+1, -e-1]	8.59×10^{-5}
	P [x; 3 | -6, 6, 15]	7.91×10^{-5}
	E [0; 9 | -e-1, -78]	3.94×10^{-5}
	E [-x; 6 | 6, -e-1, 6, e+1, 6]	2.21×10^{-5}
$D^*(2010)^+$	$2.01022 \pm 1.4 \times 10^{-4}$	
	P [0; 0 | e+1, -18, (-102)]	4.53×10^{-7}
	P [x; 3 | -6, 6, 6, (-21)]	5.72×10^{-6}
	E [0; 9 | -e-1, -63, (6)]	3.23×10^{-7}
	E [-x; 6 | 6, -e-1, 6, -12]	1.62×10^{-4}
$D_1(2420)^0$	$2.4213 \pm 6.0 \times 10^{-4}$	
	P [0; 0 | e+1, -e-1, 6, -e-1, 6]	4.56×10^{-4}
	P [x; 3 | -9, -102]	3.68×10^{-6}
	E [0; 9 | -6, e+1, -e-1, 9, -e-1]	4.37×10^{-4}
	E [-x; 6 | e+1, 27, e+1, -e-1, e+1]	4.10×10^{-4}
$D_2^*(2460)^0$	$2.4626 \pm 7.0 \times 10^{-4}$	
	P [0; 0 | e+1, -e-1, e+1, 18, -9]	5.21×10^{-6}
	E [0; 9 | -6, e+1, -15]	9.58×10^{-5}
	E [-x; 6 | e+1, 348]	1.02×10^{-5}
$D_2^*(2460)^+$	$2.4644 \pm 1.9 \times 10^{-3}$	
	P [0; 0 | e+1, -e-1, e+1, 24]	7.45×10^{-5}
	P [x; 3 | -9, -e-1, -e-1, (e+1, 18)]	2.40×10^{-6}
	E [0; 9 | -6, e+1, -18]	1.14×10^{-4}
	E [-x; 6 | e+1, 663]	1.95×10^{-6}
D_s^+	$1.96845 \pm 3.3 \times 10^{-4}$	
	P [0; 0 | e+1, -54, (-e-1, -15)]	3.13×10^{-7}
	P [x; 3 | -6, e+1, 6, (-63)]	6.81×10^{-7}
	E [0; 9 | -e-1, 42, e+1, -e-1]	2.34×10^{-4}
	E [-x; 6 | 6, -e-1, -e-1, -6]	2.00×10^{-4}
D_s^{*+}	$2.1123 \pm 5.0 \times 10^{-4}$	
	P [x; 3 | -6, -12, -e-1]	4.00×10^{-4}
	E [0; 9 | -e-1, -9, 6, -e-1, (-18, -45)]	3.42×10^{-9}
	E [-x; 6 | e+1, e+1, -e-1, e+1, -e-1, e+1, -e-1]	4.70×10^{-4}
$D_{s0}^*(2317)^+$	$2.3178 \pm 6.0 \times 10^{-4}$	
	P [0; 0 | e+1, -e-1, -27]	4.57×10^{-4}
	E [0; 9 | -e-1, -e-1, e+1, -e-1, -39]	1.50×10^{-5}
$D_{s1}(2460)^+$	$2.4595 \pm 6.0 \times 10^{-4}$	
	P [0; 0 | e+1, -e-1, e+1, 12, (15)]	1.19×10^{-6}
	P [x; 3 | -9, -6, e+1, (-9)]	5.71×10^{-5}
	E [0; 9 | -6, e+1, -12, e+1, (12)]	4.66×10^{-6}
	E [-x; 6 | e+1, 189]	5.06×10^{-5}
$D_{s1}(2536)^+$	$2.53528 \pm 2.0 \times 10^{-4}$	
	P [0; 0 | e+1, -e-1, e+1, -e-1, e+1, e+1, -6]	3.89×10^{-5}
	E [0; 9 | -6, 6, -36]	1.87×10^{-5}
	E [-x; 6 | e+1, -21, e+1, -e-1, (-e-1)]	1.88×10^{-5}
$D_{s2}^*(2573)^+$	$2.5726 \pm 9.0 \times 10^{-4}$	
	P [x; 3 | -12, e+1, 15]	8.95×10^{-5}
	E [0; 9 | -6, 9, 6]	2.24×10^{-4}

Table 6: Continued fraction representations of masses of the bottom mesons (including strange and charmed mesons) (x = -1.75083890054)

Particle	Mass ± SD [GeV] Continued fraction representation(s)	Numerical error [GeV]
B^+	$5.27917 \pm 2.9 \times 10^{-4}$ P [x; 3 | 6, -9, 6, 6]	8.81×10^{-5}
B^0	$5.27950 \pm 3.0 \times 10^{-4}$ P [x; 3 | 6, -9, 6, (33)]	4.56×10^{-6}
$B^{*0,+}$	$5.3251 \pm 5.0 \times 10^{-4}$ P [x; 3 | 6, -6, -6, e+1, e+1]	1.09×10^{-4}
$B_2^*(5747)^{0,+}$	$5.743 \pm 5.0 \times 10^{-3}$ E [0; 9 | 9, -e-1, -12]	2.95×10^{-4}
B_s^0	$5.3663 \pm 6.0 \times 10^{-4}$ P [x; 3 | 6, -6, e+1, e+1, (9)]	4.93×10^{-6}
$B_s{}^{*0}$	$5.4154 \pm 1.4 \times 10^{-3}$ P [x; 3 | 6, -e-1, -e-1, 12]	2.19×10^{-5}
$B_{s2}^*(5840)^0$	$5.8397 \pm 6.0 \times 10^{-4}$ P [x; 3 | e+1, e+1, -e-1, e+1, -9, (-6)]	4.08×10^{-5}
B_c^+	$6.277 \pm 6.0 \times 10^{-3}$ P [x; 3 | e+1, 6, -153] E [0; 9 | 6, 6, -e-1, e+1, (63)]	1.21×10^{-5} 1.71×10^{-6}

leads to a value between the principal nodes -6 and -9. From this is follows that in the continued fractions, the free link n_0 can only take the values ±6 and ±9.

Idea 4 – Effect of canceling denominators

Elementary particles can be divided in two groups: the vast majority with an extremely short half-life, and a small set with comparable longer lifetime. When analyzing the more stable particles with Müller's standard model, already a striking tendency can be discovered that especially the sum of the free link and the first denominators tends to be zero.

Examples:

The τ can be interpreted as proton resonance and the full continued fraction representation, as calculated by the computer is: P [0; 0 | e+1, 6, -e-1, e+1, -e-1, -e-1, (6)]. Note that in the end, every determination of a continued fraction results in an infinite periodical alternating sequence of the denominators e+1 and -e-1, which is always omitted here. Without significantly changing the mass value, the fraction can be rewritten: P [0; 0 | e+1, 6, -e-1, e+1, -e-1, -e-1, (e+1, -6)], and then the sum of all denominators equals zero.

The full continued fraction for the charged pion is:
E [0; 6 | -6, -e-1, e+1, -e-1, 48, (-e-1, 6, -24, e+1, -e-1, 12)]. It can be seen that the free link and the first 3 denominators cancel successively. Then this changes. A minimal manipulation leads to:
E [0; 6 | -6, -e-1, e+1, -e-1, 48, (-e-1, 6, -48, e+1, -6, e+1)].

The full continued fraction for the neutral pion is:
E [0; 6 | -6, -6, -6, 6, -e-1, (12, -12, e+1, -e-1, e+1, 45, 6)]. Here we have only to eliminate the 11^{th} denominator (45) and the sum equals zero.

Table 7: Continued fraction representations of masses of the $c\bar{c}$ mesons (x = -1.75083890054)

Particle	Mass ± SD [GeV] Continued fraction representation(s)	Numerical error [GeV]
$\eta_c(1S)^0$	$2.9803 \pm 1.2 \times 10^{-3}$ P [x; 3 | -30, e+1, -e-1] E [0; 9 | -9, e+1, (-216)] E [-x; 6 | e+1, -e-1, 18, -e-1, e+1]	6.56×10^{-5} 7.34×10^{-7} 8.84×10^{-4}
$J/\psi(1S)^0$	$3.096916 \pm 1.1 \times 10^{-5}$ E [-x; 6 | e+1, -e-1, e+1, 6, -e-1, e+1, 6, e+1, (-18)]	1.19×10^{-8}
$\chi_{c0}(1P)^0$	$3.41475 \pm 3.1 \times 10^{-4}$ P [x; 3 | 63, e+1, (57)] E [0; 9 | -15, e+1, -e-1, (-12)]	6.99×10^{-8} 9.48×10^{-6}
$\chi_{c1}(1P)^0$	$3.51066 \pm 7.0 \times 10^{-5}$ no continued fraction found	outlier
$h_c(1P)^0$	$3.52541 \pm 1.6 \times 10^{-4}$ P [x; 3 | 36, 6, (-24)]	1.94×10^{-6}
$\chi_{c2}(1P)^0$	$3.55620 \pm 9.0 \times 10^{-5}$ P [x; 3 | 33, -9, e+1, -e-1, e+1] E [0; 9 | -18, 21, -e-1]	7.52×10^{-5} 5.36×10^{-5}
$\eta_c(2S)^0$	$3.637 \pm 4.0 \times 10^{-3}$ E [0; 9 | -21, (66)]	5.00×10^{-6}
$\psi(2S)^0$	$3.68609 \pm 4.0 \times 10^{-5}$ E [0; 9 | -24, e+1, e+1, e+1, e+1]	6.30×10^{-6}
$\psi(3770)^0$	$3.77292 \pm 3.5 \times 10^{-4}$ E [0; 9 | -30, e+1, (-12)]	5.90×10^{-5}
$\chi_{c2}(2P)^0$	$3.9272 \pm 2.6 \times 10^{-3}$ P [x; 3 | 15, -27] E [0; 9 | -51, -9, e+1]	1.47×10^{-4} 1.10×10^{-4}
$\psi(4040)^0$	$4.0390 \pm 1.0 \times 10^{-3}$ P [x; 3 | 12, e+1, -e-1, (495)] E [0; 9 | -108, -e-1]	3.14×10^{-8} 5.66×10^{-4}
$\psi(4160)^0$	$4.1530 \pm 3.0 \times 10^{-3}$ P [x; 3 | 12, -e-1, -e-1, (6)] E [0; 9 | 915]	1.88×10^{-5} 1.36×10^{-5}
$\psi(4415)^0$	$4.421 \pm 4.0 \times 10^{-3}$ P [x; 3 | 9, 81] E [0; 9 | 42, -6]	4.82×10^{-5} 3.64×10^{-4}

The full continued fraction for the η^0 is:
P [0; 0 | -6, e+1, -e-1, 6, -e-1, 12, (-9, -12, -e-1, e+1, -e-1, -e-1, e+1, -e-1, e+1, e+1)].
Again the first 4 denominators form a zero sum, then the 7^{th} denominator (-9) interrupts this canceling. Without significant change of the numerical value, this fraction could be shortened and rewritten: P [0; 0 | -6, e+1, -e-1, 6, -e-1, 12, (-12, e+1)].

When interpreting η^0 as electron resonance, again adding the free link to the first 5 denominators gives zero:
E [0; 6 | e+1, -e-1, e+1, -6, -e-1, e+1, (24)]. We can add and rewrite: E [0; 6 | e+1, -e-1, e+1, -6, -e-1, e+1, (24, -e-1, -24)].

A completely different case is the neutron; here the con-

Table 8: Continued fraction representations of masses of the $b\bar{b}$ mesons (x = -1.75083890054)

Particle	Mass ± SD [GeV] Continued fraction representation(s)	Numerical error [GeV]
$\Upsilon(1S)^0$	$9.46030 \pm 2.6 \times 10^{-4}$	
	P [0; 3 | -e-1, -12, -87]	1.02×10^{-5}
	E [-x; 9 | -e-1, e+1, -12, -63]	9.33×10^{-6}
$\chi_{b0}(1P)^0$	$9.8594 \pm 5.0 \times 10^{-4}$	
	E [0; 9 | e+1, -e-1, -e-1, e+1, -9, -e-1]	1.96×10^{-4}
	E [-x; 9 | -e-1, e+1, 6, -e-1, 6, e+1]	3.40×10^{-4}
$\chi_{b1}(1P)^0$	$9.8928 \pm 4.0 \times 10^{-4}$	
	E [0; 9 | e+1, -e-1, -e-1, 6, (-75)]	4.52×10^{-6}
	E [-x; 9 | -e-1, e+1, e+1, e+1, -12]	3.00×10^{-4}
$\chi_{b2}(1P)^0$	$9.9122 \pm 4.0 \times 10^{-4}$	
	P [0; 3 | -e-1, -6, e+1, 15, -e-1]	8.26×10^{-5}
	E [0; 9 | e+1, -e-1, -e-1, 12, -6]	1.07×10^{-5}
	E [-x; 9 | -e-1, e+1, e+1, 6]	2.21×10^{-6}
$\Upsilon(2S)^0$	$1.002326 \times 10^1 \pm 3.1 \times 10^{-4}$	
	P [0; 3 | -e-1, -e-1, -e-1, e+1, -75]	1.86×10^{-6}
	E [0; 9 | e+1, -e-1, -6, e+1, e+1, e+1, (-18)]	1.28×10^{-6}
	E [-x; 9 | -e-1, e+1, e+1, -e-1, 6, -e-1, e+1, -e-1, e+1]	2.49×10^{-4}
$\chi_{b0}(2P)^0$	$1.02325 \times 10^1 \pm 6.0 \times 10^{-4}$	
	P [0; 3 | -e-1, -e-1, 327]	1.29×10^{-6}
	E [0; 9 | e+1, -e-1, -30]	9.85×10^{-5}
	E [-x; 9 | -e-1, 6, -e-1, -e-1, -e-1, -e-1]	2.80×10^{-4}
$\chi_{b1}(2P)^0$	$1.02555 \times 10^1 \pm 5.0 \times 10^{-4}$	
	P [0; 3 | -e-1, -e-1, 30]	2.78×10^{-4}
	E [0; 9 | e+1, -e-1, -54]	4.85×10^{-4}
	E [-x; 9 | -e-1, 6, -6, e+1, -e-1, -6]	8.02×10^{-5}
$\chi_{b2}(2P)^0$	$1.02686 \times 10^1 \pm 5.0 \times 10^{-4}$	
	P [0; 3 | -e-1, -e-1, 21, -e-1, 9]	1.11×10^{-5}
	E [0; 9 | e+1, -e-1, -93]	2.07×10^{-5}
	E [-x; 9 | -e-1, 6, -6, 9, (-12)]	4.33×10^{-6}
$\Upsilon(3S)^0$	$1.03552 \times 10^1 \pm 5.0 \times 10^{-4}$	
	P [0; 3 | -e-1, -e-1, 6, e+1, 6]	3.94×10^{-5}
	E [-x; 9 | -e-1, 6, -30, -e-1]	1.75×10^{-4}
$\Upsilon(4S)^0$	$1.05794 \times 10^1 \pm 1.2 \times 10^{-3}$	
	P [0; 3 | -e-1, -e-1, e+1, -e-1, e+1, -15]	9.28×10^{-5}
	E [0; 9 | e+1, -e-1, 6, e+1, 21]	4.37×10^{-5}
$\Upsilon(10860)^0$	$1.0876 \times 10^1 \pm 1.1 \times 10^{-2}$	
	E [0; 9 | e+1, -e-1, e+1, 24]	8.32×10^{-5}
$\Upsilon(11020)^0$	$1.1019 \times 10^1 \pm 8.0 \times 10^{-3}$	
	P [0; 3 | -6, e+1, -e-1, 6, e+1]	3.60×10^{-3}
	E [0; 9 | e+1, -e-1, e+1, -6, (-18)]	3.89×10^{-5}

tinued fraction is: P [0; 0 | 1974, -e-1, -e-1, (-24)]. As the first denominator is very high, the following denominators can make only minor changes of the numerical value of the fraction. So here it would be easily possible adding denominators to force the sum to be zero. Actually many particle representations fall in that category, so from looking only at these examples, the fundamental idea of a vanishing sum of denominators does not come out at all.

Hypothesis:
From all these examples we can theorize that for a permanently stable particle such as the proton and electron, the sum of the free link and all partial denominators must be zero.

3.2 Rules for constructing continued fractions

With these physical ideas, we can express the proton and electron through a very limited set of 10 pairs of continued fractions (Table 12), which can all be written down. For every continued fraction, the phase shift p can be calculated, so that equations (2) and (3) hold. Then, new rules for the interpretation of elementary particle masses can be derived. First, a mass can be either a proton or an electron resonance, and second, this newly found phase shift must now be considered.

When interpreting particle masses as proton resonance states we write (x is the new phase shift):

$$\ln \frac{m_{particle}}{m_{proton}} = (0 \text{ or } x) + S \tag{4}$$

and for electron resonances holds:

$$\ln \frac{m_{particle}}{m_{electron}} = (0 \text{ or } -x) + S. \tag{5}$$

The basic rule that the phase shift can be zero, is fundamental and will not be changed.

Now for every of these 10 different phase shifts, the new model must be checked. We have to find out to what extent other elementary particles are compatible to one of these 10 new versions of the model and still accumulate in spectral nodes. There is a set of 18 particle masses, which cannot be expressed as proton or electron resonances with phase shift zero; these are: μ^-, K^0, B^+, B^0, $B^{*0,+}$, B_s^0, $B_s{}^{*0}$, $B_{s2}{}^*(5840)^0$, $J/\psi(1S)^0$, $\chi_{c1}(1P)^0$, $h_c(1P)^0$, $\Lambda(1520)^0$, Σ^0, $\Sigma(1385)^+$, Ξ^-, Λ_c^+, $\Sigma_b{}^{*0,+}$ and $\Sigma_b{}^{*-}$. The question is now: which of the 10 possible phase shifts can reproduce these 18 masses best, with the lowest number of outliers?

By trial and error it was found that there is indeed such a "best possibility", providing only one outlier:

$$\ln \frac{m_{electron}}{m_{proton}} = x + (-6) + \cfrac{e}{12 + \cfrac{e}{-6}} \tag{6}$$

$$\ln \frac{m_{proton}}{m_{electron}} = -x + 6 + \cfrac{e}{-12 + \cfrac{e}{6}}. \tag{7}$$

The phase shift x equals -1.75083890054 and the numerical errors are very small (see Tables 1 and 9).

Tables 1 to 11 show the continued fraction representations for the considered data set (117 particles, 107 different masses) All possible fractions are given for both, proton and electron resonances with the phase shifts 0 and ±x. For completeness, Table 12 displays the 10 alternative continued fraction representations together with the calculated phase shifts

and the number of outliers when trying to reproduce the aforementioned set of 18 masses.

A single outlier is a very satisfying result when comparing to 14% outliers, which have been found with the standard version of Müller's model [9]. Since the spectra of electron and proton resonances overlap, most particles can even expressed as both, proton and electron resonances. This demonstrates that it makes only sense to analyze high accuracy data, otherwise easily a continued fraction representation can be found.

As expected, the principle of "Yin and Yang" has not been found anymore in this set of particles. There are no other pairs of particles with opposite oscillation information. It seems to be that this fundamental concept is only applicable to longterm stable systems or processes. Further research on other data sets should confirm this.

3.3 Model discussion

Is the principle of "Yin and Yang" really necessary to obtain continued fraction representations for most elementary particle masses? The critical reader could argue that alone the additional consideration of electron resonances greatly enhances the chances to express particle masses via standard continued fractions (with phase shift 0 and 3/2). This is true, however, the author has found that the 14% outliers were very little reduced when considering such additional electron resonances. So another phase shift is definitively required.

But, are the electron resonances really necessary? Would it not be possible to write only

$$\ln \frac{m_{particle}}{m_{proton}} = (0 \text{ or } p) + S \qquad (8)$$

where p is just any other phase shift different from the standard value 3/2 (between 0 and ±3)? This was exactly the author's first attempt to modify Müller's model. It was found that such phase shift does not exist.

For that reason the problem can only be solved through a new physical or philosophical idea. Every good physical theory consists of two parts, equivalent to a soul and a body. The soul represents a fundamental physical law or a philosophical principle, while always mathematics is the body.

From this viewpoint the author is particularly satisfied having found the "Yin-Yang" principle as an adequate extension of the proton resonance concept. It clearly justifies the importance of electron resonances and distinguishes the model from numerology.

Regarding the selection of the appropriate phase shift, a very critical reader could note that there is only one outlier difference between

$$\ln \frac{m_{electron}}{m_{proton}} = [x_1; -9 \mid -9, 18] \qquad (2 \text{ outliers})$$

and the best variant

$$\ln \frac{m_{electron}}{m_{proton}} = [x_2; -6 \mid 12, -6], \qquad (1 \text{ outlier})$$

Table 9: Continued fraction representations of masses of the N, Δ, Λ, Σ, Ξ and Ω baryons (x = -1.75083890054)

Particle	Mass ± SD [GeV] Continued fraction representation(s)	Numerical error [GeV]
p^+	$9.38272013 \times 10^{-1} \pm 2.3 \times 10^{-8}$ E [-x; 6 | -12, 6]	2.22×10^{-12}
n^0	$9.39565346 \times 10^{-1} \pm 2.3 \times 10^{-8}$ P [0; 0 | 1974, -e-1, -e-1, (-24)]	7.85×10^{-11}
$\Delta(1232)^{-,0,+,++}$	$1.2320 \pm 1.0 \times 10^{-3}$ P [0; 0 | 9, e+1, -e-1, e+1] P [x; 3 | -e-1, e+1, -e-1, 6, e+1, -e-1] E [-x; 6 | 75]	4.29×10^{-4} 7.12×10^{-4} 8.61×10^{-4}
Λ^0	$1.115683 \pm 6.0 \times 10^{-6}$ P [0; 0 | 15, e+1, 15, -6]	9.92×10^{-8}
$\Lambda(1405)^0$	$1.4051 \pm 1.3 \times 10^{-3}$ P [0; 0 | 6, e+1] P [x; 3 | -e-1, 6, -e-1, -e-1]	2.50×10^{-5} 6.44×10^{-4}
$\Lambda(1520)^0$	$1.5195 \pm 1.0 \times 10^{-3}$ P [x; 3 | -e-1, 15, e+1] E [-x; 6 | 12, -e-1, e+1, -e-1]	5.71×10^{-4} 4.36×10^{-4}
Σ^+	$1.18937 \pm 7.0 \times 10^{-5}$ P [0; 0 | 12, -6, e+1, -e-1, 6]	5.70×10^{-6}
Σ^0	$1.192642 \pm 2.4 \times 10^{-5}$ E [-x; 6 | 606]	1.24×10^{-5}
Σ^-	$1.197449 \pm 3.0 \times 10^{-5}$ P [0; 0 | 12, -e-1, 6, -e-1, e+1, -e-1, (93)] E [-x; 6 | 321, -e-1]	5.89×10^{-9} 1.22×10^{-5}
$\Sigma(1385)^+$	$1.3828 \pm 4.0 \times 10^{-4}$ E [-x; 6 | 18, -15 (-e-1)]	8.96×10^{-5}
$\Sigma(1385)^0$	$1.3837 \pm 1.0 \times 10^{-3}$ P [0; 0 | 6, e+1, -e-1, e+1, -e-1] E [-x; 6 | 18, -12, (e+1, 60)]	6.88×10^{-4} 2.95×10^{-8}
$\Sigma(1385)^-$	$1.3872 \pm 5.0 \times 10^{-4}$ P [0; 0 | 6, e+1, -e-1, e+1, e+1] E [-x; 6 | 18, -6, e+1]	3.03×10^{-4} 1.66×10^{-4}
Ξ^0	$1.31486 \pm 2.0 \times 10^{-4}$ P [0; 0 | 9, -e-1, e+1, -6] P [x; 3 | -e-1, e+1, -93] E [-x; 6 | 27, -9, e+1]	1.42×10^{-4} 2.86×10^{-5} 1.53×10^{-4}
Ξ^-	$1.32171 \pm 7.0 \times 10^{-5}$ P [x; 3 | -e-1, e+1, 45, e+1]	5.35×10^{-5}
$\Xi(1530)^0$	$1.53180 \pm 3.2 \times 10^{-4}$ P [0; 0 | 6, -6, (165)] E [0; 9 | -e-1, e+1, -e-1, e+1, -e-1, -e-1, -e-1]	1.35×10^{-6} 5.19×10^{-5}
$\Xi(1530)^-$	$1.5350 \pm 6.0 \times 10^{-4}$ P [0; 0 | 6, -6, 9, (-12)] P [x; 3 | -e-1, 21, 6] E [0; 9 | -e-1, e+1, -e-1, e+1, -6, (-54)]	1.09×10^{-5} 1.01×10^{-4} 1.18×10^{-6}
Ω^-	$1.67245 \pm 2.9 \times 10^{-4}$ P [0; 0 | e+1, e+1, -e-1, e+1, -e-1, -e-1] P [x; 3 | -e-1, 9, e+1, -9] E [0; 9 | -e-1, e+1, 48]	1.09×10^{-4} 1.50×10^{-4} 1.23×10^{-4}

Table 10: Continued fraction representations of masses of the charmed baryons (x = -1.75083890054)

Particle	Mass ± SD [GeV] Continued fraction representation(s)	Numerical error [GeV]
Λ_c^+	$2.28646 \pm 1.4 \times 10^{-4}$ E [-x; 6 | e+1, 6, 9, -e-1, (-e-1)]	8.64×10^{-6}
$\Lambda_c(2595)^+$	$2.5954 \pm 6.0 \times 10^{-4}$ P [x; 3 | -12, 9, e+1] E [0; 9 | -6, 15, (66)] E [-x; 6 | e+1, -12, e+1, -9]	5.64×10^{-4} 1.23×10^{-6} 1.13×10^{-4}
$\Sigma_c(2455)^{++}$	$2.45403 \pm 1.8 \times 10^{-4}$ P [x; 3 | -9, -6, -39] E [0; 9 | -6, e+1, -9, e+1, -e-1] E [-x; 6 | e+1, 105]	8.51×10^{-7} 2.02×10^{-5} 7.84×10^{-5}
$\Sigma_c(2455)^+$	$2.4529 \pm 4.0 \times 10^{-4}$ P [0; 0 | e+1, -e-1, e+1, 6, e+1, -e-1, e+1] P [x; 3 | -9, -6, -9] E [-x; 6 | e+1, 96]	2.84×10^{-4} 1.07×10^{-4} 1.02×10^{-4}
$\Sigma_c(2455)^0$	$2.45376 \pm 1.8 \times 10^{-4}$ P [x; 3 | -9, -6, -24] E [0; 9 | -6, e+1, -9, e+1, -e-1, e+1] E [-x; 6 | e+1, 102, (e+1)]	3.06×10^{-5} 1.48×10^{-4} 8.05×10^{-5}
$\Sigma_c(2520)^{++}$	$2.5184 \pm 6.0 \times 10^{-4}$ P [0; 0 | e+1, -e-1, e+1, -e-1, -18] E [0; 9 | -6, 6, -e-1, e+1, (18)] E [-x; 6 | e+1, -27, e+1, (6)]	1.44×10^{-4} 1.05×10^{-5} 1.68×10^{-5}
$\Sigma_c(2520)^+$	$2.5175 \pm 2.3 \times 10^{-3}$ P [0; 0 | e+1, -e-1, e+1, -e-1, -15, e+1] E [0; 9 | -6, 6, -e-1, e+1, (-6)] E [-x; 6 | e+1, -27]	1.01×10^{-4} 7.02×10^{-5} 4.20×10^{-4}
$\Sigma_c(2520)^0$	$2.5180 \pm 5.0 \times 10^{-4}$ P [0; 0 | e+1, -e-1, e+1, -e-1, -15] E [0; 9 | -6, 6, -e-1, e+1, (-21)] E [-x; 6 | e+1, -27, 6]	2.46×10^{-4} 8.75×10^{-6} 2.10×10^{-5}
Ξ_c^+	$2.4678 \pm 4.0 \times 10^{-4}$ P [0; 0 | e+1, -e-1, e+1, 60] P [x; 3 | -9, -e-1, -e-1, e+1, e+1] E [0; 9 | -6, e+1, -33] E [-x; 6 | e+1, -933]	5.29×10^{-5} 2.82×10^{-4} 8.89×10^{-6} 1.45×10^{-6}
Ξ_c^0	$2.47088 \pm 3.4 \times 10^{-4}$ P [0; 0 | e+1, -e-1, e+1, -162] P [x; 3 | -9, -e-1, -9, (-9)] E [0; 9 | -6, e+1, -141] E [-x; 6 | e+1, -294]	2.87×10^{-7} 1.73×10^{-5} 6.33×10^{-6} 5.91×10^{-6}
$\Xi_c'^+$	$2.5756 \pm 3.1 \times 10^{-3}$ P [x; 3 | -12, e+1, 6] E [0; 9 | -6, 9, e+1] E [-x; 6 | e+1, -12, -e-1, e+1]	4.33×10^{-4} 1.02×10^{-3} 1.40×10^{-3}
$\Xi_c'^0$	$2.5779 \pm 2.9 \times 10^{-3}$ P [x; 3 | -12, e+1, e+1] E [-x; 6 | e+1, -12, -e-1]	5.26×10^{-4} 8.16×10^{-4}
$\Xi_c(2645)^{0,+}$	$2.6459 \pm 5.0 \times 10^{-4}$ P [x; 3 | -12, -e-1, 9] E [0; 9 | -6, -39, (-330)] E [-x; 6 | e+1, -9, e+1, 6]	7.47×10^{-6} 1.13×10^{-8} 2.50×10^{-4}
Ω_c^0	$2.6952 \pm 1.7 \times 10^{-3}$ P [x; 3 | -15, e+1, -e-1, e+1] E [0; 9 | -6, -9, e+1, (-12)] E [-x; 6 | e+1, -6, e+1]	6.84×10^{-4} 3.15×10^{-6} 9.61×10^{-4}
$\Omega_c(2770)^0$	$2.7659 \pm 2.0 \times 10^{-3}$ E [0; 9 | -6, -e-1, (93)] E [-x; 6 | e+1, -6, e+1, e+1]	9.99×10^{-6} 3.47×10^{-4}

Table 11: Continued fraction representations of masses of the bottom baryons (x = -1.75083890054)

Particle	Mass ± SD [GeV] Continued fraction representation(s)	Numerical error [GeV]
Λ_b^0	$5.6202 \pm 1.6 \times 10^{-3}$ P [x; 3 | 6, e+1, -e-1, e+1, 9] E [0; 9 | 9, -27]	1.25×10^{-4} 3.49×10^{-4}
Σ_b^+	$5.8078 \pm 2.7 \times 10^{-3}$ E [0; 9 | 9, -e-1, e+1, -e-1, (-27)]	2.47×10^{-6}
Σ_b^-	$5.8152 \pm 2.0 \times 10^{-3}$ E [0; 9 | 9, -e-1, e+1, -e-1, e+1, (-e-1, 24)]	4.30×10^{-6}
$\Sigma_b{}^{*+}$, $\Sigma_b{}^{*0}$	$5.8290 \pm 3.4 \times 10^{-3}$ P [x; 3 | e+1, e+1, -e-1, e+1]	8.39×10^{-4}
$\Sigma_b{}^{*-}$	$5.8364 \pm 2.8 \times 10^{-3}$ P [x; 3 | e+1, e+1, -e-1, e+1, -6]	7.39×10^{-5}
$\Xi_b^{-,0}$	$5.7905 \pm 2.7 \times 10^{-3}$ E [0; 9 | 9, -e-1, e+1, 9]	2.20×10^{-4}

Table 12: List of the 10 possible continued fraction representations of the electron mass when considering the rules that denominators must be small and their sum including the free link equals zero, together with their associate phase shifts and the number of outliers when considering the following set of 18 particles: μ^-, K^0, B^+, B^0, $B^{*0,+}$, B_s^0, $B_s{}^{*0}$, $B_{s2}{}^*(5840)^0$, $J/\psi(1S)^0$, $\chi_{c1}(1P)^0$, $h_c(1P)^0$, $\Lambda(1520)^0$, Σ^0, $\Sigma(1385)^+$, Ξ^-, Λ_c^+, $\Sigma_b{}^{*0,+}$ and $\Sigma_b{}^{*-}$

Continued fraction representation for $\ln \frac{m_{electron}}{m_{proton}} = x + S$	phase shift x	number of outliers
P [x; -9 | 15, -6]	1.29770965366	3
P [x; -9 | -6, 15]	1.95172884111	5
P [x; -9 | 18, -9]	1.33097940724	4
P [x; -9 | -9, 18]	1.79175802145	2 μ^-, Σ^0
P [x; -6 | -6, 12]	-1.04460536299	6
P [x; -6 | 12, -6]	-1.75083890054	1 $\chi_{c1}(1P)^0$
P [x; -6 | -9, 15]	-1.20718990898	6
P [x; -6 | 15, -9]	-1.70037040878	6
P [x; -6 | 18, -12]	-1.66836807753	3
P [x; -6 | -12, 18]	-1.2860171871	4

so one single outlier might not be sufficiently significant to make a clear decision. Here it is now worth looking at the outlier particles. In the first case, the two outliers are the muon and the Σ^0. The muon has a comparatively long mean lifetime of 2.2 μs. So it is fare more stable than the average elementary particle. Therefore it is reasonable to request that the muon mass is reproduced by the model, i.e. the muon must not be an outlier.

4 Conclusions

The here presented bipolar version of Müller's continued fraction model is so far the best description of elementary particle masses. It demonstrates two facts: first, electron and

proton can be interpreted as a manifestation of the "Yin and Yang" principle in nature. They both can be interpreted as fundamental reference points in the model of a chain of harmonic oscillations. Second, the proton resonance idea alone is an incomplete concept and we have to recognize that electron resonances also play an important role in the universe.

These results can be obtained only when strictly considering the individual measurement errors of the particles and all similar future analyses should be based on the most accurate data available.

Until now, this bipolar version of Müller's model has reproduced only one data set. It is obvious that this alone cannot be considered as a full proof of correctness of this model variant and much more data should be analyzed.

Acknowledgments

The author greatly acknowledges the financial support from the Brazilian governmental funding agencies FACEPE and CNPq.

Submitted on September 6, 2012 / Accepted on September 11, 2012

References

1. Greulich K.O. Calculation of the masses of all fundamental Elementary Particles with an accuracy of approx. 1%. *Journal of Modern Physics*, 2010, v. 1, 300–302.
2. Paasch K. The logarithmic potential and an exponential mass function for Elementary Particles. *Progress in Physics*, 2009, v. 1 36–39.
3. Shah G.N. and Mir T.A. Are Elementary Particle masses related? *29th International Cosmic Ray Conference Pune*, 2005, v. 9, 219–222.
4. Tatischeff B. Use of nuclei fractal properties for help to determine some unknown particle spins and unknown nuclei excited level spins. arXiv: 1112.1586v1.
5. Tatischeff B. Fractals and log-periodic corrections applied to masses and energy levels of several nuclei. arXiv: 1107.1976v1.
6. Tatischeff B. Fractal properties applied to hadron spectroscopy. arXiv: 1105.2034v1.
7. Tatischeff B. Fractal properties in fundamental force coupling constants, in atomic energies, and in elementary particle masses. arXiv: 1104.5379v1.
8. Tatischeff B. and Brissaud I. Relations between elementary particle masses. arXiv: 1005.0238v1.
9. Ries A., Fook M.V.L. Fractal structure of nature's preferred masses: Application of the model of oscillations in a chain system. *Progress in Physics*, 2010, v. 4, 82–89.
10. Müller H. Fractal scaling Models of resonant oscillations in chain systems of harmonic oscillators. *Progress in Physics*, 2009, v. 2, 72–76.
11. Müller H. Fractal scaling models of natural oscillations in chain systems and the mass distribution of the celestial bodies in the solar system. *Progress in Physics*, 2010, v. 1, 62–66.
12. Müller H. Fractal scaling models of natural oscillations in chain systems and the mass distribution of particles. *Progress in Physics*, 2010, v. 3, 61–66.
13. Ries A. The radial electron density in the Hydrogen atom and the model of oscillations in a chain system. *Progress in Physics*, 2012, v. 3, 29–34.
14. Nakamura K. et al. Review of Particle Physics. *Journal of Physics G*, 2010, v. 37, 075021. `http://pdg.lbl.gov`
15. Press W.H., Teukolsky S.A., Vetterling W.T., Flannery B.P. Numerical recipes in C. Cambridge University Press, Cambridge, 1992.

Galaxy S-Stars Exhibit Orbital Angular Momentum Quantization per Unit Mass

Franklin Potter

Sciencegems.com, 8642 Marvale Drive, Huntington Beach, CA 92646 USA. E-mail: frank11hb@yahoo.com

The innermost stars of our Galaxy, called S-stars, are in Keplerian orbits. Quantum celestial mechanics (QCM) predicts orbital angular momentum quantization *per unit mass* for each of them. I determine the quantization integers for the 27 well-measured S-stars and the total angular momentum of this nearly isolated QCM system within the Galactic bulge.

1 Introduction

The innermost stars of our Galaxy, called S-stars, are in Keplerian orbits about a proposed [1] black hole of mass 4.3 ± 0.3 million solar masses. Their orbital planes appear to have random orientations, their orbital eccentricities range from 0.131 to 0.963 with no apparent pattern, and their origins of formation remain an issue. The star labelled S0-2 has the smallest semi-major axis of about 1020 AU and has been monitored for one complete revolution of its orbit, thereby allowing a determination of the position of the Galactic center Sgr A* at a distance of 8.33 ± 0.36 kpc.

In this brief report I use the orbital distances of the 27 well-measured S-stars revolving about the Galactic Center as a test of the orbital angular momentum quantization *per unit mass* predicted by the quantum celestial mechanics (QCM) introduced by H.G. Preston and F. Potter in 2003 [2, 3]. For the derivation of QCM from the general relativistic Hamilton-Jacobi equation, see the published articles online [2, 4].

In a Schwarzschild metric approximation, their proposed gravitational wave equation (GWE) reduces to a Schrödinger-like equation in the r-coordinate while the angular coordinates (θ, ϕ) dictate the angular momentum quantization per unit mass. In particular, a body of mass μ orbiting a central mass M has an orbital angular momentum L that obeys

$$\frac{L}{\mu} = m\,c\,H, \tag{1}$$

where m is the quantization integer and c is the speed of light. We assume that over millions of years the orbit has reached a QCM equilibrium distance r that agrees in angular momentum value with its Newtonian value $L = \mu\sqrt{GMr}$.

H is the Preston gravitational distance, a different constant for each separate gravitationally bound system, equal to the system's total angular momentum L_T divided by its total mass M_T

$$H = \frac{L_T}{M_T c}. \tag{2}$$

Note that H is not a universal constant, unlike $\hbar$, and that QCM is not quantum gravity. Also recall that the GWE in the free particle limit becomes the standard Schrödinger equation of quantum mechanics.

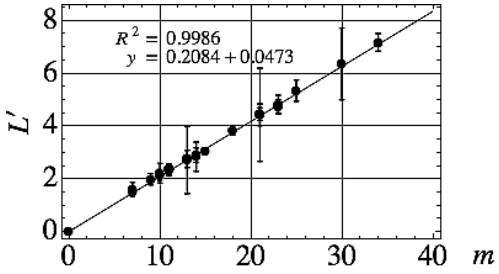

Fig. 1: QCM fit of S-stars at the Galactic Center.

2 S-star Orbital Quantization

The pertinent orbital parameters [5] for the 27 S-stars are listed in Table 1. Note that some uncertainties in both the semi-major axis column and in the eccentricity column are quite a large percentage of the mean values. These uncertainties will become smaller as more of these stars complete their orbits in the decades to come. More than an additional 100 S-stars are being studied in order to determine their orbital parameters. S0-16, whose orbital parameters are still being determined, has come the closest [1] to the Galactic Center Sgr A* at 45 AU (6.75×10^{12} m) with a tangential velocity of 1.2×10^7 m/sec!

I assume that each S-star is in a QCM equilibrium orbit in order to use the Newtonian values for the plot of $L' = L/\mu c$ versus m in Figure 1. The linear regression measure R^2 = 0.9986 indicates an excellent fit. I did not take the proposed black hole mass for M but used one solar mass instead as a reference. The slope $H = 6.59 \times 10^7$ meters for one solar mass, which becomes $H_{BH} = 1.30 \times 10^{11}$ meters (0.87 AU) for the proposed central black hole mass. For comparison, the Schwarzschild radius for this BH is 1.27×10^{10} meters.

Stars having the same QCM values for m, such as the six stars with $m = 11$, have orbits in different planes. I.e., their orbital angular momentum vectors point in different directions. There might be orbital resonances among stars with different m values even though their orbital planes have quite different orientations. With much more S-star orbital data to be determined, future fits to the QCM angular momentum quantization constraint should be very interesting.

S-star	m	a ["]	ϵ
S0-2	7	0.123 ± 0.001	0.880 ± 0.003
S0-38	7	0.139 ± 0.041	0.802 ± 0.041
S0-21	9	0.213 ± 0.041	0.784 ± 0.028
S0-5	10	0.250 ± 0.042	0.842 ± 0.017
S0-14	10	0.256 ± 0.010	0.963 ± 0.006
S0-18	10	0.265 ± 0.080	0.759 ± 0.052
S0-9	11	0.293 ± 0.050	0.825 ± 0.020
S0-13	11	0.297 ± 0.012	0.490 ± 0.023
S0-4	11	0.298 ± 0.019	0.406 ± 0.022
S0-31	11	0.298 ± 0.044	0.934 ± 0.007
S0-12	11	0.308 ± 0.008	0.900 ± 0.003
S0-17	11	0.311 ± 0.004	0.364 ± 0.015
S0-29	13	0.397 ± 0.335	0.916 ± 0.048
S0-33	13	0.410 ± 0.088	0.731 ± 0.039
S0-8	13	0.411 ± 0.004	0.824 ± 0.014
S0-6	14	0.436 ± 0.153	0.886 ± 0.026
S0-27	14	0.454 ± 0.078	0.952 ± 0.006
S0-1	15	0.508 ± 0.028	0.496 ± 0.028
S0-19	18	0.798 ± 0.064	0.844 ± 0.062
S0-24	21	1.060 ± 0.178	0.933 ± 0.010
S0-71	21	1.061 ± 0.765	0.844 ± 0.075
S0-67	21	1.095 ± 0.102	0.368 ± 0.041
S0-66	23	1.210 ± 0.126	0.178 ± 0.039
S0-87	23	1.260 ± 0.001	0.880 ± 0.003
S0-96	25	1.545 ± 0.209	0.131 ± 0.054
S0-97	30	2.186 ± 0.844	0.302 ± 0.308
S0-83	34	2.785 ± 0.234	0.657 ± 0.096

Table 1: Galaxy Center S-star orbital parameters.

3 Total Angular Momentum

If there exists the BH at the center, from the value of H_{BH} we calculate the predicted QCM total angular momentum L_T of this system to be about 3.35×10^{56} kg m^2/s. The rotating BH can contribute a maximum angular momentum of J = GM^2/c, about 1.64×10^{55} kg m^2/s, meaning that the orbiting stars dominate the angular momentum of this system.

Spectroscopic measurements to determine S-star types indicate that their masses lie between 10 and 30 solar masses, so assuming about 100 such stars randomly distributed within 10 times the orbital radius of S0-83, one estimates an average total contribution of about 1.4×10^{56} kg m^2/s, large enough to accommodate the QCM predicted total angular momentum value. Therefore, most of the system angular momentum is in the orbital motion of the S-stars.

Just how big radially is this gravitationally bound system involving the S-stars according to the QCM fit? Obviously, the angular momentum totals indicate that this gravitationally bound system does not extend significantly into the Galactic bulge, otherwise, the system's predicted H value will increase by many orders of magnitude with increases in radial distance. The Preston gravitational distance for the Galaxy, H_{Gal} = 1.2×10^{17} meters, may be the partition distance between this nearly isolated inner system and the rest of the Galaxy.

Therefore, this S-star system behaves as a nearly isolated system obeying QCM in the larger system called the Galaxy (or perhaps the Galaxy Bulge). Such QCM smaller systems within larger QCM systems already exist in the Solar System, e.g., the satellite systems of the planets [2], including the Jovian systems and the moons of Pluto [6]. Our Solar System [6] is a QCM system out on one spiral arm of the Galaxy, which is itself a QCM system requiring a different metric [4]. This hierarchy of QCM systems even applies to clusters of galaxies [7] and the Universe [8].

4 Final Comments

QCM predicts the orbital angular momentum quantization exhibited by the 27 S-stars nearest the Galactic Center. The result does not disagree with the proposed black hole mass of about 4.3 million solar masses there. The consequence is that the S-stars seem to be in their own nearly isolated QCM gravitationally bound system within the larger system of the Galaxy and the Galaxy bulge.

Acknowledgements

Generous support from Sciencegems.com is deeply appreciated.

Submitted on September 04, 2012 / Accepted on September 07, 2012

References

1. Ghez A. M., Salim S., Hornstein S. D., Tanner A., Lu J. R., Morris M., Becklin E. E., Duchêne G. Stellar Orbits around the Galactic Center Black Hole. *The Astrophysical Journal*, 2005, v. 620 (2), 744–757. arXiv: astro-ph/0306130.
2. Preston H. P., Potter F. Exploring Large-scale Gravitational Quantization without h-bar in Planetary Systems, Galaxies, and the Universe. arXiv: gr-qc/030311v1.
3. Potter F., Preston H. G. Quantum Celestial Mechanics: large-scale gravitational quantization states in galaxies and the Universe. *1st Crisis in Cosmology Conference: CCC-I*, Lerner E. J. and Almeida J. B., eds., AIP CP822, 2006, 239–252.
4. Potter F., Preston H. G. Gravitational Lensing by Galaxy Quantization States. arXiv: gr-qc/0405025v1.
5. Gillessen S., Eisenhauer F., Trippe S., Alexander T., Genzel R., Martins F., Ott T. Monitoring Stellar Orbits around the Massive Black Hole in the Galactic Center. arXiv: 0810.4674v1.
6. Potter F. Pluto Moons exhibit Orbital Angular Momentum Quantization per Mass. *Progress in Physics*, 2012, v. 4, 3–4.
7. Potter F., Preston H. G. Quantization State of Baryonic Mass in Clusters of Galaxies. *Progress in Physics*, 2007, v. 1, 61–63.
8. Potter F., Preston H. G. Cosmological Redshift Interpreted as Gravitational Redshift. *Progress in Physics*, 2007, v. 2, 31–33.

Does the Equivalence between Gravitational Mass and Energy Survive for a Quantum Body?

Andrei G. Lebed

Department of Physics, University of Arizona, 1118 E. 4th Street, Tucson, AZ 85721, USA. E-mail: lebed@physics.arizona.edu

We consider the simplest quantum composite body, a hydrogen atom, in the presence of a weak external gravitational field. We show that passive gravitational mass operator of the atom in the post-Newtonian approximation of general relativity does not commute with its energy operator, taken in the absence of the field. Nevertheless, the equivalence between the expectations values of passive gravitational mass and energy is shown to survive at a macroscopic level for stationary quantum states. Breakdown of the equivalence between passive gravitational mass and energy at a microscopic level for stationary quantum states can be experimentally detected by studying unusual electromagnetic radiation, emitted by the atoms, supported and moved in the Earth gravitational field with constant velocity, using spacecraft or satellite.

1 Introduction

Formulation of a successful quantum gravitation theory is considered to be one of the most important problems in modern physics and the major step towards the so-called "Theory of Everything". On the other hand, fundamentals of general relativity and quantum mechanics are so different that there is a possibility that it will not be possible to unite these two theories in a feasible future. In this difficult situation, it seems to be important to suggest a combination of quantum mechanics and some non-trivial approximation of general relativity. In particular, this is important in the case where such theory can be experimentally tested. To the best of our knowledge, so far only quantum variant of the trivial Newtonian approximation of general relativity has been tested experimentally in the famous COW [1] and ILL [2] experiments. As to such important and nontrivial quantum effects in general relativity as the Hawking radiation [3] and the Unruh effect [4], they are still very far from their direct and unequivocal experimental confirmations.

The notion of gravitational mass of a composite body is known to be non-trivial in general relativity and related to the following paradoxes. If we consider a free photon with energy E and apply to it the so-called Tolman formula for gravitational mass [5], we will obtain $m^g = 2E/c^2$ (i.e., two times bigger value than the expected one) [6]. If a photon is confined in a box with mirrors, then we have a composite body at rest. In this case, as shown in Ref. [6], we have to take into account a negative contribution to m^g from stress in the box walls to restore the Einstein equation, $m^g = E/c^2$. It is important that the later equation is restored only after averaging over time. A role of the classical virial theorem in establishing of the equivalence between averaged over time gravitational mass and energy is discussed in detail in Refs. [7, 8] for different types of classical composite bodies. In particular, for electrostatically bound two bodies with bare masses m_1 and m_2, it is shown that gravitational field is coupled to a combination $3K + 2U$, where K is kinetic energy, U is the Coulomb potential energy. Since the classical virial theorem states that the following time average is equal to zero, $\left\langle 2K + U \right\rangle_t = 0$, then we conclude that averaged over time gravitational mass is proportional to the total amount of energy [7, 8]:

$$\left\langle m^g \right\rangle_t = m_1 + m_2 + \left\langle 3K + 2U \right\rangle_t / c^2 = E/c^2. \qquad (1)$$

2 Goal

The main goal of our paper is to study a quantum problem about passive gravitational mass of a composite body. As the simplest example, we consider a hydrogen atom in the Earth gravitational field, where we take into account only kinetic and Coulomb potential energies of an electron in a curved spacetime. We claim three main results in the paper (see also Refs. [9, 10]). Our first result is that the equivalence between passive gravitational mass and energy in the absence of gravitational field survives at a macroscopic level in a quantum case. More strictly speaking, we show that the expectation value of the mass is equal to E/c^2 for stationary quantum states due to the quantum virial theorem. Our second result is a breakdown of the equivalence between passive gravitational mass and energy at a microscopic level for stationary quantum states due to the fact that the mass operator does not commute with energy operator, taken in the absence of gravitational field. As a result, there exist a non-zero probability that a measurement of passive gravitational mass gives value, which is different from E/c^2, given by the Einstein equation. Our third result is a suggestion of a realistic experiment to detect this inequivalence by measurements of electromagnetic radiation, emitted by a macroscopic ensemble of hydrogen atoms, supported and moved in the Earth gravitational field, using spacecraft or satellite.

3 Gravitational Mass in Classical Physics

Below, we derive the Lagrangian and Hamiltonian of a hydrogen atom in the Earth gravitational field, taking into account couplings of kinetic and potential Coulomb energies of an electron with a weak centrosymmetric gravitational field. Note that we keep only terms of the order of $1/c^2$ and disregard magnetic force, radiation of both electromagnetic and gravitational waves as well as all tidal and spin dependent effects. Let us write the interval in the Earth centrosymmetric gravitational field, using the so-called weak field approximation [11]:

$$ds^2 = -\left(1+2\frac{\phi}{c^2}\right)(cdt)^2 + \left(1-2\frac{\phi}{c^2}\right)(dx^2+dy^2+dz^2), \qquad \phi = -\frac{GM}{R}, \tag{2}$$

where G is the gravitational constant, c is the velocity of light, M is the Earth mass, R is a distance between a center of the Earth and a center of mass of a hydrogen atom (i.e., proton). We pay attention that to calculate the Lagrangian (and later — the Hamiltonian) in a linear with respect to a small parameter $\phi(R)/c^2$ approximation, we do not need to keep the terms of the order of $[\phi(R)/c^2]^2$ in metric (2), in contrast to the perihelion orbit procession calculations [11] .

Then, in the local proper spacetime coordinates,

$$x' = \left(1-\frac{\phi}{c^2}\right)x, \quad y' = \left(1-\frac{\phi}{c^2}\right)y, \qquad z' = \left(1-\frac{\phi}{c^2}\right)z, \quad t' = \left(1+\frac{\phi}{c^2}\right)t, \tag{3}$$

the classical Lagrangian and action of an electron in a hydrogen atom have the following standard forms:

$$L' = -m_e c^2 + \frac{1}{2}m_e(\mathbf{v}')^2 + \frac{e^2}{r'}, \quad S' = \int L'dt', \tag{4}$$

where m_e is the bare electron mass, e and $\mathbf{v}'$ are the electron charge and velocity, respectively; r' is a distance between electron and proton. It is possible to show that the Lagrangian (4) can be rewritten in coordinates (x, y, z, t) as

$$L = -m_e c^2 + \frac{1}{2}m_e\mathbf{v}^2 + \frac{e^2}{r} - m_e\phi - \left(3m_e\frac{\mathbf{v}^2}{2} - 2\frac{e^2}{r}\right)\frac{\phi}{c^2}. \tag{5}$$

Let us calculate the Hamiltonian, corresponding to the Lagrangian (5), by means of a standard procedure, $H(\mathbf{p},\mathbf{r}) = \mathbf{pv} - L(\mathbf{v},\mathbf{r})$, where $\mathbf{p} = \partial L(\mathbf{v},\mathbf{r})/\partial\mathbf{v}$. As a result, we obtain:

$$H = m_e c^2 + \frac{\mathbf{p}^2}{2m_e} - \frac{e^2}{r} + m_e\phi + \left(3\frac{\mathbf{p}^2}{2m_e} - 2\frac{e^2}{r}\right)\frac{\phi}{c^2}, \tag{6}$$

where canonical momentum in a gravitational field is $\mathbf{p} = m_e\mathbf{v}(1-3\phi/c^2)$. [Note that, in the paper, we disregard all tidal effects (i.e., we do not differentiate gravitational potential with respect to electron coordinates, $\mathbf{r}$ and $\mathbf{r}'$, corresponding to a position of an electron in the center of mass coordinate system). It is possible to show that this means that we consider the atom as a point-like body and disregard all effects of the order of $|\phi/c^2|(r_B/R) \sim 10^{-26}$, where r_B is the Bohr radius (i.e., a typical size of the atom).] From the Hamiltonian (6), averaged over time electron passive gravitational mass, $< m_e^g >_t$, defined as its weight in a weak centrosymmetric gravitational field (2), can be expressed as

$$\begin{aligned} < m_e^g >_t &= m_e + \left\langle \frac{\mathbf{p}^2}{2m_e} - \frac{e^2}{r} \right\rangle_t \frac{1}{c^2} + \left\langle 2\frac{\mathbf{p}^2}{2m_e} - \frac{e^2}{r} \right\rangle_t \frac{1}{c^2} \\ &= m_e + \frac{E}{c^2}, \end{aligned} \tag{7}$$

where $E = \mathbf{p}^2/2m_e - e^2/r$ is an electron energy. We pay attention that averaged over time third term in Eq. (7) is equal to zero due to the classical virial theorem. Thus, we conclude that in classical physics averaged over time passive gravitational mass of a composite body is equivalent to its energy, taken in the absence of gravitational field [7, 8].

4 Gravitational Mass in Quantum Physics

The Hamiltonian (6) can be quantized by substituting a momentum operator, $\hat{\mathbf{p}} = -i\hbar\partial/\partial\mathbf{r}$, instead of canonical momentum, $\mathbf{p}$. It is convenient to write the quantized Hamiltonian in the following form:

$$\hat{H} = m_e c^2 + \frac{\hat{\mathbf{p}}^2}{2m_e} - \frac{e^2}{r} + \hat{m}_e^g\phi, \tag{8}$$

where we introduce passive gravitational mass operator of an electron to be proportional to its weight operator in a weak centrosymmetric gravitational field (2),

$$\hat{m}_e^g = m_e + \left(\frac{\hat{\mathbf{p}}^2}{2m_e} - \frac{e^2}{r}\right)\frac{1}{c^2} + \left(2\frac{\hat{\mathbf{p}}^2}{2m_e} - \frac{e^2}{r}\right)\frac{1}{c^2}. \tag{9}$$

Note that the first term in Eq. (9) corresponds to the bare electron mass, m_e, the second term corresponds to the expected electron energy contribution to the mass operator, whereas the third nontrivial term is the virial contribution to the mass operator. It is important that the operator (9) does not commute with electron energy operator, taken in the absence of the field. It is possible to show that Eqs. (8), (9) can be also obtained directly from the Dirac equation in a curved spacetime, corresponding to a weak centrosymmetric gravitational field (2). For example, the Hamiltonian (8), (9) can be obtained [9, 10] from the Hamiltonian (3.24) of Ref. [12], where different physical problem is considered, by omitting all tidal terms.

Below, we discuss some consequences of Eq. (9). Suppose that we have a macroscopic ensemble of hydrogen atoms with each of them being in a ground state with energy E_1.

Then, as follows from Eq. (9), the expectation value of the gravitational mass operator per one electron is

$$< \hat{m}_e^g >= m_e + \frac{E_1}{c^2} + \left\langle 2\frac{\hat{\mathbf{p}}^2}{2m_e} - \frac{e^2}{r} \right\rangle \frac{1}{c^2} = m_e + \frac{E_1}{c^2}, \quad (10)$$

where the third term in Eq. (10) is zero in accordance with the quantum virial theorem [13]. Therefore, we conclude that the equivalence between passive gravitational mass and energy in the absence of gravitational field survives at a macroscopic level for stationary quantum states.

Let us discuss how Eqs. (8), (9) break the equivalence between passive gravitational mass and energy at a microscopic level. First of all, we recall that the mass operator (9) does not commute with electron energy operator, taken in the absence of gravitational field. This means that, if we create a quantum state of a hydrogen atom with definite energy, it will not be characterized by definite passive gravitational mass. In other words, a measurement of the mass in such quantum state may give different values, which, as shown, are quantized. Here, we illustrate the above mentioned inequivalence, using the following thought experiment. Suppose that at $t = 0$ we create a ground state wave function of a hydrogen atom, corresponding to the absence of gravitational field,

$$\Psi_1(r,t) = \Psi_1(r)\exp(-iE_1 t/\hbar). \quad (11)$$

In a weak centrosymetric gravitational field (2), wave function (11) is not anymore a ground state of the Hamiltonian (8), (9), where we treat gravitational field as a small perturbation in an inertial system [7–12]. It is important that for inertial observer, in accordance with Eq. (3), a general solution of the Schrodinger equation, corresponding to the Hamiltonian (8), (9), can be written as

$$\begin{aligned}\Psi(r,t) = (1-\phi/c^2)^{3/2}\sum_{n=1}^{\infty} a_n \Psi_n[(1-\phi/c^2)r] \\ \times\exp[-im_e c^2(1+\phi/c^2)t/\hbar] \\ \times\exp[-iE_n(1+\phi/c^2)t/\hbar].\end{aligned} \quad (12)$$

We pay attention that wave function (12) is a series of eigenfunctions of passive gravitational mass operator (9), if we take into account only linear terms with respect to the parameter ϕ/c^2. Here, factor $1-\phi/c^2$ is due to a curvature of space, whereas the term $E_n(1+\phi/c^2)$ represents the famous red shift in gravitational field and is due to a curvature of time. $\Psi_n(r)$ is a normalized wave function of an electron in a hydrogen atom in the absence of gravitational field, corresponding to energy E_n. [Note that, due to symmetry of our problem, an electron from $1S$ ground state of a hydrogen atom can be excited only into nS excited states. We also pay attention that the wave function (12) contains a normalization factor $(1-\phi/c^2)^{3/2}$.]

In accordance with the basic principles of the quantum mechanics, probability that, at $t > 0$, an electron occupies excited state with energy $m_e c^2(1+\phi/c^2) + E_n(1+\phi/c^2)$ is

$$\begin{aligned} P_n &= |a_n|^2, \\ a_n &= \int \Psi_1^*(r)\Psi_n[(1-\phi/c^2)r]d^3\mathbf{r} \\ &= -(\phi/c^2)\int \Psi_1^*(r) r\Psi_n'(r)d^3\mathbf{r}. \end{aligned} \quad (13)$$

Note that it is possible to demonstrate that for a_1 in Eq. (13) a linear term with respect to gravitational potential, ϕ, is zero, which is a consequence of the quantum virial theorem. Taking into account that the Hamiltonian is a Hermitian operator, it is possible to show that for $n \neq 1$:

$$\begin{aligned}\int \Psi_1^*(r) r\Psi_n'(r)d^3\mathbf{r} = \frac{V_{n,1}}{\hbar\omega_{n,1}}, \\ \hbar\omega_{n,1} = E_n - E_1, \quad n \neq 1,\end{aligned} \quad (14)$$

where $V_{n,1}$ is a matrix element of the virial operator,

$$V_{n,1} = \int \Psi_1^*(r)\hat{V}(\mathbf{r})\Psi_n(r)d^3\mathbf{r}, \quad \hat{V}(\mathbf{r}) = 2\frac{\hat{\mathbf{p}}^2}{2m_e} - \frac{e^2}{r}. \quad (15)$$

It is important that, since the virial operator (15) does not commute with the Hamiltonian, taken in the absence of gravitational field, the probabilities (13)–(15) are not equal to zero for $n \neq 1$.

Let us discuss Eqs. (12)–(15). We pay attention that they directly demonstrate that there is a finite probability,

$$P_n = |a_n|^2 = \left(\frac{\phi}{c^2}\right)^2 \left(\frac{V_{n,1}}{E_n - E_1}\right)^2, \; n \neq 1, \quad (16)$$

that, at $t > 0$, an electron occupies n-th ($n \neq 1$) energy level, which breaks the expected Einstein equation, $m_e^g = m_e + E_1/c^2$. In fact, this means that measurement of passive gravitational mass (i.e., weight in the gravitational field (2)) in a quantum state with a definite energy (11) gives the following quantized values:

$$m_e^g(n) = m_e + E_n/c^2, \quad (17)$$

corresponding to the probabilities (16). [Note that, as it follows from quantum mechanics, we have to calculate wave function (12) in a linear approximation with respect to the parameter ϕ/c^2 to obtain probabilities (16), (22), (23), which are proportional to $(\phi/c^2)^2$. A simple analysis shows that an account in Eq. (12) terms of the order of $(\phi/c^2)^2$ would change electron passive gravitational mass of the order of $(\phi/c^2)m_e \sim 10^{-9}m_e$, which is much smaller than the distance between the quantized values (17), $\delta m_e^g \sim \alpha^2 m_e \sim 10^{-4}m_e$, where α is the fine structure constant.] We also point out that, although the probabilities (16) are quadratic with respect to gravitational potential and, thus, small, the changes of the

passive gravitational mass (17) are large and of the order of $\alpha^2 m_e$. We also pay attention that small values of probabilities (16), $P_n \sim 10^{-18}$, do not contradict the existing Eötvös type measurements [11], which have confirmed the equivalence principle with the accuracy of the order of 10^{-12}-10^{-13}. For our case, it is crucial that the excited levels of a hydrogen atom spontaneously decay with time, therefore, one can detect the quantization law (17) by measuring electromagnetic radiation, emitted by a macroscopic ensemble of hydrogen atoms. The above mentioned optical method is much more sensitive than the Eötvös type measurements and we, therefore, hope that it allows to detect the breakdown of the equivalence between energy and passive gravitational mass, revealed in the paper.

5 Suggested Experiment

Here, we describe a realistic experiment [9, 10]. We consider a hydrogen atom to be in its ground state at $t = 0$ and located at distance R' from a center of the Earth. The corresponding wave function can be written as

$$\begin{aligned}\tilde{\Psi}_1(r,t) = (1-2\phi')^{3/2}\Psi_1[(1-\phi'/c^2)r] \\ \times\exp[-im_e c^2(1+\phi'/c^2)t/\hbar] \\ \times\exp[-iE_1(1+\phi'/c^2)t/\hbar],\end{aligned} \tag{18}$$

where $\phi' = \phi(R')$. The atom is supported in the Earth gravitational field and moved from the Earth with constants velocity, $v \ll \alpha c$, by spacecraft or satellite. As follows from Ref. [7], the extra contributions to the Lagrangian (5) are small in this case in an inertial system, related to a center of mass of a hydrogen atom (i.e., proton). Therefore, electron wave function and time dependent perturbation for the Hamiltonian (8), (9) in this inertial coordinate system can be expressed as

$$\begin{aligned}\tilde{\Psi}(r,t) = (1-2\phi')^{3/2}\sum_{n=1}^{\infty}\tilde{a}_n(t)\Psi_n[(1-\phi'/c^2)r] \\ \times\exp[-im_e c^2(1+\phi'/c^2)t/\hbar] \\ \times\exp[-iE_n(1+\phi'/c^2)t/\hbar],\end{aligned} \tag{19}$$

$$\hat{U}(\mathbf{r},t) = \frac{\phi(R'+vt)-\phi(R')}{c^2}\left(3\frac{\hat{\mathbf{p}}^2}{2m_e} - 2\frac{e^2}{r}\right). \tag{20}$$

We pay attention that in a spacecraft (satellite), which moves with constant velocity, gravitational force, which acts on each hydrogen atom, is compensated by some non-gravitational forces. This causes very small changes of a hydrogen atom energy levels and is not important for our calculations. Therefore, the atoms do not feel directly gravitational acceleration, **g**, but feel, instead, gravitational potential, $\phi(R'+vt)$, changing with time due to a spacecraft (satellite) motion in the Earth gravitational field. Application of the time-dependent quantum mechanical perturbation theory gives the following solutions for functions $\tilde{a}_n(t)$ in Eq. (19):

$$\tilde{a}_n(t) = \frac{\phi(R')-\phi(R'+vt)}{c^2}\frac{V_{n,1}}{\hbar\omega_{n,1}}\exp(i\omega_{n,1}t),\ n\neq 1, \tag{21}$$

where $V_{n,1}$ and $\omega_{n,1}$ are given by Eqs. (14), (15); $\omega_{n,1} \gg v/R'$.

It is important that, if excited levels of a hydrogen atom were strictly stationary, then a probability to find the passive gravitational mass to be quantized with $n \neq 1$ (17) would be

$$\tilde{P}_n(t) = \left(\frac{V_{n,1}}{\hbar\omega_{n,1}}\right)^2\frac{[\phi(R'+vt)-\phi(R')]^2}{c^4},\ n\neq 1. \tag{22}$$

In reality, the excited levels spontaneously decay with time and, therefore, it is possible to observe the quantization law (17) indirectly by measuring electromagnetic radiation from a macroscopic ensemble of the atoms. In this case, Eq. (22) gives a probability that a hydrogen atom emits a photon with frequency $\omega_{n,1} = (E_n - E_1)/\hbar$ during the time interval t. [We note that dipole matrix elements for $nS \to 1S$ quantum transitions are zero. Nevertheless, the corresponding photons can be emitted due to quadrupole effects.]

Let us estimate the probability (22). If the experiment is done by using spacecraft or satellite, then we may have $|\phi(R'+vt)| \ll |\phi(R')|$. In this case Eq. (22) is reduced to Eq. (16) and can be rewritten as

$$\tilde{P}_n = \left(\frac{V_{n,1}}{E_n-E_1}\right)^2\frac{\phi^2(R')}{c^4} \simeq 0.49\times 10^{-18}\left(\frac{V_{n,1}}{E_n-E_1}\right)^2, \tag{23}$$

where, in Eq. (23), we use the following numerical values of the Earth mass, $M \simeq 6\times 10^{24}$ kg, and its radius, $R_0 \simeq 6.36\times 10^6$ m. It is important that, although the probabilities (23) are small, the number of photons, N, emitted by macroscopic ensemble of the atoms, can be large since the factor $V_{n,1}^2/(E_n-E_1)^2$ is of the order of unity. For instance, for 1000 moles of hydrogen atoms, N is estimated as

$$N_{n,1} = 2.95\times 10^8\left(\frac{V_{n,1}}{E_n-E_1}\right)^2,\ N_{2,1} = 0.9\times 10^8, \tag{24}$$

which can be experimentally detected, where $N_{n,1}$ stands for a number of photons, emitted with energy $\hbar\omega_{n,1} = E_n - E_1$.

6 Summary

To summarize, we have demonstrated that passive gravitational mass of a composite quantum body is not equivalent to its energy due to quantum fluctuations, if the mass is defined to be proportional to a weight of the body. We have also discussed a realistic experimental method to detect this inequivalency. If the corresponding experiment is done, to the best of our knowledge, it will be the first experiment, which directly tests some nontrivial combination of general relativity and quantum mechanics. We have also shown that

the corresponding expectation values are equivalent to each other for stationary quantum states. It is important that our results are due to different couplings of kinetic and potential energy with an external gravitational field. Therefore, the current approach is completely different from that discussed in Refs. [12, 14, 15], where small corrections to electron energy levels are calculated for a free falling hydrogen atom [14, 15] or for a hydrogen atom supported in a gravitational field [12]. Note that phenomena suggested in the paper are not restricted by atomic physics, but also have to be observed in solid state, nuclear, and particle physics.

Acknowledgements

We are thankful to N. N. Bagmet (Lebed), V. A. Belinski, and Li-Zhi Fang for useful discussions. This work was supported by the NSF under Grant DMR-1104512.

Submitted on September 04, 2012 / Accepted on September 07, 2012

References

1. Colella R., Overhauser A. W., Werner S. A. Observation of gravitationally induced quantum interference. *Physical Review Letters*, 1975, v. 34 (23), 1472–1474.
2. Nesvizhevsky V. V., Borner H. G., Petukhov A. K., Abele H., Baebler S., Rueb F. J., Stoferle Th., Westphal A., Gagarski A. M., Petrov G. A., Strelkov A. V. Quantum states of neutrons in the Earth's gravitational field. *Nature*, 2002, v. 415 (January 17), 297–299.
3. Hawking S. W. Black hole explosions? *Nature*, 1974, v. 248 (March 1), 30–31.
4. Unruh W.G. Notes on black-hole evaporation. *Physical Review D*, 1976, v. 14 (4), 870–892.
5. Landau L. D., Lifshitz E. M. The Classical Theory of Fields. Butterworth-Heineman, Amsterdam, 2003.
6. Misner C. W., Putnam P. Active Gravitational Mass. *Physical Review*, 1959, v. 116 (4), 1045–1046.
7. Nordtvedt K. Post-Newtonian gravity: its theory-experiment interference. *Classical and Quantum Gravity*, 1994, v. 11 , A119–A132.
8. Carlip S. Kinetic energy and the equivalence principle. *American Journal of Physics*, 1998, v. 66 (5), 409–413.
9. Lebed A. G. Is Gravitational Mass of a Composite Quantum Body Equivalent to its Energy? arXiv: gr-qc/1111.5365v1; Breakdown of the Equivalence between Energy Content and Weight in a Weak Gravitational Field for a Quantum Body. arXiv: gr-qc/1205.3134v1.
10. Lebed A. G. "Breakdown of the Equivalence between Passive Gravitational Mass and Energy for a Quantum Body", in the Proceedings of the 13th Marcel Grossmann Meeting on Recent Developments in Theoretical and Experimental General Relativity, to be published. arXiv: gr-qc/1208.5756v1.
11. Misner C. W., Thorne K. S., Wheeler J. A. Gravitation. W. H. Freeman and Co, San Francisco, 1973.
12. Fischbach E., Freeman B. S., Cheng W. K. General-relativistic effects in hydrogenic systems. *Physical Review D*, 1981, v. 23 (10), 2157–2180.
13. Park D. Introduction to the Quantum Theory. Dover Publications, New York, 2005.
14. Pinto F. Rydberg Atoms in Curved Space-Time. *Physical Review Letters*, 1993, v. 70 (25), 3839–3843.
15. Parker L. One-Electron Atom in Curved Space-Time. *Physical Review Letters*, 1980, v. 44 (23), 1559–1562.

Genesis of the "Critical-Acceleration of MOND" and Its Role in "Formation of Structures"

Hasmukh K. Tank
Indian Space Research Organization, 22/693, Krishna Dham-2, Vejalpur, Ahmedabad-380015, India
E-mail: tank.hasmukh@rediffmail.com, hasmukh.tank1@gmail.com

As an attempt to explain the "flattening of galaxies rotation-curves", Milgrom proposed a Modification of Newtonian Dynamics MOND, in which he needed a new constant of nature a_0 , termed as "critical-acceleration-of MOND", in his best-fit empirical formula. But so far it has been an ad-hoc introduction of a new constant. Whereas this article proposes: (i) a genesis of this constant; (ii) explains its recurrences in various physical situations; and (iii) its role in determining the size and radii of various structures, like: the electron, the proton, the nucleus-of-atom, the globular-clusters, the spiral-galaxies, the galactic-clusters and the whole universe. In this process we get a new interpretation of "the cosmological-red-shift", that the linear part of the cosmological-red-shift may not be due to "metric-expansion-of-space"; and even the currently-believed "accelerated-expansion" may be slowing down with time.

1 Introduction

The observations of "flattening of galaxies rotation curves" are generally explained by assuming the presence of "dark-matter", but there is no way to directly detect it other than its presumed gravitational effect. M. Milgrom [1] proposed an alternative explanation for the "galaxies rotation curves", by modifying Newton's law of gravitation, for which he needed an ad-hoc introduction of a new constant of nature a_0, termed as "critical-acceleration of MOND", of the order of magnitude: 1.2×10^{-10} meter per seconds squared. But so far it has been an ad-hoc introduction of a new constant; and there has been no explanation for why its value is this much. Sivaram noticed its recurrences in various physical situations. This author has been of the opinion that the matching of values of the "anomalous decelerations of the four space-probes": Pioneer-10, Pioneer-11, Galileo and Ulysses and the "deceleration of cosmologically-red-shifting-photons" can not be an accidental coincidence. Now, this article presents a genesis of this "critical-acceleration of MOND". And based on this genesis, the formation of various structures, like the electron, the proton, the nucleus-of-atom, the globular-clusters, the spiral-galaxies, the galactic-clusters and the whole universe, are explained here.

2 Genesis of the "critical acceleration of MOND"

R.K. Adair, in his book "Concepts in Physics" [2] has given a derivation, that the sum of "gravitational-potential-energy" and "energy-of-mass' of the whole universe is, strikingly, zero! i.e.

$$M_0c^2 - \frac{GM_0M_0}{R_0} = 0 \tag{1}$$

where M_0 and R_0 are total-mass and radius of the universe respectively, and G is Newton's gravitational constant; i.e.

$$\frac{GM_0m}{R_0} = mc^2. \tag{2}$$

Where m is mass of any piece of matter. That is, the relativistic-energy of any piece of matter of mass m is equal to its "cosmic-gravitational-potential-energy". So the "cosmic-gravitational-force" experienced by every piece of matter is:

$$\frac{GM_0m}{R_0^2} = m\frac{c^2}{R_0}. \tag{3}$$

We know that $R_0H_0 = c$, so, $R_0 = c/H_0$. Here H_0 is Hubble's constant; i.e.

$$\frac{GM_0m}{R_0^2} = mH_0c \tag{4}$$

where m is mass of any object; and H_0c is a "cosmic-constant-of-acceleration". $H_0c = 6.87 \times 10^{-10}$ meter/second^2. In the next section we will see the recurrences of this "cosmic-constant-of-acceleration" in various physical situations.

3 Observable recurrences of "the cosmic-constant-of-acceleration"

Inter-galactic-photons experience the "cosmological red-shift". We can express the cosmological red-shift z_c in terms of de-acceleration experienced by the photon [3, 4], as follows:

$$z_c = \frac{f_0 - f}{f} = \frac{H_0D}{c}$$

i.e.

$$\frac{h\Delta f}{hf} = \frac{H_0D}{c}$$

i.e.

$$h\Delta f = \frac{hf}{c^2}(H_0c)D. \tag{5}$$

Here: h is Plancks constant, f_0 is frequency of photon at the time of its emission, f is the red-shifted frequency measured on earth, H_0 is Hubble's constant, and D the luminosity-distance.

That is, the loss in energy of the photon is equal to its mass (hf/c^2) times the acceleration $a = H_0c$, times the distance D travelled by it. Where: H_0 is Hubble-parameter. And the value of constant acceleration a is: $a = H_0c$, $a = 6.87 \times 10^{-10}$ meter/sec^2.

Now, we will verify that the accelerations experienced by the Pioneer-10, Pioneer-11, Galileo and Ulysses space-probes do match significantly with the "cosmic-constant-of-acceleration". Slightly higher value of decelerations of the space-probes is then explained.

Carefully observed values of de-accelerations [5]:
For Pioneer-10:

$$a = (8.09 \pm 0.2) \times 10^{-10} \ \ m/s^2 = H_0c. \tag{6}$$

For Pioneer-11:

$$a = (8.56 \pm 0.15) \times 10^{-10} \ \ m/s^2 = H_0c. \tag{7}$$

For Ulysses:

$$a = (12 \pm 3) \times 10^{-10} \ \ m/s^2 = H_0c. \tag{8}$$

For Galileo:

$$a = (8 \pm 3) \times 10^{-10} \ \ m/s^2 = H_0c. \tag{9}$$

For Cosmologically-red-shifted-photon,

$$a = 6.87 \times 10^{-10} \ \ m/s^2 = H_0c. \tag{10}$$

This value of acceleration is also the "critical acceleration" of modified Newtonian dynamics MOND,

$$a_0 = H_0c \tag{11}$$

and the rate of "accelerated-expansion of the universe"

$$a_{exp} = H_0c. \tag{12}$$

According to Weinberg, mass of a fundamental-particle can be obtained from the "fundamental-constants" as follows: Mass of a fundamental-particle,

$$m = \left(\frac{h^2H_0}{cG}\right)^{1/3}$$

i.e.

$$\frac{Gm}{(h/mc)^2} = H_0c. \tag{13}$$

That is, the self-gravitational-acceleration of Weinberg's [7] "fundamental-particle" is also equal to the "cosmic-constant-of-acceleration".

Reason why the apparent value of deceleration of the cosmic-photon is slightly small:

When the extra-galactic-photon enters our own milky-way-galaxy, the photon also experiences the gravitational-blue-shift, because of the gravitational-pull of our galaxy. The photon of a given frequency, if it has come from a near-by-galaxy, then it gets more blue-shifted, compared to the photon which has come from very-very far-distant-galaxy; so the galaxy which is at closer distance, appears at more closer distance, than the galaxies at far-away-distances. That is, the cosmic photon decelerated during its long inter-galactic-journey, and then accelerated because of the gravitational-pull of our milky-way galaxy; so we measure slightly lesser value of H_0; $H_0c = 6.87 \times 10^{-10}$ meter per seconds squared. But if we could send the Hubble-like Space-Telescope out-side our milky-way-galaxy, then the value of H_0c will match perfectly with the value of deceleration of all the four space-probes; $= 8.5 \times 10^{-10}$ meters per seconds squared.

Currently, the whole values of "anomalous accelerations of the space-probes" are "explained" in terms of radiation-pressure, gas-leakage... etc. So here we can explain the slight differences in their values of decelerations in terms of radiation-pressure, gas-leakage etc! Thus, the matching of values of decelerations of all the four space-probes is itself an interesting observation; and its matching with the deceleration of cosmologically-red-shifting-photons can not be ignored by a scientific mind as a coincidence. There is one more interesting thing about the value of this deceleration as first noticed by Milgrom, that: with this value of deceleration, an object moving with the speed of light would come to rest exactly after the time T_0 which is the age of the universe.

4 Formation of structures

Sivaram [6] has noticed that:

$$\begin{gathered}\frac{G\,M_0}{R_0^2} = \frac{G\,m_p}{r_p^2} = \frac{G\,m_e}{r_e^2} = \frac{G\,m_n}{r_n^2} \\ = \frac{G\,M_{gc}}{R_{gc}^2} = \frac{G\,M_{gal}}{R_{gal}^2} = \frac{G\,M_{cg}}{R_{cg}^2}\end{gathered} \tag{14}$$

$$= \text{the "critical-acceleration" of MOND} = H_0c.$$

(Here: M_0 and R_0 are mass and radius of the universe respectively, m_p and r_p are mass and radius of the proton, m_e and r_e are mass and radius of the electron, m_n and r_n are mass and radius of the nucleus of an atom, M_{gc} and R_{gc} are mass and radius of the globular-clusters, M_{gal} and R_{gal} are mass and radius of the spiral-galaxies, and M_{cg} and R_{cg} are mass and radius of the galactic-clusters respectively).

That is, the self-gravitational-pulling-force experienced by all the above bodies will be: Self-gravitational-force F = (mass of the body, say a galaxy) times (a constant value of deceleration H_0c).

For the formation of a stable structure, the "self-gravitational-acceleration" of a body of mass m should be equal to

the value of "cosmic-constant-of-acceleration" H_0c. In the expressions of eq. 14 above we found that: at the "surface" of the electron, the proton, the nucleus-of-atom, the globular-clusters, the spiral-galaxies, and the galactic-clusters this condition is beautifully satisfied. That is:

$$\frac{GM}{R^2} = H_0c. \tag{15}$$

Where M and R represent mass and radius of the above objects. And the size and radius of the above structures get decided as follows: i.e.

$$\frac{GM}{R^2} = H_0c = \frac{c^2}{R_0}$$

i.e.

$$R^2 = \frac{GM}{c^2}R_0$$

i.e.

$$R = (r_G R_0)^{1/2} \tag{16}$$

where r_G is "gravitational-radius" of the above objects. This is how all the structures get formed, beginning from the electron to the galactic-clusters.

5 Explanation for the "flattening of galaxies rotation-curves"

As seen in the expression-15, the condition for the formation of a stable structure is: $GM/R^2 = H_0c$ where M and R are mass and radius of a galaxy. That is, the centripetal acceleration at the surface of a structure is:

$$\frac{v^2}{R} = \frac{GM}{R^2} = H_0c \tag{17}$$

i.e.

$$v^2 = RH_0c. \tag{18}$$

Now, by dividing both the sides of the above expression by a distance r greater than R, the acceleration towards the center of spiral-galaxy experienced by a star at a distance r form the center is:

$$\frac{v^2}{r} = \frac{R}{r}H_0c. \tag{19}$$

Where $r > R$.

So, the velocity of the stars at the out-skirts of spiral galaxies is:

$$v = \left[\left(\frac{GM}{c^2}\frac{GM_0}{c^2}\right)^{1/2} a_0\right]^{1/2} \tag{20}$$

i.e.

$$v = \left[\left(\frac{GM}{c^2}R_0\right)^{1/2} \frac{c^2}{R_0}\right]^{1/2} \tag{21}$$

i.e.

$$v = \left[\frac{M}{M_0}\right]^{1/4} c, \tag{22}$$

a constant velocity. The above expression-22 is equal to Milgrom's expression: $(v^2/r) = [(GM/r^2)a_0]^{1/2}$ because $a_0 = GM_0/R_0^2$. This is how we can explain the "flattening of galaxies rotation-curves".

6 Conclusion

We presented here the genesis or root of the "critical acceleration of MOND", that it follows from the equality of "gravitational potential-energy" and "energy-of-mass" of the universe; and showed that there are as many as fifteen physical situations where we find recurrences of this "cosmic-constant-of-acceleration". The sizes of various structures like the electron, the proton, the nucleus-of-atom, the globular-clusters, the spiral-galaxies, the galactic-clusters and the whole universe get decided based on the condition that: the "self-gravitational-acceleration" of them all should be equal to the "cosmic-constant-of-acceleration" H_0c. The flattening of galaxies rotation curves at the out skirts of spiral galaxies also emerge from the above-mentioned equality.

We are sure that the space-probes Pioneer-10 et al. did show decelerations of the order H_0c. Now, similar to the space-probes, if the cosmologically red-shifting photons also decelerate due to the "cosmic-gravitational-force" then the linear part of the cosmological-red-shift may not be due to the "metric-expansion-of-space"; only the recently-discovered accelerated-expansion may be due to the "metric-expansion-of-space"; and its rate H_0c suggests that even the receding galaxies may be getting decelerated like the space-probes! Thus we may be able to explain even the "accelerated-expansion of the universe" without any need for dark-energy.

Submitted on: September 6, 2012 / Accepted on: September 13, 2012

References

1. Milgrom M. A modification of the Newtonian dynamics as a possible alternative to the hidden mass hypothesis. *Astrophysical Journal*, 1983, v. 270, 365.
2. Adair R.K. Concepts in Physics. Academic Press, New York, (1969), p. 775.
3. Tank H.K. A new law emerging from the recurrences of the "critical-acceleration" of MOND, suggesting a clue to unification of fundamental forces. *Astrophysics and Space Science*, 2010, v. 330, 203–205.
4. Tank H.K. Some clues to understand MOND and the accelerated expansion of the universe. *Astrophysics and Space Science*, 2011, v. 336, no. 2, 341–343.
5. Anderson J.D., Laing P.A., Lau E.L., Liu A.S., Nieto M.M., and Turyshev, S.G. Indication, from Pioneer 10, 11, Galileo, and Ulysses Data, of an Apparent Anomalous, Weak, Long-Range Acceleration. *Physical Review Letters*, 1998, v. 81, 2858–2861 [(Comment by Katz J.I.: *Physical Review Letters*, 1999, v. 83, 1892; Reply: *Physical Review Letters*, 1999, v. 83, 1893].
6. Sivaram C. Some aspects of MOND and its consequences for cosmology. *Astrophysics and Space Science*, 1994, v. 215, 185–189.
7. Weinberg S. Gravitation and Cosmology. John Wiley & Sons, (1972), p. 620.

Identical Bands and ΔI = 2 Staggering in Superdeformed Nuclei in A ∼ 150 Mass Region Using Three Parameters Rotational Model

A.M. Khalaf*, M.M. Taha†, and M. Kotb‡

*Physics Department, Faculty of Science, Al-Azhar University, Cairo, Egypt. E-mail: Profkhalaf@gmail.com
†Mathematics and Theoretical Physics Department, NRC, Atomic Energy Authority, P.No. 13759, Cairo, Egypt. E-mail: mahmoudmt@hotmail.com
‡Physics Department, Faculty of Science, Al-Azhar University, Cairo, Egypt. E-mail: mahmoudkottb@gmail.com

By using a computer simulated search program, the experimental gamma transition energies for superdeformed rotational bands (SDRB's) in $A \sim 150$ region are fitted to proposed three-parameters model. The model parameters and the spin of the bandhead were obtained for the selected ten SDRB's namely: ^{150}Gd (yrast and excited SD bands), ^{151}Tb (yrast and excited SD bands), ^{152}Dy (yrast SD bands), ^{148}Gd (SD-1,SD-6), ^{149}Gd (SD-1), ^{153}Dy (SD-1) and ^{148}Eu (SD-1). The Kinematic $J^{(1)}$ and dynamic $J^{(2)}$ moments of inertia are studied as a function of the rotational frequency $\hbar\omega$. From the calculated results, we notic that the excited SD bands have identical energies to their Z+1 neighbours for the twinned SD bands in N=86 nuclei. Also the analysis done allows us to confirm $\Delta I = 2$ staggering in the yrast SD bands of ^{148}Gd, ^{149}Gd, ^{153}Dy, and ^{148}Eu and in the excited SD bands of ^{148}Gd, by performing a staggering parameter analysis. For each band, we calculated the deviation of the gamma ray energies from smooth reference representing the finite difference approximation to the fourth derivative of the gamma ray transition energies at a given spin.

1 Introduction

The superdeformed (SD) nuclei is one of the most interesting topics of nuclear structure studies. Over the past two decades, many superdeformed rotational bands (SDRB's) have been observed in several region of nuclear chart [1]. At present although a general understanding of these SDRB's have been achieved, there are still many open problems. For example the spin, parity and excitation energy relative to the ground state of the SD bands have not yet been measured. The difficulty lies with observing the very weak discrete transitions which link SD levels with normal deformed (ND) levels. Until now, only several SD bands have been identified to exist the transition from SD levels to ND levels. Many theoretical approaches to predict the spins of these SD bands have been proposed [2–11].

Several SDRB's in the $A \sim 150$ region exhibit a rather surprising feature of a $\Delta I = 2$ staggering [12–25] in its transition energies, *i.e*. sequences of states differing by four units of angular momentum are displaced relative to each other. The phenomenon of $\Delta I = 2$ staggering has attached much attention and interest, and has thus become one of the most frequently considerable subjects. Within a short period, a considerable a mounts of effort has been spent on understanding its physical implication based on various theoretical ideas [9, 26–41]. Despite such efforts, definite conclusions have not yet been reached until present time.

The discovery of the phenomenon of identical bands (IB's) [42, 43] at high spin in SD states in even-even and odd-A nuclei aroused a considerable interest. It was found that the transition energies and moments of inertia in neighboring nuclei much close than expected. This has created much theoretical interest [44, 45]. The first interpretation [46] to IB's was done within the framework of the strong coupling limit of the particle-rotor model, in which one or more particles are coupled to a rotating deformed core and follow the rotation adiabatically. Investigation also suggest that the phenomena of IB's may result from a cancelation of contributions to the moment of inertia occurring in mean field method [47].

In the present paper we suggest a three-particle model to predict the spins of the rotational bands and to study the properties of the SDRB's and to investigate the existence of $\Delta I = 2$ staggering and also investigate the presence of IB's observed in the $A \sim 150$ mass region.

2 Nuclear SDRB's in framework of three parameters rotational model

In the present work, the energies of the SD nuclear RB's $E(I)$ as a function of the unknown spin I are expressed as:

$$E(I) = E_0 + a[[1 + b\hat{I}^2]^{1/2} - 1] + c\hat{I}^2 \qquad (1)$$

with $\hat{I}^2 = I(I+1)$, where a, b and c are the parameters of the model. The rotational frequency $\hbar\omega$ is defined as the derivative of the energy E with respect to the angular momentum $\hat{I}$

$$\begin{aligned} \hbar\omega &= \frac{dE}{d\hat{I}} \\ &= [2c + ab[1 + bI(I+1)]^{1/2}](I(I+1))^{-1/2}. \end{aligned} \qquad (2)$$

Two possible types of nuclear moments of inertia have been suggested which reflect two different aspects of nuclear dynamics. The kinematic moment of inertia $J^{(1)}$, which is

Table 1: The adopted best parameters a, b, c of the model and the band-head spin assignment I_0 of our ten SDRB's. The rms deviations are also shown.

SD Band	$E\gamma(I+2 \to I)$ (keV)	I_0 ($\hbar$)	a (keV)	b (keV)	c (keV)	χ
^{148}Gd (SD-1)	699.9	31	-0.313446E+07	0.163069E-04	0.311027E+02	7.387009E-01
(SD-6)	802.2	39	-0.106162E+06	0.107495E-03	0.105003E+02	2.104025E-01
^{150}Gd (SD-1)	815.0	47	-0.148586E+06	-0.517219E-04	0.954401E-01	5.250988E-01
(SD-2)	727.9	31	-0.617154E+06	-0.134929E-04	0.163288E+01	1.734822E+00
^{152}Dy (SD-1)	602.4	26	-0.144369E+06	0.207972E-04	0.733270E+01	5.217181E-01
^{149}Gd (SD-1)	617.8	27.5	-0.825976E+05	-0.698261E-04	0.285641E+01	4.559227E-01
^{148}Eu (SD-1)	747.7	29	-0.131028E+06	0.432608E-04	0.928191E+01	7.010767E-01
^{151}Tb (SD-1)	726.5	30.5	-0.852833E+06	-0.546382E-05	0.364770E+01	2.023767E+00
(SD-2)	602.1	26.5	-0.136986E+07	-0.431179E-05	0.289128E+01	6.644767E-01
^{153}Dy (SD-1)	721.4	30.5	-0.671437E+06	-0.386442E-05	0.464507E+01	2.171267E+00

equal to the inverse of the slope of the curve of energy E versus $\hat{I}$:

$$\begin{aligned} J^{(1)} &= \hbar^2 \hat{I}(\frac{dE}{d\hat{I}})^{-1} \\ &= \frac{\hbar^2}{ab}[1+bI(I+1)]^{1/2} + \frac{1}{2c} \end{aligned} \tag{3}$$

and the dynamic moment of inertia $J^{(2)}$, which is related to the curvature in the curve of E versus $\hat{I}$:

$$\begin{aligned} J^{(2)} &= \hbar^2(\frac{d^2E}{d\hat{I}^2})^{-1} \\ &= \frac{\hbar^2}{ab}[1+bI(I+1)]^{3/2} + \frac{1}{2c}. \end{aligned} \tag{4}$$

For the SD bands, one can extract the rotational frequency, dynamic and kinematic moment of inertia by using the experimental interband E2 transition energies as follows:

$$\hbar\omega = \frac{1}{4}[E_\gamma(I+2) + E_\gamma(I)], \tag{5}$$

$$J^{(2)}(I) = \frac{4\hbar^2}{\Delta E_\gamma}, \tag{6}$$

$$J^{(1)}(I-1) = \frac{\hbar^2(2I-1)}{E_\gamma}, \tag{7}$$

where

$$\begin{aligned} E_\gamma &= E(I) - E(I-2), \\ \Delta E_\gamma &= E_\gamma(I+2) - E_\gamma(I). \end{aligned}$$

It is seen that whereas the extracted $J^{(1)}$ depends on I proposition, $J^{(2)}$ does not.

3 Analysis of the ΔI = 2 staggering effects

It has been found that some SD rotational bands in different mass region show an unexpected $\Delta I = 2$ staggering effects in the gamma ray energies [12–25]. The effect is best seen in long rotational sequences, where the expected regular behavior of the energy levels with respect to spin or to rotational frequency is perturbed. The result is that the rotational sequence is split into two parts with states separated by $\Delta I = 4$ (bifurcation) shifting up in energy and the intermediate states shifting down in energy. The curve found by smoothly interpolating the band energy of the spin sequence I, I+4 ,I+8. . . is somewhat displaced from the corresponding curve of the sequence I+2, I+6, I+10. . . .

To explore more clearly the $\Delta I = 2$ staggering, for each band the deviation of the transition energies from a smooth reference ΔE_γ is determined by calculating the fourth derivative of the transition energies $E_\gamma(I)$ at a given spin I by

$$\begin{aligned} \Delta E_\gamma(I) &= \tfrac{3}{8}\Big(E_\gamma(I) - \tfrac{1}{6}[4E_\gamma(I-2) + 4E_\gamma(I+2) \\ &\quad -E_\gamma(I-4) - E_\gamma(I+4)]\Big). \end{aligned} \tag{8}$$

This expression was previously used in [15] and is identical to the expression for $\Delta^4 E_\gamma(I)$ in Ref. [33]. We chose to the use the expression above in order to be able to follow higher order changes in the moments of inertia of the SD bands.

4 Superdeformed identical bands

A particularly striking feature of SD nuclei is the observation of numerous bands with nearly identical transition energies in nuclei differing by one or two mass unit [42–45]. To determine whether a pair of bands is identical or not, one must compare the dynamical moment of inertia or compare the E2 transition energies of the two bands.

5 Numerical calculations and discussions

Nine SDRB's observed in nuclei of mass number $A \sim 150$ have been analyzed in terms of our three parameter model. The experimental transition energies are taken from Ref. [1]. The studied SDRB's are namely:

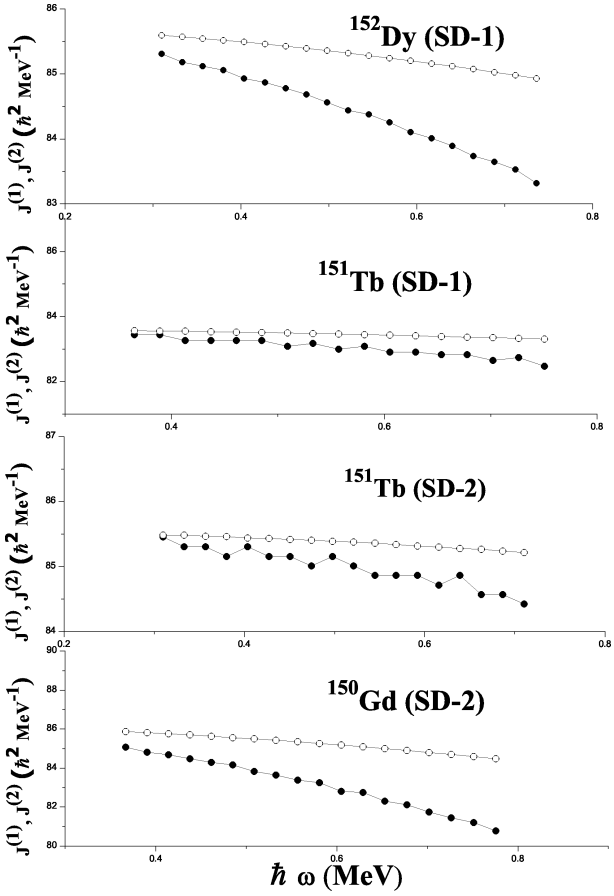

Fig. 1: Calculated Kinematic $J^{(1)}$ (open circles) and dynamic $J^{(2)}$ (closed circles) moments of inertia as a function of rotational frequency $\hbar\omega$ for the set of identical bands ^{151}Tb(SD-1), ^{152}Dy(SD-1), ^{150}Gd(SD-3) and ^{151}Tb(SD-2).

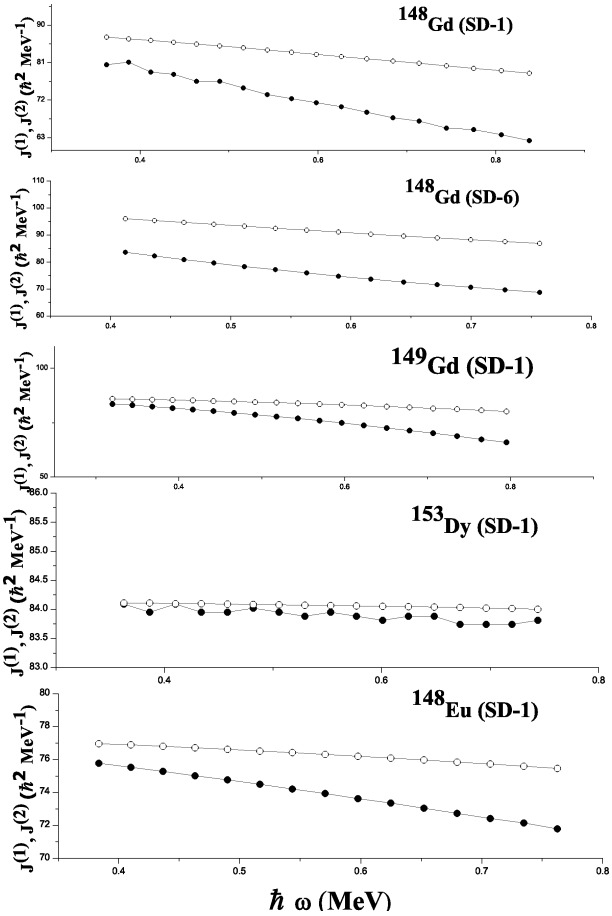

Fig. 2: Calculated Kinematic $J^{(1)}$ (open circles) and dynamic $J^{(2)}$ (closed circles) moments of inertia as a function of rotational frequency $\hbar\omega$ for the SDRB's ^{148}Gd(SD-1, SD-6), ^{149}Gd(SD-1), ^{153}Dy(SD-1) and ^{148}Eu(SD-1).

^{150}Gd(SD1, SD2), ^{151}Tb(SD1, SD2), ^{152}Dy(SD1), ^{148}Gd(SD1, SD6), ^{149}Gd(SD1), ^{153}Dy(SD1) and ^{148}Eu(SD1). The difference between the SD bands in various mass region are obviously evident through the behavior of the dynamical $J^{(2)}$ and kinematic $J^{(1)}$ moments of inertia seems to be very useful to the understanding of the properties of the SD bands. The bandhead moment of inertia J_0 at $J^{(2)} = J^{(1)}$ is a sensitive guideline parameter for the spin proposition.

A computer simulated search program has been used to get a minimum root mean square (rms) deviation between the experimental transition energies E_γ^{exp} and the calculated ones derived from our present three parameter model E_γ^{cal}:

$$\chi = \frac{1}{N}\left[\sum_{i=1}^{n}\left|\frac{E_\gamma^{cal}(I_i) - E_\gamma^{exp}(I_i)}{\delta E_\gamma^{exp}(I_i)}\right|^2\right]^{1/2} \qquad (9)$$

where N is the number of data points enters in the fitting procedure and $\delta E_\gamma^{exp}(i)$ is the uncertainties in the $\gamma-$transitions. For each SD band the optimized best fitted four parameters a, b, c and the bandhead spin I_0 were obtained by the adopted fit procedure. The procedure is repeated for several sets of trail values a, b, c and I_0. The spin I_0 is taken as the nearest integer number, then another fit with only a, b and c as free parameters is made to determine their values. The lowest bandhead spin I_0 and the best parameters of the model a, b, c for each band is listed in Table(1). The SD bands are identified by the lowest gamma transition energies $E_\gamma(I_0 + 2 \rightarrow I_0)$ observed.

The dynamical $J^{(2)}$ and kinematic $J^{(1)}$ moments of inertia using our proposed model at the assigned spin values are calculated as a function of rotational frequency $\hbar\omega$ and illustrated in Figs. (1,2). $J^{(2)}$ mostly decrease with a great deal of variation from nucleus to nucleus. The properties of the SD bands are mainly influenced by the number of the high-N intruder orbitals occupied. For example the large slopes of $J^{(2)}$ against $\hbar\omega$ in ^{150}Gd and ^{151}Tb are due to the occupation of $\pi 6_2$, $\nu 7_2$ orbitals, while in ^{152}Dy the $\pi 6_4$ level is also occupied and this leads to a more constant $J^{(2)}$ against $\hbar\omega$. A plot of

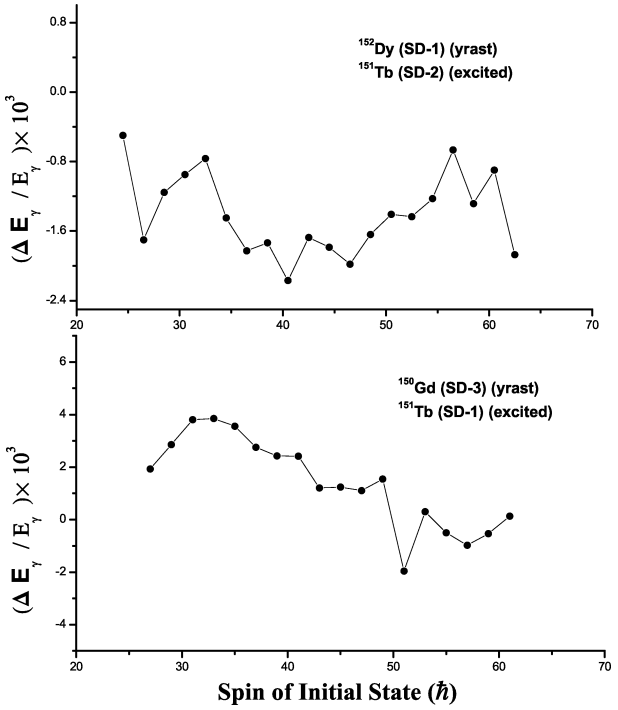

Fig. 3: Percentage differences $\Delta E_\gamma/E_\gamma$ in transition energies $E_\gamma = E(I) - E(I-2)$ as a function of spin I for the set of identical bands (^{151}Tb(SD-2), ^{152}Dy(SD-1)) and (^{150}Gd(SD-2), ^{151}Tb(SD-1)).

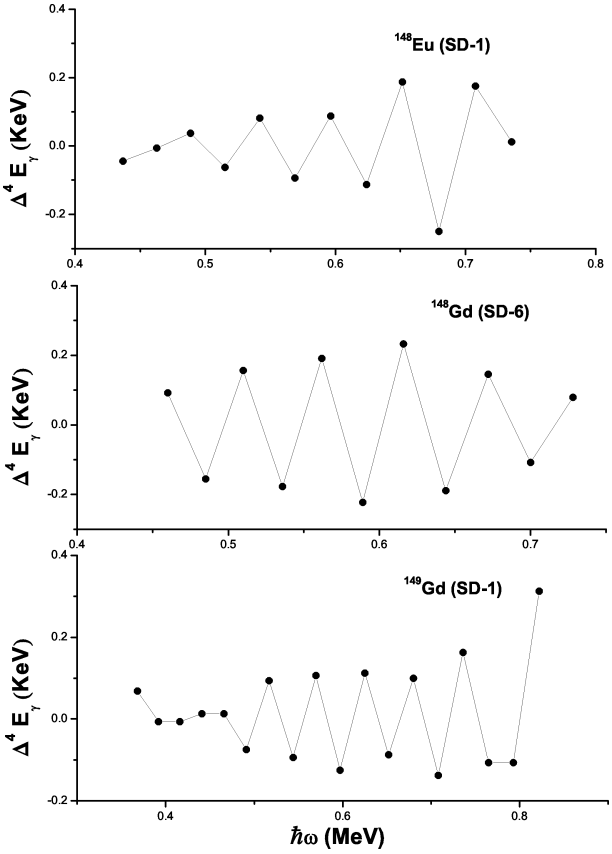

Fig. 4: The calculated $\Delta^4 E_\gamma$ staggering as a function of rotational frequency $\hbar\omega$ of the SDRB's ^{148}Eu(SD-1), ^{148}Gd(SD-6), ^{149}Gd(SD-1).

$J^{(2)}$ against $\hbar\omega$ for the excited SD band in ^{151}Tb gives a curve that is practically constant and which closely follows the $J^{(2)}$ curved traced out by the yrast SD band in ^{152}Dy but which is very different from the yrast SD band in ^{151}Tb. Similarly the ^{150}Gd excited SD band has $J^{(2)}$ values which resemble those observed in the ^{151}Tb yrast SD band. It is concluded that the N=86 isotones SD nuclei have identical supershell structures:

Nucleus	Yrast band	Excited band
$^{150}_{64}Gd$	$\pi(3)^{\bar{0}}[(4)^{10}(5)^{12}](i_{13/2})^2$	$\pi(3)^{\bar{1}}[(4)^{10}(5)^{12}](i_{13/2})^3$
$^{151}_{65}Tb$	$\pi(3)^{\bar{0}}[(4)^{10}(5)^{12}](i_{13/2})^3$	$\pi(3)^{\bar{1}}[(4)^{10}(5)^{12}](i_{13/2})^4$
$^{152}_{66}Dy$	$\pi(3)^{\bar{0}}[(4)^{10}(5)^{12}](i_{13/2})^4$	$\pi(3)^{\bar{1}}[(4)^{10}(5)^{12}](i_{13/2})^5$

6 Identical bands in the isotones nuclei N=86

A particularly striking feature of SD nuclei is the observation of a numerous bands with nearly identical transition energies in neighboring nuclei. Because of the large single particle SD gaps at Z=66 and N=86, the nucleus ^{152}Dy is expected to be a very good doubly magic SD core. The difference in $\gamma-$ray energies ΔE_γ between transition in the two pairs of N=86 isotones (excited ^{151}Tb (SD-2), yrast ^{152}Dy (SD-1)) and (excited ^{150}Gd (SD-2), yrast ^{151}Tb (SD-1)) were calculated.

The gamma transition energies of the excited band (SD-2) in ^{151}Tb are almost identical to that of the yrast band (SD-1) in ^{152}Dy. This twin band has been associated with a [301]1/2 hole in the ^{152}Dy core. The orbitals $\pi 6_2$ and $\nu 7_2$ are occupied in ^{151}Tb, while in ^{152}Dy the $\pi 6_4$ level is occupied and this leads to a more constant in dynamic moment of inertia $J^{(2)}$. Clearly the $J^{(2)}$ values for the excited SD bands are very similar to the yrast SD bands in their Z+1, N=86 isotones. The plot of percentage differences $\Delta E_\gamma/E_\gamma$ in transition energies versus spin for the two pairs (^{151}Tb(SD-2), ^{152}Dy(SD-1)) and (^{150}Gd(SD-2), ^{151}Tb(SD-1)) are illustrated in Fig. (3).

7 ΔI = 2 Staggering

Another result of the present work is the observation of a $\Delta I = 2$ staggering effects in the $\gamma-$ray energies, where the two sequences for spins $I = 4j, 4j+1$ (j=0,1,2,...) and $I = 4j+2$ (j=0,1,2,...) are bifurcated. For each band the deviation of the $\gamma-$ray energies from a smooth reference ΔE_γ is determined by calculating the fourth derivative of the $\gamma-$ray energies $\Delta E_\gamma(I)$ at a given spin $\Delta^4 E_\gamma$. The staggering in the $\gamma-$ray energies is indeed found for the SD bands in ^{148}Eu(SD-1), ^{148}Gd(SD-6) and ^{149}Gd(SD-1) in Fig. (4).

Submitted on June 11, 2012 / Accepted on June 25, 2012

References

1. Balraj Singh, Roy Zywine, Richard B. Firestone. Table of Superdeformed Nuclear Bands and Fission Isomers. *Nuclear Data Sheets*, 2002, v. 97, 241–592.
2. Becker J.A. et al. Level spin and moments of inertia in superdeformed nuclei near A = 194. *Nuclear Physics*, 1990, v. A520 c187–c194.
3. Draper J.E., et al. Spins in superdeformed bands in the mass 190 region. *Physical Review*, 1994, v. c42 R1791–R1795.
4. Khalaf A.M., et al. Band Head of the Superdeformed Bands in the $A \sim 150$ Mass region Nuclei. *Egypt Journal of Physics*, 2002, v. 33 (1), 67–87.
5. Khalaf A.M., et al. Spin Prediction and Systematics of Moments of inertia of superdeformed Nuclear Rotational Band in the Mass Region $A \sim 190$. *Egypt Journal of Physics*, 2002, v. 33 (3), 585–602.
6. Khalaf A.M., et al. Deascription of Rotational Bands in Superdeformed Nuclei by Using Two-parameter Empirical Formula. *Egypt Journal of Physics*, 2003, v. 34 (2), 159–177.
7. Khalaf A.M., et al. Properties of Superdeformed Rotational Bands of Odd Nuclei in the Mass-190 Region Using Harris Expansion. *Egypt Journal of Physics*, 2003, v. 34 (2), 195–215.
8. Khalaf A.M., et al. Analysis of Rotational Bands in Superdeformed Nuclei Using sdg Interacting Boson Model. *Egypt Journal of Physics*, 2004, v. 34 (1), 79–104.
9. Khalaf A.M., and Sirag M.M. Prediction of Nuclear Superdeformed Rotational Bands Using Incremental Alignments. *Egypt Journal of Physics*, 2006, v. 37 (3), 277–293.
10. Khalaf A.M., Allam M.A., and Saber E. Signature Partners in Odd Superdeformed Nuclei in Mass Region $A \sim 190$. *Egypt Journal of Physics*, 2008, v. 39 (1), 41–65.
11. Khalaf A.M., Allam M.A., and Sirag M.M. Bandhead Spin Determination and Moments of inertia of Superdeformed Nuclei in Mass Region 60-90 Using Variable Moment of inertia Model. *Egypt Journal of Physics*, 2010, v. 41 (2), 13–27.
12. Khalaf A.M., and Sirag M.M. Analysis of $\Delta I = 2$ Staggering in Nuclear Superdeformed Rotational Bands. *Egypt Journal of Physics*, 2004, v. 35 (2), 359–375.
13. Sirag M.M. A Reexamination of $\Delta I = 2$ Energy Staggering in Nuclear Superdeformed Rotational Bands. *Egypt Journal of Physics*, 2007, v. 38 (1), 1–14.
14. Flibolte S., et al. $\Delta I = 4$ bifurcation in a superdeformed band: Evidence for a C4 symmetry. *Physical Review Letters*, 1993, v. 71 4299–4302.
15. Cederwall B., et al. New features of superdeformed bands in ^{194}Hg. *Physical Review Letters*, 1994, v. 72 3150–3153.
16. Flibolte S., et al. Multi-particle excitations in the superdeformed ^{149}Gd nucleus. *Nuclear Physics*, 1995, v. A584 (2), 373–396.
17. Carpenter M.P., et al. Identification of the unfavored N=7 superdeformed band in ^{191}Hg. *Physical Review*, 1995, v. C51 2400–2405 .
18. Farris L.P., et al. Neutron blocking and delayed proton pair alignment in superdeformed ^{195}Pb. *Physical Review*, 1995, v. C51 R2288–R2292.
19. Bernstien L.A., et al. Superdeformation in ^{154}Er. *Physical Review*, 1995, v. C52 R1171–R1174.
20. Angelis G., et al. Spectroscopy in the second well of the ^{148}Gd nucleus: Two quasiparticle and collective excitations. *Physical Review*, 1996, v. C53 679–688.
21. Fischer S.M., et al. Alignment additivity in the two-quasiparticle superdeformed bands of ^{192}Tl. *Physical Review*, 1996, v. C53 2126–2133.
22. Semple A.T., et al. Energy Staggering in Superdeformed Bands in ^{131}Ce, ^{132}Ce, and ^{133}Ce. *Physical Review Letters*, 1996, v. 76 3671–3674.
23. Krucken R., et al. Test of ΔI=2 staggering in the superdeformed bands of ^{194}Hg.*Physical Review*, 1996, v. C54 R2109–R2113.
24. Cederwall B., et al. Properties of superdeformed bands in ^{153}Dy. *Physics Letters*, 1995, v. B346 (3-4), 244–250.
25. Haslip D.S., et al. ΔI= 4 Bifurcation in Identical Superdeformed Bands. *Physical Review Letters*, 1997, v. 78 3447–3450.
26. Hamamoto I. and Moltelran B. Superdeformed rotational bands in the presence of $Y_4$4 deformation. *Physics Letters*, 1994, v. B333 294–298.
27. Pavlicherkov I.M. and Flibolte S. C_4 Symmetry and bifurcation in superdeformed bands. *Physical Review*, 1995, v. C51 R460-R464.
28. Macchiavelli A.O., et al. C_4 Symmetry effects in nuclear rotational motion. *Physical Review*, 1995, v. C51 R1-R4.
29. Sun Y., Zhang J. and Guidry M. ΔI= 4 Bifurcation without Explicit Fourfold Symmetry. *Physical Review Letters*, 1995, v. 75 3398–3401.
30. Burzynski K., et al. Hexadecapole interaction and the ΔI = 4 staggering effect in rotational bands. *Physica Scripta*, 1995, v. T56 228–230.
31. Magierski P., Burzynski K. and Dobaczewski J. The ΔI=4 bifurcation in superdeformed bands. *Acta Physics Polonica*, 1995, v. B26 291–296.
32. Mikhailov I.N. and Quentin P. Band Staggering in Some Superdeformed States and Intrinsic Vortical Motion. *Physical Review Letters*, 1995, v. 74 3336–3340.
33. Reviol W., Jin H.Q. and Riendinger L.L. Transition energy staggering and band interaction in rare-earth nuclei. *Physical Letters*, 1996, v. B371 19–24.
34. Pavlicherkov I.M. Nonadiabatic mean field effects in the ΔI=2 staggering of superdeformed bands. *Physical Review*, 1997, v. C55 1275–1281.
35. Magierski P., et al. Quadrupole and hexadecapole correlations in rotating nuclei studied within the single-j shell model. *Physical Review*, 1997, v. C55 1236–1245.
36. Kota V.K.B. Interacting boson model basis and Hamiltonian for ΔL=4 staggering. *Physical Review*, 1996, v. C53 2550–2553.
37. Liu Y.X., et al. Description of superdeformed nuclear states in the interacting boson model. *Physical Review*, 1997, v. C56 1370–1379.
38. Hara K. and Lalazissis. Analysis of ΔI=2 staggering in nuclear rotational spectra. *Physical Review*, 1997, v. C55 1789–1796.
39. Toki H. and Wu L.A. ΔI= 4 Bifurcation in Ground Bands of Even-Even Nuclei and the Interacting Boson Model. *Physical Review Letters*, 1997, v. 79 2006–2009.
40. Luo W.D., et al. Microscopic study of a C4-symmetry hypothesis in A 150 superdeformed nuclei: Deformed Woods-Saxon mean field. *Physical Review*, 1995, v. C52 2989–3001.
41. Donou F., Frouendorf S. and Merg J. Can hexadecapole deformation lead to ΔI = 2 staggering in superdeformed bands. *Physics Letters*, 1996, v. B387 667–672.
42. Byrski T., et al. Observation of identical superdeformed bands in N=86 nuclei. *Physical Review Letters*, 1990, v. 64 1650–1653.
43. Backtash C., Hars B. and Nazarewicz N. Identical Bands in Normally Deformed and Superdeformed Nuclei. *Annual Review of Nuclear and Particle Science*, 1995, v. 45 485–541.
44. Chen Y.J., et al. Theoretical simulation for identical bands. *European Physical Journal*, 2005, v. A24 185–191.
45. He X.T., et al. The $i_{13/2}$ proton intruder orbital and the identical superdeformed bands in 193, 194, ^{195}Tl. *European Physical Journal*, 2005, v. A23 217–222.
46. Nazarewicz W., et al. Natural-parity states in superdeformed bands and pseudo SU(3) symmetry at extreme conditions. *Physical Review Letters*, 1990, v. 64 1654–1657.
47. Rigollet C., Bonche P. and Flocard H. Microscopic study of the properties of identical bands in the A=150 mass region C. Rigollet. *Physical Review*, 1999, v. C59 3120–3127.

Emergence of Particle Masses in Fractal Scaling Models of Matter

Hartmut Müller

Advanced Natural Research Institute in memoriam Leonhard Euler, Munich, Germany. www.anr-institute.com

Based on a fractal scaling model of matter, that reproduces systematic features in the distribution of elementary particle rest masses, the paper presents natural oscillations in chain systems of harmonic quantum oscillators as mechanism of particle mass generation.

1 Introduction

The origin of particle masses is one of the most important topics in modern physics. In this paper we won't discuss the current situation in the standard theory and the Higgs mechanism. Based on a fractal scaling model [1] of natural oscillations in chain systems of harmonic oscillators we present an alternative mechanism of mass generation.

Possibly, natural oscillations of matter generate scaling distributions of physical properties in very different processes. Fractal scaling models [2] of oscillation processes are not based on any statements about the nature of the link or interaction between the elements of the oscillating chain system. Therefore the model statements are quite generally, what opens a wide field of possible applications.

Within the last 10 years many articles were published which show that scaling is a widely distributed natural phenomenon [3–7]. As well, scaling is a general property of inclusive distributions in high energy particle reactions [8] – the quantity of secondary particles increases in dependence on the logarithm of the collision energy.

Particularly, the observable mass distribution of celestial bodies is connected via scaling with the mass distribution of fundamental particles [9], that can be understood as contribution to the fundamental link between quantum – and astrophysics.

Based on observational data, Haramein, Hyson and Rauscher [10,11] discuss a scaling law for all organized matter utilizing the Schwarzschild condition, describing cosmological to subatomic structures. From their point of view the universality of scaling suggests an underlying polarizable structured vacuum of mini white and black holes. They discuss the manner in which this structured vacuum can be described in terms of resolution of scale analogous to a fractal scaling as a means of renormalization at the Planck distance.

In the framework of our model [1], particles are resonance states in chain systems of harmonic quantum oscillators and the masses of fundamental particles are connected by the scaling exponent $\frac{1}{2}$. For example, the logarithm of the proton-to-electron mass ratio is $7\frac{1}{2}$, but the logarithm of the W-boson-to-proton mass ratio is $4\frac{1}{2}$. This means, they are connected by the equation:

$$\ln(m_w/m_{proton}) = \ln(m_{proton}/m_{electron}) - 3 \qquad (1)$$

The logarithm of the W-boson-to-electron mass ratio is $4\frac{1}{2} + 7\frac{1}{2} = 12$:

$$\ln(m_w/m_{electron}) = 12. \qquad (2)$$

Already within the eighties the scaling exponent $\frac{3}{2}$ was found in the distribution of particle masses by V. A. Kolombet [12]. In addition, we have shown [9] that the masses of the most massive bodies in the Solar System are connected by the scaling exponent $\frac{1}{2}$. The scaling exponent $3 \times \frac{1}{2}$ arises as consequence of natural oscillations in chain systems of similar harmonic oscillators [2]. If the natural frequency of one harmonic oscillator is known, one can calculate the complete fractal spectrum of natural frequencies of the chain system. Spectral nodes arise on the distance of $\frac{1}{2}$ logarithmic units. Near spectral nodes the spectral density reaches local maximum and natural frequencies of the oscillating chain system are distributed maximum densely. We suspect, that stable particles correspond to main spectral nodes which represent rational number logarithms.

The colossal difference between the life times of stable and "normal" particles is amazing. The life-time of a proton is minimum 10^{34} times larger than the life of a neutron, although the mass difference between them is only 0.13% of the proton rest mass. From this point of view seems that the stability of a particle is not connected with its mass.

In the framework of the standard theory, the electron is stable because it's the least massive particle with non-zero electric charge. Its decay would violate charge conservation. The proton is stable, because it's the lightest baryon and the baryon number is conserved. Therefore the proton is the most important baryon, while the electron is the most important lepton and the proton-to-electron mass ratio can be understood as a fundamental physical constant. Within the standard theory, the W- and Z-bosons are elementary particles which mediate the weak force. The rest masses of all these particles are measured with high precision. The precise rest masses of other elementary or stable particles (quarks, neutrinos) are nearly unknown and not measured directly.

The life-times of electron and proton seem not measurable. In addition, there is no comparison between the life of a proton ($\tau_{proton} > 10^{30}$ years) and the age of the visible universe ($\tau_{universe} > 10^{10}$ years). Though, there is an interesting scale similarity between the product of the proton life $\tau_{proton} > 10^{30}$ years and the proton mass generating frequency ω_{proton}, on

the one side, and the product of the age $\tau_{\text{universe}} > 10^{10}$ years of the visible universe and the Planck frequency ω_{Planck}, on the other side:

$$\omega_{\text{proton}} = \text{E}_{\text{proton}}/\hbar = 938\,\text{MeV}/\hbar = 1.425 \cdot 10^{24}\ \text{Hz}$$
$$\omega_{\text{proton}}\tau_{\text{proton}} > 10^{60} \tag{3}$$

$$\omega_{\text{Planck}} = \sqrt{(\text{c}^5/\hbar\text{G})} = 1.855 \cdot 10^{43}\ \text{Hz}$$
$$\omega_{\text{Planck}}\tau_{\text{universe}} > 10^{60}. \tag{4}$$

If both products are of the same scale, we can write:

$$\omega_{\text{proton}}\tau_{\text{proton}} \cong \omega_{\text{Planck}}\tau_{\text{universe}}. \tag{5}$$

Because the frequencies ω_{proton} and ω_{Planck} are fundamental constants, the equation (5) means that possibly exists a fundamental connection between the age of the visible universe and the proton life-time.

2 Methods

Based on the continued fraction method [13] we will search the natural frequencies of a chain system of many similar harmonic oscillators in this form:

$$\omega_{\text{jk}} = \omega_{00}\exp(S_{\text{jk}}). \tag{6}$$

ω_{jk} is a set of natural frequencies of a chain system of similar harmonic oscillators, ω_{00} is the natural angular oscillation frequency of one oscillator, S_{jk} is a set of finite continued fractions with integer elements:

$$S_{\text{jk}} = n_{\text{j0}} + \cfrac{1}{n_{\text{j1}} + \cfrac{1}{n_{\text{j2}} + \ddots + \frac{1}{n_{\text{jk}}}}} = [n_{\text{j0}}; n_{\text{j1}}, n_{\text{j2}}, \ldots, n_{\text{jk}}], \tag{7}$$

where $n_{\text{j0}}, n_{\text{j1}}, n_{\text{j2}}, \ldots, n_{\text{jk}} \in \text{Z}$, $\text{j} = 0, \infty$. We investigate continued fractions (7) with a finite quantity of layers k, which generate discrete spectra, because in this case all S_{jk} represent rational numbers. Possibly, the free links n_{j0} and the partial denominators $n_{\text{j1}}, n_{\text{j2}}, \ldots, n_{\text{jk}}$ could be interpreted as some kind of "quantum numbers". The present paper follows the Terskich [13] definition of a chain system, where the interaction between the elements proceeds only in their movement direction. Model spectra (7) are not only logarithmic-invariant, but also fractal, because the discrete hyperbolic distribution of natural frequencies ω_{jk} repeats itself on each spectral layer.

The partial denominators run through positive and negative integer values. Ranges of relative low spectral density (spectral gaps) and ranges of relative high spectral density (spectral nodes) arise on each spectral layer. In addition to the first spectral layer, fig. 1 shows the second spectral layer k = 2 with $|n_{\text{j1}}| = 2$ (logarithmic representation). Maximum spectral density areas (spectral nodes) arise automatically on the distance of integer and half logarithmic units.

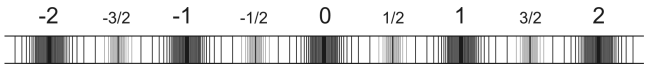

Fig. 1: The spectrum (7) on the first layer k = 1, for $|n_{\text{j0}}| = 0, 1, 2, \ldots$ and $|\text{n}_{j1}| = 2, 3, 4, \ldots$ and, in addition, the second spectral layer k = 2, with $|n_{\text{j1}}| = 2$ and $|n_{\text{j2}}| = 2, 3, 4, \ldots$ (logarithmic representation).

Fractal scaling models of natural oscillations are not based on any statements about the nature of the link or interaction between the elements of the oscillating chain system. For this reason we assume that our model could be useful also for the analysis of natural oscillations in chain systems of harmonic quantum oscillators. We assume that in the case of natural oscillations the amplitudes are low, the oscillations are harmonic and the oscillation energy E depends only on the frequency ($\hbar$ is the Planck constant):

$$E = \hbar\omega. \tag{8}$$

In the framework of our model (6) all particles are resonance states of an oscillating chain system, in which to the oscillation energy (8) corresponds the particle mass m:

$$m = \omega\hbar/\text{c}^2. \tag{9}$$

In this connection the equation (9) means that quantum oscillations generate mass. Under consideration of (6) now we can create a fractal scaling model of the mass spectrum of model particles. This mass spectrum is described by the same continued fraction 7, for $\text{m}_{00} = \omega_{00}\,\hbar/\text{c}^2$:

$$\ln(\text{m}_{\text{jk}}/\text{m}_{00}) = [n_{\text{j0}}; n_{\text{j1}}, n_{\text{j2}}, \ldots, n_{\text{jk}}]. \tag{10}$$

The frequency spectrum (7) and the mass spectrum (10) are isomorphic. The mass spectrum (10) is fractal and consequently it has a clear hierarchical structure, in which continued fractions (7) of the form $[n_{\text{j0}}; \infty]$ and $[n_{\text{j0}}; 2, \infty]$ define main spectral nodes, as fig. 1 shows.

3 Results

Based on (10) in the present paper we will calculate a list of model particle masses which correspond to the main spectral nodes and compare this list with rest masses of well measured stable and fundamental particles – hadrons, leptons, gauge bosons and Higgs bosons.

The model mass spectrum (10) is logarithmically symmetric and the main spectral nodes arise on the distance of 1 and $\frac{1}{2}$ logarithmic units, as fig. 1 shows. The mass m_{00} in (10) corresponds to the main spectral node $S_{00} = [0; \infty]$, because $\ln(m_{00}/m_{00}) = 0$. Let's assume that m_{00} is the electron rest mass 0.510998910(13) MeV/c^2 [14]. In this case (10) describes the mass spectrum that corresponds to the natural frequency spectrum (7) of a chain system of vibrating electrons. Further stable or fundamental model particles correspond to further main spectral nodes of the form $[n_{\text{j0}}; \infty]$ and $[n_{\text{j0}}; 2]$. Actually, near the node $[12; \infty]$ we find the W- and Z-bosons,

S	calculated (10) mass-interval $m_{jk}c^2$ (MeV)	corresponding particle	particle mass mc^2 (MeV) [14, 15]	$\ln(m/m_{00})$	d
$[0;\infty]$	0.451 – 0.579	electron (m_{00})	0.510998910 ± 0.000000013	0.000	0.000
$[7;2,\infty]$	815 – 1047	proton	938.27203 ± 0.00008	7.515	0.015
$[7;2,\infty]$	815 – 1047	neutron	939.565346 ± 0.000023	7.517	0.017
$[12;\infty]$	73395 – 94241	W-boson	80398 ± 25	11.966	−0.034
$[12;\infty]$	73395 – 94241	Z-boson	91187.6 ± 2.1	12.092	0.092
$[12;2,\infty]$	121008 – 155377	Higgs-boson?	125500 ± 540	12.411	−0.089
$[13;\infty]$	199509 – 256174	EWSB?			
$[51;2,\infty]$	$(1.048 - 1.345) \times 10^{22}$	Planck mass	$1.22089(6) \times 10^{22}$	51.528	0.028

Table 1: The calculated S-values (7) of $\frac{1}{4}$ logarithmic units width and the corresponding calculated model mass-intervals of main spectral nodes for the electron calibrated model mass spectrum. The deviation $d = \ln(m/m_{00}) - S$ is indicated.

but near the node $[7;2,\infty]$ the proton and neutron masses, as table 1 shows.

Theoretically, a chain system of vibrating protons generates the same spectrum (10). Also in this case, stable or fundamental model particles correspond to main spectral nodes of the form $[n_{j0};\infty]$ and $[n_{j0};2,\infty]$, but relative to the electron calibrated spectrum, they are moved by $-7\frac{1}{2}$ logarithmic units. Actually, if m_{00} is the proton rest mass 938.27203(8) MeV/c^2 [14], then the electron corresponds to the node $[-7;-2,\infty]$, but the W- and Z-bosons correspond to node $[4;2,\infty]$.

Consequently, the core claims of our model don't depend on the selection of the calibration mass m_{00}, if it is the rest mass of a fundamental resonance state that corresponds to a main spectral node. As mentioned already, this is why the model spectrum (10) is logarithmically symmetric.

Because a chain system of any similar harmonic oscillators generates the spectrum (10), m_{00} can be much less than the electron mass. Only one condition has to be fulfilled: m_{00} has to correspond to a main spectral node of the model spectrum (10). On this background all particles can be interpreted as resonance states in a chain system of harmonic quantum oscillators, in which the rest mass of each single oscillator goes to zero. In the framework of our oscillation model this way can be understood the transition of massless to massive states.

Within our model particles arise as resonance states in chain systems of harmonic quantum oscillators and their mass distribution is logarithmically symmetric. In [1] we have investigated the distribution of hadrons (baryons and mesons) in dependence on their rest masses. We have shown that all known baryons are distributed over an interval of 2 logarithmical units, of $[7;2,\infty]$ to $[9;2,\infty]$. Maximum of baryons occupy the logarithmic center $[8;2,\infty]$ of this interval. Maximum of mesons occupy the spectral node $[8;\infty]$ that split up the interval of $[0;\infty]$ to $[12;\infty]$ between the electron and the W- and Z-bosons proportionally of $\frac{2}{3}$. In addition, we have shown that the mass distribution of leptons isn't different of the baryon and meson mass distributions, but follows them. The rest mass of the most massive lepton (tauon) is near the maximum of the baryon and meson mass distributions.

In the framework of our model [1], the Planck frequency ω_{Planck} corresponds to a main spectral node of the model mass spectrum (10). Actually, relative to the proton mass generating frequency ω_{proton} the Planck frequency ω_{Planck} corresponds to the main node $[44;\infty]$ of the frequency spectrum (6):

$$\ln\frac{\omega_{Planck}}{\omega_{proton}} = \ln\frac{1.855\times10^{43}}{1.425\times10^{24}} \cong 44. \tag{11}$$

Relative to the electron mass generating frequency ω_e the Planck frequency ω_{Planck} corresponds to the spectral node $[51;2,\infty]$:

$$\ln\frac{\omega_{Planck}}{\omega_e} = \ln\frac{1.855\times10^{43}}{7.884\times10^{20}} \cong 51.5 = 44 + 7.5. \tag{12}$$

The Planck frequency ω_{Planck} is e^{44} times larger than the proton mass generating frequency ω_{proton} and the same relationship is between the Planck mass m_{Planck} and the proton rest mass m_{proton}:

$$\ln\frac{m_{Planck}}{m_{proton}} = \ln\frac{2.177\times10^{-8}}{1.673\times10^{-27}} \cong 44$$
$$m_{Planck} = \sqrt{(\hbar c/G)} = 2.177\times10^{-8}\ \text{kg}. \tag{13}$$

The Planck mass $m_{Planck} \cong 21.77\ \mu g$ corresponds to the main node $[44;\infty]$ of the proton calibrated mass spectrum (10) and therefore, probably, m_{Planck} is the rest mass of a fundamental particle. In the framework of our model [1] the gravitational constant G is connected directly with the fundamental particles masses. Now we can calculate G based on the proton rest mass m_{proton}:

$$G = \frac{\hbar c}{(e^{44}m_{proton})^2} \tag{14}$$

Resume

In the framework of the present model discrete scaling mass distributions arise as result of natural oscillations in chain systems of harmonic quantum oscillators. With high precision, the masses of known fundamental and stable particles are connected by the model scaling factor $\frac{1}{2}$. Presumably, the complete mass distribution of particles is logarithmically symmetric and, possibly, massive particles arise as resonance states in chain systems of quantum oscillators.

Within our model any chain system of harmonic quantum oscillators generates the same mass spectrum (10) and the corresponding to the spectral node $[12; 2, \infty]$ observated particle mass of 125 GeV [15] can be interpreted as resonance state in a chain system of oscillating protons, for example.

Acknowledgements

The author is deeply grateful to S. E. Shnoll, V. A. Panchelyuga and V. A Kolombet for valuable discussions and support.

Submitted on September 29, 2012 / Accepted on September 30, 2012

References

1. Müller H. Fractal scaling models of natural oscillations in chain systems and the mass distribution of the celestial bodies in the Solar System. *Progress in Physics*, 2010.
2. Müller H. Fractal scaling models of resonant oscillations in chain systems of harmonic oscillators. *Progress in Physics*, 2009.
3. Ries A., Fook M. V. L. Fractal Structure of Nature's Preferred Masses: Application of the Model of Oscillations in a Chain System. *Progress in Physics*, 2010.
4. Ries A., Fook M. V. L. Application of the Model of Oscillations in a Chain System to the Solar System. *Progress in Physics*, 2011.
5. Kelvin K. S. Wu, Ofer Lahav, Martin J. Rees. The large-scale smoothness of the Universe. *Nature*, Vol. 397, 1999.
6. Barenblatt G. I. Scaling. Cambridge University Press, 2003.
7. Tatischeff B. Fractals and log-periodic corrections applied to masses and energy levels of several nuclei. arXiv:1107.1976v1, 2011.
8. Feynman R. P. Very High-Energy Collisions of Hadrons, *Phys. Rev. Lett.* 23, 1969, 1415.
9. Müller H. Fractal scaling models of natural oscillations in chain systems and the mass distribution of the celestial bodies in the Solar System. *Progress in Physics*, 2010.
10. Haramein N., Hyson M., Rauscher E. A. Proceedings of The Unified Theories Conference. 2008. Scale Unification: A Universal Scaling Law for Organized Matter, in Cs Varga, I. Dienes & R.L. Amoroso (eds.), The Noetic Press, ISBN 9780967868776.
11. Haramein N. Scaling Law for Organized Matter in the Universe. *Bull. Am. Phys. Soc.* AB006, Ft. Worth, October 2001.
12. Kolombet V. Macroscopic fluctuations, masses of particles and discrete space-time. *Biofizika*, 1992, v. 36, pp. 492–499 (in Russian)
13. Terskich V. P. The continued fraction method. Leningrad, 1955 (in Russian).
14. Particle listings. Astrophysical constants. Particle Data Group, www.pdg.lbl.gov.
15. Pier Paolo Giardino et al. Is the resonance at 125 GeV the Higgs boson? arXiv:1207.1347v1, 2012.

Resonance and Fractals on the Real Numbers Set

Victor A. Panchelyuga, Maria S. Panchelyuga

Institute of Theoretical and Experimental Biophysics, Pushchino, Russia.
Research Institute of Hypercomplex Systems in Geometry and Physics, Friazino, Russia. E-mail: panvic333@yahoo.com

The paper shown that notions of resonance and roughness of real physical systems in applications to the real numbers set lead to existence of two complementary fractals on the sets of rational and irrational numbers accordingly. Also was shown that power of equivalence classes of rational numbers is connected with well known fact that resonance appear more easily for pairs of frequencies, which are small natural numbers.

1 Introduction

Well known that resonance is relation of two frequencies p and q, expressed by rational number $r \in \mathbb{Q}$:

$$r = \frac{p}{q}, \tag{1}$$

where $p, q \in \mathbb{N}$ and $\mathbb{N}$ is the set of natural numbers, $\mathbb{Q}$ is set of rational numbers. If r is irrational number, i.e. $r \in \mathbb{Q}^*$, where $\mathbb{Q}^*$ is set of irrational numbers, resonance is impossible.

Resonance definition as $r \in \mathbb{Q}$ leads to the next question. For real physical system p, q and, consequently, r cannot be a fixed number due to immanent fluctuations of the system. Consequently, condition $r \in \mathbb{Q}$ cannot be fulfilled all time because of irrational numbers, which fill densely neighborhood of any rational number. By these reasons, resonance condition $r \in \mathbb{Q}$ cannot be fulfilled and resonance must be impossible. But it is known that in reality resonance exists. The question is: in which way existence of resonance corresponds with it's definition as $r \in \mathbb{Q}$?

Also is known that resonance appear more easily for such $r \in \mathbb{Q}$ for which p and q are small numbers. As will be shown this experimental fact is closely connected with the question stated above.

2 Rational numbers distribution

The question stated above for the first time was considered by Kyril Dombrowski [1]. He suppose that despite the fact that rational numbers distributed densely along the number axis this distribution may be in some way non-uniform. In cited work K. Dombrowski used proposed by Khinchin [2] procedure of constructing of rational numbers set, based on the following continued fraction:

$$\left\{Q_i^{a_i}\right\} = \cfrac{1}{a_1 \pm \cfrac{1}{a_2 \pm \cfrac{1}{\dots \; a_i \pm \cfrac{1}{\dots}}}} \tag{2}$$

where $a_1, a_2, \dots, a_i = \overline{1, N}$, $i = \overline{1, N}$. Continued fraction (2) gives rational numbers, which belongs to interval $[0, 1]$. Is known that exists one-to-one correspondence between [0,1] and $[1, \infty)$ intervals. I.e., any regularities obtained from (2) on the interval $[0, 1]$ will be also true and for interval $[1, \infty)$.

In case $N \to \infty$ expression (2) leads to

$$\left\{Q_i^{a_i} \middle| N \to \infty\right\} \to \mathbb{Q}.$$

Apparently, in this case no distribution available, because rational numbers distributed along number axis densely.

For case of real physical system, condition $N \to \infty$ means that any parameters of the system must be defined with infinite accuracy. But in reality parameters values of the systems cannot be defined with such accuracy even if we have an ideal, infinite-accuracy measuring device. Such exact values simply don't exist because of quantum character of physical reality.

All this means that for considered physical phenomenon – resonance – we need to limit parameter i in (2) by some finite number N. Fig. 1 presents numerical simulation of (2) for the first two cases of finite N: $N = 1$, $N = 2$, and $N = 3$. In the case $N = 1$ (Fig. 1*a*) we have only one value $i = 1$, and from (2) we can obtain:

$$\left\{Q_1^{a_1}\right\} = \frac{1}{a_1}, \quad i = 1, \quad a_1 = \overline{1, \infty}. \tag{3}$$

In the case of $N = 2$, analogously:

$$\left\{Q_i^{a_i}\right\} = \frac{1}{a_1 \pm \cfrac{1}{a_2}} = \frac{a_2}{a_1 a_2 \pm 1}, \quad i = 1, 2, \quad a_1, a_2 = \overline{1, \infty}. \tag{4}$$

For the case $N = 3$ we have

$$\left\{Q_i^{a_i}\right\} = \frac{1}{a_1 \pm \cfrac{1}{a_2 \pm \cfrac{1}{a_3}}} = \frac{a_2 a_3 \pm 1}{a_1(a_2 a_3 \pm 1) \pm a_3}, \tag{5}$$

$$i = 1, 2, 3; \quad a_1, a_2, a_3 = \overline{1, \infty}.$$

It's easy to see that final set presented in Fig. 1c has a fractal character. Vicinity of every line in Fig. 1b is isomorphic to

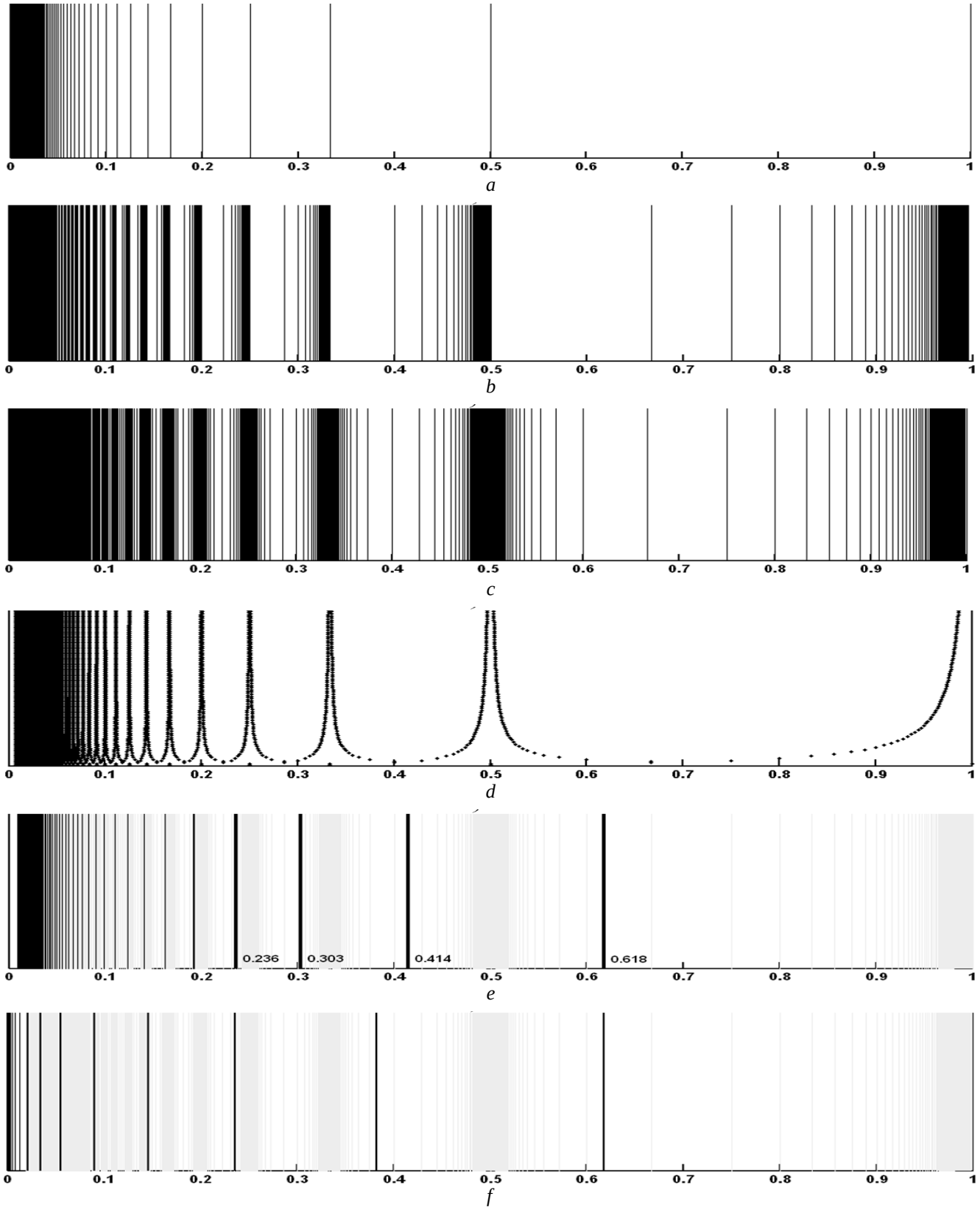

Fig. 1: Rational (a) – (d) and irrational (e) – (f) numbers distribution.

whole set in Fig. 1a. Consequently, vicinity of every line in Fig. 1c is isomorphic to whole set in Fig. 1b. Apparently that such regularity will be repeated on every next step of the algorithm and we can conclude that (2), in the case of $N \to \infty$, gives an example of mathematical fractal, which in the case of finite N gives an pre-fractal, which can be considered as physical fractal.

From Fig. 1c we can conclude that rational numbers for the case of finite N distributed along number axis inhomogeneously. This conclusion proves density distribution of rational numbers, constructed on the base of set presented in Fig. 1c, and given in Fig. 1d.

Summarizing, we can state that roughness of parameters of real physical system modeled by finite N in (2) leads to inhomogeous fractal distribution of rational numbers along number axis. As follows from Fig. 1d major maxima in the distribution defined by first steps of algorithm given in (3).

3 Equivalence classes of rational numbers and resonance

Expression (1) can be rewrite in terms of wavelength λ_p and λ_q, which corresponds to frequencies p and q:

$$r = \frac{p}{q} = \frac{\lambda_q}{\lambda_p}. \qquad (6)$$

Suppose, that $\lambda_q > \lambda_p$. Then (6) means that wavelength λ_q is an integer part of λ_p. In this case resonance condition can be write in the form $\lambda_q \bmod \lambda_p = 0$, or in more general form:

$$n \bmod i = 0, \qquad (7)$$

where $i, n \in \mathbb{N}$, $i, n = \overline{1, \infty}$. All i, which satisfy (7) gives integer divisors of natural number n. Fig. 2 gives graphical representation of numbers of integer divisors of n, obtained from (7).

Analogously to previous, roughness of physical system in the case of (7) can be modeled if instead of $n \to \infty$ will be used condition $n \to N$, where N is quite large, but finite natural number. In this case we can directly calculate power of equivalence classes of n, which belong to segment $[1, N]$. Result of the calculation for $N = 5000$ is given in Fig. 3.

As follows from Fig. 3a – b the power of equivalence classes is maximal only for first members of natural numbers axis.

From our point of view this result can explain the fact that resonance appears easier when p and q are small numbers. Really, for the larger power of equivalence classes exist the greater number of pairs p and q (different physical situations), which gives the same value of r, which finally make this resonance relation more easy to appear.

An interesting result, related to the power of equivalence classes, is presented in Fig. 4. This result for the first time was described, but not explained in [3]. In Fig. 4 are presented diagrams, obtained by means of the next procedure.

Number sequence, presented in Fig. 2, was divided onto

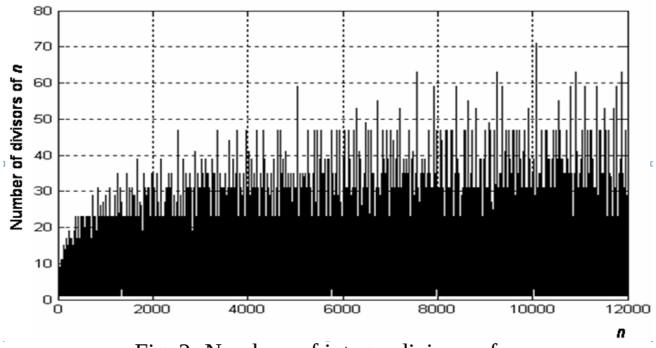

Fig. 2: Numbers of integer divisors of n.

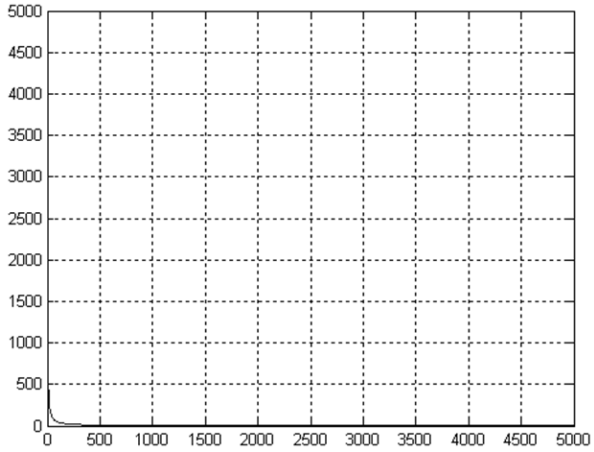

(a)

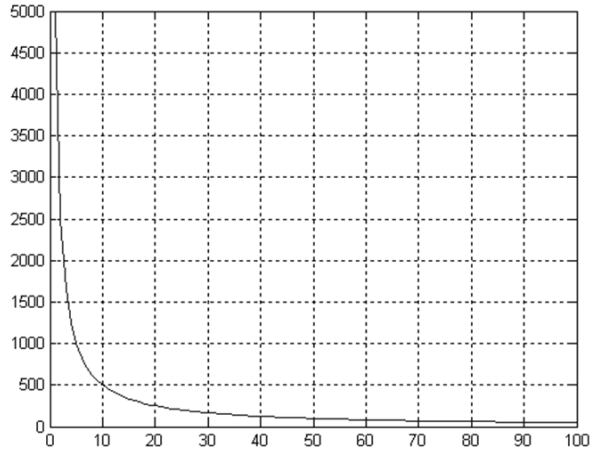

(b)

Fig. 3: Power of equivalence classes for $N = 5000$, (a); magnified part of (a) for $N = 100$, (b). X-axis: value of N, Y-axis: power of equivalence classes.

equal Δn-points segments. In this way we obtain $\frac{N}{\Delta n}$ segments. The points in the segments was numerated from 1 to Δn. Finally all points with the same number in $\frac{N}{\Delta n}$ segments were summarized.

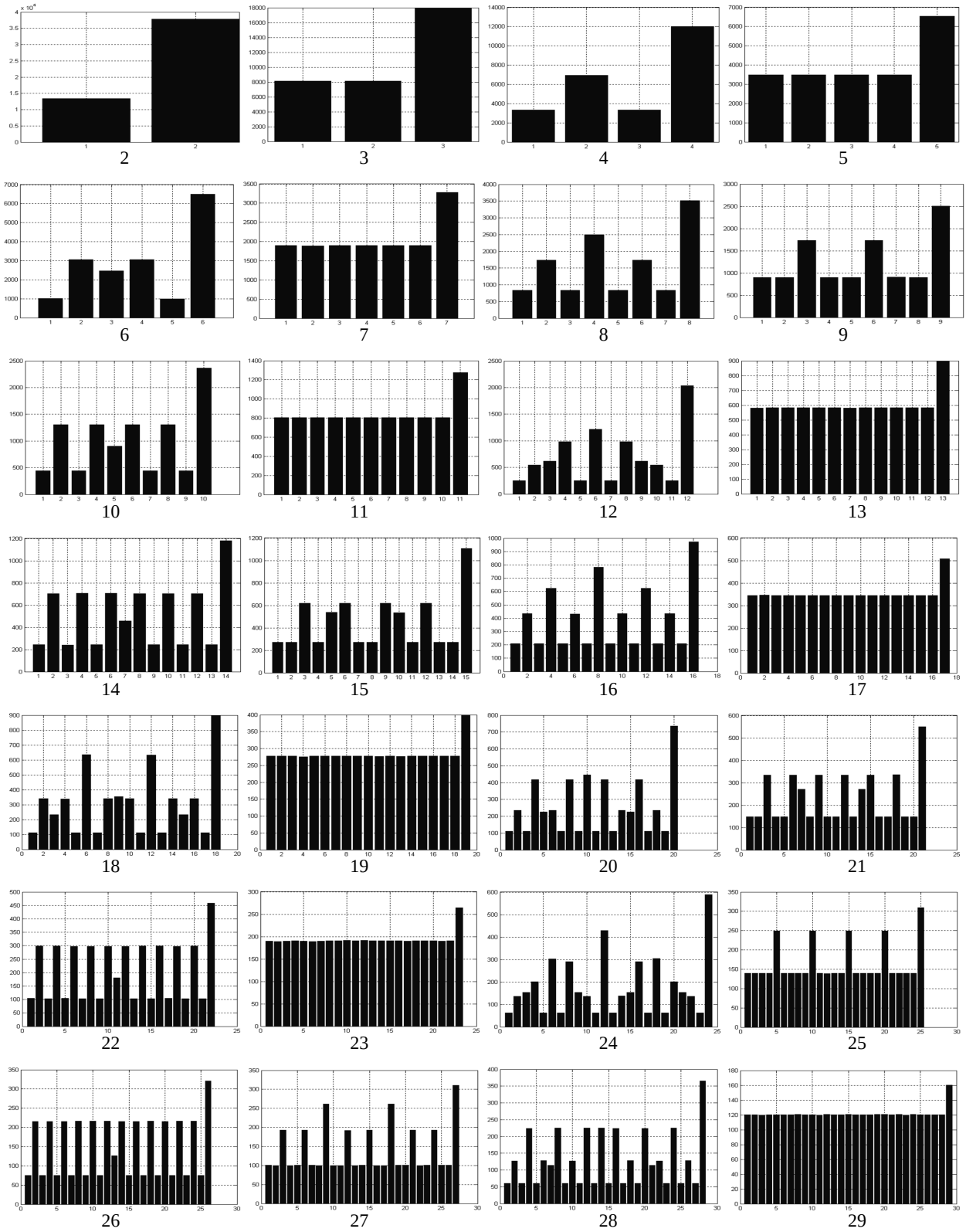

Fig. 4: Diagrams constructed on the base of sequence, presented in Fig. 2. The length of Δn-points segments pointed by number below the diagrams.

It can be seen from Fig. 4 that form of straight case when Δn is a prime number diagram always have a line. Otherwise presents some unique pattern. If we examine patterns, displayed in Fig. 4, we can find that in the role of buildings blocks, which define structure of the patterns with relatively big Δn, serve the patterns obtained for relatively small Δn. The patterns with small Δn based on numbers with greater power of equivalence classes and therefore manifests itself trough summarizing process in contradiction from relatively big values of Δn.

4 On irrational numbers distribution

Presented in Fig. 1c – d rational numbers distribution displays some rational maxima. Existence of such maxima means that in the case of rational relations, which correspond to the maxima, resonance will appear more easy and interaction between different parts of considered physical system will be more strong. If parameters of the system correspond to the maxima, such system becomes unstable, because of interaction, which is maximal for this case.

Analogously to rational maxima is interesting to consider existence of irrational maxima, which in opposition to rational one, must correspond to minimal interaction between parts of the system and to its maximal stability. Work [1] suppose that irrational maxima correspond to minima in rational numbers distribution. In the role of "the most irrational numbers" was proposed algebraic numbers, which are roots of equation

$$\alpha^2 + \alpha b + c = 0. \tag{8}$$

Assume that $c = -1$. Then

$$\alpha = \frac{1}{\alpha + b} = \frac{1}{b + \dfrac{1}{b + \dfrac{1}{b + \cdots}}} = \frac{\sqrt{b^2 + 4} - b}{2}. \tag{9}$$

Infinite continued fraction gives the worst approximation for irrational number α the smaller is its $k+1$ component. So, the worst approximation will be in the case $b = 1$:

$$\alpha_1 = \frac{1}{1 + \dfrac{1}{1 + \dfrac{1}{1 + \cdots}}} = \frac{\sqrt{5} - 1}{2} = 0.6180339. \tag{10}$$

The case $b = 1$ corresponds to co-called golden section. Farther calculations on the base of (9) give:

$$\alpha_2 = \frac{1}{2 + \dfrac{1}{2 + \dfrac{1}{2 + \cdots}}} = \frac{\sqrt{8} - 2}{2} = 0.4142135,$$

$$\alpha_3 = 0.3027756,$$

$$\alpha_4 = 0.2360679,$$

$$\cdots\cdots\cdots\cdots$$

Results of calculations are presented in Fig. 1e. Grey lines in Fig. 1e give rational numbers distribution, which is identical to Fig. 1c. Black lines give results of numerical calculation, based on (9) for $b = \overline{1, 100}$. Bold black lines point cases $\alpha_1, \ldots, \alpha_4$.

As possible to see from Fig. 1e algebraic numbers with grows of b have tendency became closer to rational maxima. This result, indicate that such numbers, possibly, are not the best candidate for "the most irrational ones" [1].

In present work we don't state the task to find explicit form of irrational numbers fractal. It is clear, that first irrational maxima must be connected with golden section. The question is about the rest of the maxima. Fig. 1f gives another attempt to construct such maxima on the base of set, given by generalized golden proportion [4]. It is obvious from Fig. 1f that this case also is far away from desired result.

5 Summary

All results described in the paper are based on the notions of resonance and roughness of real physical system. This notions in applications to set of real numbers leads to existence of rational numbers distribution, which has fractal character. Maxima of the distribution (Fig. 1d) correspond to maximal sensitivity of the system to external influences, maximal interaction between parts of the system. Resonance phenomena are more stable and appear more easy if r (1) belong to rational maxima (Fig. 1d).

Obtained rational numbers distribution (Fig. 1c – d) contains also areas where density of rational numbers are minimal. It's logically to suppose that such minima correspond to maxima in irrational numbers distribution. We suppose that such distribution exists and is complementary to distribution of rational numbers. Maxima in such distribution correspond to high stability of the system, minimal interaction between parts of the system, minimal interaction with surrounding.

Both irrational and rational numbers distribution are related to the same physical system and must be consider together.

Question about explicit form of irrational numbers distribution remains open. At the moment we can only state that main maxima in this distribution must corresponds to co-called golden section (10).

Ideas about connection between resonance and rational numbers distribution can be useful in [4–8] where used the same mathematical apparatus, but initial postulates are based on the model of chain system.

Acknowledgements

The authors is grateful to S. E. Shnoll, V. A. Kolombet, H. Müller and D. Rabounski for valuable discussions and support.

Submitted on September 29, 2012 / Accepted on September 30, 2012

References

1. Dombrowski K. Rational Numbers Distribution and Resonance. *Progress in Physics*, 2005, v. 1, 65 – 67.
2. Khinchin A. Ya. Continued fractions. M., 1978. (in Russian)
3. Shnoll S. E. at al. About regularities in discrete distributions of measuring results (cosmophysical aspects). *Biophysics*, 1992, v. 37, No. 3, 467 – 488. (in Russian)
4. Stakhov A. P. Codes of golden proportion. M., 1984. (in Russian)
5. Müller H. Fractal Scaling Models of Resonant Oscillations in Chain Systems of Harmonic Oscillators. *Progress in Physics*, 2009, v. 2, 72 – 76.
6. Müller H. Fractal scaling models of natural oscillations in chain systems and the mass distribution of the celestial bodies in the Solar system. *Progress in Physics*, 2010, v. 1, 62 – 66.
7. Müller H. Fractal scaling models of natural oscillations in chain systems and the mass distribution of particles. *Progress in Physics*, 2010, v. 3, 61 – 66.
8. Ries A., Vinicius M. Lia Fook Application of the model of oscillations in a chain system to the Solar System. *Progress in physics*, 2011, v. 1, 103 – 111.

LETTERS TO PROGRESS IN PHYSICS

LETTERS TO PROGRESS IN PHYSICS

Atomic Masses of the Synthesed Elements (No.104–118) being Compared to Albert Khazan's Data

Albert Khazan
E-mail: albkhazan@gmail.com

Herein, the Hyperbolic Law of the Periodic System of Elements is verified by new data provided by theory and experiments.

A well-known dependence exist in the Periodic Table of Elements. This dependence links atomic masses of chemical elements with their numbers in the Table. Our research studies [1, 2] produced in the recent years showed that this dependence continues onto also the region of the synthetic elements located, in the Table, from Period 7 upto the end of Period 8. As is seen in Fig. 1, our calculations can be described by an equation whose coefficient of truth approximation is $R^2 = 0.99995$. However the experimental data obtained by the nuclear physicists, who synthesed the super-heavy elements, manifest a large scattering which gives no chance to get a clear dependence in this region. This is because their experiments were produced in the hard conditions, and only single atoms were synthesed that makes no possibilities for any statistics. Despite this drawback, the nuclear physicists continue attempts to synthese more and more super-heavy elements, still giving their characteristics to be unclear exposed. At the present day, 15 super-heavy elements (No.104–118) were synthesed. Obtained portions of them are as microscopic as the single atoms [3]. Therefore, masses of the products of the reactions are estimated on the basis of calculations. Analysis of the calculated data being compared to the data obtained on the basis of our theory is given in Fig. 2. The upper arc shows the difference between the atomic masses obtained on the basis of the experimental data (which are unclear due to the large scattering) and our exact calculations. All given in the Atomic Units of Mass (A.U.M.).

In the upper arc of Fig. 2, these numerical values are converted into percents. As is seen, this arc has a more smooth shape, while there is absolutely not deviations for elements No. 105 and No. 106. Most of the deviations is less than 2%. Only 5 points reach 2.5–3.6%. Proceeding from these results, we arrive at the following conclusion. Because our calculation was true on the previous numerical values, it should be true in the present case as well. Hence, the problem rises due to the complicate techniques of the experiments, not doubts in our theory which was checked to be true along all elements of the Periodic Table. It is important to note that our theoretical prediction of element No.155 [1, 2], heavier of whom no other elements can be formed, arrived after this.

Concerning the experimental checking of our theory. There are super-heavy elements which were synthesed already later as my first research conclusions were published in 2007 [1]. These new elements — their characteristics obtained experimentally (even if with large scattering of the numerical values) — can be considered as the experimental verification of the theory I suggested [1, 2], including the Hyperbolic Law in the Periodic Table of Elements, and the upper limit of the Table in element No.155.

Submitted on September 01, 2012 / Accepted on September 13, 2012

References

1. Khazan A. Upper Limit in the Periodic Table of Elements. Progress in Physics, 2007, v. 1, 38–41.
2. Khazan A. Upper Limit in Mendeleev's Periodic Table — Element No. 155. American Research press, Rehoboth (NM), 2012.
3. Web Elements: the Periodic Table on http://webelements.com

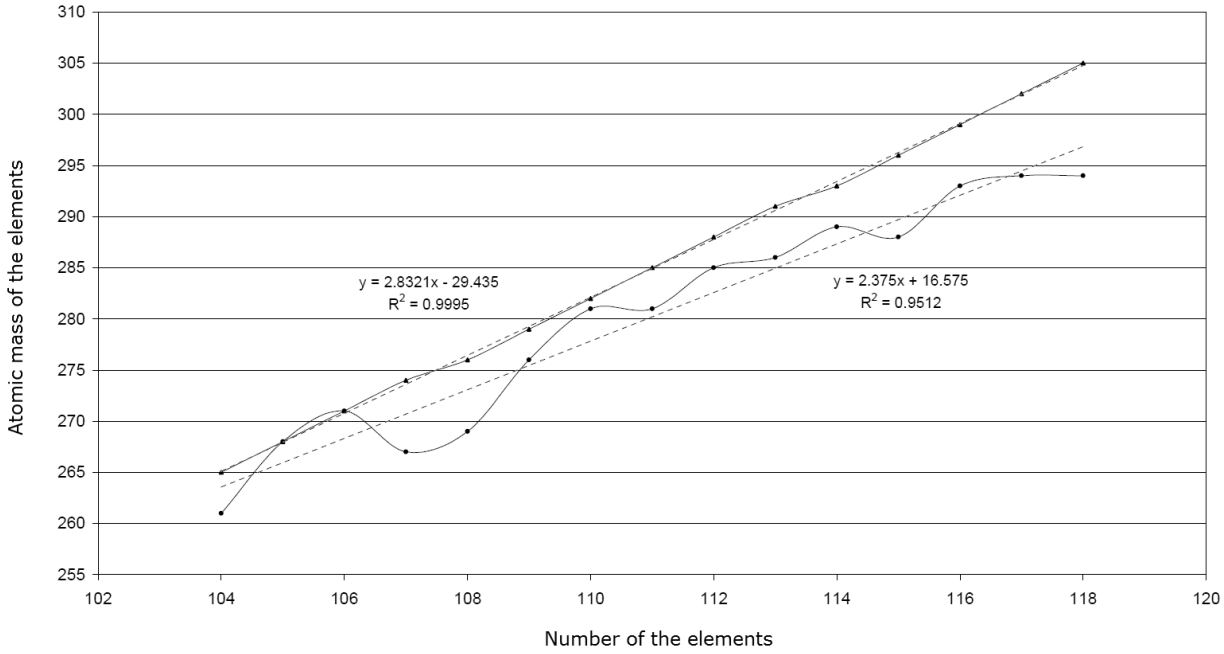

Fig. 1: Dependence of the atomic masses of the elements on their number in the Periodic Table. The experimental data (obtained with large scattering of the numerical values) are shown as the curved arc. Our calculations are presented with the straight line.

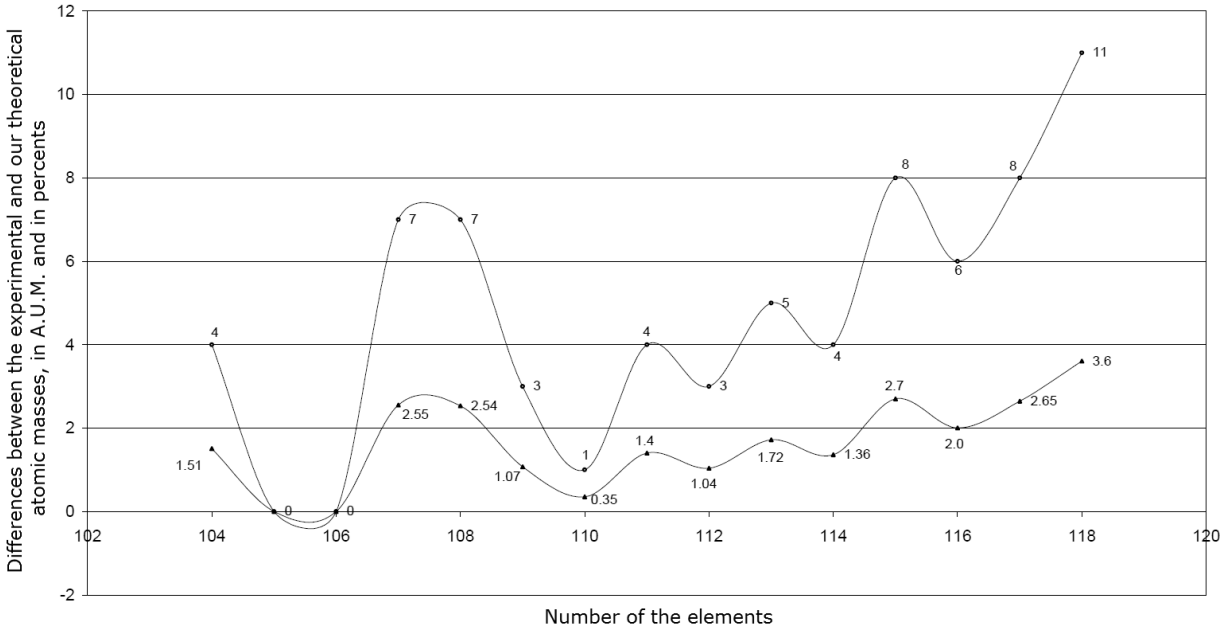

Fig. 2: Differences between the atomic masses (experimental and our theoretical), obtained in the region of the super-heavy (synthetic) elements No.104–No.188. The upper arc manifests the differences in A.U.M. (g/mole). The lower arc — the same presented in percents.

Progress in Physics is an American scientific journal on advanced studies in physics, registered with the Library of Congress (DC, USA): ISSN 1555-5534 (print version) and ISSN 1555-5615 (online version). The journal is peer reviewed and listed in the abstracting and indexing coverage of: Mathematical Reviews of the AMS (USA), DOAJ of Lund University (Sweden), Zentralblatt MATH (Germany), Scientific Commons of the University of St.Gallen (Switzerland), Open-J-Gate (India), Referential Journal of VINITI (Russia), etc. Progress in Physics is an open-access journal published and distributed in accordance with the Budapest Open Initiative: this means that the electronic copies of both full-size version of the journal and the individual papers published therein will always be acessed for reading, download, and copying for any user free of charge. The journal is issued quarterly (four volumes per year).

Electronic version of this journal: http://www.ptep-online.com

Postal address:
Department of Mathematics and Science,
University of New Mexico, 705 Gurley Avenue, Gallup, NM 87301, USA

Printed in the United States of America